

①

Performance of Deep Excavations in Boston

by

Michael P. Whelan

B.S., Geological Engineering
Colorado School of Mines, 1990

M.S., Environmental Engineering
Georgia Institute of Technology, 1992


Submitted to the Department of
Civil and Environmental Engineering in Partial Fulfillment of
the Requirements for the Degree of

MASTER OF SCIENCE
in Civil and Environmental Engineering
at the Massachusetts Institute of Technology

February, 1995

© copyright 1995, Massachusetts Institute of Technology
All Rights Reserved


Signature of Author


Department of Civil and Environmental Engineering
January 17, 1995

Certified by

Professor Charles C. Ladd
Thesis Supervisor

Accepted by


Professor Joseph M. Sussman
Chairman, Departmental Committee on Graduate Studies

MASSACHUSETTS INSTITUTE
OF TECHNOLOGY

Barker Eng

OCT 25 1995

PERFORMANCE OF DEEP EXCAVATIONS IN BOSTON

by
MICHAEL P. WHELAN

Submitted to the Department of Civil and Environmental Engineering on January 20, 1995 in partial fulfillment of the requirements for the Degree of Master of Science in Civil and Environmental Engineering

ABSTRACT

Lateral movements, settlements, and groundwater fluctuations resulting from excavations for a project in Boston were measured with various types of geotechnical instruments. The data collected from these instruments were studied in an attempt to relate the measured movements and water fluctuations to construction activities, and to compare the measurements with predictions from available empirically-based design charts. This study is one component of a three-phase research project entitled "Design and Performance of Deep Excavations", which is being conducted by MIT and aims to develop improved methods of predicting ground movements associated with deep excavations in "soft" clays.

The research focused on a single, well-instrumented section near the west end of the excavation under consideration. At this location, the excavation was about 40 feet deep and 200 feet wide, and the soil profile included an approximately 30-foot-thick layer of cohesive fill and organic deposits and over 60 feet of Boston Blue Clay (BBC). The cut was supported by two types of walls: a sheetpile wall on one side, and a concrete diaphragm wall on the other side, where an adjacent structure needed to be protected. Both walls were supported by tiebacks. Behind the sheetpile wall, the tiebacks were approximately 25 to 85 feet long and grouted in the crust of the BBC. Behind the diaphragm wall, the tiebacks were about 125 to 170 feet long and grouted in bedrock.

Construction records were used to define the history of construction at the chosen cross-section as precisely and accurately as possible. This allowed geotechnical data to be correlated to construction events that may have influenced soil movements and groundwater levels. Graphs were prepared which plotted geotechnical data against time and graphically summarized the schedule of excavation and tieback installation.

Existing design charts and the MOVEX computer program were used to compare measured settlements and wall deflections to predicted movements, at each side of the excavation. Although the deflection of the South (sheetpile) wall was underpredicted, the settlements were slightly over-predicted, probably due to consolidation of the underlying soils induced by deep pumping. The predictions failed to duplicate the behavior of the North diaphragm wall, which was pulled back into the retained soil by the tiebacks. However, settlements measured behind the North wall exceeded predictions, probably because of soil consolidation in possible conjunction with disturbance of the BBC induced by tieback installation.

Thesis Supervisor: Prof. Charles C. Ladd
Title: Edmund K. Turner Professor of Civil and Environmental Engineering

ACKNOWLEDGEMENTS

This research would have been impossible were it not for all the people who assisted me in my efforts to make some sense out of an amazingly vast collection of data.

First of all, my sincere thanks goes out to the staff in the Management Consultant's main office. Dave Druss helped us get this whole effort going, and remained involved to the very end by making a final technical review of this thesis. Charles Daugherty served as the official liaison to MIT, and introduced me to the project's Field Office, where I spent so many autumn afternoons. I also want to thank Dan Bobrow for his willingness to teach me GTILT, Touraj Saffari for helping me with AutoCAD files, and Pat Dowling for her patience with my desire to root through all of the data file boxes.

The engineers and staff at the Field Office were extremely generous of their time, knowledge, and experience, and would have been hard pressed to make sense out of all the data were it not for my numerous discussions with them. I wish to thank them for always pointing me toward the right person or file cabinet, or, if I was still confused about something, sitting down with me to try and hash it out.

During all of this, of course, MIT served as my "home base", and I must say that I will really miss all of the folks there who made life as enjoyable as it was. Special thanks must go first to the small - but powerful - research team. Lucy Jen remained a good friend throughout my entire stay here, ever since the early days of geotech lab (although I still claim that she was responsible for that now-legendary dropped sample). Rob Jameson, a relative newcomer, proved an invaluable friend and has especially earned my eternal gratitude for all his help during - and after - my return trip from Seattle. Rob did a noble job of acting as the thesis' curator throughout the many rounds of painful surgery that it was forced to undergo.

My advisor, Professor Ladd, was always encouraging and I greatly appreciate his ability to keep things moving, and his willingness to put up with my tendency to make the scheduling as complicated as possible. It was a long haul, but he got me through, as he promised. I also thank Professor Whittle for his suggestions on the work.

Let me add a special thanks to Professor Ladd for his efforts on behalf of this document, even months after I left the MIT campus. His tireless efforts have preserved the integrity of the thesis and prevented it from ending up in complete tatters at the hands of lawyers and bureaucracies.

I leave behind so many friends at MIT. It's great to be finally heading west, but I'll miss you all. Jason Bialon, Doug Cauble, Samir Chauhan, Mike Geer, Violeta Ivanova, Dante Legaspi, Marika Santagata, Joe Sinfield, and the whole cast: thanks for good times, kind words, and those pizzas. Hope you all enjoy the free movies.

The last person I'll thank is the one that I'm leaving with. Lara, I love you. Thank you for being so strong and putting up with so many trials this last year. It was never easy, yet you kept me going more than you'll ever realize. And now, finally, *finally*, we can return to the west, where we always belonged.... to the Emerald City, to snowcapped peaks in every direction, and to the "Ocean That Has No Memory"...

Mike Whelan

TABLE OF CONTENTS

Abstract	3
Acknowledgements.....	5
Table of Contents	7
List of Tables	11
List of Figures.....	13
1. Introduction	21
1.1. Background	21
1.2. Overview of Braced Excavation	22
1.2.1. General.....	22
1.2.2. Typical Support Methods and Construction Sequence	23
1.3. Scope of Thesis.....	25
2. Soil Movements and Their Prediction.....	33
2.1. Introduction.....	33
2.2. Recommendations from Case Studies.....	34
2.3. Semi-Empirical Design Charts.....	36
2.4. Studies of Specific Excavations with the Finite-Element Technique	38
3. Description of the Construction Project in Boston	47
3.1. Site Layout	47
3.2. Subsurface Soil Profile.....	48
3.3. Support of Excavation	49
3.3.1. Sheetpile and Diaphragm Walls.....	50
3.3.2. Tiebacks.....	51
3.3.2.1. Sheetpile Wall Tiebacks	52
3.3.2.2. Slurry Wall Tiebacks (rock anchors).....	55
3.3.3. Boat Section Structure and Tiedowns.....	57
3.4. Excavation Dewatering and Pressure Relief.....	58
4. Geotechnical Instrumentation and Selection of Test Section	75
4.1. Geotechnical Instrumentation.....	75
4.2. Selection of Instrumented Section for Analysis.....	76
4.2.1. Selection Criteria.....	76
4.2.2. Review of Available Instrumented Sections.....	77
4.2.3. Review of Construction Histories	78
4.2.4. Review of Soil Movement	78
4.2.5. Selection of ISS-4	80

5. Soil Stratigraphy and Soil Properties at ISS-4.....	95
5.1. Soil Stratigraphy	95
5.2. Groundwater Regime.....	96
5.3. Overburden Stresses	97
5.4. Index and Engineering Properties of Main Deposits.....	98
5.4.1. Recent Fill Deposits.....	98
5.4.1.1. Granular and Miscellaneous Fills	99
5.4.1.2. Cohesive Fill	99
5.4.2. Organic Deposits	101
5.4.3. Boston Blue Clay	102
5.4.3.1. General	102
5.4.3.2. Index Properties.....	103
5.4.3.3. Stress History and Undrained Strength Profiles	104
5.4.3.4. Stress History Developed by MIT	106
5.4.3.5. Compressibility Parameters	107
5.4.3.6. Coefficients of Consolidation and Permeability	107
5.4.3.7. Undrained Shear Strength	108
5.4.3.8. Drained Shear Strength.....	109
5.4.3.9. Coefficient of Earth Pressure at Rest (K_0)	109
5.4.4. Glacial Deposits	109
5.4.4.1. General	109
5.4.4.2. Glaciomarine Deposits	110
5.4.4.3. Glacial Till	111
5.4.5. Bedrock	111
6. Conditions and Construction History at ISS-4.....	133
6.1. Objectives	133
6.2. Geometry and Structural Features.....	133
6.2.1. SOE Walls and Tiebacks.....	134
6.2.2. Geotechnical Instrumentation	135
6.3. Tieback Lock-off Loads and Elastic Moduli	135
6.3.1. Data Collection and Sources.....	136
6.3.2. Averaged Tieback Loads	136
6.3.3. Effective Moduli of Tiebacks	137
6.4. Excavation History	138
6.4.1. Data Collection and Sources.....	138
6.4.2. Finalized Excavation History	140
7. Instrument Monitoring Data from ISS-4.....	151
7.1. Presentation of Data.....	151
7.1.1. Data-vs.-Time Plots.....	152
7.1.2. Presentation of Data in “Time Period Summaries”	154
7.2. Discussion of Instrumentation Data.....	156
7.2.1. Settlements and Wall Movements	156
7.2.1.1. North Side of Excavation	

(behind concrete diaphragm wall).....	156
7.2.1.2. South Side of Excavation (behind sheetpile wall).....	160
7.2.2. Groundwater Levels Around and Below Excavation.....	166
7.2.2.1. Pore Pressures in the Lower Aquifer.....	166
7.2.2.2. Groundwater Levels North of Excavation.....	168
7.2.2.3. Groundwater Levels South of Excavation.....	169
7.2.3. Heave and Pore Pressures Within Excavation.....	170
8. Further Analyses and Comparison of Data to Predictions.....	209
8.1. Further Analysis of Instrumentation Data.....	209
8.1.1. Responses to Pressure Relief Drawdowns.....	209
8.1.1.1. Pore Pressure Dissipation in BBC.....	209
8.1.1.2. Settlements of Soil Layers.....	211
8.1.2. Pore Pressure Reductions due to Excavation Unloading.....	213
8.2. Comparison of Movements to Predictive Techniques.....	214
8.2.1. Purpose and Objectives.....	214
8.2.2. Normalized Settlements.....	214
8.2.3. Prediction of Settlements and Wall Deflections using MOVEX.....	215
8.2.3.1. The MOVEX Computer Program.....	215
8.2.3.2. Results of MOVEX Analyses.....	217
9. Summary and Conclusions.....	231
9.1 Summary.....	231
9.2 Conclusions.....	235
9.2.1. Factors Influencing Wall and Soil Movements.....	235
9.2.2. Comparison of Measured Wall and Soil Movements to Predictions.....	236
9.2.2.1. North Side of Excavation (Diaphragm Wall A).....	236
9.2.2.2. South Side of Excavation (Sheetpile Wall).....	237
9.2.2.3. Trends Common to Both Walls.....	237
9.2.3. Groundwater and Soil Movements Within the Excav.....	237
9.3. Recommendations.....	238
9.3.1. Excavation Conditions and Excavation History.....	238
9.3.2. Presentation of Geotechnical Instrumentation Data.....	238
10. List of References.....	241
Appendix A - Review of Geotechnical Instrumentation.....	245
A.1. Purpose of Geotechnical Instrumentation.....	245
A.2. Instruments Which Measure Lateral Deformations (Inclinometers).....	245
A.3. Instruments Which Measure Vertical Deformations.....	248
A.3.1. Deformation Monitoring Points.....	248

A.3.2. Probe Extensometers	249
A.3.3. Heave Gages	251
A.4. Instruments Which Measure Groundwater Levels and Pore Pressures	252
Appendix B - Engineering Properties of Cohesive Soils	275
Appendix C - Excavation Support System: SOE Walls and Tiebacks.....	295
Appendix D - Available Information on Excavation History	315
Appendix E - Data Plots Provided by Contractor	321
Appendix F - Analysis of Consolidation and Settlement	331
Appendix G - Analysis using MOVEX.....	341

LIST OF TABLES

Table 1.1. Research Tasks and Schedule During Phase I of Current Research Project, Covering the First Year	27
Table 1.2. Research Tasks and Schedule During Phase II of Current Research Project, Covering the Second Year	28
Table 1.3. Research Tasks and Schedule During Phase III of Current Research Project, Covering the Third Year	29
Table 3.1. Summary of Installations for the Tieback Installation and Testing Program (Contractor's Geotechnical Consultant, 1992c).	60
Table 3.2. Summary of Test Results from the Tieback Installation and Testing Program (Contractor's Geotechnical Consultant, 1992c).	61
Table 4.1. Positive and Negative Attributes of the Eight Instrumented Sections.	82
Table 4.2. Summary of Deflections and Installations for Near-wall Inclometers (Page 1 of 2).	83
Table 4.2. Summary of Deflections and Installations for Near-wall Inclometers, continued (Page 2 of 2).	84
Table 5.1. Engineering Properties of Miscellaneous Fill.	112
Table 5.2. Engineering Properties of Cohesive Fill (2 pages).	113
Table 5.3. Engineering Properties of Organic Deposits (2 pages).	115
Table 5.4. Engineering Properties of Marine Clay (BBC) (3 pages).	117
Table 5.5. Engineering Properties of Glaciomarine Deposits.	120
Table 5.6. Engineering Properties of Glacial Till.	121
Table 5.7. Engineering Properties of Bedrock.	122
Table 6.1. Summary of Dimensions, Lock-off Loads, and Elastic Moduli of Tiebacks.	141
Table 6.2. List of all Geotechnical Instruments Located at the ISS-4 Test Section.	142
Table 6.3. Summary of Excavation History at ISS-4.	143
Table A.1. Information Table for ISS-4 Inclometers.	255
Table A.2. Information Table for ISS-4 Deformation Monitoring Points.	256
Table A.3. Information Table for ISS-4 Multi-Point Heave Gages and Probe Extensometers.	257
Table A.4. Information Table for ISS-4 Groundwater Monitoring Instruments.	258
Table A.5. (page 1 of 6) Location Data for Geotechnical Instruments.	259
Table A.5. (page 2 of 6) Location Data for Geotechnical Instruments.	260
Table A.5. (page 3 of 6) Location Data for Geotechnical Instruments.	261
Table A.5. (page 4 of 6) Location Data for Geotechnical Instruments.	262
Table A.5. (page 5 of 6) Location Data for Geotechnical Instruments.	263
Table A.5. (page 6 of 6) Location Data for Geotechnical Instruments.	264

LIST OF FIGURES

Figure 1.1. General Movement Trends Around Braced Cuts (Clough, 1985)	30
Figure 1.2. Types of Excavation Support Systems (from NAVFAC, 1982).	31
Figure 2.1. Summary of Soil Settlements Behind In-Situ Walls (Peck, 1969).	41
Figure 2.2. Dimensionless Settlement Profiles Recommended for Estimating Settlement Distribution Adjacent to Excavations in Different Soil Types (Clough and O'Rourke, 1990).	42
Figure 2.3. Relationship Between Factor of Safety Against Basal Heave and Nondimensionalized Maximum Lateral Wall Movement (Mana and Clough, 1981). a. Case History Data. b. Analytical Results.	43
Figure 2.4. Chart for Estimating Maximum Lateral Wall Movements and Ground Surface Settlements for Support Systems in Clays (Clough et al., 1989).	44
Figure 2.5. Envelopes for Normalized Ground Settlement Profiles (Mana and Clough, 1981).	45
Figure 2.6. Estimation of Maximum Lateral Wall Deflections from Numerical Experiments for Excavation in Boston Blue Clay (Hashash and Whittle, 1994).	46
Figure 3.1. Plan View of the Project Alignment. (Dimensions are approximate rather than exact.)	62
Figure 3.2. Cross-Section A-A from Figure 3.1, Through the Boat Section (Station 77+00), Showing Two Types of Support Wall: a Diaphragm (Slurry) Wall on the North and a Sheetpile Wall on the South.	63
Figure 3.3. The Soil Profile along the Project Alignment showing the Elevation of Final Excavation Subgrade (MHD Geotechnical Consultant, 1991b).	64
Figure 3.4. The North and South Support-of-Excavation (SOE) Walls, including Tieback Levels and Final Excavation Subgrade on each side.	65
Figure 3.5. Location of the Tieback Installation and Testing Program (Contractor's Geotechnical Consultant, 1992a).	66
Figure 3.6. Arrangement of Tiebacks for the Tieback Installation and Testing Program (Contractor's Geotechnical Consultant, 1992a).	67
Figure 3.7. Equipment Used for Applying Stresses to Tiebacks and for Measuring Applied Loads (Xanthakos, 1991).	68
Figure 3.8. Structure of a Typical Boat Section Tiedown.	69
Figure 3.9. Locations of Dewatering and Pressure Relief Wells (Contractor's Geotechnical Consultant, 1992b).	70
Figure 3.10. Plan View of a Typical Dewatering and Pressure Relief Well, Showing its Placement Relative to the Sheeting and Wale (Contractor's Geotechnical Consultant, 1992b).	71
Figure 3.11. Elevation View of a Typical Dewatering and Pressure Relief Well, Showing Screened Lengths in the Upper and Lower Contractor's Geotechnical Consultant, 1992b).	72

Figure 3.12. Definition of the Factor of Safety against Hydrostatic Uplift (MHD, 1992).	73
Figure 4.1. Cross-Sectional View of a “Typical” Instrumented Section Through the Project Alignment, Showing Locations and Depths of Geotechnical Instruments (MDPW, 1991).	85
Figure 4.2 Plan View of the Excavation, showing Positions of Geotechnical Instrumentation and Instrumented Sections.	87
Figure 4.3. The Excavation Support System used at ISS-8, between Station 90+00 and the Circular Cofferdam.	89
Figure 4.4. Summary of Construction History at Instrumented Sections ISS-1 to ISS-8.	90
Figure 4.5. Lateral Wall Deflections at Three Elevations Plotted Against Station Number. Deflections are Those Measured on the Date of Excavation to Final Subgrade.	91
Figure 4.6. An Illustration of the Typical Deformations of Two Different Wall Types. (a) Sheetpile Wall. (b) Diaphragm (Slurry) Wall.	92
Figure 4.7 (a). Settlement Troughs Measured Behind the North Wall at Various Instrumented Sections. (Settlements are shown for different times in the construction history of each section: 1. Excavation of Lift 1; 2. Excavation of Final Subgrade; 3. Invert Mat Pour.)	93
Figure 4.7 (b). Settlement Troughs Measured Behind the South Wall at Various Instrumented Sections. (settlements are shown for different times in the construction history of each section: 1. Excavation of Lift 1; 2. Excavation of Final Subgrade; 3. Invert Mat Pour.)	94
Figure 5.1. Locations of Exploratory Borings in the Project Area Conducted by MHD’s Geotechnical Consultant. (Also shown: zone numbers, the location of the Special Testing Site, and locations of salt and fill stockpiles which existed in the 1980’s.)	123
Figure 5.2. Information on Subsurface Stratigraphy at the ISS-4 Section. a. Borings Conducted by MHD Geotechnical Consultant (1991). b. Selected ISS-4 Soil Profile. c. Instrument Installation Logs	125
Figure 5.3. Initial Piezometric Levels in the Upper and Lower Aquifers Plotted Against Station Numbers, and at Special Test Site. Data from MHD Geotechnical Consultant (1991a, b, and 1993).	126
Figure 5.4. Initial In-Situ Stresses Throughout the ISS-4 Soil Profile.	127
Figure 5.5. Total Unit Weight, Water Content, and Atterberg Limit Profiles for BBC near the ISS-4 Cross-Section.	128
Figure 5.6. OCR and Undrained Strength Profiles for Marine Clay throughout the Project Alignment. From MHD Geotechnical Consultant (1991b) and Special Testing Program (MHD Geotechnical Consultant, 1993).	129
Figure 5.7. Selected Effective Stress Profile at ISS-4 Determined by MIT from Re-evaluation of Consolidation Test Data on BBC.	130

Figure 5.8. Elevation vs. CR (Compression Ratio) and RR (Recompression Ratio) Measured by Consolidation Tests on BBC, by MHD Geotechnical Consultant (1991a).	131
Figure 5.9. Comparison of Undrained Shear Strength Profile as Estimated by MIT using the SHANSEP Method with UUC and Lab Vane Strength Data.	132
Figure 6.1. Cross-Sectional View of Excavation at ISS-4 Test Section (approx. Sta.77+20), showing Tiebacks, SOE Walls, and Geotechnical Instrumentation. View is Looking East; North is to the Left.	144
Figure 6.2. Plan View of the ISS-4 Area, showing Building A and Geotechnical Instrumentation.	145
Figure 6.3. Dimensions and Engineering Properties of Arbed AZ-18 Sheet Piling (ISPC, 1990).	146
Figure 6.4. Cumulative Lock-Off Load vs. Lateral Position along Diaphragm Wall A (Sta. 76+00 to 77+67).	147
Figure 6.5. Cumulative Lock-Off Load vs. Lateral Position along the South Sheetpile Wall (Sta. 76+00 to 78+00).	148
Figure 6.6. Example of a Load-Elongation Plot for a Series of Adjacent Tiebacks in a Single Tier. (Note: These plotted tiebacks are in the sheetpile wall immediately east of Diaphragm Wall A, and were not considered in later analyses of ISS-4.)	149
Figure 6.7. Graphical Summary of Construction Activities and Lift Excavations at ISS-4.	150
Figure 7A.1. Wall Deflections vs. Time, Measured by INC-102 (in Diaphragm Wall A).	174
Figure 7A.2. Wall Deflections vs. Time, Measured by INC-101 (behind the south sheetpile wall).	175
Figure 7A.3. Lateral Deflections vs. Time, Measured by IPE-113 (south of excavation).	176
Figure 7A.4. Surface Settlements behind the North (diaphragm) Wall vs. Time.	177
Figure 7A.5. Surface Settlements behind the South (sheetpile) Wall vs. Time.	178
Figure 7A.6. Settlements Within the Boston Blue Clay, Measured by the IPE-113 Probe Extensometer (south of excavation).	179
Figure 7A.7. Piezometric Pressures in the Lower Aquifer vs. Time, Measured by Four Deep Piezometers (below the BBC).	180
Figure 7A.8. Groundwater Level vs. Time, Measured by Shallow Observation Wells OW-002 and 016 (North side of excavation).	181
Figure 7A.9. Piezometric Pressures at Base of Upper Aquifer vs. Time, Measured by VWPZ-67 and 68, which have the same location and tip elevation. (North side of excavation)	182
Figure 7A.10. Groundwater Level in Upper Aquifer vs. Time, Measured by OSPZ-106 (South side of excavation).	183
Figure 7A.11. Marine Clay Heave vs. Time, Measured by MPHG-110 (inside of excavation).	184

Figure 7A.12. Marine Clay Heave vs. Time, Measured by MPHG-109 (inside of excavation).....	185
Figure 7A.13. Marine Clay Heave vs. Time, Measured by MPHG-501 (inside of excavation).....	186
Figure 7A.14. Marine Clay Heave vs. Time, Measured by MPHG-107 (inside of excavation).....	187
Figure 7A.15. Piezometric Pressure in Marine Clay vs. Time, Measured by VWPZ-135 and 136 (inside the excavation).....	188
Figure 7A.16. Piezometric Pressure in Marine Clay vs. Time, Measured by VWPZ-133 and 134 (inside the excavation).....	189
Figure 7A.17. Piezometric Pressure in Marine Clay vs. Time, Measured by VWPZ-131 and 132 (inside the excavation).....	190
Figure 7A.18. Boston Blue Clay Heave vs. Elevation, as Measured by Four MPHG's Within the Excavation.	191
Figure 7B.1(a). Sheet 1 of Time Period Summary for Step 1.0, Showing Excavation Geometry on 5/7/1993.	192
Figure 7B.1(b). Sheet 2 of Time Period Summary for Step 1.0, Showing Surface Settlements and Inclinometer Deflections on 5/7/1993.	193
Figure 7B.2(a). Sheet 1 of Time Period Summary for Step 2.0, Showing Excavation Geometry on 6/29/1993.	194
Figure 7B.2(b). Sheet 2 of Time Period Summary for Step 2.0, Showing Surface Settlements and Inclinometer Deflections on 6/29/1993.	195
Figure 7B.3(a). Sheet 1 of Time Period Summary for Step 3.0, Showing Excavation Geometry on 7/9/1993.	196
Figure 7B.3(b). Sheet 2 of Time Period Summary for Step 3.0, Showing Surface Settlements and Inclinometer Deflections on 7/9/1993.	197
Figure 7B.4(a). Sheet 1 of Time Period Summary for Step 4.0, Showing Excavation Geometry on 8/9/1993.	198
Figure 7B.4(b). Sheet 2 of Time Period Summary for Step 4.0, Showing Surface Settlements and Inclinometer Deflections on 8/9/1993.	199
Figure 7B.5(a). Sheet 1 of Time Period Summary for Step 5.0, Showing Excavation Geometry on 9/2/1993.	200
Figure 7B.5(b). Sheet 2 of Time Period Summary for Step 5.0, Showing Surface Settlements and Inclinometer Deflections on 9/2/1993.	201
Figure 7B.6(a). Sheet 1 of Time Period Summary for Step 6.0, Showing Excavation Geometry on 10/6/1993.	202
Figure 7B.6(b). Sheet 2 of Time Period Summary for Step 6.0, Showing Surface Settlements and Inclinometer Deflections on 10/6/1993.	203
Figure 7B.7(a). Sheet 1 of Time Period Summary for Step 7.0, Showing Excavation Geometry on 3/11/1994.	204
Figure 7B.7(b). Sheet 2 of Time Period Summary for Step 7.0, Showing Surface Settlements and Inclinometer Deflections on 3/11/1994.	205
Figure 7B.8(a). Sheet 1 of Time Period Summary for Step 8.0, Showing Excavation Geometry on 5/31/1994.	206

Figure 7B.8(b). Sheet 2 of Time Period Summary for Step 8.0, Showing Surface Settlements and Inclinometer Deflections on 5/31/1994.	207
Figure 8.1. “Simplified” Excess Pore Pressure Wedge used for Consolidation Analysis, based on Measured Piezometric Water Elevations at Different Times and Three Elevations in the ISS-4 Soil Column.	220
Figure 8.2. Plot of Effective Stresses and Preconsolidation Pressures Versus Elevation, Before and After Consolidation of Cohesive Soil Layers.	221
Figure 8.3. Settlements Measured by IPE-113 Plotted Versus Elevation.	222
Figure 8.4. Pore Pressure Reductions Measured by Piezometers Within the Excavation Plotted Against Excavation-Induced Total Vertical Stress Reductions.	223
Figure 8.5. Normalized Settlements Along Project Alignment (Prior to Construction of Invert Mat) Plotted on Peck’s (1969) Design Chart.	224
Figure 8.6. Normalized Settlement Distribution Along Project Alignment (Prior to Construction of Invert Mat) Plotted With Settlement Trough Envelopes Suggested by Mana and Clough (1981).	225
Figure 8.7. Factor of Safety Calculation Used by MOVEX for Layered Soils (Smith, 1987).	226
Figure 8.8. “Alpha Factors” Suggested by Mana and Clough (1981) which Relate Excavation Parameters to Maximum Lateral Wall Movement. (a.) Effect of Strut Stiffness. (S =Strut Stiffness per Horizontal unit of Length; h =Vertical Strut Spacing; γ =Total Unit Weight of Soil.) (b.) Effect of Depth to Underlying Firm Layer. (c.) Effect of Excavation Width.	227
Figure 8.9. Factor of Safety Versus Anisotropic Strength Ratio (from Smith, 1987).	228
Figure 8.10. Comparison of Settlements and Wall Deflections Measured at ISS-4 and Predicted by the MOVEX Computer Program.	229
Figure A.1. A. Inclinometer Design from Project Standard Drawings. B. Principle of Operation of a Typical Inclinometer.	265
Figure A.2. Types of Deformation Monitoring Points (DMP’s) used to Monitor the Excavation.	266
Figure A.3. Three Types of Probe Extensometer. A. Mechanical Probe with telescoping access tube. From Dunicliff (1988). B. Induction Coil Probe. Steel rings around the corrugated access tube act as measurement points. From Dunicliff (1988). C. Magnetic Reed Switch Probe with Spider Magnet Measurement Points. From Project Standard Drawings.	267
Figure A.4. Principle of Operation of a Magnetic Probe Extensometer. From MHD Instrumentation Consultant (1992).	268
Figure A.5. Inclinometer/Probe Extensometer. From Project Standard Drawings.	269
Figure A.6. Multi-Point Heave Gage. From Project Standard Drawings.	270
Figure A.7. Observation Well. From Project Standard Drawings.	271
Figure A.8. Open Standpipe Piezometer. From Project Standard Drawings.	272

Figure A.9. A. Vibrating Wire Piezometer Installation. From Project Standard Drawings. B. Details of the Piezometer. From Geokon, Inc.	273
Sheet B1. Summary of ω_N, Atterberg Limit, and S_u Data on Cohesive Fill (data from MHD Geotechnical Consultant, 1991a).....	276
Sheet B2. Summary of Oedometer Data on Cohesive Fill (MIT interpretation of data from MHD Geotechnical Consultant, 1991a).....	277
Sheet B3. SPT Blow Count Data on Cohesive Fill.....	278
Sheet B4. Summary of ω_N, Atterberg Limit, and S_u Data on Organic Deposits (data from MHD Geotechnical Consultant, 1991a).....	279
Sheet B5. Plasticity Chart: Organic Deposits.....	280
Sheet B6. Summary of Oedometer Data on Organic Deposits (MIT interpretation of data from MHD Geotechnical Consultant, 1991a).....	281
Sheet B7. Water Content, Virgin Compression Ratio, and NC Coefficient of Consolidation Data on BBC (Data from MHD Geotechnical Consultant, 1991a).....	282
Sheet B8. Elevation vs. Mean Natural Water Content from Borings Near ISS-4.....	283
Sheet B9. Plasticity Chart for Boston Blue Clay in the Region Surrounding ISS-4. ...	284
Sheet B10. Summary of Stress History Data for BBC: Sta. 71 to 79.....	285
Sheet B11. Compression Graph from Consolidation Test OED-14.....	286
Sheet B12. Strain Energy Plot of Recompression Range, from OED-14.....	287
Sheet B13. Strain Energy Plot, Maximum Past Pressure Range, from OED-14.	288
Sheet B14. Compression Graph from Consolidation Test OED-34.....	289
Sheet B15. Strain Energy Plot of Recompression Range, from OED-34.....	290
Sheet B16. Strain Energy Plot, Maximum Past Pressure Range, from OED-34.	291
Sheet B17. Comparison of Preconsolidation Pressures Estimated from Casagrande and Strain Energy Techniques for 17 Oedometer Tests on BBC (Fixed piston samples).....	292
Sheet B18. Vertical In-Situ Permeability Plotted Against Elevation for the Special Test Sites (MHD Geotechnical Consultant, 1993).	293
Sheet C1. Plan View of Diaphragm Wall A and Building A.	296
Sheet C2. Elevation View of Diaphragm Wall A and Tiebacks.	297
Sheet C3. Placement of Reinforcing Steel Bars Within Diaphragm Wall A.	298
Sheet C4. Face-on View of Diaphragm Wall A, showing Tieback Locations, Embedment Depths of Wall Panels, and Dates of Concrete Pours.....	299
Sheet C5. Face-on View of the Sheetpile Wall along the South side of ISS-4, showing Tieback Locations and Embedment Depth.	300
Sheet C6. Stress-Strain Plot for Tieback Tier 1 on the North Diaphragm Wall.	301
Sheet C7. Stress-Strain Plot for Tieback Tier 2 on the North Diaphragm Wall, Anchors 1-16.	302
Sheet C8. Stress-Strain Plot for Tieback Tier 2 on the North Diaphragm Wall, Anchors 17-24.	303
Sheet C9. Stress-Strain Plot for Tieback Tier 3 on the North Diaphragm Wall, Anchors 1-16.	304

Sheet C10. Stress-Strain Plot for Tieback Tier 3 on the North Diaphragm Wall, Anchors 17-24.	305
Sheet C11. Stress-Strain Plot for Tieback Tier 1 on the South Sheetpile Wall.	306
Sheet C12. Stress-Strain Plot for Tieback Tier 2 on the South Sheetpile Wall, page 1 of 3.	307
Sheet C13. Stress-Strain Plot for Tieback Tier 2 on the South Sheetpile Wall, page 2 of 3.	308
Sheet C14. Stress-Strain Plot for Tieback Tier 2 on the South Sheetpile Wall, page 3 of 3.	309
Sheet C15. Stress-Strain Plot for Tieback Tier 3 on the South Sheetpile Wall, page 1 of 3.	310
Sheet C16. Stress-Strain Plot for Tieback Tier 3 on the South Sheetpile Wall, page 2 of 3.	311
Sheet C17. Stress-Strain Plot for Tieback Tier 3 on the South Sheetpile Wall, page 3 of 3.	312
Sheet C18. Tabulation of Two Independently Estimated Tieback Moduli, and Selected Values.	313
Sheet D1. Construction Activity Table, page 1 of 2 (from Weekly Geotechnical Summary Reports).	316
Sheet D2. Construction Activity Table, page 2 of 2.	317
Sheet D3. Recopied Form of Large-Sheet SOE Wall Plans, provided by Contractor.	318
Sheet D4. Recopied Form of a Construction Progress Plan, showing dates of excavation of various lifts. (from Weekly Geotechnical Instrumentation Reports).	319
Sheet E1. <i>Inclinometer</i>: Deflection vs. Depth, from GTILT.	322
Sheet E2. <i>Inclinometer</i>: Shear Strain vs. Time, from GTILT.	323
Sheet E3. <i>DMP</i>: Settlement vs. Time.	324
Sheet E4. <i>MPHG</i>: Settlement / Heave vs. Depth.	325
Sheet E5. <i>IPE</i>: Settlement / Heave vs. Depth.	326
Sheet E6. <i>Observation Well</i>: Tabulated Data.	327
Sheet E7. <i>Observation Well</i>: Graph of Data vs. Time.	328
Sheet E8. <i>VWPZ</i>: Tabulated Data.	329
Sheet E9. <i>VWPZ</i>: Graph of Data vs. Time.	330
Sheet F1. Settlement Calculation Spreadsheet S320-O.WKS, page 1 of 3.	332
Sheet F2. Settlement Calculation Spreadsheet S320-O.WKS, page 2 of 3.	333
Sheet F3. Settlement Calculation Spreadsheet S320-O.WKS, page 3 of 3.	334
Sheet F4. Settlement Calculation Spreadsheet S320-OC.WKS, page 1 of 3.	335
Sheet F5. Settlement Calculation Spreadsheet S320-OC.WKS, page 2 of 3.	336
Sheet F6. Settlement Calculation Spreadsheet S320-OC.WKS, page 3 of 3.	337
Sheet F7. Settlement Summary Table, page 1 of 2.	338
Sheet F8. Settlement Summary Table, page 2 of 2.	339

Sheet G1. Definition of Input Parameters: ISS-4 Soil Profile and Vertical Stresses.	342
Sheet G2. Calculation of Input Undrained Shear Strengths, page 1 of 2.	343
Sheet G3. Calculation of Input Undrained Shear Strengths, page 2 of 2.	344
Sheet G4. Calculation of Wall Stiffnesses for Diaphragm Wall and Sheetpile.....	345
Sheet G5. Calculation of Strut Stiffnesses for Tiebacks Behind Sheetpile Wall.	346
Sheet G6. Calculation of Strut Stiffnesses for Tiebacks Behind Diaphragm Wall.	347
Sheet G7. Summary of MOVEX Results from "Best Estimate" Analyses.	348
Sheet G8. Summary of MOVEX Parametric Analyses, page 1 of 2.	349
Sheet G9. Summary of MOVEX Parametric Analyses, page 2 of 2.	350
Sheet G10. MOVEX Input File for ISS-4 Sheetpile Wall, page 1 of 3.....	351
Sheet G11. MOVEX Input File for ISS-4 Sheetpile Wall, page 2 of 3.....	352
Sheet G12. MOVEX Input File for ISS-4 Sheetpile Wall, page 3 of 3.....	353
Sheet G13. MOVEX Input File for ISS-4 Diaphragm Wall, page 1 of 3.....	354
Sheet G14. MOVEX Input File for ISS-4 Diaphragm Wall, page 2 of 3.....	355
Sheet G15. MOVEX Input File for ISS-4 Diaphragm Wall, page 3 of 3.....	356

CHAPTER 1

INTRODUCTION

1.1. BACKGROUND

Ground movements play an important role in the design of deep excavations in cohesive soils. Although common engineering practice must design excavation support systems to resist failure through the use of structural analysis procedures, greater damages and consequent litigation expenses often arise from associated soil movements than from overall system “failure” (Clough et al., 1989). The ability to make reliable predictions of ground movements offers the following benefits. First, it provides a basis for defining performance criteria, or acceptable levels of movement for the protection of adjacent facilities. Second, it allows identification of areas requiring special construction methods, and assists in choosing between various construction options. Third, it facilitates the design and interpretation of a geotechnical field monitoring program.

This report is one component of a research effort entitled “Design and Performance of Deep Excavations”. The research is being conducted by MIT for a project underway in Boston. The overall goal of the research is to develop improved methods for predicting ground movements associated with deep excavations in “soft” clay (Ladd and Whittle, 1993).

The research is being performed in three phases spanning a period of three years. Tables 1.1, 1.2, and 1.3 provide an overview of the research time schedule. Phase I, covering the first year, will compare ground movements predicted by existing empirical techniques and advanced finite element analyses, to comprehensive records of actual ground movements collected during construction of selected portions of the project. Phase II will use the capabilities developed in Phase I to evaluate the principal factors that influence ground movements and will develop a more reliable technique for analysis of bottom heave stability. Phase III will combine the results of the finite element and bottom heave analyses with data from case studies such as this one, to develop improved semi-empirical design charts for predicting ground movements.

1.2. OVERVIEW OF BRACED EXCAVATIONS

1.2.1. General

Excavations in soft soils require the use of a support system which consists of a wall and bracing elements. The wall serves three principal functions. First, it physically retains the soil and helps prevent instability due to basal heave. Second, the toe of the wall (the portion of the wall which is embedded below excavation subgrade) receives passive resisting force from soil on the inside of the excavation, further helping to hold the wall in place. Third, it provides resistance to bending between the levels of bracing elements.

The bracing elements serve to resist active earth pressures which act on the wall. Bracing elements can be divided into three basic types, according to the method by which they resist active soil forces. Inclined beams called *rakers* transmit soil force to the excavation subgrade, *cross-lot struts* extend across the excavation between the two support walls, and *tiebacks* extend into stable soil or rock existing behind or below the wall and resist active forces through tension.

Excavations change the stress state in the adjacent soil mass, causing movement of the surrounding ground. The changed stress state causes both elastic and plastic deformation of the soil; the adjacent retained soil mass moves laterally inward towards the excavation and undergoes settlement, as indicated in Figure 1.1. At the same time, soil within the excavation will heave upward in response to the reduced vertical stresses.

Support systems are intended to keep the sides of the excavation stable and safe with respect to basal heave, and in so doing reduce the amount of ground movement, but they can not eliminate movements altogether. Aside from the inevitable soil movements that result from the changing stresses, construction activities can also play a large role in causing deformations of walls and the ground surface (Clough and O'Rourke, 1990). Dewatering is done to maintain a dry subgrade or relieve high pressures in underlying pervious strata, but if pore pressures in the retained soil also become reduced, then consolidation settlement can occur. Construction of the support walls and installation of sheetpiles, soldier piles, or tiebacks can result in disturbance to the soil mass and possibly

loss of ground which contributes to ground settlement. Compliance of the bracing system increases lateral wall movement.

The successful control of ground movements can be one of the most important criteria in designing an effective excavation support system when the excavation is in close proximity to existing structures. Expensive damage can occur even when ground movements are small. For example, based on a statistical survey of structures built on clays and sandy soils, Skempton and MacDonald (1956) suggest that cracking initiates in typical structures when the angular ground distortion (differential settlement divided by lateral distance) exceeds $1/300$, and that "severe" structural damage can occur at a value of $1/150$.

1.2.2. Typical Support Methods and Construction Sequence

Braced excavations are made following the "top-down" procedure. The first step is the installation of bracing walls before any soil is excavated. The installation technique depends on the type of wall that is used.

One of the most common wall types consists of soldier piles and lagging. A series of steel H- or I-beams (soldier piles) are driven into the soil, spaced several feet apart. Timber planks (lagging) are placed horizontally between the vertical soldier piles as the excavation proceeds, forming a soil-retaining wall.

Another typical wall type is the sheetpile wall. Sheetpile walls are composed of a series of interlocked sections, usually made of steel. Each section is a few feet wide and typically one-quarter to one inch thick, and sections are individually driven into the soil like piles, and attached to adjacent sections by "thumb-and-finger", "ball-and-socket", or "double-hook" type interlocks along the sections' lengths (Das, 1984, p.269). The result is a continuous "wall" embedded in the soil. In general, each sheetpile section is bent such that the resulting wall is corrugated for added resistance to bending.

A third type of support wall is the diaphragm (slurry) wall. Such a wall is created by digging a trench, usually two to four feet in width, down to the level of the desired wall base. The trench is held open by a water-bentonite slurry. Reinforcing steel is placed in the

trench, into which concrete is then poured. The concrete hardens to create a reinforced concrete “wall” within the soil mass.

A fairly recent technology allows the creation of another type of diaphragm wall known as a “soil-mix” wall. An arrangement of overlapping mixing augers is advanced into the ground while cement grout is pumped into the soil through the tips of the auger stems. Mixing paddles on the auger shafts help mix the soil with the cement grout as the augers are advanced and then withdrawn. A series of auger runs creates a continuous line of overlapping soil-mix “panels”. Before the soil-grout mix sets up, I-beam soldier piles are lowered vertically into the soil-mix columns to reinforce the wall. The hardened soil cement resists earth pressures between the soldier piles through arching.

Once the support walls are in place, the excavation begins. Most excavations are deep enough that the wall is unable to retain the soil through cantilever action alone (Figure 1.2-a), therefore requiring additional support elements. The first supports are generally placed either at the top of the wall before excavation starts, or when the cut reaches a depth of six to ten feet. After the first level of supports is installed, the excavation resumes until another support level is necessary or the final subgrade is reached. Excavation stops temporarily as each required level of “bracing” elements is installed in the cut, usually every eight to twelve vertical feet. This procedure is termed “top-down” excavation.

As with walls, there are several types of bracing systems, as illustrated in Figure 1.2. Cross-lot struts (Figure 1.2-b) are the most common in narrow excavations. The struts are beams made of wood or steel, which extend across the excavation from wall to wall. Wider excavations requiring unreasonably long cross-lot struts can instead utilize rakers, which are like inclined steel struts placed between the wall and the subgrade, sometimes abutting earth berms left inside the cut (Figure 1.2-c).

Another option available for wide excavations is the use of tiebacks, which anchor the walls to the retained soil mass (Figure 1.2-d). Steel strands extend from the wall back into the soil, and the ends are grouted under pressure to form a bond with the soil mass or underlying bedrock. Tiebacks were used sparingly in the 1960’s, but became increasingly common after the early 1970’s as the technology proved its adequacy (Xanthakos, 1991).

They offer a distinct advantage over cross-lot braces or rakers in that they exist outside, rather than inside, the excavation, thus leaving the interior unobstructed and easily accessible to construction equipment.

In some cases, the permanent structure itself can provide the necessary excavation support. Such was the case for the underground parking garage constructed at Post Office Square in downtown Boston. The concrete slabs that formed each of seven parking decks were cast on-grade, and upon set up, acted essentially as cross-lot struts, permitting further excavation to the next subgrade level (Whittle et al., 1993).

1.3. SCOPE OF THESIS

This thesis represents the partial completion of Tasks 1 through 4 on the Phase I schedule for the MIT research project "Design and Performance of Deep Excavations" (See Table 1.1 and description of project in Section 1.1).

This thesis details information on the excavations performed for a construction project in Boston. Excavations in this section were supported by tiebacks in conjunction with both sheetpile and diaphragm walls. The project covers approximately 2500 feet of depressed highway alignment, consisting of a combination of cut-and-cover tunnels and a boat section. The organization of this thesis is as follows.

Chapter 2 reviews existing literature on the behavior of supported excavations and accompanying soil movements. Emphasis is placed on available empirically-derived soil movement prediction techniques. These techniques will be compared to monitoring data from the construction project, which is described in Chapter 3, with emphasis on the excavation support systems.

Discussion of the performance of the Boston excavation begins with Chapter 4, which describes the instrumentation and reviews the soil movements measured throughout the area. It also describes the basis for selecting one well-instrumented cross-section (ISS-4) for more detailed study. Chapter 5 describes the distribution and selected engineering properties of the soils at this cross-section, while Chapter 6 describes the careful reconstruction of the time history of excavation events there. Chapter 7 presents and discusses the data from geotechnical instrumentation at this location. In Chapter 8, the

measured soil movements are compared to those predicted by the techniques reviewed in Chapter 2. Chapter 9 contains the summary and conclusions.

The main text is followed by several appendices. The first provides a more detailed discussion of geotechnical instrumentation: how it is installed, how it is interpreted, and its accuracy. Other appendices provide supplementary information on the support systems used for the excavations under study, the sequencing of construction events, engineering properties of the underlying soils, and analyses to compare predicted versus measured performance.

This thesis was prepared in cooperation with the Massachusetts Highway Department and the United States Department of Transportation, Federal Highway Administration. The opinions expressed in the thesis are those of the author and do not necessarily reflect those of the Massachusetts Highway Department.

**Table 1.1. Research Tasks and Schedule During Phase I of Current Research Project,
Covering the First Year**

Phase	Tasks	First Year			Second Year			Third Year						
		1-3	4-6	7-9	10-12	13-15	16-18	19-21	22-24	25-27	28-30	31-33	34-36	
I	Evaluation of Predictive Capabilities and Limitations 1. Select test sections a. Uniform conditions b. Mixed conditions 2. Summarize monitoring data & construction activities a. Uniform conditions b. Mixed conditions 3. Select engineering properties a. To use design charts b. For FE input parameters 4. Comparison of predicted and measured performance using design charts 5. FE predictions of performance and comparison with measured data a. Initial properties/ boundary conditions b. Modified parameters 6. Preliminary evaluation of stability analyses for bottom heave 7. Progress (X) and technical (O) reports	X												

**Table 1.3. Research Tasks and Schedule During Phase III of Current Research Project,
Covering the Third Year**

Phase	Tasks	First Year				Second Year				Third Year			
		1-3	4-6	7-9	10-12	3-15	16-18	19-21	22-24	25-27	28-30	31-33	34-36
III	Design Recommendations for Predicting Ground Movements 1. Complete other case histories of deep excavations 2. Complete interpretation of results from numerical experiments, including additional FE analyses 3. Develop new design charts for predicting ground movements based on results of II 4, III 1 and III 2. 4. Develop recommendations regarding conditions leading to excessive movements, effectiveness of remedial measures, and guidelines for construction monitoring 5. Progress (X) and final technical (O) reports												

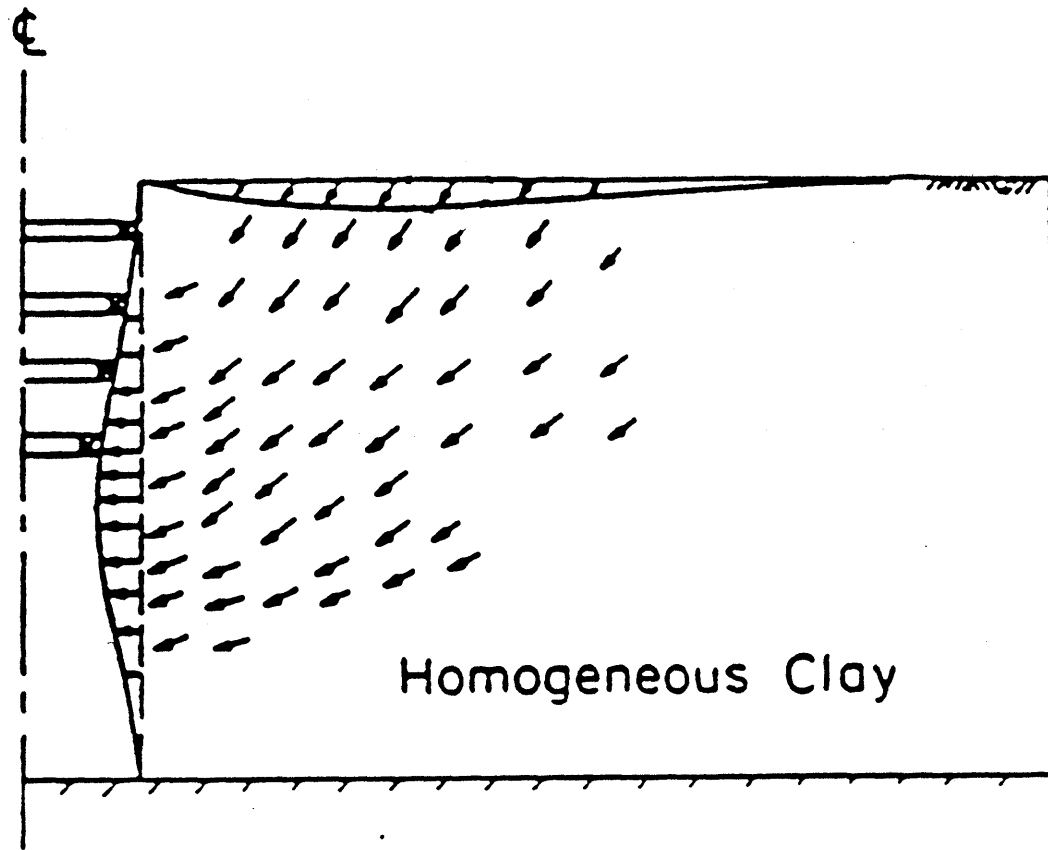
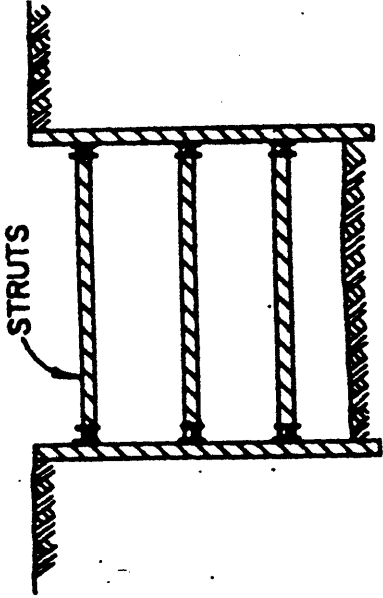
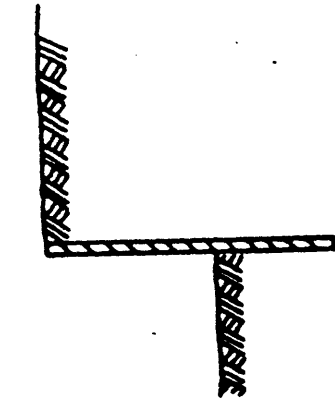


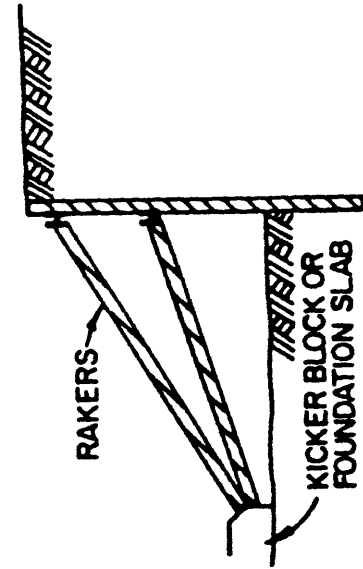
Figure 1.1. General Movement Trends Around Braced Cuts (Clough, 1985)



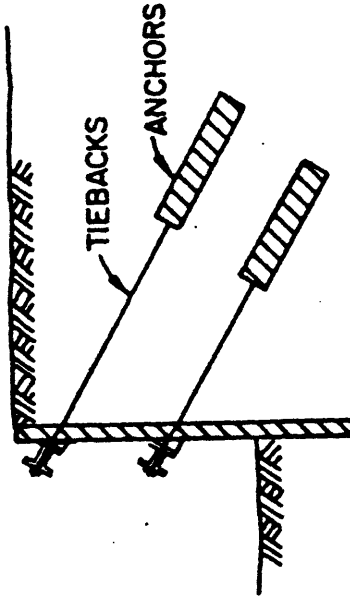
A. CANTILEVER WALL



B. CROSS-LOT BRACED WALL



C. RAKER SYSTEM



D. ANCHOR OR TIEBACK WALL

Figure 1.2. Types of Excavation Support Systems (from NAVFAC, 1982).

CHAPTER 2

SOIL MOVEMENTS AND THEIR PREDICTION

2.1. INTRODUCTION

The ability to quantitatively predict ground movements around braced excavations is not very well developed, and geotechnical engineers essentially have to rely on engineering judgment and intelligent guesswork when estimating ground movements for a given support system design. Guidance is provided by a number of existing design charts, which are developed through the use of two possible sources of information. On one hand, empirically-based design charts summarize ground deformation data collected from specific excavation histories. On the other, mathematical modeling and computer simulations allow a more theoretical analysis, usually via the "finite element" technique. Finite element analysis uses mathematical soil models to predict soil deformations for specific cases and allows an assessment of how the deformations relate to various construction factors. Each methodology has strengths and weaknesses:

"...methods which are based on field data collected from case histories provide a useful guide for estimating a likely range of movements, but cannot be used reliably for site-specific predictions. Finite element methods have the ability to analyze complex design problems, but have questionable accuracy due to one or more of the following factors: inadequate site investigation to properly define relevant soil properties; use of simplistic soil models that do not describe the actual behavior of natural clays; and no consideration of changes in the groundwater conditions during excavation" (Ladd and Whittle, 1993)

This chapter briefly reviews the development of soil movement prediction techniques and design charts, with emphasis placed on braced excavations in soft clays such as those that underlie the construction project in Boston. The discussion focuses on the most relevant studies, and has been divided into three categories of prediction

methodology. First, design recommendations based solely on empirical charts developed from a synthesis of case histories are reviewed. The second category is 'semi-empirical' studies, which combine case history data with theoretical (e.g., finite-element) analyses to make general recommendations. Finally, the third category is the use of the finite-element technique for modeling and predicting deformations at specific excavations.

2.2. RECOMMENDATIONS FROM CASE STUDIES

Peck (1969) was the first to use a collection of existing data to develop an empirical chart for estimating the magnitude and distribution of surface settlements behind braced excavation walls. His chart, shown in Figure 2.1, summarizes the observed surface settlements adjacent to a number of excavations in various soils which used sheetpile walls or soldier piles and lagging. The resulting settlement troughs are divided into three separate zones, which were distinguished by soil type and strength, quality of workmanship, and stability against basal heave. His chart predicts that the maximum settlement would most commonly occur at the wall and would generally equal one to two percent of the excavation's depth. Settlements for the first two zones on the graph extend to distances between two and four times the excavation depth.

Peck's compilation of soil deformation data has been supplemented by more recent case studies. Goldberg et al. (1976) provided a more updated collection of data, which included measurements of surface settlements and lateral wall deflections for excavations supported by sheetpiles and concrete diaphragm walls. They found that maximum surface settlements and lateral wall deflections were typically less than 0.35% of excavation depth in granular soils and stiff to hard clays, regardless of wall type. In 'soft' clays, movements higher than 1% were commonly seen when 'flexible' (i.e., sheetpile) walls were used; behind 'stiff' (braced diaphragm) walls, settlements and wall deflections were substantially lower, usually less than 0.25% of excavation depth. Settlements troughs in granular soils extended to no more than twice the excavation depth, in agreement with Peck, but settlements sometimes extended farther for clays. They attributed this to consolidation in the clay due to groundwater drawdown.

O'Rourke (1981) also studied ground movements caused by braced excavations in sand and clay, and correlated surface displacements and wall deformations to support design and construction techniques. Based on a survey of seven case studies of crosslot-braced cuts in clay, he concluded that when braces are stiff and installed promptly, deep-seated bulging occurs; when braces are inadequately stiff and are installed late, the wall deflects in a cantilever mode. O'Rourke's review of case histories also allowed him to assess the effectiveness of common excavation support techniques. He concluded that preloading struts and using earth berms were only moderately effective in controlling soil movements, and emphasized the importance of over-excavation below the lowest support level by stating that wall deflections, on average, vary in proportion to the 4th power of over-excavation depth.

Clough and O'Rourke (1990) provide a thorough review of the available techniques for soil movement prediction, updated with more recent developments in excavation support technology (such as tieback supports and soil cement walls). They used case history data to develop settlement trough predictions for different soil types. They recommend three different settlement profiles, shown in Figure 2.2, which apply to excavations in different soil conditions. The triangular wedge for sands and hard clays develops as the wall tends to deflect in a cantilever mode. The trapezoidal settlement profile which characterizes soft to medium clays occurs as a result of deep-seated inward soil movements and "bowing" of the wall into the excavation.

Clough and O'Rourke (1990) also reviewed the effects of construction techniques and support system design on ground movements. An especially important parameter is the depth of excavation below a given brace level. They cite the example of an excavation in San Francisco Bay Mud, having a depth of 15 m and an average strut spacing of about 5 m. A location with a 10-meter initial excavation experienced 100% greater wall movement than other locations without over-excavation. With regards to the design of the support members themselves, they concluded that the spacing of excavation support members has a greater effect on ground movements than does their stiffness. In addition, the stiffness of the support wall reduces movements most effectively in soft soils when the factor of safety against basal heave is low. They also stated that the use of earth berms

inside the excavation to counteract unbalanced soil forces is much more effective in 'stiff' soils than it is in soft to medium clays.

2.3. SEMI-EMPIRICAL DESIGN CHARTS

Although field data provide valuable information on "typical" measured soil movements from specific sites, analytical studies and mathematical modeling can give a deeper understanding of the parameters that affect soil movements in a great variety of excavation scenarios. These two types of information can complement each other, and some researchers have combined field information with theoretical analyses to create "semi-empirical" design charts.

Mana and Clough (1981) developed such a chart for braced excavations in clays by combining an evaluation of carefully selected case studies with finite element analyses. Out of a total of about 130 case histories, they chose only the eleven that had sufficiently 'simple' histories, in which soil movements were "generated primarily by the excavation stress relief", and not by any secondary construction factors. They found that the factor of safety against basal heave, as originally defined by Terzaghi (1943), had a strong influence on wall deflections. Their empirical correlation between lateral wall movements and basal heave factor of safety is plotted in Figure 2.3 (a). Both the magnitude and rate of inward wall movement were found to increase greatly as the factor of safety against basal heave became lower than 1.5.

Mana and Clough (1981) continued their study by comparing the case history field data with the results of finite element computer analyses using a non-linear, perfectly plastic soil model. The empirical correlation between wall deflections and basal heave factor of safety was verified, as indicated in Figure 2.3 (b). This analysis was extended by Clough et al. (1989), who used additional finite element modeling to plot the combined effects of basal heave stability and a "system stiffness" term which combines wall stiffness (EI) and strut spacing (h). Their chart appears in Figure 2.4.

Design charts such as these either summarize information that was gathered from a variety of different excavations, and lump all the data into one or a few simplified categories, or assume "typical" ranges for several variables at once. For example, by

combining wall stiffness and strut spacing - which can be dealt with independently during the design process - into one term, the Clough et al. (1989) chart masks the individual effect of each. This adversely influences the applicability of the design chart to a specific excavation scenario, since the chart can not distinguish the effects of different variables on ground movements. Instead, a number of parameters that affect movements but are under the control of the design engineer - such as wall stiffness, excavation geometry, and strut spacing, stiffness, and preloading - have to be studied individually, so that the influence of each can be assessed.

For this reason Mana and Clough (1981) devised a procedure to account for the individual effects of a number of construction parameters in predicting soil and wall movements. Their parametric analysis considered the following variables: wall and strut stiffness, depth of underlying firm layer, excavation width, strut preloading, and soil strength and modulus. The results of each individual parametric analysis was combined in a single formula which provided a means of estimating maximum wall movement. Using their formula requires finding a first estimate of wall movement based on a calculation of basal heave factor of safety, and then modifying this first estimate through the use of influence coefficients for each of the variables they considered.

In addition to dealing with predicted wall movements, Mana and Clough (1981) also conducted a semi-empirical analysis of settlements, using their 11 selected case studies and further use of finite element techniques. In general, maximum surface settlements seen in the field equaled 0.5 to 1.0 times the maximum wall deflections, in fairly good agreement with the conclusions of Goldberg et al.(1976). Computer models allowed them to relate surficial settlement distribution to basal heave safety factor; the resulting idealized settlement profiles are plotted in Figure 2.5. A narrower settlement trough is seen for situations with lower factors of safety.

Milligan (1983) studied idealized soil deformation scenarios with the "velocity field" analysis technique. This is a geometrical analysis which relates lateral wall movements to surficial displacements of the retained soil body. Milligan stated that for a retained soil that exhibits perfectly undrained behavior, like a low-permeability clay, "the

profile of the settlement of the surface behind the wall will be exactly the same as the profile of the horizontal deflection of the wall".

2.4. STUDIES OF SPECIFIC EXCAVATIONS WITH THE FINITE-ELEMENT TECHNIQUE

Finite element analyses involve recreating a construction activity and the affected soil mass in a mathematical simulation; computers utilize pre-defined soil model parameters and algorithms in conjunction with a carefully defined spatial geometry and time history to iteratively calculate ground movements around the excavation. The technique first became used for excavations in the early 1970's (Clough and Duncan, 1971) and has become increasingly powerful over the past twenty years as more realistic soil models have been developed and numerous case studies have been used to 'calibrate' the accuracy of the simulations.

To date, finite element analyses have been used mostly to make "after-the-fact" predictions. In other words, these back-analyses modeled excavations that had already occurred, and the results compared to actual soil deformation measurements made at the site. Although such studies do not provide advance information on soil movements for that excavation, they do allow for parametric analyses which can provide valuable design guidelines for future work in similar soil conditions.

Perhaps the most challenging aspect of making accurate finite element analyses is to realistically model the constitutive behavior of the soil. Early work, which usually assumed elastic soil behavior, the Modified Cam Clay model, or variations thereof, experienced problems with accurately predicting both wall movements and settlements. While Mana and Clough (1981) used the SOILSTRUCT computer program and a non-linear, perfectly plastic soil model to create general-use design recommendations, the relative simplicity of their soil model made it less suited to studies of specific excavations.

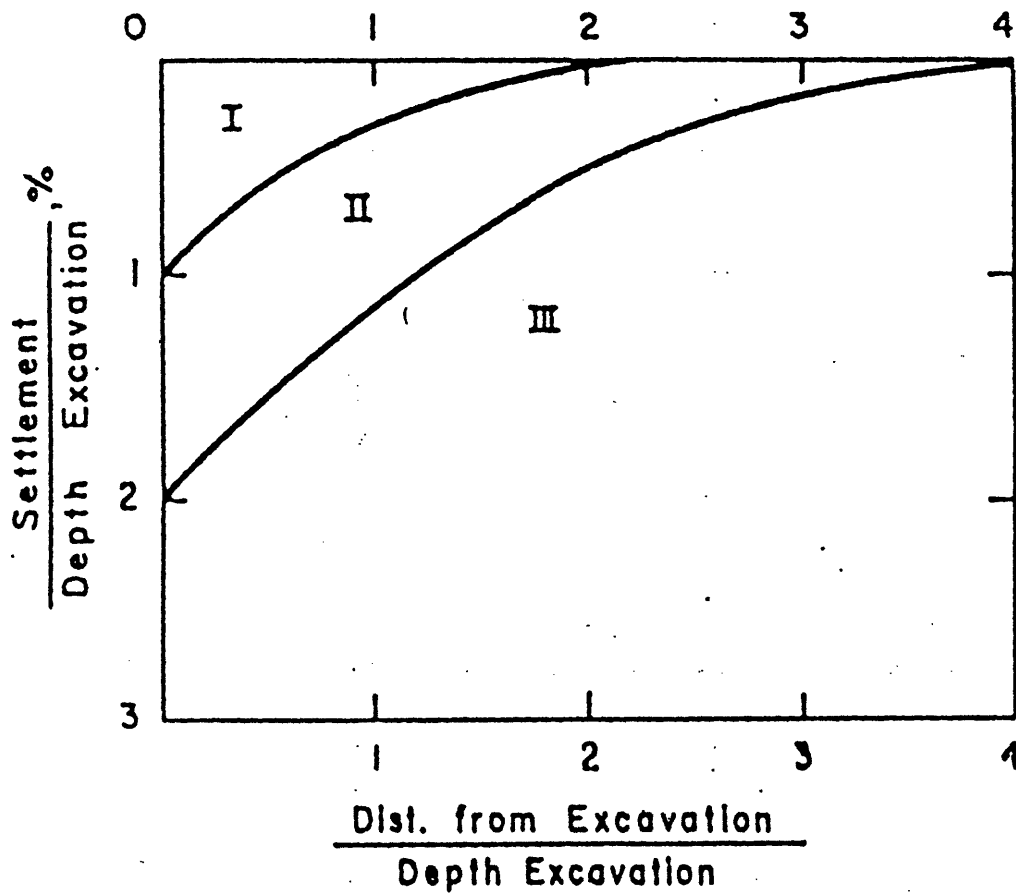
Since then much progress has been made in finite-element analyses, through the development and use of increasingly powerful soil models, and increased understanding of significant modeling parameters. Finno and Harahap (1991) used an effective-stress, anisotropic bounding surface soil model to study a 40-foot deep excavation through soft

clays in Chicago. They were able to obtain good agreement between measured and predicted wall deflections, while predicted settlements agreed “reasonably well” with those measured, until incipient shear surfaces developed behind the walls in the field. The effects of sheetpile installation on soil movements were successfully modeled. The accuracy of Finno and Harahap’s predictions was attributed to their use of an anisotropic soil model which included the effects of partial drainage and consolidation in the finite-element mesh, the precise representation of excavation history, and the fact that they accounted for displacements within the soil mass away from the walls in addition to those immediately adjacent to the walls.

Recent efforts at MIT have led to development of even more accurate soil models. The MIT-E3 model (Whittle and Kavvadas, 1994) describes most rate-independent aspects of clay constitutive behavior, including anisotropy, small strain non-linearity, and hysteresis associated with load reversals. This model was used to model ground movements around the Post Office Square excavation in downtown Boston (Whittle et. al., 1993). An underground parking garage was being constructed at this site; the eight floor slabs acted as struts for the concrete diaphragm walls that framed the excavation. Predicted movements matched the measured deformations reasonably well, when temperature-induced shrinkage of the concrete floor slabs and effects of dewatering were accounted for accurately.

An extension of this work with MIT-E3 was the development of design charts for prediction of diaphragm wall deflection in Boston Blue Clay (Hashash and Whittle, 1994). These charts, shown in Figure 2.6, resulted from a series of parametric analyses done with the MIT-E3 model, which assessed the influence of wall length, support (cross-lot brace) spacing, and stress history profile. All analyses used a symmetric excavation with a 20 m half-width, a maximum depth of 40 m, and a “wished-in-place” 1-m thick wall. The parametric analyses led to the following conclusions regarding excavation performance in soft clays: 1. Wall length (and therefore embedment) was found to have a strong influence on the potential for bottom instability. Although wall length has a minimal impact on pre-failure deformations, short- to medium- length walls are susceptible to development of a basal heave mechanism. 2. The FEM analyses indicated that the initial unsupported

excavation depth has only a “transient” effect on subsequent wall deflections and settlements. This contradicts the conclusions of Clough and O’Rourke (1990), who stressed the importance of these early deflections on later deflection magnitudes. 3. The soil stress history was found to have a major impact on predicted deformations. As OCR was increased, deformations reduced significantly and failure mechanisms were much less likely to develop.



I - Sand and Soft to Hard Clay, Avg. Workmanship

II - Very Soft to Soft Clay

1. Limited Depth of Clay Below Bott. Exc.

2. Significant Depth of Clay Below Bott. Exc.,
But $N_b < N_{cb}$ *

III - Very Soft to Soft Clay to a Significant Depth
Below Exc. Bott. and $N_b > N_{cb}$

* N_b = Stability No. Using C "Below Base Level" = $\frac{\gamma H}{C_b}$
 N_{cb} = Critical Stab No. for Basal Heave

Figure 2.1. Summary of Soil Settlements Behind In-Situ Walls (Peck, 1969).

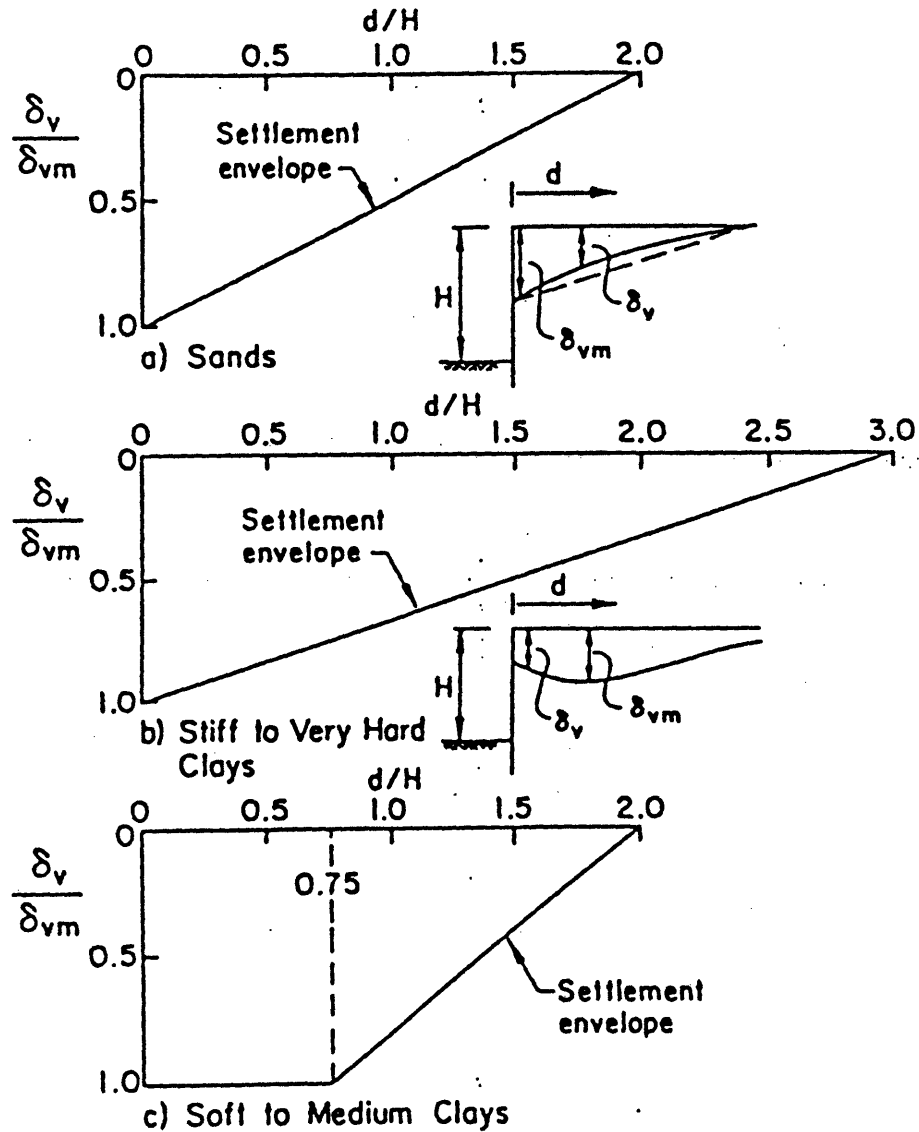
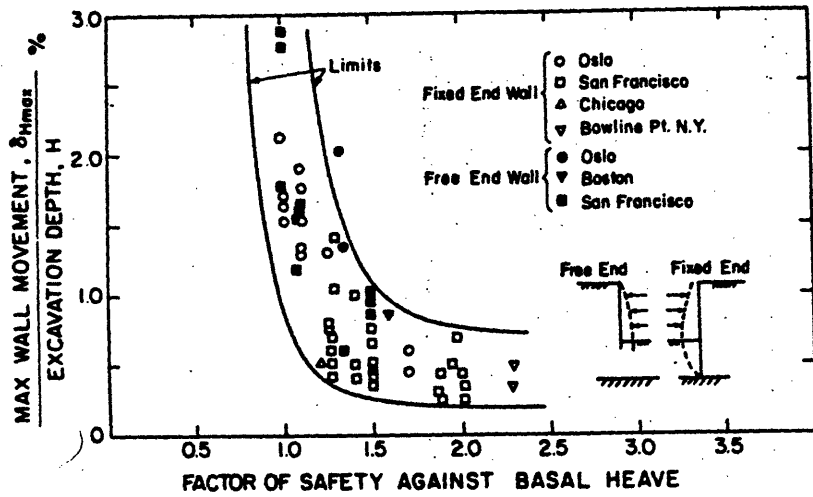
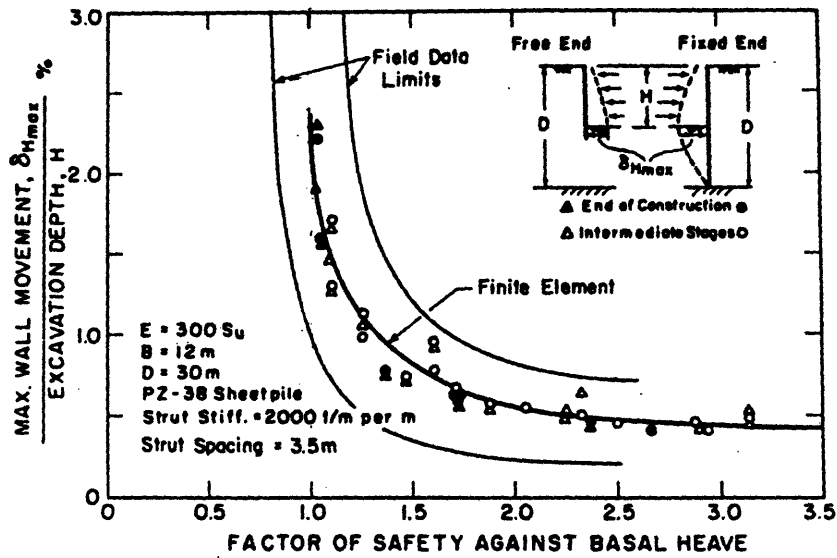


Figure 2.2. Dimensionless Settlement Profiles Recommended for Estimating Settlement Distribution Adjacent to Excavations in Different Soil Types (Clough and O'Rourke, 1990).



a. Relationship Between Factor of Safety Against Basal Heave and Nondimensionalized Maximum Lateral Wall Movement for Case History Data



b. Analytically Defined Relationship Between Factor of Safety Against Basal Heave and Nondimensionalized Maximum Lateral Wall Movement

Figure 2.3. Relationship Between Factor of Safety Against Basal Heave and Nondimensionalized Maximum Lateral Wall Movement (Mana and Clough, 1981). a. Case History Data. b. Analytical Results.

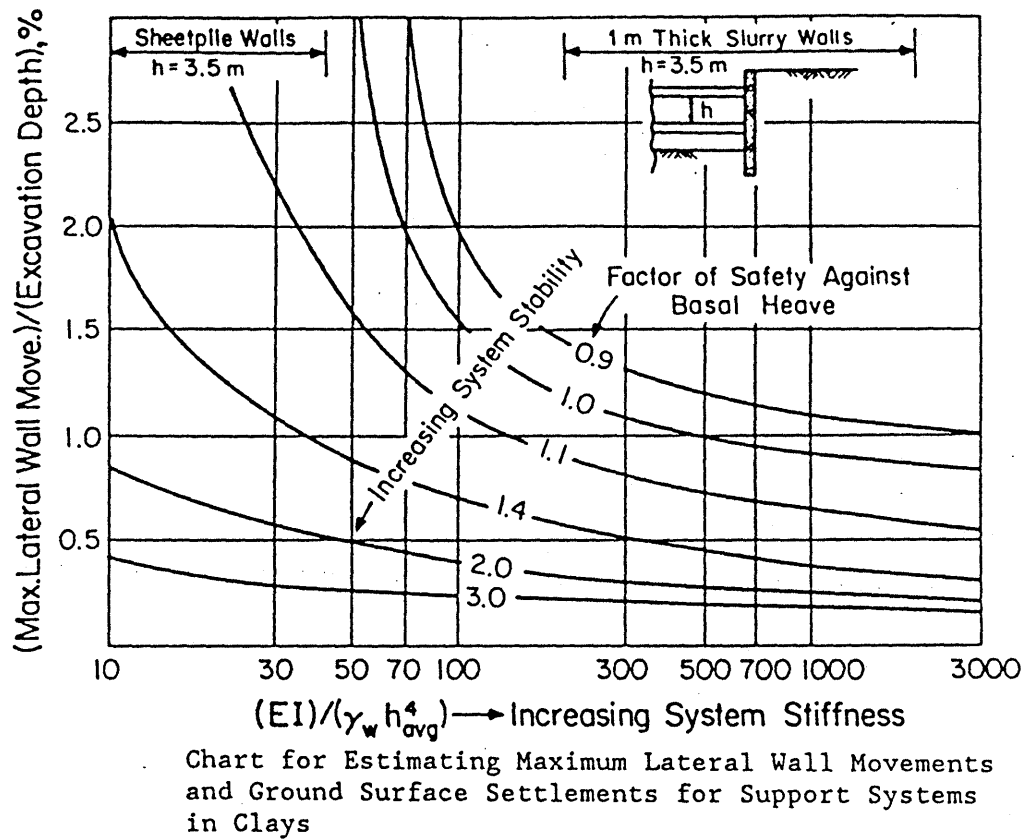
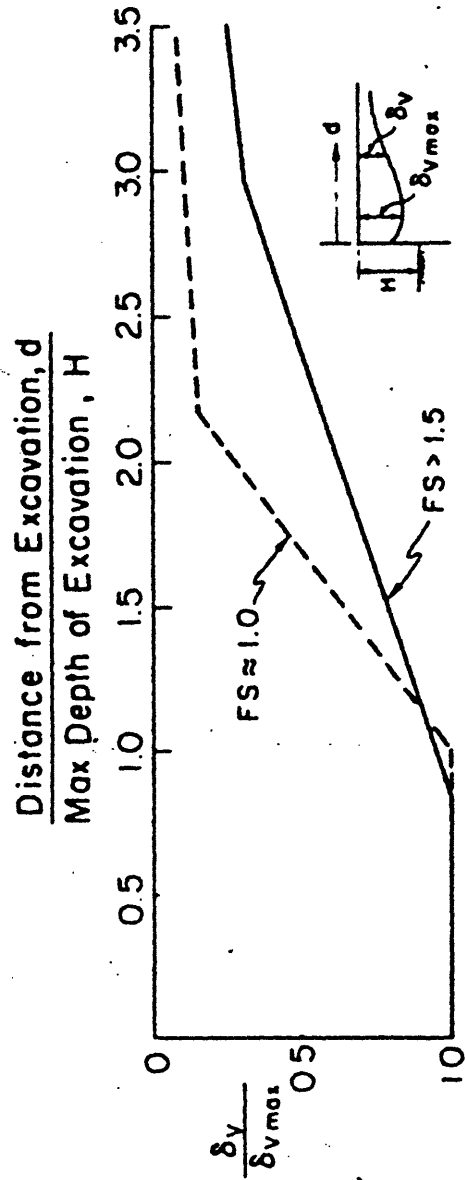


Figure 2.4. Chart for Estimating Maximum Lateral Wall Movements and Ground Surface Settlements for Support Systems in Clays (Clough et al., 1989).



-Envelopes to Normalized Ground Settlement Profiles

Figure 2.5. Envelopes for Normalized Ground Settlement Profiles (Mana and Clough, 1981).

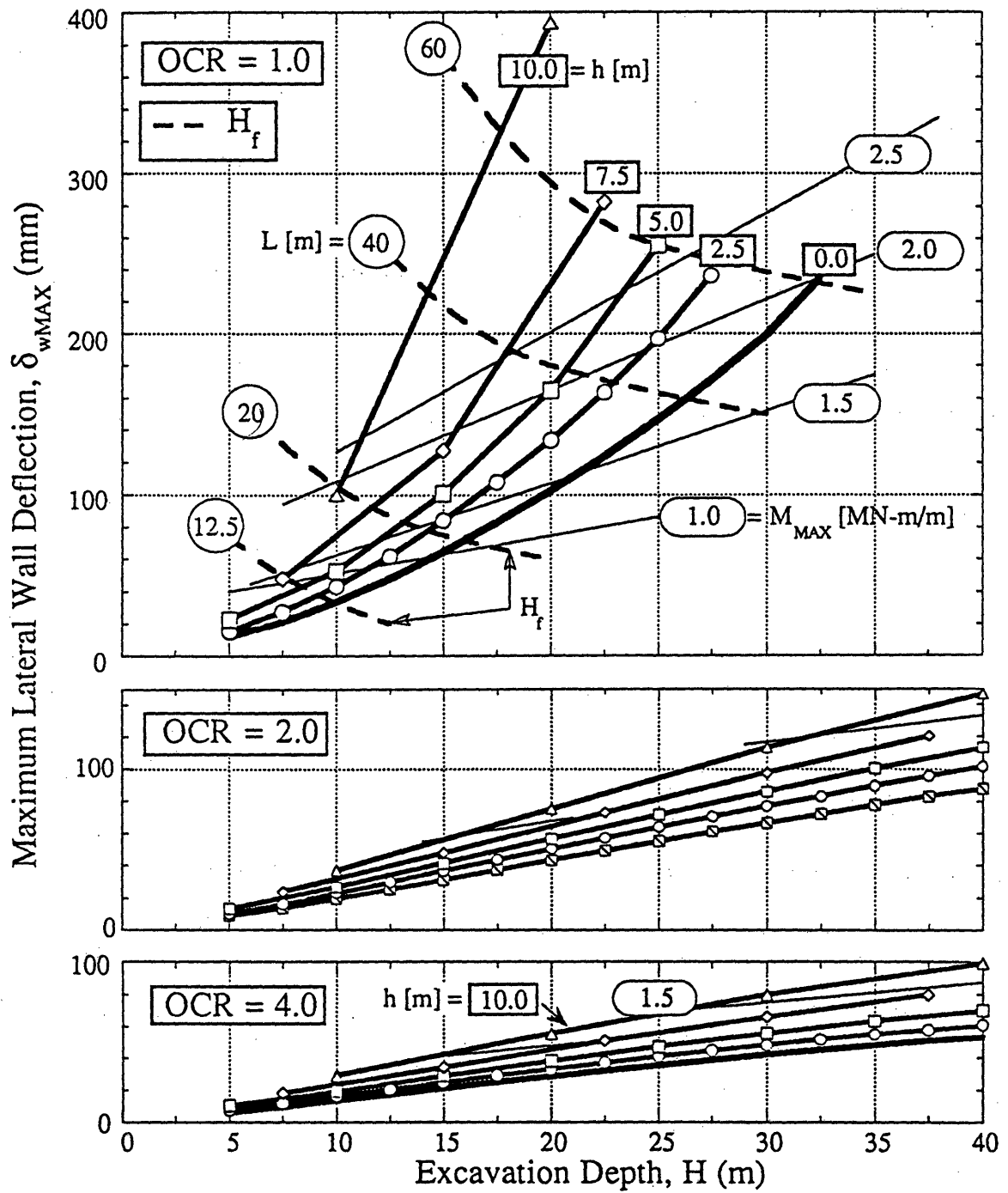


Figure 2.6. Estimation of Maximum Lateral Wall Deflections from Numerical Experiments for Excavation in Boston Blue Clay (Hashash and Whittle, 1994).

CHAPTER 3

DESCRIPTION OF THE CONSTRUCTION PROJECT IN BOSTON

3.1. SITE LAYOUT

The Construction Project in Boston has been divided into numerous sections for separate design and construction contracts. The section under study in this thesis is a 2500 ft-long stretch of highway. As shown in Figure 3.1, this section of highway begins approximately at Sta. 70+50, the western end of the alignment, and terminates at Sta. 96, the eastern end. The final roadway structure will consist of a depressed boat section between Sta. 72+70 and 81+40, with cut-and-cover tunnels to the east and west. The eastern terminus of the excavation is within a circular cofferdam with concrete diaphragm walls, where a vent building is located.

The excavation for the project is about 200 ft wide at its western end (Sta. 70+50), and gradually narrows toward the east, reaching a width of approximately 80 feet at the eastern terminus (Sta. 96). At the west end of the alignment, the excavation is 41 ft deep; the subgrade rises slightly to about El. 74 at Sta. 75+00 (excavation depth = 36 ft), and then deepens toward the east as it approaches the terminus, where the depth reaches about 63 ft.

The alignment passes through land that was originally tidal flats and shallow marine bays before being artificially filled in the nineteenth and twentieth centuries to its current grade. The surface topography is therefore fairly flat, at an elevation of about 109 to 112 ft (project datum, which is 100 ft below National Geodetic Vertical Datum sea level). South of the excavation and west of Sta. 76+00, the surface elevation was nearly ten feet higher than the area's average elevation. A pre-excavated trench was made along the south side of the excavation here to reduce the adjacent elevation to the typical value of 110 ft. In this area, the north side was also pre-excavated, to El. 104 ft. This was done to reduce earth pressures on the walls, since especially soft marine clay was presumed to exist in this portion of the alignment (MHD, 1991b). The pre-excavated trenches on both sides were no less than 30 ft wide, measured from the excavation's edge.

The alignment passes through an industrial area containing manufacturing buildings and fisheries, several of which are in close proximity to the excavation. As Figure 3.1 illustrates, Buildings A (Sta.77), B (Sta.81-83), C (Sta.82), D (Sta.86), and E (Sta.92) all come within 150 ft of the excavation.

Cross-section A-A, shown in Figure 3.2, is through the boat section and shows the size, width, and depth of the cut at this location. This cross-section is particularly informative because it provides a typical view of two different excavation support systems: a diaphragm (slurry) wall on the north side and a sheetpile wall on the south. These support systems are representative of excavation support at the cut-and-cover tunnels as well, and are discussed further in Section 3.3.

3.2. SUBSURFACE SOIL PROFILE

A geotechnical consultant was contracted by the Massachusetts Highway Department to perform an investigation of geotechnical characteristics of the site and to provide recommendations associated with the planned construction. The results of this investigation have been published in two reports: a Geotechnical Engineering Report published in October 1991 (MHD Geotechnical Consultant, 1991b) and an accompanying Geotechnical Data Report published in April 1991 (MHD Geotechnical Consultant, 1991a). The information in Section 3.2 is abstracted from these reports.

The soil profile for the entire alignment is shown in Figure 3.3. The profile is based on a review of test borings performed by the MHD Geotechnical Consultant as part of their subsurface investigation for the project. They performed sixty-two borings throughout the project area, and their study included ten others which they had performed for an investigation of the section immediately west of the project. They also gathered available data from borings in the vicinity that had been done by other companies for different projects.

As Figure 3.3 illustrates, the project site surface is everywhere underlain by a deposit of recent fill. This combination of granular and cohesive fill is about 20 ft thick throughout most of the alignment, but increases to as much as 50 ft at the eastern end, where dredging activities were done earlier in the century. Below the fill, a layer of

organic silt exists throughout most of the alignment area, with a maximum thickness of 15 ft. This deposit represents the original tidal mud flats of Boston Harbor.

The organic stratum is underlain by a thick sequence of soils deposited as a result of the Pleistocene glaciation. Its most prominent constituent is a layer of marine clay, known locally as Boston Blue Clay (BBC), which extends throughout most of the Boston area and plays a prominent role in almost all of the city's geotechnical design work. The thickness of BBC reaches a maximum value of about 70 ft at the project's western terminus. The deposit tapers toward the east (the direction of the harbor) due to a rise in the underlying bedrock surface, as well as to the fact that much of the upper BBC was removed during waterfront dredging operations. The thickness of BBC decreases to 10 ft at the section's extreme eastern end. Under the BBC lies a largely granular glaciomarine deposit and a veneer of glacial till covering argillitic bedrock.

The elevation of final subgrade along the excavation is also shown in Figure 3.3. Throughout the alignment's western half, the final subgrade very nearly reaches the top of the Boston Blue Clay or cuts into it by up to 10 ft. As the subgrade level slopes down toward the eastern terminus, it cuts well into the clay deposit, eventually reaching the underlying glacial till and bedrock.

The engineering properties of the different soils underlying the site are discussed in detail in Chapter 5. Groundwater exists in two aquifers separated by the impermeable BBC aquitard. Hydrostatic pressures exist in the upper aquifer, which consists of the fills and organic deposits. The lower aquifer exists in the glacial deposits and fractured bedrock underlying the clay, and is termed a "confined" aquifer due to its position underneath the confining BBC layer (Fetter, 1988). The piezometric elevation of the lower aquifer is about five to ten feet lower than the water table in the upper aquifer. Section 5.2 details initial measurements of pore water pressures in both aquifers.

3.3. SUPPORT OF EXCAVATION

Figure 3.2 shows the cross-sectional view A-A (from Figure 3.1) along the project alignment. This cross-section is located at Station 77+00, near building A. The figure presents the soil profile, the size and depth of the final excavation, the support of

excavation walls (sheetpile and slurry walls), the tiebacks, and the completed boat section structure. The following sections provide detailed descriptions of the features illustrated in this figure.

3.3.1 Sheetpile and Diaphragm Walls

The design of support of excavation (SOE) walls accounts for the presence of the nearby buildings that appear in Figure 3.1. The distribution of the two wall types along both sides of the excavation is illustrated in Figures 3.3 (plan view) and 3.4 (face view of walls).

The majority of the excavation is supported by sheetpile walls, embedded 10 to 25 ft below final subgrade. An example of a sheetpile wall appears on the right (South) side of the Figure 3.2 cross-section. Arbed AZ-18 sheeting was used throughout nearly the entire area. The sheetpile walls are braced with a series of tiebacks grouted in the BBC stratum.

Near adjacent buildings, the excavation is supported by reinforced concrete diaphragm walls, which are substantially more rigid than the sheetpile walls and are intended to prevent excessive soil movements. As Figure 3.1 shows, diaphragm walls are located adjacent to Buildings A, B, D, and E. All four diaphragm walls are three feet thick and consist of several separately constructed panels, each being 17 to 23 feet wide. Each panel has a cage of reinforcing steel within the concrete. Unlike the sheetpiles, which are embedded no more than 25 feet below subgrade, the diaphragm walls extend fully through the clay deposit, and are keyed at least two feet into the bedrock.

Like the sheeting, the diaphragm walls are braced with tiebacks. However, the tiebacks behind the diaphragm walls are longer and are inclined at a steeper angle, so that they extend through the clay into the cohesionless glacial soils and bedrock beneath. These tiebacks are grouted in the rock and are therefore commonly referred to as 'rock anchors', in order to distinguish them from the clay-grouted tiebacks behind the sheeting. A diaphragm wall and its rock anchors appears on the left (North) side of the cross-section in Figure 3.2, next to Building A.

There is one area of the excavation where the SOE system is significantly different from the wall-and-tieback arrangement described above. At the extreme eastern end of the alignment, between about Sta. 90+50 and the circular cofferdam, the excavation's upper bracing level consists of cross-lot pipe struts, arranged in triangular clusters of three, rather than tiebacks. The locations of these struts are shown as the triangular symbols in Figure 3.4. Additionally, in the immediate vicinity of Building E's northern corner, both sides of the excavation are supported by "T"-buttressed concrete diaphragm walls, which are structurally stiffer than the straight diaphragm walls used elsewhere along the alignment. This especially stiff support design was used in this area because of the large depth of excavation (54 ft to 63 ft) and the need to protect Building E.

3.3.2. Tiebacks

The elevations of the tieback levels are shown for the entire excavation in Figure 3.4. Three levels of wale-and-tieback support are used throughout the western third of the alignment, with four and five levels becoming necessary as the excavation deepens to the east. The tiebacks are laterally distributed so as to provide the necessary amount of resisting force per linear foot, while at the same time avoiding foundations for nearby former and existing buildings.

The vertical downward inclinations of the tiebacks were selected by weighing several competing requirements. According to Xanthakos (1991), increasing the inclination angle of tiebacks offers the advantages of keeping the tiebacks below nearby underground structures and utility pipes, as well as minimizing the length of tendon required to reach depths with sufficient overburden stresses or a competent anchoring stratum. However, larger angles of inclination require an increase in total anchor capacity (to provide the same resistance to horizontal earth pressures) and also cause an increase in the downward vertical force on the wall that must be resisted by wall friction and end bearing. On the other hand, a minimum inclination of about 15 degrees is required to facilitate installation of the tiebacks and the grout under gravity forces. Typical angles of inclination in construction practice are 15 to 30 degrees; if a steeper angle is needed, 45 degrees is a common choice.

3.3.2.1. Sheetpile wall tiebacks

Along steel sheetpiles, the predominant wall types in the excavation, each tieback is locked to a horizontal wale on the interior side of the sheeting. All sheetpile wall tiebacks are installed at an average downward angle of 20 degrees. In general, tieback tiers were vertically separated by 10 to 12 ft. The horizontal spacing of the tiebacks tended to become smaller with depth: while the uppermost tier had tieback spacings ranging from 10.5 to 16.5 ft, the lowermost tier tiebacks were most frequently separated by five to nine feet.

Typical sheetpile wall tiebacks are shown on the right side of Figure 3.2. These tiebacks are anchored with grout in the upper ten to twenty feet of the Boston Blue Clay deposit, taking advantage of the strength of the BBC's heavily overconsolidated crust (as will be described in Section 5.4.3). The length of the bonded zone in the clay is at least 40 feet.

Before any excavation started, the design and performance of tiebacks grouted in Boston Blue Clay was evaluated through the Tieback Installation and Test Program (TITP), conducted by the contractor and its engineering consultants during the month of August, 1992. The program took place near the center of the excavation alignment between Sta. 72 and 73, as shown in Figure 3.5, and involved installation and grouting of ten tiebacks, five each in an Upper and Lower row, as shown in Figure 3.6. The following information is abstracted from a pair of reports by the Contractor's Geotechnical Consultant (1992c) on the TITP results, one report for each row of test tiebacks.

All ten tiebacks had grouted bond lengths of 40 feet, unbonded lengths of 60 to 65 feet, and were inclined 30 degrees from horizontal; they were grouted in the upper 20 ft of the marine clay in the overconsolidated crust. Tieback holes were drilled by advancing a 7-inch-O.D. steel casing to the base of the organic layer (the top of the clay), drilling with a rotary drag bit and flushing externally with water. A 6-inch-diameter hole was then drilled without the casing in the marine clay. Upon completion of drilling, the hole was filled with cement grout (0.5 water-cement ratio), and the strand assembly lowered into place. Each tieback consisted of six to eight 0.6-inch diameter, seven-wire, 270 ksi strands, which

were attached to a tube-a-manchette for post-grouting. After emplacing the tieback strands, the steel casing was withdrawn from the hole.

The tiebacks were postgrouted two or three times after installation. The first postgrout was done 20 to 48 hours after tieback installation and primary grouting; ensuing postgrouts were done on successive days. Each postgrout involved the injection of cement grout (0.6 to 0.75 water-cement ratio) through a 'tube-a-manchette', a 1-inch diameter PVC pipe with perforations at 2.5-foot centers. Each perforation was covered with a rubber one-way valve sleeve which allowed post grout out only when the grout pressures were high enough to displace the existing primary grout. A 'packer' was used in the tube to permit passage of the grout from only one perforation at a time. Grout was injected through each valve until either the pressures reached 800 psi or one full sack of cement (1.6 cubic ft) had been added. This procedure was repeated until all valves were postgrouted, except for two of the test tiebacks, for which the packer was not used and instead the grout was pumped through all perforations at once. Table 3.1 is a summary of the ten installations.

About one week after postgrouting, the tiebacks were tested by measuring anchor elongation under different loads. According to the TITP specifications (Contractor's Geotechnical Consultant, 1992a), tieback elongation was measured using dial gages which were accurate to 0.001 inch. Loads were applied with a hydraulic jack, and a pressure gage on the jack provided a measure of the load (See Figure 3.7). A second measure of applied loads was provided by a load cell, placed in axial alignment with the bearing plate, hydraulic jack, jack chair, and tieback tendon.

The two tiebacks at the ends of each wale were tested to failure in pull-out capacity tests, in which the tieback loads were increased in 20-ton increments up to 100 tons and 10-ton increments thereafter. These tests defined the maximum pullout load for the tiebacks in each row, and the design load was taken to be 50% of this load. The remaining three tiebacks in each wale were performance and creep tested. A performance test involves applying a cyclical progression of increasing loads, with each cycle reaching a load that is higher than the previous one by 25% of the chosen design load, until 150% of the design load is reached. The final maximum load is held for ten minutes. A creep test

involves loading the tieback in a monotonically increasing progression, again in increments equal to 25% of the design load, and holding the load constant at each stage for increasingly long periods of time. The last increment of the creep test is at 150% of the design load, and is held for 100 minutes.

The results of the tieback tests are summarized in Table 3.2. From the performance of the end tiebacks in the capacity tests, the contractor selected 170 tons as the failure load, based on the load cell values, which were generally lower and therefore considered to be conservative. The design load was defined as one-half of the failure load, equaling 85 tons. Subsequent performance and creep tests verified that the remaining anchors could hold up to 150% of the 85-ton design load, except for the two anchors for which a packer was not used in the post-grout stage. Anchor number 9, in fact, failed during hold at 150% design load.

Based on this testing program, it was concluded that the installation procedure used for test tiebacks was appropriate for sheetpile wall tiebacks, and that 85-ton design capacities could be achieved. The following recommendations were made: 1. Two post-grouts be performed on each tieback, except for tiebacks with less than ten feet of bond length in the clay's overconsolidated crust, which should be post-grouted three times. 2. At least 12 hours should elapse between post grouts, and the packer system should be used for the post-grouting. 3. Performance tests be conducted on the first three tiebacks installed, and on ten percent of the remaining tiebacks. 4. Proof testing to 150% design load be done on every tieback. A proof test is a relatively fast test in which the anchor is loaded to 133% or 150% anchor design load, in increments of 25%. Each load increment is held for no more than a minute, only long enough to obtain a reading of elongation. The final load is then held for ten minutes.

The following Acceptance Criteria, from recommendations by the Post-Tensioning Institute (1986), were applied to all tiebacks:

1. The total elastic movement obtained from a performance test should exceed 80 percent of the theoretical elastic elongation of the stressing length, but be less than the theoretical elastic elongation of the stressing length plus 50 percent of the bond length.

2. The total movement obtained from a proof test, measured between 50 percent of the design load and the test load, should exceed 80 percent of the theoretical elastic elongation of the free stressing length for that respective load range.

3. The creep rate should not exceed 0.080 inches per log cycle during the final log cycle of the performance test, proof test, and/or creep test -- regardless of tendon length and load.

4. The initial lift-off reading, taken after lock-off of each tieback, should be within five percent of the specified lock-off load.

3.3.2.2. Diaphragm wall tiebacks (rock anchors)

The tiebacks which hold the diaphragm walls are more steeply inclined than those for the sheeting; they dip at an angle of 45 degrees, and are long enough to extend into the upper part of the bedrock, thus being termed *rock anchors*. Refer to the left side of Figure 3.2 for an illustration of these tiebacks. The rock anchors were tremied with cement grout (water/cement ratio = 0.4 to 0.45); no pressurized post grouting was done. The tremie grout was allowed six days to cure before testing and stressing the anchor. Testing on the Diaphragm Wall A anchors included performance tests on the first three anchors and 5% of anchors thereafter, and proof tests to 133% design load on all anchors. (Design load typically ranged from 227 to 440 kips at Building A.) Acceptance Criteria were in accordance with PTI recommendations as listed in Section 3.3.2.1. Rock anchors, like the sheetpile wall tiebacks, were spaced 10 to 12 ft vertically, and were more widely spaced in the upper tier than in the lower tiers. Tier 1 horizontal spacings ranged from 8.5 to 12.75 ft, while spacings in the remaining tiers ranged between about six and seven feet. This spacing distance is slightly lower than that for the sheetpile wall tiebacks (See Section 3.3.2.1).

The drilling procedure for rock anchor tiebacks behind slurry walls underwent modification as excavation and construction work progressed along the alignment. Since excavation started at the west end of the alignment and progressed east, the first location at which rock anchors were installed was Diaphragm Wall A, the westernmost of the slurry walls, adjacent to Building A. Here, initially, the length of each tieback hole was

drilled with a downhole hammer, using wash water and high pressure air to flush cuttings out of the casing, a technique which is generally used for drilling in rock and hard till. 6-inch-OD casing was advanced along with the drill bit, and was usually kept six inches ahead of the bit, although the bit was occasionally allowed to protrude beyond the casing. The air pressure was maintained below 200 psi. The tieback installation contractor used this method through the overburden soils (fill, organics, marine clay, and glaciomarine deposits) as well as in the glacial till and rock. With this method, there was no need for drilling stoppages while the drill rods were pulled out and the drill bit replaced once the till and rock was reached.

Certain events were observed when the tiebacks were being installed with this approach in the lower part of Diaphragm Wall A and at Diaphragm Wall B. During drilling, air and wash water were seen escaping from adjacent tieback holes and from tieback holes in higher tiers, indicating communication of water and pressurized air through the Boston Blue Clay. This communication was observed while the drill bit was advancing through the clay deposit; since the clay is highly impermeable to air and water, it was suspected that the clay was being fractured under pressure, and hence greatly disturbed, by the use of the rock bit and pressurized air. Occasional fracture-inducing build-ups of air pressure ahead of the casing might have been caused by clogging of the casing by entrapped spoil, temporarily preventing the air flow from returning up the casing. From time to time, field engineers noticed stoppages in the return flow of air, which were frequently followed by sudden "bursts" of air as the flow through the casing resumed.

Due to concerns about potential clay disturbance, the drilling procedure was modified. First, the air flow used during drilling was reduced by about 40%, but when communication between holes continued to be observed at Buildings A and B, it was decided to use a drag bit to drill through the overburden soils, as was used for sheetpile tiebacks at the south wall. Water, rather than pressurized air, was used to flush cuttings out of the casing. This method permits a cleaner cut of soft and clayey soils, with much less disturbance. The tieback installation contractor changed to this procedure on August 5, 1993, when most of the tiebacks at Building A were in place and installation at

Diaphragm Wall B was well underway. The new procedure was then used for all subsequent drilling behind slurry walls.

3.3.3. Boat Section Structure and Tiedowns

The highway is founded on a ten- to twelve-foot-thick reinforced concrete slab. Under the boat section base slab, a grid of tension piles, or “tiedowns”, serve to resist unbalanced hydrostatic uplift pressures. A total of 600 tiedowns are spaced 14 to 18 ft apart in a grid containing 50 rows, each row spanning the width of the excavation and containing 10 to 14 tiedowns. Using tiedowns allowed the thickness of the concrete base slab to be reduced by approximately 15 feet, which substantially reduced the volume of poured concrete and the depth of final excavation.

Figure 3.8 illustrates the structure of the tiedowns. Each tiedown consisted of an assembly of seven 1-3/8-inch diameter DYWIDAG steel threaded bars inside of a 8-inch I.D. HDPE corrugated sheath. Centralizers and spacers were used along the length of the bars to keep them in the center of the borehole and separated from one another for maximum contact with the grout.

The drilling technique for the tiedown boreholes underwent revision as the work progressed through the boat section. If, as was frequently the case, the tiedown installation was done before final subgrade was reached, a 15-inch diameter pipe sleeve was installed into the soil down to the level of the eventual subgrade. The borehole drilling plan involved creation of a continuous 2.5-foot diameter soilcrete column down to the top of bedrock. A pilot hole was then drilled through the 15-inch pipe sleeve and on down to the bedrock, using a four-inch diameter drill bit, and the soilcrete column was formed by jet grouting the length of the hole. This jet grouted column was intended to serve in lieu of a casing, holding the borehole open and preventing flow of pressurized water from the lower aquifer. After the soilcrete set up, a 12-1/4-inch diameter bit was used to drill through it and on into the bedrock, penetrating the rock by at least 25 feet. When the drill rods were removed, the hole was grouted with a water-cement mixture (properties unspecified). At this point the sheathed assembly of bars was lowered into a grouted

borehole; as the assembly was lowered into place, the inside of the HDPE sheath was filled with grout as well.

The first tiedown installation activities took place at the southwestern end of the boat section in July of 1993. In December of 1993, jet grouting was stopped after having been completed throughout the western half of the boat section, through Row 34 (Sta. 77+00). Tiedown bars themselves had been installed only in the first few (westernmost) tiedown rows.

Rather than attempting to install tieback bars in the completed soilcrete columns, all tieback locations were redone by installing 15-inch ID permanent steel casings, each offset about two feet from the existing soilcrete column locations. Initially, for approximately the first two rows (near Sta. 73), the casings were "spun" into the soil all the way down to bedrock using rotary drilling methods, but a slight 'wobbling' effect resulted in a poor seal between the casing and the soil, allowing flow of pressurized water from the lower aquifer up along the outside of the casing. For this reason, subsequent casings were driven to bedrock.

The tiedown bars were long enough to extend above the ground surface after installation, permitting later connection to bearing plates on the completed boat section base slab. The tiedowns were post-tensioned after the base slab was constructed. Each tiedown was designed to hold a load of 350 kips, except for those at the edges of the structure, which had a 645-kip capacity in order to resist uplift forces arising from inward bending of the boat section walls (Druss, 1994b). Tiedowns were not necessary under the cut-and-cover tunnel slabs, which resisted unbalanced hydrostatic pressures through the weight of the closed structure and the soil backfill above it.

3.4. EXCAVATION DEWATERING AND PRESSURE RELIEF

The presence of the water table only five to ten feet below ground surface in the excavated area necessitated a dewatering and pressure relief program for the excavation. Dewatering was required from both the upper aquifer, in order to maintain a dry working subgrade, and from the lower aquifer, to relieve hydrostatic pressures acting upward on the base of the clay layer.

A series of nearly 40 dewatering and pressure relief wells were installed after the sheetpile walls were driven. As Figure 3.9 illustrates, the wells were placed throughout the entire alignment, along the inside of the support walls on both sides of the cut, in spaces between the sheeting and wales (as shown in Figure 3.10). Each well consisted of a 6-inch-diameter PVC pipe which was screened throughout the fill and organics above the clay and throughout the glacial deposits below the clay, extending about five feet into the underlying bedrock. The well casing was solid through the BBC deposit. Figure 3.11 provides an elevation view of a typical dewatering/pressure relief well, showing the screened lengths. A single submersible pump was placed in the well casing.

Pore water pressures in the permeable glacial deposits and weathered bedrock underlying the clay were reduced in order to maintain a factor of safety against hydrostatic uplift equal to or greater than 1.2 at each stage of the excavation (MHD, 1992). This factor of safety is defined by the formula given in Figure 3.12, and is essentially a ratio between the weight of soil above the glaciomarine deposit and the hydrostatic pressure within that deposit. As overburden material was excavated, the weight of the soil and clay counteracting the lower aquifer's hydrostatic pressure decreased, thus reducing the factor of safety against hydrostatic uplift.

Because the sheetpiles penetrated only partially into the clay, pressure reductions in the deep aquifer from wells within the excavation would result in pore pressure drawdowns outside of the cut as well. Such external drawdowns were to be minimized so that compression of the deep deposits and subsequent surface settlements would be as small as possible. However, all of the wells shown on Figure 3.9 were screened in the lower aquifer, like the "typical" well in Figure 3.11. Therefore pressure relief wells were placed throughout the alignment. The initiation of pressure relief pumping in portions of the alignment resulted in large pressure reductions in the lower aquifer. The subsequent history of pressure relief pumping is discussed in Section 7.2.2.1, where it is related to measured data from deep piezometers.

Table 3.1. Summary of Installations for the Tieback Installation and Testing Program (Contractor's Geotechnical Consultant, 1992c).

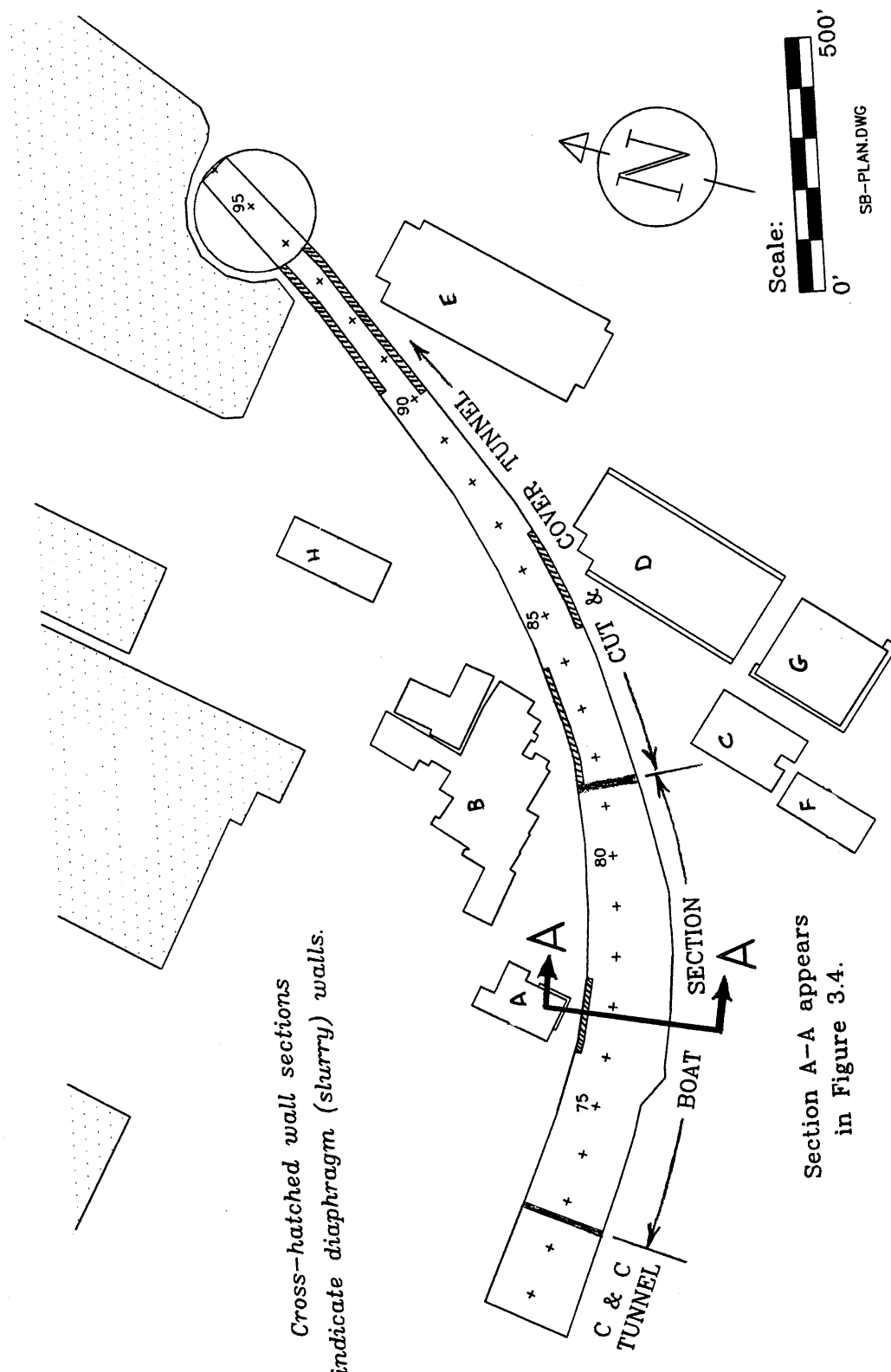
Tieback No.	Angle Measured from Horizontal (Degrees)	No. of 0.6" Ø Strands	Free Length ¹ (ft)	Bond Length ² (ft)	Elev. Top of Bond Zone	No. of Post Grouts	Average Post Grout Volume per Linear Foot Bond Length (ft ³)			
							1 st	2 nd	3 rd	Total Vol.
UPPER TIER	1	8	72.6	40	73.5	2	0.5	0.6	NA	1.1
	2	6	61.9	40	78	2	0.6	0.6	NA	1.2
	3	6	67.6	40	75	2	0.6	0.6	NA	1.2
	4	6	70	40	74.5	3 ³	0.5	0.5	0.5	1.5
	5	8	73	40	73	3	0.6	0.2	0.1	0.9
LOWER TIER	6	8	70.3	40	62	3	0.6	0.6	0.5	1.7
	7	6	70.3	40	62	3	0.6	0.7	0.6	1.9
	8	6	70.3	40	62	3	0.6	0.6	0.6	1.8
	9	6	70.3	40	61	3 ³	0.8	0.8	0.8	2.4
	10	8	70.3	40	62	2	0.7	0.4	NA	1.1

1. Tieback free length measured from anchor head to top of bond zone.
2. Tieback bond length in stiff to medium clay. Top of clay at about Elev. 78.
3. All tiebacks, except Nos. 4 and 9, were post grouted by pumping neat cement grout into each valve of the tube-a-manchette with a packer. A packer was not used at tieback Nos. 4 and 9.
4. Tube-a-manchette valves spaced at 2-1/2' centers.
5. Post grout consists of Type III cement and water with water cement ratio between 0.6 and 0.75.

Table 3.2. Summary of Test Results from the Tieback Installation and Testing Program (Contractor's Geotechnical Consultant, 1992c.)

Tieback No.	Type of Test	Maximum Test Load		Total Elongation (inches)	Bond Length (ft)	Anchor Elongation Per Log Cycle of Time at 150% Design Load (inches)	
		from Jack (tons)	from Load Cells (tons)			1 - 10 min.	10 - 100 min.
UPPER TIER	1	193	172	7.88	40	Not	Performed
	2	(Failure Load) 148	127	6.44	40	0.031	0.051
	3	147	128	6.32	40	0.010	0.014
	4	136	128	7.14	40	0.018	0.029
LOWER TIER	5	207 (Failure Load)	Inoperative	8.49	40	Not	Performed
	6	210±	179	7.41	40	Not	Performed
UPPER TIER	7	(Strands Yield) 142	128	7.07	40	0.009	0.027
	8	145	128	7.23	40	0.009	0.029
	9	142	128	8.04 (Note 3)	40	Not	Performed
	10	150 (Failure Load)	170	7.66	40	Not	Performed

1. These results used to determine a failure load of 170 tons and design load of 85 tons. See discussion in text.
2. Tiebacks Nos. 2 through 4 were loaded to 1.5 times 85-ton design load as indicated by load cell.
3. Performance test at Tieback No. 4 stopped after 4 min. hold at maximum test load because jack ram travel exceeded. Strands rehooked. Tieback failed at 99 tons (Jack reading) during reloading.



Cross-hatched wall sections indicate diaphragm (slurry) walls.

Section A-A appears in Figure 3.4.

Figure 3.1. Plan View of the Project Alignment in Boston. (Dimensions are approximate rather than exact.)

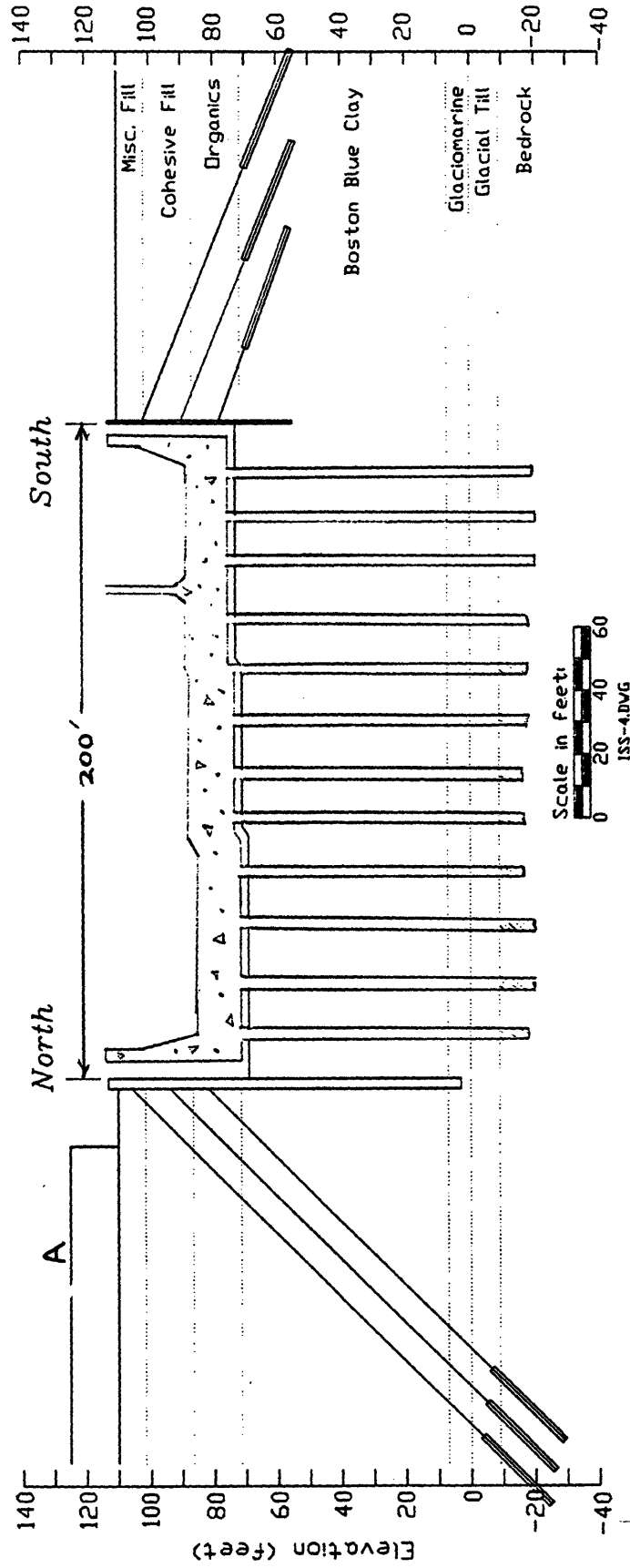


Figure 3.2. Cross-Section A-A from Figure 3.1, Through the Boat Section (Station 77+00), Showing Two Types of Support Wall: a Diaphragm (Slurry) Wall on the North and a Sheetpile Wall on the South.

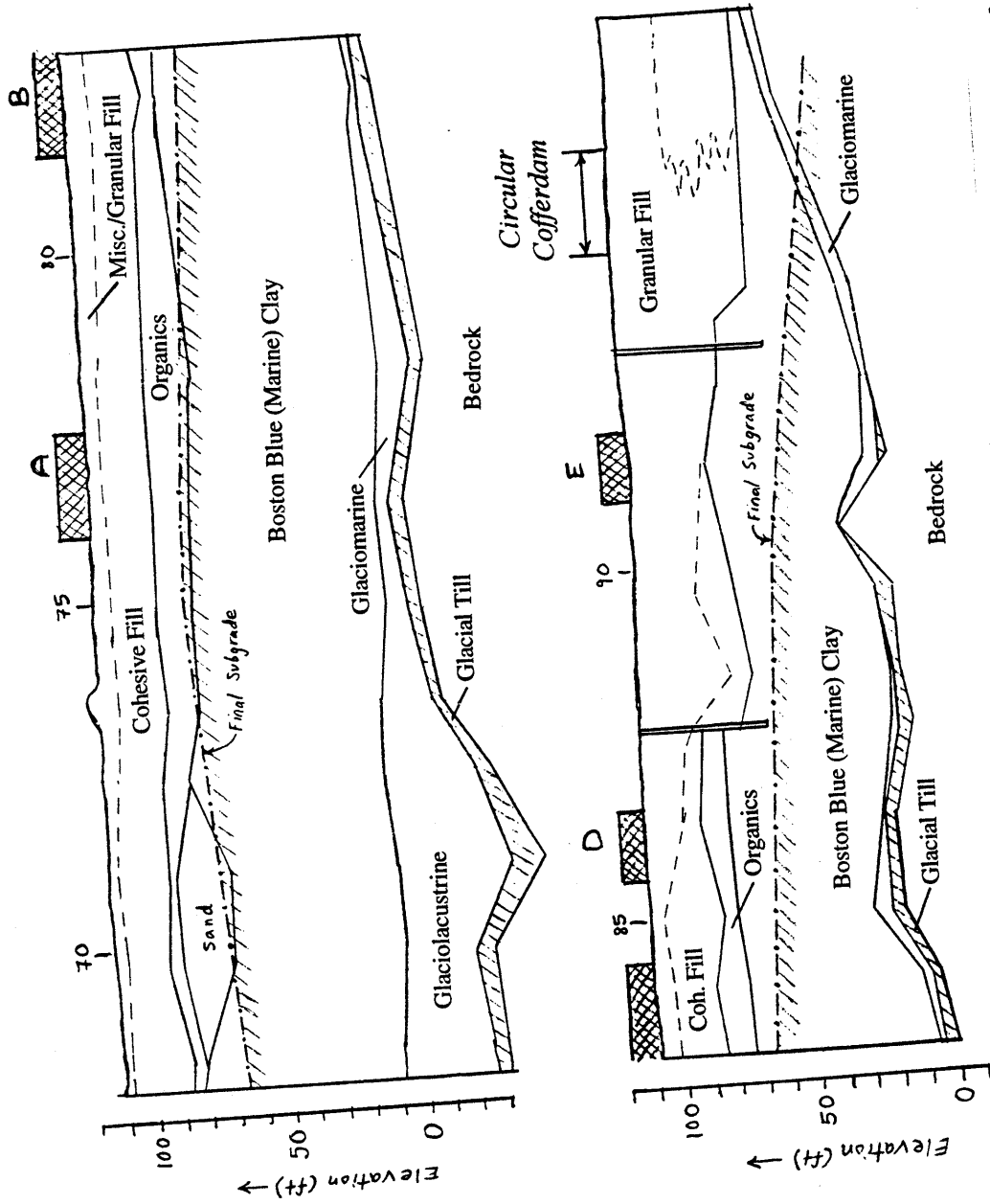
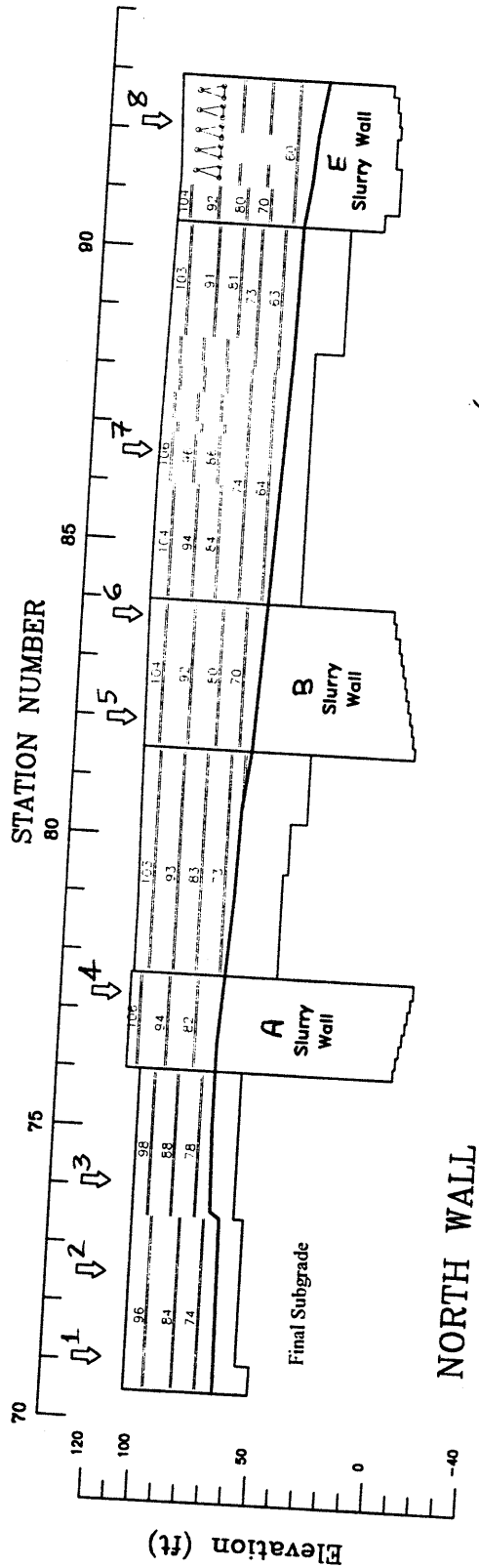
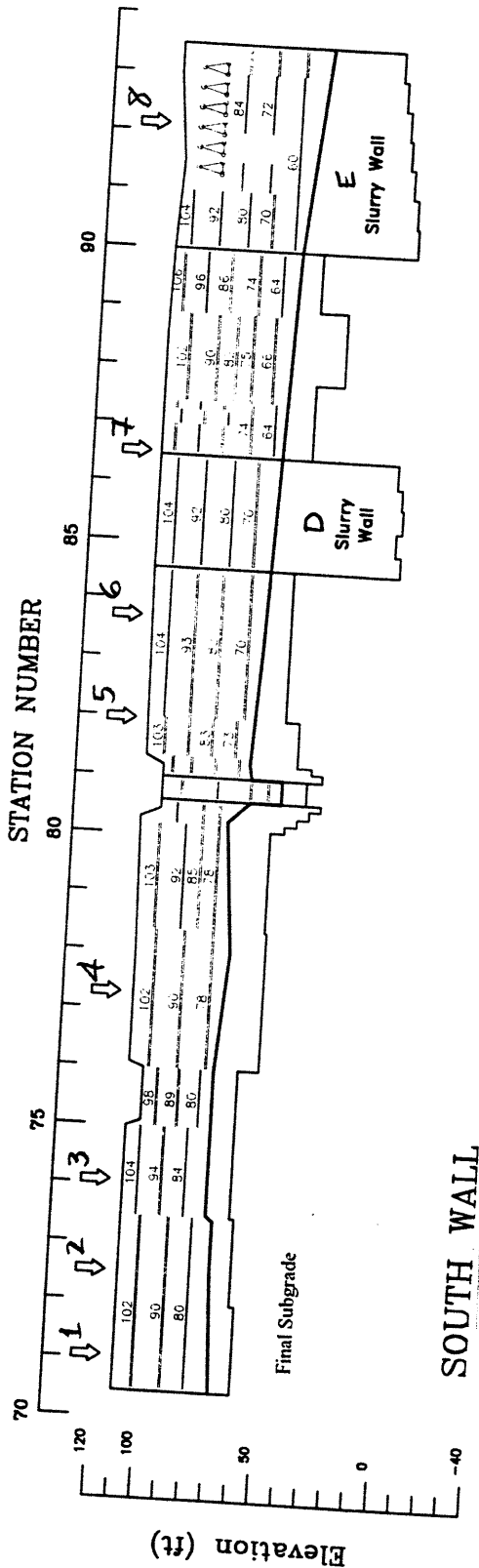


Figure 3.3. The Soil Profile along the Project Alignment showing the Elevation of Final Excavation Subgrade (based on MHD Geotechnical Consultant, 1991b).



↕6 = Location and Number of Instrumented Section



SOE.DWG

Figure 3.4. The North and South Support-of-Excavation (SOE) Walls, including Tieback Levels and Final Excavation Subgrade on each side.

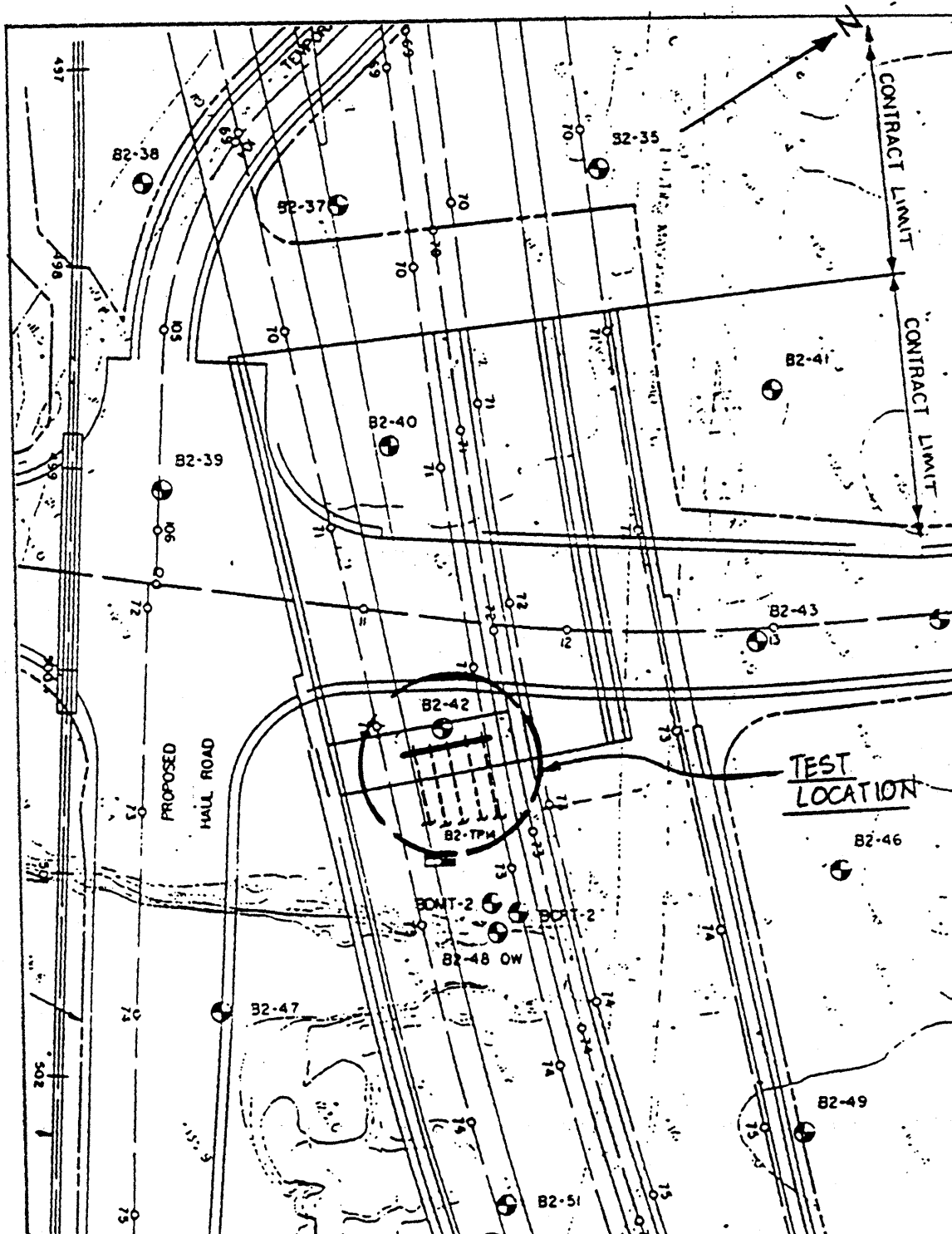


Figure 3.5. Location of the Tieback Installation and Testing Program (Contractor's Geotechnical Consultant, 1992a).

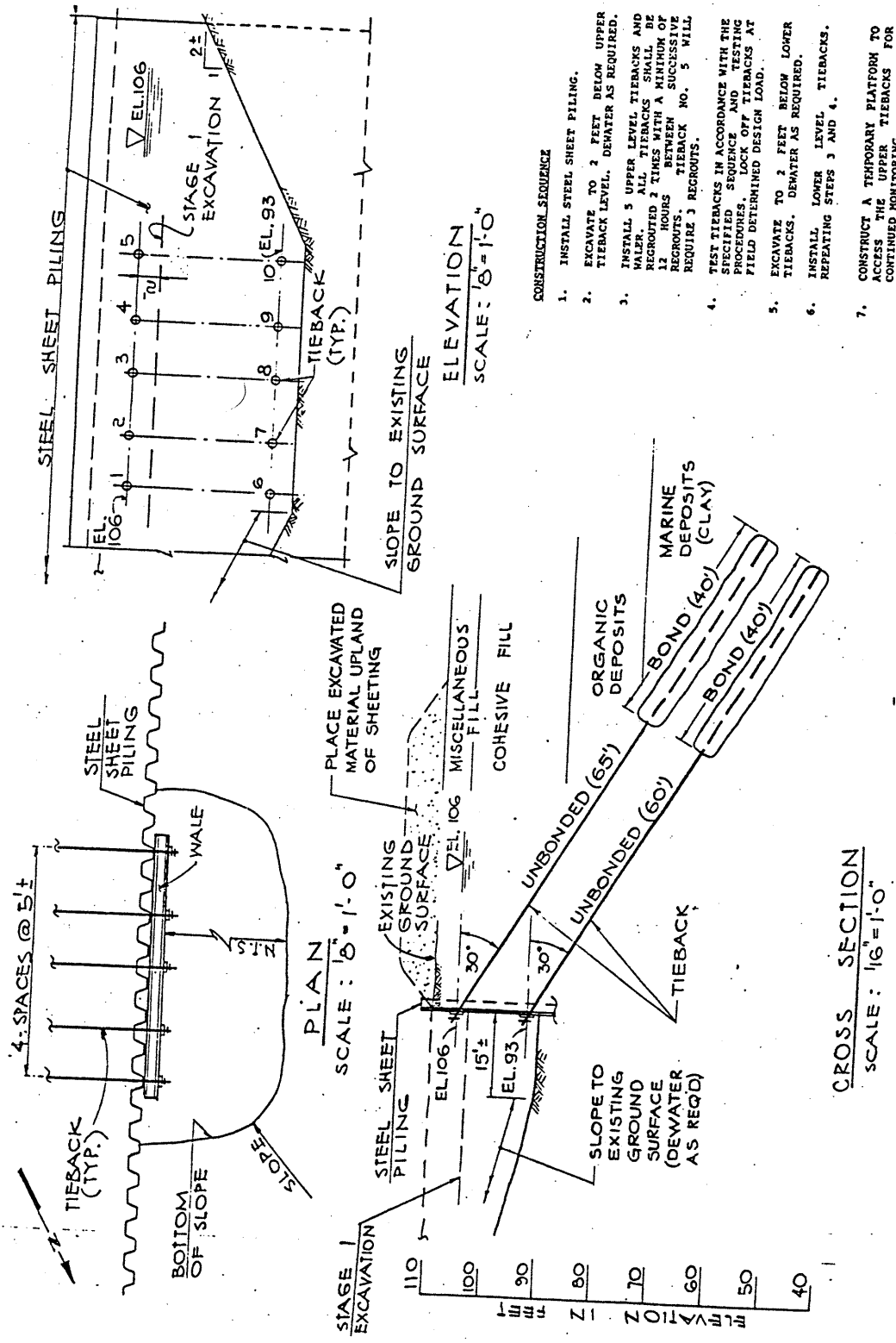


Figure 3.6. Arrangement of Tiebacks for the Tieback Installation and Testing Program
 (Contractor's Geotechnical Consultant, 1992a).

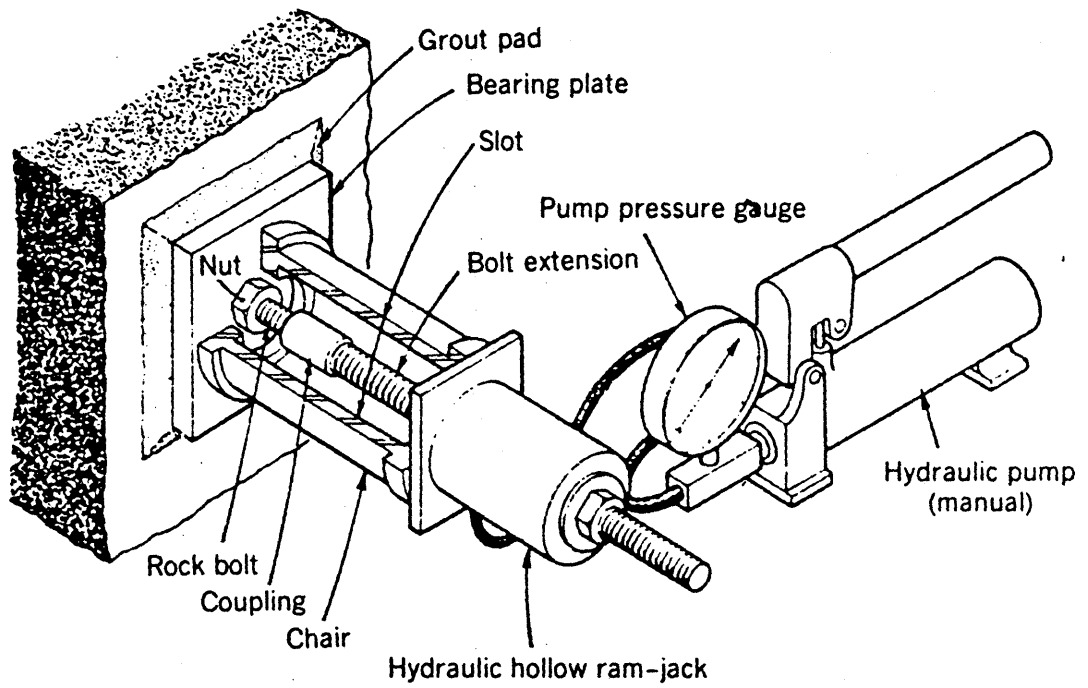
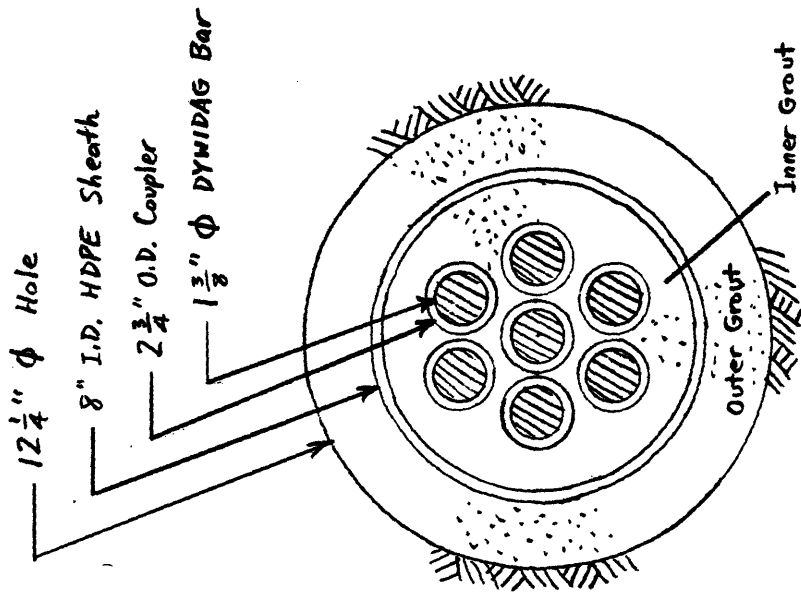
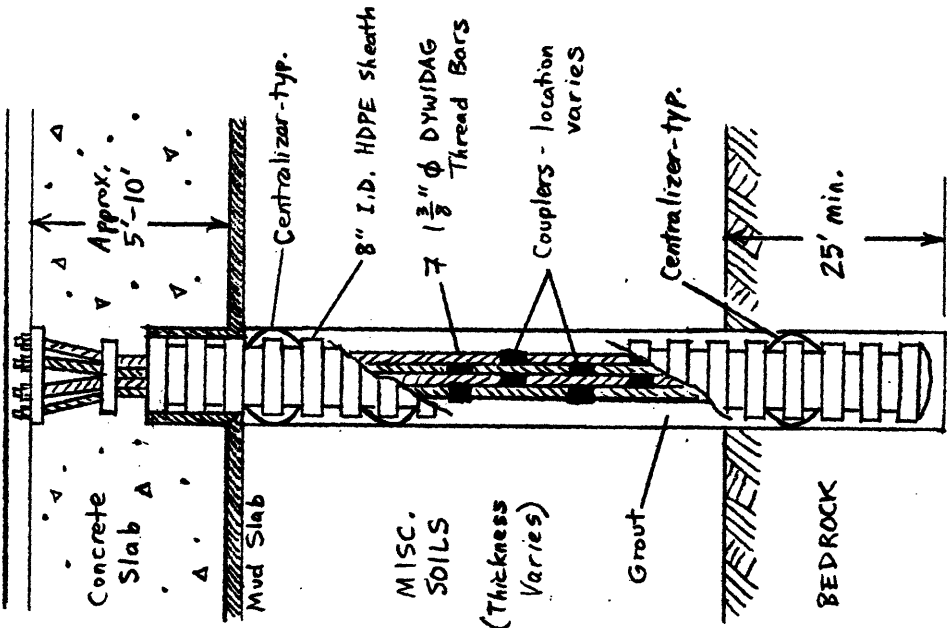


Figure 3.7. Equipment Used for Applying Stresses to Tiebacks and for Measuring Applied Loads (Xanthakos, 1991).



CROSS-SECTIONAL VIEW



ELEVATION VIEW

Figure 3.8. Structure of a Typical Boat Section Tiedown.

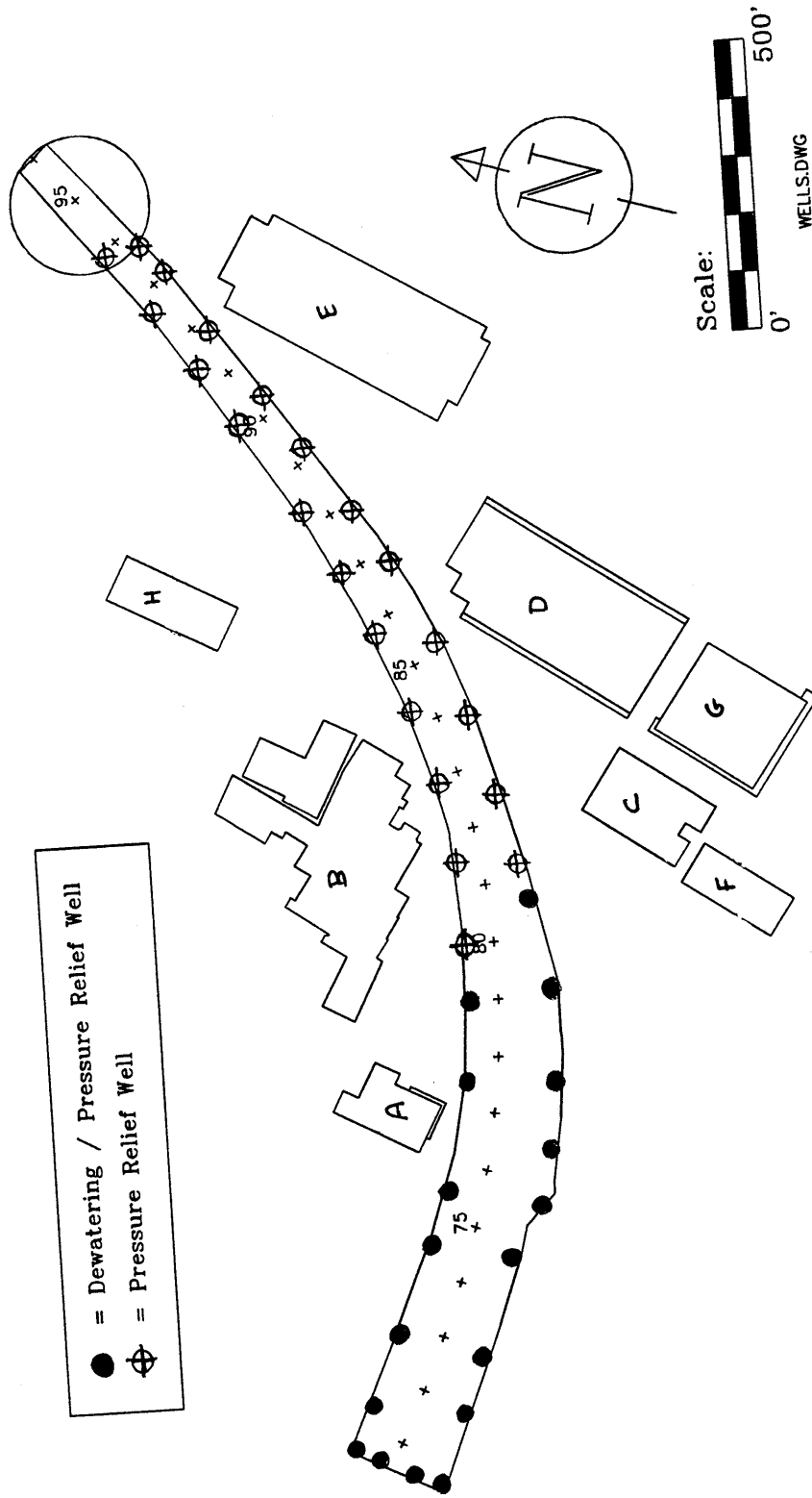


Figure 3.9. Locations of Dewatering and Pressure Relief Wells (Contractor's Geotechnical Consultant, 1992b)

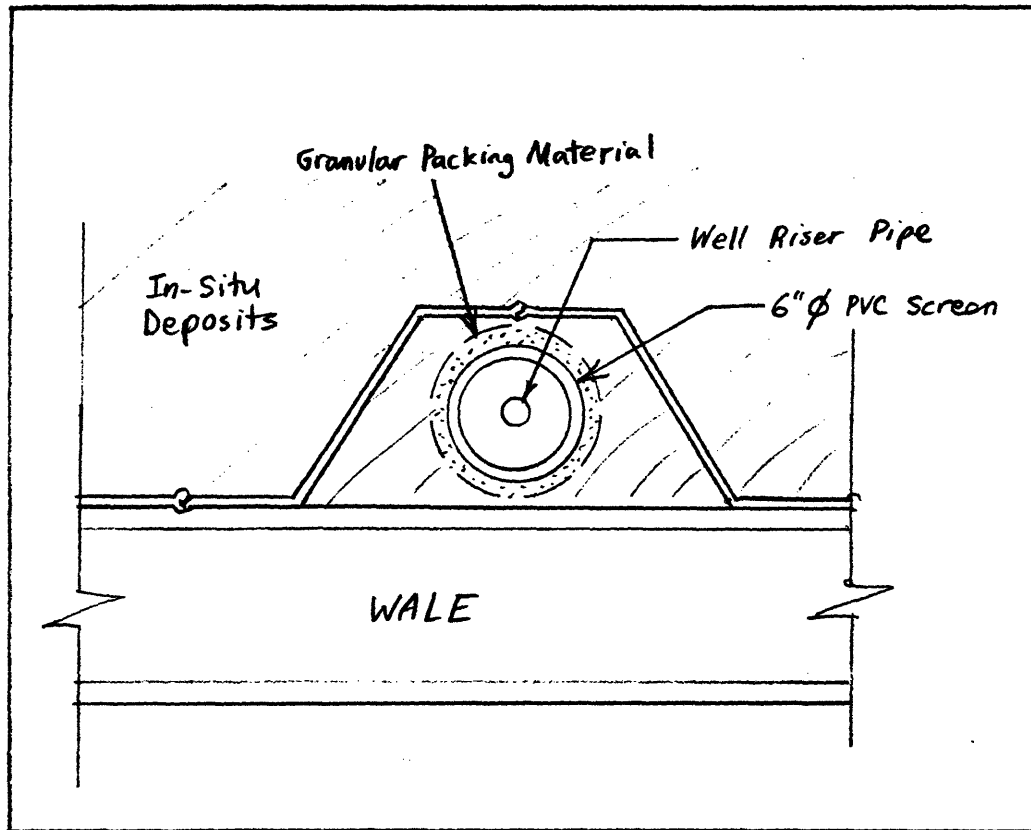


Figure 3.10. Plan View of a Typical Dewatering and Pressure Relief Well, Showing its Placement Relative to the Sheet piling and Wale (Contractor's Geotechnical Consultant, 1992b).

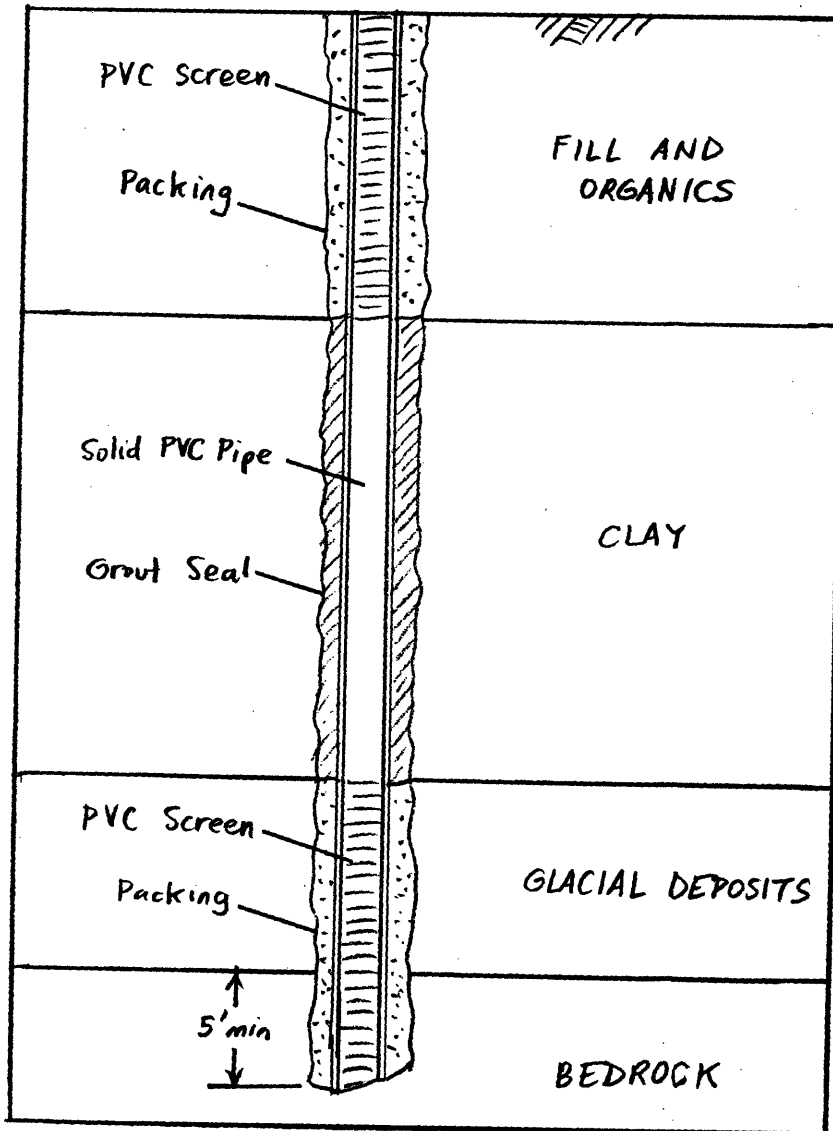


Figure 3.11. Elevation View of a Typical Dewatering and Pressure Relief Well, Showing Screened Lengths in the Upper and Lower Aquifers (Contractor's Geotechnical Consultant, 1992b).

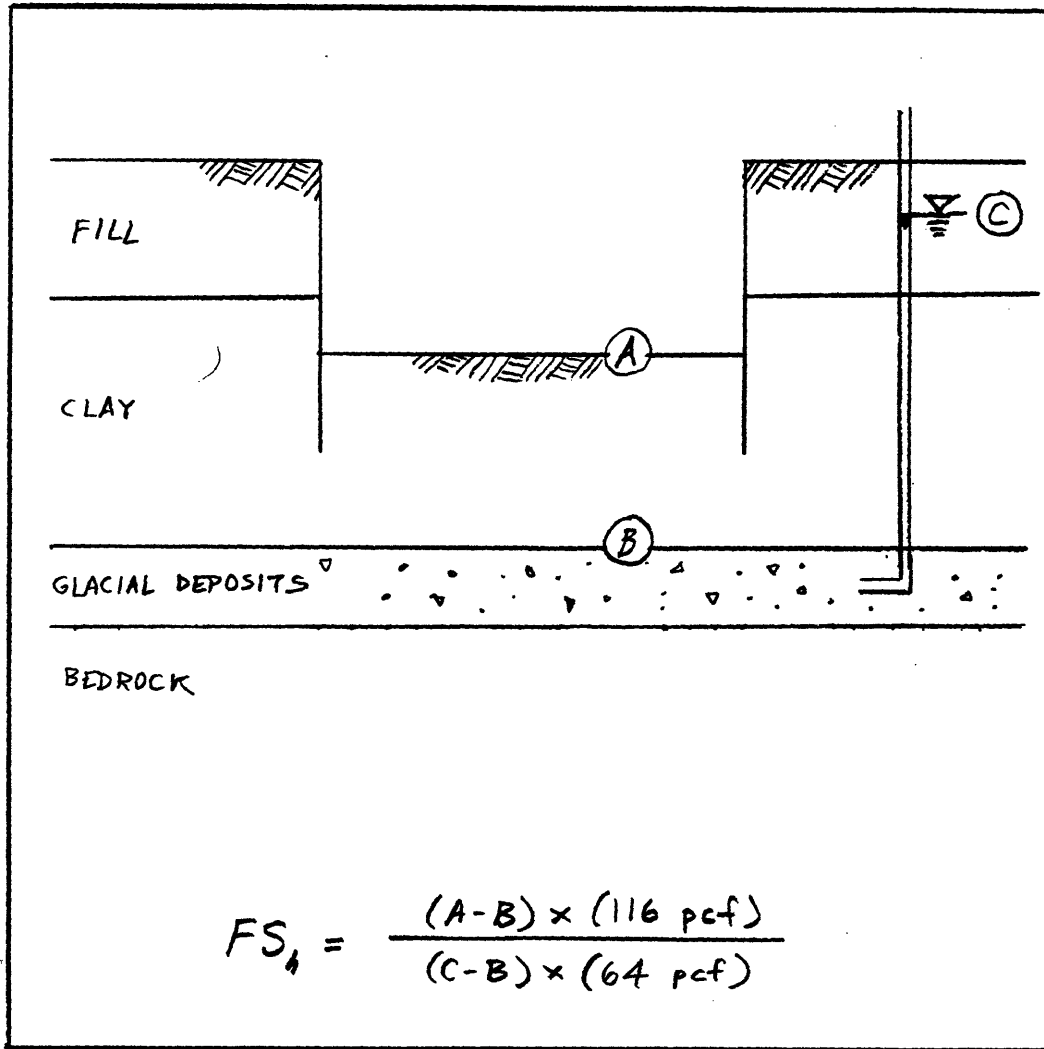


Figure 3.12. Definition of the Factor of Safety against Hydrostatic Uplift (MHD, 1992)

CHAPTER 4

GEOTECHNICAL INSTRUMENTATION AND SELECTION OF TEST SECTION

4.1. GEOTECHNICAL INSTRUMENTATION

During construction of the contract area under study, soil movements and pore pressures adjacent to the excavation were continuously monitored by an array of geotechnical instruments located inside and outside of the cut. Figure 4.1 shows a “typical” cross-section through the excavation, with the locations and depths of various geotechnical instrument types that were used throughout the alignment. The following quantities were measured:

1. *Horizontal (lateral) deflections vs. depth* were measured by Inclometers (labeled INCL's in Figure 4.1) and Inclometer/Probe Extensometers (IPE's). Lateral deflections of SOE walls were measured by inclinometers placed against or just behind sheetpile walls, or within diaphragm walls.

2. *Surficial settlements* were measured with Deflection Monitoring Points (DMP's) which came in two types: Type 2 DMP's, placed on vertical surfaces of existing structures such as building sides and sidewalk curbs, and Type 4 DMP's, placed on the ground surface.

3. *Vertical deformations (settlements or heave) vs. depth* were measured with Probe Extensometers (PBEX's and IPE's) outside of the excavation and with Multi-Point Heave Gages (MPHG's) within the excavation.

4. *Groundwater conditions* were monitored with a variety of instruments at different depths in the soil profile. Elevation of the water table was measured by Observation Wells (OW's). Shallow porewater pressures were measured by Open Standpipe Piezometers (OSPZ's). Deeper porewater pressures were measured by Vibrating Wire Piezometers (VWPZ's).

Appendix A presents a more detailed discussion of the design and capabilities of these geotechnical instruments.

Figure 4.2 shows the plan location of geotechnical instruments throughout the project area. It can be seen from this figure that instruments are generally arranged in clusters, or instrumented sections. The positioning of the instrumented sections included all locations where buildings were adjacent to the alignment, in general accordance with the recommendations of Dunnicliff (1988). For the purposes of this research, the instrumented sections were assigned the labels ISS-1 through ISS-8.

4.2. SELECTION OF INSTRUMENTED SECTION FOR ANALYSIS

4.2.1. Selection Criteria

A single well-instrumented “test section” was chosen for detailed analysis. Soil movements measured at this section would be compared to predictions based on existing empirical and semi-empirical design methods (Chapter 2). Later, as part of Task 5 in Phase I of the research project (Table 1.1), the soil movements, wall deflections, and pore pressure changes measured at the selected test section are going to be compared with the results of future Finite Element simulations using the MIT-E3 soil model (Jen, work in progress). Three criteria were used in selecting the instrumented section that would be best suited for this study. First, it needed to be sufficiently instrumented to allow a complete record of soil movements and groundwater levels beside and within the cut. Ideally the test section would have at least one inclinometer and two settlement points behind both the North and South walls, one or more observation wells or piezometers on each side, and some heave gages and additional piezometers within the excavation. Second, the excavation sequence and geometry, the excavation support system, the soil profile, and the soil movements recorded at the chosen section should be representative of conditions along the alignment; i.e., they should not represent ‘anomalous’ behavior relative to the rest of the area. Third, conditions to either side of the section along the alignment should be fairly consistent so that the finite element analysis can reasonably assume an infinitely long excavation (plane strain conditions).

4.2.2. Review of Available Instrumented Sections

The first step in choosing the most suitable instrumented section was to examine the layout of instruments in the project area, as shown in Figure 4.2. This allowed some instrumented sections to be immediately assigned less desirable status. Such sections included: ISS-1 and ISS-6, which had few or no surface settlement points (DMP's); ISS-2, which had no instrumentation inside the cut; and ISS-7 and 8, which were each lacking inclinometers on one side. Because ISS-5 and 6 were close together and poorly defined as individual sections, the possibility of combining these two instrumented sections into a wider single section was considered.

The excavation geometry and distribution of wall types also provided a basis for comparing instrumented sections. As shown in Figure 3.3, the soil profile along the alignment remains fairly constant and therefore did not influence the selection process. The width of the excavation decreased toward the east, such that ISS-1, at the west end, was wider than the rest of the alignment, while ISS-8 was the narrowest section. In addition, the excavation at ISS-8 was supported by a unique and much less flexible support system than those used throughout the rest of the area: walls on both sides were "T"-buttressed diaphragm walls, and triads of steel pipe were used as strong cross-lot struts, emplaced to protect Building E on the South side. This anomalous support geometry, which is diagrammed in Figure 4.3, made ISS-8 a poor choice for further study and thus eliminated it from further consideration. Among the remaining sections, four (ISS-4 through 7) were asymmetrical, having a combination of two wall types: a sheetpile wall on one side and a slurry wall on the other. ISS-1 through 3, on the other hand, were symmetrical sections with sheetpile walls on both sides.

This survey of the eight available instrumented sections is summarized in Table 4.1, which lists the positive and negative features of each section with respect to the available instruments, the excavation geometry, and the support system at each.

4.2.3. Review of Construction Histories

The schedule of construction events was another important factor in selecting a representative instrumented section. Figure 4.4 uses a graphical format to show a simplified version of the construction histories at each of the eight sections. The symbols marked "T1", "T2", etc. show the dates of lock-off for different tieback levels. "EFS" indicates the dates of excavation to final subgrade. Final subgrade was excavated twice at ISS-2 because large soil movements measured in that area were countered by partially backfilling the excavation for a number of months. The excavation histories at this location was therefore anomalous.

4.2.4. Review of Soil Movements

Lateral deflections of the wall and adjacent soil mass, as well as surficial settlement profiles throughout the alignment, were plotted so that soil movements along the alignment could be readily viewed, thus facilitating the identification of representative vs. anomalous movements. Summary plots of each variable were prepared by plotting wall deflections and surface settlements versus station number. Each plot shows movements that were measured on the date of excavation to the final subgrade level at each instrumented section or individual instrument.

Lateral wall deflections measured by inclinometers within or immediately adjacent to the support of excavation (SOE) walls, on the date of the final subgrade excavation, are plotted against station number in Figure 4.5. Values of H (excavation depth) varied along the alignment, and are summarized in Table 4.2. West of the boat section (Sta. 70+50 to 73+50), the excavation depth ranged between 37 and 40 ft. Through the boat section, the depth increased eastward from 32 ft (at Sta. 73+50 along the North wall) to nearly 45 ft (at Sta 81+00). East of the boat section, the excavation continued to deepen to the east, reaching a maximum depth of 59 at the eastern terminus (Sta. 93+00).

Three sets of deflection values are plotted on the graphs in Figure 4.5: the wall deflection measured at the final subgrade elevation, the deflection measured at the top of the wall, and the overall maximum wall deflection. The graphs show the locations of the diaphragm (slurry) walls, and it can be seen that these walls deflect in a much different

manner than do the sheetpile walls. The different behaviors of the two wall types is further illustrated in Figure 4.6. First, the maximum wall deflections are lower for the diaphragm walls than they are for the sheetpile walls, in accordance with the higher stiffness of 3 ft.-wide reinforced concrete relative to thin (Arbed type AZ-18) steel sheeting. While maximum outward wall deflections never exceed two inches at the slurry walls, they are rarely less than five inches behind sheetpiles. Second, the tops of the slurry walls always show an “inward” deflection (negative on the plots), meaning that the top of the wall has been pulled back into the retained soil by the force from the tiebacks. Such deflections are very rarely seen elsewhere at this construction project or in general practice.

Figure 4.5 shows wall deflections in excess of nine inches west of Sta. 74 along the north wall. The wall movements in this region were well in excess of those seen elsewhere along the alignment, and could be attributed to a number of possible factors including: 1.) disturbance of the soil by tieback drilling with highly pressurized air and water, which was done behind sheetpiles only at that location on the North side before lower pressures were used for subsequent installations; 2.) the removal of existing foundation piles from the soil just behind the North wall at that location, resulting in further disturbance; 3.) the possibility of unusually low undrained strengths for the BBC in that area. As mentioned in Section 4.2.3, the large movements that occurred in this area necessitated a partial backfilling of the excavation, as well as a reduction of active earth pressures by removal of soil from behind the sheeting. The large wall movements and disrupted excavation schedule of this area of the excavation made sections ISS-1 and ISS-2 poor choices for further consideration and analysis.

Interpretation of the wall movement data in Figure 4.5 is complicated by the fact that many inclinometers were installed well after excavation started in their vicinity. Such inclinometers therefore recorded only partial wall deflections, since some deflection must have occurred before their installation. Table 4.2 provides inclinometer installation dates relative to the start of excavation activities. This table lists only the inclinometers that record wall, rather than soil mass, movements: that is, only those that are positioned immediately behind the SOE walls (within two feet) or are actually on or inside the walls (i.e., either welded on the excavation side of sheetpile walls, or within the concrete slurry

of diaphragm walls). Eight inclinometers were installed more than a month after excavation started. Inclinometer INC-111 (North wall, Sta.78+65), for example, was installed 99 days after excavation of the first lift, at which point the second tier of tiebacks had already been drilled and installed. The deflection measured by this instrument at excavation to final subgrade is 2.8 inches, which is an anomalously low number (especially for sheetpiles - see Figure 4.5) but is well explained by the late installation date.

Surface settlements behind the SOE walls are plotted in Figure 4.7-a for the North side and Figure 4.7-b for the South side. Settlement data measured on three (and, in one case, four) dates are shown for each instrumented section that included DMP's or Probe Extensometers (in IPE's). The three selected dates represent the following construction events: excavation of the first lift, excavation to the final subgrade level, and the pouring of the concrete invert. The plot for the North side of ISS-2 includes settlements from a fourth date, representing the second excavation to final subgrade level, which followed the partial backfilling that was done to control excessive soil movements at that location.

Plots for the North side of ISS-5 and the South side of ISS-6 are uninformative due to the lack of DMP's at these sections. 'Typical' wedge-shaped settlement troughs are seen for most of the other sections except for ISS-3 and 7 North. In addition to showing the distribution of settlements with distance from the wall, the plots also give an idea of how the settlements developed over time. Most settlement occurred during the process of excavation, between excavation of the first lift and the excavation to final subgrade. In general, less than one inch of settlement occurred between the excavation to final subgrade and the invert pour.

Section 8.2.2 provides more discussion of these settlement profiles and how they compare to empirically predicted settlement distributions.

4.2.5. Selection of ISS-4

Based on the criteria discussed above, ISS-3 and ISS-4 were judged to be the most suitable instrumented sections for further study. These instrumented sections have the following features:

1. Both were sufficiently instrumented, having full complements of instrumentation types both inside the cut and outside the cut and on both sides (unlike all the other sections).

2. Both experienced wall deflections and settlements that were judged representative of those seen throughout the excavation (unlike ISS-1 and -2).

3. The inclinometers at both were installed before or within a few days of the start of excavation activities (unlike ISS-7).

4. Excavations at both were carried out in a relatively simple manner, without any backfilling or other special measures being necessary (unlike ISS-1 and -2).

Of the two, ISS-4 was selected as the best section to be studied in detail, because, unlike ISS-3, it offered the chance to study soil movements behind both types of SOE walls: the slurry wall on the north side adjacent to Building A, and the sheetpile wall on the south side. This provided the opportunity to analyze two very different types of wall behavior at one section.

The remainder of this thesis will therefore focus on data and interpretations from ISS-4. Instrument records from ISS-3 may be studied in the future, depending upon the results of the planned finite element analysis at ISS-4.

Table 4.1. Positive and Negative Attributes of the Eight Instrumented Sections.

Instrumented Section	Station and Wall Type	Positive Characteristics	Negative Characteristics
ISS-1	Sta. 71+20 Sheetpiles - both sides	Instrumented within excavation	No settlement points Excessively high wall movements on north side Complex excavation history (backfilling) Too close to end of excavation
ISS-2	Sta. 72+50 Sheetpiles - both sides	Fully instrumented outside excavation	No instruments within excavation Excessively high wall movements on north side Complex excavation history (back filling)
ISS-3	Sta. 74+20 Sheetpiles - both sides	Fully instrumented within excavation Fully instrumented outside excavation Representative soil movements	
ISS-4	Sta. 77+20 Slurry wall - north	Fully instrumented within excavation Fully instrumented outside excavation Representative soil movements	Limited extent of slurry wall to the east
ISS-5	Sta. 82+00 Slurry wall - north	Representative soil movements	Few instruments within excavation No piezometers on south side
ISS-6	Sta. 83+50 Slurry wall - north	Representative soil movements	Few instruments within excavation No nearby DMP's or VWPZ's on south side INC-114 (South) installed 36 days late
ISS-7	Sta. 86+20 Slurry wall - south		Few instruments within excavation No inclinometer on south side INC-117 (North) installed 23 days late
ISS-8	Sta. 92+30 Slurry wall - both sides		'T'-shaped diaphragm walls and pipe struts are unique to the alignment Few instruments within excavation No inclinometer on north side No piezometers on south side

WALL DEFLECTIONS -- SUMMARY

NORTH WALL

Inst.	Sta.	Excav. Depth (H)	Subgrade		Top		Max. inward	
			Wall Deflect. *	Normal. Defl. (%)	Wall Deflect. *	Normal. Defl. (%)	Wall Deflect. *	Normal. Defl. (%)
IPE-108	71.09	38	5.1	1.12	9.7	2.13	10.8	2.37
INC-502	72.5	37	6.3	1.42	8.7	1.96	9.2	2.07
IPE-110	73.25	37	6.1	1.37	9.5	2.14	9.5	2.14
IPE-105	74.25	32	3.6	0.94	5.4	1.41	5.4	1.41
INC-102	77.09	39	-0.6	-0.13	-5.3	-1.13	0.4	0.09
INC-111	78.65	41	2.8	0.57	1.5	0.30	2.9	0.59
INC-113	80.55	43	4.6	0.89	0.4	0.08	5.0	0.97
INC-104	82.02	47	0.7	0.12	-2.3	-0.41	0.9	0.16
IPE-111	83.46	50	1.6	0.27	-0.5	-0.08	1.9	0.32
INC-116	84.48	51	4.7	0.77	1.6	0.26	5.7	0.93
INC-117	86.22	53	5.1	0.80			5.1	0.80
INC-118	87.3	53	5.1	0.80	0.4	0.06	5.5	0.86
INC-120	88.76	54	(data not obtained)					
INC-122	89.93	54	(data not obtained)					

SOUTH WALL

Inst.	Sta.	Excav. Depth (H)	Subgrade		Top		Max. inward	
			Wall Deflect. *	Normal. Defl. (%)	Wall Deflect. *	Normal. Defl. (%)	Wall Deflect. *	Normal. Defl. (%)
IPE-107	71	40	3.2	0.67	4.6	0.96	5.4	1.13
INC-109	71.7	39	2.2	0.47	2.3	0.49	2.5	0.53
INC-501	72.33	38						
IPE-109	73.25	38	4.4	0.96	4.3	0.94	5.5	1.21
IPE-104	74.25	36	5.6	1.30	3.8	0.88	5.8	1.34
INC-101	77.01	38	5.1	1.12	2.8	0.61	5.3	1.16
INC-110	78.31	40	2.5	0.52	1.2	0.25	2.6	0.54
INC-112	79.99	38	1.9	0.42	-0.7	-0.15	2.2	0.48
INC-103	81.94	45	4.6	0.85	0.5	0.09	5.2	0.96
INC-114	82.98	47	5.9	1.05	0.6	0.11	6.7	1.19
INC-115	83.52	48	4	0.69	1.9	0.33	5.9	1.02
INC-105	85.21	49	1.1	0.19	-2.5	-0.43	1.2	0.20
INC-119	88.59	53	(data not obtained)					
INC-121	89.55	53	(data not obtained)					
IPE-112	92	59	(data not obtained)					

* Deflections were measured on date of excavation to final subgrade (EFS)
 Deflections are in inches; depths are in feet
 Normalized deflections equal wall deflection (inches) divided by H (as a %)

Table 4.2. Summary of Deflections and Installations for Near-wall Inclinerometers (Page 1 of 2).

NORTH WALL

Inst.	Installed after excav. began?			On / in wall	Wall Type	Comments
	yes / no	# days after	progress at inst.			
IPE-108	no			no	sp	
INC-502	no			no	sp	
IPE-110	no			no	sp	
IPE-105	no			no	sp	
INC-102	YES	1	Ex T1	YES	d/w	Bent inwards
INC-111	YES	99	In T2	YES	sp	
INC-113	YES	51	In T1	YES	sp	
INC-104	no			YES	d/w	Bent inwards at top
IPE-111	no			np	d/w	Zig-zag: due to grout?
INC-116	YES	86	In T1	YES	sp	Bent 3" by tractor
INC-117	YES	23	LO T1	YES	sp	Accidentally cut 10' above s.g.
INC-118	YES	146	LO T2	YES	sp	Slight damage, well above s.g.
INC-120				YES	sp	
INC-122				YES	sp	

SOUTH WALL

Inst.	Installed after excav. began?			On / in wall	Wall Type	Comments
	yes / no	# days after	progress at inst.			
IPE-107	no			no	sp	
INC-109	YES	56	LO T2	no	sp	
INC-501	no			no	sp	Destroyed after 3/4/93
IPE-109	no			no	sp	
IPE-104	no			no	sp	
INC-101	YES	2	Ex T1	no	sp	
INC-110	YES	142	In T2	YES	sp	
INC-112	YES	50	In T1	YES	sp	
INC-103	no			no	sp	
INC-114	YES	36	In T1	YES	sp	
INC-115	no			YES	sp	Damaged?
INC-105	no			YES	d/w	Bent outwards at top
INC-119				YES	sp	
INC-121				YES	sp	
IPE-112				no	d/w	

Ex = excavate to tier level
 In = drill and install tiebacks
 LO = lock-off tiebacks

sp = sheetpile wall
 d/w = diaphragm wall

Table 4.2, Summary of Deflections and Installations for Near-wall Inclinerometers, continued (Page 2 of 2).

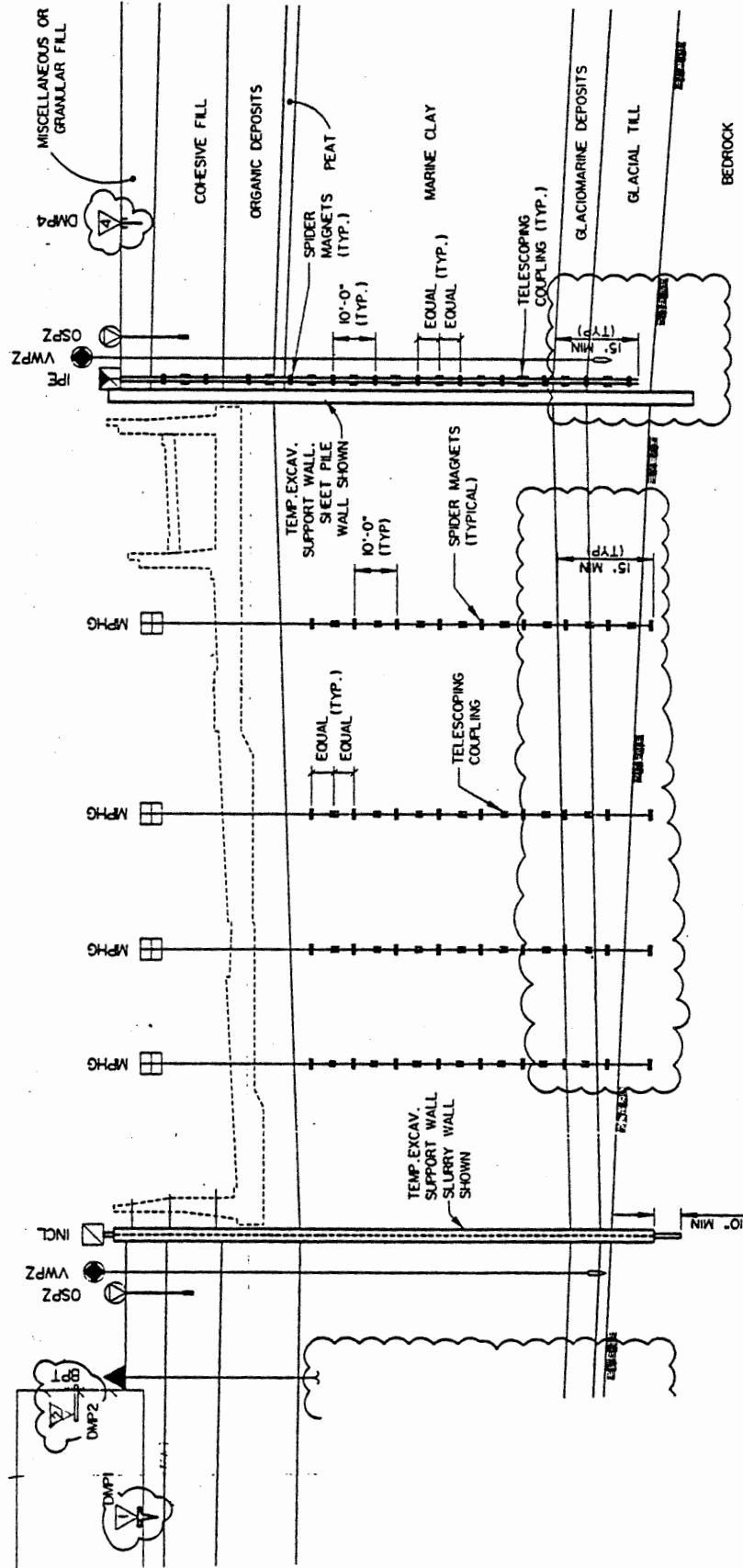


Figure 4.1. Cross-Sectional View of a "Typical" Instrumented Section Through the Project Alignment, Showing Locations and Depths of Geotechnical Instruments (MDPW, 1991).

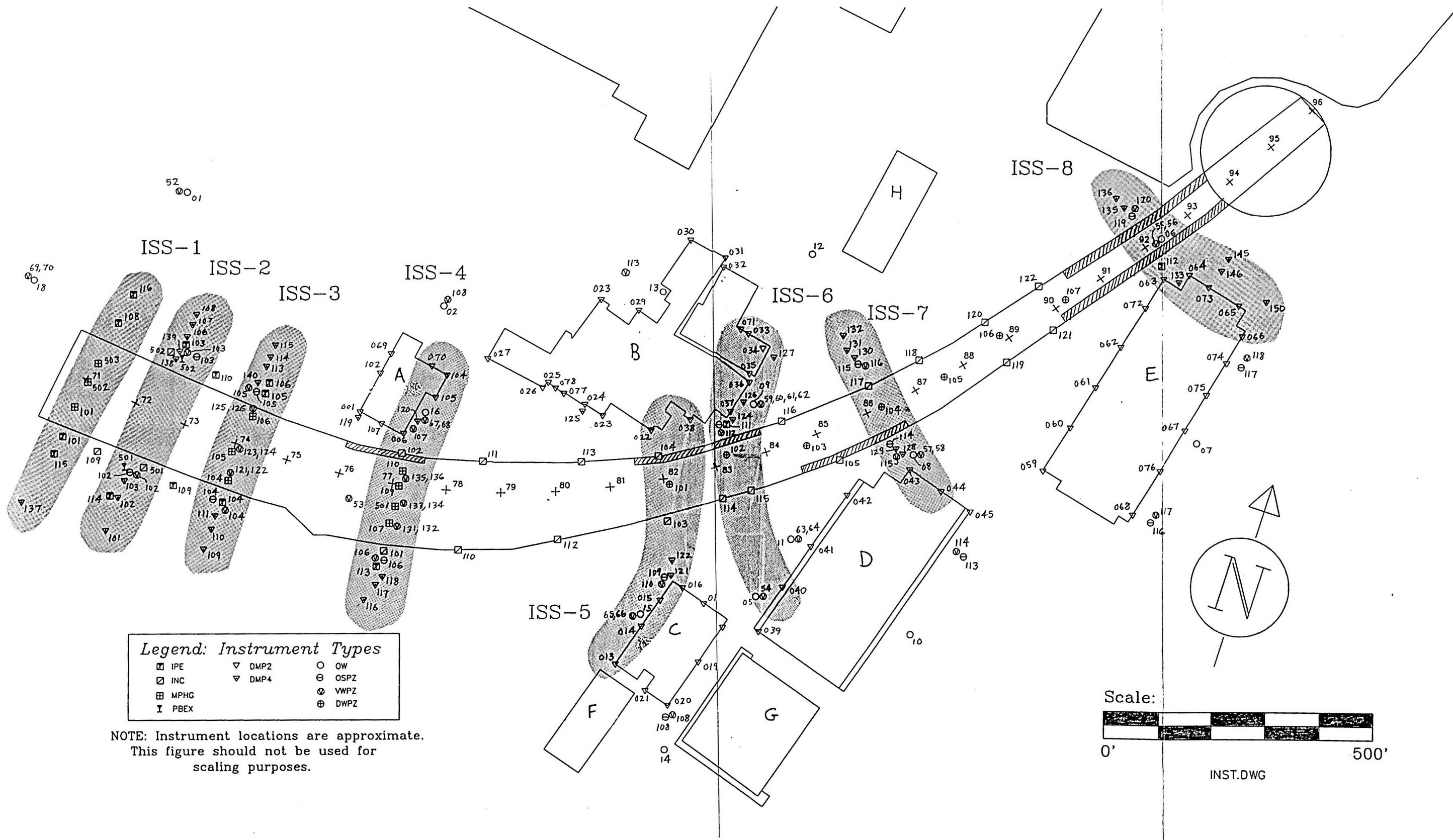


Figure 4.2 Plan View of the Excavation, showing Positions of Geotechnical Instrumentation and Instrumented Sections.

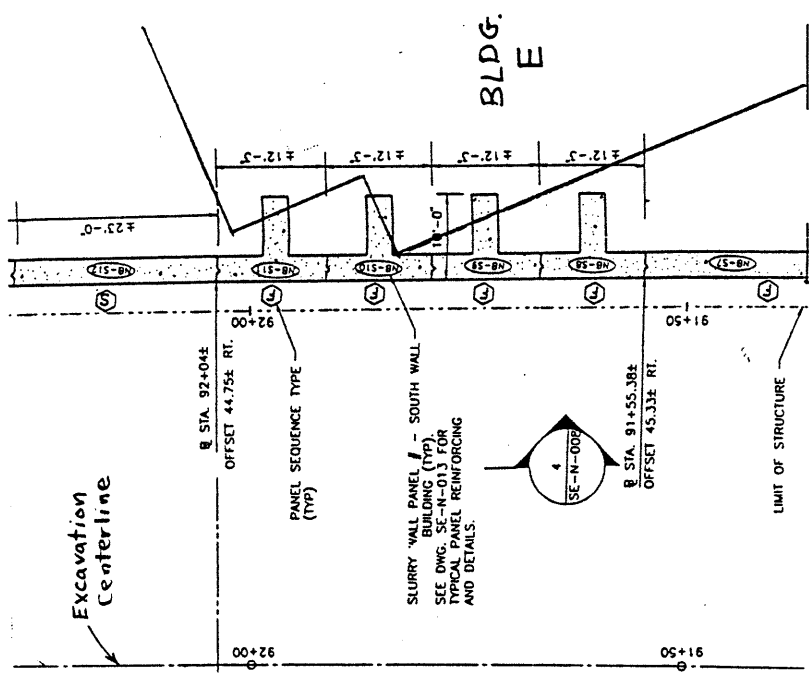
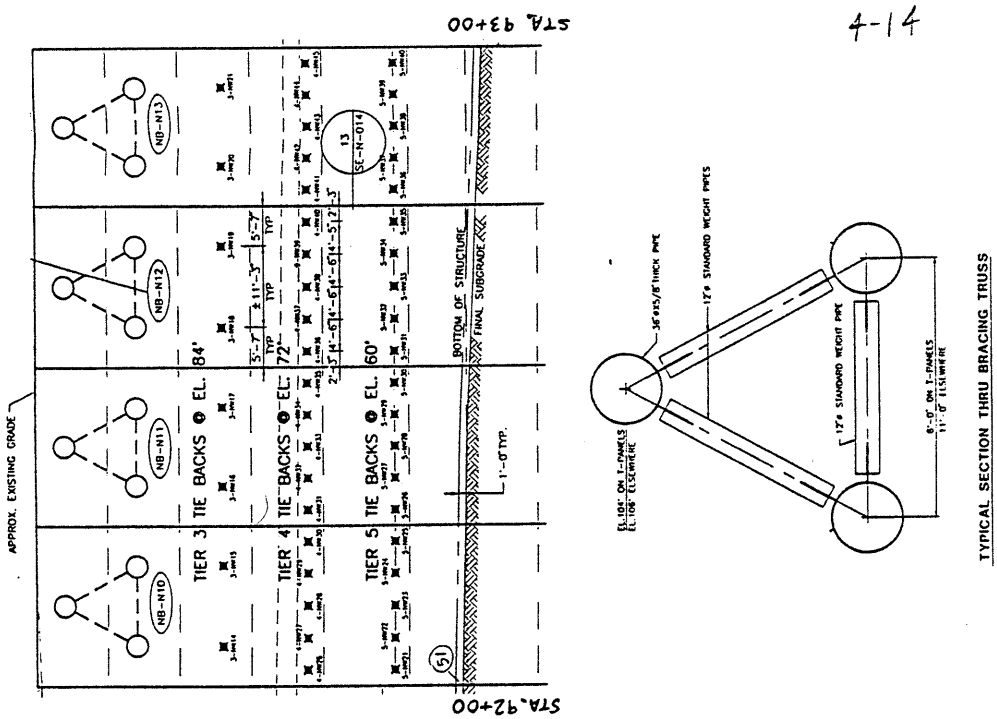


Figure 4.3. The Excavation Support System used at ISS-8, between Station 90+00 and the Circular Cofferdam.

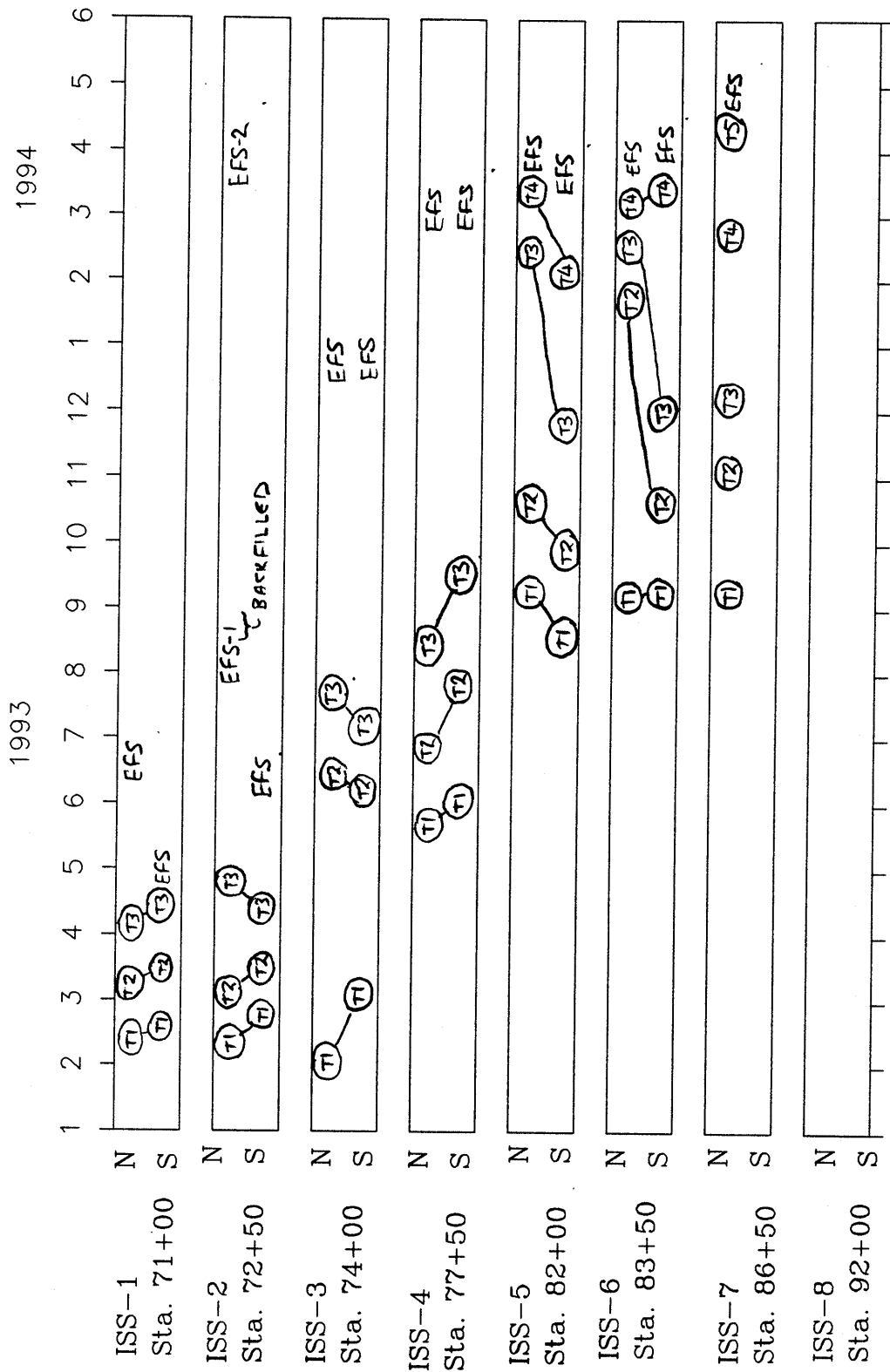
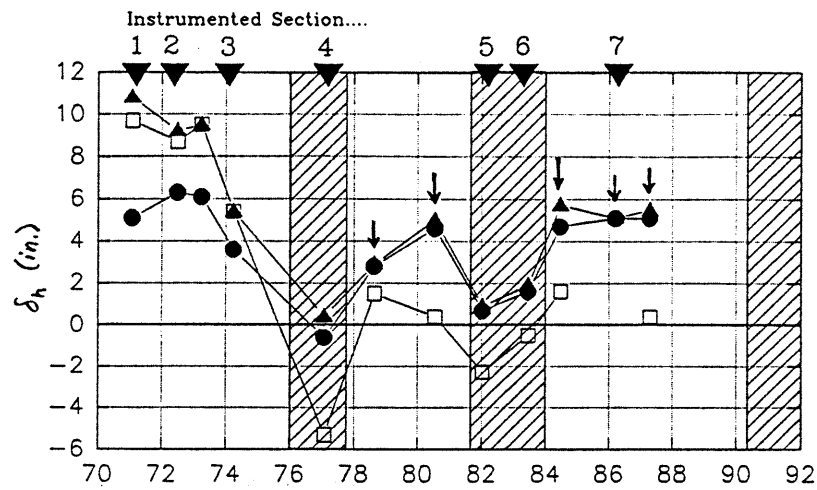
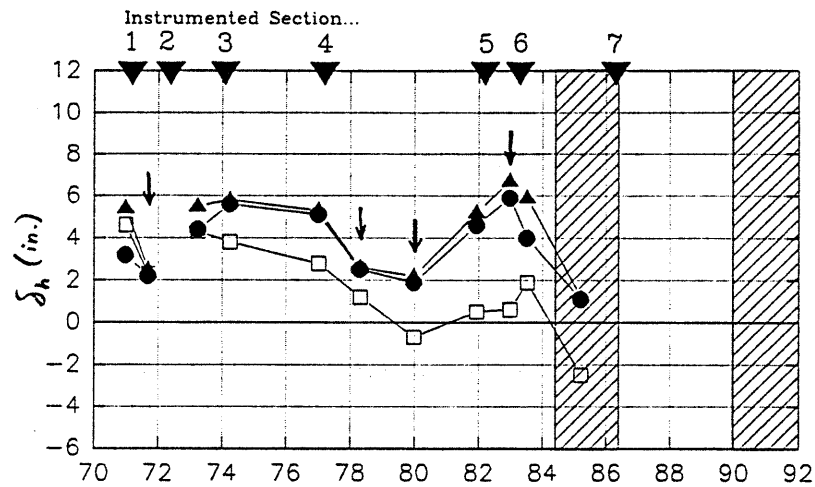


Figure 4.4. Summary of Construction History at Instrumented Sections ISS-1 to ISS-8.



WALL DEFLECTIONS -- NORTH SIDE



WALL DEFLECTIONS -- SOUTH SIDE

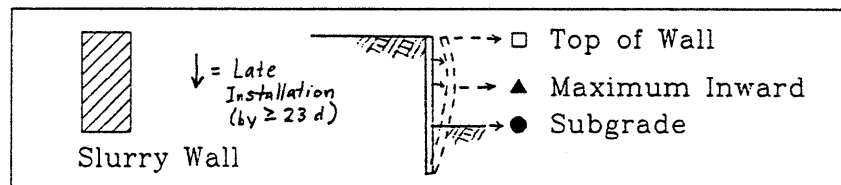
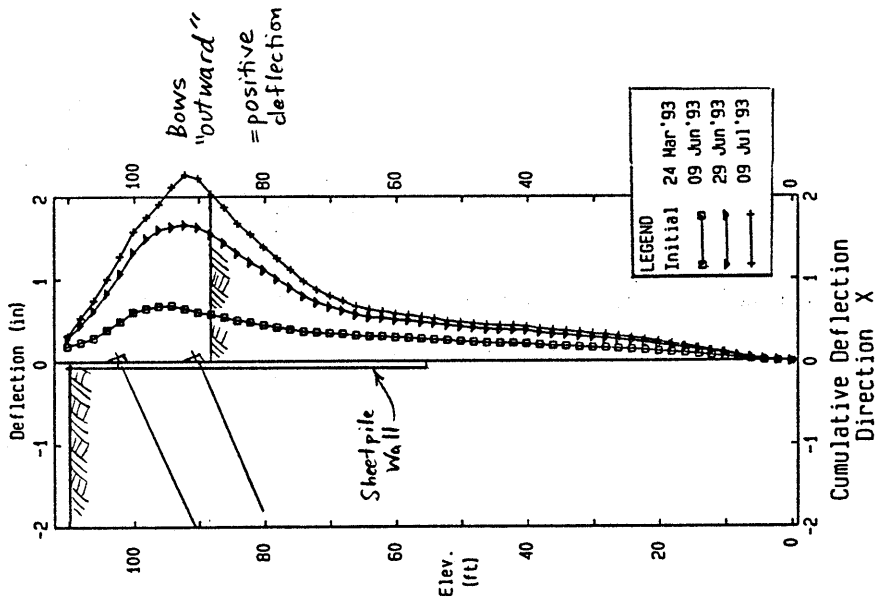
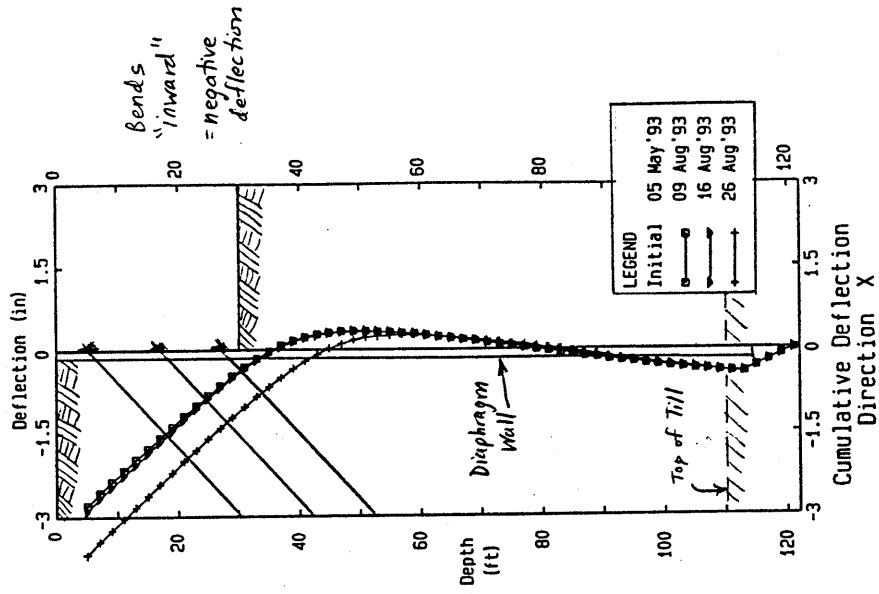


Figure 4.5. Lateral Wall Deflections at Three Elevations Plotted Against Station Number. Deflections are Those Measured on the Date of Excavation to Final Subgrade.



INC-101



INC-102

Figure 4.6. An Illustration of the Typical Deformations of Two Different Wall Types. (a) Sheetpile Wall. (b) Diaphragm (Slurry) Wall.

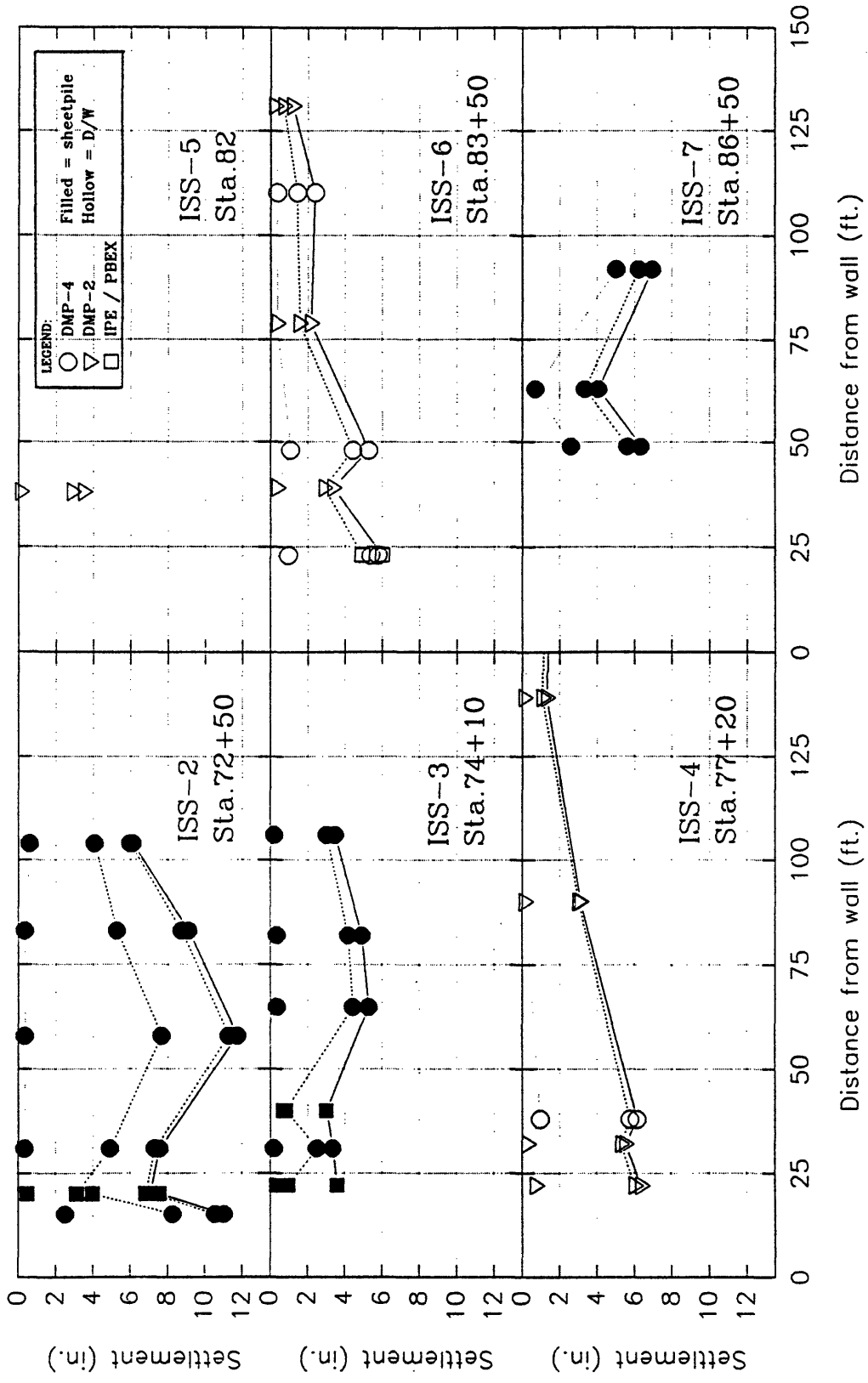


Figure 4.7 (a). Settlement Troughs Measured Behind the North Wall at Various Instrumented Sections. (Settlements are shown for different times in the construction history of each section: 1. Excavation of Final Subgrade; and 3. Invert Mat Pour.)

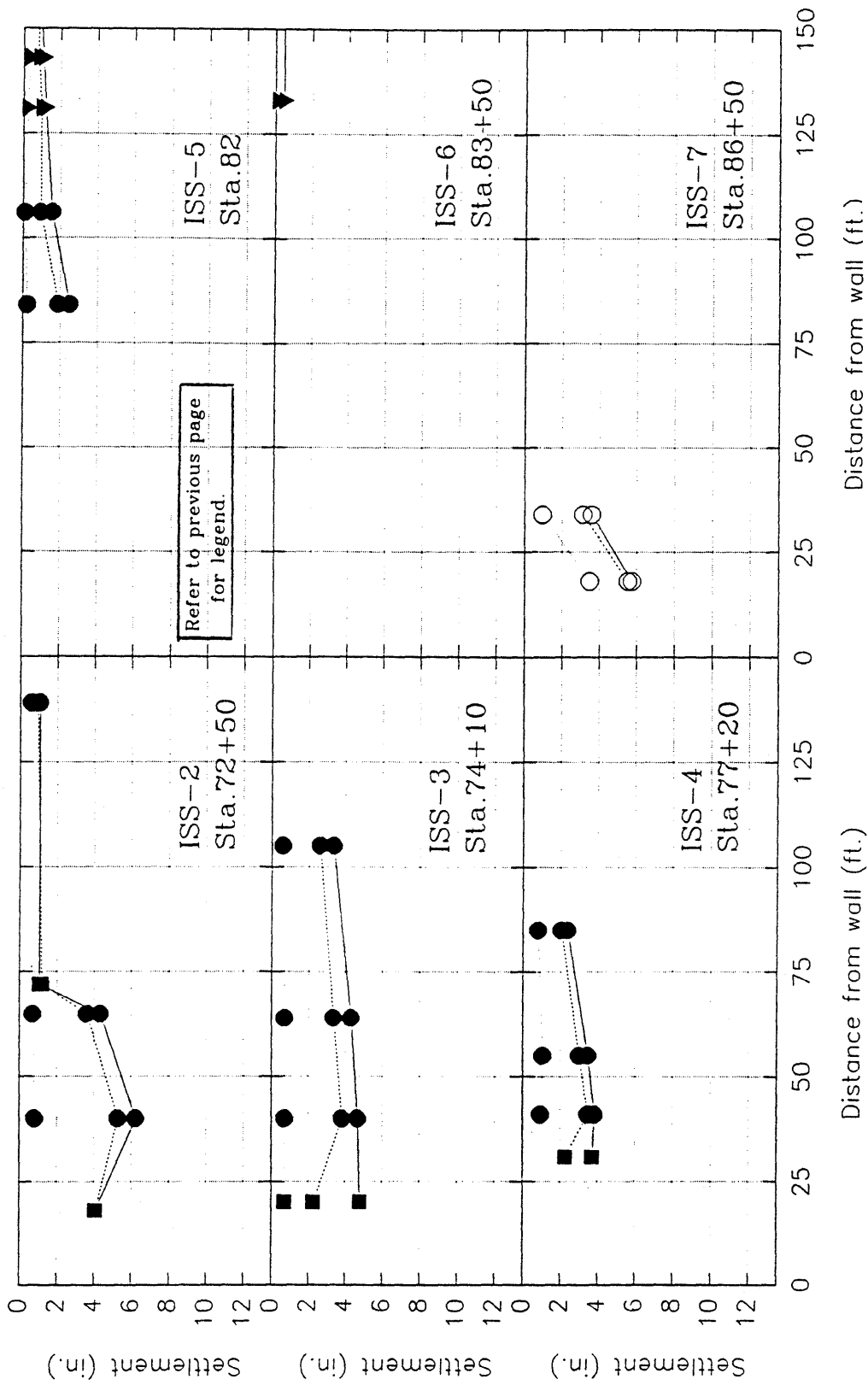


Figure 4.7 (b). Settlement Troughs Measured Behind the South Wall at Various Instrumented Sections. (Settlements are shown for different times in the construction history of each section: 1. Excavation of Lift 1; 2. Excavation of Final Subgrade; and 3. Invert Mat Pour.)

CHAPTER 5

SOIL STRATIGRAPHY AND SOIL PROPERTIES AT ISS-4

In addition to their investigation of the project area's geology and stratigraphy (discussed in Section 3.2), MHD's geotechnical consultant carried out a program of in-situ and laboratory testing on the various soil units present in the area for the purpose of defining their pertinent engineering properties, such as strength, compressibility, and permeability. The geotechnical consultant also conducted a Special Testing Program for the purpose of further evaluating the engineering properties of Boston Blue Clay in the vicinity. The Special Test Program used a combination of special laboratory shear and consolidation tests and several types of in-situ tests, as described more fully in Section 5.4.3.1.

Figure 5.1 shows the locations of exploratory borings conducted by MHD's geotechnical consultant for their investigation of soil units in the project area. They assigned each boring a number which was preceded by the prefix "B2-" to indicate the most recent series of borings. For convenience, Figure 5.1 shows only the number of each boring, without the prefix, and this text will henceforth refer to the borings by their numbers only. Figure 5.1 also indicates the location of the Special Testing Program.

This chapter reviews the findings of the investigations by MHD's geotechnical consultant for the overall project area. The presentation also includes results from further analyses by MIT on the stress history, compressibility, flow, and undrained strength properties of the cohesive soil units at the location of ISS-4.

5.1. SOIL STRATIGRAPHY

The selected soil profile at ISS-4 was developed using two sources of data: selected borings from subsurface investigations, and instrument installation logs for nearby inclinometers and deep piezometers. The locations of borings and instrumentation near the ISS-4 cross-section which were used in developing the soil profile are shown in Figures 5.1 and 6.2, respectively. The installation logs were made by the instrumentation

subconsultant to the project contractor. The stratigraphic information from these two sources is summarized in Figure 5.2-a and 5.2-c. A simplified, averaged soil profile was produced from these data, and is shown in Figure 5.2-b. In selecting appropriate thicknesses for the strata, elevations of soil unit interfaces from nearby borings were averaged. Due to their greater variability and less precise nature, information from the installation logs was used only to make a qualitative check of the selected average profile.

The soil profile consists primarily of a sequence of three cohesive soil layers underlying 8.5 ft of granular fill: 15 ft of cohesive fill, 15 ft of an organic deposit, and 64.5 ft of Boston Blue Clay. The cohesive soils are underlain by glacial deposits and bedrock.

5.2. GROUNDWATER REGIME

The average groundwater levels from eight observation wells installed in the upper aquifer by MHD's geotechnical consultant are graphed against station number in Figure 5.3; they are the upper of the two curves. The observed water levels indicated water table elevations of approximately 102 to 108 feet, generally decreasing eastward toward the harbor (MHD Geotechnical Consultant, 1991b). The sea level of Boston Harbor typically ranges between Elevations 95.5 and 104.8 ft (project datum), but the tidal fluctuations seen in the harbor were seen only in the easternmost of the observation wells, while little or no tidal influence was seen elsewhere. Some of the water table variations between different wells were attributed to the heterogeneous nature of the fill deposits and to the presence of either impervious pavement or open ground surface at different locations.

Pore pressures measured in the lower aquifer by vibrating wire piezometers indicated piezometric elevations between approximately 96 and 100 ft, i.e., five or more feet lower than the levels in the upper aquifer. These water levels are shown as the lower set of points in Figure 5.3.

Groundwater and piezometric levels were also measured at the Special Testing Program Site. Here, one observation well and one vibrating wire piezometer was placed in the upper and lower aquifers, respectively, while three piezometers were placed at different depths within the Boston Blue Clay. The average measurements from the instruments in the upper and lower aquifers are shown in Figure 5.3, along with the

instrument data from the project alignment. The groundwater level measured by the Special Testing Program observation well was somewhat lower than levels measured in the project alignment's observation wells. The piezometers in the clay indicated small excess pore pressures which had not yet dissipated following the placement of overburden fill materials (MHD Geotechnical Consultant, 1993).

Based on the piezometric data shown in Figure 5.3, best estimates for initial water pressures at ISS-4 (Stations 76+50 to 78+00) are as follows:

Piezometric Elevation=106 ft in the upper aquifer.

Piezometric Elevation=100 ft in the lower aquifer.

5.3. OVERBURDEN STRESSES

In-situ vertical total stresses (σ_{vo}), pore water pressures (u_o), and effective vertical stresses (σ'_{vo}) were calculated for the selected ISS-4 profile, using the equation

$$\sigma_{vo}' = \sigma_{vo} - u_o \quad (5-1)$$

The average ISS-4 soil profile appears in Figure 5.2-b and the selected total unit weights appear in Figure 5.4.

The selected initial piezometric water elevations (PWE's) for the upper and lower aquifers are given in Section 5.2. The upper aquifer PWE of 106 ft was used to calculate pore pressures in the miscellaneous and cohesive fills and the organic deposit. The lower aquifer PWE of 100 ft was used to calculate u_o in the glaciomarine deposit and glacial till underlying the Boston Blue Clay. Pore pressures within the clay were assumed to vary linearly from the top to the bottom of the deposit. The unit weight of water was assumed to equal 63 pcf because of the presence of salt.

The following table summarizes the selected unit weights of the six soil units, and the calculated values of σ_{vo} , u_o , and σ'_{vo} at the interfaces between the deposits. The stresses are also shown graphically in Figure 5.4.

Soil Unit	γ_t (pcf)	Stresses at base of deposit (psf)		
		σ_{vo}	u_o	σ'_{vo}
Misc. Fill (above WT)	110	440	0	440
Misc. Fill (below WT)	120	980	284	697
Cohesive Fill	110	2630	1229	1402
Organics	108	4250	2174	2077
Boston Blue Clay	116	11732	5859	5873
Glaciomarine	135	12677	6300	6377
Glacial Till	145	13982	6867	7115

Based on the values of effective stress at the top and bottom of the clay, and the clay's 64.5-ft thickness, the following equation gives σ'_{vo} in the clay as a function of elevation:

$$\sigma'_{vo} \text{ (psf)} = 6285 - 58.85 \text{ (Elev.)} \quad (5-2)$$

5.4. INDEX AND ENGINEERING PROPERTIES OF MAIN DEPOSITS

The following discussion provides a detailed review of laboratory and in-situ testing conducted by MHD's geotechnical consultant for their geotechnical study of the project area. Their recommendations provided a proper perspective on the overall variability in properties along the alignment. For this discussion, only those soil strata that are present at ISS-4 will be emphasized. These testing results and recommendations, as well as values selected by MIT for its site-specific analysis of the ISS-4 cross-section, are summarized in Tables 5.1 through 5.7.

5.4.1. Recent Fill Deposits

MHD's geotechnical consultant (1991) distinguished three different fill sub-units along the project alignment. The first is Granular Fill, and is primarily composed of a brown coarse to fine sand. The second, Miscellaneous Fill, is a mixture of brown sand and grey-black silt containing a variety of construction debris like cinders, wood blocks, and

bricks. Both sub-units were considered to be non-cohesive. The third fill sub-unit is Cohesive Fill, a mixture of clay and organic silt which was dredged from Boston Harbor.

5.4.1.1. Granular and Miscellaneous Fills

Granular Fill is infrequent at the ISS-4 section, but is predominant east of Sta. 87 and intermittently over the rest of the project area. As Figure 3.5 shows, the Miscellaneous Fill is present only sporadically throughout the area. MHD's geotechnical consultant did not go into much detail in their discussions of the Miscellaneous Fill. They compared the Granular and Miscellaneous Fills west of Sta. 87 to the thicker, predominantly Granular Fill deposits east of Sta. 87, stating that the former deposits are "generally denser, consistent with [their] placement above sea level, proximity to vehicular traffic, and the presence of oversized and miscellaneous materials" (p.34, MHD Geotechnical Consultant, 1991b).

Table 5.1 lists the engineering properties of the Miscellaneous Fill according to the study. In-situ permeability tests led MHD's geotechnical consultant to conclude that the permeability of this deposit was "highly variable, and dependent on local conditions and gradation" (p.35, MHD Geotechnical Consultant, 1991b).

Additional in-situ pump testing was conducted in October, 1991, after the initial geotechnical exploration phase. Pumping Test Number 3 consisted of the installation of a pumping well screened both in the upper fill and in the underlying bedrock (MHD Geotechnical Consultant, 1992). The well was placed in the vicinity of Sta. 90, and several observation wells and piezometers were installed around it for measurement of water levels and pressures during pumping and subsequent recovery. This well was located in an area where the Granular Fill, rather than the Miscellaneous Fill, was predominant, but the resulting permeability is listed in Table 5.1 for the purposes of comparison.

5.4.1.2. Cohesive Fill

Due to its predominance throughout the project alignment, and to the fact that it is locally very soft, the Cohesive Fill was an important deposit from a geotechnical point of view. Therefore, MHD's geotechnical consultant presented a detailed discussion of this soil layer. MIT carefully evaluated their laboratory and field data, with emphasis placed on

test results from undisturbed samples taken in the vicinity of ISS-4. The available data are presented graphically in Sheets B1, B2, and B3 in Appendix B, and are summarized along with selected engineering properties of the Cohesive Fill in Table 5.2.

Unit weights, water contents, and Atterberg Limits were obtained from laboratory tests conducted on undisturbed samples taken from nine different boreholes. Atterberg Limits and water contents are presented graphically in Sheet B1. Table 5.2 lists average values from all samples, as well as averages from only those samples collected at Borings 49, 60, and 61, which are in the vicinity of ISS-4. (Boring locations are shown in Figure 5.1.) Based on the data from these borings, a liquid limit (w_L) of 50% and a plasticity index (I_p) of 26.5% were selected as being most representative of cohesive fill at ISS-4, which places the soil on the boundary between CL and CH clays on the standard Plasticity Chart.

According to MHD's geotechnical consultant, five of the eight CIUC tests performed on Cohesive Fill used consolidation pressures that were 1.3 to 1.8 times higher than the actual effective overburden stress, and consequently resulted in overly high strengths. The higher pressures were used because, at the time of testing, the water table in the fill was assumed to be at El. 100 ft, while in fact it was 4 to 8 feet higher as revealed by observation well data collected later. Sheet B1 summarizes additional strength data from UU, torvane, and miniature lab vane testing; these data were used by MIT to select the "best-estimate" undrained strengths given in Table 5.2.

Sheet B2 summarizes preconsolidation pressures interpreted by MIT from oedometer tests conducted by MHD's geotechnical consultant for borings 40, 41, 60, and 61. Samples from borings 60 and 61 yielded substantially lower values of σ_p' than did borings 40 and 41; the higher preconsolidation pressure at 40 may be due to the past existence of salt stockpiles at that location (Figure 5.1). Overall, the deposit appears to be overconsolidated, and a constant OCR of 1.7 was selected by MIT for the Cohesive Fill, based on the samples from 60 and 61.

Table 5.2 lists values of c_v (the coefficient of consolidation) estimated for different loading stages in the oedometer tests. Further analysis by MIT of the lab tests and variable-head field pumping tests resulted in two different estimates of c_v for

overconsolidated Cohesive Fill: 1.0 and 15.0 ft²/day. Due to uncertainty in the estimate, it is recommended that both values be used in analysis.

Sheet B3 illustrates SPT-N values measured during drilling of several borings throughout the project alignment. The somewhat higher N-values near the top of the Cohesive Fill suggest the existence of a stronger crust. Among those borings near ISS-4, the fill near the north side of the excavation (represented by borings 49, 52, 60, and 62) appears to be weaker between depths of 11 and 16 ft than does the fill in the “middle” and south areas of ISS-4.

5.4.2. Organic Deposits

The Organic stratum represents materials that were naturally deposited in the tidal marsh environment which existed before filling activities began. The organic deposits exist primarily west of Sta. 87 (as Figure 3.5 indicates). The deposit actually contains two sub-units: a cohesive grey to black Organic Silt, which is by far the predominant component, and a thin, intermittent layer of peat. For simplicity, the thin peat layer and the overlying organic silt were considered to be a single organic layer in the selected ISS-4 soil profile.

Results of laboratory tests on the organic soils are summarized in Table 5.3. Sheet B4 in Appendix B plots water contents and Atterberg Limits measured for samples from ten different borings, most in the vicinity of ISS-4 (i.e., borings 49, 55, 59, 60, 61, and 62, as shown in Figure 5.1). Although this deposit is termed an organic soil, the Atterberg limits actually lie to either side of the A-line on the Plasticity Chart (Sheet B5), making it more properly classified a CH-OH material.

MIT evaluated the stress history and undrained strength of the Organic deposits using data from laboratory tests performed by MHD’s geotechnical consultant. Maximum past pressures (σ'_p) were determined mainly by the Casagrande technique. Section 5.4.3.4 provides more discussion of this method of analysis, which was also performed for the Boston Blue Clay. Sheet B6 plots σ'_p data from three tests at ISS-4 (Borings 60 and 61), one of which was highly disturbed, and one test each to the west (Boring 48) and east (Boring 68) of ISS-4. These data indicated that the organic deposit was slightly overconsolidated, with an average value of 3.5 ksf determined for σ'_p . Since

precompression of tidal mud flat deposits probably occurs due to desiccation during deposition, the assumption of a constant σ'_p is not unreasonable.

The SHANSEP equation was used to compute undrained shear strengths for the deposit, assuming normalized parameters of $S=0.25$ and $m=0.8$ (which apply to the DSS mode of shear). Refer to Section 5.4.3.7 for a more thorough discussion of this method. The resulting calculated strengths plot slightly below, but in fairly good agreement with, the trend of UU results measured by MHD's geotechnical consultant (Sheet B4).

MHD's geotechnical consultant did not perform any in-situ pumping tests in the organic deposits, so the permeability estimates came from laboratory consolidation tests, using the methodology described in Ladd et al. (1994).

5.4.3. Boston Blue Clay

5.4.3.1. General

The Boston Blue Clay is a deposit of great geotechnical importance throughout most of the Boston area owing to its wide areal distribution, its thickness, and its low overconsolidation ratio at depth. On this project, it is the most predominant of three separate marine deposits, which together represent a period of time near the end of Pleistocene glaciation, about 12,000 to 14,000 years ago, when continental glaciers were retreating from the Boston region and sea levels were rising (Kaye, 1982). In addition to the Marine Clay (BBC), the marine deposit sequence includes discontinuous, thin layers of sand and silt. At ISS-4, the clay is the only substantial sub-unit of the three.

Because of its importance to geotechnical design issues, MHD's geotechnical consultant devoted a large portion of their investigation to the Marine Clay deposit. Consolidation properties and stress history profiles of the deposit were investigated with numerous conventional, incremental-load oedometer tests and some Constant Rate of Strain (CRS) tests. Undrained strengths were tested by UU and CIUC tests. Additional in-situ tests, including piezocone and Menard pressuremeter tests, were also conducted.

In conjunction with the project's Geotechnical Investigation, MIT and others collaborated on a Special Testing Program in Boston (MHD Geotechnical Consultant, 1993). The goal of the Special Testing Program was to evaluate the strength,

compressibility, and flow properties of Boston Blue Clay deposits in the vicinity of the Boston excavations, as well as to appraise the usefulness of advanced in-situ and laboratory testing techniques for defining these properties. A variety of in-situ testing devices were utilized, including the self-boring pressuremeter, the field vane, the piezocone, the dilatometer, and the earth pressure cell. Undisturbed samples were obtained using fixed-piston and block sampling techniques, and a comprehensive laboratory program was performed using specialized testing techniques such as the lateral stress oedometer, constant rate-of-strain consolidation, and computer-automated K_o -consolidated undrained triaxial compression and extension tests. Samples were taken from a selected "Special Test Site", located about 500 ft from the western end of the project alignment. The location of the Special Test Site is shown in Figure 5.1. Results from the Special Testing Program are included with results from the project geotechnical investigations in Table 5.4.

Results from laboratory and in-situ tests are summarized in Table 5.4, except for stress history and undrained strength profiles developed by MHD's geotechnical consultant, which are shown in Figure 5.6.

5.4.3.2. Index Properties

Total unit weights, water contents, and Atterberg limits for Boston Blue Clay in the vicinity of ISS-4 are plotted in Figure 5.5. The data were gathered from 23 selected borings which were in the immediate vicinity of ISS-4 and within about 500 ft along the alignment in both directions. This figure therefore provides a summary of how the unit weight and index properties vary with elevation at and around ISS-4 (Also see Sheets B7 and B8). The natural water content (ω_N) range equaled $40 \pm 4\%$. The range for liquid limit (ω_l) equalled $51 \pm 5\%$; the range for plasticity index (I_p) was $28.5 \pm 4.5\%$.

Sheet B9 shows the values of ω_l plotted against corresponding values of I_p , based on the data provided in Figure 5.5 and Sheet B7. It can be seen that the data range plots just above the A-line, as is typical for marine illitic clays.

5.4.3.3. Stress History and Undrained Strength Profiles

Stress history and undrained strength profiles were developed by MHD's geotechnical consultant for five zones along the project alignment as well as for the Special Test Site. Undrained strengths were measured in the laboratory with UU and CIUC tests and also calculated via the SHANSEP technique. The resulting overconsolidation ratio (OCR) and strength profiles are shown in Figure 5.6. The plotted strengths are from SHANSEP calculations, using the measured OCR's and normalized strength parameters of $S=0.20$ and $m=0.75$ (values from MIT CK₀U-DSS tests on resedimented BBC). The solid lines labeled "1" through "4" represent OCR and strength profiles from different zones along the alignment, each with distinct stress history and strength characteristics. The labeling of the lines on Figure 5.6 corresponds to the labeled groups of borings in Figure 5.1.

For the most part, the profiles are fairly typical for BBC in the Boston area: a stiff overconsolidated crust overlies a softer, nearly normally consolidated clay at depth. In general, undrained strengths decreased with depth in the crust, while increasing with depth in the near-normally consolidated deeper region. However, substantial variations in stress history and strength were found along the alignment, a phenomenon "not known to have been observed previously in the Boston area" (p.54, MHD Geotechnical Consultant, 1991b). For example, the strength profile for area 3 is unique due to its lack of a stronger crust in the upper part of the deposit. Profile number 1, from the region west of Sta. 74, is also unique in that it features an unusually low OCR profile and is therefore substantially weaker throughout much of its thickness than the other areas. However, undrained strengths for Boring 40 (at Sta. 71) were anomalously high. Clearly, clay strengths undergo great variations over relatively small distances, particularly within the western half of the project area.

The "low" strengths seen at most locations in the western part of the area remain unexplained. However, the anomalously high strengths seen at Boring 40 can be attributed to consolidation under the weight of 30- to 40-foot-high salt stockpiles which existed in the area until the early 1980's. The approximate location of the stockpiles is shown on Figure 5.1 and appears to overlie Boring 40. Also, for a few years in the mid-80's,

stockpiles of fill materials excavated from South Station were placed in the area indicated on the figure. The fill in these piles was 'spread out' in 1987, forming a higher ground elevation immediately southwest of the excavation. Although there is very little information available on these stockpiles, they may well have influenced local clay strengths.

Figure 5.6 includes, in dashed lines, OCR and undrained strength profiles at the Special Test Site. The dashed line marked "SHANSEP DSS" was calculated using the SHANSEP equation, normalized strength parameters as shown in Table 5.4, and the measured stress history profile. The hatched zone labeled "STP Compression Tests" covers the range of strengths measured by Recompression- and SHANSEP- type triaxial compression tests in the Special Test Program.

The STP DSS profile agrees most closely with that from zone number 4, representing the eastern part of the alignment where strengths were relatively high. The Special Test Site stress history profile was obtained from preconsolidation pressure measurements in "excellent" and "very good"-quality laboratory consolidation tests (mostly CRS and K_o -triaxial). Compression curves from clay below El 40 were often S-shaped, showing that the deeper clays are structured.

Results from the Special Test Program (MHD Geotechnical Consultant, 1993) produced three conclusions that, in hindsight, could have affected the evaluation of preconsolidation pressures obtained from incremental oedometer tests.

1. *Sample extrusion:* The STP showed that samples extruded from tubes in the conventional manner can cause excessive disturbance, and hence lower values of σ_p' than samples that were pre-cut around the perimeter of the tube before extrusion.

2. *Samples in the crust with very rounded compression curves:* The STP showed that the strain energy technique (Becker et al., 1987) usually produced more reliable estimates of σ_p' than the conventional Casagrande technique (see Section 5.4.3.4).

3. *Samples with S-shaped compression curves:* The STP showed that continuous loading (as done with CRS and K_o -triaxial consolidation) is needed to obtain compression curves having well-defined values of σ_p' for the more structured clay.

5.4.3.4. Stress History Developed by MIT

Preconsolidation pressure data estimated by MHD's geotechnical consultant from laboratory consolidation testing had a great deal of scatter. In the crust, one of the major reasons for the scatter was the fact that the compression curves were frequently very rounded. MIT decided to re-evaluate the test data using two σ_p' estimation techniques. The first technique, the Casagrande (1936) construction, is the most commonly used method in geotechnical practice. It was used by MHD's geotechnical consultant for their estimates of σ_p' and also by MIT for comparison estimates. The second method used by MIT was the Strain Energy technique, developed by Becker et al. (1987) and considered by MIT to be generally more reliable.

Sheet B10 in Appendix B shows a plot of σ_p' vs. elevation estimated by the Casagrande method for BBC in zones 1, 2, and 3 in the vicinity of ISS-4. The plot includes values selected by MHD's geotechnical consultant (solid symbols) and independently by MIT (hollow symbols); the two sets of results commonly show substantial differences. The values determined by both parties show considerable scatter, making selection of a "best-fit" σ_p' profile difficult.

Sheets B11 through B16 in Appendix B show examples of MIT's Strain Energy constructions compared to Casagrande constructions, for two tests having very rounded compression curves. Strain Energy analyses were made for 17 oedometer tests run using standard loading plotted at EOP (as shown in Sheets B11 and B14). The Strain Energy estimates were done using tabulated void ratio data and computer-generated plots of SE vs. σ_{vo}' , with linear regression used to define slopes for initial reloading and virgin compression (based on the maximum value of CR). Values of σ_p' were calculated from the intersection of the two linear regression lines.

The results of the Strain Energy analyses are plotted against the Casagrande results in Sheet B17. These data are from Borings 40, 48, 49, and 61, which are near ISS-4 (Figure 5.1). On average, the Strain Energy-based σ_p' values exceeded the MIT-selected Casagrande values by about 10% and the MHD geotechnical consultant values by even more.

The selected σ_p' profile from MIT's re-evaluation is shown in Figure 5.7. This profile is based on consolidation test data from the three borings (49, 60, and 61; see Figure 5.1) closest to ISS-4 and agrees very well with seven of the nine estimated values of preconsolidation pressure. It is interesting to note that the two outliers are from boring 49, which MHD's geotechnical consultant (1991a) included with zone 2, whereas borings 60 and 61 are part of zone 3 (see Figure 5.1). However, the OCR profile for zone 3 corresponds to a linear increase in σ_p' with depth, whereas MIT's profile based on Strain Energy analyses produces a decreasing σ_p' within the upper crust of the deposit.

Figure 5.7 also shows the preconsolidation pressure profile obtained from very extensive consolidation tests for the Special Testing Program (MHD Geotechnical Consultant, 1993). The difference again highlights the large spatial changes in stress history within the BBC.

5.4.3.5. Compressibility Parameters

Figure 5.8 shows values of CR_{max} (Virgin Compression Ratio at maximum slope) and RR (Recompression Ratio) plotted against elevation. Additional data are plotted on Sheet B7. The data in Figure 5.8 and Sheet B7 were obtained from oedometer and CRS tests conducted on samples from eight borings located between Stations 71 and 86 along the alignment. The RR values plotted in Figure 5.8 were obtained from unload-reload cycles at stress levels less than the in situ σ_p' . The selected RR value of 0.025 ± 0.010 also considers unload-reload cycles from the virgin compression line and final unloading curves. The selected values of each parameter are provided in Table 5.4, along with values from the Special Test Program.

5.4.3.6. Coefficients of Consolidation and Permeability

The vertical coefficient of consolidation (c_v) was measured using conventional oedometer tests and CRS tests (see Sheet B7), and values of c_h were estimated from in-situ piezocone and dilatometer porewater dissipation tests done for the Special Test Program (See Table 5.4). The c_h values given by the piezocone tests were appreciably higher than the laboratory results, which MHD's geotechnical consultant attributed to

“horizontal drainage effects encountered in full-scale field conditions versus tests on small-scale laboratory samples” (p.45, MHD Geotechnical Consultant, 1991b). Generally, it is difficult to directly relate in-situ measurements of c_v or c_h to laboratory measurements, due to the different flow regimes, loading systems, and stress histories. MHD’s geotechnical consultant recommended a range of c_v equal to 50 to 300 x 10⁻⁴ cm²/sec, applicable to one-dimensional analysis for BBC heave and recompression.

CRS testing done as part of the Special Test Program provided values of k_{vo} , the in-situ vertical permeability. Sheet B18 shows a plot of k_{vo} from CRS tests against elevation; this plot appears as Figure 12 in the STP Report (MHD Geotechnical Consultant, 1993). The average value of k_{vo} is approximately 12.0x10⁻⁸ cm/sec. Ladd et al. (1994) summarized k_{vo} data for BBC under the I-95 test embankment at Station 246 in Saugus, MA. The I-95 BBC appears to have a lower permeability below the crust.

5.4.3.7. Undrained Shear Strength

The stress history for the ISS-4 BBC profile was used to calculate undrained strengths via the SHANSEP procedure (Ladd and Foott, 1974). This uses the following equation:

$$s_u = S \sigma_{vo}' (\text{OCR})^m \tag{5-3}$$

where S and m are Normalized Strength Parameters which vary according to clay type and shearing mode (i.e., compression, direct simple shear, or extension). The following table summarizes the parameters which apply to BBC, as based on CK_oU testing (Ladd, 1994).

Shearing Mode	S	m
Compression	0.28	0.68
DSS	0.19	0.75
Extension	0.145	0.95
Average	0.205	0.77

The undrained strength profile shown in Figure 5.9 was computed using the average parameters. This profile is typically about 30% higher than mean strengths measured in laboratory UUC and miniature vane tests run on samples from borings near ISS-4.

5.4.3.8. Drained Shear Strength

The effective stress failure envelope was defined through a series of K_0 -consolidated tests on BBC conducted for the Special Test Program (MHD Geotechnical Consultant, 1993). Both SHANSEP and Recompression tests were performed. The drained strength envelope is defined with the following parameters for drained compression:

SHANSEP Tests		Recompression Tests	
c'/σ'_p	ϕ'	c'/σ'_p	ϕ'
0.017	28.5°	0.044	29°

5.4.3.9. Coefficient of Earth Pressure at Rest (K_0)

Laboratory and in-situ tests (pressuremeter and earth pressure cell) conducted as part of the Special Testing Program indicated decreasing values of K_0 with depth. A relationship between K_0 and OCR is provided in Table 5.4.

5.4.4. Glacial Deposits

5.4.4.1. General

Underlying the Boston Blue Clay is a sequence of soils deposited during one or possibly numerous episodes of continental glaciation, the latest of which ended about 12,000 years ago. The various deposits, which include Glaciomarine, Glaciolacustrine, Glaciofluvial, and Glacial Till (lodgement and ablation types), represent different stages of glacial advance and melting.

The Glaciolacustrine soils are the uppermost of the glacial deposits and lie to the west of Sta.76 (Figure 5.1). Between Sta. 69 and 74, these deposits occasionally reach a

thickness of nearly 30 feet. They were deposited in the relatively calm environment of glacial meltwater ponds and lakes, and are accordingly more fine-grained than the other “higher-energy” glacial deposits. The Glaciolacustrine deposit consists of fine sands, silts, and interbedded clays.

Like the Glaciolacustrine deposits, the Glaciofluvial soils are present primarily below the western end of the project alignment, west of Sta. 73. Since they were deposited in the high-energy environment of meltwater rivers and torrents, they tend to be better-sorted and coarser-grained than the finer Glaciolacustrine soils, and consist largely of coarse to fine sand, with some gravel.

The Glaciolacustrine and Glaciofluvial deposits are not present in the vicinity of ISS-4. Of the four glacially-deposited soil types, only the Glaciomarine and Glacial Till deposits exist within the ISS-4 soil profile. Detailed summaries of the engineering properties of these two deposits are provided in Tables 5.5 and 5.6, respectively. The following is a brief discussion of each.

5.4.4.2. Glaciomarine Deposits

The Glaciomarine deposits overlie the Glacial Till throughout most of the project area. They represent glacial outwash materials that were deposited in the newly formed marine environment. The Glaciomarine soil has been described as “till-like”, due to the fact that it frequently appears as an unsorted mixture of gravel, coarse sand, fine sand, silt, and clay.

Although most of the Glaciomarine deposit were characterized as cohesionless, some zones within the deposit were more cohesive in nature. These cohesive zones existed under the extreme eastern area of the alignment, but not at ISS-4. Table 5.5 therefore presents properties of the cohesionless Glaciomarine materials.

Two pressuremeter tests were successfully completed in the Glaciomarine soils. Although one in-situ pumping test was performed for the purpose of estimating permeability, it was done at Boring 89, where the deposit is cohesive. Permeability values for the cohesionless portion of the deposit were provided by correlations to grain-size distributions and are listed in the table.

5.4.4.3. Glacial Till

The movement of the continental glaciers over the landscape, and their tendency to grind and scour the existing bedrock surface, left a heterogeneous, unsorted, and relatively stiff deposit of Glacial Till over the bedrock surface. The till is essentially a mixture of all grain sizes, from gravel to clay, and tends to have angular grains due to their origin in the glacial 'grinding' action. According to MHD's geotechnical consultant, the till is generally a mixture of two distinct components: a) a fine gravel and coarse to fine sand, and b) more limited zones which consist largely of finer sand and silt. Permeabilities are expected to undergo wide local variations, in accordance with the dichotomy of grain size distributions.

5.4.5. Bedrock

The sequence of glacial soils is underlain by bedrock which is classified as part of the Cambridge Formation, a thinly bedded argillite. The bedrock was found to have a highly variable Rock Quality Designation (RQD), indicating widely varying degrees of weathering and fracturing. Table 5.7 lists the results of in-situ tests performed in the bedrock, using both Menard Pressuremeters for determining the rock's elastic modulus, and borehole pumping tests conducted with the drill casing seated at the top of the rock. Only initial moduli were determined from the pressuremeter tests because the rock stiffness exceeded the sensitivity of the measuring device. There appears to be a direct, though non-linear, correlation between initial elastic modulus and RQD.

The in-situ permeability measurements are supplemented by a permeability estimate provided by Pumping Test # 3 (MHD Geotechnical Consultant, 1992). This Pumping Test was described in Section 5.4.1.1 (on the Granular and Miscellaneous Fills).

Table 5.1. Engineering Properties of Miscellaneous Fill

Property	Value(s) or Range	Location / Condition ¹	Source ²	Comments
γ_t	110 pcf 120 pcf	Above Water Table Saturated	MIT assumption	
ϕ	32°		Correlations to grain size and SPT-N values	
K_u	0.31		Correlations to grain size and SPT-N values	
K_p	3.3		Standard Rankine & Jaky equations, using ϕ	
K_o	0.50		"	
Permeability (k)	10^{-5} to 10^{-2} cm/s 10^{-3} to 10^{-2} cm/s 5×10^{-2} cm/s	Between Sta. 87 & 95 " Near Sta. 90	10 in-situ pumping tests Correlations to grain size Pumping Test # 3	see description in text

NOTES:

1. Values representative of entire project area unless specified otherwise
2. All data and analyses by MHD Geotechnical Consultant (MHD Geo. Cslt.) unless specified otherwise

Table 5.2. Engineering Properties of Cohesive Fill (Page 1 of 2: continued on next page)

Property	Value(s)/Range ^{1,4}	Location / Condition ²	Source ³	Comments
γ_t	110 pcf		MHD Geo. Cslt. recommendation, based on average from lab tests	Use this value for ISS-4 analyses
ω_N (%)	110.3 ± 7.9 pcf	ISS-4 area	Lab tests from Borings 49, 60, 61	
Atterberg Limits:	38 ± 10	ISS-4 area	9 undisturbed samples	See Sheet B1
	44 ± 11		Lab tests from Borings 49, 60, 61, 68	
ω_1 (%)	48 ± 8.5	ISS-4 area	10 undisturbed samples	
	52.5 ± 7.5			
I_p (%)	50		3 lab tests from Borings 49, 60, 61	
	25.5 ± 5.5		MIT selected value	
ω_p (%)	27.5 ± 5	ISS-4 area	10 undisturbed samples	
	26.5			
	23.5		3 lab tests from Borings 49, 60, 61	
Cu (undrained strength)	640 to 2040 psf		MIT selected value	Soil Classification: CL-CH
	520 to 860 psf		Based on selected values of ω_1 and I_p	
	200 to 1000 psf		8 CIUC tests	
	= 0.2 σ_v'		4 UU tests	
ϕ'			MHD Geo. Cslt. Recommended Range	5 tests may have over-estimated strength (see text)
			MHD Geo. Cslt. "Lower Bound" Recommendation	
c'		DSS Shearing	Based on MIT re-evaluation of test data from MHD Geo. Cslt.	In Table VIII, MHD Geo. Cslt. (1991b)
		Compression		
Normalized SHANSEP Parameters			CIUC tests	Approx. "lower bound" to UU, σ_v' and lab vane data (See Sheet B1)
			"	
	Select parameters from resedimented BBC		MIT estimate	

Table 5.2, continued (page 2 of 2)

OCR	1.3 to 5.1 1.7		4 oedometer tests by MHD Geo. Cslt. MIT analysis of MHD Geo. Cslt. oedometer data from borings 60 and 61	Believed to be over-estimated Use for ISS-4 analyses. See Sheet B2.
CR	0.17 ± 0.07 0.17		Oedometer data, borings 40, 41, 60, 61 Mid-range value	See Sheet B2.
RR	0.025		Oedometer data, borings 40, 41, 60, 61	See Sheet B2.
e_o	1.22		Given $\omega_N = 44\%$	
C_c	0.38		Given CR=0.17	
C_r	0.055		Given RR=0.025	
c_v	$30 \times 10^{-4} \text{ cm}^2/\text{s}$ $10 \times 10^{-4} \text{ cm}^2/\text{s}$ $20 \times 10^{-4} \text{ cm}^2/\text{s}$	Unload to 1/2 σ_v' Unload to 1/8 σ_v' Reload	4 oedometer tests by MHD Geo. Cslt.	Estimated by MHD Geo. Cslt.
	$10.5 \pm 5.8 \times 10^{-4} \text{ cm}^2/\text{s}$	Normally Consol.	"	"
	1.0 ft ² /day	Overconsolidated	Assumes $c_v(\text{OC}) = 10c_v(\text{NC})$ [MIT assumption]	From MIT re-evaluation. See Sheet B2.
	15 ft ² /day	Overconsolidated	Field pumping tests by MHD Geo. Cslt.	Due to uncertainty, try analyses with both values.
Permeability : k_{vo} (cm/s)	approx. 10^{-8} cm/s		MHD Geo. Cslt. estimate from 4 oedometer tests	
	5×10^{-6} to 4×10^{-4}	Range	Six in-situ rising head pumping tests	Representative of k_h ?
	10^{-6} to 10^{-4} cm/s	MHD Geo. Cslt. Recommended Range		Actual permeability expected to be "highly variable".
	.01 - .0007 ft/day (= 25 - 350×10^{-9} cm/sec)	MIT Recommended Range	Both oedometer and in-situ tests	Use for ISS-4
C_k	0.38		Assumed to equal C_c	

- NOTES:**
1. Averages are given with Standard Deviations (based on population)
 2. Values representative of entire project area unless specified otherwise
 3. All data and analyses by MHD Geotechnical Consultant (MHD Geo. Cslt.) unless specified otherwise
 4. Values given in bold and shaded are recommended values for ISS-4 analyses

Table 5.3. Engineering Properties of Organic Deposits (Page 1 of 2: continued on next page)

Property	Value(s)/Range ^{1,4}	Location / Condition ²	Source ³	Comments
γ_t	110 pcf 108.2 ± 6.8 pcf 117.9 ± 2.5	Overall, ISS-4 area Peat, ISS-4 area	Based on average from 17 lab tests (Table VIII, MHD Geo. Cslt., 1991b) 8 lab tests 2 lab tests	Text cites average of 106 pcf rather than 110 pcf. <i>Higher than average</i>
ω_N (%)	108 pcf 55.0 ± 9.0		10 borings	Use for ISS-4 analyses See Sheet B4 for data
Atterberg Limits:				
ω_1 (%)	71.0 ± 12.5		10 borings	See Sheet B4 for data
I_p (%)	38.5 ± 7.0		10 borings	Material classification: CH-OH (See Sheet B5)
ω_p (%)	32.2 ± 6.2		Based on calculated values of ω_1 and I_p	See Sheet B4 for data
Cu (undrained strength)	700 to 1500 psf		MHD Geo. Cslt. Recommended Range	In Table VIII, MHD Geo. Cslt. (1991b)
	730 psf 790 psf	ISS-4: Top of deposit ISS-4: Base of deposit	MIT SHANSEP analysis using $S=0.25$ and $m=0.8$ (DSS mode of shearing)	Assuming $\sigma'_p = 3.5$ ksf; agrees fairly well with UU data (See Sheet B4)
ϕ' c'	$41 \pm 3^\circ$ approx. 0		CIUC tests by MHD Geo. Cslt. “	
Normalized SHANSEP Parameters	$S=0.32; m=0.8$ $S=0.20; m=0.8$ $S=0.25; m=0.8$	Compression Extension DSS	MIT estimate “ “	MIT tests on organic deposits along New England coastline
OCR	1.1 to 2.7		MHD Geo. Cslt. estimate, from 5 oedometer tests	Slightly overconsolidated
σ'_p	3.45 ± 0.4 ksf 3.5 ksf	Constant throughout deposit	MIT re-evaluation of MHD Geo. Cslt. oedometer tests, using Casagrande method MIT estimate	See Sheet B6 Indicates OCR=1.7 to 2.3 given σ'_{vc} of 1.5 to 2 ksf

Table 5.3, continued (page 2 of 2)

CR	0.24 ± .09		Based on borings 48, 60, 61, and 68 'Mid-range' value	See Sheet B6 Use for ISS-4 analyses
RR = SR	0.24 0.02		"	See Sheet B6.
e_o	1.46		Given $\omega_N = 55\%$	
C_c	0.59		Given CR=0.24	
$C_r = C_s$	0.049		Given RR=SR=0.02	
c_v	35×10^{-4} cm ² /s 10×10^{-4} cm ² /s 25×10^{-4} cm ² /s 5×10^{-4} cm ² /s	Unload to 1/2 σ_v' Unload to 1/8 σ_v' Reload Virgin Compression	MHD Geo. Cslt. estimate from 5 oedometer tests " "	
	6.2×10^{-4} cm ² /s = .058 ft ² /d	Normally Cons.	5 oedometer tests	See Sheet B6
	62×10^{-4} cm ² /s = .58 ft ² /d	Overconsolidated	5 oedometer tests	Assuming $c_r(OC) = 10c_r(NC)$
C_α (Coeff. of secondary compression) (% ϵ / log t)	slightly over 1% 0.2%	Normally Consolidated Recompression	MHD Geo. Cslt. estimate from 5 oedometer tests "	
Permeability : k_{vo}	approx. 10^{-8} cm/s		MHD Geo. Cslt. estimate from 5 oedometer tests	"Consistent" for all tests; expect somewhat higher k_h
	1.14×10^{-4} ft/d		MIT estimate	Computed via methodology in Ladd et al. (1994)
C_k	0.59		MIT estimate	
K_o	0.55(OCR)^{0.45}		MIT estimate	

- NOTES:**
1. Averages are given with Standard Deviations (based on population)
 2. Value representative of entire project area unless specified otherwise
 3. All data and analyses by MHD Geotechnical Consultant (MHD Geo. Cslt.) unless specified otherwise
 4. Values given in bold and shaded are recommended values for ISS-4 analyses

Table 5.4. Engineering Properties of Marine Clay (Boston Blue Clay) (Page 1 of 3; continued on next page)

Property	Value(s) / Range ¹	Location / Condition ²	Source ³	Comments
γ_t	116 ± 3 pcf		Average from all MHD Geo. Cslt. lab tests	See Figure 5.5
Normalized Strength Parameters (SHANSEP)	S=0.28 n=0.68	STP ⁴ Compression	SHANSEP CKoUC	Piezocone tip stress correlation was the only in-situ test to show good correlation with undrained strength measurements
	S=0.30 n=0.68	"	Recompression CKoUC	
	S=0.14 n=0.83	Extension	SHANSEP CKoUE	
	S=0.14 n=0.98	"	Recompression CKoUE	
	S=0.20 n=0.77	DSS, OC crust	SHANSEP DSS	
	S=0.18 n=0.66	DSS, low OCR	SHANSEP DSS	
ϕ'	33 ± 2°		CIUC tests by MHD Geo. Cslt.	
	30° to 34°	STP	CK _o U tests for STP	
c_v (cm ² /sec)	5 to 50 x 10 ⁻⁴	All load conditions	Conventional oedometer tests	
	100 x 10 ⁻⁴	Initial Unloading		MHD Geo. Cslt.: "Not significantly different than c_v from oedometer tests".
	10 to 30 x 10 ⁻⁴	Continued Unloading	2 CRS tests, Boring 60	
	20 to 30 x 10 ⁻⁴	Reloading		$c_h = 100$ to 180×10^{-4}
	5 to 60 x 10 ⁻⁴	STP ⁴	5 piezocone porewater dissipation tests	
	15 to 60x10 ⁻⁴	STP: "upper" clay, OCR=3-20	Lab tests with unload cycles above σ'_p	
	2 to 40x10 ⁻⁴	STP: "lower" clay, OCR=1-3	"	See Figure 11, STP report
c_v (NC)	50 to 300 x 10 ⁻⁴		MHD Geo. Cslt. recommended value	
	20 x 10 ⁻⁴	El. 60-70	MIT estimate from MHD Geo. Cslt. data	
	14 x 10 ⁻⁴	El. 40-60	"	See Sheet B7
	9 x 10 ⁻⁴	El. 17-40	"	
	15 x 10 ⁻⁴	below El. 17	"	
c_v (OC)	= 10 x c_v (NC)			

Table 5.4, continued (Page 2 of 3; continued on next page)

CR	0.21 to 0.33	Lower clay, western part of alignment	Oedometer tests and one CRS test by MHD Geo. Cslt.	See Sheet B7 for more detailed values
	appx. 0.15 to 0.25 0.13 to 0.76	STP ^d Crust Lower Clay	Special Testing Program Oedometer, CRS, CKoU lab tests	See Fig. 10, STP report. Deeper clays are structured, resulting in S-shaped curves leading to scatter in CR values See Sheet B7
RR (= SR)	0.17 ± 0.005 0.23 ± 0.02	Crust (> El.40) Lower Clay (< El.40)	Selected by MIT	
	0.008	Unload to 1/2 σ_v'		
	0.011	Unload to 1/8 σ_v'		
	0.004	Reload to 1/4 σ_v'		
	0.008	Reload to 1/2 σ_v'		
	0.012	Reload to σ_v'		
Coeff. second. compression / swell (C_{cs})	0.013 ± 0.002 0.026 ± 0.008	STP ^d Unload below σ_p' Unload above σ_p'	Consolidation tests by MHD Geo. Cslt.	Secant values 30-40% coefficients of variation
	0.025 ± 0.010	All clay	Selected by MIT	
	0.05% ϵ per log t	Unload / Recom. portion of test	Conventional oedometer tests	
	2 x 10 ⁻⁸ ± 50%		Conventional oedometer tests	
Permeability: k_v (cm/sec)	12.0 ± 6.5 x 10 ⁻³	STP	22 CRS tests	See Sheet B18
	=(2 to 5) x k_v		MHD Geo. Cslt. estimate	Based on presence of horizontal banding & sedimentary nature Note variability Not including value of 492x10 ⁻⁷
k_h (cm/sec)	13.1 ± 15.5 x 10 ⁻⁷	STP	11 Piezocone / Dilatometer tests	

Table 5.4, continued (Page 3 of 3)

K _o	Boring 76, El.77 STP, El.68 Boring 76, El.65 STP, El.48 STP, El.34 STP, El.0	Menard Pressuremeter EPC (Earth Pressure Cell) Menard Pressuremeter EPC EPC EPC	Disturbance to borehole?
1.36 0.97 0.65 0.87 0.83 0.48	STP	Average from controlled strain-rate, K _o - consolidated triaxial tests	Exceed values predicted by Jaky equation
0.53 ± .03 K _o (OC)/K _o (NC) = (OCR) ⁿ n = 0.390 ± .045	Normally cons. Overconsolidated	"	

NOTES:

1. Averages are given with Standard Deviations (based on population)
2. Values are representative of entire project area unless specified otherwise
3. All data and analyses by MHD Geotechnical Consultant (MHD Geo. Cslt.) for project area, unless specified otherwise
4. "STP" stands for Special Testing Program
5. Values given in bold and shaded are recommended values for ISS-4 analyses

Table 5.5. Engineering Properties of Glaciomarine Deposits (cohesionless zones)

Property	Value(s) or Range	Location / Condition ¹	Source ²	Comments
γ_t	135 pcf	Cohesionless zones	Correlations to grain size and SPT-N values	
ϕ	42°		"	
K_a	0.20		Standard Rankine & Jaky equations, using ϕ	
K_p	5.0		"	
K_o	1.1		Menard Pressuremeter test	
	1.2	Boring 60, El. 2.7	"	
	1.0	Boring 61, El. -7.6	"	
Initial Modulus	1300 ksf	Boring 60, El. 2.7	"	Unload/Reload moduli
	2500 ksf	Boring 61, El. -7.6	"	2-4 times higher
	2000 ksf			
Permeability (k)	10^{-3} to 10^{-1} cm/s	Cohesionless zones	Correlations to grain size; "local experience"	Considered to be "relatively isotropic"
	10^{-3} cm/s			

- NOTES:**
1. Values are representative of entire project area unless specified otherwise
 2. All data and analyses by MHD Geotechnical Consultant (MHD Geo. Cslt.) unless specified otherwise
 3. Values given in bold and shaded are recommended for ISS-4 analysis

Table 5.6. Engineering Properties of Glacial Till

Property	Value(s) or Range	Location / Condition ¹	Source ²	Comments
SPT N-value	110 ± 50			
γ_T	145 pcf		Correlations to grain size and SPT-N values	
ϕ	45°		"	
K_a	0.17		Standard Rankine & Jaky equations, using ϕ	
K_p	5.8		"	
K_o	1.0		"	
Permeability (k)	10^{-6} to 10^{-3} cm/s	General range	Pressuremeter tests at nearby Boston sites	See text
	10^{-2} cm/s	Possible value in more pervious zones	Correlations to grain size; "local experience"	Considered to be "relatively isotropic"
	10^{-4} cm/s			More pervious zones may exist locally

NOTES:

1. Values are representative of entire project area unless specified otherwise
2. All data and analyses by MHD Geotechnical Consultant (MHD Geo. CsIt.) unless specified otherwise
3. Values given in bold and shaded are recommended for ISS-4 analysis

Table 5.7. Summary of In-Situ Tests Performed in Bedrock

A. Pressuremeter Tests

Boring No.	Station	Elevation (ft)	RQD (%)	Initial Modulus
61	78	-24.1	0	3,000 ksf
60	77+50	-7.6	47	15,000 ksf
30	67	-39.2	80	75,000 ksf

Recommended Value: 12,000 ksf

B. Permeability Tests

Boring No.	Station	Elevation (ft)	RQD (%)	k_b (cm/sec)
86	94	18 to 23	100, 75	2 to 60 x 10 ⁻⁴
89	95	17.5 to 22.5	77, 73	0.07 to 0.3 x 10 ⁻⁴
90	96	36 to 41	7, 38, 28	1 to 20 x 10 ⁻⁴
91	96	29.5 to 32	20, 62	1 to 6 x 10 ⁻⁴

TW-3 ¹	90	-4.9 to 15.1	not recorded	3 x 10 ⁻⁴
-------------------	----	--------------	--------------	----------------------

Recommended Value: 5x10⁻⁴

NOTES: 1. TW=Test Well, installed for Pumping Tests. Refer to description in text.

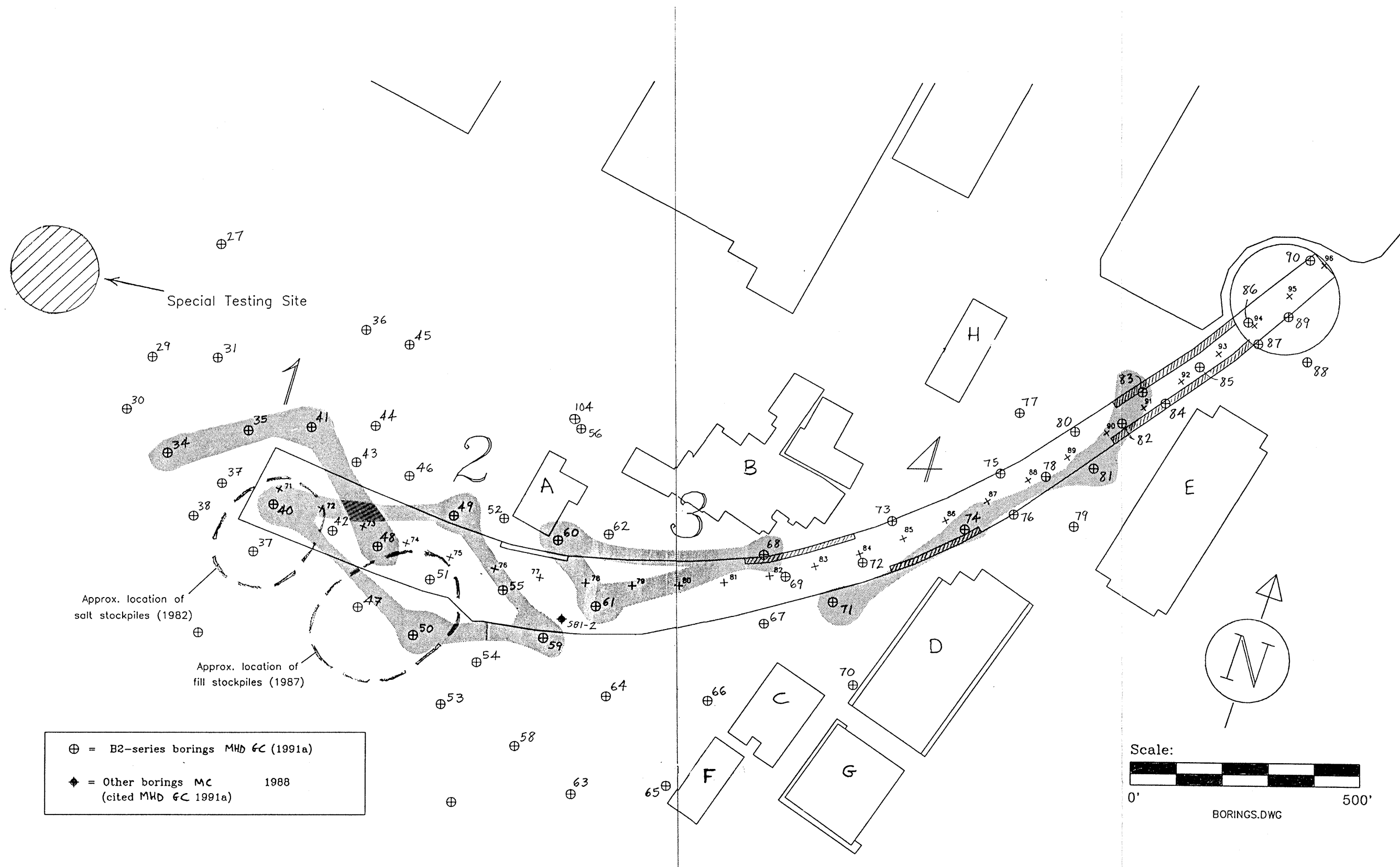


Figure 5.1. Locations of Exploratory Borings in the Project Area Conducted by MHD's Geotechnical Consultant. (Also shown: zone numbers, the location of the Special Testing Site, and locations of salt and fill stockpiles which existed in the 1980's.)

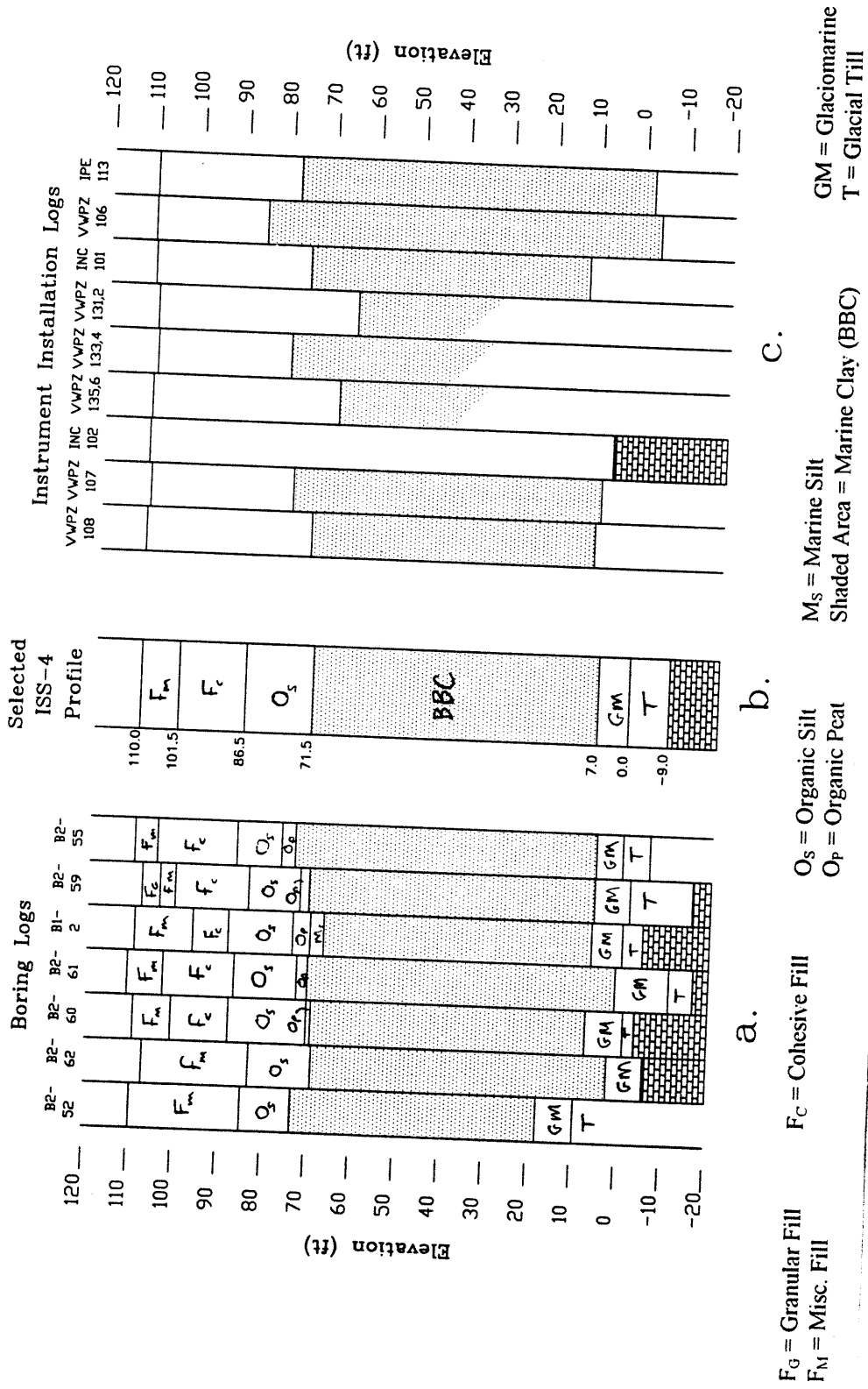


Figure 5.2. Information on Subsurface Stratigraphy at the ISS-4 Section. a. Borings Conducted by MHD Geotechnical Consultant (1991). b. Selected ISS-4 Soil Profile. c. Instrument Installation Logs

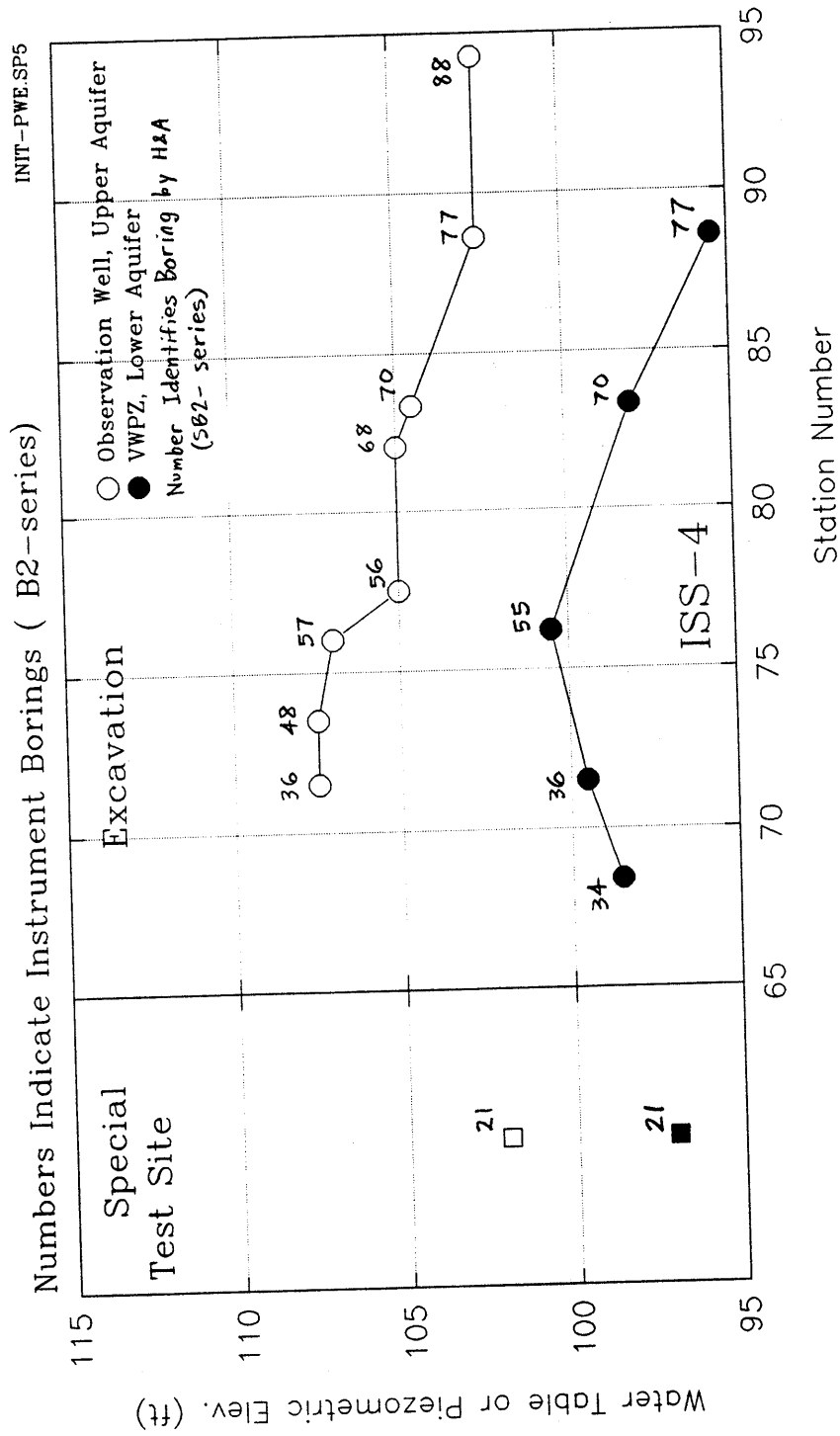


Figure 5.3. Initial Piezometric Levels in the Upper and Lower Aquifers Plotted Against Station Numbers, and at Special Test Site. Data from MHD Geotechnical Consultant (1991a, b, and 1993).

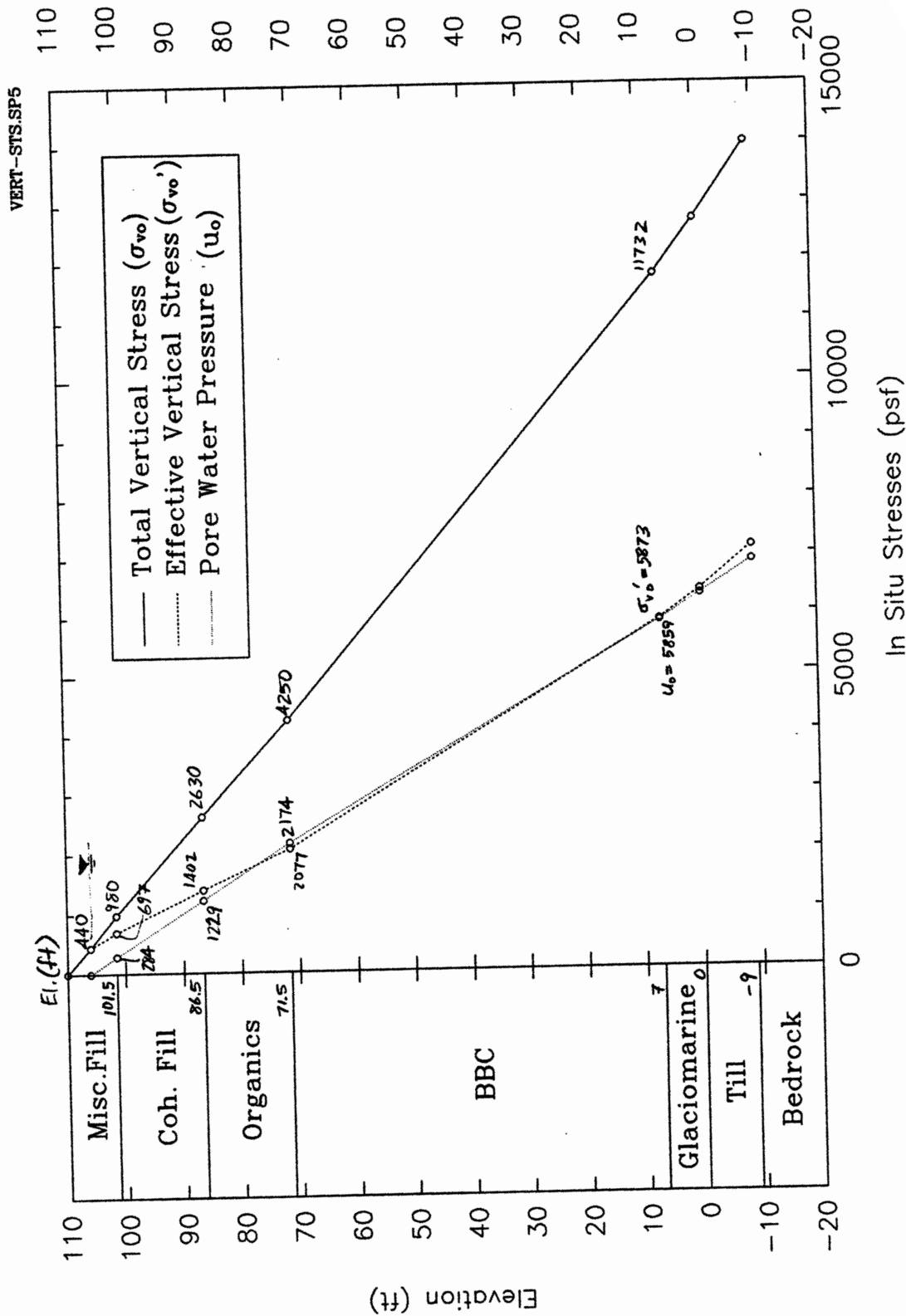


Figure 5.4. Initial In-Situ Stresses Throughout the ISS-4 Soil Profile.

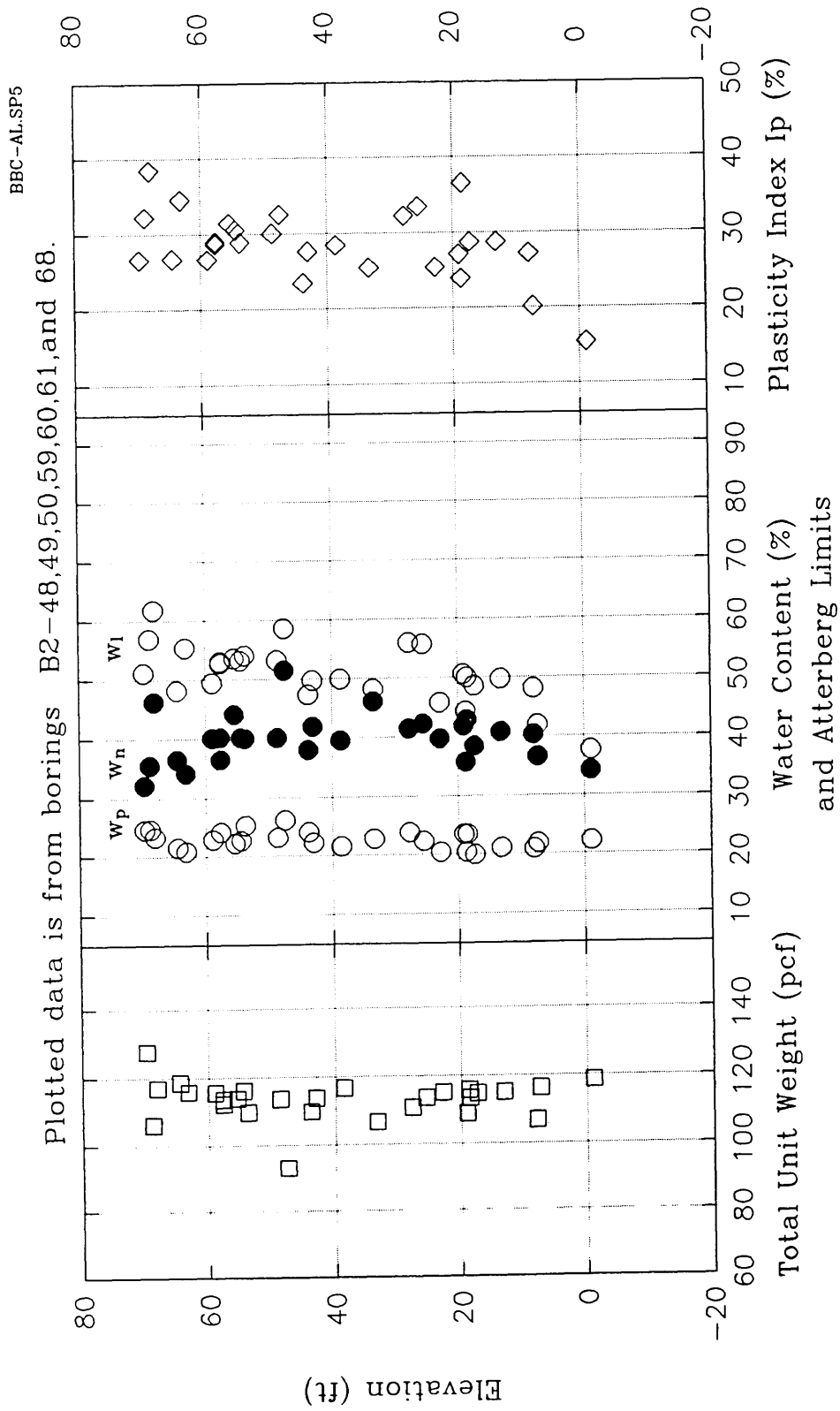


Figure 5.5. Total Unit Weight, Water Content, and Atterberg Limit Profiles for BBC near the ISS-4 Cross-Section.

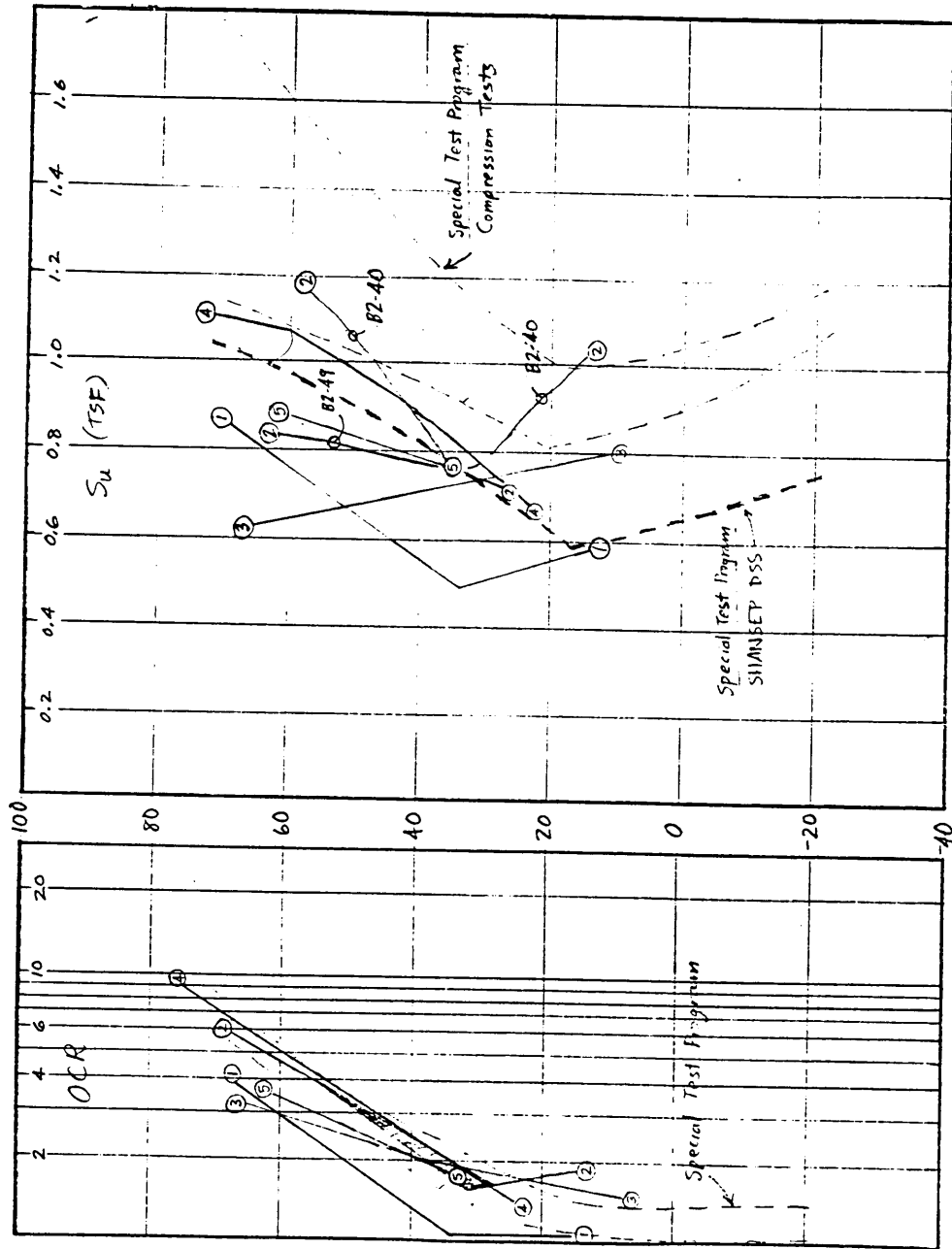


Figure 5.6. OCR and Undrained Strength Profiles for Marine Clay throughout the Project Alignment. From MHD Geotechnical Consultant (1991b) and Special Testing Program (MHD Geotechnical Consultant, 1993).

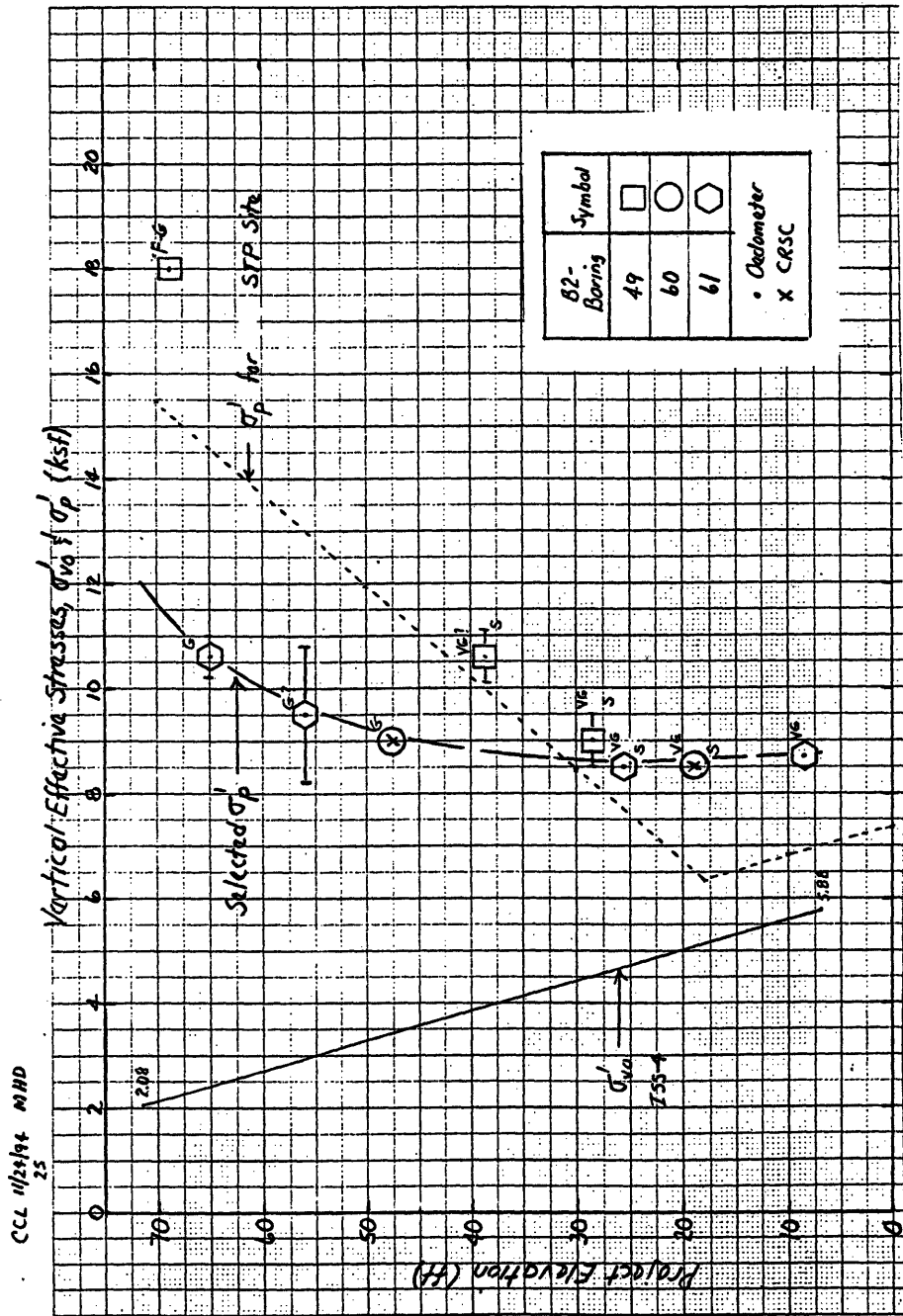
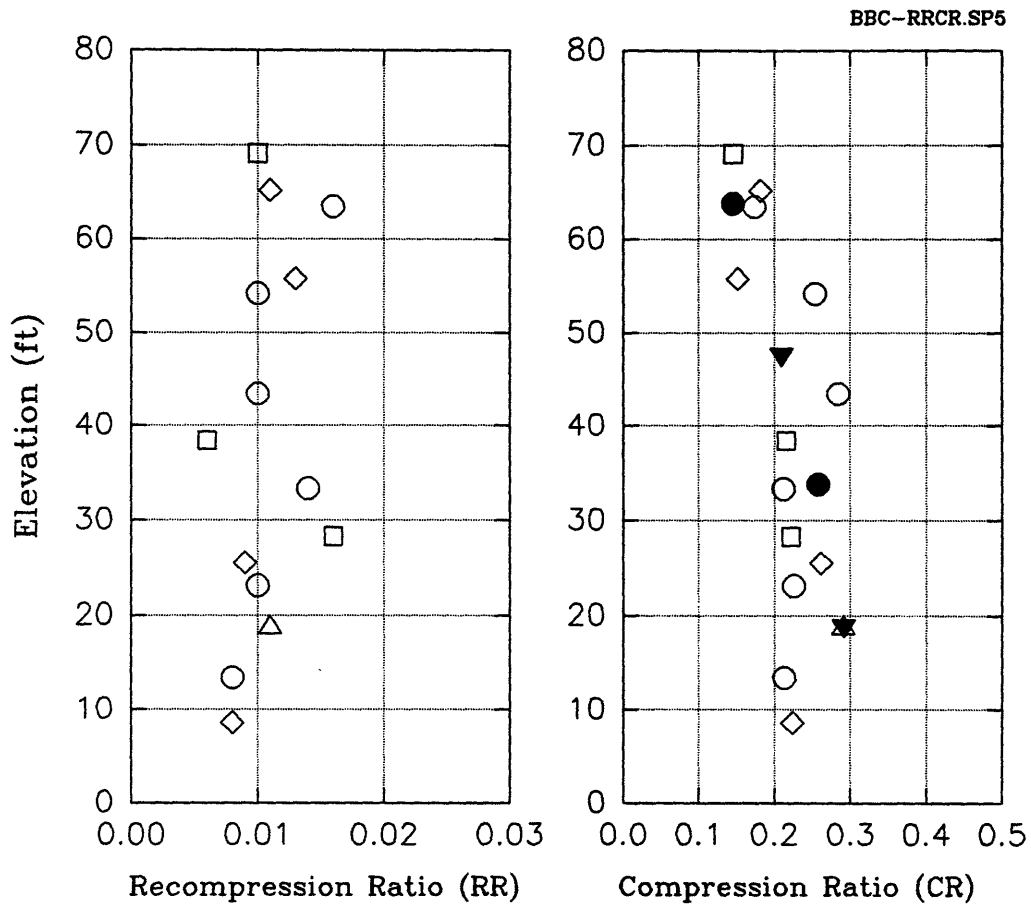


Figure 5.7. Selected Effective Stress Profile at ISS-4 Determined by MIT from Re-evaluation of Consolidation Test Data on BBC.



Legend:

○	B2-48	Hollow symbols: Oedometer Test Filled symbols: CRS Test
□	B2-49	
△	B2-50	
▼	B2-60	
◇	B2-61	

Figure 5.8. Elevation vs. CR (Compression Ratio) and RR (Recompression Ratio) Measured by Consolidation Tests on BBC, by MHD Geotechnical Consultant (1991a).

CCL 11/26/94 MHD

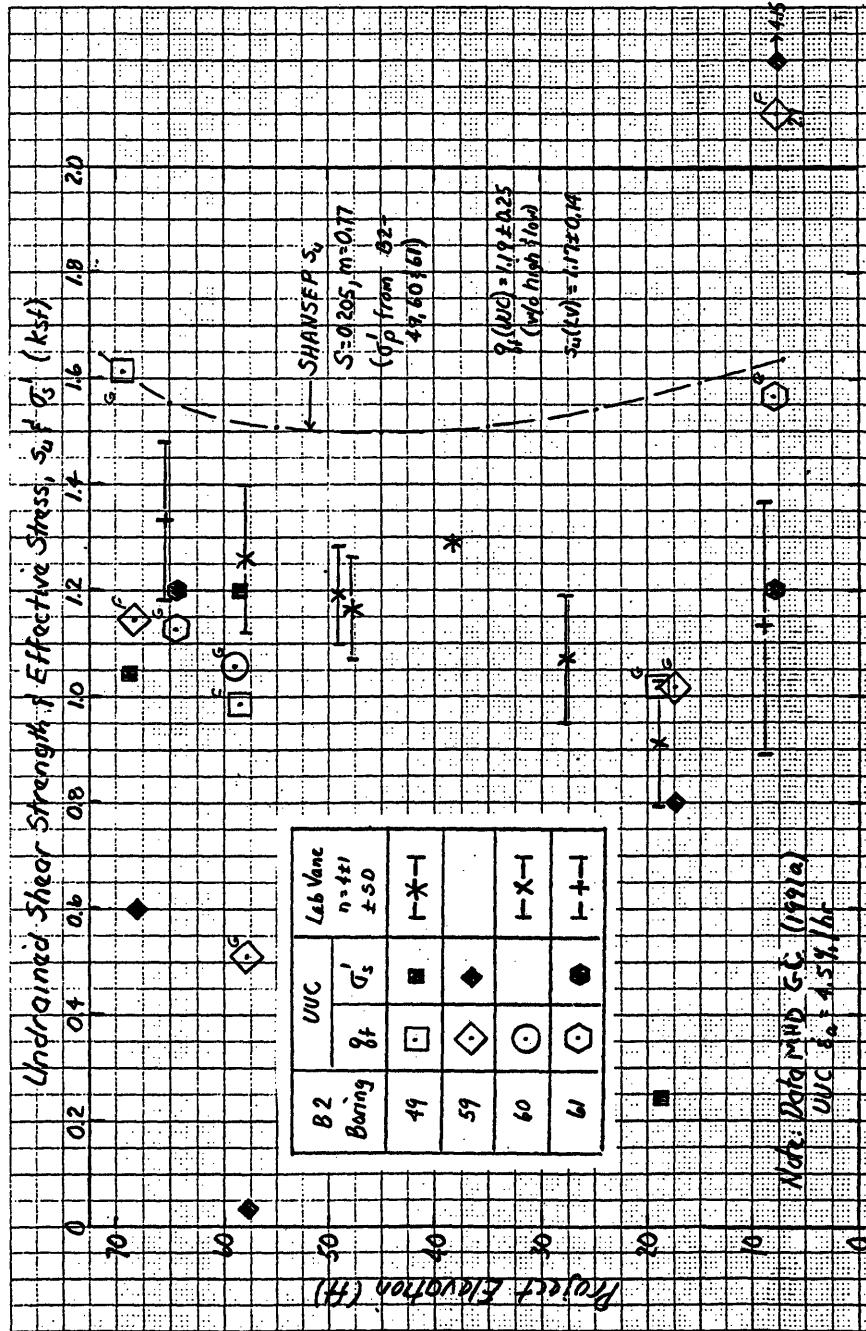


Figure 5.9. Comparison of Undrained Shear Strength Profile as Estimated by MIT using the SHANSEP Method with UUC and Lab Vane Strength Data.

CHAPTER 6

CONDITIONS AND CONSTRUCTION HISTORY AT ISS-4

6.1. OBJECTIVES

The first step in a careful study of instrumentation records from an excavation is development of a thorough knowledge of the excavation's geometry, structure, soil conditions, and construction history. Such knowledge is essential for an understanding of parameters and events which can influence the measured soil movements and water elevations. Pertinent information includes, as examples, the locations of instruments relative to the excavation, the structure of the SOE walls, the depth of the cut at various times, and the arrangement and load-carrying capacity of the tiebacks. This information can then be used in estimating soil deformations from design charts (Chapter 2) and for making an accurate two-dimensional reconstruction for finite-element modeling.

In addition to the original site geometry and layout, the sequence of construction events at and around ISS-4 is reconstructed in detail. Making sense of geotechnical instrumentation data for a project like this requires a careful definition of the changing geometry of the excavation subgrade as a function of time. Finite element modeling requires an even more extensive understanding of excavation history, since the exact cross-sectional geometry of the cut needs to be recreated with an element mesh as accurately as possible for all stages in the excavation process.

6.2. GEOMETRY AND STRUCTURAL FEATURES

Figure 6.1 represents the ISS-4 cross-section at approximately Sta. 77+20. This cross-section shows all of the important spatial details of the excavation support structure and the geotechnical instrumentation. A plan view of the ISS-4 area is provided in Figure 6.2.

The geometry shown in Figure 6.1 is intended to reflect representative conditions in the vicinity of the instrumented section, and does not necessarily depict absolute

dimensions precisely at Station 77+20. This is true for those dimensions that are spatially variable, including the embedment depths of the walls, the tieback lengths, and the soil profile. This “averaging” was done over a distance approximately 50 feet to either side of Sta. 77+20.

6.2.1. SOE Walls and Tiebacks

ISS-4 is at a boat section, and is located at the same location as Section A-A in Figure 3.1. As Figure 6.1 illustrates, there is a slurry wall (Diaphragm Wall A) on the north side of the cut and a sheetpile wall on the south side. The length and inclination of the tiebacks are different for the two wall types. A detailed description of the two types of SOE walls and the tiebacks was presented in Section 3.3.

Diaphragm Wall A is intended to protect Building A from excessive settlements. It is a 3-foot wide reinforced concrete wall, approximately 160 ft in length, and spans between Stations 76+00 and 77+60. It was constructed in eight separate panels, each about 17 or 21 feet long. The panels are reinforced by steel cages made of horizontal and vertical bars which lie no less than three inches inside of the diaphragm wall faces. Additional shear reinforcement is provided throughout by horizontal bars across the wall's thickness, and there are extra steel reinforcements in the vicinity of anchor holes. Sheets C1 and C2 show plan and elevation views of Diaphragm Wall A, respectively. The reinforcing steel in the wall is diagrammed in Sheet C3. The concrete was poured for the two end panels of the wall before the adjacent steel sheeting was driven; the sheetpiles were then driven before the concrete set, with one end extending about one foot into the fluid concrete.

The panels for Diaphragm Wall A are keyed two feet into the argillitic bedrock. Sheet C4 illustrates the embedment depths of the eight panels and the dates on which concrete was poured for each. Also shown in this figure are the three levels of tiebacks, which have a vertical inclination of 45 degrees and are grouted in the glacial till and bedrock. The free and grouted lengths of the three tieback tiers are listed in Table 6.1.

The sheetpile wall on the south side of ISS-4 is size AZ-18 steel sheeting. Figure 6.3 lists dimensions and engineering properties of AZ-18 sheet piles. The sheeting is

embedded to a tip elevation of 55 feet in the section of interest (between Sta. 76 and 78), which equals an embedment of 15 to 19 feet below subgrade. Like the north wall, there are three levels of tiebacks supporting the south wall. The top two tiers have an inclination of 22 degrees from horizontal, while the third tier is inclined 20 degrees (Table 6.1); all tiebacks are grouted in the upper 15 feet of the clay, in the overconsolidated “crust”. Sheet C5 shows the section of the south wall between Stations 76 and 78.

6.2.2. Geotechnical Instrumentation

The entire set of geotechnical instrumentation in the region surrounding ISS-4 is illustrated in Figure 6.2. (Even though they are considered to be part of the ISS-4 cluster, instruments VWPZ-108, VWPZ-53, OW-02, and OW-17 are too far away from the cross section to appear in Figure 6.1.) Table 6.2 lists all of the instruments at ISS-4. The settlement points on the western side of Building A are not included in this list because of their lateral distance from the ISS-4 centerline. VWPZ-53, however, is included, because of the fact that deep piezometer readings are fairly independent of location (see Chapter 7).

Information on the individual instruments, such as their locations, depths, and installation dates, is given in Tables A.1 through A.4 in Appendix A. All instruments were installed before any activity started on the site, except for the inclinometers, which were placed a day or two after excavation began on the first lift.

6.3. TIEBACK LOCK-OFF LOADS AND ELASTIC MODULI

The importance of the tiebacks as structural support members requires detailed knowledge of their dimensions, locations, and installation and testing procedures. Section 3.3.2 presented a detailed discussion of the structure and installation of tiebacks throughout the project alignment; this section will focus on key properties of the tiebacks in the vicinity of ISS-4, particularly with respect to their lock-off loads and stress-strain properties. Tiebacks between Sta. 76 and 78 were considered as being within the range of ISS-4.

6.3.1. Data Collection and Sources

MHD's Management Consultant provided data sheets for all tiebacks between Sta. 76+00 and 78+00, within approximately 100 ft of the ISS-4 centerline (Station 77+20). These data sheets were created by the contractor's field engineers, who were present for drilling, grouting, and locking off activities. Representatives from the drilling subcontractor also filled out similar sheets for each installed tieback.

Every tieback data sheet included information on: stressing and bond lengths, design and as-built lock-off loads, and load vs. deformation data for proof tests (performed on every tieback) and performance tests (done on 5 to 10% of tiebacks). The as-built data provided in these sheets were used for analyses of average load per unit length and modulus of elasticity, which will be discussed in the next two sections. The free and grouted lengths which appear in Table 6.1 were also obtained from the sheets, and represent as-built values.

6.3.2. Equivalent Tieback Loads

Tieback lockoff loads were based on design assumptions of the earth pressures that must be resisted by the wall. A line of tiebacks at a single elevation provides a combined loading condition which approximates an equivalent linear load on the wall at that level. Because the tiebacks do not have a uniform horizontal spacing, the magnitude of individual lock-off loads differs from one anchor to the next. Although the lock-off load of every individual tieback at ISS-4 was known from the data sheets, it is the equivalent linear load, or load per unit length, which is needed for accurate two-dimensional modeling of the cross section in finite element analyses.

The equivalent load per linear foot of wall was obtained from the lateral spacing of the tiebacks and from the load that each one of them carries. Plotting the cumulative, rather than the absolute, lock-off loads against station yields a nearly straight line, whose slope equals the tieback load per unit length. This analysis was done for all three tieback tiers on the North and South sides of ISS-4. The graphs are shown in Figures 6.4 and 6.5, for the North and South walls, respectively. Linear regressions on the slopes gave the

tieback loads per unit length, which are listed in Table 6.1 along with the correlation coefficients from the regressions. It can be seen that the cumulative load vs. station lines were extremely close to being linear.

6.3.3. Effective Moduli of Tiebacks

The load and elongation data from proof and performance tests done on each anchor were included on the field data sheets. Loads (in kips) and elongations (in inches) were converted to stress and strain so that an “effective” modulus could be computed for the tiebacks. Figure 6.6 shows an example of a load-displacement plot for a series of adjacent tiebacks in a single tier. Load was divided by the total cross-sectional area of the tieback strands, given the number of individual strands in the tieback and a diameter of 0.6 inches for each strand. Elongation was converted to strain by dividing by the free (unbonded) length of the tendon.

An “effective” modulus was defined for each tier of tiebacks by finding the average slope of the stress-strain curves for all tiebacks in a given tier, within 100 feet of the ISS-4 centerline. The modulus was estimated graphically by choosing a “best-fit” slope through the lines. Some judgement was required because the curves tended to be slightly rounded, with a modulus that decreased at higher loads. Stress-strain curves for all three tiers on the North and South sides of ISS-4, with “best-fit” lines included, are provided in Sheets C6 through C18 in Appendix C. The effective moduli are listed in Table 6.1.

It should be noted that these moduli are based on elongation measurements that combine the effects of tendon stretching and deformation of the grouted zone, and can therefore be considered “effective” values. The contribution of grouted zone deformation to the measured displacements explains the fact that these elastic moduli are lower than typical modulus values for steel tendons, listed as 23,000 to 30,000 ksi by Xanthakos (1991). This is especially true for the south wall tiebacks, which are grouted in stiff clay rather than bedrock. Deformation of the grouted zone may also be the cause of the curves’ slightly rounded shapes.

6.4. EXCAVATION HISTORY

6.4.1. Data Collection and Sources

Defining the excavation history at ISS-4 proved to be a time-consuming process, as complete records of excavation progress in three spatial dimensions were scattered and sometimes incomplete. While most of the time history was defined using information contained in the weekly geotechnical reports submitted to MHD's Management Consultant, field engineer reports and construction photographs were also necessary to clarify ambiguities. Several sources of information were used in defining the excavation history, in three spatial dimensions, at ISS-4. The following is a review of these sources and the steps that were taken to completely define the history at this section.

1. Dates of tier excavations, tieback installations, and lock-offs were obtained from a *construction activity table*, provided in updated form in each weekly geotechnical instrumentation report sent to and filed by MHD's Management Consultant. Dates in the table pertained to events that occurred at the walls, immediately adjacent to inclinometers. Sheets D1 and D2 in Appendix D are one of the last construction activity tables, which contains a nearly complete listing of all pertinent dates.

2. The contractor provided large-sheet *SOE wall plans*, on which they had distinguished individual excavated lifts and excavation dates for each. These drawings showed the lateral extent of each lift along the walls. For convenience, the large-scale sheets were recopied by hand onto more manageable 8.5 x 11-inch sheets. One of these smaller sheets was made for each side of the excavation in the vicinity of ISS-4, and is provided as Sheet D3.

3. *Tieback installation records* for the vicinity of ISS-4 were obtained from the Management Consultant, as described in Section 6.3.1. Along with the lock-off loads, these records included dates of tieback installation and lock-off. The dates of these events could then be defined within approximately 50 feet to either side of ISS-4, ensuring accurate two-dimensional modeling of installation history along the walls.

4. A photographer was hired to shoot a set of *site photographs* once a month. These photos were usually taken from a helicopter and showed aerial views of selected

areas. They were kept on file at the project field office and could be used to help define subgrade geometry on certain dates. However, the photographs provided an incomplete record of the construction sequence at ISS-4, given their once-a-month frequency and the fact that the ISS-4 area was not photographed in every monthly set.

5. In addition to the construction activity tables, each weekly geotechnical instrumentation report included a *construction progress plan*. This was a large-scale plan drawing of the entire alignment, including instrument locations, on which the week's excavated sections and tieback installations were sketched and labeled. These plans were particularly helpful because, unlike the construction activity tables, they identified excavation events that occurred in the center of the excavation. As was done with the contractor's SOE wall plans, these large sheet plans were recopied onto more convenient 8.5 x 11-inch sheets. Several weeks' worth of progress plans were often copied onto a single sheet for further convenience; an example of such a recopied sheet is provided in Sheet D4. Not all of the progress plans were found, so only part of the excavation history could be determined from them.

6. The previously mentioned sources allowed most details of the excavation time history to be defined, but they still left some unanswered questions due to missing, ambiguous, or conflicting data. *Daily field engineer reports* on file at the project field office allowed confirmation or resolution of almost all information that was still unknown or ambiguous. Each construction day, field engineers monitored site activities and submitted individual reports. Usually, engineers were assigned to particular areas or activity types for a period of a few weeks. For example, one engineer might be observing spoil removal and transport, while another might be responsible for tieback installation activities in the western third of the alignment. A few weeks later, they would generally be reassigned to different areas. By knowing a range of dates to study and the name of the engineer documenting the type of activity under consideration, the relevant field engineer reports could be readily located, although it was still a rather time-consuming process.

6.4.2. Finalized Excavation History

The end result of this information search was a complete time history of the ISS-4 cross-section, including all excavation steps, installation and lock-off dates for support walls and tiebacks, and intermediate subgrade geometries. Table 6.3 presents a summary of all construction events, listing the relevant dates in chronological order.

Figure 6.7 illustrates all construction activities that occurred as the final subgrade was approached. This information will be used in re-creating the excavation's geometry through time with a finite-element mesh. The step-by-step nature of the excavation can be seen; it is clear that the excavation sequencing was much more complex than a simple series of flat subgrades at increasing depth, which is what many previous finite element simulations modeled. In addition to making cuts along either wall of the excavation for tieback installation, lifts were also cut from the center of the cross-section, for the purpose of laying down temporary haul roads for transportation of materials and spoil, to and from other parts of the alignment.

Another important feature of the ISS-4 excavation history is the prolonged suspension of excavation activity during the period when boat section tiedowns were installed, followed by excavation to the final subgrade.

Table 6.1. Summary of Dimensions, Lock-off Loads, and Elastic Moduli of Tiebacks.

	Anchor Head elev. (ft)	Vertical Angle (°)	Free Length (ft)	Fixed (GROUTED) Length (ft)	Lock-off Load per Unit Length (k/ft)	Lin. Regression r^2	Effective E (ksi)	# strands	Lateral spacing (ft)
NORTH (DIAPHRAGM) WALL									
Tier 1	106	45	165 - 169	30	27.4	1.000	22,200	9 - 10	10.5
Tier 2	94	45	149 - 152	30	51.5	0.999	21,100	10 - 11	6.5
Tier 3	82	45	125 - 132	32	64.7	1.000	20,200	11 - 12	6.5
SOUTH (SHEETPILE) WALL									
Tier 1	102	22	84 - 86	40	13.6	0.996	20,500	5 - 6	14.5
Tier 2	90	22	53 - 55	40	30.4	1.000	16,600	6	6
Tier 3	78	20	23 - 25	40	29.9	1.000	14,200	6	6

Data are from field data sheets provided by M.C.. For linear regressions, see Sheets C6 through C19 in Appendix C.

Table 6.2. List of all Geotechnical Instruments Located at the ISS-4 Test Section.

	NORTH SIDE	INSIDE EXCAVATION	SOUTH SIDE	
Inclinometers	INC-102		INC-101 IPE-113	Soil Movement Instruments
Deflection (Settlement) Monitoring Points	DMP4-120 DMP2-006 DMP2-107 DMP2-105 DMP2-104 DMP2-070		DMP4-118 DMP4-117 DMP4-116	
Heave Measurements (Spider Magnets)		MPHG-110 MPHG-109 MPHG-501 MPHG-107	IPE-113	
Observation Wells	OW-002 OW-16			Groundwater Instruments
Piezometers	VWPZ-108 VWPZ-67 VWPZ-68 VWPZ-107	VPWZ-135 VPWZ-136 VPWZ-133 VWPZ-134 VWPZ-131 VWPZ-132 VWPZ-53	VWPZ-106 OSPZ-106	
Load Cells		- none -		

Table 6.3. Summary of Excavation History at ISS-4.

SUMMARY OF EXCAVATION EVENTS				
				ISS-4
				Sta. 77-78
EVENT				
Date(s)	North Wall	Center	South Wall	
Install and Post-grout TTP anchors:				
7/23 - 8/1/92		Upper level, anchors 1 and 5.		
8/11 - 8/15/92		Upper level, anchors 2 through 4.		
8/26 - 8/30/92		All Lower level anchors		
ISS-4 Excavation:				
12/7 - 12/9/92			Drive Sheet Piles	
3/22/93			Excavate Lift 1 (100')	
3/24 - 4/9/93	Excavate Bl _{da} , A Slurry Wall			
3/31 - 4/13/93	Pour concrete, Bl _{da} , A Slurry Wall			
4/13/93			Install Tier 1 tiebacks	
5/4 - 5/5/93	Excavate Lift 1 (103')			
5/17 - 5/21/93		Excavate Lift 1, Center (94')		
5/18 - 5/24/93	Install Tier 1 tiebacks			
5/28 - 6/1/93	Lock Off Tier 1 tiebacks			
6/1 - 6/3/93	Excavate Lift 2 (92')			
6/5/93			Lock Off Tier 1 tiebacks	
6/7 - 6/14/93	Install Tier 2 tiebacks			
6/15/93			Excavate Lift 2 (89')	
6/25/93		Excavate Lift 2, Center (85')		
6/30 - 7/1/93			Install Tier 2 tiebacks	
7/1 - 7/2/93	Lock Off Tier 2 tiebacks			
7/12 - 7/13/93	Excavate Lift 3 (80')			
7/27 - 8/5/93	Install Tier 3 tiebacks			
7/30 - 7/31/93			Lock Off Tier 2 tiebacks	
8/11 - 8/16/93			Excavate Lift 3 (partial, 80')	
8/16 - 8/17/93			Install Tier 3 tiebacks	
8/20/93	Lock Off Tier 3 tiebacks			
9/17 - 9/20/93			Lock Off Tier 3 tiebacks	
9/28 - 9/30/93		Excavate Lift 3, Center (78')		
10/13 - 10/14/93			Grade Haul Road (78')	
Rock Anchors (tiedowns):				
1/29 - 2/8/94	Install anchors, North and Center			
2/14 - 2/22/94			Install anchors, South side	
Completion of excavation:				
3/2 - 3/4/94	Excavate Final Subgrade			
5/17/94			Pour South Invert	
5/26/94	Pour North Invert			

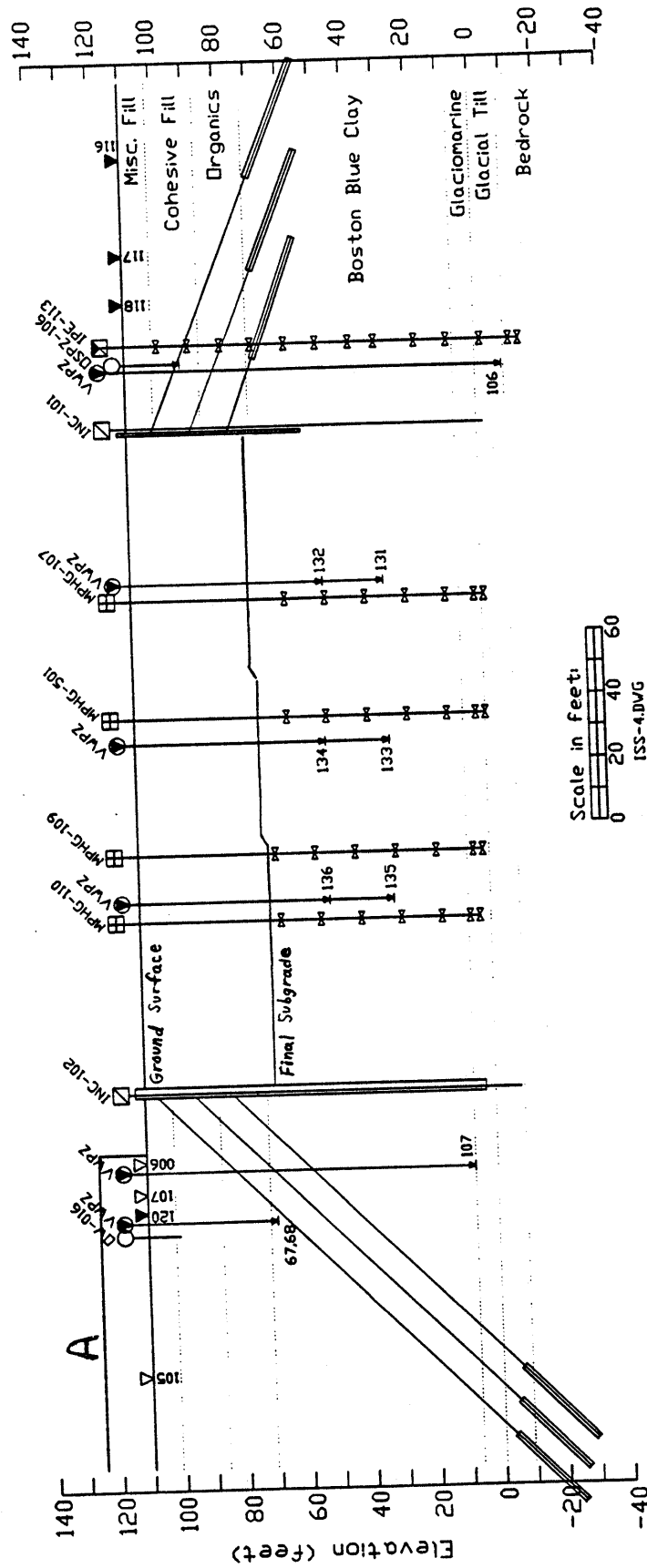


Figure 6.1. Cross-Sectional View of Excavation at ISS-4 Test Section (approx. Sta. 77+20), showing Tiebacks, SOE Walls, and Geotechnical Instrumentation. View is Looking East; North is to the Left.

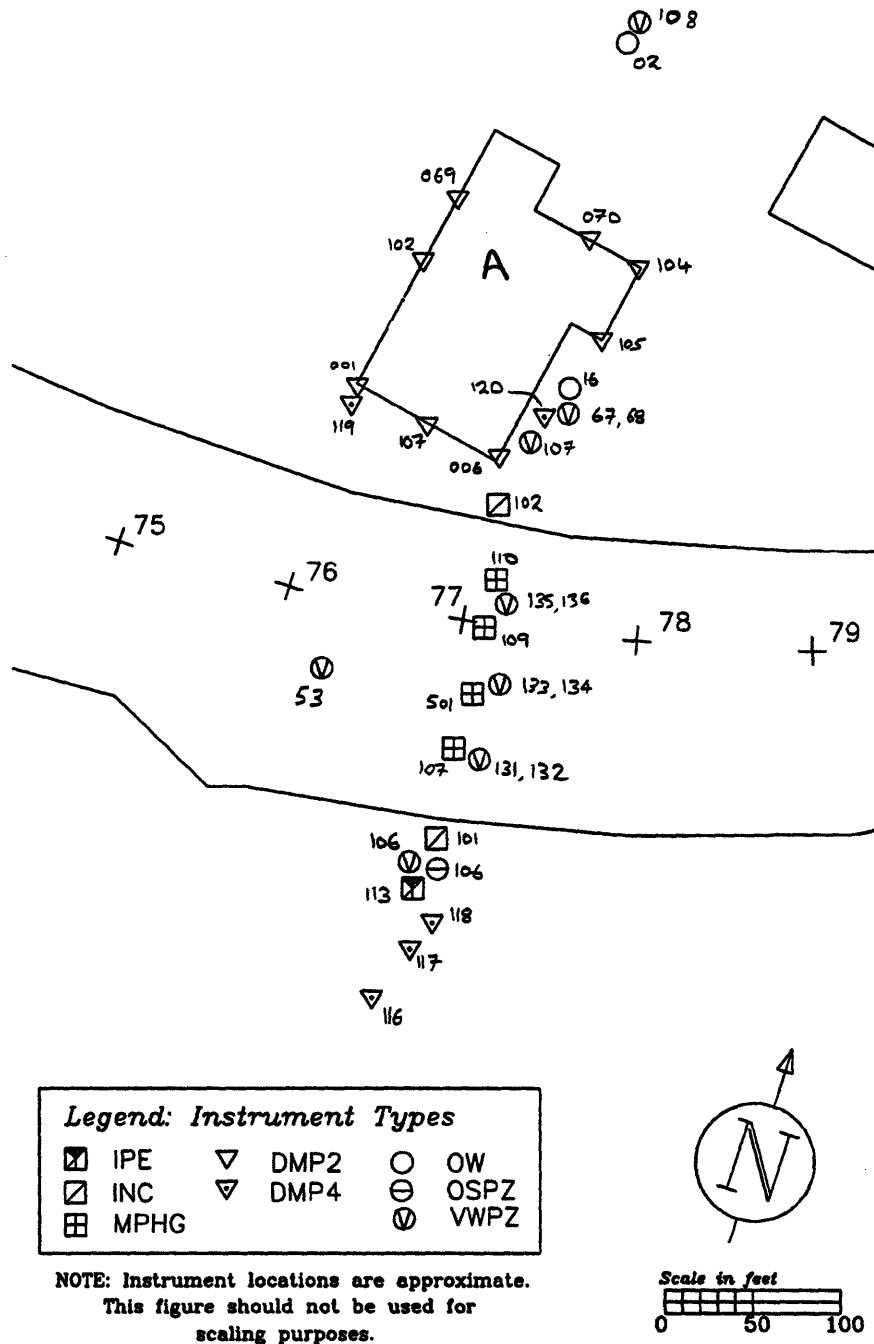


Figure 6.2. Plan View of the ISS-4 Area, showing Building A and Geotechnical Instrumentation.

Profile	S = Single pile D = Double pile	Mass per ft lb/ft	Sectional area in ²
	per S per D per ft of wall	50.00 100.00 24.17	14.69 29.38 7.08
<p>The interlocking joints of AZ-profiles are made for mutual connections For corner arrangements special connectors are in stock.</p>			

coating area ¹⁾ ft ² /ft	Develop. perim. in	Section modulus S _y ²⁾ in ³	moment of inertia		Radius of gyration r in	Profile
			I _y in ⁴	I _z in ⁴		
5.64	32.4	69.3	517.5	870.2	5.93	AZ 18
		138.6			5.93	per S
		33.5			250.4	5.93
1) Excludes inside of interlocks 2) Considered neutral axe: y-y						

Figure 6.3. Dimensions and Engineering Properties of Arbed AZ-18 Sheet Piling (ISPC, 1990).

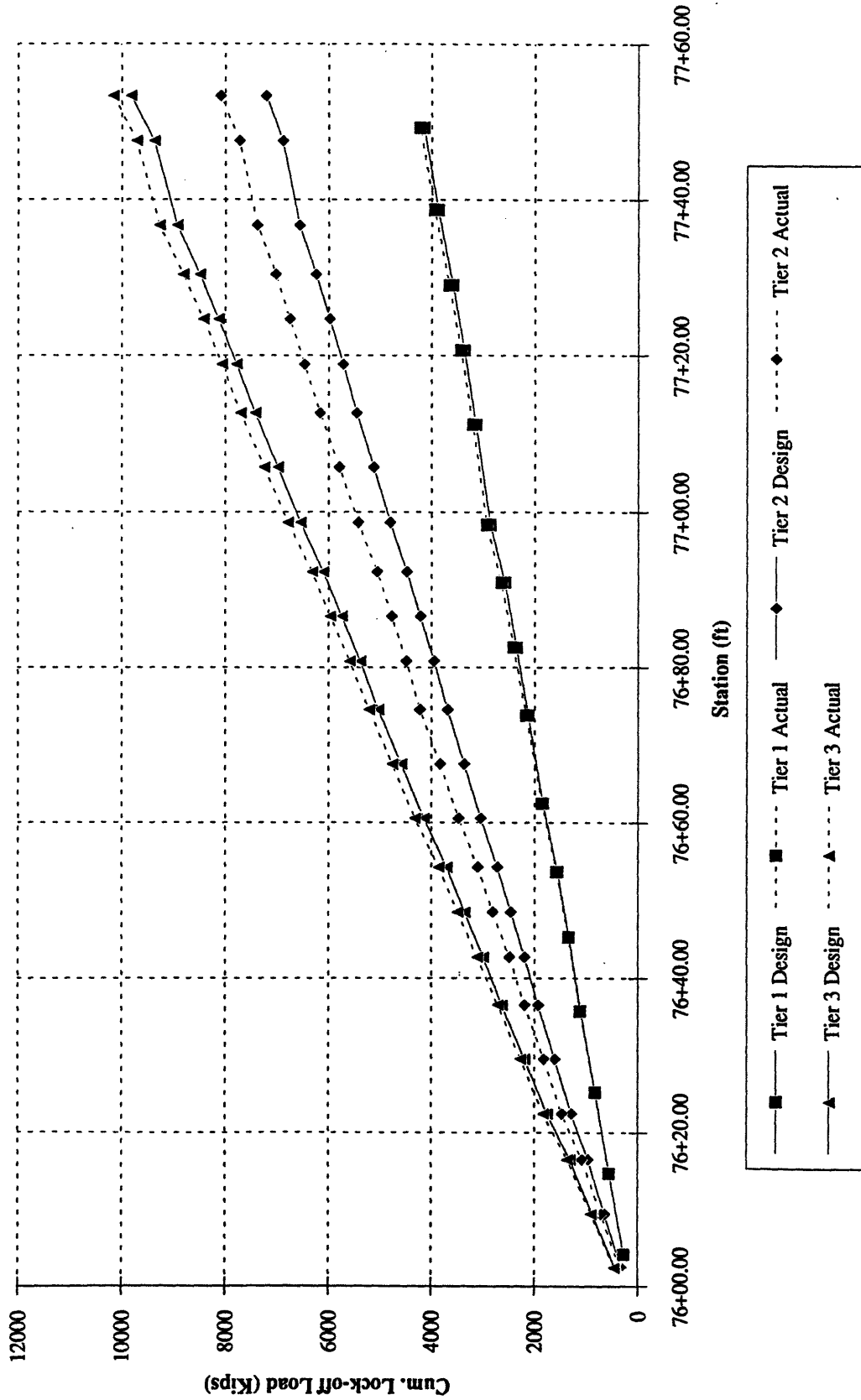


Figure 6.4. Cumulative Lock-Off Load vs. Lateral Position along Diaphragm (Slurry) Wall A (Sta. 76+00 to 77+67).

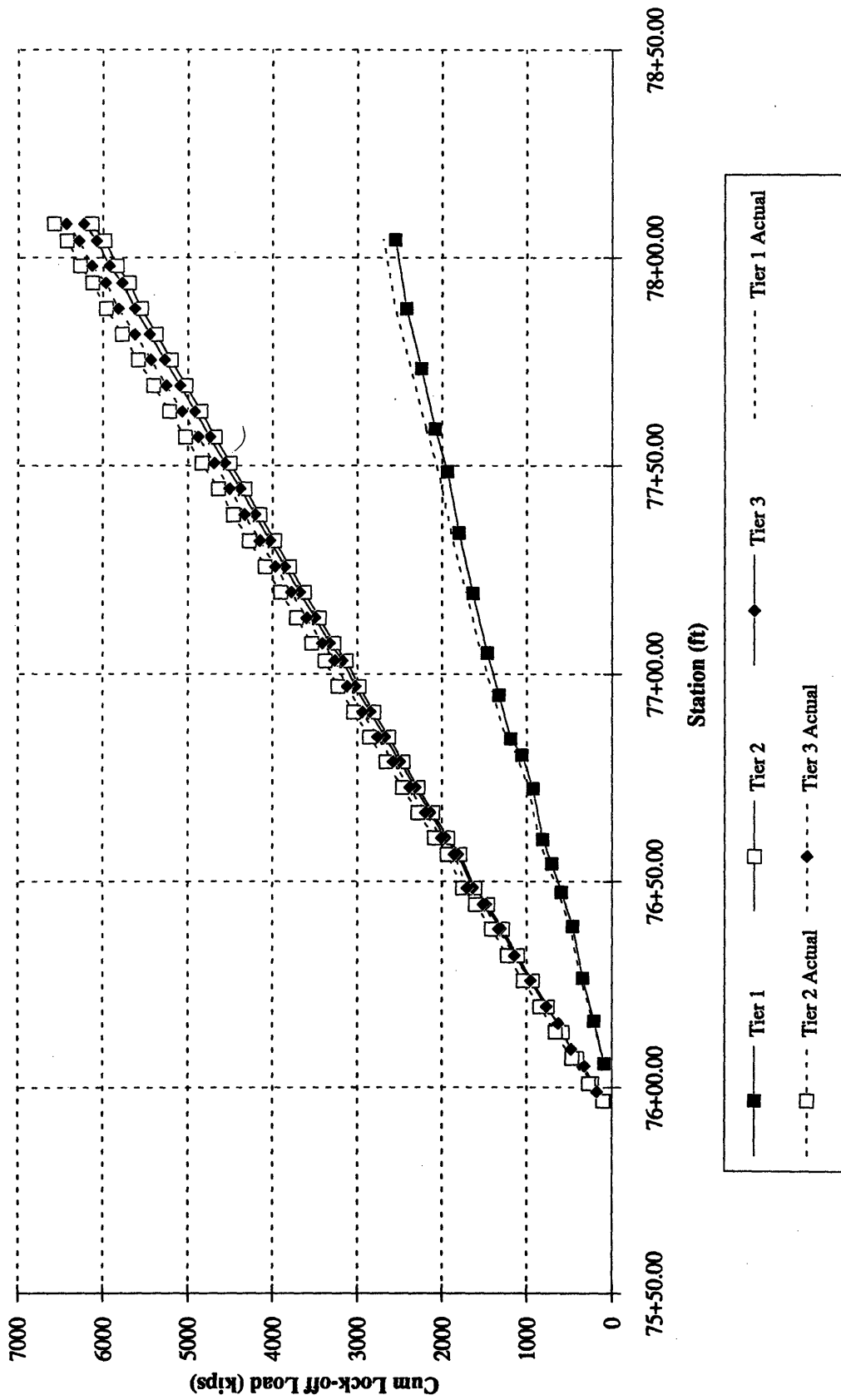


Figure 6.5. Cumulative Lock-Off Load vs. Lateral Position along the South Sheeppile

Wall (Sta. 76+00 to 78+00).

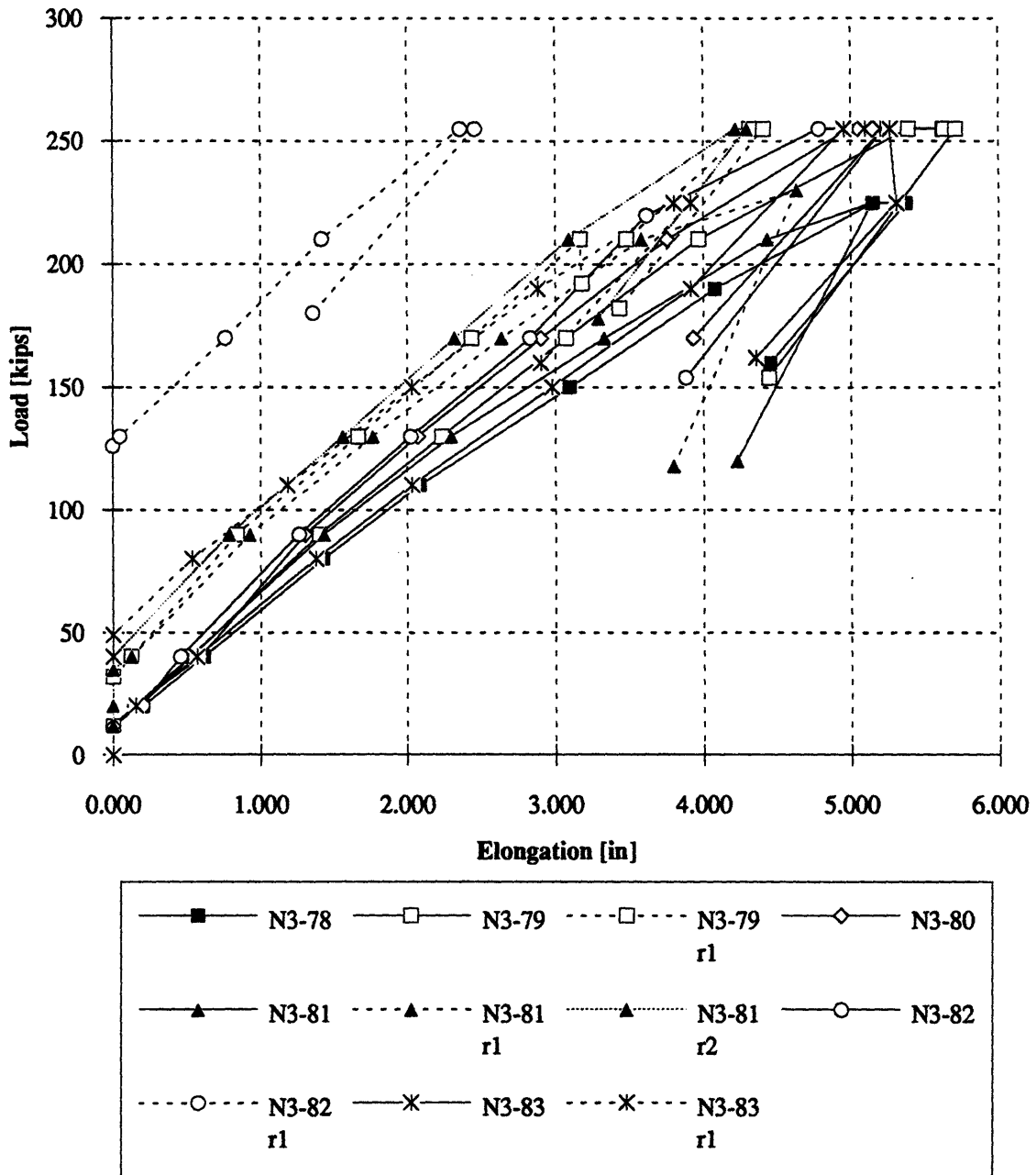


Figure 6.6. Example of a Load-Elongation Plot for a Series of Adjacent Tiebacks in a Single Tier. (Note: These plotted tiebacks are in the sheetpile wall immediately east of Slurry Wall A, and were not considered in later analyses of ISS-4.)

Horiz. Scale 1" = 20' outside
 1" = 40' inside

ISS-4 Sta. 77+10

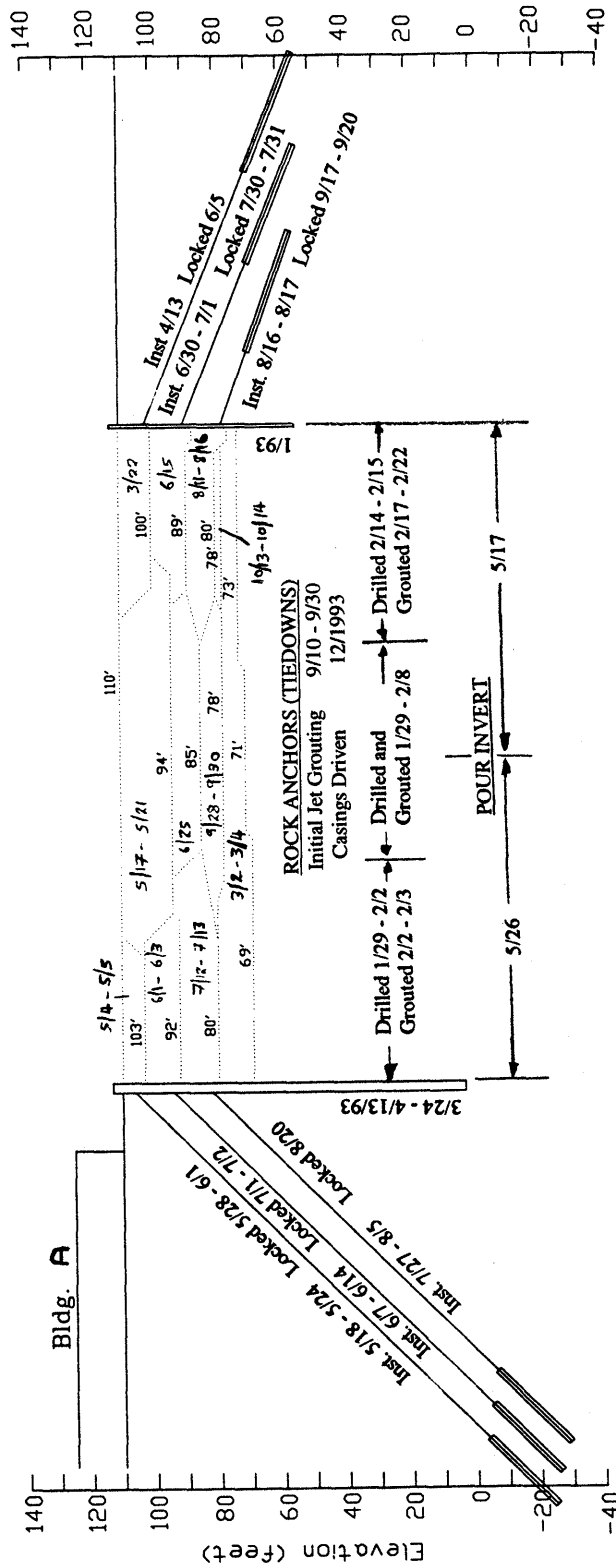


Figure 6.7. Graphical Summary of Construction Activities and Lift Excavations at ISS-4.

CHAPTER 7

INSTRUMENT MONITORING DATA FROM ISS-4

7.1. PRESENTATION OF DATA

There were 33 geotechnical instruments monitored at the ISS-4 cross-section, and complete records were gathered for this research from all of them. The data records were provided by MHD's Management Consultant (MC) and existed in both printed and digital form. Every week, a geotechnical data report was prepared by the primary construction contractor and its instrumentation subcontractors. These weekly reports, in addition to providing much of the excavation history information that was discussed in Section 6.4, contained complete sets of data from every operating instrument in the project area. Instrument data were graphed, usually against time, and listed in tables for some instruments as well; every weekly report was a cumulative tabulation, such that the last several months of data, or even the entire history of data for some instruments, were given in each one. Appendix E provides examples of the graphs and tables in these weekly reports.

The weekly reports were accompanied by data stored digitally on 3.5-inch diskettes. All the disks were stored chronologically by the MC and copied into a computerized memory system accessible through a users network.

Although instruments were read on a regular (usually weekly) basis by the contractor via its instrumentation consultant, the MHD representative also performed independent supplementary readings on a monthly basis, as "checks" on the contractor's data. The two monitoring teams were distinguished by the initials "CC" and "MC". "CC" means Construction Contractor and its instrumentation subcontractor, who installed the instruments and did the weekly readings. "MC" in this context represents both the firm acting as MHD's MC, and another firm responsible for all optical surveying work, such as DMP (settlement) readings. In general, the data from the two groups were in close

agreement, and this report deals mostly with the more frequent CC readings. MC readings are, however, combined with the CC data for DMP's (settlements).

MIT prepared a new set of data plots which facilitate the process of interpreting soil and groundwater behavior during the excavation process. The data are plotted in two ways: the Figure 7A series presents plots of data versus time, and the Figure 7B series presents "Time Period Summaries" showing construction activities, wall movements, and surface settlements over selected time intervals. The next two sections describe the motivations and procedures that led to these two series of figures.

7.1.1. Data-vs.-Time Plots

The instrument-vs.-time plots provided in the geotechnical data reports, while very informative, were not ideal for careful study and interpretation of data. MIT prepared a set of new graphs which appear as Figures 7A.1 to 7A.17. Data plots from the contractor are included in Appendix E (Note: These data plots are typical of geotechnical practice in the U.S.). The MIT plots represent possible advantages in the following ways:

1. *Contractor*: The plots of instrument readings vs. time usually did not indicate the times of excavation and construction events. *MIT*: The stepwise lowering of subgrade by lift excavations and the times of tieback installations and lock-offs are depicted graphically on a easily visualized timeline. The elevation of the subgrade as it changed with time is represented by a line, and the dates of tieback installation and lockoff are marked by the letters "T" and "L", respectively.

2. *Contractor*: It was sometimes difficult to locate or define individual dates on the time axes. *MIT*: All time axes are subdivided into a convenient time scale of months.

3. *Contractor*: A separate graph was often provided for each individual instrument. *MIT*: The researchers feel that it would often be helpful to plot two or more associated instruments on the same graph. Therefore, many of the MIT graphs combine two or more instruments at once. This is true for two cases: 1. All settlement points at ISS-4 that were on the same side of the cut are combined onto one MIT graph (Figures 7A.4 and 7A.5). 2. Groundwater monitoring instruments that are located either at different depths in the same

borehole or in similar locations or soil deposits, are shown together in the MIT graphs (Figures 7A.7 through 7A.9 and Figures 7A.15 through 7A.17).

4. *Contractor*: Lateral movements measured with inclinometers were plotted against time in the form of shear strain, defined as the relative lateral displacement between two consecutive data points along the inclinometer length, divided by their two-foot separation distance. This was done to facilitate assessment of the overall stability of the excavation. Shear strains at two or three different depths were combined on the same graph. *MIT*: Lateral displacements, rather than shear strains, are plotted against time, because this variable was considered more informative for MIT's research. Displacements measured at three to five different depths are included on each graph, which are presented in Figures 7A.1 through 7A.3.

The seventeen data-vs.-time plots in the Figure 7A series are presented in groupings based on instrument type and location. They are arranged in the same order as they will be discussed in this chapter. Each of the seventeen graphs has the same format, and all cover the same span of time: from August 1992 to the end of May 1994. These limiting dates bracket all important construction activities that occurred at ISS-4, up to the pouring of concrete invert slabs. August 1, 1992 is a logical starting point because almost all of the instruments were installed and read for the first time after that date.

The first three figures plot lateral deflections measured by the three inclinometers. These are followed by two figures (7A.4 and 7A.5) showing surface settlements measured by Deformation Monitoring Points, to the north and south of the excavation, respectively. Figure 7A.6 is a graph of settlements measured by the IPE-113 probe extensometer, behind the south wall. The next four figures (7A.7 through 7A.10) present groundwater levels and piezometric water elevations measured outside of the excavation and in the lower aquifer beneath the Boston Blue Clay. The remaining seven figures are for instruments located within the excavation. Figures 7A.11 through 7A.14 present clay heave measured by four multi-point heave gages, and Figures 7A.15 through 7A.17 show pore pressures within the clay recorded by three pairs of piezometers. Figure 7A.18 plots heave versus elevation at representative times for the multi-point heave gages.

7.1.2. Presentation of Data in “Time Period Summaries”

The planned finite element analyses (Task 5 in Table 1.1) will recreate as accurately as possible the geometry, soil properties, and excavation history of the ISS-4 cross-section, for comparison of numerically-predicted wall and surface movements and pore pressure changes to those actually measured by the geotechnical instrumentation. Therefore the ISS-4 instrumentation data should be presented in a way that will allow convenient comparison to analysis results that apply to particular times in the excavation’s history. Such data presentations should show developments at the ISS-4 section for specific time intervals: not only measured wall movements and settlements for each period, but also any changes in the support system and excavation geometry that occurred due to construction activities.

Inclinometer and settlement point measurements at ISS-4 were therefore combined with the construction history in a series of “Time Period Summaries”, which show excavation progress and recorded movements for selected dates throughout the excavation process. A total of eight Time Period Summaries were prepared, and are shown in Figures 7B.1 through 7B.8. Each summary figure consists of two sheets, labeled (a) and (b). Sheet (a) shows the excavation’s geometry on the pertinent date and indicates the construction activities that occurred since the date of the previous summary. Sheet (b) shows surface settlements and inclinometer deflections for the given date. The remaining instrumentation data from heave gages, observation wells, and piezometers can be found in the data-vs.-time plots presented in the Figure 7A series.

Each Time Period Summary, therefore, represents a single date in the excavation history at ISS-4, and summarizes developments that occurred throughout a block, or “step”, of time between that date and the date of the previous Summary. The eight Time Period Summaries together cover the entire sequence of construction events at ISS-4, up to the pouring of the concrete invert slabs.

The dates that served as divisions between “Steps” were chosen carefully. Utilizing arbitrary increments of time, such as two month periods, was initially considered but eventually presented serious problems. It was desired to make Time Period Summaries that were “self-contained”. This means that each one would show changes that resulted

only from the construction events that occurred during that “step” of time. As it turned out, matching the instrumentation monitoring schedules to the construction sequence was a complicated task. The problem was that most inclinometers and settlement points had completely independent monitoring schedules, and the monitoring frequencies were quite variable. Frequently, most of the instruments would be read shortly after a particular excavation event, except for one or more which were not read until several days or even weeks later, by which time another excavation event had occurred. The eight selected dates provided readings from every inclinometer and DMP within a short enough period of time that no excavation events occurred between monitoring dates for these instruments. Thus all of the soil movements shown in a given summary were influenced equally by only the excavation events shown in that summary.

Together, Figures 7B.2-a and -b comprise a single Time Period Summary, and serve to illustrate the major features of the summaries. Sheet (a) shows the condition of the support system and excavation on June 29, 1993, which was selected as the final date of the “Step 2.0” time period. The geometry of the subgrade as it existed on this date is shown by the solid line inside the excavation. Dotted lines inside the excavation define individual lifts that were excavated during the Step 2.0 time interval, between the end of the Step 1.0 interval (May 7, 1993) and the end of Step 2.0. The inclined lines behind the support walls and outside of the cut represent tiebacks. A single solid line indicates the drilling of holes for that tier of tiebacks and the placement of steel tendons within the hole. The presence of a thicker zone at the end of a tieback line indicates that the tiebacks at that level have been grouted and locked off. All construction activities that took place during the Step 2.0 time interval are listed in the box on the upper right-hand corner of sheet (a). The sheet also includes the positions and depths of all geotechnical instruments at the cross-section.

Sheet (b) presents surface settlements and lateral inclinometer deflections measured during the Step 2.0 time interval. Settlements are plotted against distance from the excavation’s edge on the upper part of the sheet. The excavation depth and installed tiebacks at the end of Step 2.0 are illustrated on the inclinometer plots.

7.2. DISCUSSION OF INSTRUMENTATION DATA

This section will discuss the behavior of the ISS-4 excavation support system, the soil movements around and inside the cut, and the changing groundwater conditions, as measured by the geotechnical instruments emplaced in the area. The discussion is divided into three subsections which deal with different instrument types, purposes, or locations. The first part of the discussion deals with wall movements and surficial settlements at and behind the SOE walls, and will focus first on the area north of the excavation, and then on the area to the south. The second part deals with pore pressures and groundwater levels to either side of the excavation and in the confined aquifer underneath it. Finally the third part involves instrumentation inside of the cut, including heave gages and piezometers in the clay. In each subsection, events will be described in roughly chronological order.

7.2.1. Settlements and Wall Movements

7.2.1.1. North side of excavation (behind concrete diaphragm wall)

Figure 7A.1 shows lateral deflections plotted against time for the Building A slurry wall, measured by Inclinator INC-102, which exists within the wall. Settlements behind slurry wall A, measured on and near Building A, are plotted against time in Figure 7A.4.

As shown in Table A.2, the first settlement measurements from three of the six settlement points were taken in August and September of 1992. The other three DMP's were not monitored until March 17, 1993, which was selected as the reference "zero" reading for Figure 7A.4 because it was desired to reference all six DMP's to the same date and this provided the first chance to do so. The figure shows that approximately one half inch of settlement had occurred at DMP2-006 and DMP4-120 (the settlement points closest to the excavation) before any construction work at ISS-4 had even started. Most of this settlement appears to have occurred in late January 1993, which coincided with a sharp drawdown of over 30 ft in the lower aquifer, shown in Figure 7A.7. This drawdown resulted from the initiation of pressure relief dewatering activities, and is described further in Section 7.2.2. Resulting minor compression of the granular glacial deposits comprising the lower aquifer, in conjunction with partial consolidation near the bottom of the marine clay, are possible causes of this early half-inch of settlement seen behind the north wall.

While slight settlements were occurring over the long term before excavation commenced, it can be seen from Figure 7A.4 that the installation of slurry wall A, in late March and early April of 1993, resulted in little to no nearby settlement. Clough & Davidson (1977) state that construction of a slurry wall can lead to nearby soil movements resulting from loosening of soil at the sides of the trench. However, the construction of this slurry wall resulted in little to no nearby ground losses and deformations.

The first reading of INC-102 was taken on 5/7/93, about two days after the first lift along the wall was excavated. Figure 7B.1-b, from Time Period Summary number 1.0, shows that the slurry wall had not deflected appreciably by that date. A half inch of deflection into the retained soil was measured along the entire wall, quickly sloping back to zero below Elevation -1; this appears to be an artifact of either the data processing or the concrete mix setting up, and is not considered to represent actual soil movements.

The excavation of the first lift at the north wall caused the slurry wall to deflect inwards (meaning, in the direction of the excavation) by about one half inch on 5/25. The inclinometer trace, illustrated in the Step 2.0 Time Period Summary (Figure 7B.2-b), shows that slight cantilever movement occurred. By the time of the 6/29 reading at INC-102, the first tier of tiebacks had been locked off, the second lift had been excavated (to El. 92), and the second tier of tiebacks installed. The combined effect on the wall from all these activities is revealed in the 6/29 trace, shown in the Step 2.0 summary. The top of the wall had bent back into the retained soil by one inch, due to the force from the locked-off first tier of tiebacks. The wall appears to have experienced an almost negligible inward deflection of, at most, one quarter of an inch about twenty feet below the second lift subgrade. This mode of deflection was representative of the slurry wall's behavior throughout the rest of the excavation history: the wall experienced little to no deflection inwards toward the cut, but instead was pulled back into the soil mass by tieback forces. Time Period Summaries for Steps 2.0 through 6.0 show continued deflection of the top of the wall back into the soil, reaching over two inches after lock-off of Tier 2, nearly four inches after lock-off of Tier 3, and increasing to almost five inches by October 6 (Step 6.0, in Figure 7B.6-b).

Surface settlements had reached nearly two inches behind the North wall by 6/25. As was true for the inclinometer data, the settlement distribution measured on 6/25 was similar to those that were measured throughout the rest of the excavation process, a point which is reinforced by the graph of settlements vs. time in Figure 7A.4. The settlement trough on 6/25, illustrated in the Time Period Summary for Step 2.0 (Figure 7B.2-b), tapers off from a two-inch maximum deflection measured by the DMP's closest to the excavation's edge, to little or no settlements measured at the DMP's on the far side of Building A. This settlement trough deepened as the excavation continued, until by Step 6.0, on October 5, the maximum measured settlement was in excess of four inches close to the wall, tapering off to half an inch at the far side of the building, 150 feet from the excavation's edge.

The combination of substantial surface settlements and negative wall deflections (back into the retained soil mass) is not encountered in the existing literature. Case studies reveal that positive settlements behind diaphragm walls are generally accompanied by inward wall movements. Milligan (1983) used theoretical considerations to show that the profiles of wall deflections and surface settlements would be equivalent for an undrained (constant volume) excavation in soft, homogeneous clays. This leads to the expectation that wall "pull-back", or negative deflection, would be accompanied by heave, rather than settlement, behind the wall. The reason for the opposite occurring at slurry wall A must be attributable to other 'construction factors'. Construction activities are well known to contribute to soil movements, as much as or even more than the effects of excavation unloading alone (Clough & Davidson, 1977; Clough & O'Rourke, 1990). In this case, however, the tieback loads - which can be considered a 'construction factor' - were enough to not only resist the soil pressures, but in fact reverse the direction of wall movement.

The settlements might be attributed to two factors: first, groundwater drawdowns in the upper and lower aquifers (discussed further in Section 7.2.2), and second, soil disturbance during drilling for tieback installation. Section 3.4.2.2 described field observations of air and water escaping from adjacent tieback holes during drilling with a down-hole hammer and pressurized air, indicating drilling-induced disturbance and

fracturing of the Marine Clay. This disturbance could have induced sudden porewater pressure increases, leading to consolidation settlements as the pressures subsequently dissipated.

The plots of wall deflections and settlements against time suggest, to some extent, a correlation between deformations and the cycles of tieback excavation, installation, and lock-off. In the case of the wall movements, the correlation is fairly clear. Figure 7A.1 shows quick increases in 'pull-back' wall deflections of at least one inch occurring on tieback lock-off dates for tiers 2 and 3. Similar movement is not seen for the Tier 1 lockoff, possibly because the effect was masked by other events (such as the excavation of Lift 2) which occurred during the four week span between the consecutive monitoring dates of 5/25 and 6/22. Before the Tier 2 lock-off, between the Tier 2 and Tier 3 lock-offs, and following the Tier 3 lock-off, the wall continued to deflect, but at a slower rate.

These trends are more subtle for the surface settlements (Figure 7A.4), but are discernible upon close study of the graphs. In this case, the settlement rate tended to increase between tieback installation and lock-off, and then slow down after lock-off was performed. The indication that accelerated settlements follow tieback installations, rather than lift excavations, suggests that ground loss during drilling was the main cause of settlements, rather than excavation-induced strains in the soil mass. The trend can be seen faintly for the three DMP's nearest to the cut (DMP2-006, DMP2-107, and DMP4-120), between Tier 1 installation in late May and Tier 2 lock-off at the start of July. The aforementioned effect is not so apparent, however, for the Tier 3 events, during which the settlements increased at a fairly consistent rate.

After Tier 3 lock-offs in August of 1993, excavation-related activity at ISS-4 was halted for several months. The graphs of wall deformations and surface settlements against time, however, show that deflections continued to occur during this time period, albeit at a lessened rate. The top of the slurry wall continued to move gradually back into the soil; at the elevation of Tier 1, the deflection increased from 4.6 inches on October 1, to 5.3 inches on March 1, 1994, when excavation resumed, reaching final subgrade. Lower points on the wall underwent negligible deflections during this period.

Meanwhile, Figure 7A.4 also shows continued movements of all six DMP's after lock-off of Tier 3 was completed. During this period, settlements occurred at rates that appear to decrease with distance from the wall, thus increasing the total differential settlement experienced by the Building A. However, these differential settlements increased at a slower rate than they did during the excavation phase. The latter part of the graph shows settlement curves that appear to reflect exponential decay toward an asymptote; suggesting the possibility that the continued settlements are the result of consolidation in the clays, caused both by pumping from the lower aquifer and by dissipation of disturbance-induced excess pore pressures in the drilled regions of the clay.

In summary, the settlement curves can be divided into three parts. The first part covers the period of time preceding excavation, up until May of 1993. During that time, very slight settlements developed equally at all six DMP's, not exceeding one half inch, and which appear to be related to pumping from the deep aquifer. The second phase occurred between the beginning of May and the end of September, when the first three lifts were excavated. This period was distinguished by differential settlements, as points close to the wall settled substantially faster than points far from the wall. Differential settlements across Building A reached four inches by the start of October. This settlement phase may be related to loss of ground caused by installation of the tiebacks. Finally, the third settlement phase involved a gradual tapering off of settlement rates and a substantially reduced rate of differential settlement which appears to be related to consolidation-type settlements due to soil disturbance from tieback installation and to deep pumping.

Excavation to the final subgrade elevation of 69 ft occurred on March 2, 1993. The settlements were not visibly affected by this excavation, but Figure 7A.1 shows that there was a slight increase in inward wall movements at and below subgrade elevations. This is indicative of very slight bowing of the slurry wall.

7.2.1.2. South side of excavation (behind sheetpile wall)

Two inclinometers were emplaced behind the south wall at ISS-4. One of them, INC-101, was two feet behind the sheetpile wall, while the other, IPE-113, was about 26

feet back from the wall. Graphs of lateral deflections vs. time as measured by each instrument are shown in Figures 7A.2 and 7A.3, respectively. Since IPE-113 was also a probe extensometer, it was capable of measuring settlements below the surface at a number of different depths. Figure 7A.6 contains a graph of settlements vs. time for selected IPE-113 spider magnets, at the top, middle, and base of the Boston Blue Clay deposit. Figure 7A.5 shows surface settlements at three DMP's behind the south wall plotted against time. All three were Type-4 DMP's, meaning that they were emplaced in the ground surface rather than in building sides (See description in Appendix A).

In general, movements at and behind the South wall of ISS-4 were more complex than those seen on the North side and discussed in Section 7.2.1.1. In fact, there are a few instances of wall and soil movements that are rather difficult to explain. The following paragraphs will review the instrumentation measurements and discuss possible explanations for what was seen.

The three DMP's, DMP4-116, 117, and 118, were all surveyed for the first time on September 4, 1992. This date is therefore used as the reference 'time zero' on the Figure 7A.5 graph. This graph shows the gradual development of approximately one inch of settlement at all three DMP's before excavation began in late March of 1993, which is similar to, but in excess of, initial settlements that occurred at Building A (Figure 7A.4). A half inch of the south side's settlements occurred relatively quickly in mid-January of 1993, corresponding to a sudden drawdown of pore pressures in the lower aquifer (Figure 7A.11). As was discussed for Building A, the pre-excavation settlements can be partially attributed to consolidation and compression of the clay and underlying glacial soils.

The sheetpile wall at ISS-4 was driven in December, 1992, as indicated on the timelines. The sheetpile driving activities appear to have had little effect on adjacent settlements either at the surface (Figure 7A.5) or at depth, as indicated by IPE-113 spider magnets (Figure 7A.6).

Excavation of the first lift along the South wall, to an elevation of 100 ft, caused one inch of cantilever-type deflection at the top of the sheetpile wall. This is shown by the INC-101 trace measured on 4/6 and illustrated in the Time Period Summary for Step 1.0 (Figure 7B.1-b). The actual deflection that occurred in response to this excavation

increment may have been greater than indicated by the 4/6 inclinometer trace, since the instrument's formal initial reading was taken two days after the excavation was made.

Subsequent lock-off of Tier 1 tiebacks pulled the top of the wall back to its original position, as can be seen on the 6/9 trace in the Step 2.0 plots (Figure 7B.2-b). When the second lift was excavated, on June 15, INC-101 bulged outward about 1.5 inches at the second tier subgrade by 6/29. This change in deformation style from 'cantilever' to 'bulging' as the cut deepened was in accordance with trends for braced excavations described by O'Rourke (1981) and Clough & O'Rourke (1990).

Meanwhile, by the time the second lift had been excavated, IPE-113 had moved toward the excavation by about one inch at the top. In addition, the instrument had started to experience a slight 'waviness', apparent in all three traces illustrated in Figure 7B.2-b. Such a deflection pattern probably did not reflect soil movements, but was more likely a byproduct of the instrument's installation. "Waviness" was frequently seen in the Inclinometer/Probe Extensometers at this construction project. It was attributed to the relatively soft annular grout in the borehole (as required by the installation specifications), which allowed flexure of the inclinometer casing. Further discussion of the "warping" phenomenon among the IPE's appears in Appendix A.

On 7/9, IPE-113 developed a pronounced 'kink', which, in this case, can be attributed to construction activities rather than to characteristics of the instrument itself. The plot for IPE-113 which appears in the Step 3.0 Time Period Summary (Figure 7B.3-b) includes locations of the tiebacks. It is apparent that the 1.5-inch kink at Elevation 80 is aligned with the second level of tiebacks behind the sheetpile wall. The kink appeared between the dates of 6/29 and 7/9, and the second tier of tiebacks was installed on 7/1, so the kink probably reflects disturbance to the instrument caused by the drilling of a nearby tieback hole. The IPE-113 probe extensometer (settlement measurements) showed a slight effect from the second tier tieback installation, as well: a half inch of settlement occurred at the top of the Marine Clay on the date of second tier installation (See Figure 7A.6). This amount of settlement exceeds the downward component of the casing flexure at that elevation, and can therefore be considered to represent "actual" soil settlement.

Installation of the third tier of tiebacks did not cause any additional kinks in the casing, as shown in the traces on the Step 5.0 Time Period Summary (Figure 7B.5-b). The second and third tier tiebacks were placed in horizontal alignment, so the instrument was theoretically equidistant from tiebacks in both. However, it is possible that the advancement of casing for the Tier 2 tiebacks is what caused the kink at that time. Since IPE-113 appears to “intersect” the third tier tiebacks near the top of the bonded zone (see (a) sheets of the 7B. series), the casing would not have been advanced past the instrument during installation of this tier. This may explain why a similar kink was not seen during Tier 3 installation.

While no ‘kinking’ was seen, the probe extensometer did show developing settlements at the top of the clay around the time of third tier tieback installation (Figure 7A.6). Settlement here increased by nearly a full inch, and by lesser amounts throughout the deposit. It is hard to tell if these movements were responses to the tieback installation or to the excavation of the third lift, since both events occurred within a few days of each other.

The graph of wall deflections vs. time is characterized by two periods of accelerated wall deflections, clearly shown in Figure 7A.2. The first event occurred in July and saw the wall bow outward by a maximum of nearly 3.5 inches at the intermediate subgrade level (El.90). See Step 4.0 (Figure 7B.4-b) for an illustration of the wall’s deflection on 7/21. The second deformation event occurred in late August, and involved an increase in wall deflections to over five inches. This event appears from Figure 7A.2 to be the more drastic of the two, since lateral deflections increased by as much as three inches between consecutive readings. Figure 7B.5-b (the Step 5.0 Time Period Summary) provides a clear illustration of the increased wall movement that occurred between 8/9 and 9/2.

Both deflection events started after excavation of a new lift and peaked before lock-off of the tiebacks at that level. In both cases, consecutive inclinometer readings were taken on dates before and after the lock-offs, and the measured deflections after the lock-offs were nearly equal to or less than the deflections before. For example, the second tier tiebacks were locked off on July 30 and 31, and the consecutive inclinometer data points

from 7/21 and 8/5 indicate that the stressing of tiebacks reversed the direction of wall deformation. In a similar fashion, the third tier lock-off period of September 17 through 20 was immediately followed by a reading on 9/21, which showed, once again, stoppage or reversal of the previously developing deflections recorded on 9/2.

The fact that the increases in wall deflection for the second and third lifts correlate with excavation events is evidence that they reflect the reaction of the retained soil mass to excavation unloading. The continued, gradual development of lateral deflections which peaked in late July may be indicative of time-dependent continuing 'creep'-like behavior. The nature of movements leading up to and following the early September peak is more difficult to determine due to the infrequency of inclinometer readings during this period, but they may have been similar to events during the July event.

More information on the causes of these increased deflections is provided by study of the other instruments. Some substantial and surprising differences are revealed between the two wall deformation events. The July event was evident not only at INC-101, but also in the lateral deflections of IPE-113 and the surface settlements (Figure 7A.3 and 7A.5, respectively). IPE-113 moved an additional 1.5 inches toward the cut, while DMP-118 and 117 underwent a half inch of settlement. Such associated settlements and lateral deformations adjacent to a deep excavation are consistent with large-scale movements within the soil mass. The August deformation event, on the other hand, was curiously "unrepresented" in the plots of surface settlements and IPE-113 lateral deflections, which is especially surprising considering the magnitude of the event as measured at INC-102. The IPE-113 probe extensometer magnets did show approximately one inch of added clay settlement in late August; it is hard to explain why there were no accompanying large surface settlements (e.g., Figure 7A.5) or increased movements at the rest of the instruments, unless the apparent movement was due to data inaccuracy.

After excavation of the cut's central portion from El. 85 to El. 78 in late September for regrading of a mid-excavation haul road (See Step 6.0, Figure 7B.6), about five months passed without any further excavation or tieback installation occurring at ISS-4. During this period, surface settlements continued to gradually increase at a constant rate for all three DMP's, as Figure 7A.5 illustrates. While Building A experienced

continued differential settlement at that time, the south side of the excavation was experiencing “global” settlements. The continuing settlements were possibly the result of ongoing compression and consolidation of the underlying soils from pumping-induced pore pressure reductions and groundwater drawdown. The installation of the tiedowns, which caused intermittent hydraulic depressurizations, also may have been a contributing factor. The different settlement behaviors on the two sides of the excavation might be attributable to the different degrees of soil disturbance induced in the overburden soils by tieback drilling. Whereas the drilling of tiebacks at slurry wall A might have involved a great deal of disturbance and fracturing within the organic and BBC deposits, the tieback holes behind the south wall were drilled with a drag bit and water wash, which provided a ‘cleaner’ cut through the overburden soils and upper clay.

Meanwhile, the two inclinometers experienced slight to negligible deflection through the last months of 1993. Following this period of low activity, the sheetpile wall experienced increased movement during the first two months of 1994: as Figure 7A.2 shows, Inclinometer 101 moved an inch and a half at the elevation of the upper tiebacks between late December of 1993 and early March of 1994, with appreciable but smaller movements at the other levels as well. The increased movement appears to have started at the very end of December 1993, but the rate of movement is difficult to define because of the lack of data between early January and early March of 1994. In a similar fashion, IPE-113 underwent an increased rate of movement beginning in mid-January of 1994 (Figure 7A.3). Both events occurred well before the final lift was excavated, and the only construction activity that occurred at ISS-4 at the times of increased movements was the driving of tiedown casings in December. However, anomalous inclinometer behavior (i.e., “spikes” of outward movement) was observed on numerous occasions during tiedown installation. This behavior might have been caused by the observed artesian flow from the tiedown holes prior to grouting and reduction of the water pressures acting on the passive side of the retaining walls.

In March of 1994, INC-101 underwent approximately one inch of ‘reversed’ movement back into the retained soil, at the elevation of Tier 1. Meanwhile, the other tiers did not experience any further deflection. The ‘reversed’ movement of the uppermost tier

is very odd; two possible causes - restressing of existing tiebacks or installation of new tiebacks -- are ruled out because neither activity was performed at this time.

7.2.2. Groundwater Levels Around and Below Excavation

The soil profile at ISS-4 and throughout the project alignment contains two aquifers separated by the highly impermeable aquitard of Boston Blue Clay (BBC). The upper aquifer consists of granular and cohesive fills which overlie the organic and marine deposits, while the lower aquifer is in the relatively permeable glacial deposits and weathered bedrock underlying the marine clay. The initial piezometric level in the upper aquifer was 106 ft, while in the lower aquifer, it was 100 ft. (See Section 5.2 for a more detailed discussion of initial piezometric elevations.)

The locations, depths, and identification numbers of the groundwater monitoring instruments are shown in the cross-section in Figure 6.1. This section will discuss measurements by instruments that are either above or below the BBC and represent groundwater conditions adjacent to and below the excavation. Figures 7A.7 through 7A.10 show graphs versus time of piezometric elevation measured by these instruments. A discussion of pore pressure measurements made within the clay on the inside of the excavation follows in Section 7.2.3.

7.2.2.1. Pore Pressures in the Lower Aquifer

Piezometric pressures in the lower aquifer were measured by four independent vibrating wire piezometers in the vicinity of ISS-4. Measurements from all four are plotted against time in Figure 7A.7. It is clear from this graph that pressures were essentially the same at all four piezometers, even though they were separated by an average distance of over 200 feet. This indicates that pore pressure fluctuations in the lower aquifer were transmitted rapidly throughout the area due to the high hydraulic diffusivities in the soils and upper bedrock beneath the clay. Hydraulic diffusivity is a measure of the rate at which a cone of pore pressure drawdown spreads radially outward from a point of pumping and is equal to the permeability divided by the storage coefficient (Fetter, 1988).

The high measured diffusivities had the important ramification of making it very difficult to reduce pressures underneath the excavation without also causing large pressure reductions over a large distance outside of the excavation. Given the lateral spacing of the instruments, the pressure changes shown in Figure 7A.7 occurred over an area at least 400 ft wide. Therefore, they cover an area much larger than ISS-4 alone. They do not correlate to any excavation or construction events at ISS-4 or the surrounding area. For example, although the construction of Slurry Wall A involved penetration into the lower aquifer soils, its effect on the deep piezometric pressures was slight, at best. The piezometric pressures in the lower aquifer were instead most influenced by pumping of groundwater from the glacial soils, which was done in order to relieve hydrostatic pressures below the excavation (as discussed in Section 3.4). The pressure fluctuations reflect in a general sense the history of dewatering and pressure relief activities.

The first noteworthy event on Figure 7A.7 is a large 30- to 35-foot drop in the pore water elevation (PWE) to about 65 ft at the start of 1993. This drawdown was caused by the initiation of pressure relief pumping. In response to the large drawdowns, pressure relief pumping rates were reduced at the end of January, 1993. The reduction of pumping rates apparently helped to recover some of the lowered pressures, but the pressures remained depressed and continued to fluctuate erratically between PWE's of 75 and 90 ft, with sudden five- to ten-foot changes occurring frequently, for the rest of the monitoring history.

An added cause of sustained pressure reductions in the lower aquifer was "passive" flow from the upper well screens. This first occurred in early- to mid-1993, when the excavation reached a depth below the piezometric elevation of the lower aquifer (El. 100), allowing water from the lower aquifer to flow out of the exposed upper screens. Refer to Figure 3.11 for a diagram of the screened sections of the wells. In August, the contractor sealed off all exposed upper well screens with grout, thus stopping the "passive" flow.

7.2.2.2. *Groundwater Levels North of Excavation*

Groundwater pressures in the upper aquifer north of Slurry Wall were monitored at two depths. Observation Wells 002 and 016, plotted in Figure 7A.8, measured the elevation of the actual water table. VWPZ-67 and -68 were emplaced just above the Marine Clay, about 40 feet below the ground surface. These piezometers, plotted in Figure 7A.9, were essentially duplicates of one another, since they were in the same borehole and at the same elevation. The plots from the two are therefore equivalent.

The two observation well plots show that the water table was drawn down during excavation activities. OW-016 was nearer to the excavation than OW-002, and displayed three to four feet of drawdown, whereas OW-002 showed slightly less drawdown. The fact that drawdowns increased closer to the excavation wall suggests that groundwater may have been leaking into the cut. Project field engineers had observed slow leakage of this sort; e.g., through tieback holes or sheetpile interlocks.

Disregarding the numerous temporary water level fluctuations, the graphs in Figure 7A.8 can be divided roughly into three segments. The first segment precedes the start of excavation in May, 1993, and features a fairly constant water table elevation. Between May and the later months of 1993, the graphs slope downward as the water level gradually dropped, as mentioned previously. After excavation had ceased for a while, the water table reached a fairly constant value once again.

The graphs for VWPZ-67 and 68, the piezometers in the top of the clay (Figure 7A.9), underwent a similar history in which drawdowns occurred during the period of excavation and tapered off later. However, the plots for these instruments differed from the observation wells in that the total drawdown was substantially greater (11 feet by mid-1994), and that the drawdown developed over a different time scale. By August of 1993, the piezometers recorded a drawdown of about three to four feet, similar to what was measured by the observation wells. However, pore water pressures jumped about three feet in August, after which drawdown resumed along an exponentially decreasing curve. This suggests the development of an increasing hydraulic gradient downward through the upper aquifer, in response to the large pressure reductions that had occurred in the lower aquifer. Section 8.1.1 presents the results of calculations done to determine if the

drawdowns measured by VWPZ-67 and 68 could be attributed to drainage into the depressurized lower aquifer.

The large temporary increase which peaked at the beginning of September is difficult to explain. At its maximum value, the piezometric pressure increased by four or five feet; it then underwent a six-foot reduction through September. There is no comparable peak in the observation well measurements, which discounts the possibility of increased precipitation. One explanation for this temporary increase is that it was caused by the installation and grouting of nearby tiebacks. Immediately east of Slurry Wall A, between August 30 and September 3, the third tier of tiebacks was installed through the sheetpile wall. The sheetpile-wall tiebacks were pressure grouted in the upper part of the Marine Clay, within 50 ft of VWPZ-67 and 68, and the resulting temporary increase in local pore pressures may have influenced readings from these piezometers.

7.2.2.3. Groundwater Levels South of Excavation

Behind the south wall of ISS-4, there was only one instrument that monitored water levels in the upper aquifer: Open Standpipe Piezometer (OSPZ) 106. Measurements from OSPZ-106 are graphed in Figure 7A.10, and represent the elevation of the water table.

This instrument recorded a four- to five-foot drawdown that occurred at the time of the first lift excavation in late March of 1993. This event coincides with some larger, more sudden fluctuations in data, on the order of eight to ten feet, which are considered to be incorrect, anomalous data. After the four- to five-foot drawdown, water levels continued to undergo occasional fluctuations, but overall stayed relatively constant at an elevation of 102 feet. It is difficult to explain why there would be such a considerable reaction to the first lift excavation, but no changes in response to subsequent excavation events. One possibility is that excavation of the first lift exposed enough sheeting to permit leakage of water, which initially caused a sudden drop in groundwater levels. When the rate of leakage flow through the wall reached a steady value, the water levels could have stabilized at their lower value. Also, the presence of relatively impermeable cohesive fill

below about El. 100 could have limited the amount of groundwater drawdown resulting from wall leakage.

The four foot drop in PWE recorded in February of 1994 is considered to be anomalous.

7.2.3. Heave and Pore Pressures Within Excavation

The interior of the excavation at ISS-4 was instrumented with four multi-point heave gages and three pairs of vibrating wire piezometers. These instruments were installed to monitor pore pressure changes and heave in the basal soils in response to excavation unloading and hydrostatic uplift from pressures in the lower aquifer. Figures 7A.11 through 7A.14 show graphs of settlements vs. time, measured by the heave gages at three selected spider magnets located at the top, center, and bottom of the Boston Blue Clay. Figure 7A.18 is a plot showing spider magnet heave vs. depth, and provides added insight into the development of heave throughout the clay. Figures 7A.15 through 7A.17 are graphs of pore pressures in the clay as measured by the three pairs of piezometers. Refer to Figure 6.1 for the locations, elevations, and identification numbers of these instruments within the excavation.

The timelines below the instrumentation graphs illustrate the changing elevation of excavation subgrade. As Figure 6.8 showed, the cut was excavated in three separate zones, each covering approximately one-third of the total excavation width. Therefore there were three separate excavation histories that could be shown in the timelines. The histories that appear in each graph were chosen according to the positions of the instruments within the cut, and for instruments such as MPHG-110 which straddled two adjacent excavation zones, the timelines for both zones are provided.

The graphs from the four multi-point heave gages are all fairly similar, and show similar responses to construction events within the excavation at ISS-4. The graphs from the six piezometers are also quite similar to each other. Rather than presenting separate descriptions of heave gage and piezometer data, this section will discuss the two types of instruments together, which provides better insight into the reasons behind the soil's behavior.

Before excavation began in this area, there was little change in the spider magnet elevations except for slowly developing settlements measured at three of the instruments. By the time that the first lifts were excavated (between late March and mid-May), slightly less than one half inch of settlement was measured in the upper clay by Heave Gages 109 and 501, while MPHG-107 experienced a bit more than three quarters of an inch of settlement. These settlements were probably caused by ongoing consolidation of the BBC due to reduction of pore pressures in the underlying confined aquifer. The data from piezometers in the clay support the possibility of clay consolidation. The graphs for the three VWPZ pairs show, first of all, slight and gradual pore pressure reductions of around five feet before any excavation occurred; and second, a gradually increasing difference between pressures measured in the upper and lower piezometers in each of the three sets. Piezometric elevations in the upper piezometer exceeded those in the lower piezometer, indicating a downward hydraulic gradient in the clay which increased as the differential heads grew. This gradient would have developed as a response to the pressure reductions in the lower aquifer, and the decreased pore pressures in the clay would cause consolidation.

The MPHG's started to record heave in the clay once excavation commenced. While the excavation deepened, the rate of heave increased, in response to reduction of vertical overburden stresses in the clay. In a one-dimensional situation, a reduction of vertical stress will initially induce excess negative pore pressures in the soil. These negative pore pressures dissipate as water enters the soil matrix - essentially the reverse of consolidation drainage. The effective stresses decrease as dissipation occurs, resulting in expansion of the soil mass, or heave. The accelerated heave was particularly pronounced for MPHG-110 (Figure 7A.11), when the third lift was excavated from the northern portion of the cut, and for MPHG-501 (Figure 7A.13) in July and August of 1993.

It appears, in fact, that heave at the top of the clay accelerated at all four locations during July of 1993. This period coincides with lowered pumping rates from the lower aquifer, as indicated by the increase in PWE from 75 to 90 ft, shown on Figure 7A.7.

While the excavation deepened, pore pressures in the clay dropped at an increased rate, which is clearly reflected by the piezometer data. Such pressure reductions would be

expected in such an unloading scenario, as explained in the previous paragraph. The pore pressures appeared to undergo reductions whenever lifts were excavated, but remained relatively constant between excavation events. Section 8.1.2 discusses these unloading-induced pore pressure drawdowns in more detail.

The graphs of heave vs. time show a pair of sharp increases in heave rates in September and December of 1993, which exceeded previous movements recorded by these instruments. The first sharp increase was an inch to an inch and a half at the three remaining MPHGs and occurred in mid- to late-September. The second was of a similar or slightly greater magnitude and occurred in early- to mid-December. Meanwhile, pore pressures in piezometers 135 and 136 (Figure 7A.15) underwent sudden increases of 25 feet in late September and over 40 feet in December, the same times as the increased heave measurements.

These two instances of related clay heave and pore pressure increases can be correlated to events involving installation of boat section tiedowns by two different methods, as described in Section 3.4.3. The first event, in September, was very likely caused by local jet grouting for the creation of soilcrete columns that were supposed to serve in lieu of casings when tiedown holes were later drilled into bedrock. The injection of high-pressure jet grout into the clay would be expected to cause considerable disturbance to adjacent soils as well as immediate increases in pore pressure. The second event, in December, can be attributed to the driving of casings in the area, which was done after it was found that the jet-grouted columns were not functioning as well as originally anticipated. A sudden "spike" in pore pressures, followed by a more gradual drop-off, and a sharp increase in clay heave, are typical responses to pile-driving.

Although the tiedown installation activities affected all of the operating heave gages, they only had an effect on piezometers 135 and 136, while the other four did not record any similar pore pressure "spikes" (Figures 7A.16 and 7A.17). Whether or not the tiedown activities resulted in pore pressure "signatures" was probably a function of the proximity of the local tiedowns. The tiedowns were spaced 12 to 18 feet apart throughout the boat section, which limits the distance between a given piezometer and the nearest

tiedown. It seems likely that piezometers 131 through 134 just happened to lie far enough away from jet grout or pipe driving operations to not show any response to them.

In summary, the soil movements and pore pressure changes that occurred inside the clay and within the ISS-4 excavation were primarily influenced by three construction-related factors. The first of these factors was groundwater pumping from the lower aquifer by the contractor, which induced slight consolidation settlements in the BBC. The second was the reduction of vertical total stress by excavation unloading, which induced sudden pore pressure drops (or “increases in negative excess pore pressures”) that were followed by soil heave. The third factor was the preparation of tiedowns by two methods - jet grouting and casing driving - both of which left marked signatures on the data recorded by the heave gages and piezometers.

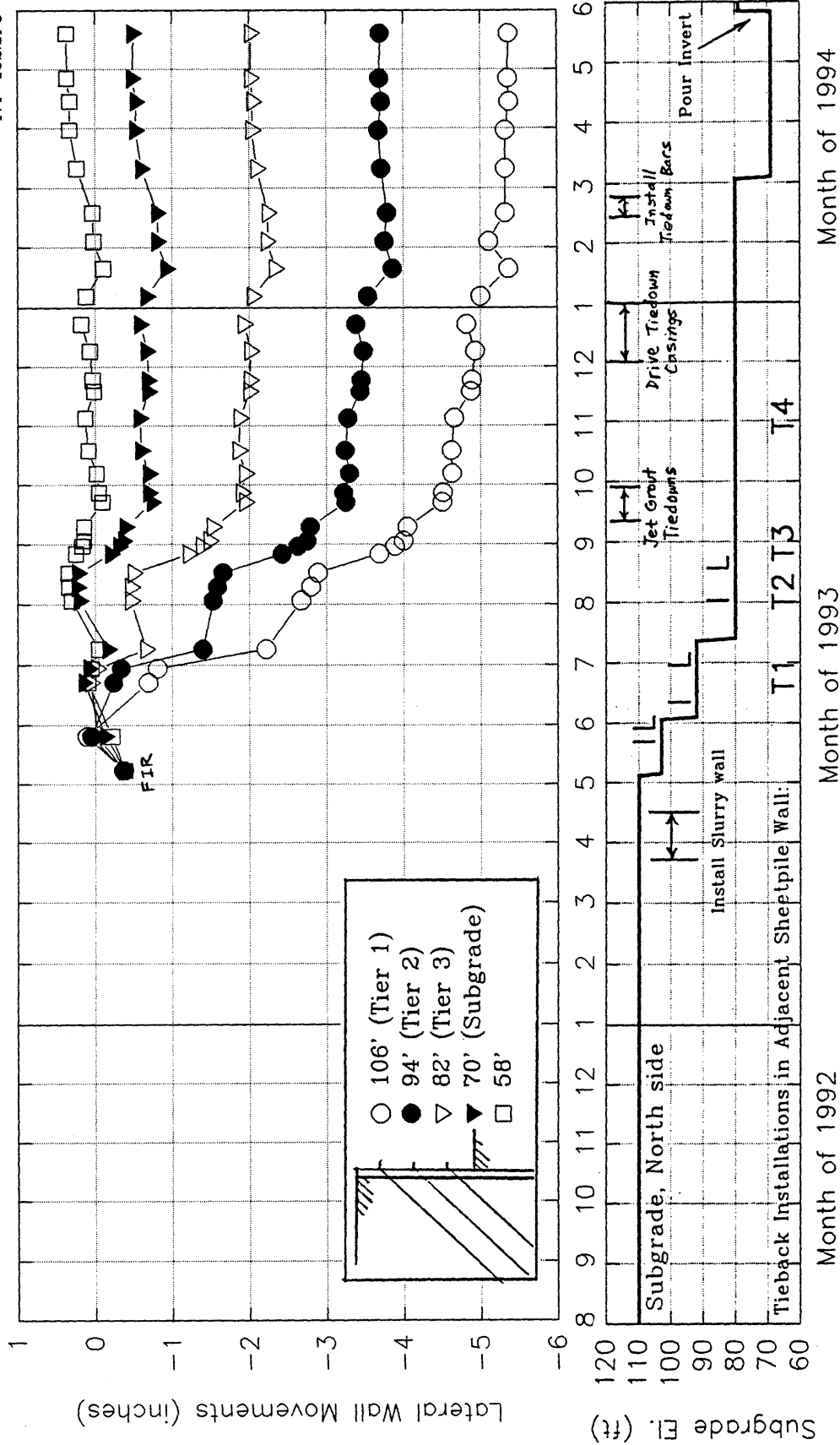


Figure 7A.1. Wall Deflections vs. Time, Measured by INC-102 (in Diaphragm Wall A)

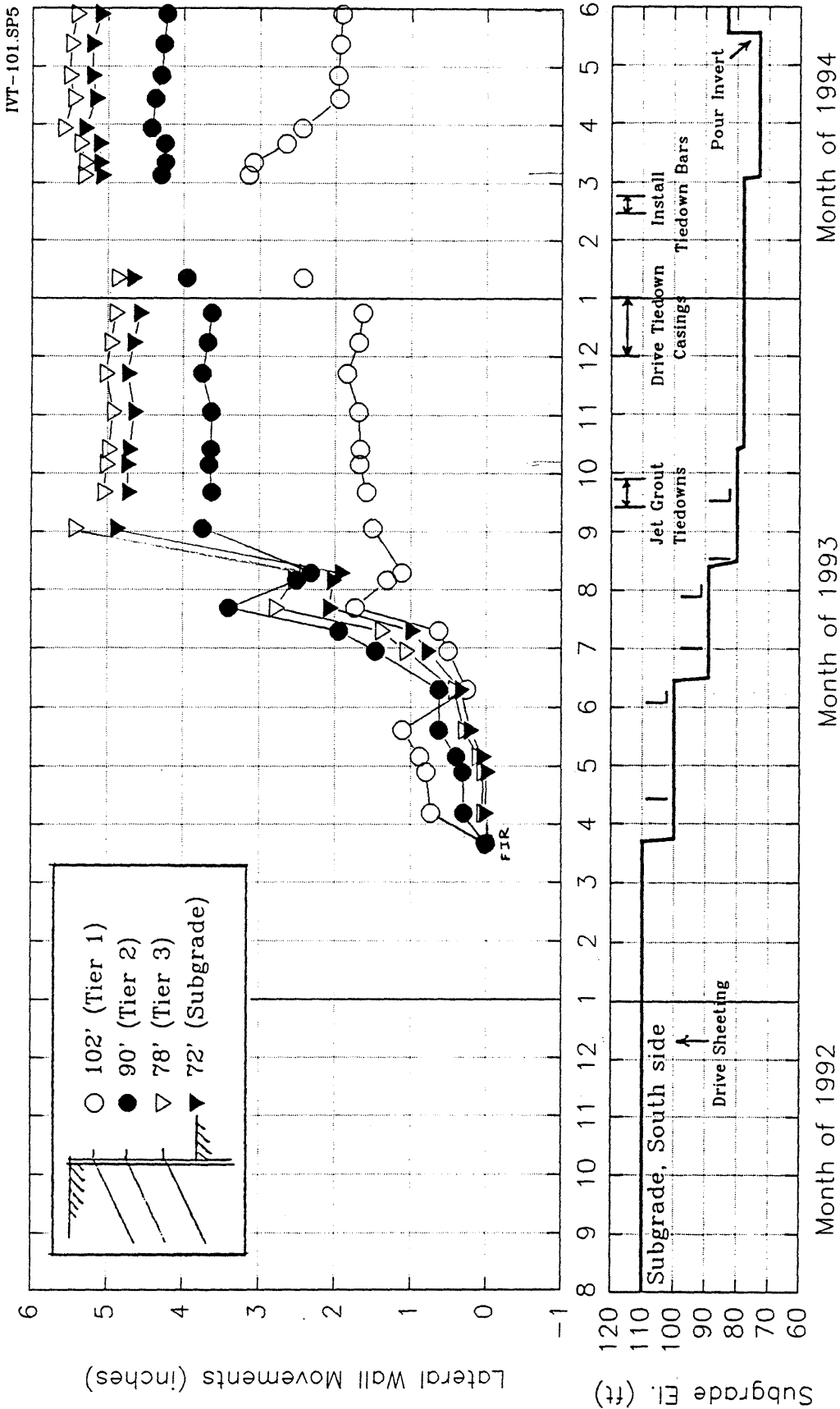


Figure 7A.2. Wall Deflections vs. Time, Measured by INC-101 (behind the south sheetpile wall).

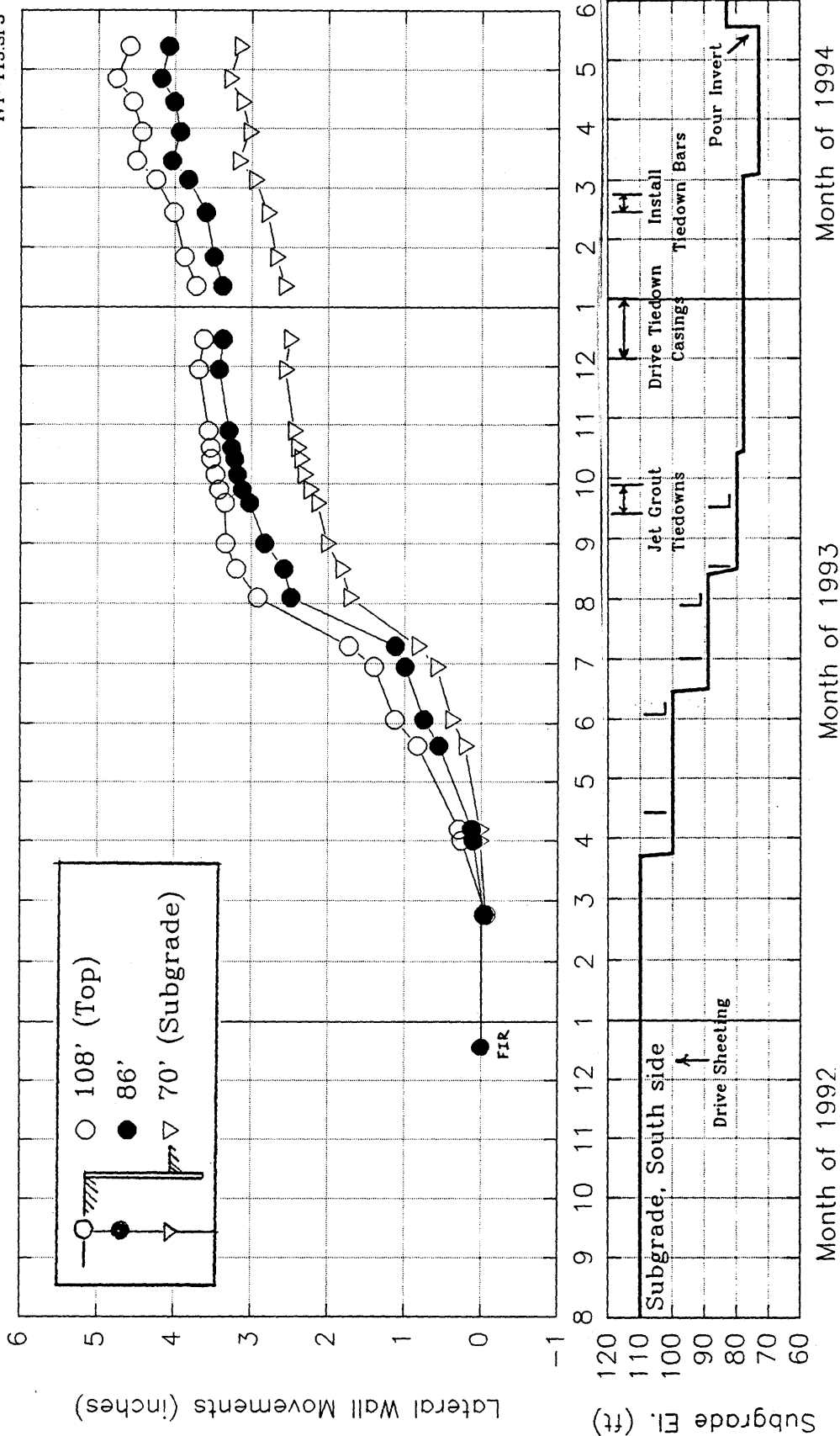


Figure 7A.3. Lateral Deflections vs. Time, Measured by IPE-113 (south of excavation).

S4-DMP-N-SP5

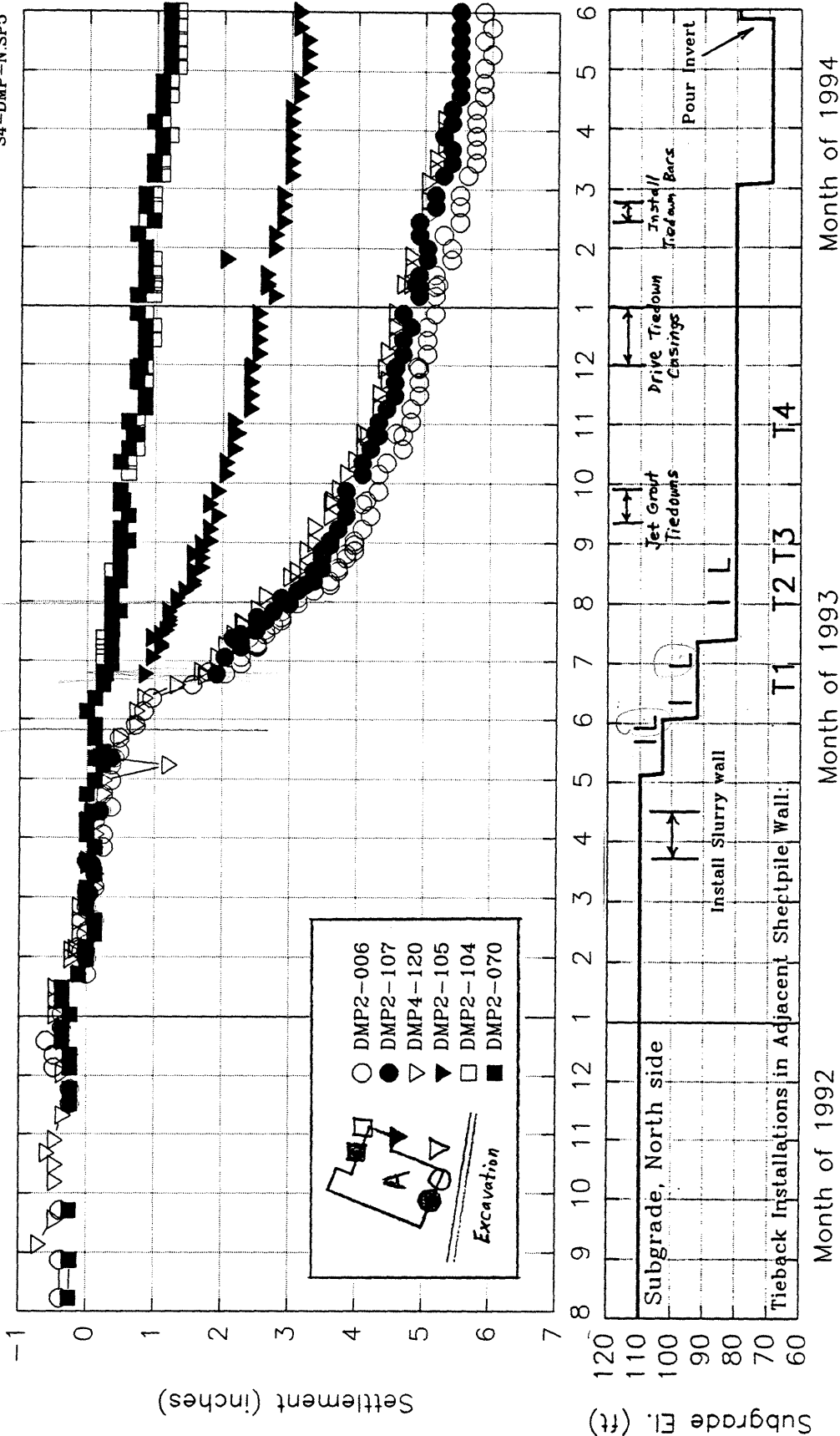


Figure 7A.4. Surface Settlements behind the North (diaphragm) Wall vs. Time.

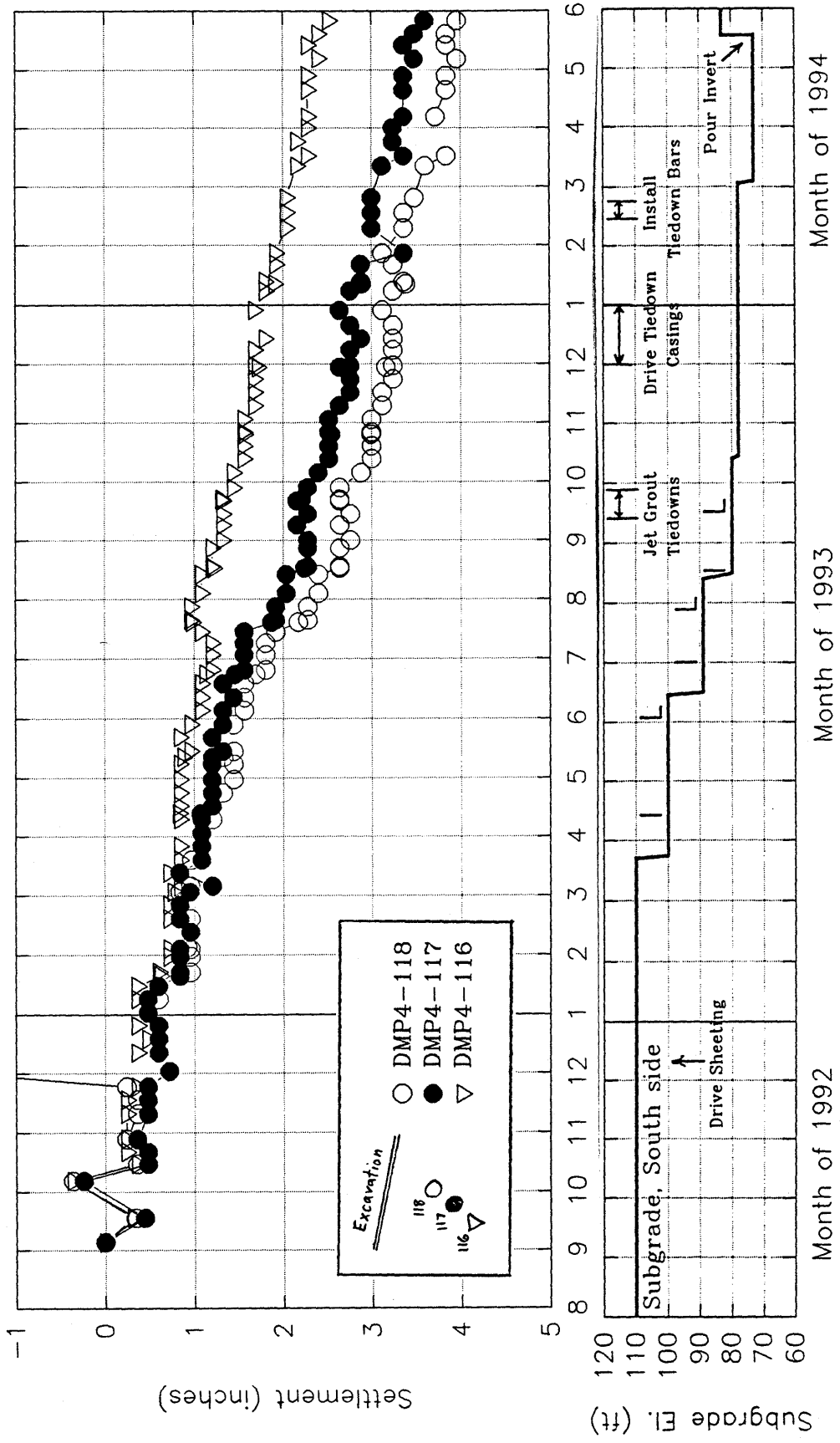


Figure 7A.5. Surface Settlements behind the South (sheetpile) Wall vs. Time.

IPE-113.SP5

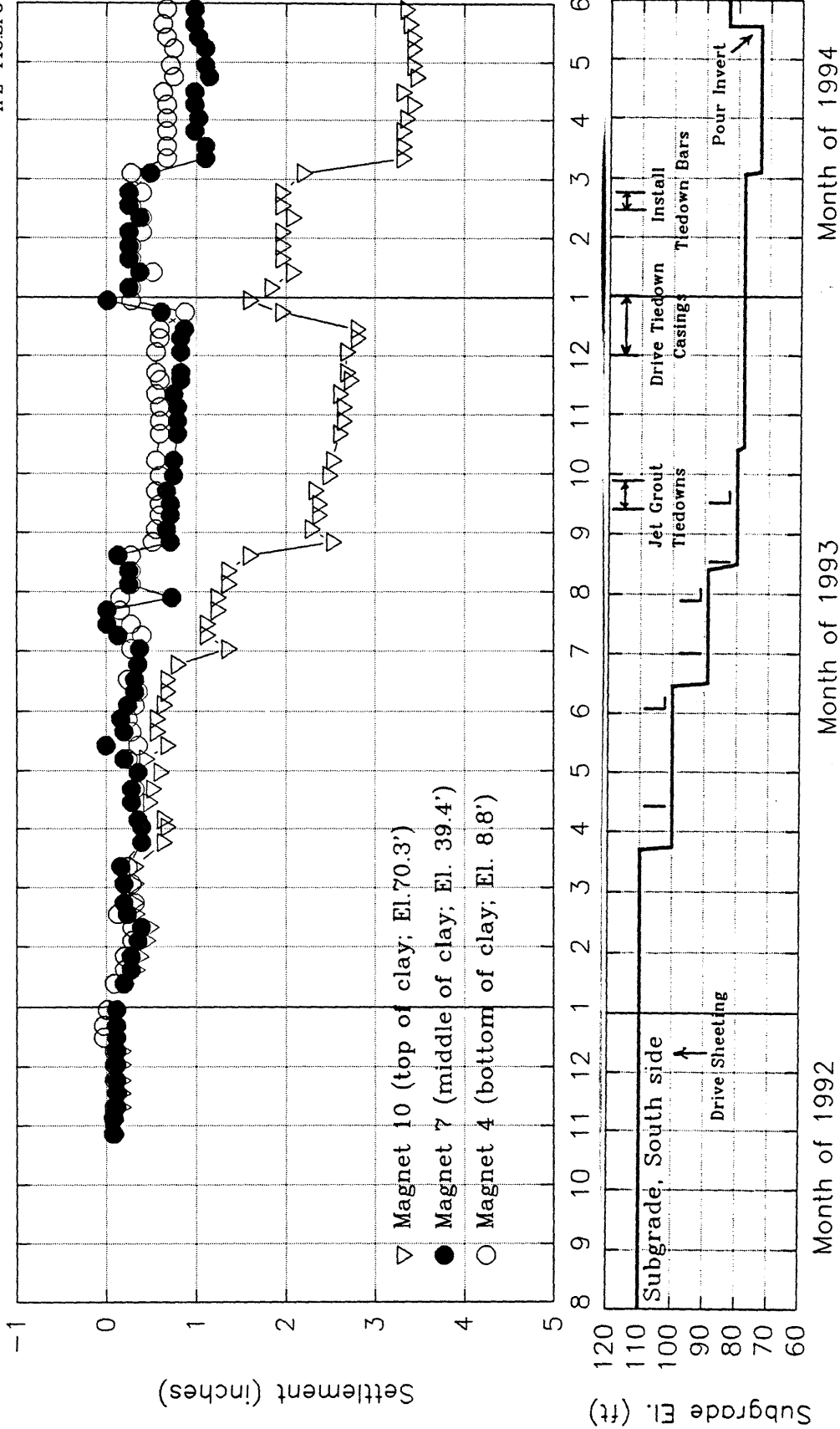


Figure 7A.6. Settlements Within the Boston Blue Clay, Measured by the IPE-113 Probe Extensometer (south of excavation).

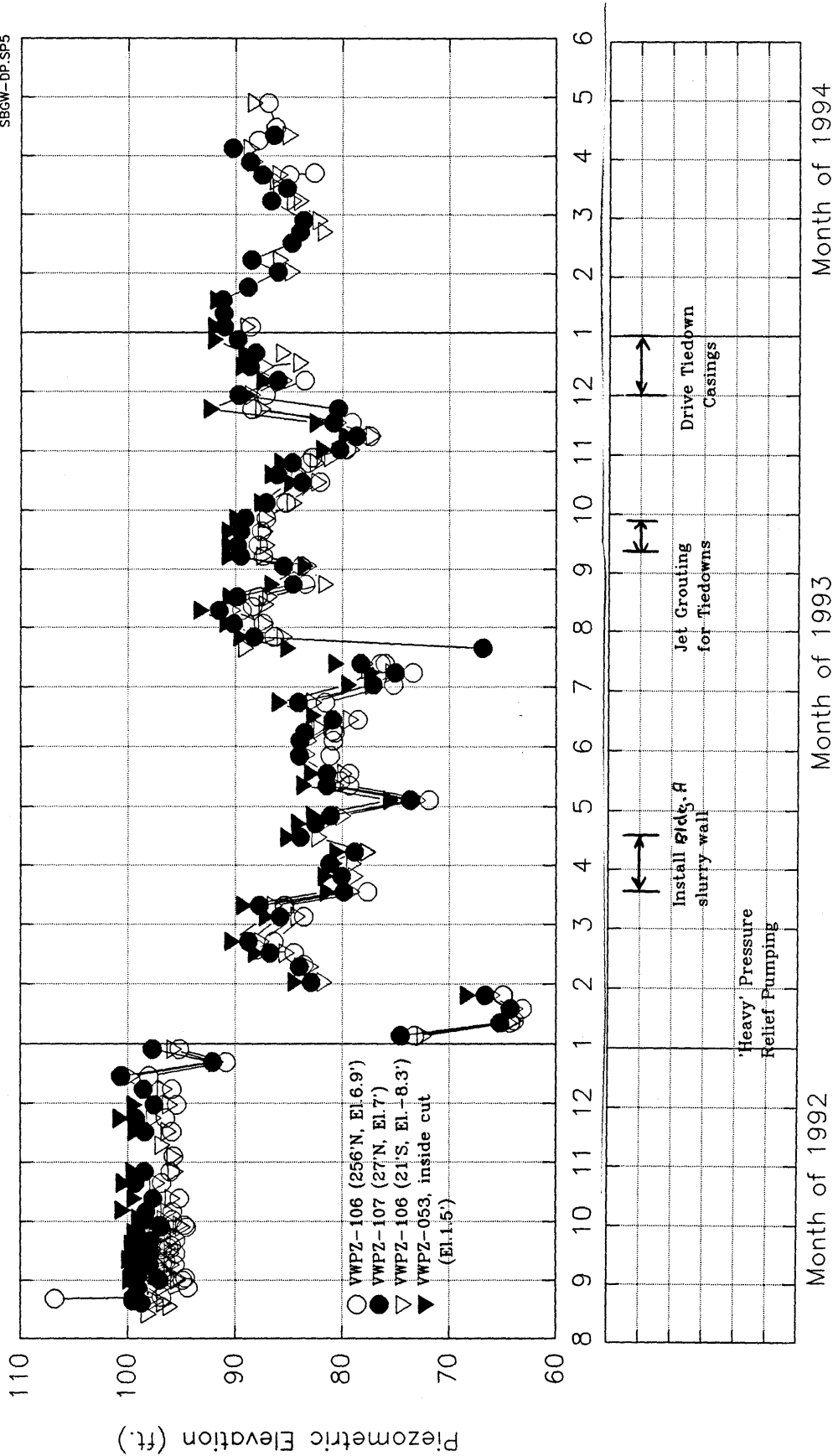


Figure 7A.7. Piezometric Pressures in the Lower Aquifer vs. Time, Measured by Four Deep Piezometers (below the BBC).

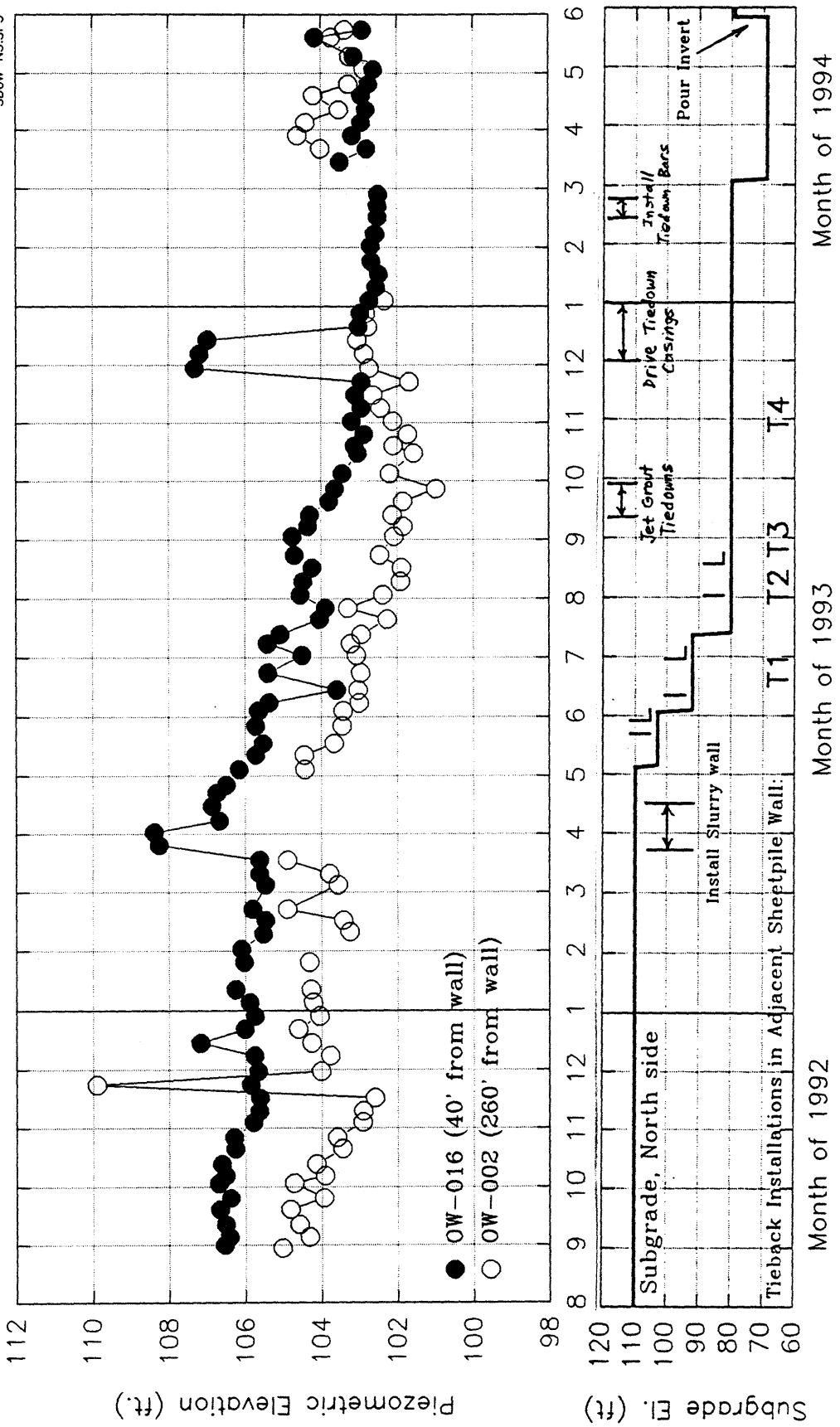


Figure 7A.8. Groundwater Level vs. Time, Measured by Shallow Observation Wells OW-002 and 016 (North side of excavation).

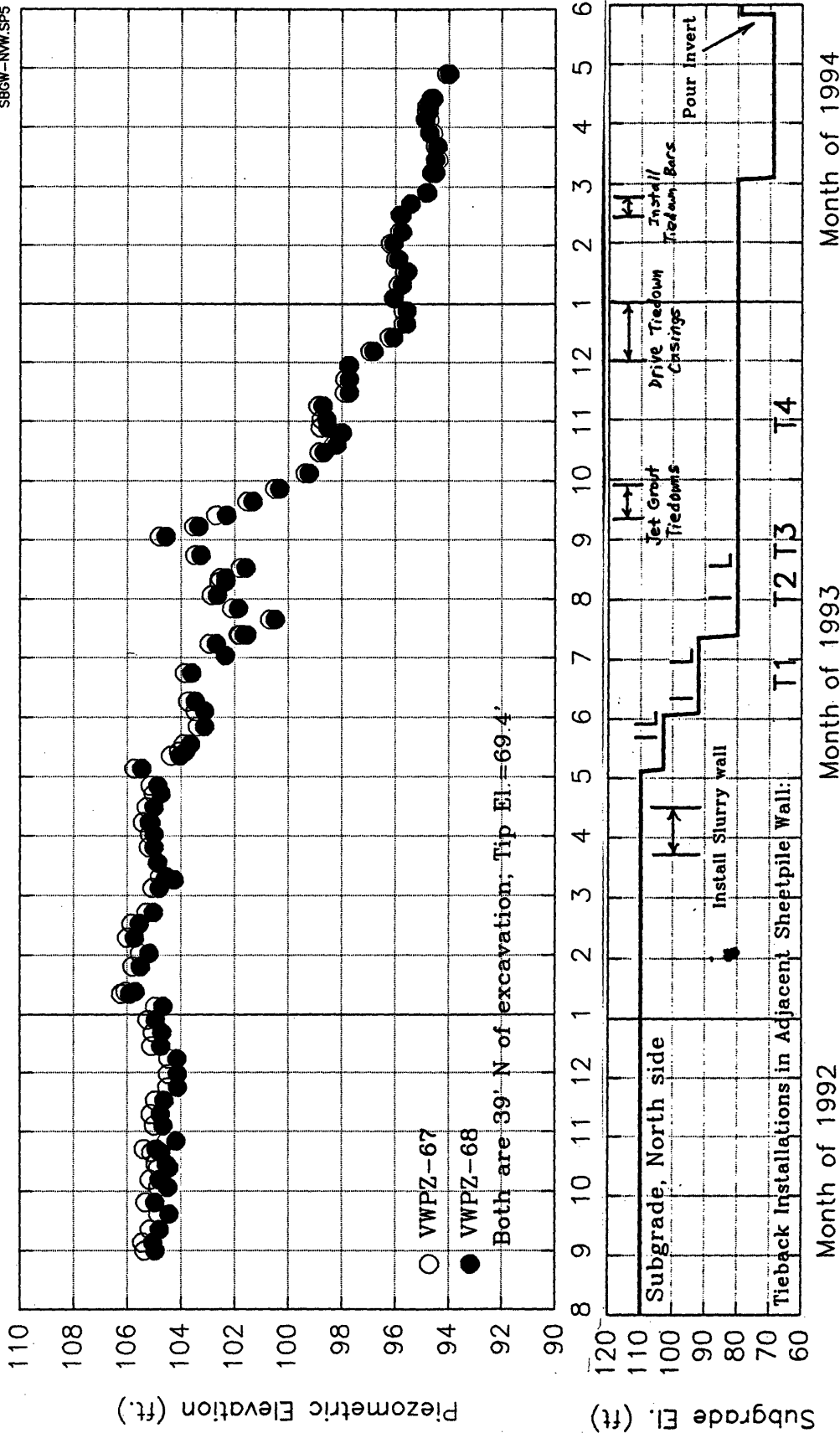


Figure 7A.9. Piezometric Pressures at Base of Upper Aquifer vs. Time, Measured by VWPZ-67 and 68, which have the same location and tip elevation. (North side of excavation)

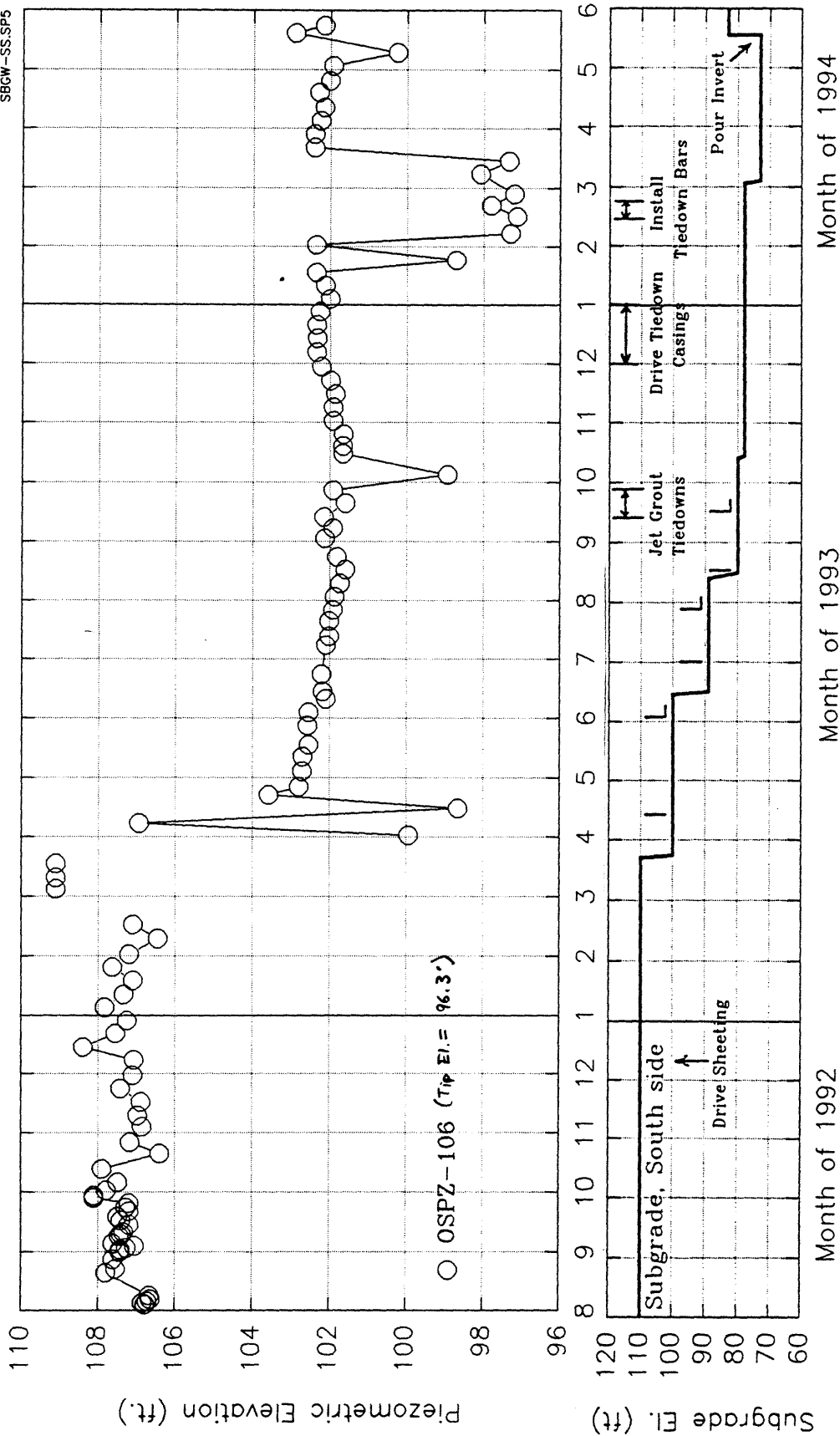


Figure 7A.10. Groundwater Level in Upper Aquifer vs. Time, Measured by OSPZ-106 (South side of excavation).

MPHG-110.SP5

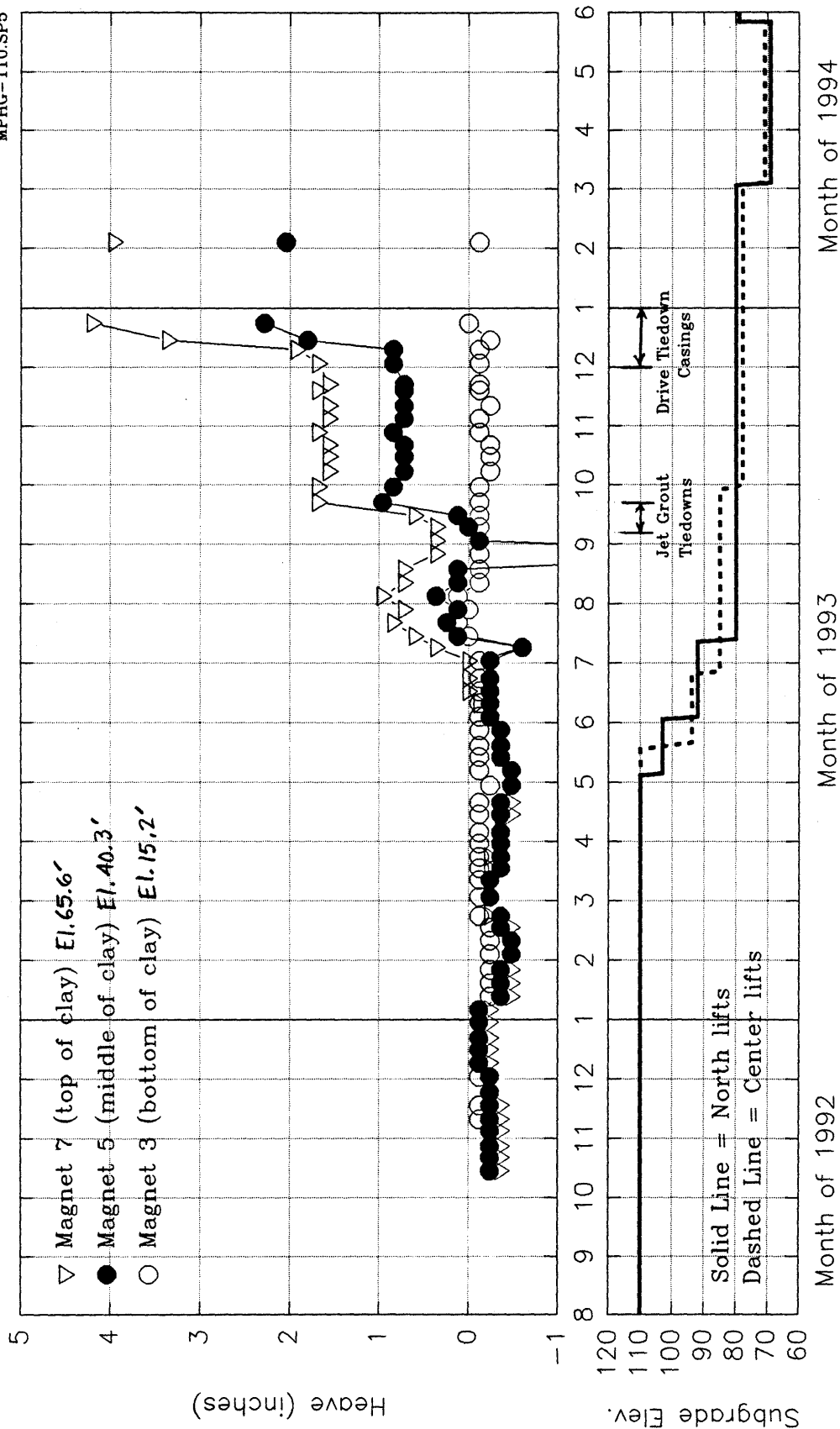


Figure 7A.11. Marine Clay Heave vs. Time, Measured by MPHG-110 (inside of excavation).

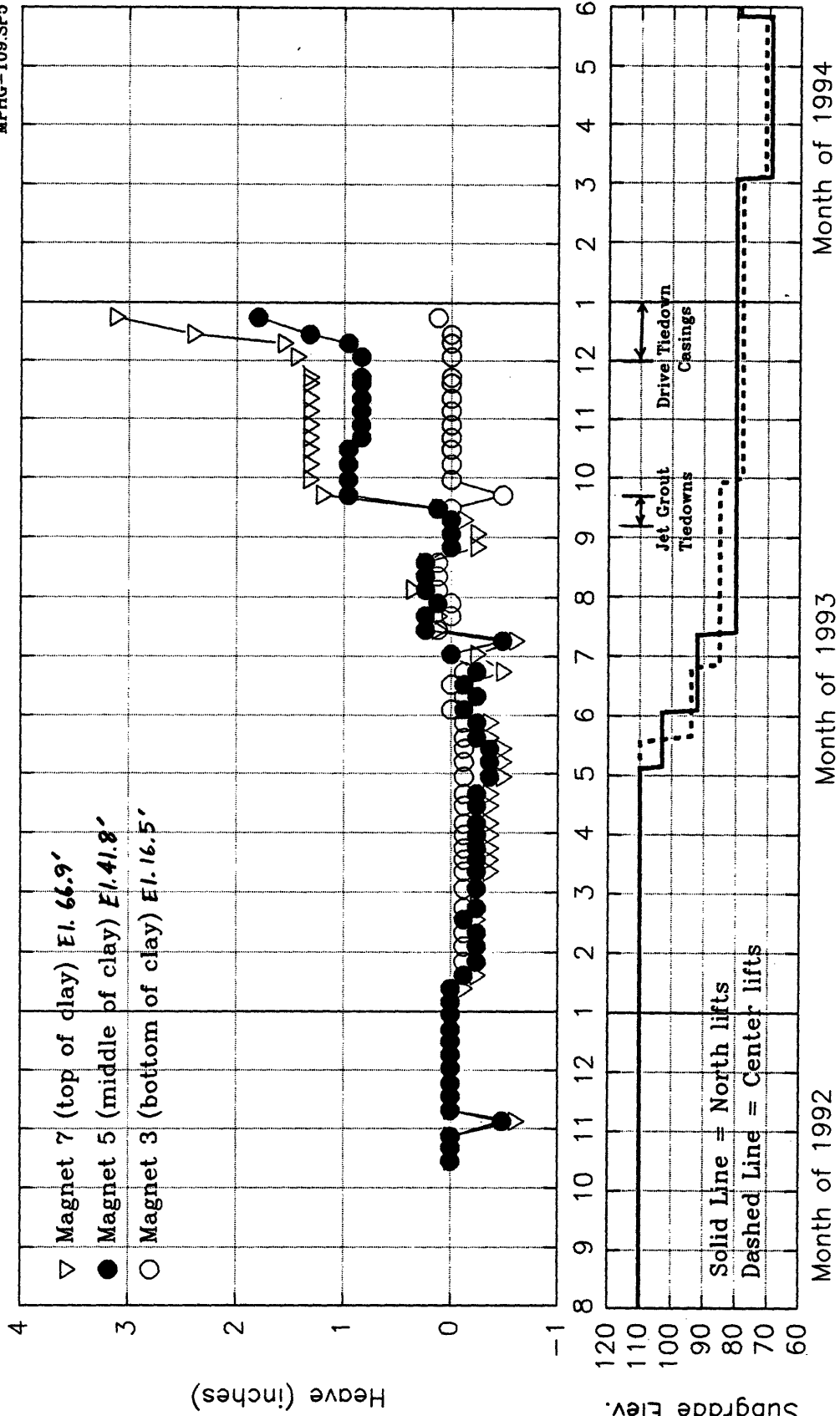


Figure 7A.12. Marine Clay Heave vs. Time, Measured by MPHG-109 (inside of excavation).

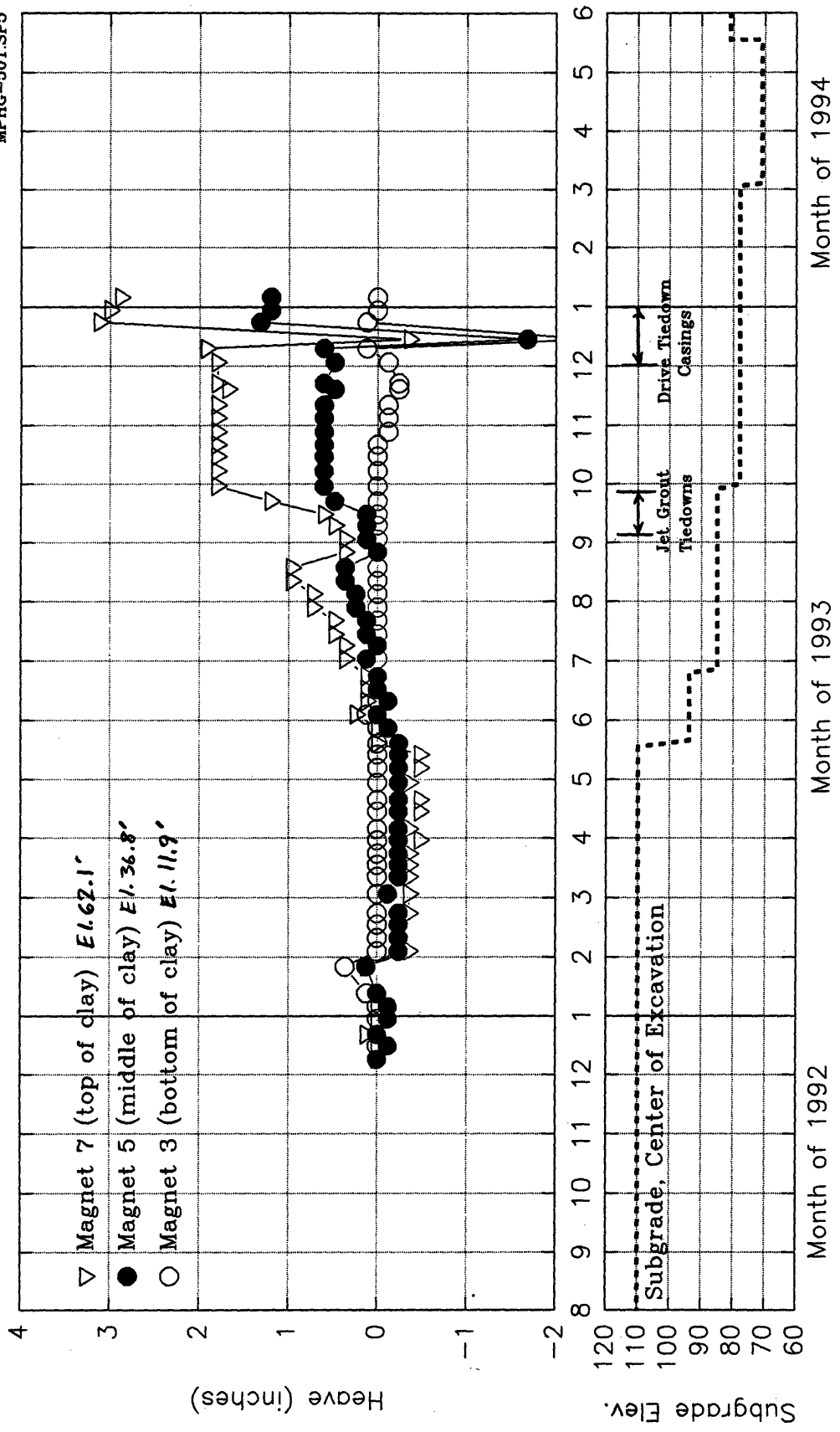


Figure 7A.13. Marine Clay Heave vs. Time, Measured by MPHG-501 (inside of excavation).

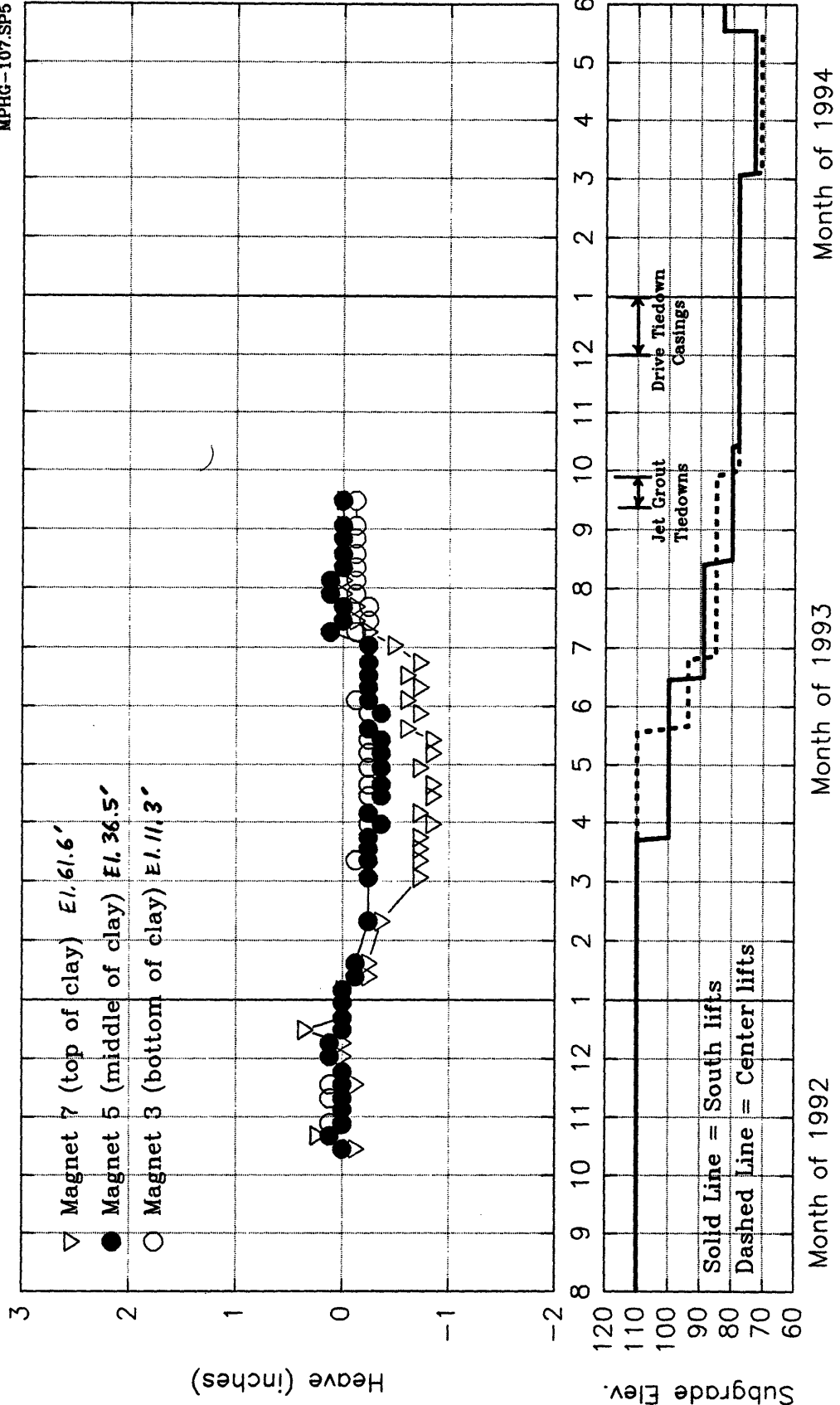


Figure 7A.14. Marine Clay Heave vs. Time, Measured by MPHG-107 (inside of excavation).

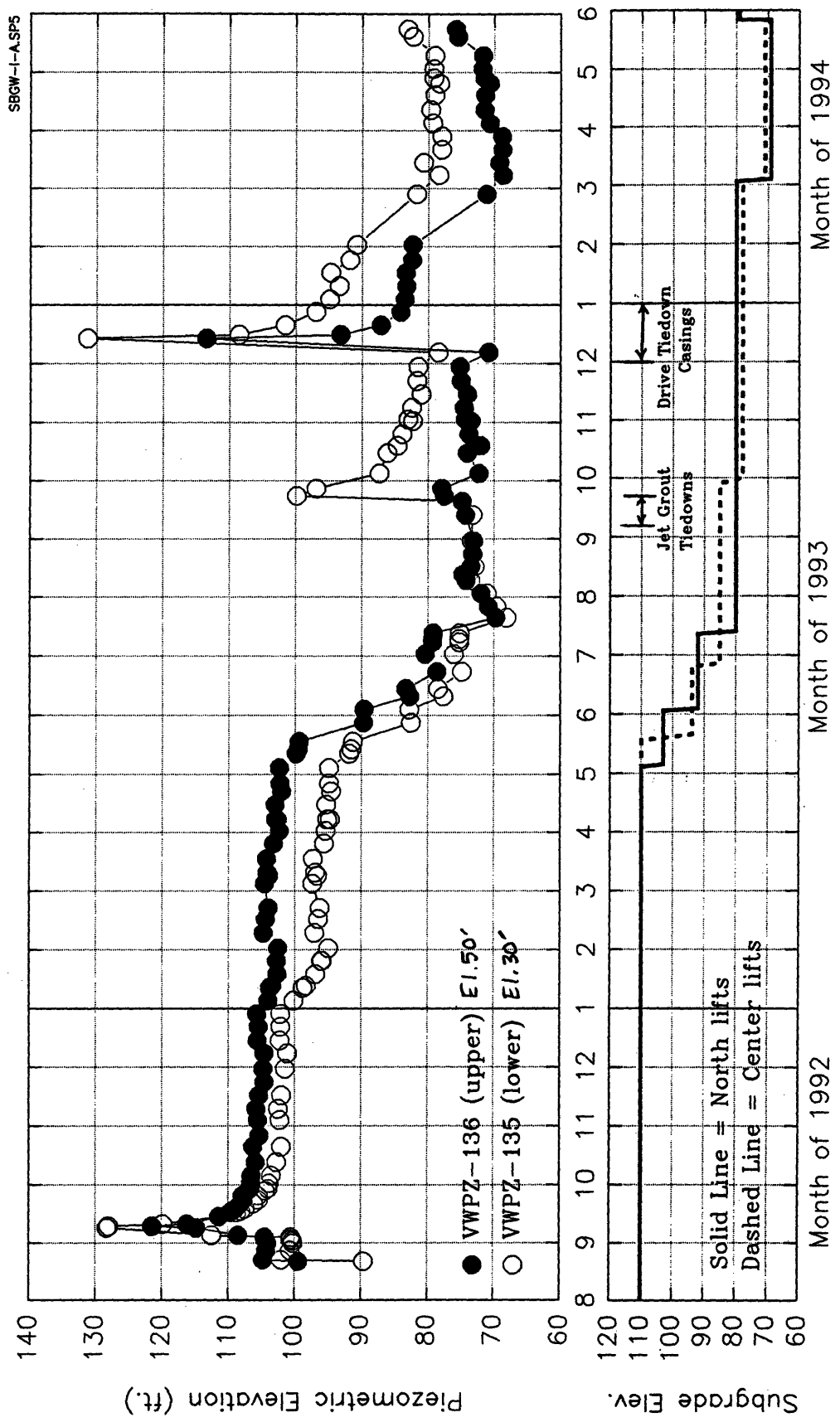


Figure 7A.15. Piezometric Pressure in Marine Clay vs. Time, Measured by VWPZ-135 and 136 (inside the excavation).

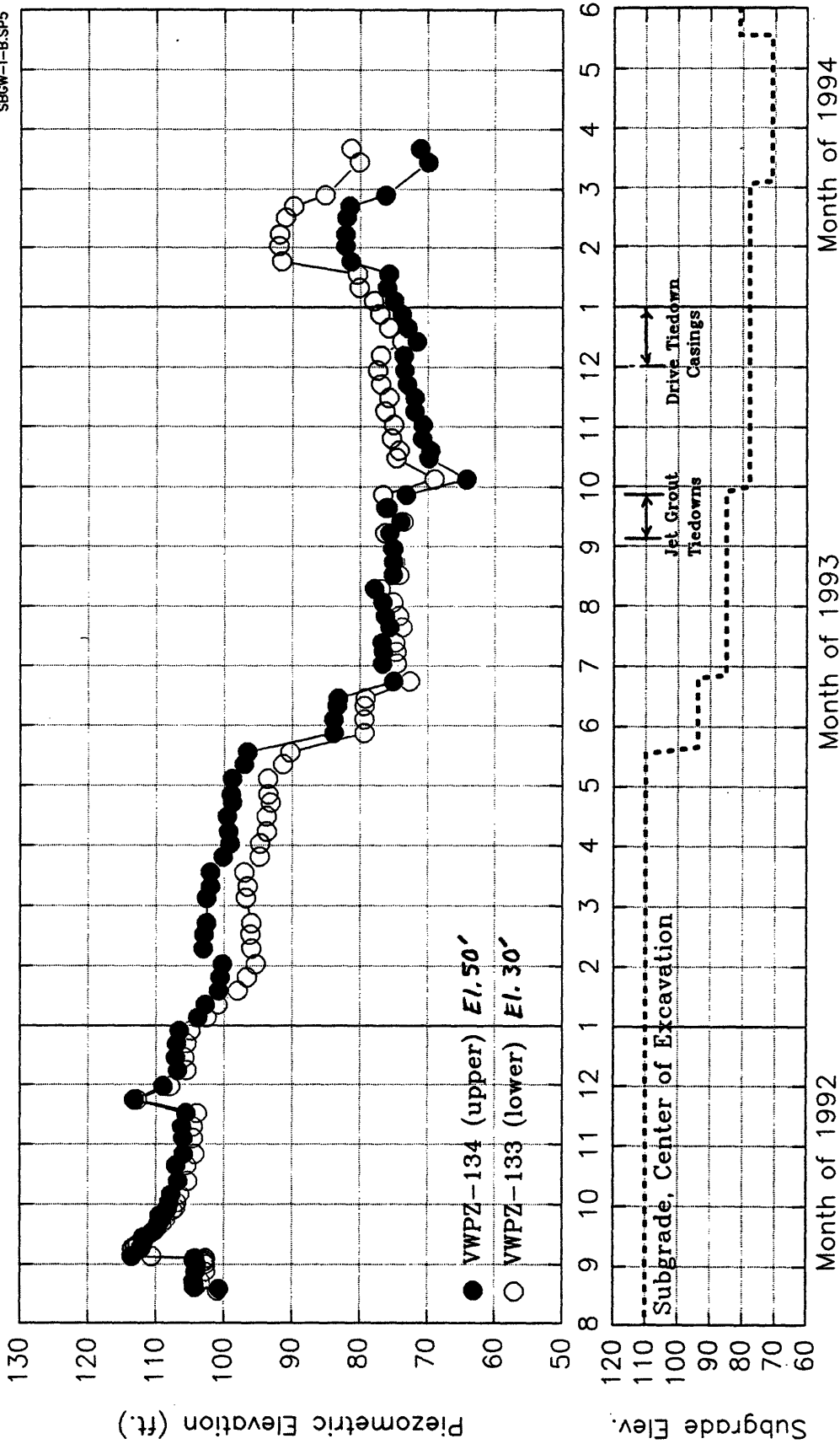


Figure 7A.16. Piezometric Pressure in Marine Clay vs. Time, Measured by VWPZ-133

and 134 (inside the excavation).

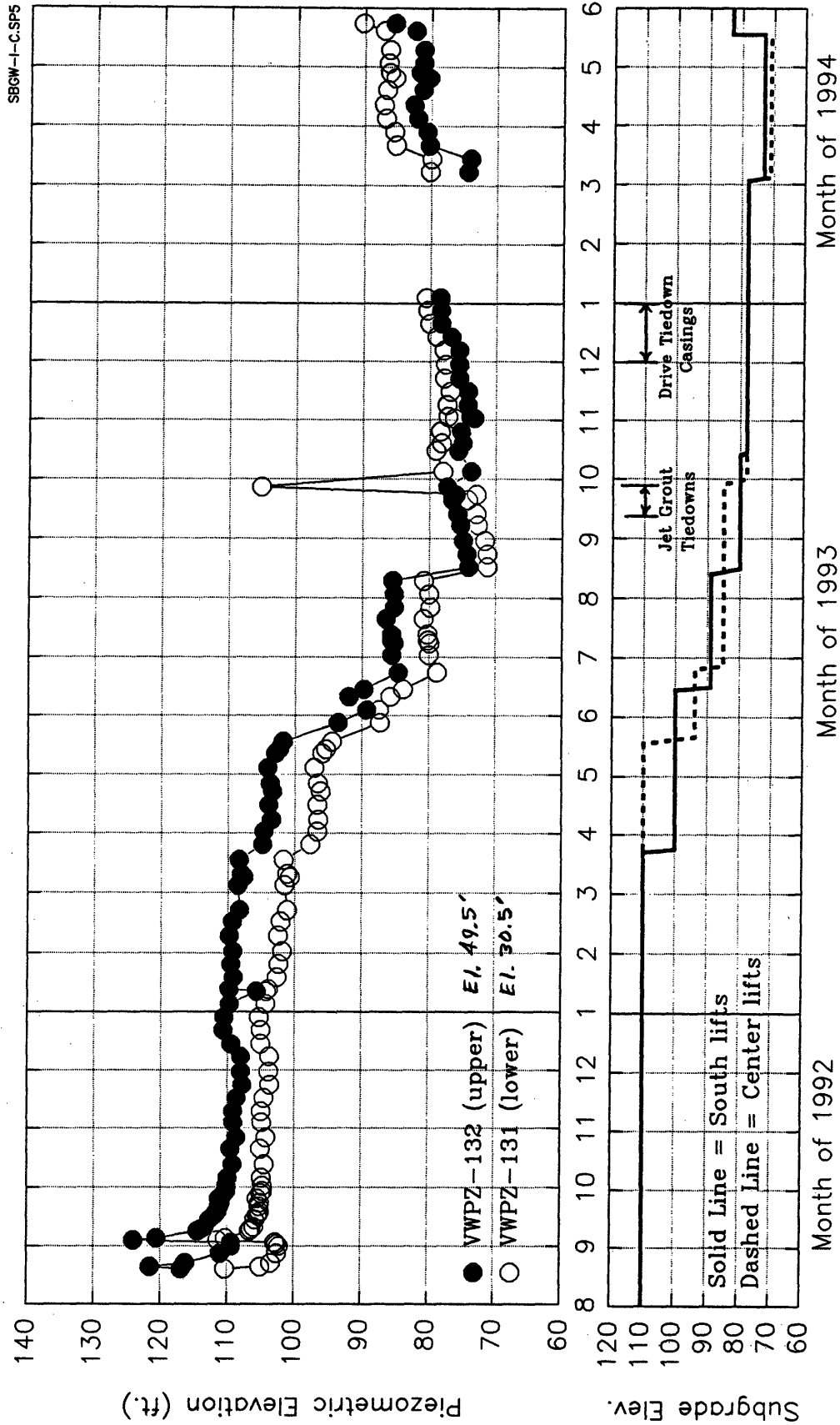


Figure 7A.17. Piezometric Pressure in Marine Clay vs. Time, Measured by VWPZ-131 and 132 (inside the excavation).

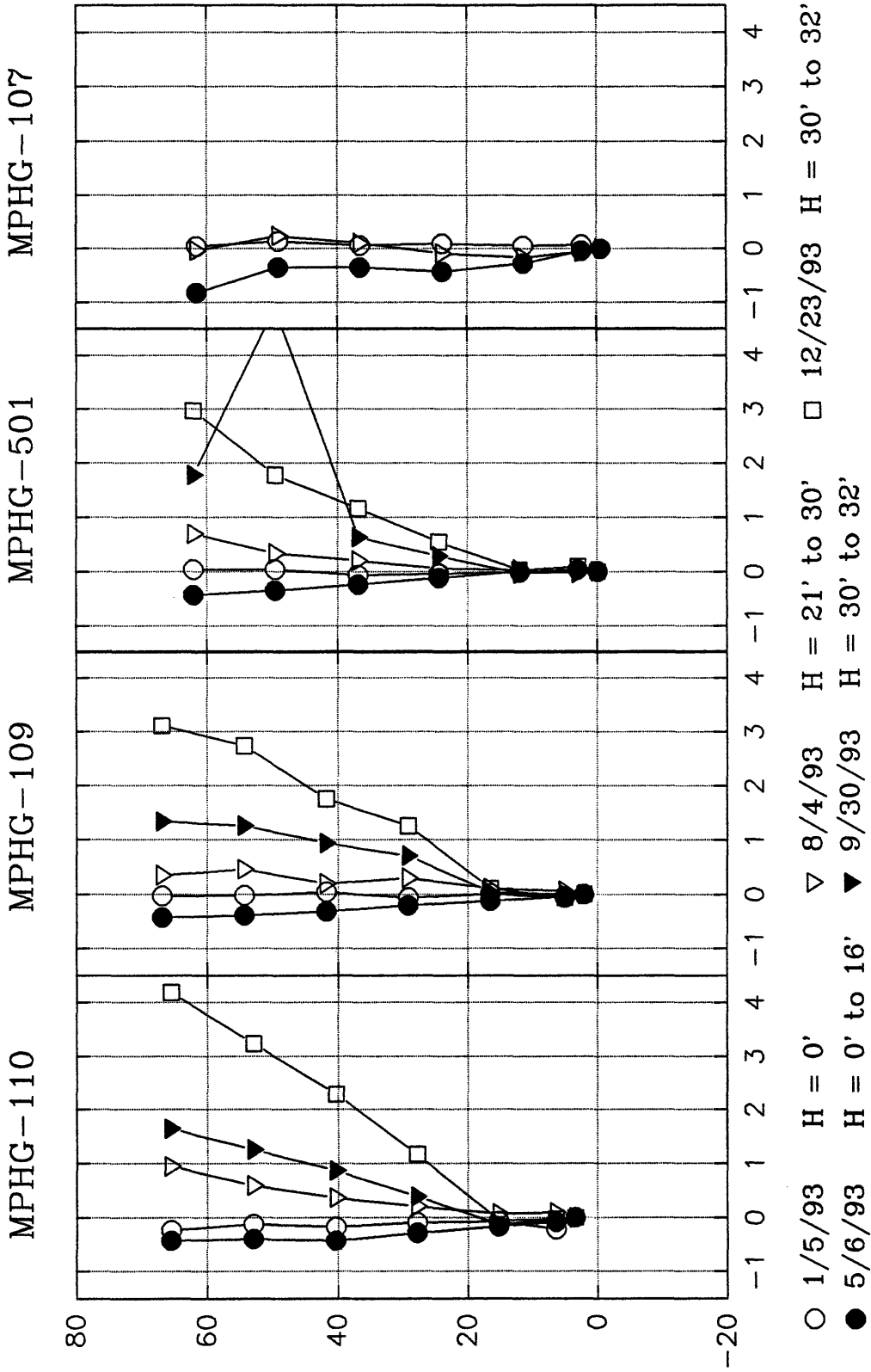


Figure 7A.18. Boston Blue Clay Heave vs. Elevation, as Measured by Four MPHG's Within the Excavation.

ISS-4	Boston
Step Number: 1.0	
Date: 5/7/1993	

Construction Events:		
1. 12/7 to 12/9	S	Drive South sheetpile walls
2. 3/22:	S	Excavate Lift 1 South (100')
3. 3/24 to 4/13:	N	Excav. and pour, B/C, A slurry wall
4. 4/13:	S	Install Tier 1-S tiebacks
5. 5/4 to 5/5:	N	Excavate Lift 1 North (103')

MPV 1/16/95

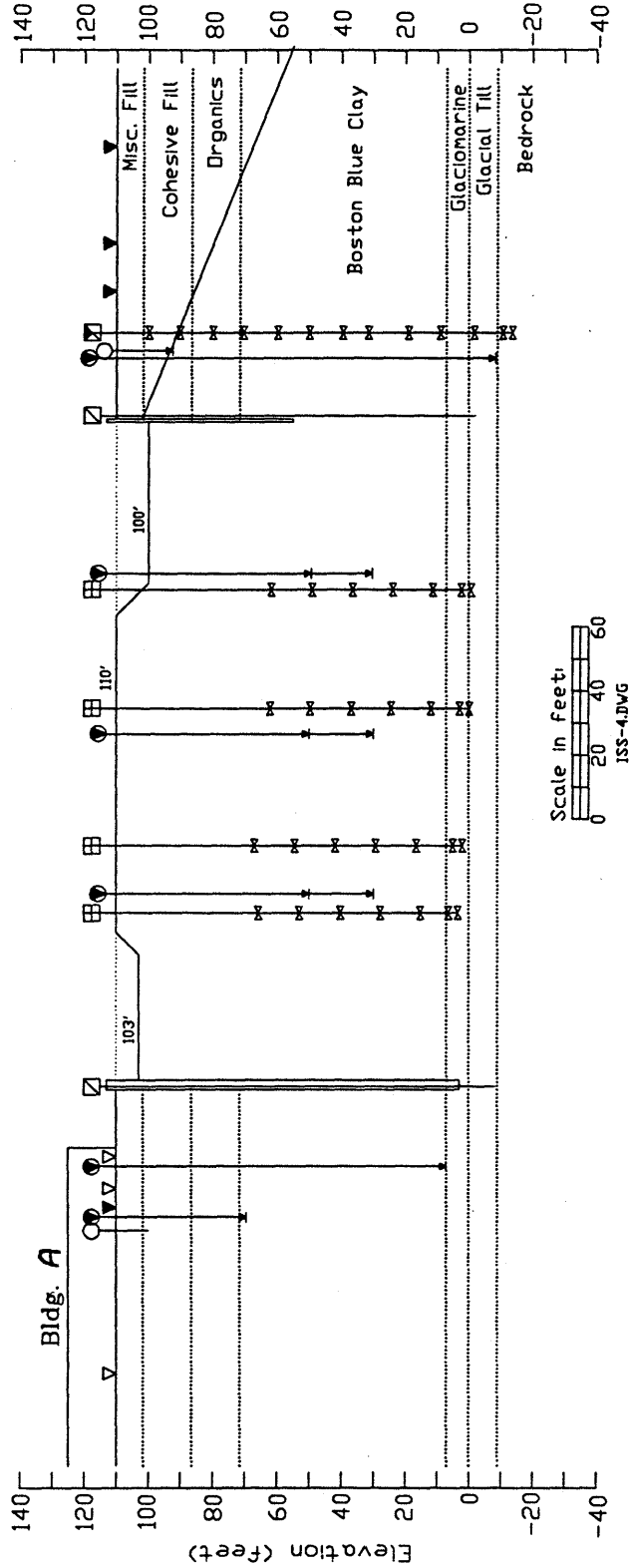


Figure 7B.1(a). Sheet 1 of Time Period Summary for Step 1.0, Showing Excavation

Geometry on 5/7/1993.

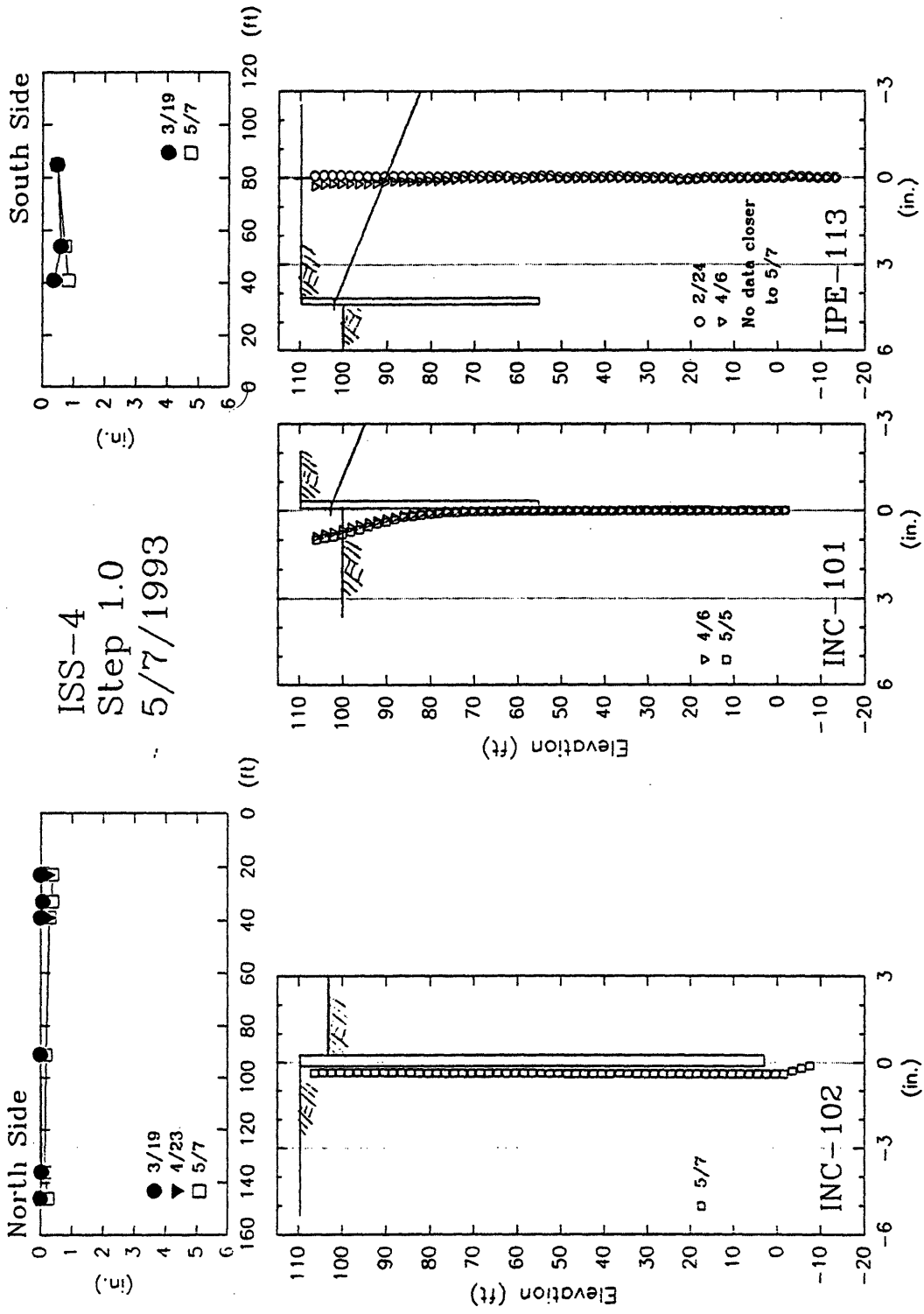


Figure 7B.1(b). Sheet 2 of Time Period Summary for Step 1.0, Showing Surface Settlements and Inclinometer Deflections on 5/7/1993.

ISS-4	Boston
Step Number: 2.0	
Date: 6/29/1993	

- Construction Events:
1. 5/17 to 5/21: C Excavate Lift 1 Center (94')
 2. 5/18 to 5/24: N Install Tier 1-N tiebacks
 3. 5/28 to 6/1: N Lockoff Tier 1-N tiebacks
 4. 6/1 to 6/3: N Excavate Lift 2 North (92')
 5. 6/5: S Lockoff Tier 1-S tiebacks
 6. 6/7 to 6/14: N Install Tier 2-N tiebacks
 7. 6/15: S Excavate Lift 2 South (89')
 8. 6/25: C Excavate Lift 2 Center (85')

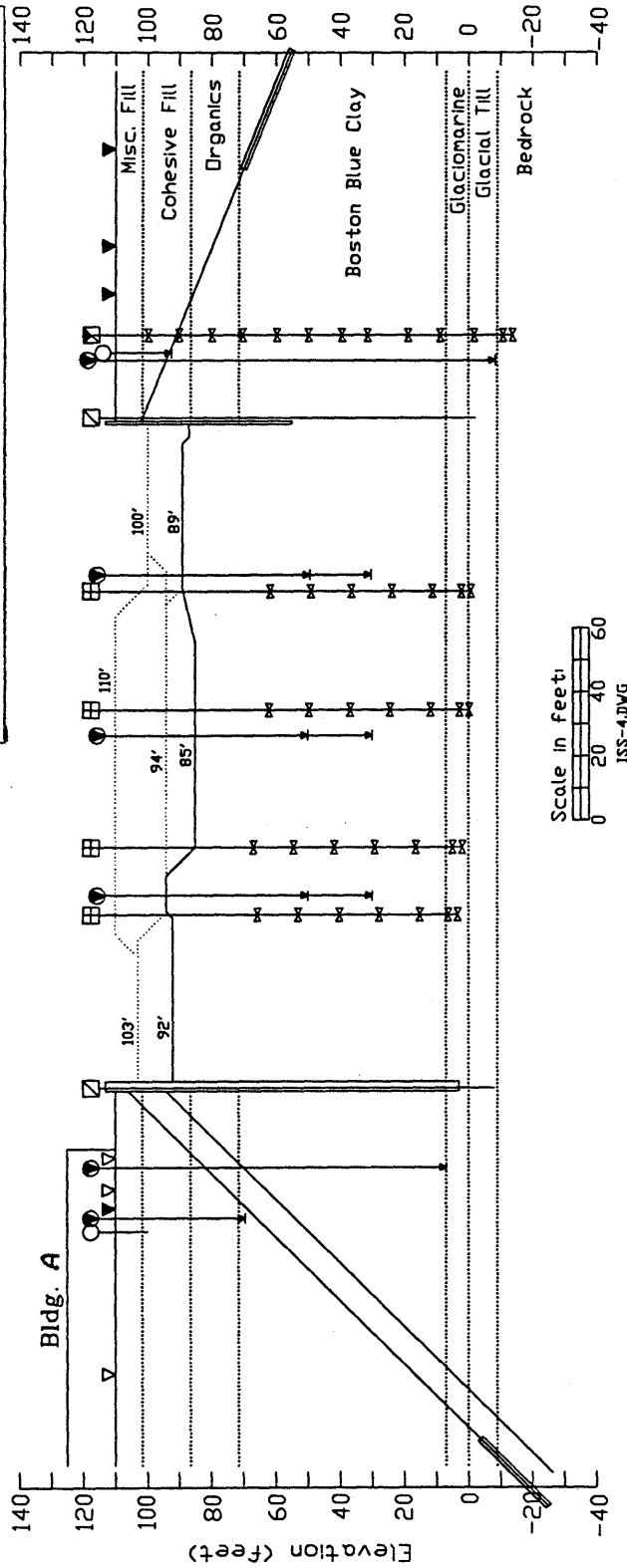


Figure 7B.2(a). Sheet 1 of Time Period Summary for Step 2.0, Showing Excavation Geometry on 6/29/1993.

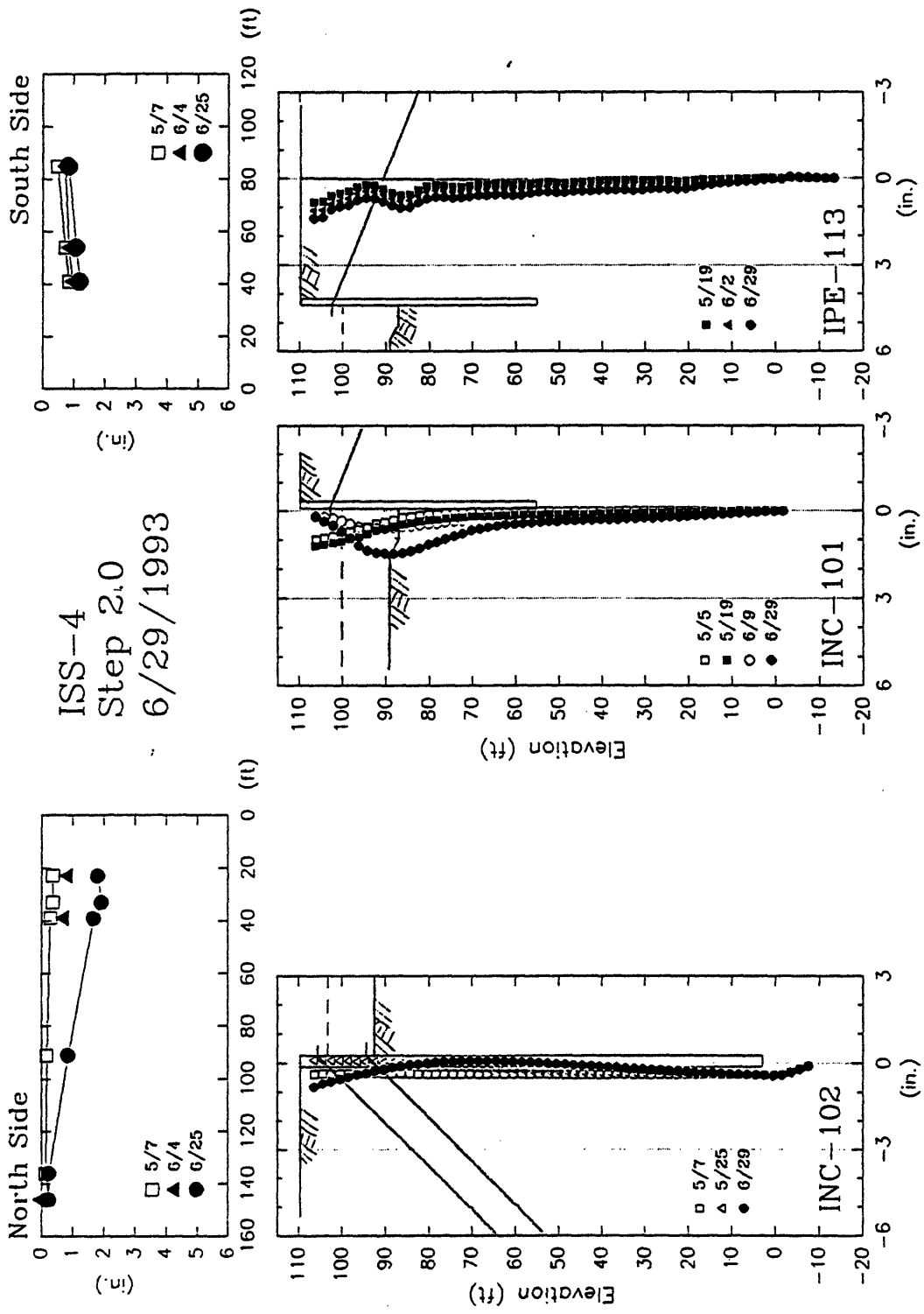


Figure 7B.2(b). Sheet 2 of Time Period Summary for Step 2.0, Showing Surface

Settlements and Inclinometer Deflections on 6/29/1993.

ISS-4 Boston

Step Number: 3.0

Date: 7/9/1993

Construction Events:

1. 6/30 to 7/1: S Install Tier 2-S tiebacks

2. 7/1 to 7/2: N Lockoff Tier 2-N tiebacks

MPV 1/16/95

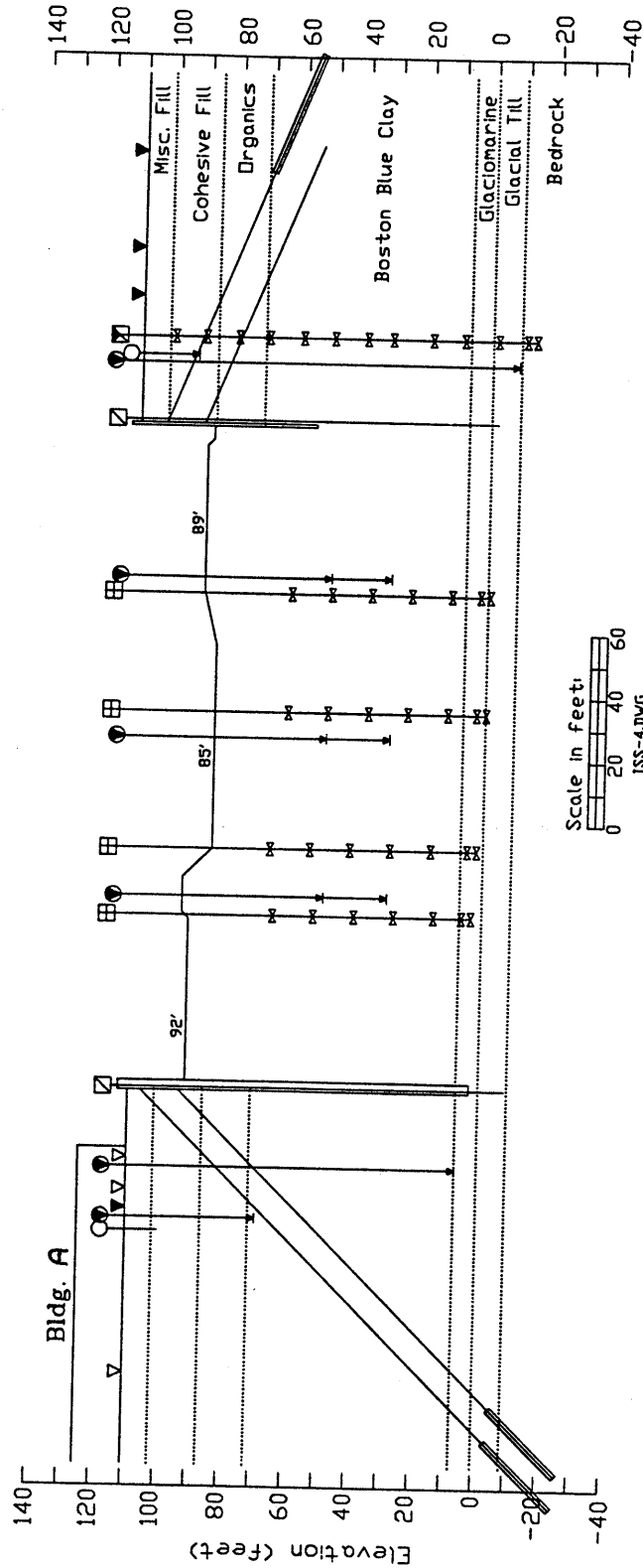


Figure 7B.3(a). Sheet 1 of Time Period Summary for Step 3.0, Showing Excavation Geometry on 7/9/1993.

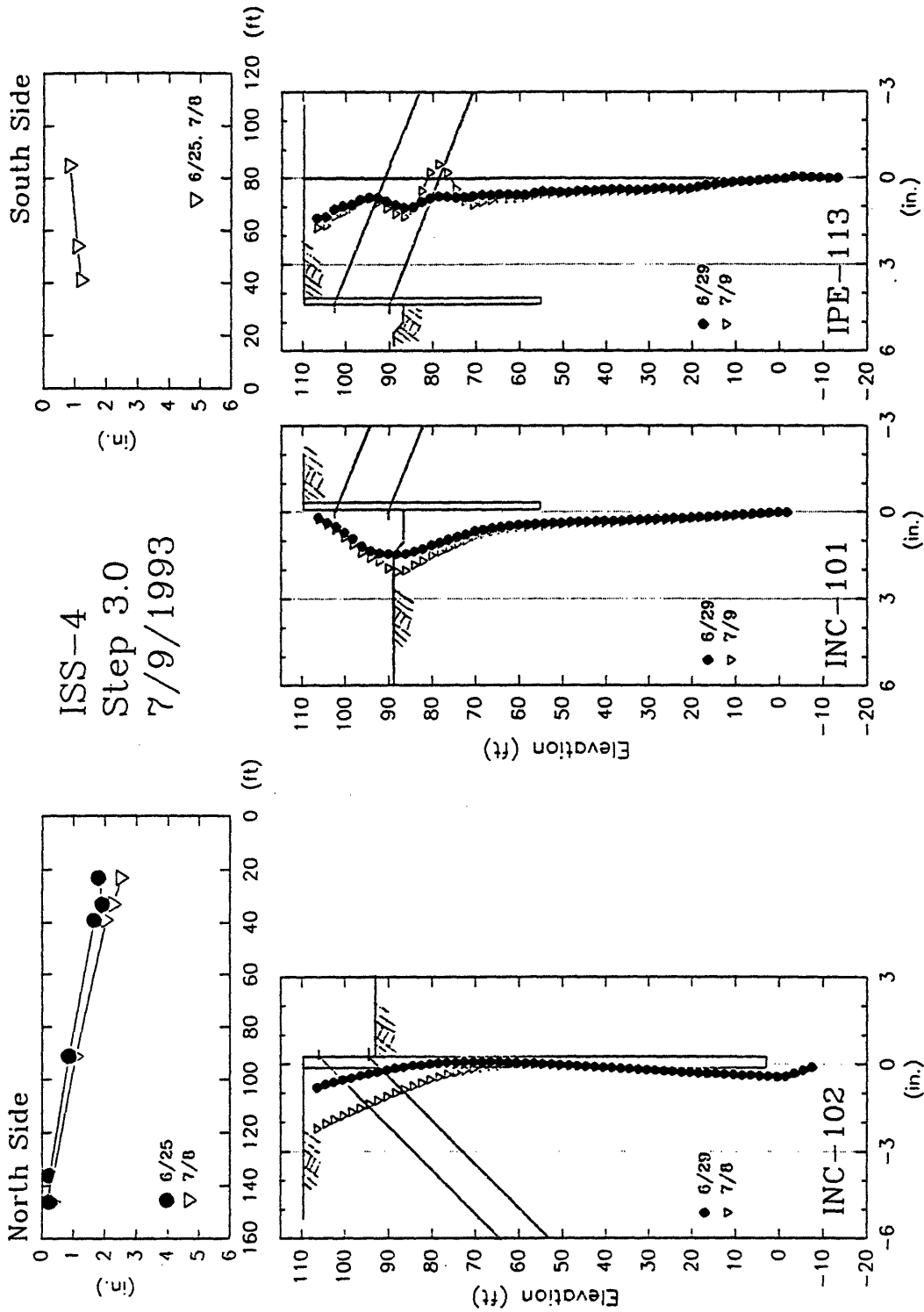


Figure 7B.3(b). Sheet 2 of Time Period Summary for Step 3.0, Showing Surface

Settlements and Inclinometer Deflections on 7/9/1993.

ISS-4	Boston
Step Number: 4.0	
Date: 8/9/1993	

Construction Events:

- 7/12 to 7/13: N
Excavate Lift 3 North (80')
- 7/30 to 7/31: S
Lockoff Tier 2-S tiebacks
- 7/27 to 8/5: N
Install Tier 3-N tiebacks

HPV 1/16/95

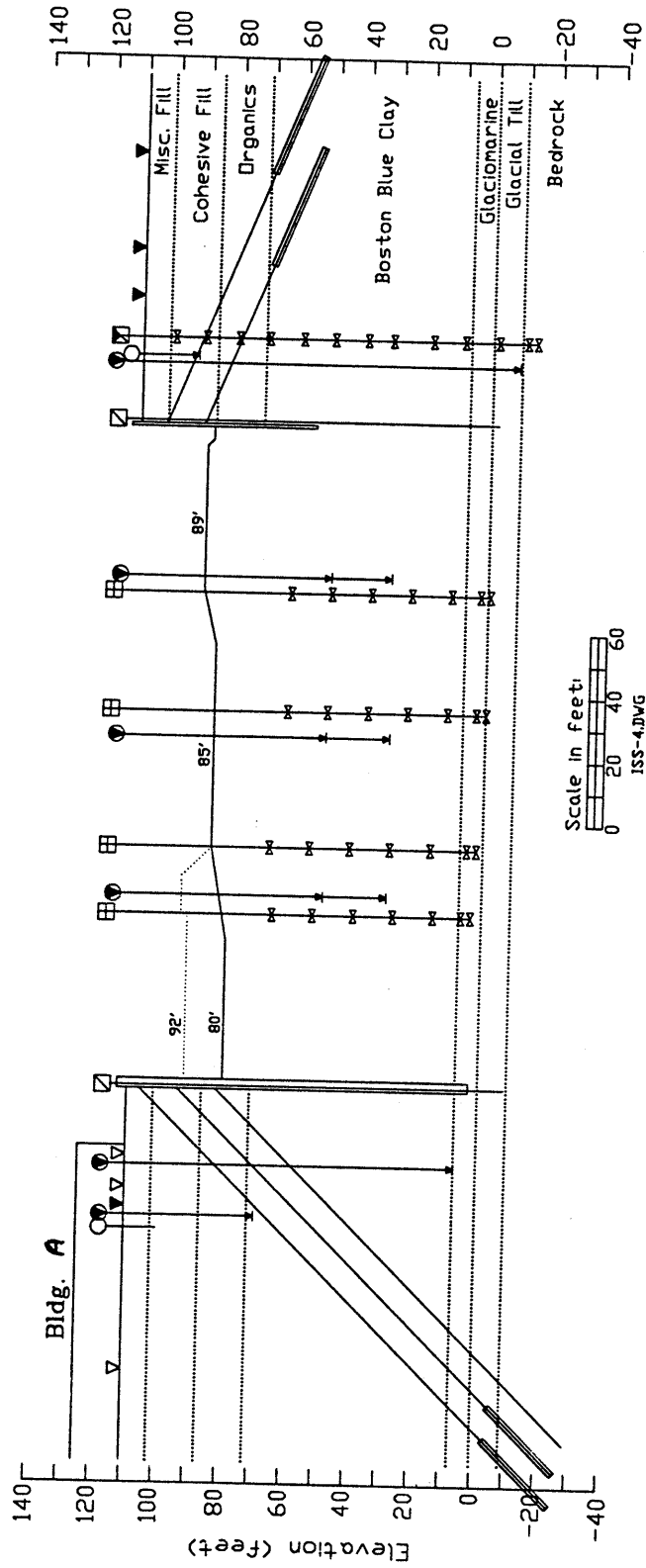


Figure 7B.4(a). Sheet 1 of Time Period Summary for Step 4.0, Showing Excavation Geometry on 8/9/1993.

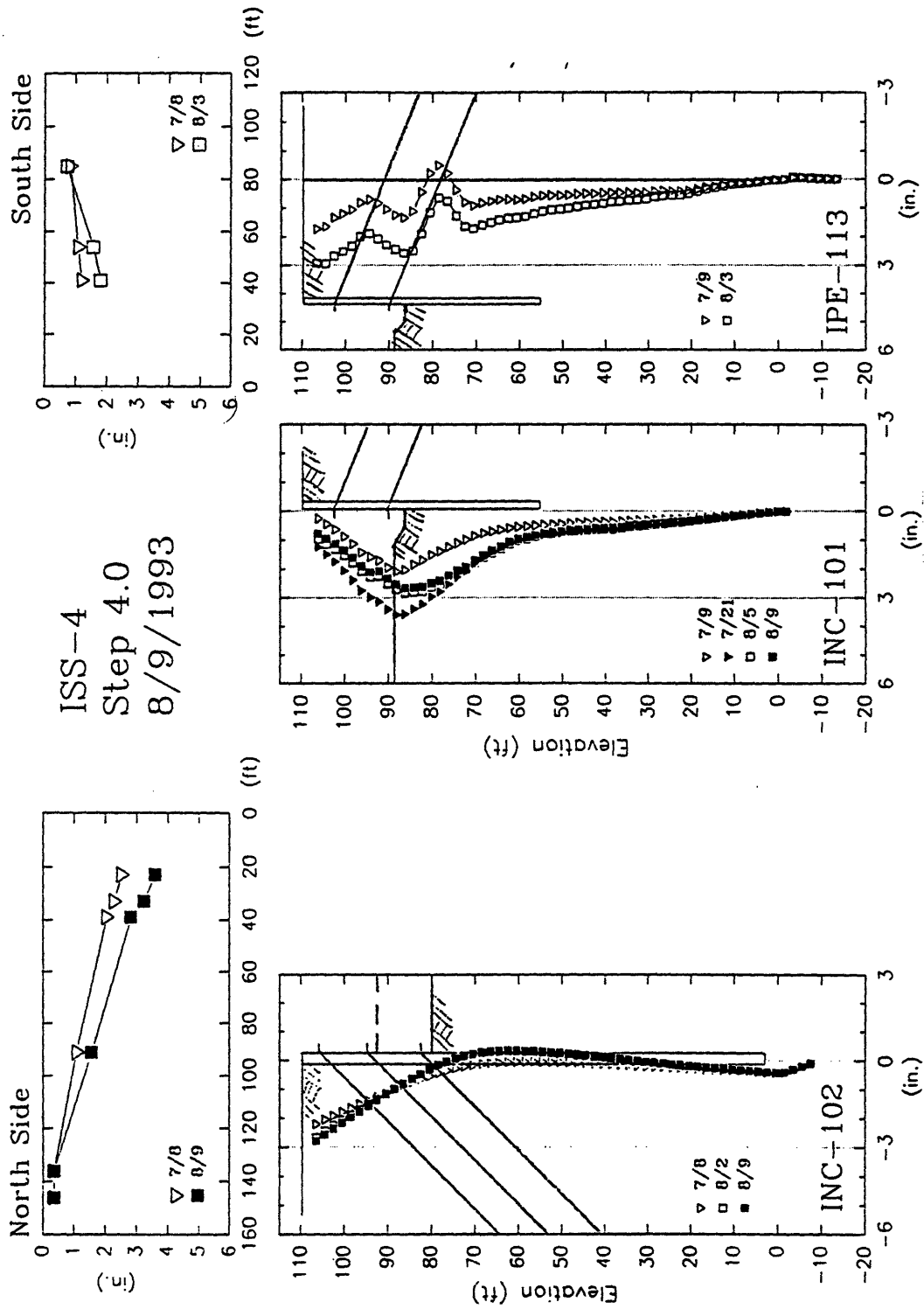


Figure 7B.4(b). Sheet 2 of Time Period Summary for Step 4.0, Showing Surface

Settlements and Inclinometer Deflections on 8/9/1993.

ISS-4 Boston

Step Number: 5.0

Date: 9/2/1993

Construction Events:

1. 8/11 to 8/16: S Excavate Lift 3 South (80')
2. 8/16 to 8/17: S Install Tier 3-S tiebacks
3. 8/20: N Lockoff Tier 3-N tiebacks

MPV 1/16/95

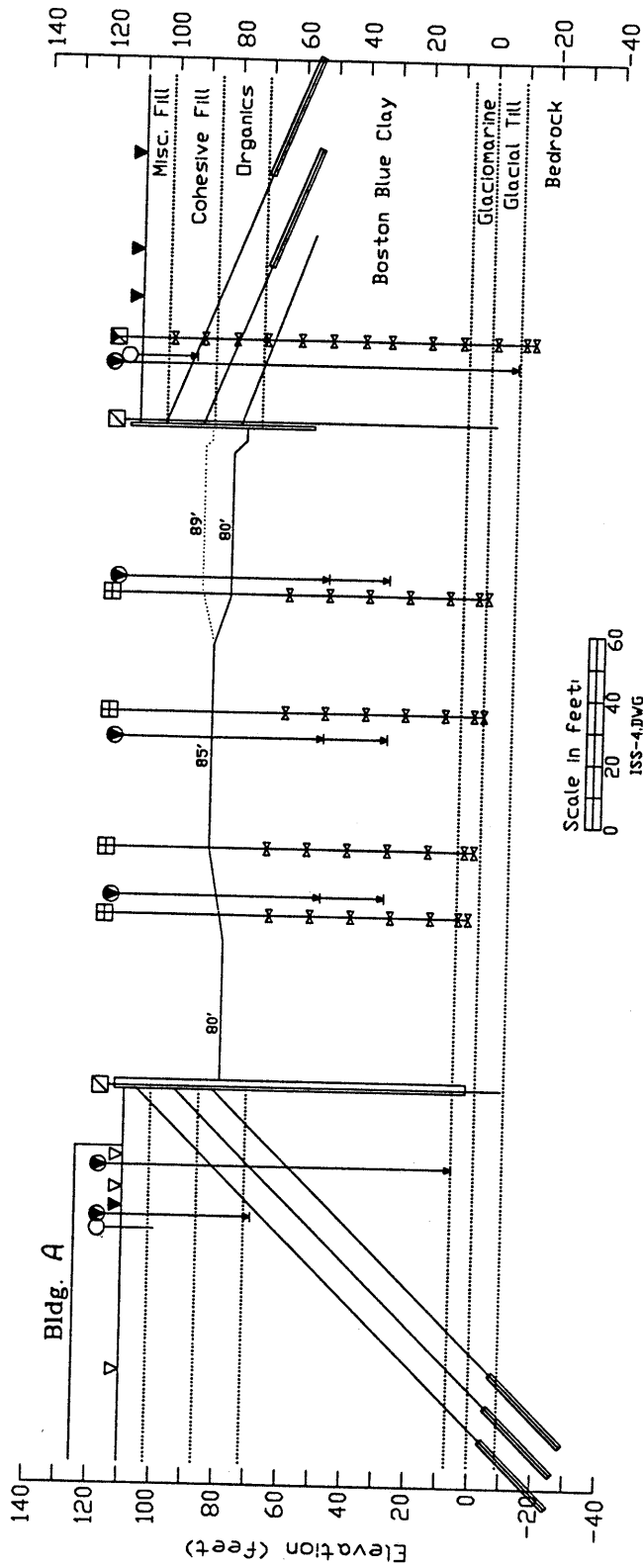


Figure 7B.5(a). Sheet 1 of Time Period Summary for Step 5.0, Showing Excavation Geometry on 9/2/1993.

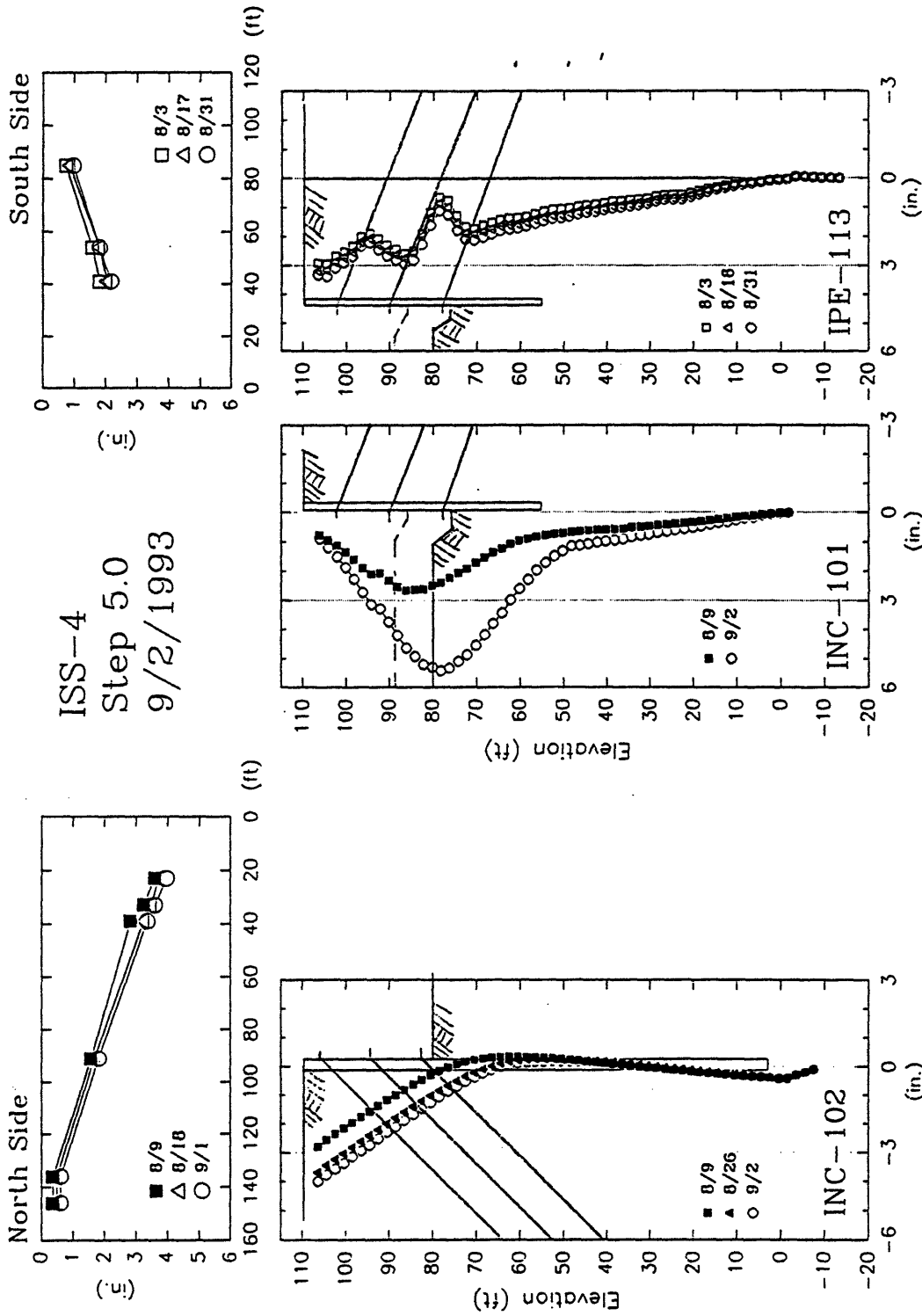


Figure 7B.5(b). Sheet 2 of Time Period Summary for Step 5.0, Showing Surface

Settlements and Inclinometer Deflections on 9/2/1993.

ISS-4	Boston
Step Number: 6.0	
Date: 10/6/1993	

Construction Events:

1. 9/10 to 9/30: Jet Grout Tiedowns
2. 9/17 to 9/20: S Lockoff Tier 3-S tiebacks
3. 9/28 to 9/30: C Excavate Lift 3 Center (78')

MPV 1/16/95

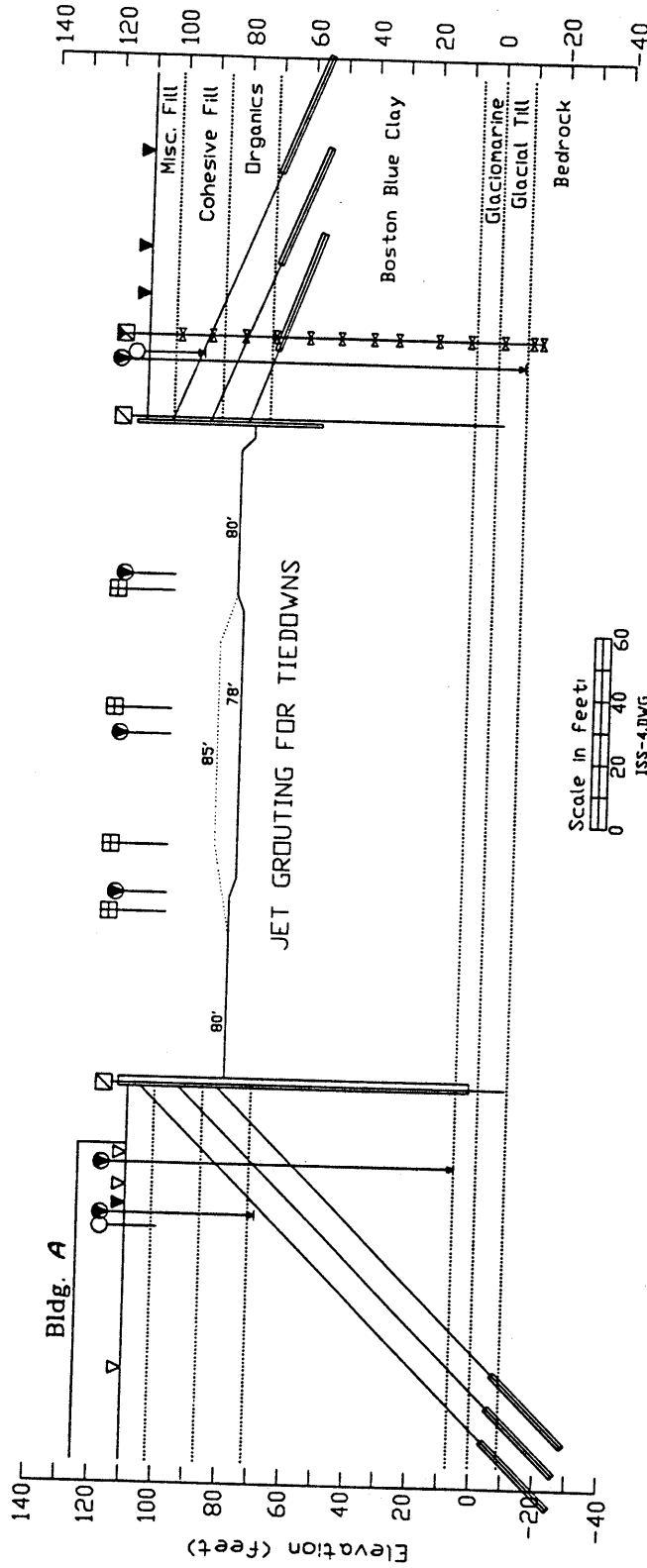


Figure 7B.6(a). Sheet 1 of Time Period Summary for Step 6.0, Showing Excavation Geometry on 10/6/1993.

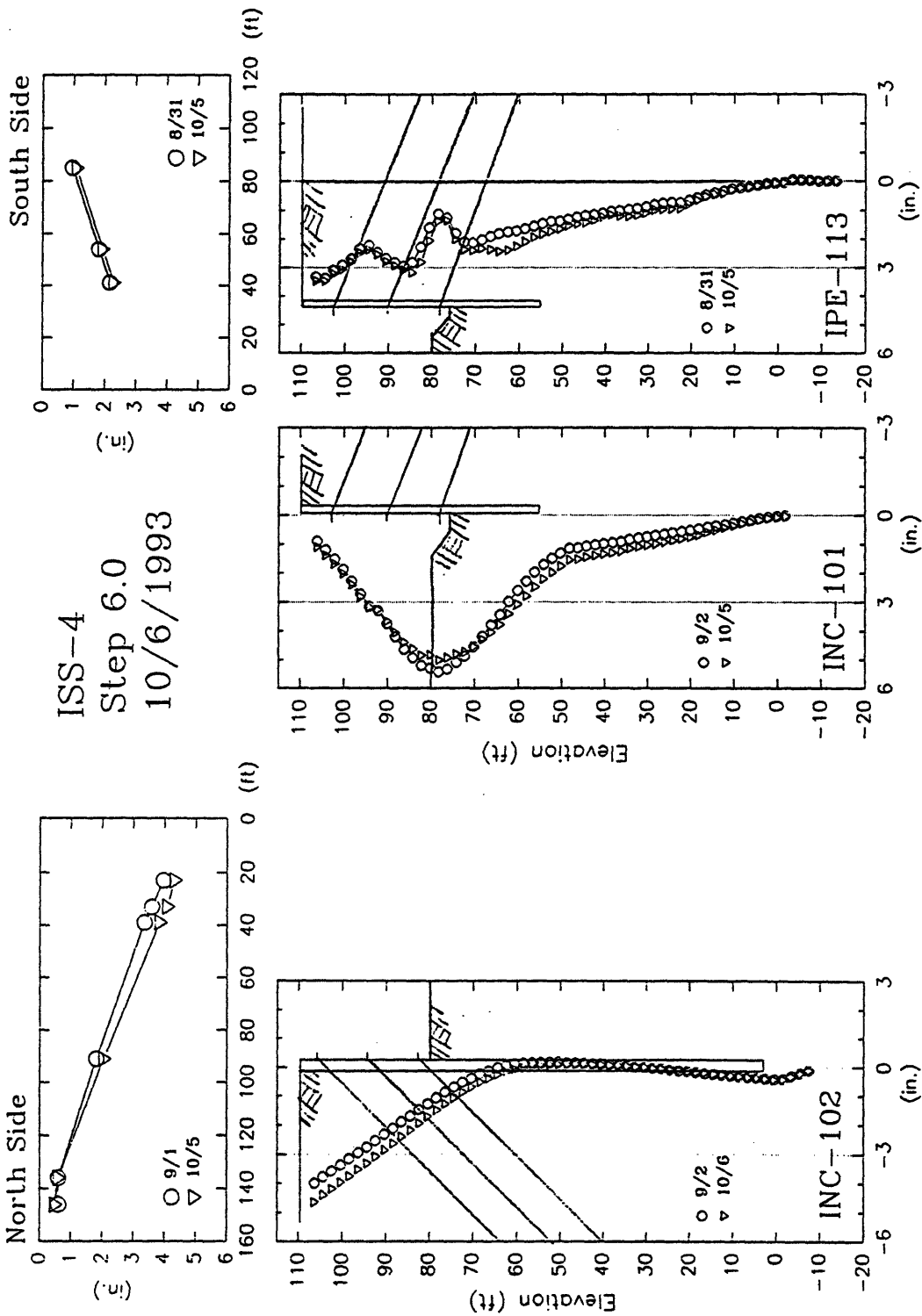


Figure 7B.6(b). Sheet 2 of Time Period Summary for Step 6.0, Showing Surface

Settlements and Inclinometer Deflections on 10/6/1993.

ISS-4	Boston
Step Number: 7.0	
Date: 3/11/1994	

Construction Events:	
1. 10/13 to 10/14:	S
2. 12/93:	
3. 1/29 to 2/8:	N
4. 2/14 to 2/22:	S
5. 3/2 to 3/4:	
Grade Haul road to El. 78'	
Drive Tiedown Casings	
Grout and Install Tiedowns, North & Center	
Grout and Install Tiedowns, South	
Excavate Final Subgrade	

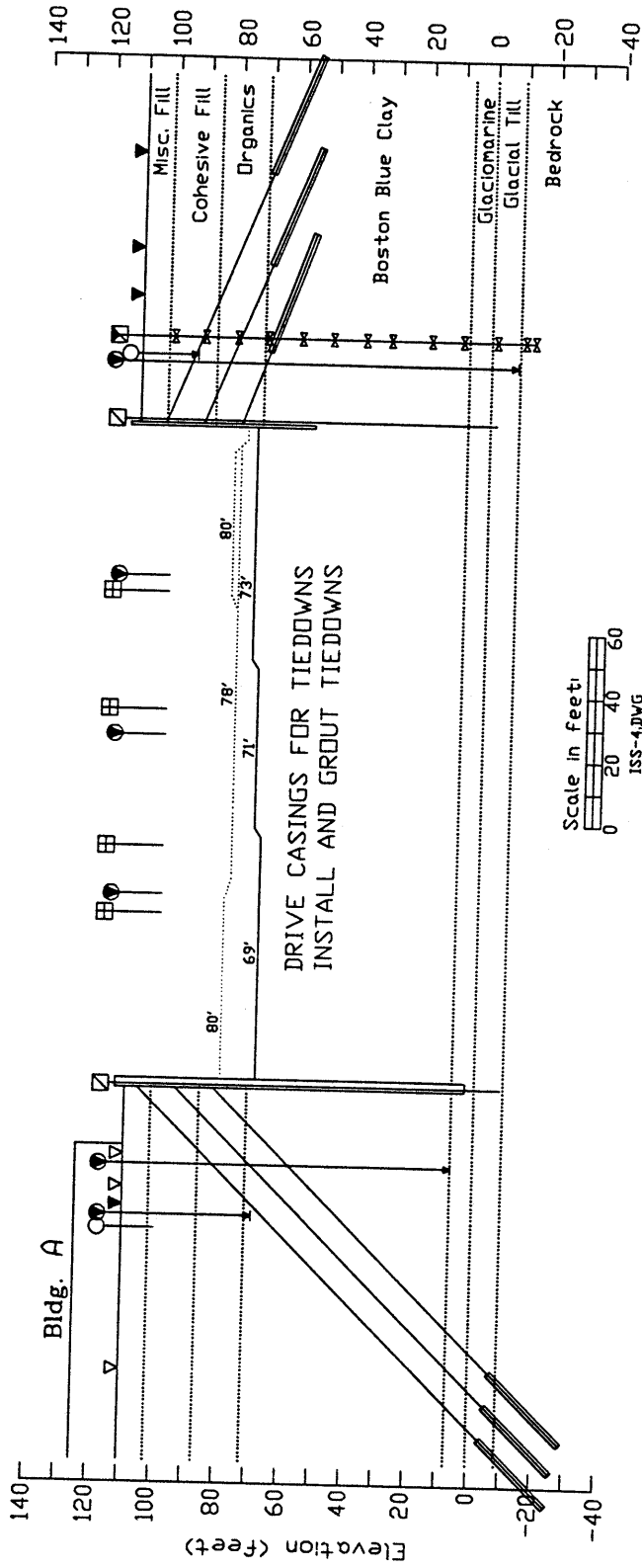


Figure 7B.7(a). Sheet 1 of Time Period Summary for Step 7.0, Showing Excavation Geometry on 3/11/1994.

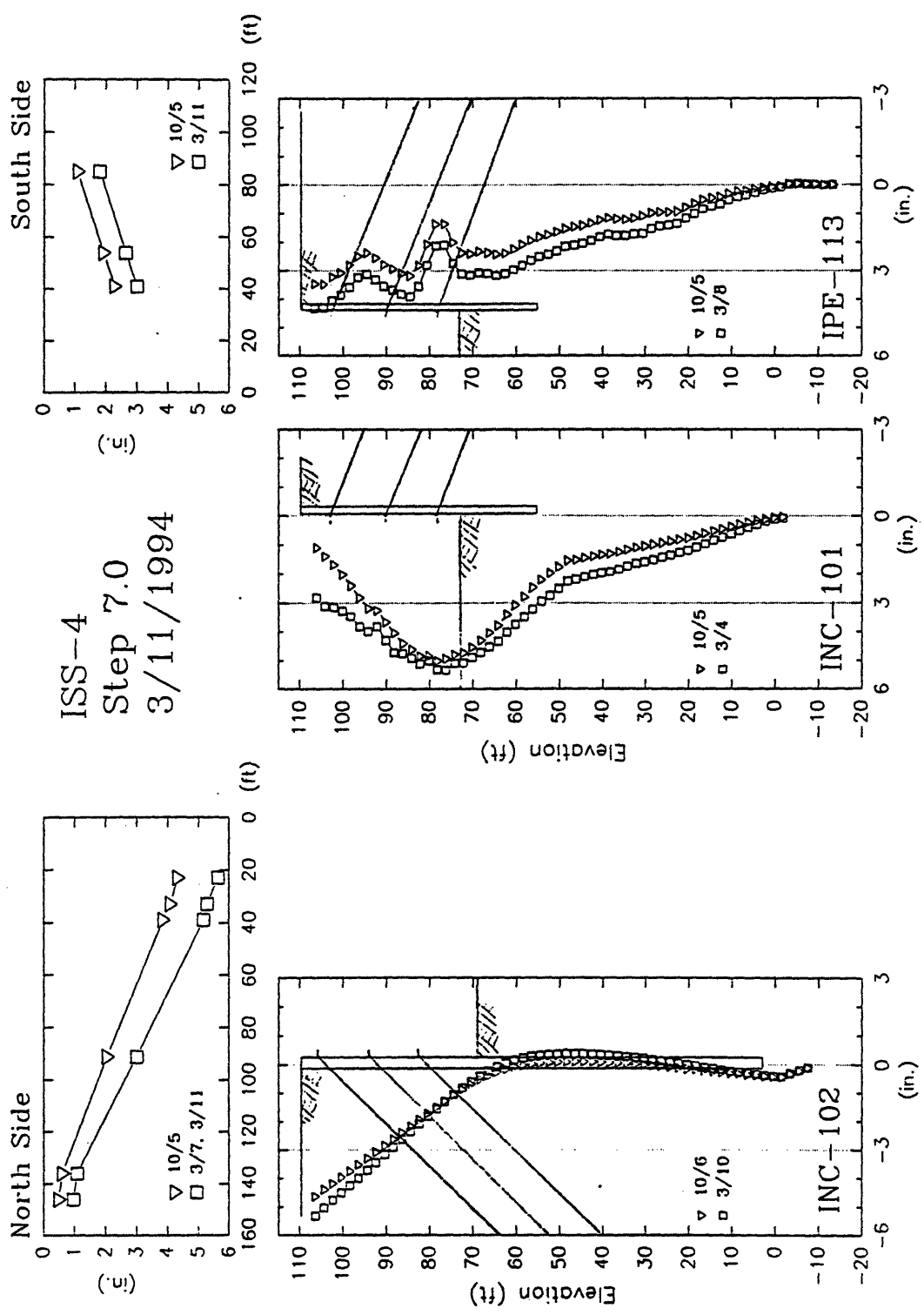


Figure 7B.7(b). Sheet 2 of Time Period Summary for Step 7.0, Showing Surface

Settlements and Inclinometer Deflections on 3/11/1994.

ISS-4 Boston

Step Number: 8.0

Date: 5/31/1994

Construction Events:

1. 5/17:	S	Pour South Invert
2. 5/26:	N	Pour North Invert

MPV 1/16/95

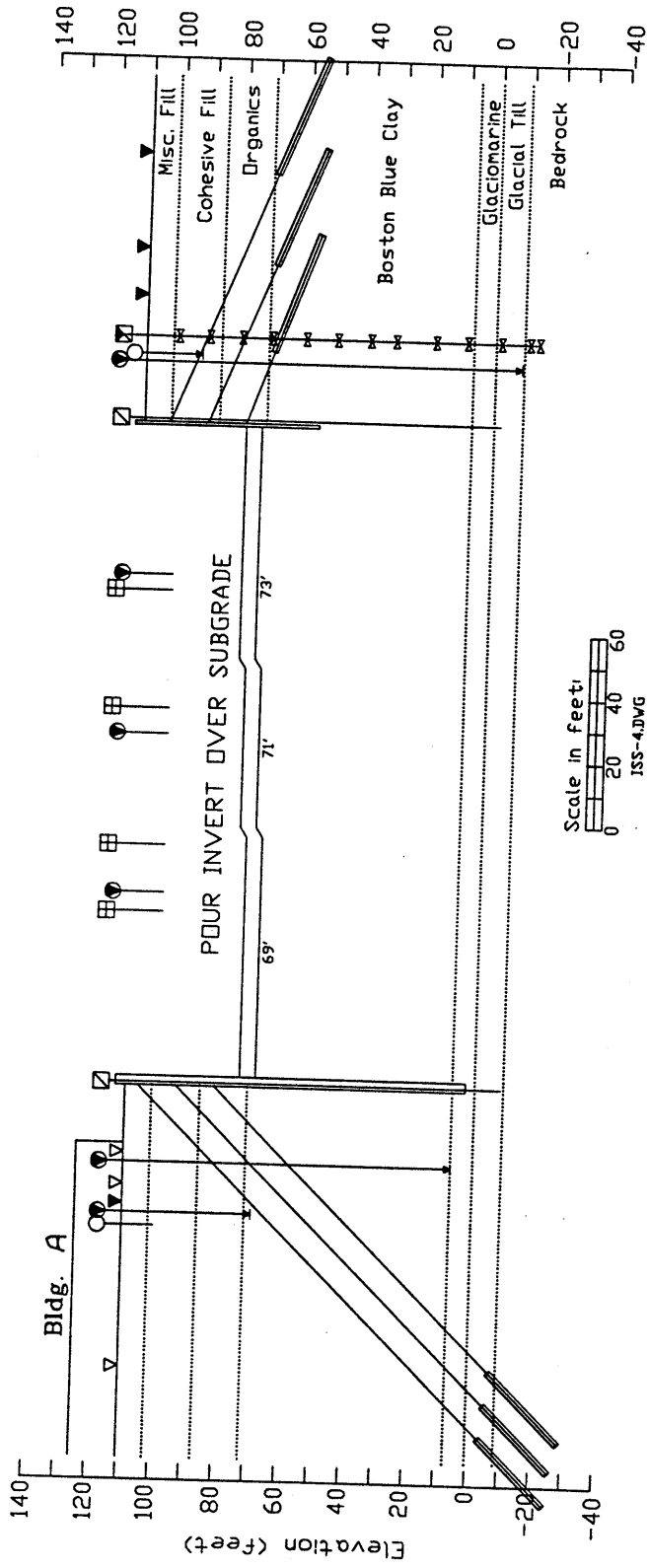


Figure 7B.8(a). Sheet 1 of Time Period Summary for Step 8.0, Showing Excavation Geometry on 5/31/1994.

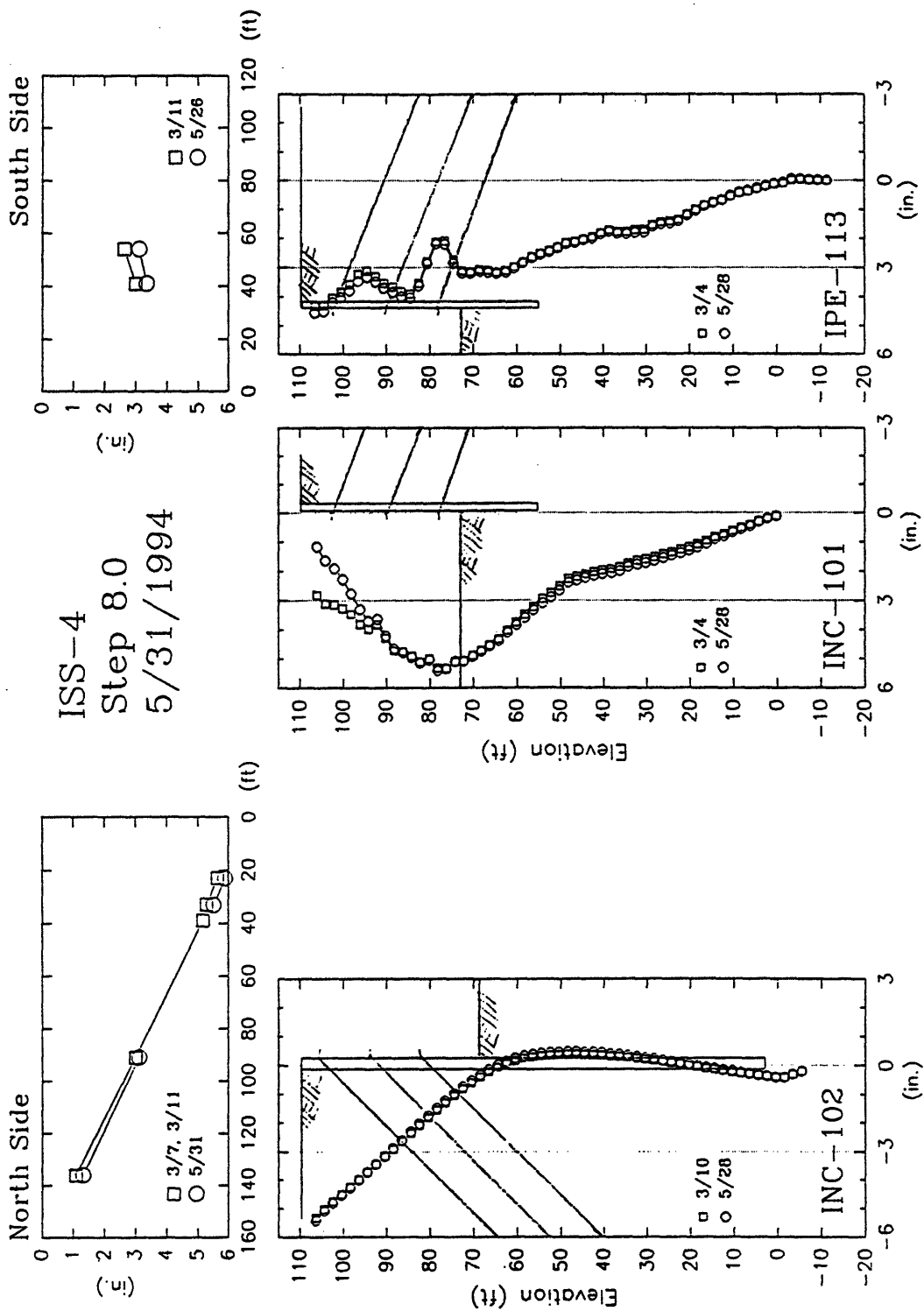


Figure 7B.8(b). Sheet 2 of Time Period Summary for Step 8.0, Showing Surface

Settlements and Inclinometer Deflections on 5/31/1994.

CHAPTER 8

FURTHER ANALYSES AND COMPARISON OF DATA TO PREDICTIONS

8.1. FURTHER ANALYSIS OF INSTRUMENTATION DATA

Chapter 7 presented a thorough discussion of observed soil deformations and groundwater changes as measured by geotechnical instrumentation at ISS-4. That discussion described the measured trends, as well as possible causes for the trends that were seen. Section 8.1 discusses additional calculations that were performed by MIT to provide a better understanding of the causes of certain phenomena seen in the instrumentation records.

8.1.1. Responses to Pressure Relief Drawdowns

Pore water pressures in the lower aquifer were reduced by the contractor so that they would not exceed the overburden stress as soil was removed from the excavation (discussed in Section 3.4). Drawdowns in the lower aquifer were in excess of 15 ft. for the better part of 1993, causing consolidation of the overlying clay as pore pressures dissipated into the underlying depressurized boundary. Calculations were performed to quantify the amount of consolidation that might be expected to occur.

8.1.1.1. Pore Pressure Dissipation in BBC

Figure 8.1 (a) shows measured piezometric water elevations (PWE's) throughout the soil profile at different times in the construction history. PWE's that appear in the figure were measured by ISS-4 instruments at three elevations. (Most of these instruments were north of the excavation.) Pore water elevations are shown for four different dates which were selected to give an overall impression of the drawdown history: 9/92 (the initial time), 7/93, 11/93, and 4/94 (representing "final" conditions). The elevation of the shallow water table in the miscellaneous fill (base at El. 101.5) underwent about three to four feet of reduction during this time period, as measured by OW-016 (Refer to Figure

7A.8). The pore water elevation in the glacial deposits below the base of the BBC (at El. 7) underwent a mean reduction of about 20 feet, as measured by deep piezometers VWPZ-107 and 106 (Figure 7A.7). These drawdowns formed the upper and lower limits of a simplified wedge of excess head, as diagrammed in Figure 8.1 (b). Between the top and bottom of this wedge, near the top of the Boston Blue Clay at El. 69.4, piezometers VWPZ-67 and 68 recorded pore pressure reductions of 3 ft in July and 7 ft in November of 1993 (Figure 7A.9).

The soils between El. 101.5 and El. 7, consisting of the Cohesive Fill, Organic Silt, and BBC, was assumed to act as a single cohesive deposit with double drainage conditions, for the purposes of this analysis. A consolidation analysis was performed to evaluate whether the measured drawdowns within the 94.5-ft-thick cohesive layer were consistent with consolidation analyses using a reasonable range of soil properties and the drawdowns measured at the upper and lower boundaries of the deposit.

The analysis of cohesive layer consolidation assumed a bipartite excess pore pressure wedge consisting of a rectangular distribution with a magnitude of 3.5 ft (due to the lowered water table), and a triangular distribution with a magnitude of 15 ft (due to deep pumping). Analyses were performed with a spreadsheet to facilitate variation of certain parameters such as time, compression and recompression ratio, and consolidation coefficient (c_v). Based on measured and calculated soil properties presented in Tables 5.2, 5.3, and 5.4, reasonable c_v values for recompression in the three cohesive units were estimated as follows:

Soil Layer	Selected Values of c_v	
	(cm^2/sec)	(ft^2/day)
Cohesive Fill	120 or 1600 x 10^{-4}	1.1 or 15
Organics	60 x 10^{-4}	0.55
Boston Blue Clay	120 x 10^{-4}	1.1

To simplify the analyses, the three-component cohesive soil layer was assigned a single c_v value of $120 \times 10^{-4} \text{ cm}^2/\text{sec}$ to match that of the predominant BBC layer, and the thicknesses of the Cohesive Fill and Organic layers were adjusted to account for their

higher or lower c_v values, as necessary (Ladd, 1994). The thickness of the Organic deposit was increased from 15 to 21 ft because its c_v was half that of the BBC. When the higher Cohesive Fill c_v was used, that layer's thickness was reduced from 15 to 4 ft.

The analysis was conducted for time durations of 200 and 320 days to match the PWE measurement dates. The time of 200 days is equivalent to the middle of July while 320 days is equivalent to the middle of November, 1993.

The calculated and measured decreases in piezometric head near El. 70 are summarized below.

Assumed c_v in the Cohesive Fill	Time		
	200 days	320 days	"infinity"
1.1 ft ² /day	0.25 ft.	0.6 ft.	8.9 ft.
15 ft ² /day	0.8 ft.	1.25 ft.	7.7 ft.
Measured in field	3 ft.	7 ft.	--

Spreadsheets for $t=320$ days, using both values of c_v in the Cohesive Fill, appear in Appendix F.

In all cases, the analyses underpredict the drawdowns measured by VWPZ-67 and 68 at El. 69.4 ft. This suggests two possibilities: that the assumed values of c_v are too low, or that drainage in the clay near VWPZ-67 and 68 was enhanced by disturbance caused during tieback drilling and installation procedures.

8.1.1.2. Settlements of Soil Layers

The calculations just described were carried a step further, by using the changes in effective stress throughout the soil profile to compute total settlements resulting from the predicted pore pressure dissipations. The previously described spreadsheet was extended for this purpose, and settlements at the ground surface and at the top of the clay were calculated for time=200, 320 days, and "infinity" (i.e. complete pore pressure dissipation). As for the analysis of PWE drawdowns, two c_v values of 1.1 and 15 ft²/day were applied to the Cohesive Fill. Again, selected spreadsheet print-outs are provided in Appendix F.

It is important to note that, for the settlement analyses, the thicknesses of the Cohesive Fill and Organic layers were not adjusted when calculating the amount of compression in each. Adjusting the layer thicknesses to account for different values of c_v , as described in Section 8.1.1.1, was only done for the calculation of pore pressure dissipation, which equals changes in effective stress.

Figure 8.2 shows a plot of effective stresses versus elevation, both before, during, and after consolidation of the cohesive soil layers, as well as the preconsolidation pressures. It can be clearly seen that even after complete consolidation under these conditions, the soil profile would remain overconsolidated throughout. Therefore, only values of Recompression Ratio (RR) were needed to compute settlement. "Best estimate" RR values were assigned according to the MIT recommendations given in Tables 5.2, 5.3, and 5.4. The influence of varying RR was assessed by doing additional analyses with RR's that were increased or decreased by 0.005. The following table provides the results of the analyses, showing calculated settlements at the surface and at the top of the BBC (in parentheses).

Time c_v in Cohesive Fill	200 days		320 days		"infinity"	
	1.1 ft ² /d	15 ft ² /d	1.1 ft ² /d	15 ft ² /d	1.1 ft ² /d	15 ft ² /d
"Best Est." RR	0.8" (0.45")	1.0" (0.55")	1.0" (0.65")	1.15" (0.65")	2.5" (1.7")	2.3" (1.6")
RR + 0.005					3.05" (2.0")	2.8" (1.9")
RR - 0.005					2.0" (1.35")	1.85" (1.3")
Measured by DMP4-116 (See Figure 7A.5)	approx. 1.1"		approx. 1.6"			

The predicted values of settlements (δ_v) are compared to the settlements measured at DMP4-116, which lies about 85 ft from the south wall. This offset distance exceeds $2H$, where H is the depth of excavation (about 40 ft at this location). According to the design chart of Clough and O'Rourke (1990) shown in Figure 8.6, DMP4-116 is outside of the range of influence of wall movements, and should therefore record settlements that result

only from consolidation. The table indicates that predicted settlements were only 20 to 30% lower than the field measurements. Varying RR by ± 0.005 induced changes of approximately 20% in the final predicted δ_v values, which is enough to account for much of the differences between predicted and measured δ_v .

Figure 8.3 presents measurements of settlement at different depths, from IPE-113 (which was 27 ft behind the South wall). These settlements were close to three inches in November. Figure 8.3 indicates that most of the settlement occurred in the cohesive fill layer and the very top of the clay. The calculated settlements, for comparison, indicate that 55 to 70% of the total δ_v would occur within the BBC. As before, some of this settlement can be attributed to deflection of the wall. However, it is also possible that installation of the tiebacks could have disturbed the soil and increased the compressibility of the BBC crust.

8.1.2. Pore Pressure Reductions due to Excavation Unloading

In an undrained, one-dimensional situation, unloading will result in negative pore pressures which equal the decrease in vertical total stress (assuming 100% saturation). These negative pore pressures develop because the undrained condition requires that the effective stress be unchanged initially; changing only as drainage occurs and the excess negative pore pressures dissipate.

This basic effect was the main cause of pore pressure reductions measured during excavation events by the six VWPZ's inside of the excavation (as discussed in Section 7.2.3). Ideally, the sudden pore pressure drops that were recorded by the piezometers (shown in Figures 7A.15 through 7A.17) would be equivalent to the total stress reduction that resulted from excavation.

The measured reductions in pore water pressure were plotted against the corresponding increments of excavation unloading to see how closely the two amounts agreed, as predicted for an ideal 1-D case. The plot is presented in Figure 8.4. The pore pressure reductions were consistently less than the total stress reductions (computed as $\Delta\sigma_v = \Delta H\gamma_t$), plotting well below the line of equivalency. This is partly attributable to a systematic overestimation of total stress reductions, caused by the fact that the excavation

was a 2-D, rather than 1-D, unloading condition. Since excavation lifts were usually only about one-third as wide as the excavation, higher subgrade elevations were generally left to one or both sides of a newly excavated lift section, hence contributing to the total stress state within the underlying soil and lessening the amount of total stress reduction. In a two- or three-dimensional unloading situation such as this, the change in octahedral stress [$\Delta\sigma_{oct} = 1/3(\Delta\sigma_1 + \Delta\sigma_2 + \Delta\sigma_3)$], which incorporates the changes in all three principal stresses, should provide a better representation than $\Delta\sigma_v$ of unload-induced stress reductions for comparison to Δu .

8.2. COMPARISON OF MOVEMENTS TO PREDICTION TECHNIQUES

8.2.1. Purpose and Objectives

As shown in Table 1.1, Task 4 of Phase I of this research project was the “comparison of predicted and measured performance using design charts”. Wall movements and surface settlements measured at the project’s excavations provide an important source of data for assessment of the predictive ability of existing empirical and semi-empirical techniques, toward the project’s ultimate goal of producing improved design charts via FEM analysis. This section will compare predicted wall and surface movements to measurements from the project excavation in general and the ISS-4 cross-section in particular.

8.2.2 Normalized Settlements

Peck’s (1969) design chart for prediction of settlement distribution was presented in Figure 2.1. Normalized settlements measured throughout the project area are plotted on his chart in Figure 8.5. These settlements pertain to the date on which the concrete invert was poured adjacent to each DMP - the last day on which the excavation existed at its maximum depth. (These settlements are also shown as the lowermost points in the Figure 4.7 plots.)

The measured, normalized settlements all fall within zones II or III, which apply to “very soft to soft clay”. Zone III represents the settlements expected for excavations underlain by a significant depth of soft clay, which is a reasonably accurate description of

the project excavations. Settlements behind diaphragm walls (indicated by the hollow symbols) tend to be lower and concentrate closer to zone II, due to the added support provided by the stiffer wall. The largest values of δ_v for sheetpile walls were measured near the western end of the alignment (ISS-1 and 2) where anomalously large movements were noted.

Settlements were normalized against excavation depth for comparison to the suggested distributions proposed by Mana and Clough (1981), shown in Figure 2.5. The plot of normalized settlements appears in Figure 8.6. The settlements behind the sheetpile walls tend to exceed the suggested envelopes by extending farther from the excavation wall than predicted. Settlements behind diaphragm walls were in closer agreement with the suggested envelopes.

The results in Figure 8.6 indicate that the normalized settlements behind sheetpile walls extend to much greater distances from the wall than predicted. This disagreement might be a result of “extraneous” construction-related factors which could have influenced and exacerbated soil movements: e.g., large pressure drawdowns in the lower aquifer and perhaps disturbance of the soil from tieback drilling activities.

8.2.3. Prediction of Settlements and Wall Deflections using MOVEX

8.2.3.1. The MOVEX Computer Program

The computer program MOVEX calculates lateral wall deflections and surface settlement distributions for braced excavations using the semi-empirical techniques developed by Mana & Clough (1981) and Clough et al. (1989). The program, presented by Smith (1987), accepts as input the undrained strength profile of the soil column, stiffness terms for the support wall and members (struts or tiebacks), and the dimensions of the excavation (including depth, width, and length, along with the vertical spacing of the support members). Given these quantities, the program then outputs maximum lateral wall deflections and surface settlement distributions for each time that the excavation reaches a new strut or tieback level.

The following procedure is used by MOVEX to calculate wall and soil movements, and is repeated by the program for each stage of the excavation. The first step undertaken

by MOVEX is to compute the factor of safety against basal heave (FSBH) based on an enhancement of the formula suggested by Terzaghi (1943). Figure 8.7 shows the formula used by the program, which accounts for soil layers with varying strength characteristics. (NOTE: The equation does not account for wall embedment depth.)

Next, MOVEX makes an initial estimate of maximum lateral wall movement by “reading” the appropriate value from the design chart developed by Clough et al. (1989), which is shown in Figure 2.4. This chart requires a “system stiffness” term which is computed using the given value of wall stiffness and the average spacing of support members at the given excavation stage. The initial estimate of wall movement is then modified by applying a series of multipliers, or “alpha factors”, as originally suggested by Mana and Clough (1981). Three alpha factors are used:

Alpha Factor	Approximate Range of Values	Parameter of Influence
α_S	0.75-1.2	Strut stiffness and spacing
α_D	0.62-1.0	Depth to ‘firm’ layer
α_B	1.0-1.8	Excavation width

Figure 8.8 shows how these alpha factors vary with their respective parameters. The alpha factors are applied to the maximum wall deflection obtained from Figure 2.4.

The maximum surface settlement is assumed to equal the final, modified estimate of maximum wall deflection. The settlement trough profile is then developed according to the suggested distribution by Mana and Clough (1981), shown in Figure 2.5.

The latest version of MOVEX which was completed by Smith (1987) also has two additional features. First, it can account for initial cantilever movements of the wall, which commonly occur before any support members are emplaced. The empirical methods used by the program do not account for such movements, so if this option is to be used, the user inputs the amount of cantilever deflection at the top of the wall and the depth to a “hinge” point. MOVEX will then add these deflections to subsequently calculated movements.

The program also allows for consideration of strength anisotropy in soils. The user can input an Anisotropic Strength Ratio (K_s), equal to the undrained strength in extension divided by the undrained strength in compression. The program then modifies its computed FSBH according to the graph shown in Figure 8.9.

8.2.3.2. Results of MOVEX Analyses

The MOVEX program was used to predict wall movements and surface settlements on the North (diaphragm wall) side and South (sheetpile wall) side of the excavation at ISS-4. Calculations required to define the input files are provided in Sheets G1 through G6 in Appendix G, and Sheets G10 through G15 provide two example output files from the program: one each for analyses of the sheetpile wall and the diaphragm wall. These output files used MIT's DSS undrained strength profiles in the BBC and overlying layers, included corrections to the strut stiffness terms to account (theoretically) for the downward inclination of the tiebacks, and assumed that the Glaciomarine and Glacial Till strata underlying the BBC formed an underlying "firm" base.

Figure 8.10 compares the predicted wall movements and settlements to those measured by geotechnical instrumentation between 10/93 and 4/94. During this period, the excavation was completed. It can be seen from this figure that sheetpile wall deflections were moderately underpredicted by MOVEX. In contrast, the behavior of Slurry Wall A - which bent back into the retained soil - was not duplicated. This is not surprising, given that the existing empirical and semi-empirical prediction methodologies do not account for this type of wall movement.

The program underestimated settlements behind the north slurry wall, but matched the settlements behind the south sheetpile wall fairly well (predicted settlements slightly exceeded the field measurements). This might reflect the different degrees of soil disturbance that occurred behind the walls in response to tieback drilling. Behind the North wall, there was evidence of considerable disturbance to the soil mass, and the BBC in particular (Section 3.4.2.2), which might have contributed to the large surface settlements that occurred there. On the other side of the excavation, tiebacks were not drilled as deep, and there was much less evidence of soil disturbance, so the "extraneous"

effects of drilling were minimized. Moreover, MOVEX makes the generally conservative assumption that the maximum vertical settlement equals the maximum lateral deflection.

Five different parametric analyses were performed with the program to gain insights into the effects of certain variables on the program results. The parametric analyses were conducted using the South sheetpile wall input file, which resulted in a reference δ_v of 4.6 in. Records from these program runs are provided on Sheets G8 and G9. The following paragraphs discuss the results of the parametric analyses.

1. *Depth to 'firm' layer.* For the reference case, with the Glaciomarine layer defined as the 'firm' layer, the maximum wall movement (and maximum settlement) equaled 4.6 inches. When the bedrock was defined as the underlying 'firm' layer, and the Glaciomarine and Till units were included in the input profile, the movements decreased to 2.6 inches. The Glaciomarine and Glacial Till are high strength layers, which, when included in the input, are factored into the average S_u below excavation used to compute FSBH (Figure 8.7). Their high strengths raise the average profile strength and the movements consequently decrease.

2. *Anisotropic Strength Ratio (ASR).* The following table shows how movements changed for different values of ASR, as Figure 8.9 indicates.

ASR	Max. Movement
0.5	7.3"
1.0	4.6"
1.25	4.1"

Since the reference case used DSS strengths rather than triaxial compression, the analysis with ASR=0.5 is not realistic.

3. *Effective Strut Length (ESL).* The "best estimate" of effective strut length for the tiebacks was selected as the free length (FL) plus one-half the bonded length (BL). This parameter was varied by using either none of the bonded length or all of it. This had only a slight influence on predicted movements:

Definition of ESL	Range of Stiffnesses (3 tiers)	Max. movement
ESL = FL	24,000 to 157,100	4.3"
ESL = FL + 0.5(BL)	19,400 to 85,700	4.6"
ESL = FL + BL	16,300 to 58,900	4.8"

4. *Initial cantilever movement.* Based on the initial cantilever-type movement of the South sheetpile wall measured by INC-101, a cantilever deflection of one inch at the top of the wall and a 25-foot-deep hinge point were input. The resulting maximum movement was unaffected. As the sketch on Sheet G9 indicates, the input cantilever deflection profile was added to the calculated wall deflections. This increased the deflections at the top of the wall, but had no influence on the lower elevations where maximum movement was predicted to occur.

5. *Width of excavation.* The table below shows how predicted movements varied with the excavation width. (All analyses assumed an excavation length of 2000 ft.)

Excavation Width	Max. Movement
50 ft.	2.9"
100 ft.	4.0"
200 ft.	4.6"
400 ft.	4.5"
1000 ft.	4.3"

A narrower excavation is predicted to experience decreased movements, as a result of a restraining influence from the other wall and supports. As the excavation widens, this restraint becomes less and less effective, and larger movements are predicted to occur. Eventually, as width continues to increase, additional gains in width have diminishing effects and the soil movements tend to reach an asymptote. This effect is illustrated by the hand-sketched graph at the bottom of Sheet G9. The program incorporates the effect of excavation width through the N_c factor, as defined on Figure 8.7.

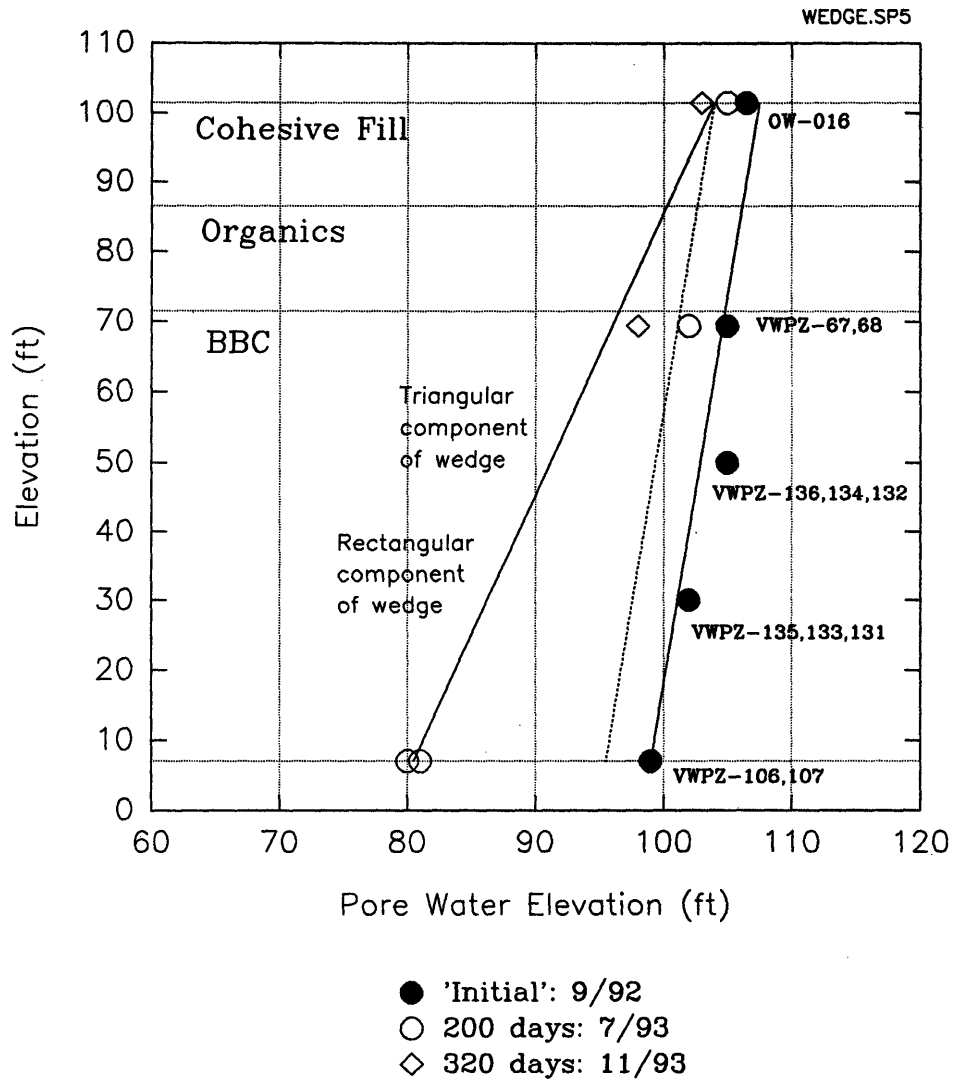


Figure 8.1. “Simplified” Excess Pore Pressure Wedge used for Consolidation Analysis, based on Measured Piezometric Water Elevations at Different Times and Three Elevations in the ISS-4 Soil Column.

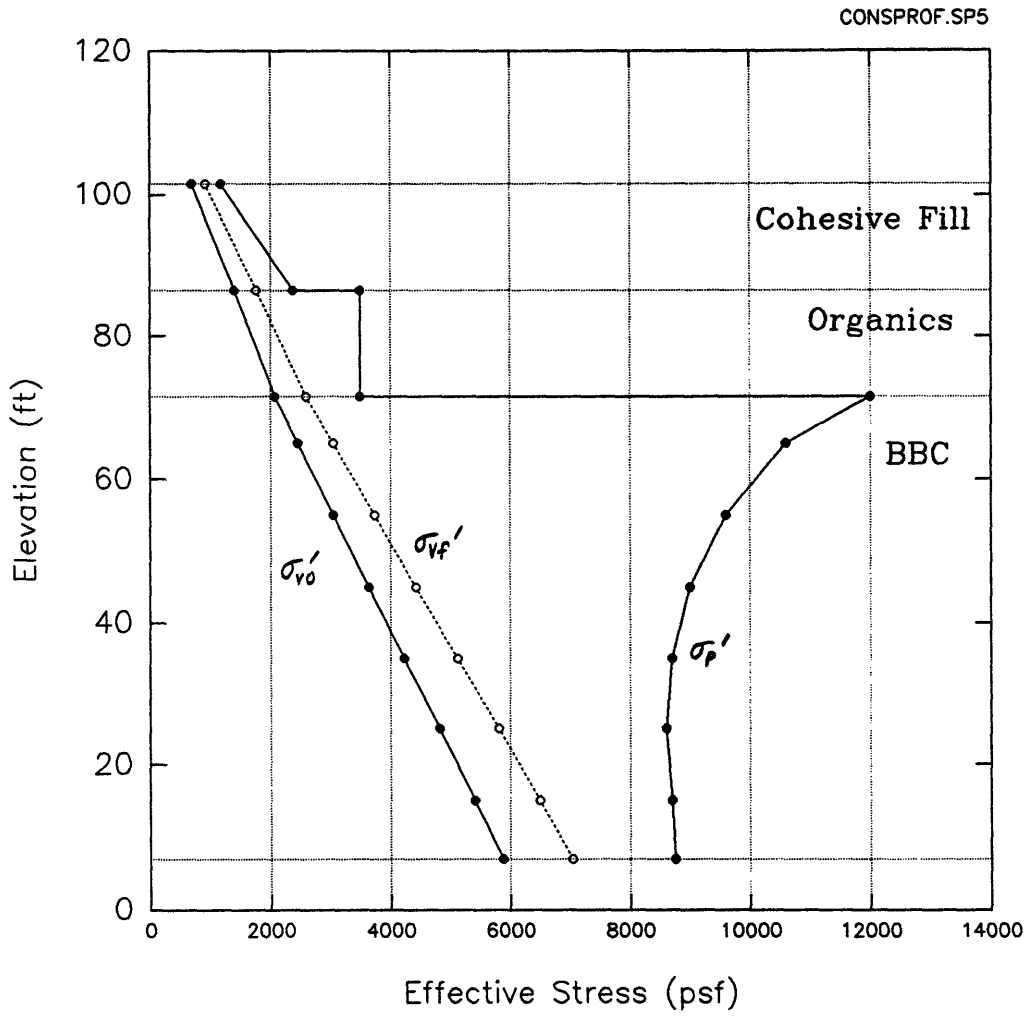


Figure 8.2. Plot of Effective Stresses and Preconsolidation Pressures Versus Elevation, Before and After Consolidation of Cohesive Soil Layers.

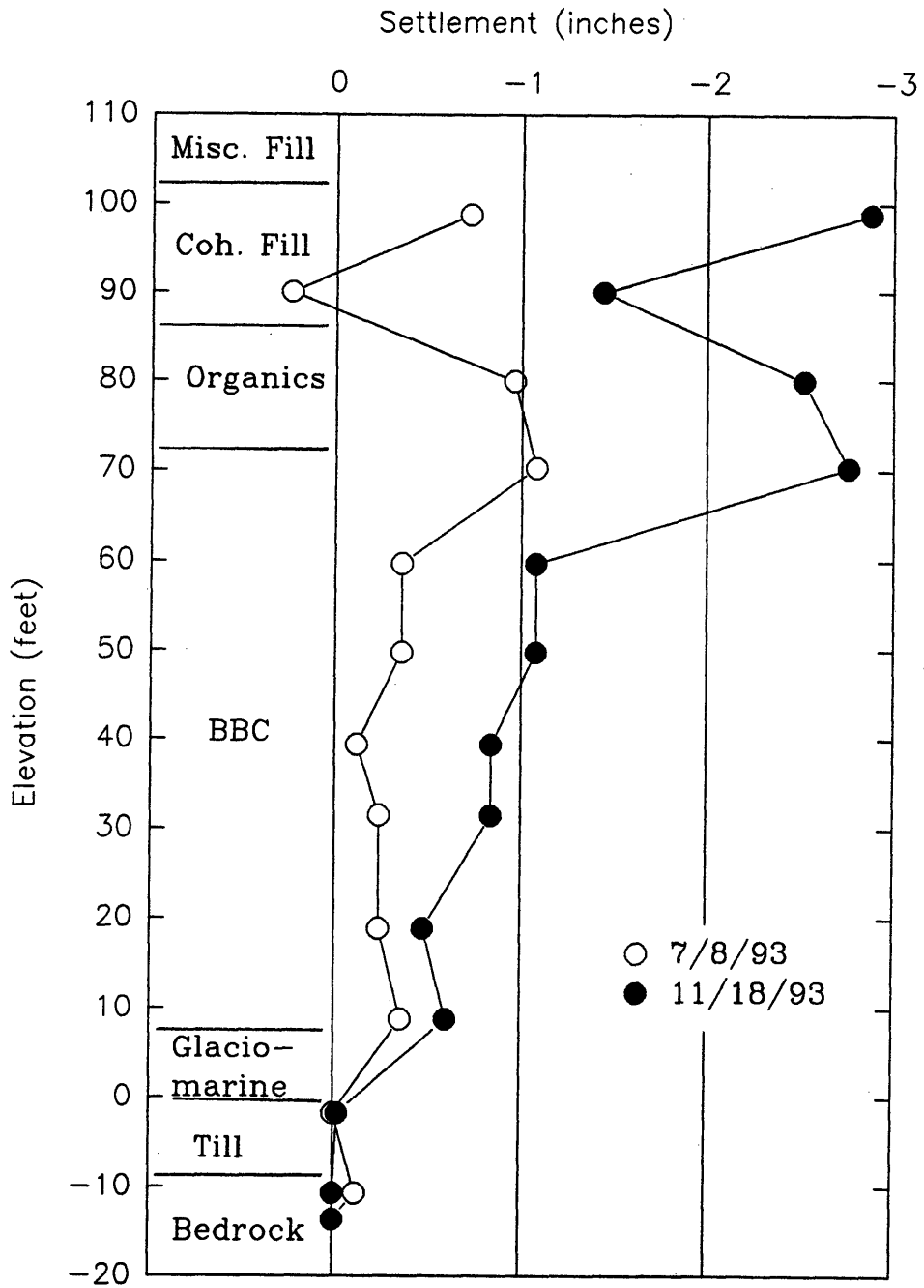
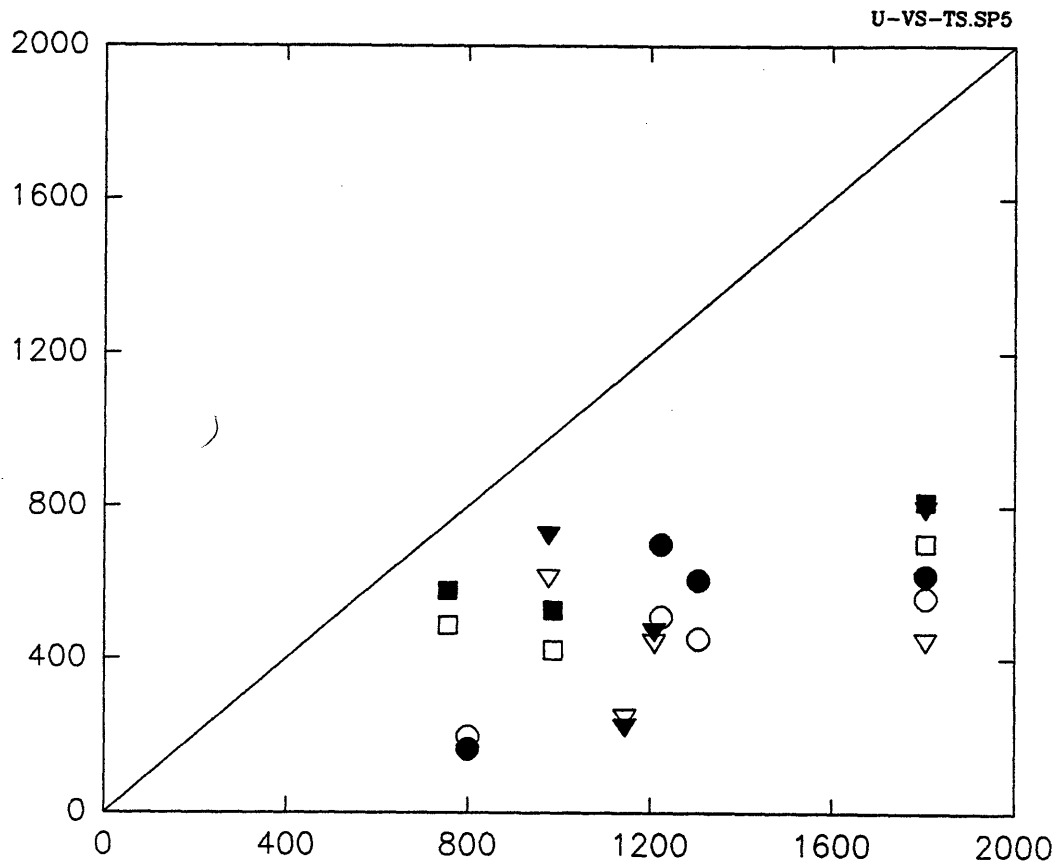


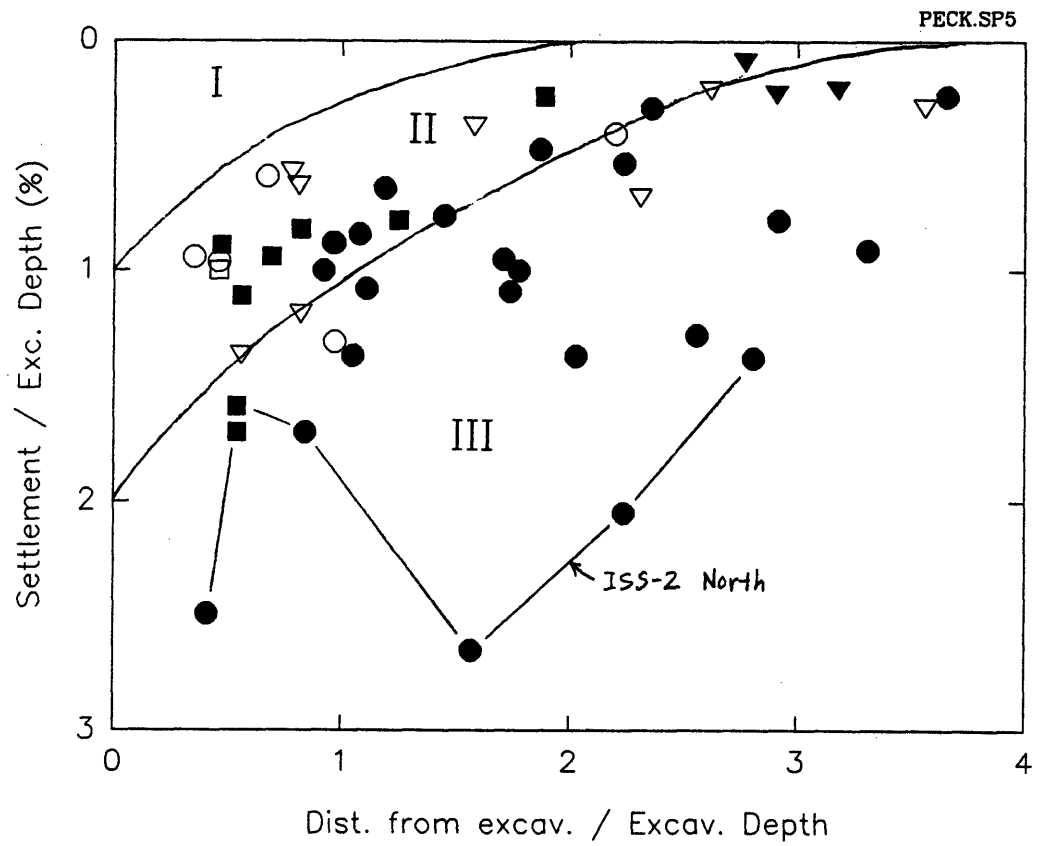
Figure 8.3. Settlements Measured by IPE-113 Plotted Versus Elevation.



- VWPZ-135, 136 (near North wall)
- VWPZ-133, 134 (near center)
- ▽ VWPZ-131, 132 (near South wall)

Filled symbols represent shallow piezometers (El. 50')
 Hollow symbols represent deep piezometers (El. 30')

Figure 8.4. Pore Pressure Reductions Measured by Piezometers Within the Excavation Plotted Against Excavation-Induced Total Vertical Stress Reductions.



	DMP-4	DMP-2	Probe Ext.
Sheetpile Wall	●	▼	■
Diaphragm Wall	○	▽	□

Refer to sheets F7 and F8 for tabulated data

Figure 8.5. Normalized Settlements Along Project Alignment (Prior to Construction of Invert Mat) Plotted on Peck's (1969) Design Chart.

NORMSETT.SP5

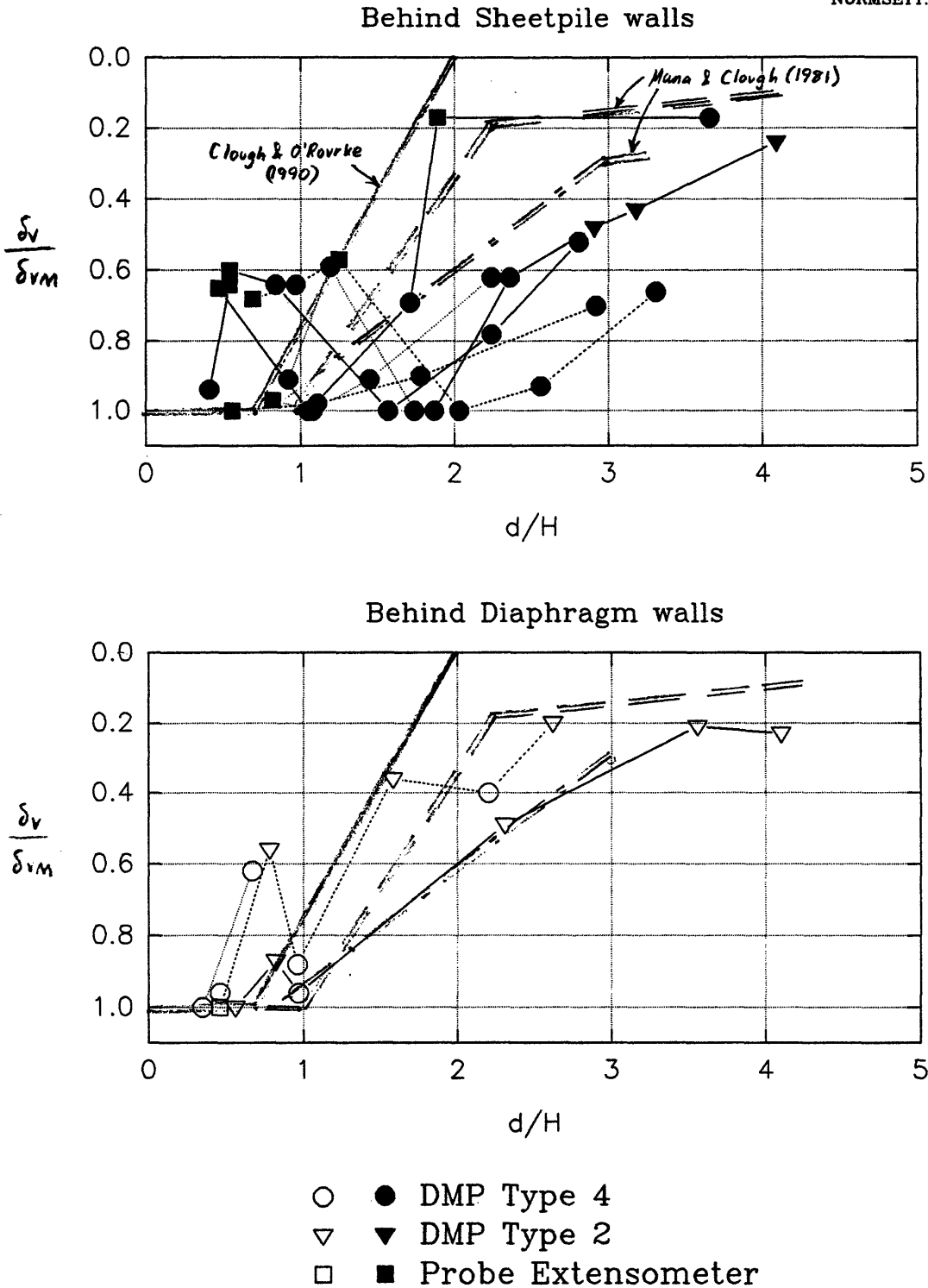
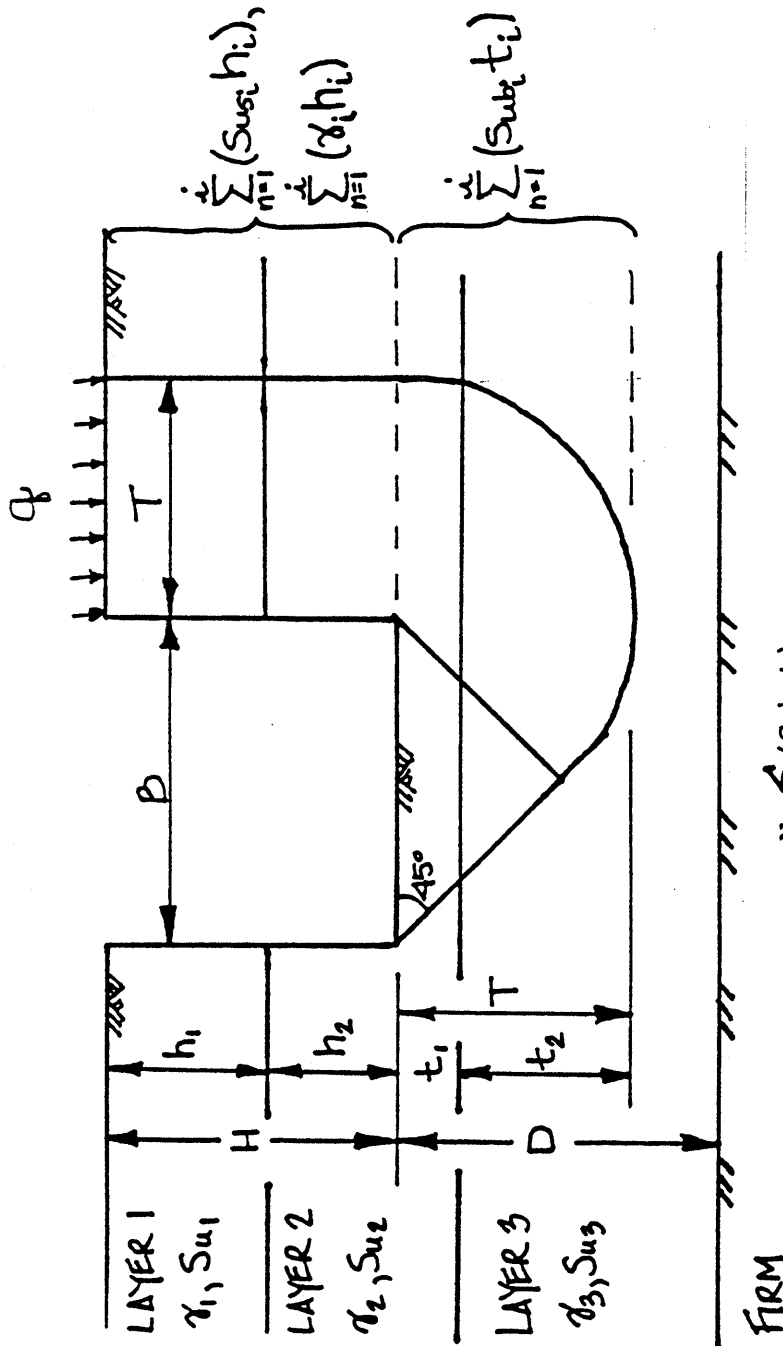


Figure 8.6. Normalized Settlement Distribution Along Project Alignment (Prior to Construction of Invert Mat) Plotted With Settlement Trough Envelopes Suggested by Mana and Clough (1981).



$$F = \frac{N_c \sum (Sub \cdot t)}{[\sum (\sigma h) + q]T - \sum (Sus h)}$$

IF $D < 0.7B$, $T=D$ IF $D > 0.7B$, $T=0.7B$

$N_c = 5 [1 + 0.2 (B/L)]$
 $L =$ excavation length

$Sus = S_u$ along side of excavation
 $Sub = S_u$ below excavation
 γ = total unit weight of soil along side of excavation
 q = surcharge load

Figure 8.7. Factor of Safety Calculation Used by MOVEX for Layered Soils (Smith, 1987).

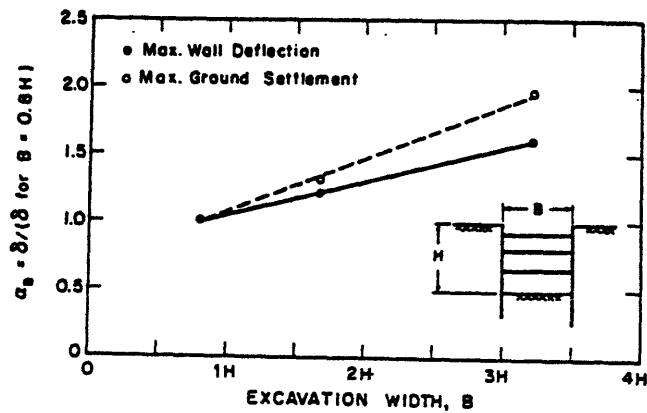
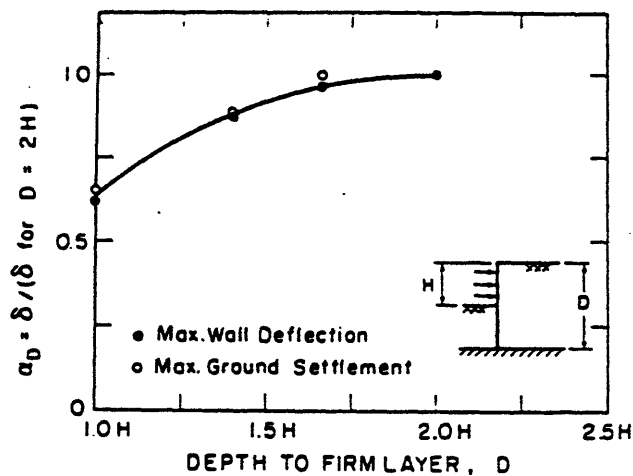
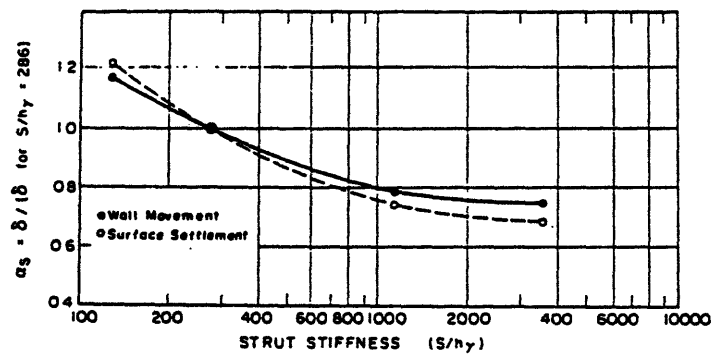


Figure 8.8. "Alpha Factors" Suggested by Mana and Clough (1981) which Relate Excavation Parameters to Maximum Lateral Wall Movement. (a.) Effect of Strut Stiffness. (S =Strut Stiffness per Horizontal unit of Length; h =Vertical Strut Spacing; γ =Total Unit Weight of Soil.) (b.) Effect of Depth to Underlying Firm Layer. (c.) Effect of Excavation Width.

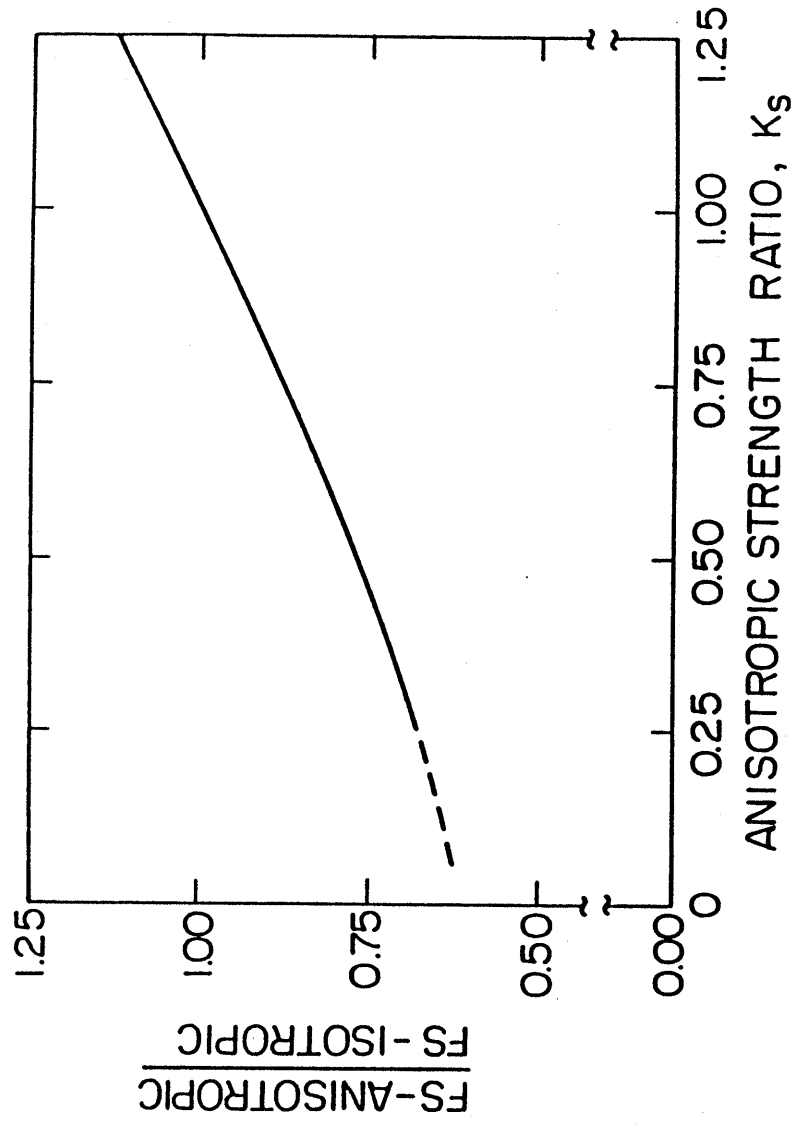


Figure 8.9. Factor of Safety Versus Anisotropic Strength Ratio (from Smith, 1987).

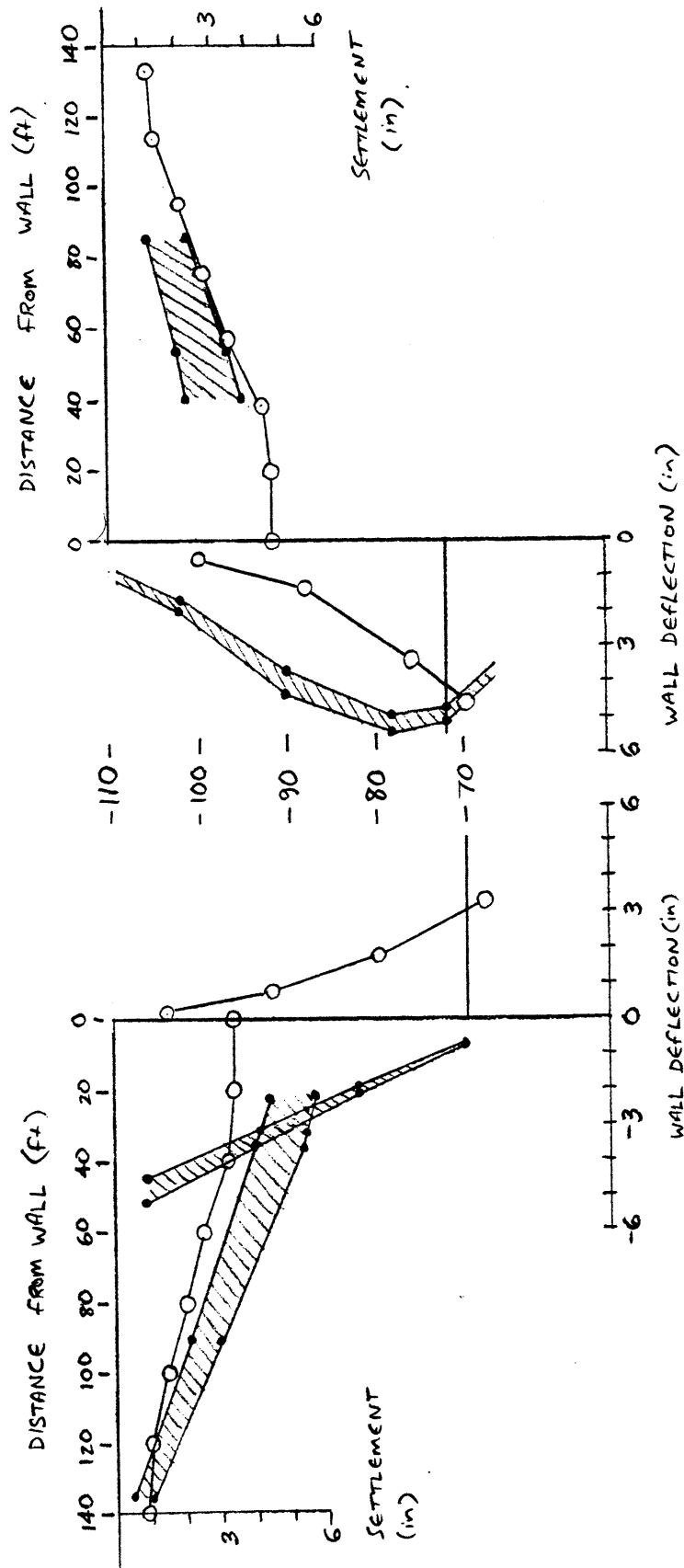


Figure 8.10. Comparison of Settlements and Wall Deflections Measured at ISS-4 and Predicted by the MOVEX Computer Program.

CHAPTER 9

SUMMARY AND CONCLUSIONS

9.1. SUMMARY

Ground movements play an important role in the design of deep excavations in cohesive soils. This thesis studies an excavation for a construction project in Boston, Massachusetts which is up to 60 ft deep and extends through a deposit of Boston Blue Clay which can be up to 100 ft thick. The presence of adjacent buildings makes the control of ground movements a primary consideration in the design of earth support systems for this excavation. This thesis focuses on ground movements and groundwater changes occurring at an excavation monitored by a thorough program of geotechnical instrumentation. An attempt is made to evaluate both the magnitudes and the causes of measured soil movements and groundwater fluctuations, and the measurements are compared to available empirically-based prediction techniques (reviewed in Chapter 2).

This study is one component of a three-phase research project entitled “Design and Performance of Deep Excavations”, which is being conducted by MIT for the Massachusetts Highway Department (MHD) and aims to develop improved methods of predicting ground movements associated with deep excavations in “soft” clays.

Chapter 3 provides a detailed description of the excavation and earth support systems utilized for the construction project. The project is approximately 2500 ft long and required an excavation which was 80 to 200 ft in width (widening towards the west) and 36 to 63 ft deep (generally deepening towards the east). Figure 3.1 presents a plan view of the excavation, and shows the locations of several pre-existing buildings adjacent to the cut.

Figure 3.3 illustrates the soil profile along the alignment’s centerline. The ground surface is underlain by recent fill deposits. Beneath a surficial layer of Miscellaneous Fill lie a sequence of three cohesive deposits: Cohesive Fill, Organics, and Boston Blue Clay (BBC). These cohesive and largely “soft” soils are inherently unstable when excavated, thus dictating the need for a support-of-excavation (SOE) system. The BBC deposit is the

predominant soil type in the area, with a thickness ranging from about 40 to 70 feet, thickest in the western half of the alignment. It has a relatively strong, overconsolidated crust but is softer and less overconsolidated at depth. Under the BBC lie two stronger, granular, glacially deposited strata, and then bedrock.

The excavation's large width made the use of tied-back walls, rather than cross-lot struts, an economical choice for excavation support. Two types of walls were used: sheetpile walls along the majority of the alignment, and stiffer diaphragm (slurry) walls along sections that were immediately adjacent to buildings. Figure 3.2 shows a cross-sectional view of the excavation at a location where both types of wall were used (due to the presence of a building near one side). Behind the sheetpile walls, the tiebacks were grouted in the stiff, overconsolidated crust of the Boston Blue Clay (BBC), while behind the diaphragm walls, they extended at a steeper angle (45 degrees) into the underlying bedrock.

The excavation was heavily instrumented by a variety of different types of geotechnical instruments. Lateral deflections at or behind (to the retained side of) the walls were measured with inclinometers (INC's). Surface settlements were measured with Deflection Monitoring Points, (DMP's). Settlements at different depths within the soil mass were measured with probe extensometers outside of the cut and Multi-Point Heave Gages (MPHG's) within the cut. Inclinometers were commonly combined with probe extensometers to form "IPE's". Groundwater elevation was measured with Observation Wells (OW's) and Open Standpipe Piezometers (OSPZ's). Deeper piezometric pressures were monitored with Vibrating Wire Piezometers (VWPZ's). Appendix A presents a detailed discussion of the design and capabilities of these instruments.

The layout of instruments throughout the project area is shown on Figure 4.2. Instruments were generally arranged in clusters, or instrumented sections. A single well-instrumented "test section" was selected for detailed analysis. The section labeled ISS-4, at Sta. 77+20, was selected using criteria which are described in detail in Chapter 4. ISS-4 offered the following major advantages: 1. It was well instrumented on both sides of, and within, the excavation. 2. It experienced soil movements and a construction history that were considered representative of the entire area. 3. It had both types of support walls: a

diaphragm wall on the north side (adjacent to Building “A”) and a sheetpile wall on the south side.

Chapter 5 presents the selected soil profile and engineering properties at ISS-4. Information on the soil deposits came from two studies executed by MHD’s Geotechnical Consultants: a geotechnical engineering investigation for the project (MHD Geotechnical Consultant, 1991a and 1991b), and a Special Testing Program, done in conjunction with MIT and others, which evaluated the engineering properties of the BBC using a variety of advanced laboratory and in-situ testing techniques (MHD Geotechnical Consultant, 1993). Figure 5.2 shows the “best estimate” soil profile for ISS-4, based on a number of borings conducted in the vicinity of the test section. Tables 5.1 through 5.7 provide summarized information on soil test results and selected engineering properties, while more detailed soil property data are presented in Appendix B.

MIT carefully evaluated strength, flow, and compressibility properties of the three cohesive soils at ISS-4, by applying various analytical techniques to available test data and by using pertinent information on similar soils at other locations. The Strain Energy technique (Becker et al., 1987) was used to estimate preconsolidation pressures from the consolidation tests on BBC. This generally gave less scattered values than Casagrande’s (1936) technique, for the upper clay crust having rounded compression curves (compare Sheet B10 and Figure 5.7). Undrained strengths were estimated using the SHANSEP method (Ladd and Foott, 1974).

The geometry, support systems, and construction history were defined for the ISS-4 test section as precisely as possible, using construction data provided by two sources: MHD’s Management Consultant and the construction contractor. Chapter 6 describes the use of construction records to define the geometry of the ISS-4 section, the tieback lockoff loads and moduli, and the construction history. Tables 6.1 and 6.3 summarize the ISS-4 tieback properties and construction history, respectively. Figure 6.1 shows a cross-sectional view of ISS-4, and Figure 6.8 graphically summarizes the construction history at that location.

Monitoring data from the geotechnical instruments at ISS-4 were provided by MHD’s Management Consultant. MIT created two types of data summary figures. First,

the data were plotted against time; these graphs are the "7A" series of figures in Chapter 7. A key feature of the MIT graphs is that each includes a graphical representation of the excavation history, for easy comparison to the geotechnical data. A total of seventeen graphs were prepared for the 7A series: Figures 7A.1 through 3 show lateral deflections of the walls and soil; Figures 4 through 6 show settlements; Figures 7 through 10 show groundwater levels and piezometric pressures around the excavation; Figures 11 through 14 show soil heave within the excavation; and Figures 15 through 17 show piezometric pressures in the BBC within the cut.

The second type of data plot was a series of eight "Time Period Summaries", the "7B" series of figures. Each Time Period Summary consists of a pair of sheets showing the excavation's geometry, construction activities (i.e., tieback installation and lock-off), surface settlements, and wall deflections for a particular time period.

Chapter 7 presents detailed discussions of the wall movements, settlements, and groundwater changes that were observed at ISS-4 throughout the construction history. This discussion attempts to define the causes of trends seen in the instrumentation data, by relating observed soil and groundwater changes to construction events: namely, excavation of lifts, installation of tiebacks, and groundwater pumping activities.

Additional calculations were done by MIT in an effort to better identify the causes of certain phenomena seen in the instrumentation records. One set of calculations models the consolidation behavior of cohesive soils at ISS-4 in response to groundwater drawdowns observed in the upper fill and in the deeper glacially deposited soils. The calculations predicted surface settlements and piezometric reductions within the cohesive layers, for two different dates in the construction history. These calculations are discussed in Section 8.1. Section 8.2 compares the observed wall and ground movements to predictions from available empirical and semi-empirical techniques. In particular, predictions made by the computer program MOVEX (Smith, 1987) were analyzed (Figure 8.10).

9.2. CONCLUSIONS

9.2.1. Factors Influencing Wall and Soil Movements

In general, current methods of predicting wall and soil movements for braced excavations make the assumption that the surface settlements (vertical deflections, δ_v) are directly relatable to the amount of horizontal wall deflection (δ_h). A common approach is that of Mana & Clough (1981) and Clough & O'Rourke (1990), which involves first utilizing empirical data and analytical experience to estimate the maximum δ_h , and then predicting maximum δ_v by assuming that it is approximately equal to the maximum δ_h . The geometry of the settlement trough can then be readily developed by using charts such as those presented in Figures 2.2 and 2.5.

Measurements from the geotechnical instruments at ISS-4 indicate that the actual development of movements is not this simple and that a variety of additional factors can significantly influence δ_h and δ_v and the relationship between the two. In particular, this research has identified three possible factors which could have influenced movements at ISS-4; these factors are discussed as follows.

1. Pumping for dewatering and pressure-relief purposes caused large drawdowns in the granular materials underlying the BBC. Piezometers placed in the relatively permeable glacial deposits underlying the BBC recorded a rapid pressure head reduction of 30 to 35 feet in January of 1993; PWE drawdowns remained between 10 and 20 feet throughout the rest of the year (Figure 7A.7). These PWE reductions resulted from pumping which was done to dewater the excavation and prevent hydrostatic uplift of soils within the cut. Drilling of holes for installation of boat section tiedowns was another likely cause of these large PWE fluctuations in the lower soil deposits.

These deep drawdowns, in conjunction with smaller drawdowns measured in the overlying Miscellaneous Fill, promoted consolidation of the cohesive soils (Cohesive Fill, Organics, and BBC) and hence surface settlements. PWE reductions within the cohesive soils were recorded by VWPZ-67 and 68, which recorded drawdowns at the top of the BBC of about 8 to 10 feet by the end of 1993 (Figure 7A.9). These drawdowns may reflect ongoing pressure dissipation and consolidation of the cohesive soils. However, consolidation calculations using reasonable estimates of consolidation coefficient (c_v)

underpredicted the degree of PWE reduction in these instruments (Section 8.1.1.1). This suggests that the assumed values c_v were too low, or possibly that drainage in the clay was enhanced (on the north side) by disturbance from tieback drilling activities.

2. Observations by field engineers during drilling of tiebacks at the north diaphragm wall (Slurry Wall A) suggested the possibility of disturbance to the cohesive soils due to the use of high air and water pressures and a down-hole hammer. At the south sheetpile wall, a drag bit was used, providing a cleaner cut and potentially less disturbance. This factor, while somewhat speculative, does provide a means of explaining large settlements behind Slurry Wall A, even though the wall was “pulled back” into the retained soil.

3. This “pull back” deflection of Slurry Wall A was not predicted by any existing design chart. The “pull back” was a result of high lock-off forces applied to the diaphragm wall tiebacks, which was sufficient to not only resist the lateral earth pressures but to reverse the direction of wall movement. Since the available design charts account for bracing *stiffness*, not *force*, they cannot predict negative wall deflections.

9.2.2. Comparison of Measured Wall and Soil Movements to Predictions

9.2.2.1. North Side of Excavation (Slurry Wall A)

Although Slurry Wall A deflected back into the retained soil mass (due to the tieback forces), positive (downward) settlements were measured behind the wall (Figure 7A.4). This behavior disagrees with common experience for excavations in cohesive soils, which predicts that the maximum settlements should approach the maximum wall deflection into the excavation, and therefore that soil *heave* should accompany wall “pull-back”. The downward settlements at Slurry Wall A could be caused by: 1. Consolidation settlement of the BBC and possibly the other cohesive soils, due to the large drawdowns in the underlying permeable soils and, to a lesser extent, the water table drawdowns in the overlying Miscellaneous Fill; and 2. Disturbance to cohesive soil deposits (Figure 6.1) from tieback drilling activities.

The computer program MOVEX was used to predict wall deformations and surface settlements from the design charts of Mana & Clough (1981) and Clough et al.

(1989). As expected, the program completely failed to predict the “pull-back” experienced by Slurry Wall A. However, due to compensating “errors”, the program slightly underpredicted the settlements behind the north side of the excavation (Figure 8.10).

9.2.2.2. South Side of Excavation (Sheetpile Wall)

While MOVEX underpredicted the deflection of the south side sheetpile wall, it nearly matched (but slightly exceeded) the amount of settlement behind the wall (Figure 8.10). These settlements appear to be the result of: 1. Motion of soil in toward the excavation, as indicated by bowing of the sheetpile wall. 2. Consolidation of the clay and cohesive soils, from the PWE drawdowns. Disturbance to the underlying soils was not as likely behind the south wall as it was behind the north wall, since a different drilling technique was used. The close agreement of predicted and measured settlements may be due to the lesser influence of this factor on the south side.

9.2.2.3. Trends Common to Both Walls

Measured wall movements on both sides of ISS-4 seemed to correlate well with construction activities. For the south wall (Figure 7A.2), excavation of lifts appeared to cause accelerated wall movements, while the ensuing lock-off of tiebacks tended to stop, slow down, or temporarily reverse the wall movements. The opposite was true for the “pulled back” north wall (Figure 7A.1), which experienced brief *increases* in movement when tiebacks were locked off, reflecting the added force of the added tieback tier.

Normalized settlements extended farther from the wall than was predicted by the design chart of Clough & O’Rourke (1990) (Figure 8.6). This seems attributable to soil consolidation from drawdowns in the lower aquifer.

9.2.3. Groundwater and Soil Movements Within the Excavation

Reductions in pore pressure measured by VWPZ’s inside the cut correspond to times of excavation unloading events (refer to Figures 7A.15 through 7A.17). The decreases in PWE are a response to excavation unloading, but appear to be somewhat less than would be expected in a 1-D unloading scenario. This is attributable to three-

dimensional stress effects, from the added weight of berms that were commonly left to the sides of newly excavated lifts. The dissipation of these excess negative pore pressures caused heave of the soils within the excavation (see Figures 7A.11 through 7A.14).

9.3. RECOMMENDATIONS

This research involved a great deal of data collection and required careful study of numerous construction records that were kept by MHD's Management Consultant and the contractors. The experience of using these records to accurately recreate the construction history and interpret geotechnical data led to the following recommendations for record keeping on future projects involving deep excavations in cohesive soils.

9.3.1. Excavation Conditions and Construction History

An accurate understanding of the construction history of an excavation is essential for proper interpretation of monitoring data. The success of reconstructing this history is dependent on the quality and clarity of construction records. It can be greatly facilitated if the contractor keeps updated summary tables which list the dates of lift excavations and of all other construction activities such as tieback installation and lock-off. The Construction Activity Tables shown on Sheets D1 and D2 served this purpose. However, the dates only provide part of the story: the depth, geometry, and extent of each lift, including those that occur near the center of the cut rather than at the sides, need to be properly defined as well for a complete understanding of the construction sequence. Information on the time history of subgrade geometry is essential for FEM (finite element) modeling.

Regular photographs of the site taken throughout the construction history are very helpful in this regard, especially if they show wide views of the excavation, and not just "close-ups". These photographs provide important information on the geometry of all excavation lifts.

9.3.2. Presentation of Geotechnical Instrumentation Data

To facilitate the study and interpretation of monitoring data, plots should incorporate the following features, all of which appear in the "7A" series of figures:

1. They should use a convenient time scale, such as months.
2. The dates of construction events should be provided along with the geotechnical data. This can be readily done with modern computer spreadsheet software. A graphical time scale showing subgrade elevation vs. time is a particularly effective way of presenting this information.
3. Data from associated instruments should be placed together on the same graph, so their records can be easily compared.

CHAPTER 10

LIST OF REFERENCES

- Becker, D. E., J. H. A. Crooks, K. Been, and M. G. Jefferies (1987). "Work as a Criterion for Determining In Situ and Yield Stresses in Clays". *Canadian Geotechnical Journal*, 24(4), 549-564.
- Casagrande, A. (1936). "The Determination of the Pre-Consolidation Load and its Practical Significance". *Proceedings of the 1st ICSMFE*, Cambridge, Vol.3, 60-64.
- Clough, G. W. (1985) "Effects of Excavation Induced Movements in Clays on Adjacent Structures". *Proceedings of the Eleventh International Conference on Soil Mechanics and Foundation Engineering*, San Francisco, Session 5A.
- Clough, G. W. and R. R. Davidson (1977). "Effects of Construction on Geotechnical Performance". *Relationship Between Design and Construction in Soil Engineering*, Ninth International Conference, International Society for Soil Mechanics and Foundation Engineering, Tokyo, July 1977, 15-53.
- Clough, G. W. and J. M. Duncan (1971). "Finite Element Analysis of Retaining Wall Behavior". *Journal of Soil Mechanics and Foundations Engineering*, ASCE, (97), 1657-1673.
- Clough, G. W. and T. D. O'Rourke (1990). "Construction Induced Movements of In-situ Walls". *Proceedings of the Specialty Conference on Design and Performance of Earth-Retaining Structures*, ASCE, 439-470.
- Clough, G. W., E. M. Smith, and B. P. Sweeney (1989). "Movement Control of Excavation Support Systems by Iterative Design". *Proceedings of the Congress on Foundation Engineering: Current Principles and Practices*, ASCE, Vol.2, New York, NY., 869-882.
- Contractor's Geotechnical Consultant (1992a). "Specifications for Tieback Installation and Test Program". Submitted to contractor.
- Contractor's Geotechnical Consultant (1992b). General Excavation Dewatering and Pressure Relief System Drawings. Submitted to contractor.
- Contractor's Geotechnical Consultant (1992c). "Tieback Test Program: Upper Level Tiebacks" and "Lower Level Tiebacks". Submitted to contractor.
- Das, Braja M (1984). *Principles of Foundation Engineering*. PWS-Kent Publishing Co., Boston, MA.
- Druss, D. (1994) "Waterproofing a Structural Slab at Ground Anchor Locations". *Proceedings of the Specialty Conference on Serviceability of Earth Retaining Structures*, ASCE, Atlanta, October.
- Dunnicliff, J. (1981). Training Course entitled "Geotechnical Instrumentation", U.S. Dept. of Transportation, Federal Highway Administration.

- Dunnicliff, J. (1988). *Geotechnical Instrumentation for Monitoring Field Performance*. Wiley.
- Fetter, C. W. (1988). *Applied Hydrogeology*. 2nd Edition. Merrill Publishing Company, Columbus, Ohio.
- Finno, R.J. and Harahap, I.S. (1991). "Finite Element Analysis of HDR-4 Excavation". *Journal of Geotechnical Engineering*, ASCE, 117 (10), October. 1590-1609.
- Goldberg, D. T., W. E. Jaworski, and M. D. Gordon (1976). "Lateral Support Systems and Underpinning". Report No. FHWA-RD-75-129, Volume 2. Washington, D.C., April.
- Hashash, Y. M. A. and A. J. Whittle (1994). "Ground Movement Prediction for Deep Excavations in Soft Clay". Submitted to the *Journal of Geotechnical Engineering*, ASCE, August.
- ISPC [International Sheet Piling Company] (1990). *Steel Sheet Piling: A Selection of the Best*. Luxembourg, January.
- Kaye, C. A. (1982). "Bedrock and Quaternary Geology of the Boston Area, Massachusetts", *Geological Society of America Reviews in Engineering Geology*, Vol. V, 25-40.
- Ladd, C. C. (1994). Private Communication.
- Ladd, C. C. and R. Foott, (1974). "New Design Procedures for Stability of Soft Clays", *Journal of the Geotechnical Engineering Division*, ASCE, No. GT7, August.
- Ladd, C. C. and A. J. Whittle (1993). "Design and Performance of Deep Excavations". Research Proposal, Department of Civil and Environmental Engineering, MIT, Cambridge, MA. Submitted to Massachusetts Bureau of Transportation, Planning, and Development on July 30, 1993.
- Ladd, C. C., A. J. Whittle, and D. E. Legaspi, Jr. (1994). "Stress-Deformation Behavior of an Embankment on Boston Blue Clay". *Vertical and Horizontal Deformations of Foundations and Embankments: Proceedings of Settlement '94*, Geotechnical Engineering Division, ASCE, College Station, Texas, June 16-18, 1730-1759.
- Lambe, T. W. and Whitman, R. V. (1969). *Soil Mechanics*. John Wiley and Sons.
- Mana, A.I. and Clough, G.W. (1981). "Prediction of Movements for Braced Cuts in Clay". *Journal of the Geotechnical Engineering Division*, ASCE, Vol.107, No.GT6, June, 759-777.
- Massachusetts Department of Public Works (1991). Standard Drawings for construction project under study.
- MHD [Massachusetts Highway Department] (1992). *Special Provisions to Construction Details of the Standard Specifications for Highways and Bridges*. Contract Document, Volume 2 of 7 (Attachment A, Div. II), April.
- MHD Geotechnical Consultant (1991a) "Final Geotechnical Data Report", Volumes I and II. Submitted to the Massachusetts Department of Public Works, April.

- MHD Geotechnical Consultant (1991b) "Final Geotechnical Engineering Report". Submitted to the Massachusetts Department of Public Works, October.
- MHD Geotechnical Consultant (1992) "Draft Report on Pumping Tests No. 3 and No. 4". Submitted to the Massachusetts Department of Public Works, January.
- MHD Geotechnical Consultant (1993) "Final Report on Special Laboratory and In-Situ Testing Program". Submitted to the Massachusetts Highway Department, March.
- MHD Instrumentation Consultant (1992). Geotechnical Instrumentation Qualifications, Material, and Installation Procedures Submittals, Numbers 1, 2, and 3.
- Milligan, G.W.E. (1983). "Soil Deformations Near Anchored Sheet-Pile Walls". *Geotechnique*, Vol.33, No.1, 41-55.
- NAVFAC (1982). *Design Manual 7.2: Foundations and Earth Structures*. Department of the Navy, May.
- O'Rourke, T. D. (1981). "Ground Movements Caused by Braced Excavations". *Journal of the Geotechnical Engineering Division*, ASCE, 107(9), 1159-1177.
- Peck, R.B. (1969). *Deep Excavations and Tunneling in Soft Ground*, State-of-the-Art Report, 7th International Conference of Soil Mechanics and Foundation Engineering, Mexico City, 225-290.
- PTI (1986). *Recommendations for Prestressed Rock and Soil Anchors*. Post-Tensioning Institute, Phoenix, AZ. 12-15.
- SINCO (Slope Indicator Company) (1991). Instruction Manual, Digitilt Inclinometer with Sensor.
- Skempton, A.W. and MacDonald, D.H. (1956). "The Allowable Settlement of Buildings". *Proceedings of the Institute of Civil Engineers*, Part III. Vol.5, 727-784.
- Smith, E. M. F. (1987). *MOVEX: Interactive Design of Braced Excavations to Limit Ground Movements*. M.S. Thesis, Virginia Polytechnic Institute.
- Terzaghi, K. (1943). *Theoretical Soil Mechanics*. John Wiley & Sons, New York.
- Whittle, A. J., Y. M. Hashash, and R. V. Whitman (1993). "Analysis of Deep Excavation in Boston". *Journal of the Geotechnical Engineering Division*, ASCE, 119(1), 69-91.
- Whittle, A. J. and M. J. Kavvas (1994). "Formulation of MIT-E3 Constitutive Model for Overconsolidated Clays". *Journal of Geotechnical Engineering*, ASCE, 120(1), 173-198.
- Xanthakos, P. P. (1991). *Ground Anchors and Anchored Structures*. John Wiley & Sons, USA.

APPENDIX A

REVIEW OF GEOTECHNICAL INSTRUMENTATION

A.1. Purpose of Geotechnical Instrumentation

Large excavations, such as the one for the project under consideration, have the potential to cause damage to adjacent facilities and adversely affect the excavation support system due to excessive deformations in the surrounding soil and large changes in the groundwater regime. Installation and careful monitoring of geotechnical instruments allows measurement of wall deflections, surface settlements, loads on support members, and changes in the pore water pressures. This has two major benefits. First, it can provide forewarning of adverse behavior such as unacceptably large settlements or groundwater drawdowns, thereby allowing remedial actions to be implemented before adjacent structures are damaged. Second, even if problems do not arise, the project's quantitative performance can be used to assess the effectiveness of the excavation and construction techniques, thus providing helpful information and lessons for future work of a similar nature.

Appendix A reviews the purpose, design, installation, and use of the various types of geotechnical instrumentation that were studied in this report. Actual specifications for instruments used in the construction project were obtained from a series of three submittals done by MHD's Instrumentation Consultant (1992). General information on the basis and design of geotechnical instruments has been abstracted from the writings of Dunnycliff (1981, 1988).

Tables A.1 through A.4 supply information on all geotechnical instruments which were installed in the vicinity of ISS-4 and which provided the data that were evaluated.

A.2. Instruments Which Measure Lateral Deformations (Inclinometers)

Lateral deflections that occur within a soil profile or along a support wall can be measured with an *inclinometer*. An inclinometer is in essence a pipe-like instrument which

measures deformations normal to the axis of the pipe by means of a probe which is lowered or raised through it (Dunnicliff, 1988). Figure A.1-a illustrates a typical inclinometer design according to the project specifications. Although inclinometers are most commonly installed vertically, as they were beside the project's braced excavation, they can also be aligned horizontally for measurement of settlements beneath structures or embankments.

An inclinometer consists of two main components. First is the *guide casing*, a long tube made of plastic, fiberglass, aluminum, or steel, having an outside diameter of two to 3-1/2 inches. 2.75-inch O.D. plastic casings were used at this project. Although casings with square cross-sections are available, they are more frequently cylindrical, with four orthogonal grooves along the length of the inside. These grooves serve as tracks for the wheeled *probe*, as do the four inside corners of a square casing. The probe is the second major component of an inclinometer. As it is pulled up through the guide casing, it measures the degree of tilt at regularly-spaced points along the casing length, generally with a force balance accelerometer, which was used for this project, or a potentiometric transducer.

Depending on the strength and consistency of the soil profile, a vertical inclinometer casing can be installed in a borehole that is either unsupported or supported by drilling mud or a drill casing. The inclinometer casing should extend down into a layer that will provide base fixity; Dunnicliff (1988) recommends a depth of 10 to 20 feet below the expected active deformation zone, while MHD's standard specifications for this project (1991) specify a depth of ten feet into the "fixed" stratum. The annular space between the inclinometer casing and the boring wall is filled with grout or granular material. If a drill casing was used to support the borehole, it must be removed once the annular space has been filled. The backfill material should have approximately the same shear strength and compressibility as the surrounding ground, as was required for the grout mix used in this project's inclinometers.

Although many of the inclinometers within the project alignment were installed in boreholes, the majority of inclinometers east of Sta. 78 were attached to the driven sheetpiles on the side facing the interior of the cut. The inclinometer casings were placed

in 5-inch O.D. steel pipes that were connected to the sheetpiles with welds and steel brackets as the excavation proceeded. Because these instruments were not protected by surrounding soil, they were more susceptible to damage from construction equipment. For example, Inclinator 117 (Sta. 86+22, North side) was cut off ten feet above the final subgrade and Inclinator 116 (Sta. 84+48, North side) was bent three inches, also about ten feet above final subgrade.

Where the excavation was supported by slurry walls rather than sheetpiles, inclinometers could conveniently be installed in the concrete mix during wall construction before set up. Inclinator 102, in Diaphragm Wall A, and inclinometer 104, in Diaphragm Wall B, were installed in this way.

The principle of inclinometer measurement is illustrated in Figure A.1-b. Lateral deflections along the length of the inclinometer casing are measured by passing a level-sensing probe through the casing. In a vertical inclinometer the probe is first lowered to the fixed base of the casing, and as it is pulled back up, measurements of inclination are taken at regular intervals. Dunncliff (1988) recommends using a measurement interval that is equal to the spacing between wheels on the probe; following this recommendation, the inclinometers at this project had a reading interval of two feet.

A single monitoring session may require more than one set of probe runs. Probes which measure only uniaxial tilt require a pair of runs in orthogonal casing grooves to measure deflection in both vertical planes. The instrumentation specifications for this construction project mandate the use of biaxial probes, which measure inclinations in both planes at once. However, even a biaxial probe should be run through the casing an additional time, rotated 180 degrees from its first orientation. This allows a convenient assessment of systematic errors in the instrument or problems with the casing through the calculation of "check-sums", the algebraic sums of the two readings taken at each depth increment. Ideally, check-sums should remain fairly constant over the casing length. Specs for this project required that the standard deviations of the check-sums not exceed 0.0005 feet. This project's inclinometers were manufactured by Slope Indicator Co., and had accuracies of approximately 0.25 inches per 100 feet of casing (SINCO, 1991).

Inclinometer data are processed through a series of simple but time-consuming arithmetic steps, and since a single error can accumulate and produce completely misleading results, this analysis should be automated. (A detailed discussion of the data reduction process is not necessary for the purposes of this presentation.) Engineers on this project utilized the GTILT computer program, by Mitre Software Corporation in Edmonton, Alberta, to reduce raw inclinometer data and to create plots of deflections.

A number of inclinometer casings at the excavation under study were equipped with spider magnets at various depths, which allowed measurement of settlements at multiple points within the soil profile. These combined instruments are known as Inclinometer/Probe Extensometers and are discussed further in Section A.3.2.

Table A.1 contains information on the three inclinometers installed at ISS-4.

A.3. Instruments Which Measure Vertical Deformations

Generally, controlling surface settlements is more important than controlling horizontal wall deflections, because settlements have the potential to directly harm adjacent structures and utilities, whereas wall movements provide a less direct indication of soil deformations that could cause damage. Thus it is important to monitor settlements carefully. Various geotechnical instruments exist for the purpose of measuring settlements not only at the surface or on structures, but also below the surface, at different points within the soil profile. Measurement of settlements at different depths allows identification of the soil strata that are compressing or heaving, thereby providing insight into the causes of the surface movements.

A.3.1. Deformation Monitoring Points

Monitoring surface settlements requires surveying the precise position of defined points, relative to unmoving or “deep” benchmarks. MHD’s Standard Special Provisions for this project specify four different types of Deformation Monitoring Points, or DMP’s, for measurement of both vertical and horizontal displacements of points on the ground surface and on structures. Figure A.2 shows drawings of the different DMP types.

Types 1 and 4 are emplaced in the ground or in paved horizontal surfaces like roads or sidewalks. Types 2 and 3 are mounted horizontally in vertical surfaces such as the sides of buildings or curbs. Type 2 consists of a screw anchor into which a bolt is threaded when surveying is being performed. Type 3 differs from Type 2 in that a shorter bolt is permanently screwed into place.

At ISS-4, only DMP types 2 and 4 were installed, to measure settlements on adjacent structures (Building A, in this case) and on the ground surface, respectively. Although horizontal deflections of DMP's can be measured, this was not done at this project. Only vertical positions, relative to deep benchmarks, were monitored. Dunnicliff (1988) gives typical expected values for the precision of DMP measurements: within 0.01 ft. for elevation measurements (as specified for surveying on this project), or 0.001 ft. for especially sensitive cases that require increased precision.

A listing of the nine DMP's used at the ISS-4 cross-section, as well as relevant information on each, is provided in Table A.2.

A.3.2. Probe Extensometers

Settlements at different depths beneath the ground surface can be monitored with *probe extensometers*, which measure the distance between two or more points along a common axis. For a vertical probe extensometer, measuring points are emplaced at different depths, and their locations determined at different times with a probe that is passed down an access tube.

A number of different types of probe extensometers exist, with a variety of measurement point and probe designs. Measurement points can either be emplaced directly in the soil, or can be attached to the access tube. The latter option requires that the tube be adequately bonded to the surrounding soil and that it allow axial expansion or compression, as can telescoping or corrugated pipes. The attached measurement points will then be able to settle or heave with the soil mass.

There are basically three different methods for detection of measurement points with a probe. They are diagrammed in Figure A.3. The first technique is mechanical. In this case, the measurement points are bumps or knobs in the pipe, or simply the edges of

the telescoping pipe sections, and the probe is equipped with latches that catch on the points or with an electrical switch that closes mechanically, signaling arrival at the point (Figure A.3-a). In the second method, the probe is equipped with a current-displacement induction coil. The measurement points are steel rings wrapped around a corrugated access tube at different locations along its length (Figure A.3-b). The electrical output current from the probe is constantly monitored, and when the probe passes through one of the steel rings, the current reaches an identifiable maximum due to induction.

The third method uses magnetic measurement points which are fixed in the soil (Figure A.3-c), and was used in the design of probe extensometers at this project. The operation principle of magnetic measurement points is illustrated in Figure A.4. The probe contains a reed switch which closes twice as it passes through the magnets, once just above and once just below each magnet's position, sending a pair of electric signals to the output device. The magnetic rings were attached to leaf spring "legs" known as *spider magnets*. After a borehole was drilled for the instrument, spider magnets were lowered in retracted position to their appropriate depths, where the leaf springs were pneumatically released, so that they caught in the sides of the borehole. A telescoping access tube was then lowered into the borehole, through the spider magnets. Finally, the borehole was filled with a grout mixture specified as "Type A", which had an unconfined compressive strength between 500 and 1000 psi.

Accurate measurement of changing measurement point elevations requires all depths to be referenced to a known or unchanging location, such as an external benchmark, or more conveniently, to points in the probe extensometer that are fixed in a rigid stratum. This project's Standard Special Provisions mandate a minimum ten foot embedment into a fixed stratum, such as the glacial till or the underlying bedrock. In accordance with Dunicliff's recommendations, the probe extensometers used for this project include, in addition to the spider magnets, a pair of datum magnets embedded in the rigid stratum at the base of the instrument, which serve as the fixed reference points. The Standard Special Provisions required an accuracy of about 0.1 inches for settlement measurements. The spider magnets and probes used in the project permitted readings to approximately the nearest 0.05 inches (MHD Instrumentation Consultant, 1992).

Throughout the project alignment, and at ISS-4 in particular, the probe extensometers were usually combined with inclinometers. The *Inclinometer/Probe Extensometer*, or IPE, is illustrated in Figure A.5. The IPE makes use of the fact that both the inclinometer and the probe extensometer utilize a vertical access tube for probe access and can therefore be easily combined, with a few adjustments to the design of each. For example, an inclinometer casing has a larger diameter than a typical probe-extensometer access tube requires, so the IPE requires larger diameter spider magnets than a probe extensometer would. Also, project specifications require “Type A” grout to fill IPE boreholes, which had to have a lower strength than the “Type B” grout used inclinometers. The lower strength was specified to give the instrument sufficient flexibility to accurately follow the soil settlements. Unfortunately, the low-strength grout, in combination with the larger borehole required to accommodate the spider magnets, led to flexure of the inclinometer casing which appear as anomalous ‘waviness’ in many of the IPE traces (discussed in section 7.2.1.2).

A.3.3. Heave Gages

Soil heave is an intrinsic response to the removal of overburden stresses as overlying soil is removed, but it can also reflect developing instabilities in the soil mass such a basal heave or bottom uplift from a pressurized underlying aquifer. A probe extensometer can be used to monitor soil heave within an excavation, as long as its height can be cut down as the excavation deepens. Such an instrument is known as a *multi-point heave gage* (MPHG) and is illustrated in Figure A.6.

The design of the MPHG is essentially the same as the Probe Extensometer. Before excavating the area around the instrument, the top of the access tube is sealed with a mechanical packer and an internal cutting tool is used to trim the access tube to an elevation below the bottom of the subsequent excavation.

Table A.3 lists information on the one IPE and the four MPHG’s installed beside and within the excavation at ISS-4. The accuracy of MPHG readings was about 0.05 to 0.10 inches, as for the Probe Extensometers and IPE’s.

A.4. Instruments which Measure Groundwater Levels and Pore Pressures

Careful monitoring of the groundwater regime in and around an excavation provides knowledge of the pressures and movements of pore water, and can be important for the following reasons:

1. Water pressures can constitute a significant fraction of the earth forces that have to be resisted by support walls, especially when the excavation reaches depths well below the water table.

2. High pore pressures in a confined aquifer beneath an excavation can cause bottom heave.

3. Pore pressure drawdowns can result in consolidation and therefore surface settlements, particularly when clay is present in the soil profile.

4. The dissipation of excess negative pore pressures induced by excavation unloading generally results in swelling of soils within the cut, which reduces strengths on the passive side of the support wall.

There are essentially two types of groundwater monitoring instruments: *observation wells* and *piezometers*. An observation well is simply an open vertical tube which is screened over all or part of its length, allowing measurement of the surrounding water table elevation. A piezometer, on the other hand, allows measurement of pore pressures at a specific depth within the soil column.

This construction project utilized observation wells and two different types of piezometer. The observation wells measured the elevation of the water table in the granular and miscellaneous fill deposits which composed the area's upper aquifer. *Open standpipe piezometers* (OSPZ's) were emplaced in the cohesive fill, a deeper component of the upper aquifer. Pore pressures in the glacial deposits of the confined lower aquifer and within the clay were measured by *vibrating wire piezometers* (VWPZ's).

Figure A.7 shows a diagram of an observation well, as installed along the project alignment. A PVC riser pipe, slotted along a five foot length, was installed in an augered borehole, and the annular space filled with 20-30 filter sand. The water level could be measured in the riser with a water level indicator, which is a probe that is lowered through the pipe by a graduated cable; when the probe contacts the water, electrical current is able

to pass between a pair of terminals so that a light and buzzer inform the operator that water has been reached. The depth of the probe can then be read from the cable. The cables used for this project had gradations every 0.01 feet.

An open standpipe piezometer is similar to an observation well, since the water level is measured by lowering a probe down a riser pipe. The difference is that the porous tip is located in a zone that is sealed off from the rest of the strata. Figure A.8 illustrates the OSPZ design used in the project area. 20 - 30 filter sand was used around the porous point, and was overlain by a four-foot thick layer of granular bentonite which sealed the porous tip from the rest of the soil profile. (Grout can also be used for this purpose.)

The design of vibrating wire piezometers used to monitor this excavation is shown in Figure A.9-a. Like the OSPZ, a four-foot-thick layer of bentonite seals the piezometer tip from the remaining soil column. The piezometer itself measures pore pressures electronically; an electrical cable, rather than a riser pipe, connects the tip to the surface. Details of the vibrating wire piezometer tip are illustrated in Figure A.9-b. The instrument contains a thin steel wire connected to a diaphragm with deflects under the applied pore pressure. This deflection applies a proportional tension to the wire. An electric pulse applied by an adjacent coil 'plucks' the wire, and then measures the resonant frequency of the resulting vibrations. The square of the vibration frequency is proportional to the wire strain and therefore to the pressure existing outside of the diaphragm.

Vibrating wire piezometers are sensitive to the existing barometric pressure and, to a lesser extent, the temperature. The manufacturer generally provides calibration coefficients for both corrections. Piezometers for this project were provided by Geokon, Inc., and had an accuracy of $\pm 0.025\%$ full scale. VWPZ's with a 100 psi range were used in the deep aquifer. The clay layer inside and below the excavation was instrumented with 50-psi-range VWPZ's, because initial pore pressures were lower and were expected to undergo reductions in response to dewatering activities (MHD Instrumentation Consultant, 1992).

The installation procedures for the three previously described instruments were fairly similar. Project specifications prohibited the use of bentonite mud while drilling the boreholes, because of the possibility of 'clogging' the surrounding soils. The hole was

drilled with a casing, which was withdrawn incrementally as the hole was filled with lifts of backfilling material such as sand, bentonite, and grout. The backfilling had to be done with great care, since the adequacy of the instruments was dependent on forming an impermeable seal around the riser pipes (Dunncliff, 1981). The vibrating wire piezometer was lowered in a water filled canvas sack into a water-filled borehole, in order to keep the instrument fully saturated at all times. Formal initial readings on the groundwater monitoring instruments involved taking the average of three successive, independent readings.

Table A.4 provides a list of all the groundwater monitoring instruments at ISS-4, including both observation wells and piezometers.

Table A.1. Information Table for ISS-4 Inclinerometers.

	Instrument	Station	Offset from Wall	(Top) Reference Elevation	Length of Data Record	Elevation of Base	Installation Date	FIR*	Skew
North Wall	INC-102	77+09	In slurry wall	112.440'	120'	-8'	4/23/93	5/5/93	-2°
	South Wall								
South Wall	INC-101	77+02	2'	112.183'	114'	-2'	3/10/93	3/24/93	-18°
	IPE-113	77+00	27'	112.6'	126'	-14'	9/3/92	12/16/92	2°

*FIR = Formal Initial Reading
Data are measured at 2-foot intervals

Table A.2. Information Table for Deformation Monitoring Points

Instrument		Station	Offset from Wall	Installation Date	First Reading	Initial Elevation (ft)
NORTH SIDE	Type 4	77+30	39'	9/4/92	9/4/92	108.95
	Type 2	77+10	23'	5/22/92	5/22/92	115.21
		76+70	33'	2/3/93	2/3/93	114.43
		77+70	91'	2/3/93	2/3/93	111.05
		77+90	136'	2/3/93	2/3/93	110.22
		77+30	146'	5/22/92	5/22/92	111.08
SOUTH SIDE	Type 4	77+08	41'	9/4/92	9/4/92	109.20
		77+03	54'	9/4/92	9/4/92	109.61
		76+90	85'	9/4/92	9/4/92	110.38

Table A.3. Information Table for Multi-Point Heave Gages and Probe Exstensometers

Instrument	Station	Offset from		Installation Date	Number of Magnets
		CL			
MPHG-110	77+09	24'N		10/9/92	7
MPHG-109	77+03	3'N		10/9/92	7
MPHG-501	77+00	40'S		12/4/92	7
MPHG-107	76+97	77'S		10/9/92	7

South Side	IPE-113	76+96	157'S	9/3/92	13
------------	---------	-------	-------	--------	----

Initial Elevation of Spider Magnets

Instrument	Initial Elevation of Spider Magnets												
	1	2	3	4	5	6	7	8	9	10	11	12	13
MPHG-110	3.38	6.37	15.21	27.8	40.28	52.95	65.58						
MPHG-109	2.01	5.02	16.51	29.17	41.78	54.35	66.92						
MPHG-501	-0.06	2.93	11.94	24.40	36.8	49.55	62.05						
MPHG-107	-0.67	2.32	11.34	23.84	36.5	49.04	61.58						

South Side	IPE-113	-13.68	-10.69	-1.74	8.84	18.87	31.51	39.37	49.84	59.68	70.26	79.91	90.03	99.84
------------	---------	--------	--------	-------	------	-------	-------	-------	-------	-------	-------	-------	-------	-------

Table A.4. Information Table for Groundwater Monitoring Instruments

Instrument	Station	Offset: from wall	Tip Elevation	Installation date	First reading date	Initial PWE Elev. (ft)
NORTH SIDE	VWPZ-108	77+44.8	256'N	6.9'	8/21/92	106.797 *
	OW-002	77+55	259'N	N/A	3/8/90	104.80
	OW-016	77+40	39'N	N/A	9/23/91	106.30
	VWPZ-67	77+40	39'N	69.4'	9/4/91	104.818
	-68			69.4'	9/4/91	105.557
VWPZ-107	77+25.5	27'N	7.0'	8/19/92	8/19/92	98.672
INSIDE EXCAVATION	VWPZ-135	77+10.1	18'S	30.0'	8/21/92	89.544
	-136			50.0'	8/21/92	99.435
	VWPZ-133	77+06.4	32'S	30.0'	8/17/92	100.9
	-134			50.0'	8/18/92	100.7
	VWPZ-131	77+02.6'	82'S	30.5'	8/19/92	110.325
	-132			49.5'	8/19/92	116.874
	VWPZ-53	76+30	40'S	1.5'	4/4/90	4/6/90
SOUTH SIDE	VWPZ-106	76+93	150'S	-8.3'	8/13/92	98.202
	OSPZ-106	77+00	151'S	96.3'	7/31/92	106.67

*96.853 on 8/22

INSTRNAME	NORTHING	EASTING	STATION	OFFSET from ξ
WVZ-065	2951472	781168	8100	245
WVZ-066	2951472	781168	8100	245
WVZ-067	2951834	780773	7740	-115
WVZ-068	2951834	780773	7740	-115
WVZ-069	2952106	780041	6915	-120
WVZ-070	2952106	780041	6915	-120
WVZ-075	0	0	0	0
WVZ-501	2951988	779919	6860	37
WVZ-107A	0	0	9340	0
WVZ-107B	0	0	9340	0
WVZ-117	2951683	782138	8669	409
WVZ-118	2951963	782309	9244	279
PREX-501	2951747	780231	7240	116
PREX-502	2951954	780321	7240	110
INCL-501	2951744	780250	7258	111
INCL-502	2951948	780333	7253	109
IPE-116	2952070	780237	7109	-180
IPE-115	2951779	780096	7197	144
IPE-114	2951702	780204	7233	109
IPE-112	2952117	782141	9204	544
INCL-101	2951589	780697	7702	131
INCL-102	2951495	780736	7709	-78
INCL-103	2951647	781222	8194	79
INCL-104	2951784	781205	8202	-59
INCL-105	2951748	781549	8521	75
INCL-109	2951778	780166	7170	115
INCL-110	2951579	780837	7831	125
INCL-111	2951776	780884	7865	-74
INCL-112	2951599	781018	7999	104
INCL-113	2951776	781064	8055	-70
INCL-114	2951674	781327	8298	75
INCL-115	2951689	781382	8352	74
INCL-117	2951909	781590	8622	-56
INCL-118	2951960	781684	8730	-57
INCL-120	2952025	781808	8876	-56
MPHG-101	2951863	780129	7102	54
MPHG-502	2951908	780153	7104	2
MPHG-102	2951912	780153	7102	-1
MPHG-103	2951947	780175	7107	-42
MPHG-104	2951725	780413	7411	-70
MPHG-105	2951779	780420	7400	17
MPHG-106	2951852	780463	7416	-66
MPHG-107	2951643	780701	7697	77
MPHG-108	2951692	780708	7697	27
MPHG-109	2951722	780719	7703	-3
MPHG-110	2951741	780728	7709	-24

Table A.5. (page 1 of 6) Location Data for Geotechnical Instruments.

INSTRNAME	NORTHING	EASTING	STATION	OFFSET
IPE-101A	2951744	780250	7258	112
IPE-102	2951954	780321	7240	-110
IPE-103	2951975	780335	7244	-135
IPE-104	2951678	780401	7415	119
IPE-105	2951890	780486	7425	-110
IPE-106	2951906	780489	7423	-126
IPE-107	2951804	780109	7110	115
IPE-108	2952012	780207	7107	-115
IPE-109	2951716	780312	7323	114
IPE-110	2951921	780390	7320	-106
IPE-113	2951565	780687	7696	157
IPE-101B	2951747	780231	7240	116
IPE-111	2951831	781335	8346	-75

Table A.5. (page 2 of 6) Location Data for Geotechnical Instruments.

INSTRNAME	NORTHING	EASTING	STATION	OFFSET
BPT-101	2951839	780651	7611	-106
BPT-102	2951834	781339	8351	-76
BPT-103	2951534	781221	8176	191
BPT-104	2951689	781521	8476	120
BPT-105	2952020	782039	9067	74
DMP4-101	2951632	780187	7246	240
DMP4-102	2951698	780210	7240	170
DMP4-103	2951725	780221	7240	140
DMP4-104	2951963	780325	7240	-120
DMP4-105	2951968	780327	7240	-125
DMP4-106	2951991	780337	7240	-150
DMP4-107	2952014	780348	7240	-175
DMP4-108	2952032	780354	7239	-195
DMP4-109	2951597	780368	7410	205
DMP4-110	2951636	780381	7410	165
DMP4-111	2951659	780389	7410	140
DMP4-112	2951904	780475	7410	-120
DMP4-113	2951938	780487	7410	-155
DMP4-114	2951953	780492	7410	-171
DMP4-115	2951975	780500	7410	-195
DMP4-116	2951510	780672	7690	213
DMP4-117	2951388	780607	7703	180
DMP4-118	2951435	781367	7708	169
DMP4-119	2951839	780679	7612	-112
DMP4-120	2951151	781292	7730	-116
DMP4-121	2951549	781235	8195	183
DMP4-122	2951574	781230	8190	160
DMP4-123	2951613	781223	8107	126
DMP4-124	2951836	781341	8355	-78
DMP4-125	2951858	781075	8063	-145
DMP4-126	2951867	781359	8382	-102
DMP4-127	2951956	781384	8475	-163
DMP4-128	2951771	781662	8627	101
DMP4-129	2951749	781672	8618	87
DMP4-130	2951951	781570	8622	-103
DMP4-131	2951961	781559	8616	-117
DMP4-132	2951991	781549	8623	-145
DMP4-135	2952232	782069	9225	-68
DMP4-136	2952252	782048	9227	-83
DMP2-001	0	0	0	0
DMP2-069	0	0	0	0
DMP2-070	0	0	0	0
DMP2-006	0	0	0	0
DMP2-022	0	0	0	0
DMP2-023	0	0	0	0
DMP2-026	0	0	0	0
DMP2-037	0	0	0	0
DMP2-024	0	0	0	0
DMP2-077	0	0	0	0

Table A.5. (page 3 of 6) Location Data for Geotechnical Instruments.

INSTRNAME	NORTHING	EASTING	STATION	OFFSET
DMP2-078	0	0	0	0
DMP2-025	0	0	0	0
DMP2-027	0	0	0	0
DMP2-028	0	0	0	0
DMP2-029	0	0	0	0
DMP2-030	0	0	0	0
DMP2-031	0	0	0	0
DMP2-036	0	0	0	0
DMP2-038	0	0	0	0
DMP2-071	0	0	0	0
DMP2-035	0	0	0	0
DMP2-032	0	0	0	0
DMP2-033	0	0	0	0
DMP2-034	0	0	0	0
DMP2-014	0	0	0	0
DMP2-016	0	0	0	0
DMP2-018	0	0	0	0
DMP2-013	0	0	0	0
DMP2-015	0	0	0	0
DMP2-019	0	0	0	0
DMP2-020	0	0	0	0
DMP2-021	0	0	0	0
DMP2-039	0	0	0	0
DMP2-040	0	0	0	0
DMP2-041	0	0	0	0
DMP2-042	0	0	0	0
DMP2-043	0	0	0	0
DMP2-044	0	0	0	0
DMP2-045	0	0	0	0
DMP2-046	0	0	0	0
DMP2-059	0	0	0	0
DMP2-060	0	0	0	0
DMP2-061	0	0	0	0
DMP2-062	0	0	0	0
DMP2-063	0	0	0	0
DMP2-064	0	0	0	0
DMP2-065	0	0	0	0
DMP2-066	0	0	0	0
DMP2-067	0	0	0	0
DMP2-068	0	0	0	0
DMP2-072	0	0	0	0
DMP2-073	0	0	0	0
DMP2-074	0	0	0	0
DMP2-075	0	0	0	0
DMP2-076	0	0	0	0
DMP4-137	0	0	7105	260
DMP4-138	2951905	780478	7247	-107
DMP4-139	2951963	780331	7246	-122
DMP4-140	2951949	780326	7413	-122

Table A.5. (page 4 of 6) Location Data for Geotechnical Instruments.

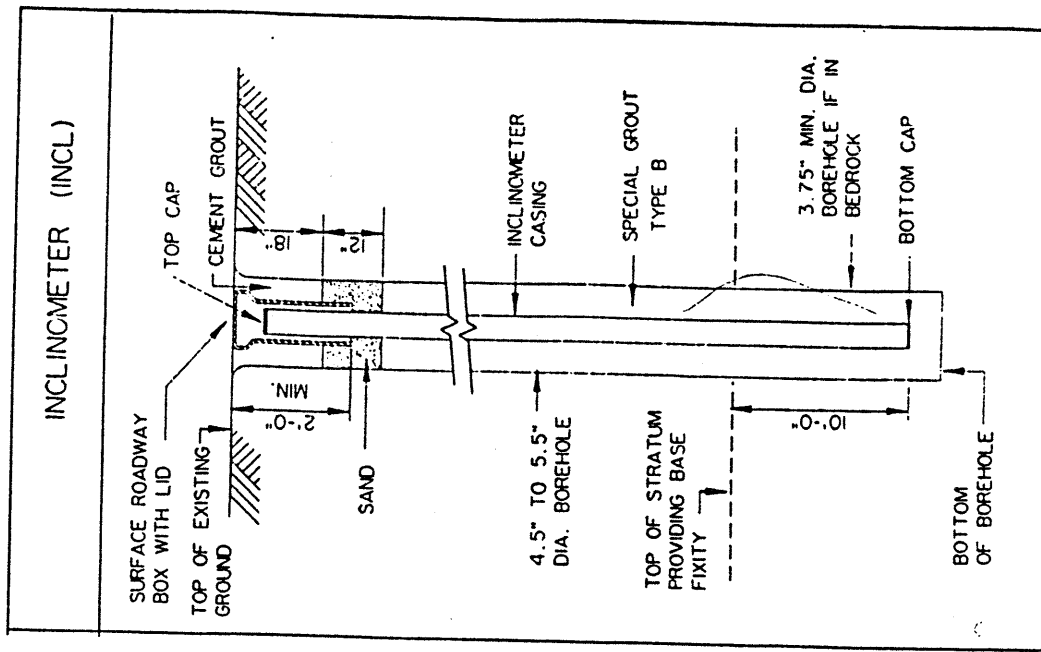
INSTRNAME	NORTHING	EASTING	STATION	OFFSET
DMP2-017	0	0	0	0
DMP2-102	0	0	0	0
DMP2-104	0	0	0	0
DMP2-105	0	0	0	0
DMP2-107	0	0	0	0
DMP2-153	0	0	0	0
DMP2-154	0	0	0	0
DMP2-155	0	0	0	0
DMP2-156	0	0	0	0
DMP2-157	0	0	0	0
DMP2-158	0	0	0	0
DMP4-143	0	0	0	0
DMP4-145	0	0	0	0
DMP4-146	0	0	0	0
DMP4-150	0	0	0	0
OSPZ-101	2951939	780096	7041	0
OSPZ-102	2951743	780256	7237	122
OSPZ-103	2951878	780409	7355	-72
OSPZ-104	2951680	780393	7407	119
OSPZ-105	2951893	780476	7415	-109
OSPZ-106	2951569	780692	7700	151
OSPZ-108	2951289	781226	8148	432
OSPZ-109	2951538	781225	8180	186
OSPZ-110	2951585	781133	8104	126
OSPZ-111	2951826	781330	8340	-71
OSPZ-113	2951573	781741	8619	313
OSPZ-114	2951778	781641	8615	84
OSPZ-115	2951942	781575	8623	-92
OSPZ-116	2951666	782128	8954	418
OSPZ-117	2951945	782298	9226	286
OSPZ-119	2952224	782069	9224	-57
OW-001	2952260	780336	7100	-395
OW-002	2952047	780805	7755	-335
OW-003	2951228	780527	7595	535
OW-004	2951772	781201	8200	-45
OW-005	2951487	781395	8300	260
OW-006	2952161	782126	9230	60
OW-007	2951797	782206	9050	350
OW-008	2951765	781697	8650	150
OW-009	2951868	781376	8400	-105
OW-010	2951450	781666	8500	400
OW-011	2951596	781453	8385	175
OW-012	2952150	781488	8630	-320
OW-013	2952072	781221	8250	-340
OW-014	2951228	781224	8100	500
OW-015	2951472	781168	8100	245
OW-016	2951834	780773	7740	-115
OW-017	2951566	780633	7645	165
OW-018	2952106	780041	6915	-120

- Destroyed
- Destroyed

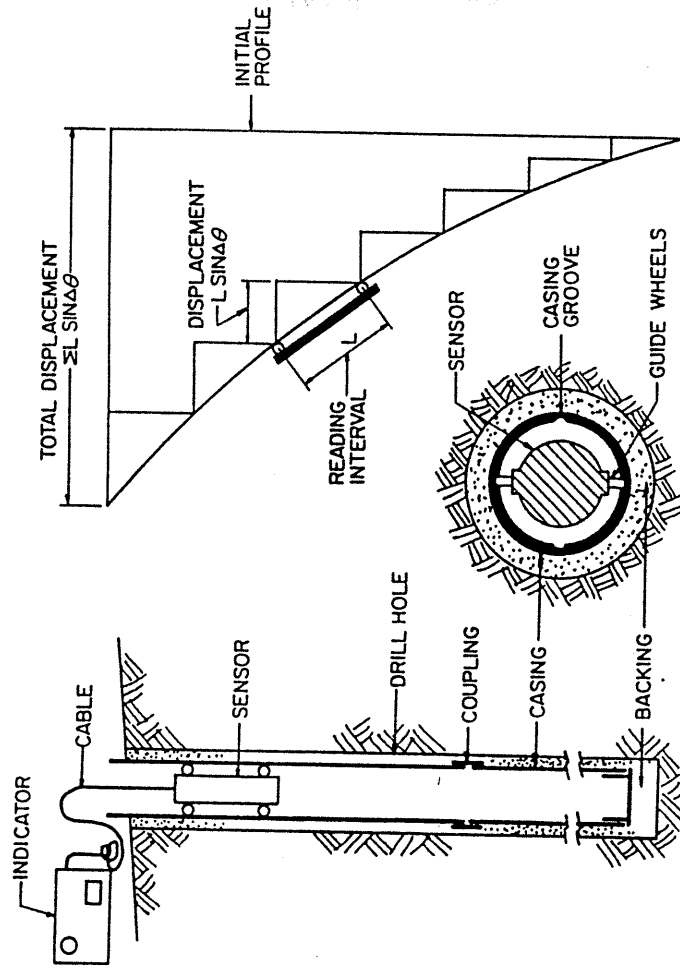
Table A.5. (page 5 of 6) Location Data for Geotechnical Instruments.

INSTRNAME	NORTHING	EASTING	STATION	OFFSET
OW-019	0	0	9040	-44
OW-020	0	0	9060	-42
OW-021	0	0	9082	-42
OW-022	2951787	780363	7344	30
OW-023	2952189	782372	9440	132
OW-024	2951752	780006	0	0
OW-501	2951772	781201	8200	-45
WVPZ-102	2951739	780234	7246	122
WVPZ-103	2951960	780329	7245	-118
WVPZ-104	2951672	780400	7416	124
WVPZ-105	2951896	780469	7407	-110
WVPZ-106	2951572	780685	7693	150
WVPZ-107	2951816	780755	7726	-103
WVPZ-108	2951816	780802	7745	-332
WVPZ-109	2951292	781228	8150	430
WVPZ-110	2951530	781218	8173	194
WVPZ-111	2951585	781330	8101	-127
WVPZ-112	2951820	781326	8334	-67
WVPZ-113	2952091	781149	8205	-371
WVPZ-114	2951578	781733	8615	304
WVPZ-115	2951772	781650	8620	93
WVPZ-116	2951935	781581	8625	-84
WVPZ-120	2952224	782090	9227	-62
WVPZ-121	2951733	780419	7414	61
WVPZ-122	2951736	780414	7408	59
WVPZ-123	2951782	780429	7407	11
WVPZ-124	2951782	780429	7407	11
WVPZ-125	2951870	780465	7412	-84
WVPZ-126	2951870	780465	7412	-84
WVPZ-131	2951637	780706	7703	82
WVPZ-132	2951637	780706	7703	82
WVPZ-133	2951686	780717	7706	32
WVPZ-134	2951686	780717	7706	32
WVPZ-135	2951735	780728	7710	-18
WVPZ-136	2951735	780728	7706	-18
WVPZ-051	2951993	779907	6845	40
WVPZ-052	2952260	780336	7100	-395
WVPZ-053	2951691	780636	7630	40
WVPZ-054	2951487	781395	8300	260
WVPZ-055	2952161	782128	9230	60
WVPZ-056	2952161	782128	9230	60
WVPZ-057	2951765	781697	8650	150
WVPZ-058	2951765	781697	8650	150
WVPZ-059	2951868	781376	8400	-105
WVPZ-060	2951868	781376	8400	-105
WVPZ-061	2951868	781376	8400	-105
WVPZ-062	2951868	781376	8400	-105
WVPZ-063	2951596	781453	8385	175
WVPZ-064	2951596	781453	8385	175

Table A.5. (page 6 of 6) Location Data for Geotechnical Instruments.



A.



B.

Figure A.1. A. Inclinometer Design from Project Standard Drawings. B. Principle of Operation of a Typical Inclinometer.

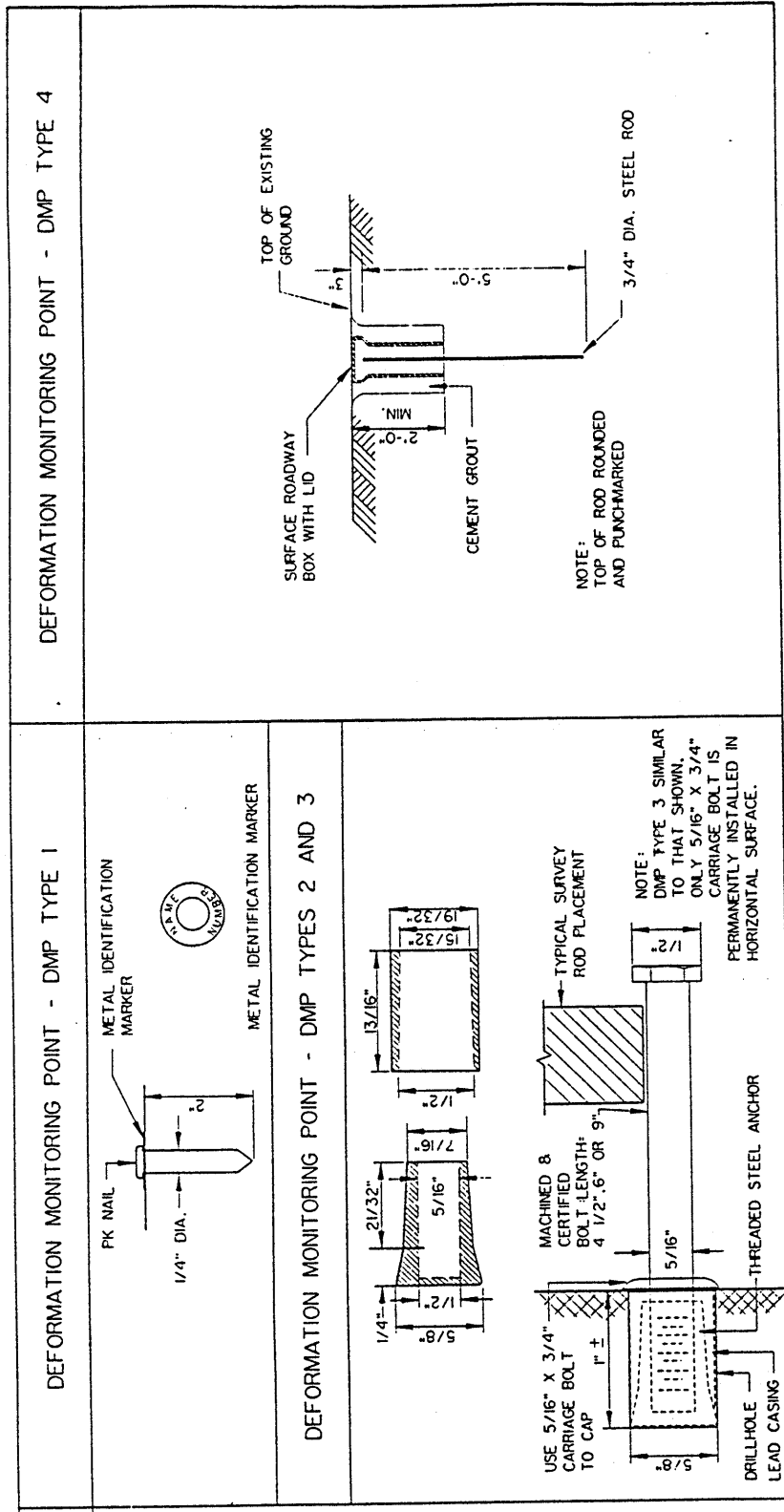


Figure A.2. Types of Deformation Monitoring Points (DMP's) used to Monitor the Excavation.

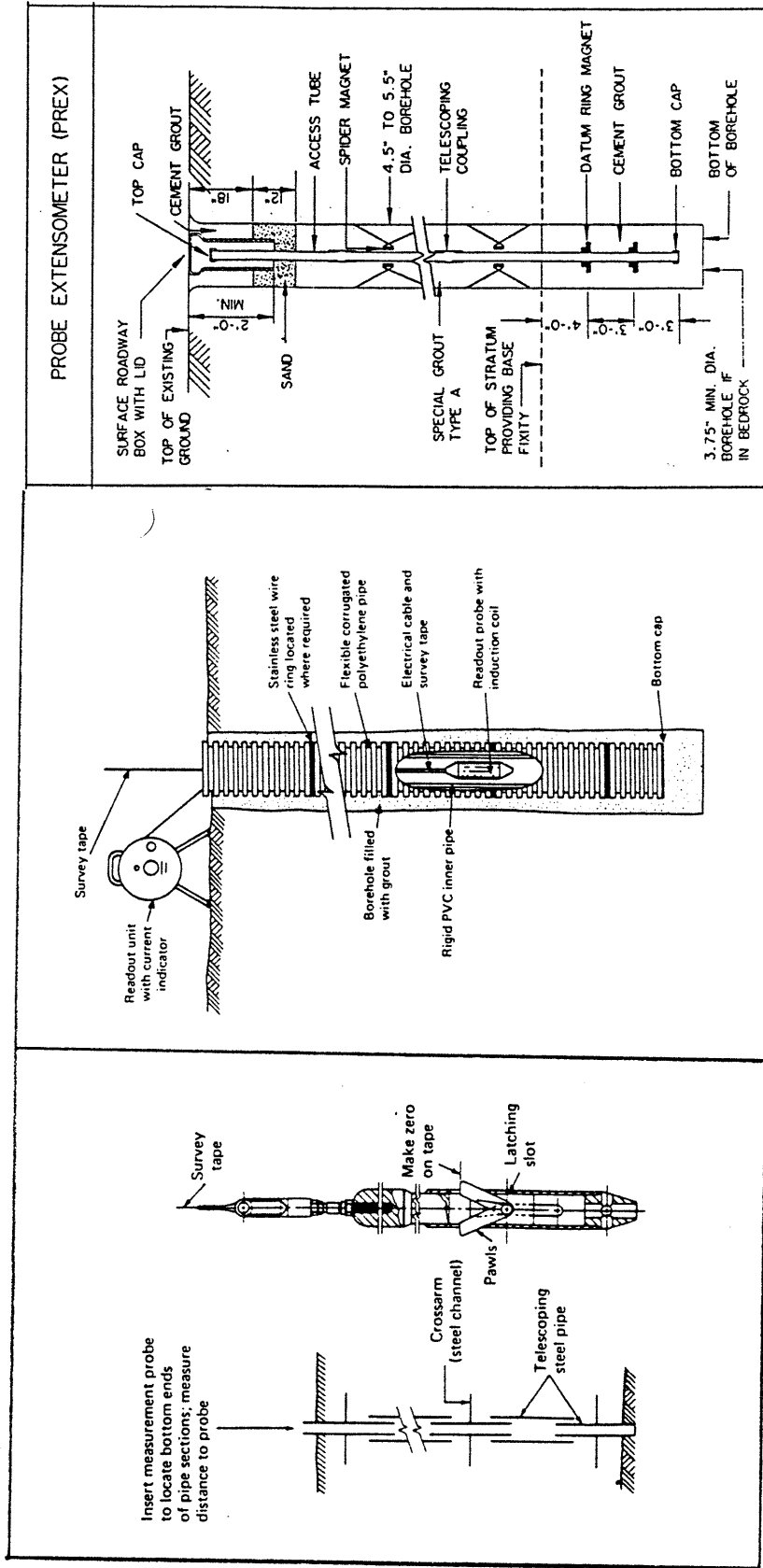


Figure A.3. Three Types of Probe Extensometer. A. Mechanical Probe with telescoping access tube. From Dunnicliff (1988). B. Induction Coil Probe. Steel rings around the corrugated access tube act as measurement points. From Dunnicliff (1988). C. Magnetic Reed Switch Probe with Spider Magnet Measurement Points. From Project Standard Drawings.

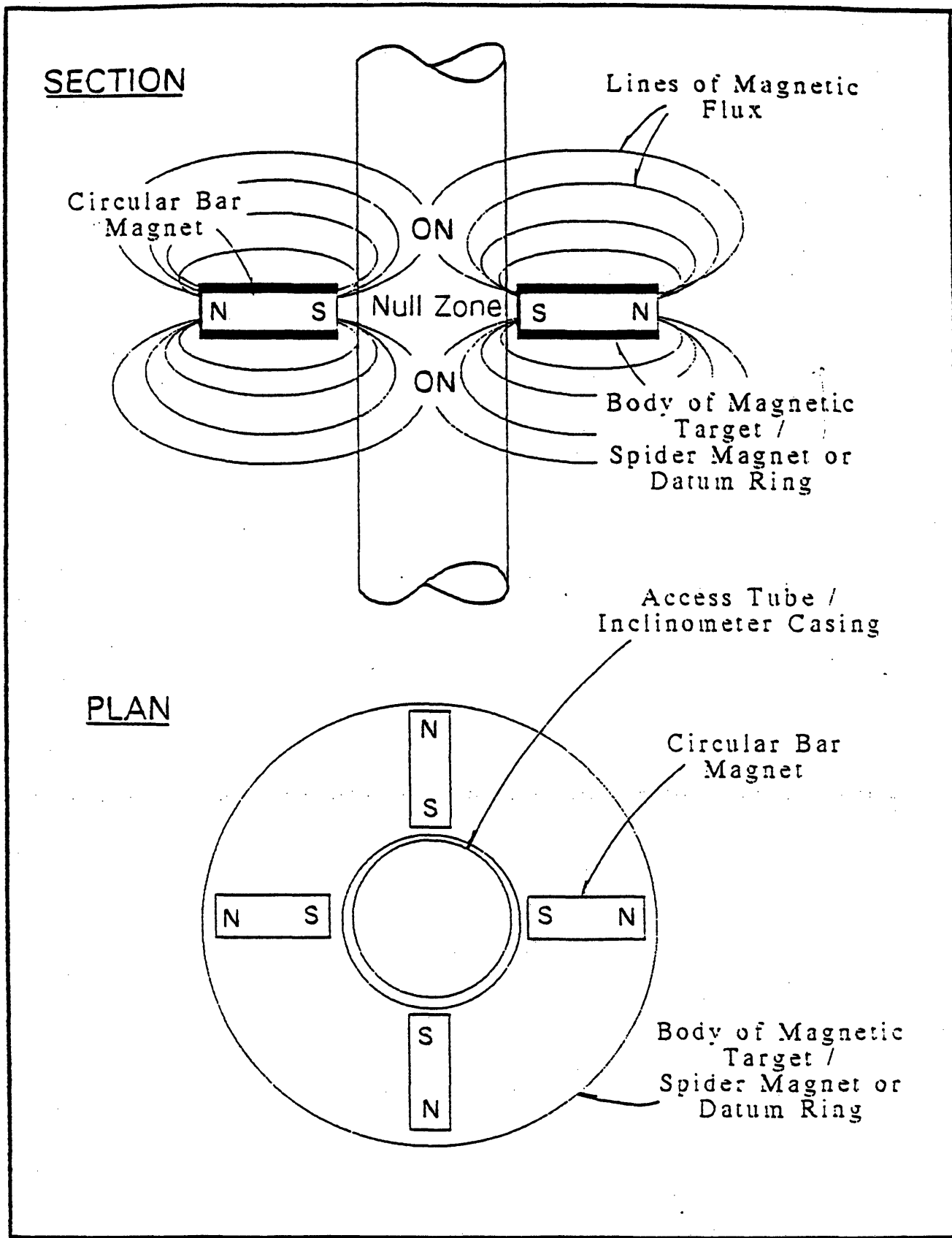


Figure A.4. Principle of Operation of a Magnetic Probe Extensometer. From MHD Instrumentation Consultant (1992).

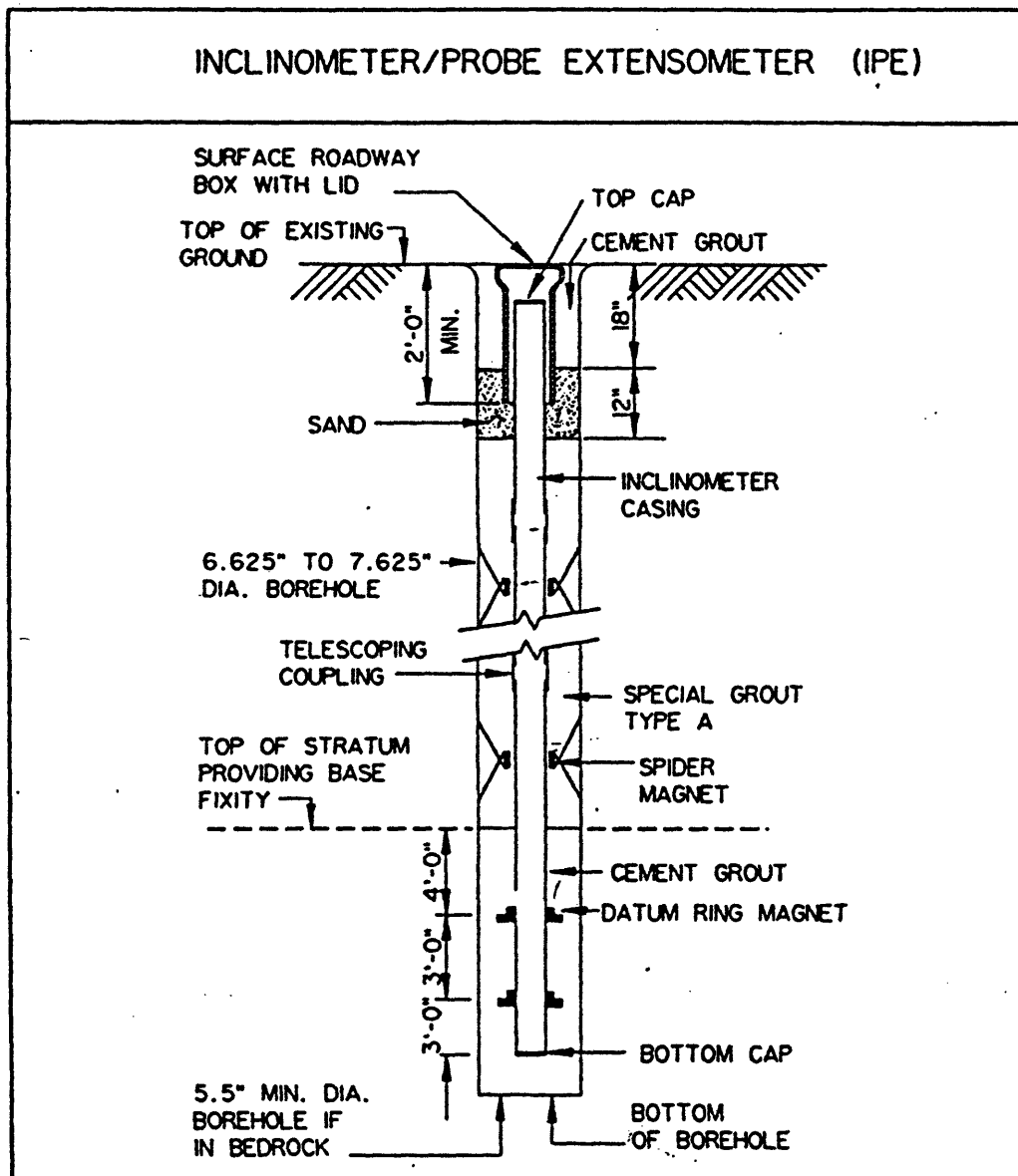


Figure A.5. Inclinator/Probe Extensometer. From Project Standard Drawings.

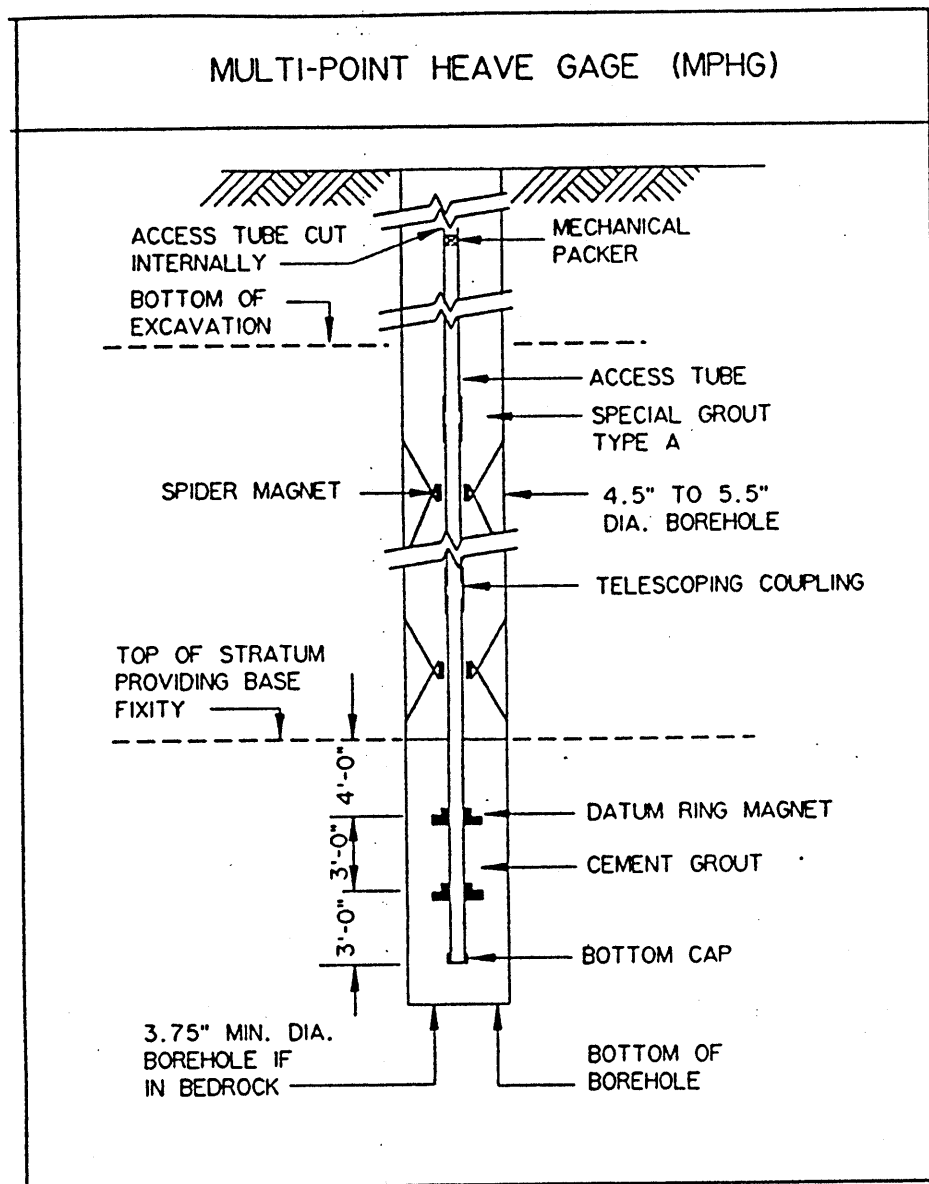


Figure A.6. Multi-Point Heave Gage. From Project Standard Drawings.

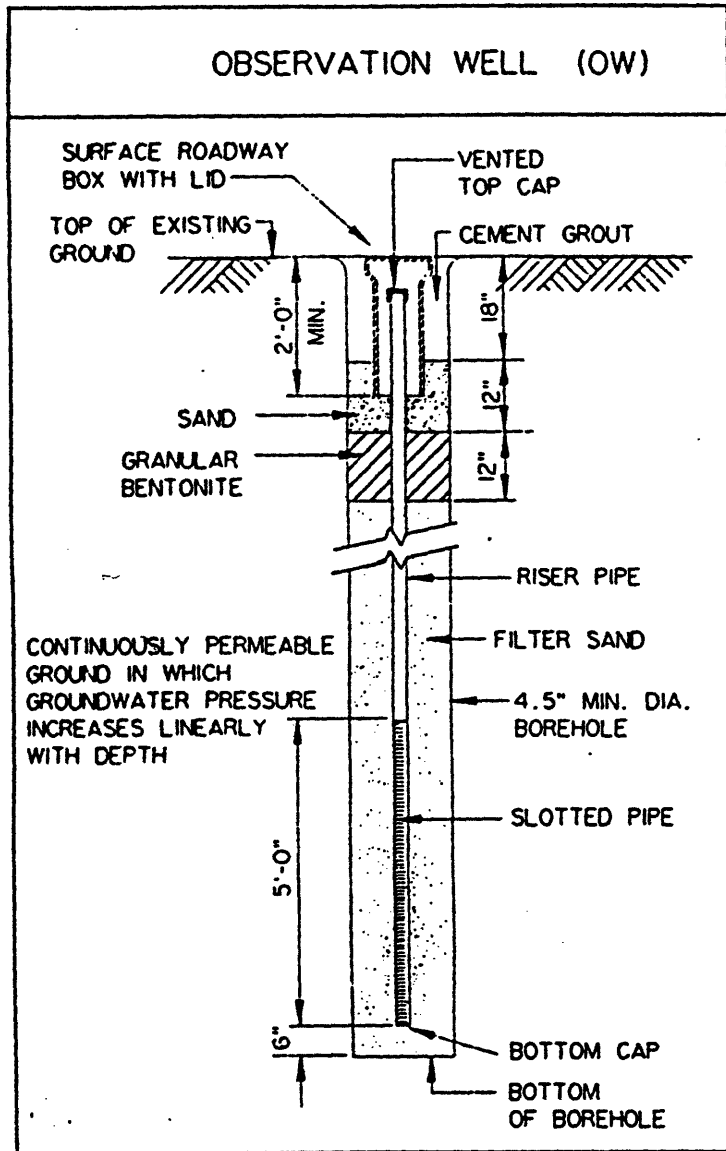


Figure A.7. Observation Well. From Project Standard Drawings.

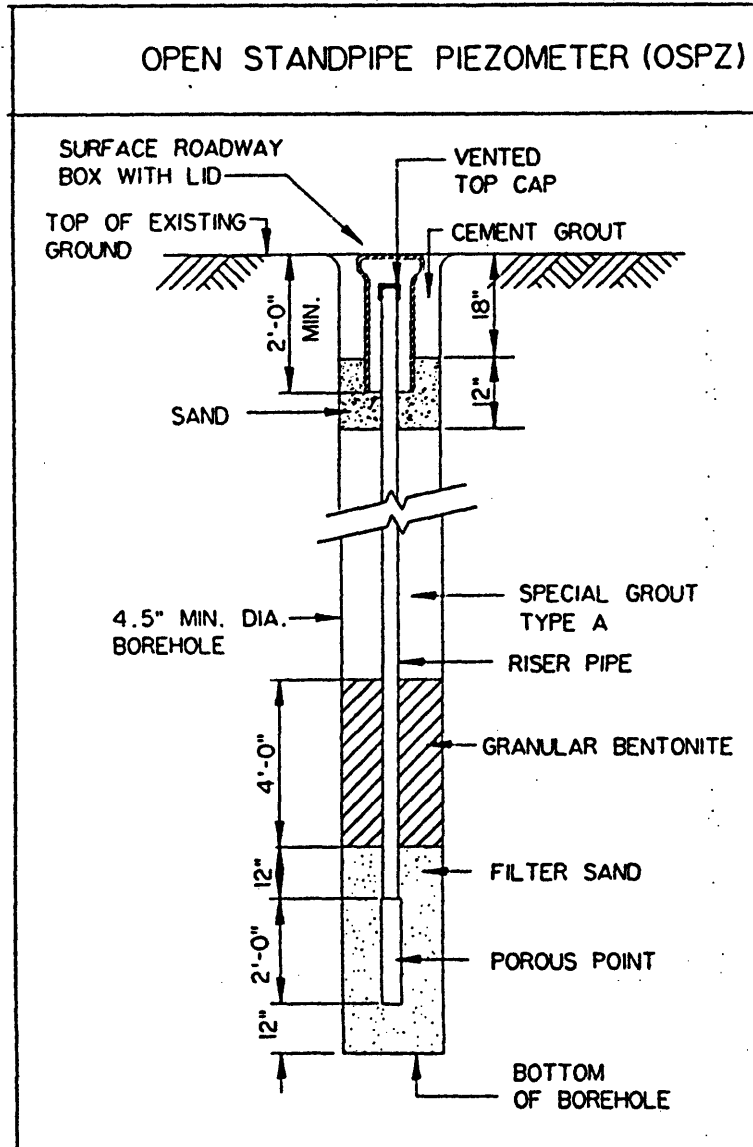


Figure A.8. Open Standpipe Piezometer. From Project Standard Drawings.

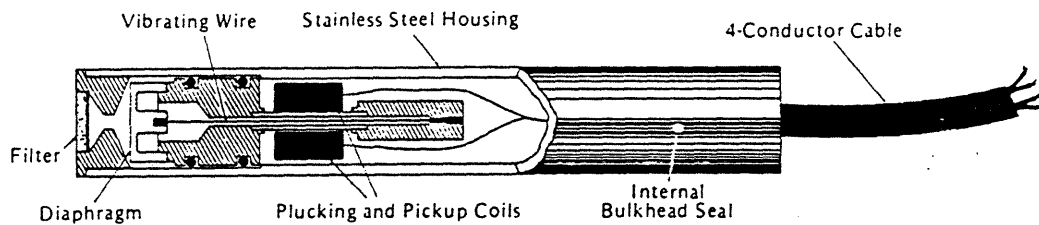
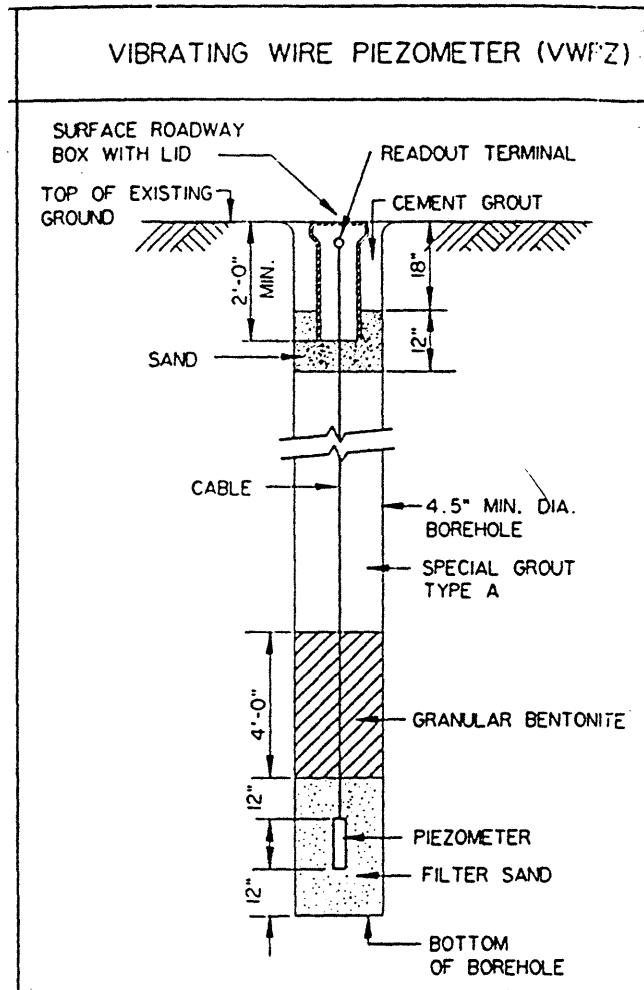
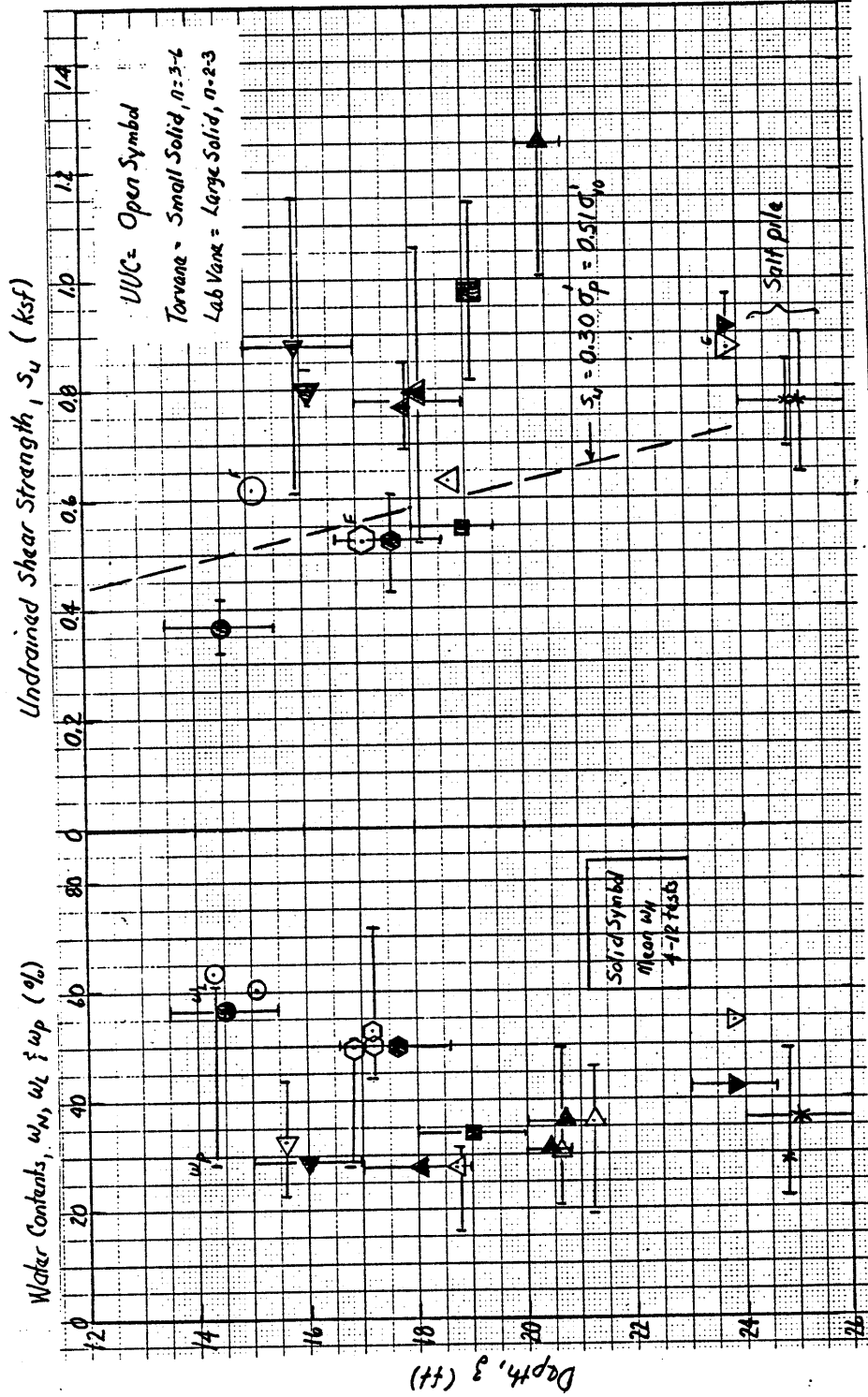


Figure A.9. A. Vibrating Wire Piezometer Installation. From Project Standard Drawings. B. Details of the Piezometer. From Geokon, Inc.

APPENDIX B: Engineering Properties of Cohesive Soils

Sheet B1. Summary of ω_N, Atterberg Limit, and S_u Data on Cohesive Fill (data from MHD Geotechnical Consultant, 1991a).	276
Sheet B2. Summary of Oedometer Data on Cohesive Fill (MIT interpretation of data from MHD Geotechnical Consultant, 1991a).	277
Sheet B3. SPT Blow Count Data on Cohesive Fill.	278
Sheet B4. Summary of ω_N, Atterberg Limit, and S_u Data on Organic Deposits (data from MHD Geotechnical Consultant, 1991a).	279
Sheet B5. Plasticity Chart: Organic Deposits.	280
Sheet B6. Summary of Oedometer Data on Organic Deposits (MIT interpretation of data from MHD Geotechnical Consultant, 1991a).	281
Sheet B7. Water Content, Virgin Compression Ratio, and NC Coefficient of Consolidation Data on BBC (Data from MHD Geotechnical Consultant, 1991a).	282
Sheet B8. Elevation vs. Mean Natural Water Content from Borings Near ISS-4.	283
Sheet B9. Plasticity Chart for Boston Blue Clay in the Region Surrounding ISS-4.	284
Sheet B10. Summary of Stress History Data for BBC: Sta. 71 to 79.	285
Sheet B11. Compression Graph from Consolidation Test OED-14.	286
Sheet B12. Strain Energy Plot of Recompression Range, from OED-14.	287
Sheet B13. Strain Energy Plot, Maximum Past Pressure Range, from OED-14.	288
Sheet B14. Compression Graph from Consolidation Test OED-34.	289
Sheet B15. Strain Energy Plot of Recompression Range, from OED-34.	290
Sheet B16. Strain Energy Plot, Maximum Past Pressure Range, from OED-34.	291
Sheet B17. Comparison of Preconsolidation Pressures Estimated from Casagrande and Strain Energy Techniques for 17 Oedometer Tests on BBC (Fixed piston samples).	292
Sheet B18. Vertical In-Situ Permeability Plotted Against Elevation for the Special Test Sites (MHD Geotechnical Consultant, 1993).	293



Boring	34	40	41	49	60	61	68	74	81
Symbol	△	*	▽	□	○	◇	△	△	▽

Fig. 1 Summary of w_N , Atterberg Limit and S_u Data on Cohesive Fill for Boston

CCL 12/1/1964 MHP

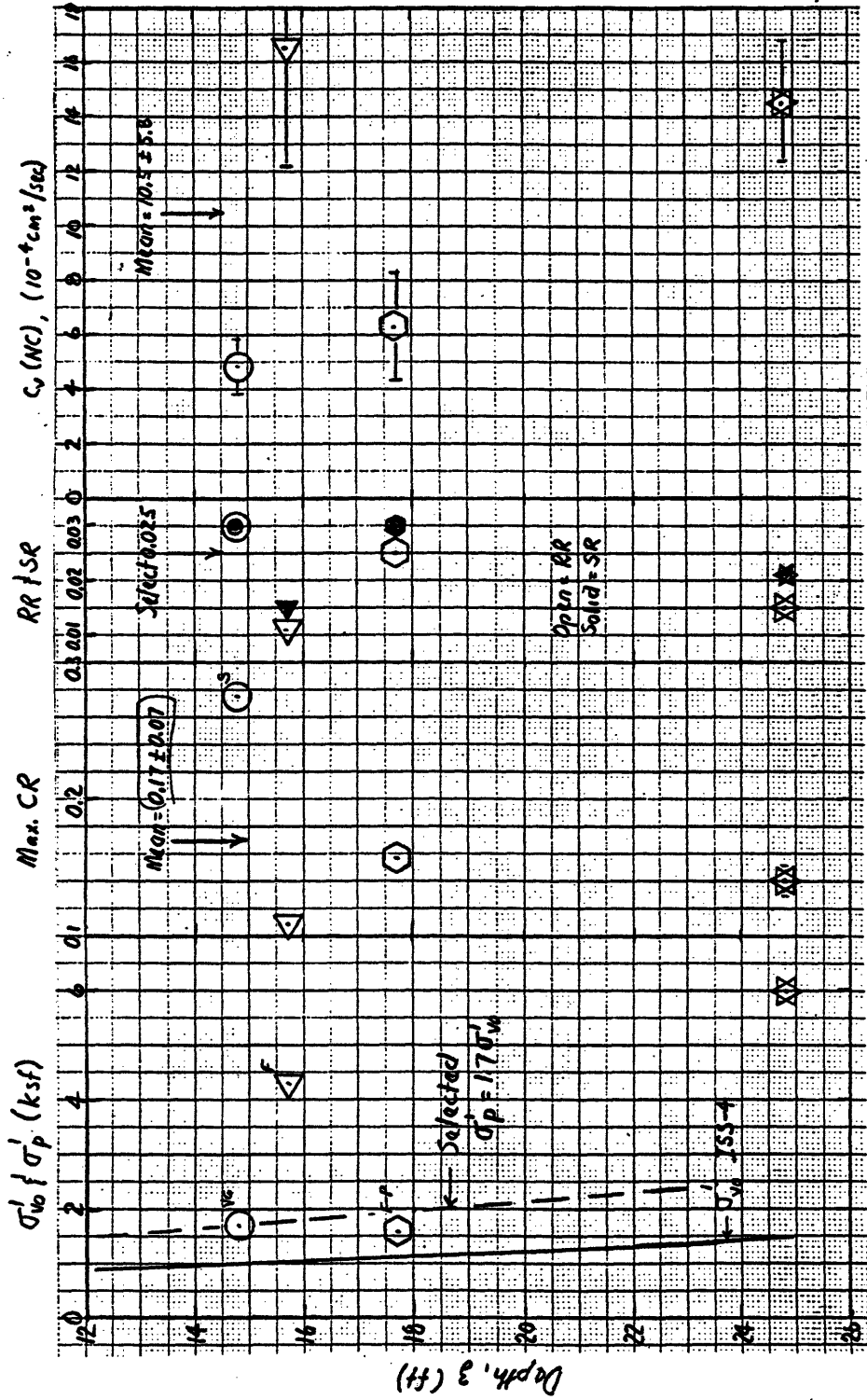


Fig. 2 Summary of Oedometer Data on Cohesive Fill for Boston (MIT interpretation of data MHD 6-6-1991)

Sheet B2

CCL 12/1/54 MHD

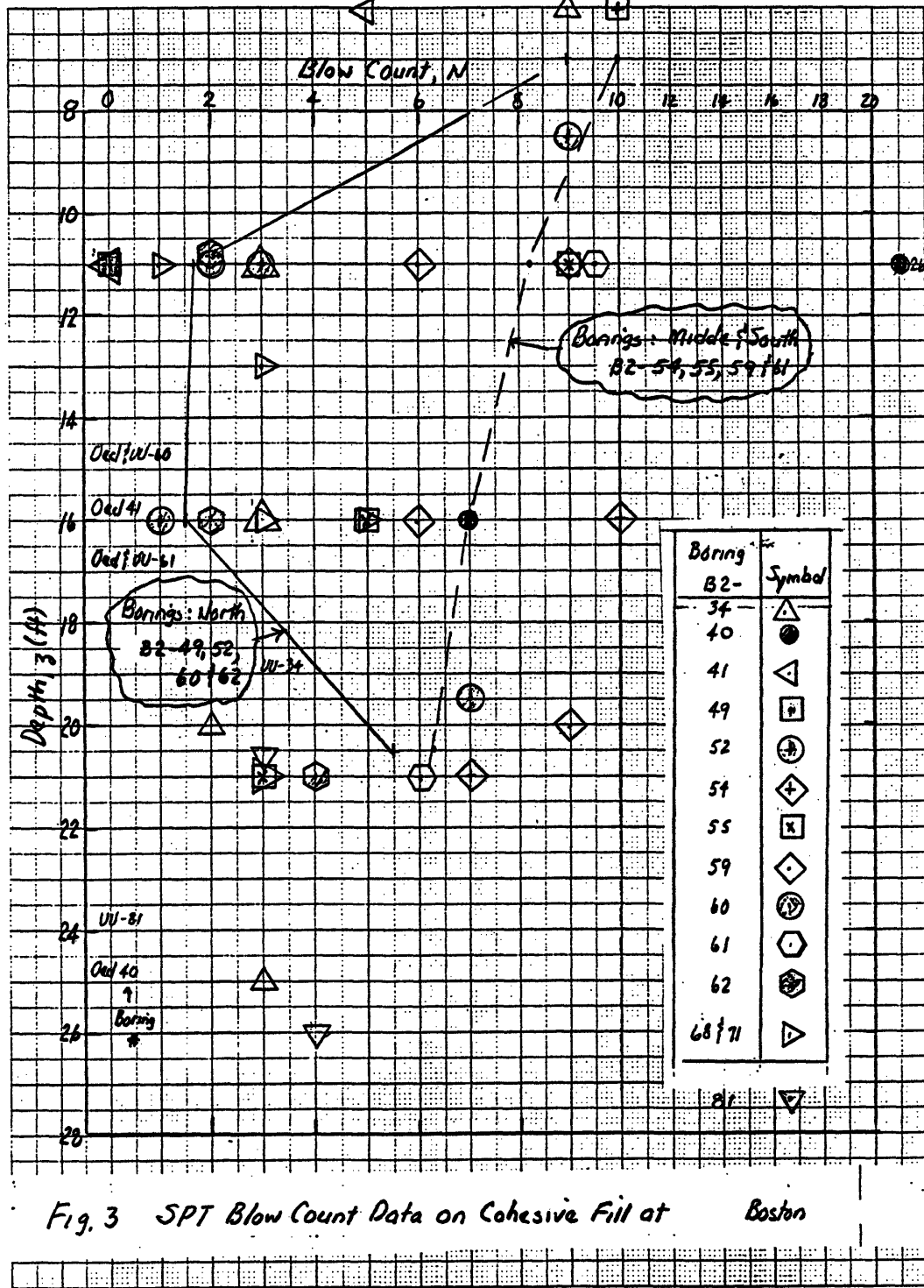


Fig. 3 SPT Blow Count Data on Cohesive Fill at Boston

CCL 11/29/94 12/8/94 MHD

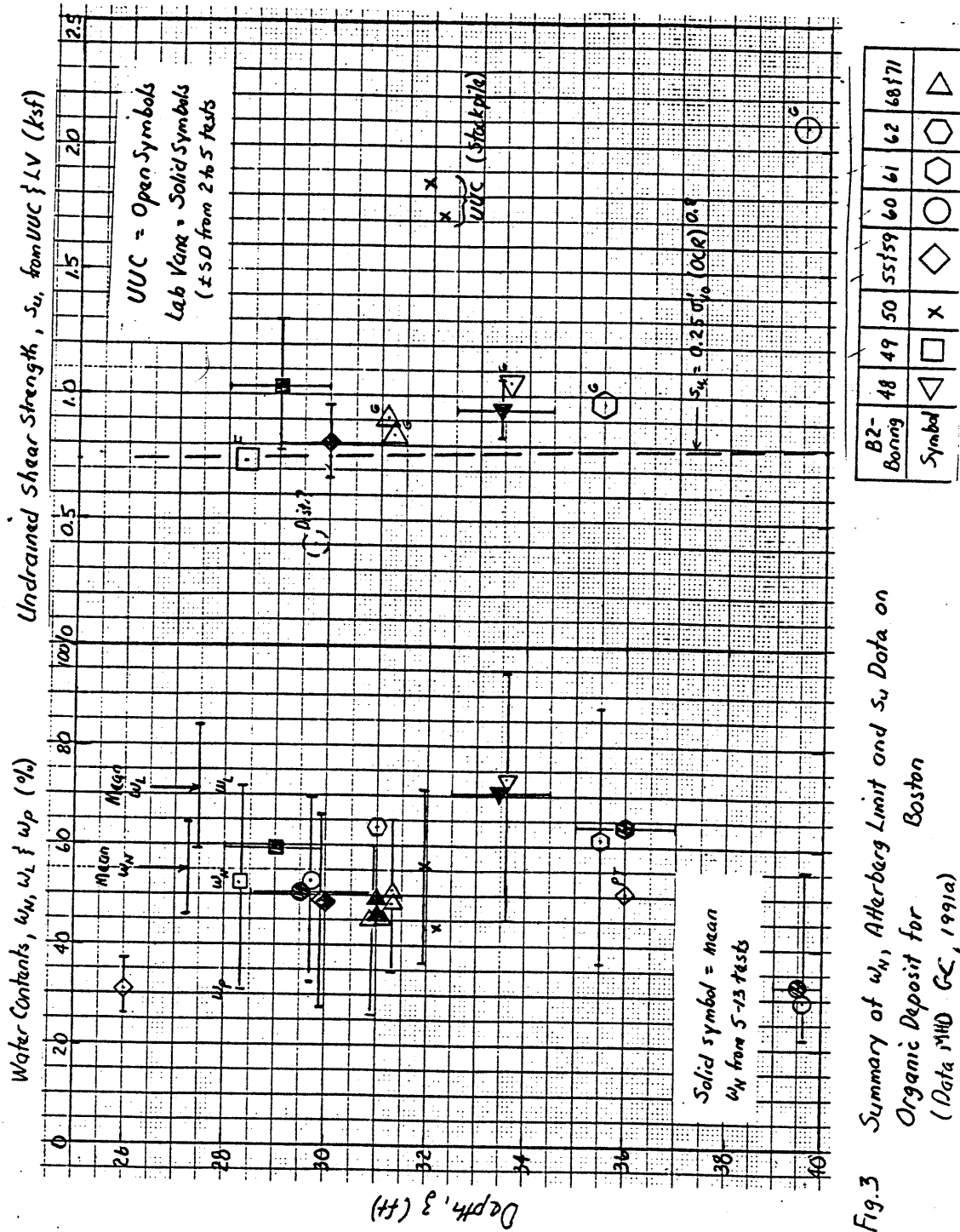


Fig. 3 Summary of w_N , Atterberg Limit and s_u Data on Organic Deposit for Boston (Data MHD GC, 1991a)

Sheet B4

CCL 12/87

CCL 11/24/94 MHD

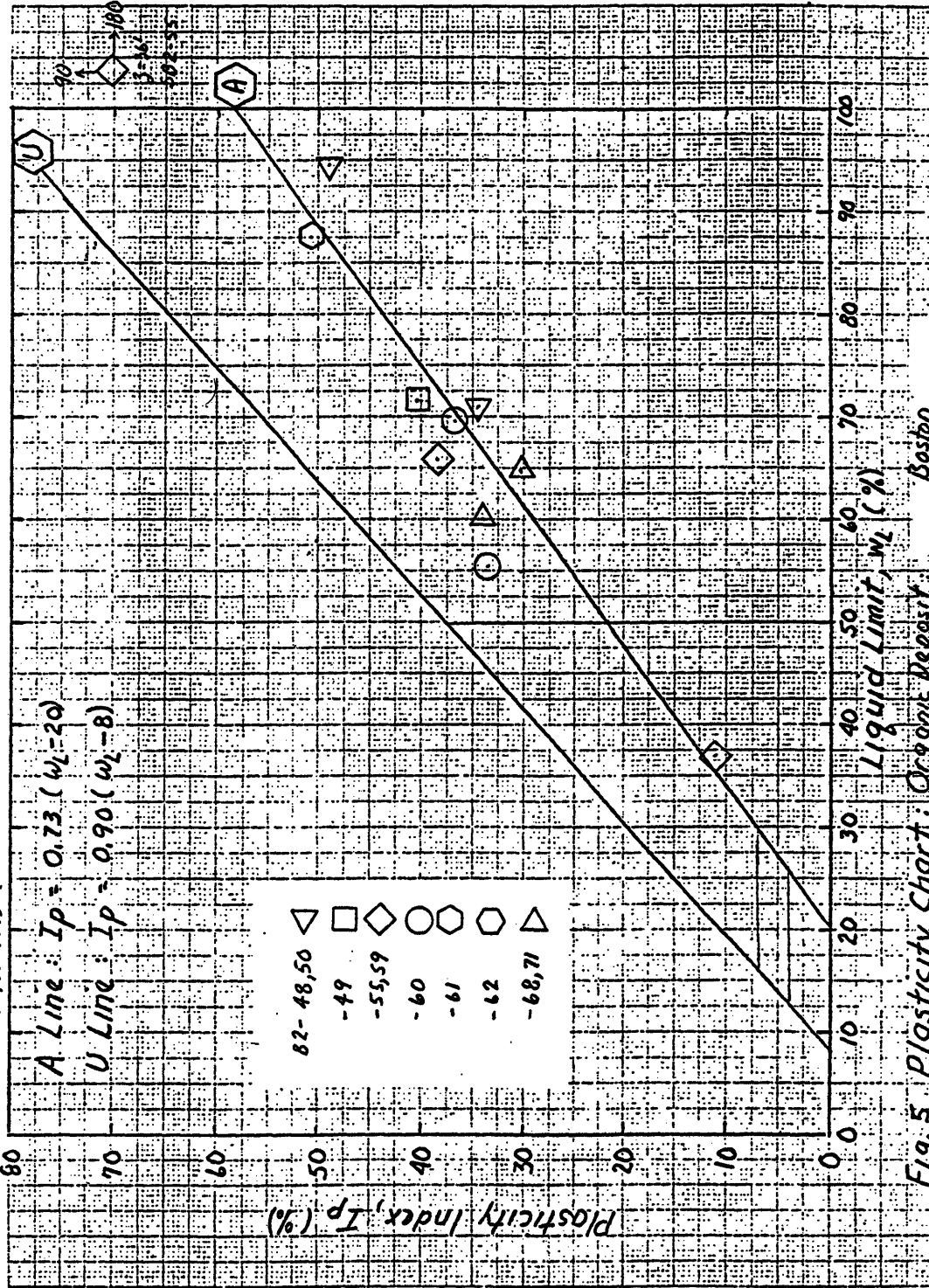
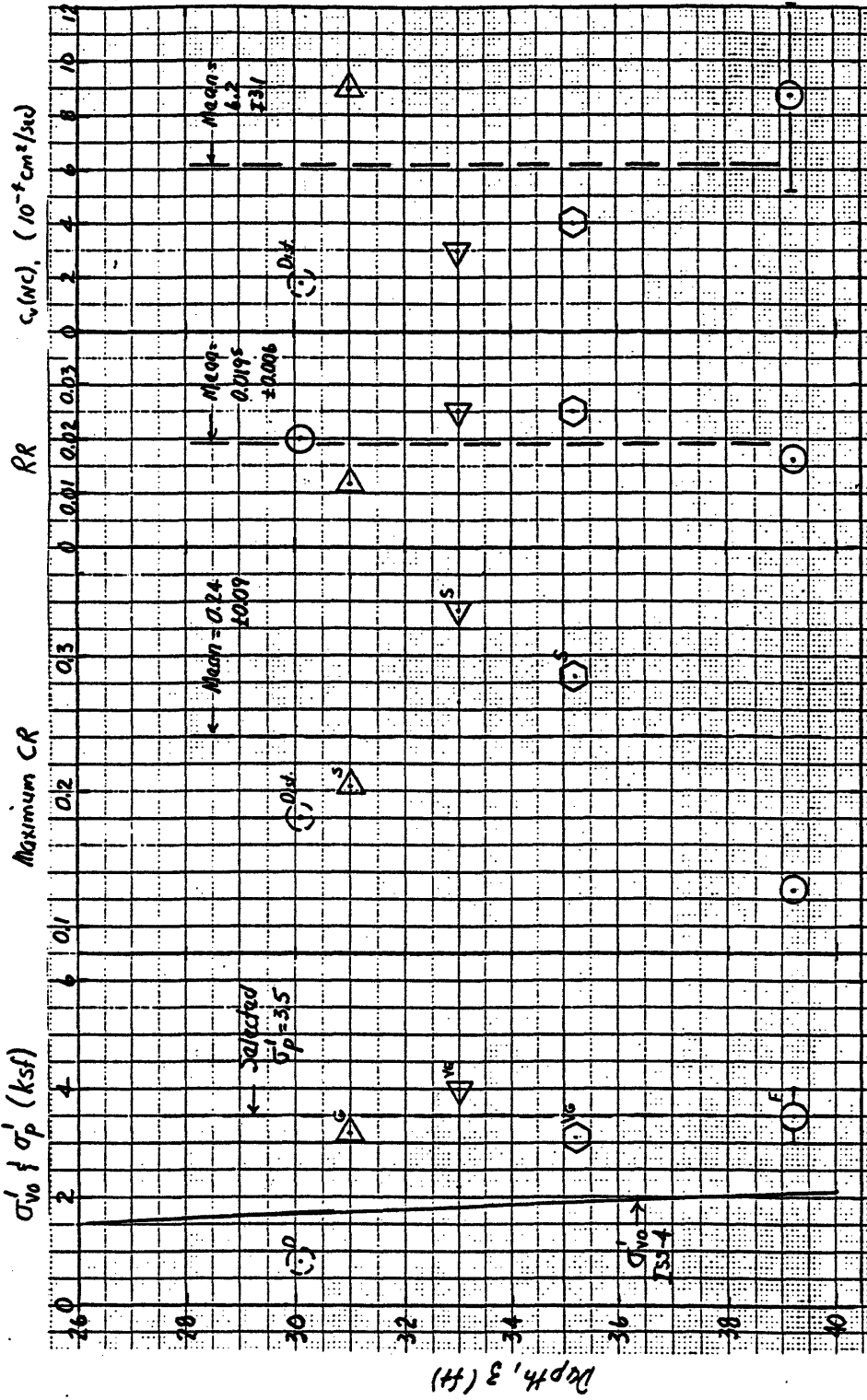


Fig. 5. Plasticity Chart: Organic Deposits Boston

(POOR QUALITY)

Sheet B5

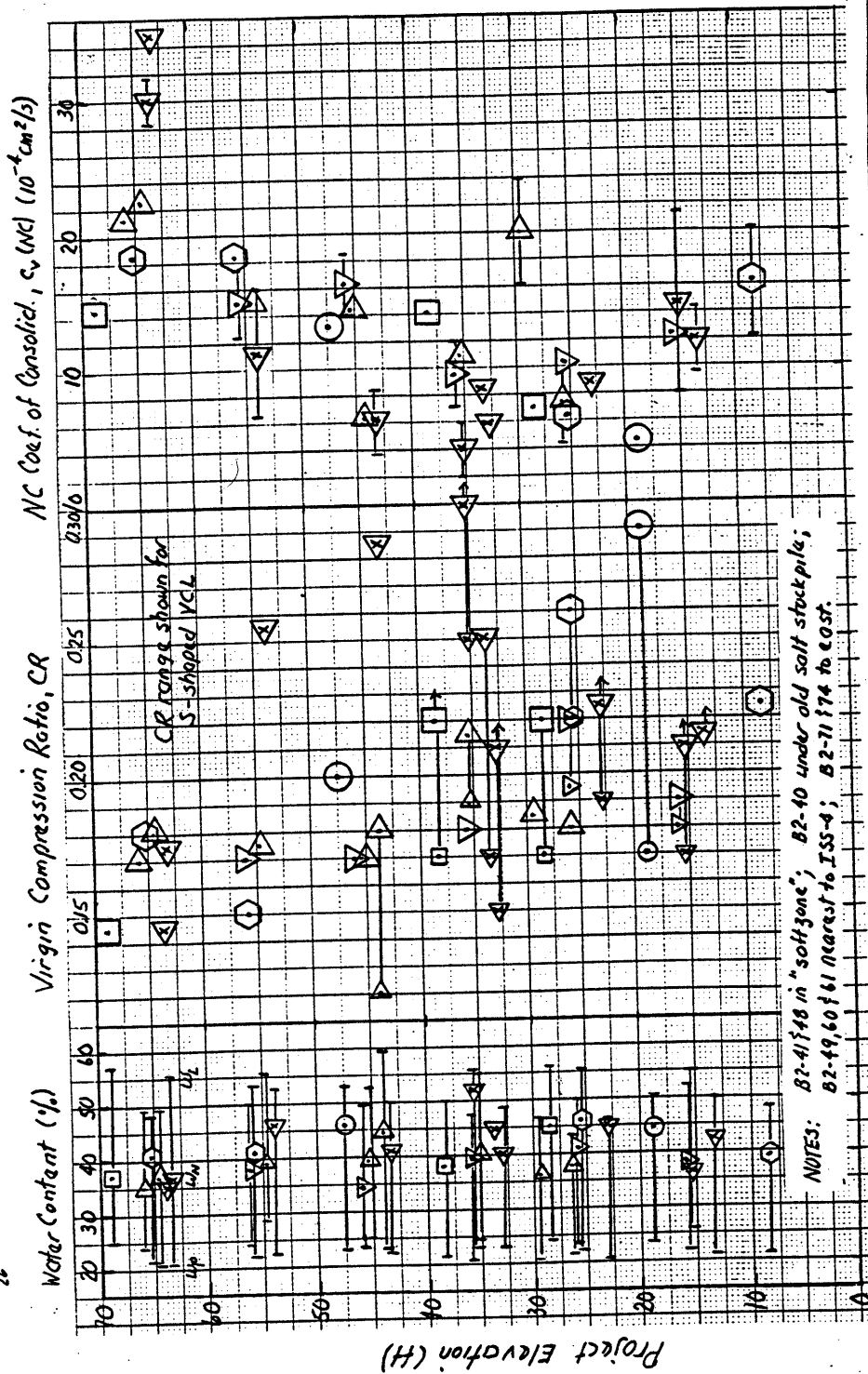
CC 1/15/10 + 12/10/10 MND



B-2 Boring	Symbol
48	∇
60	\circ
61	\square
68	\triangle

Fig. 4 Summary of Oedometer Data on Organic Deposit for Boston (MIT interpretation of data MND GG/1991a)

CCL 11/25/94 MHD
26



NOTES: B2-41748 in "soft zone"; B2-40 under old salt stockpile;
B2-49, 60 & 61 nearest to ISS-4; B2-71774 to east.

B2 Boring	41748	40	49	60	61	71774
Symbol	△	▽	□	○	◇	△

Fig. 4 Water Content, Virgin Compression Ratio and NC Coef. of Consolidation Data on BBC for Boston (Data MHD GC 1991a)

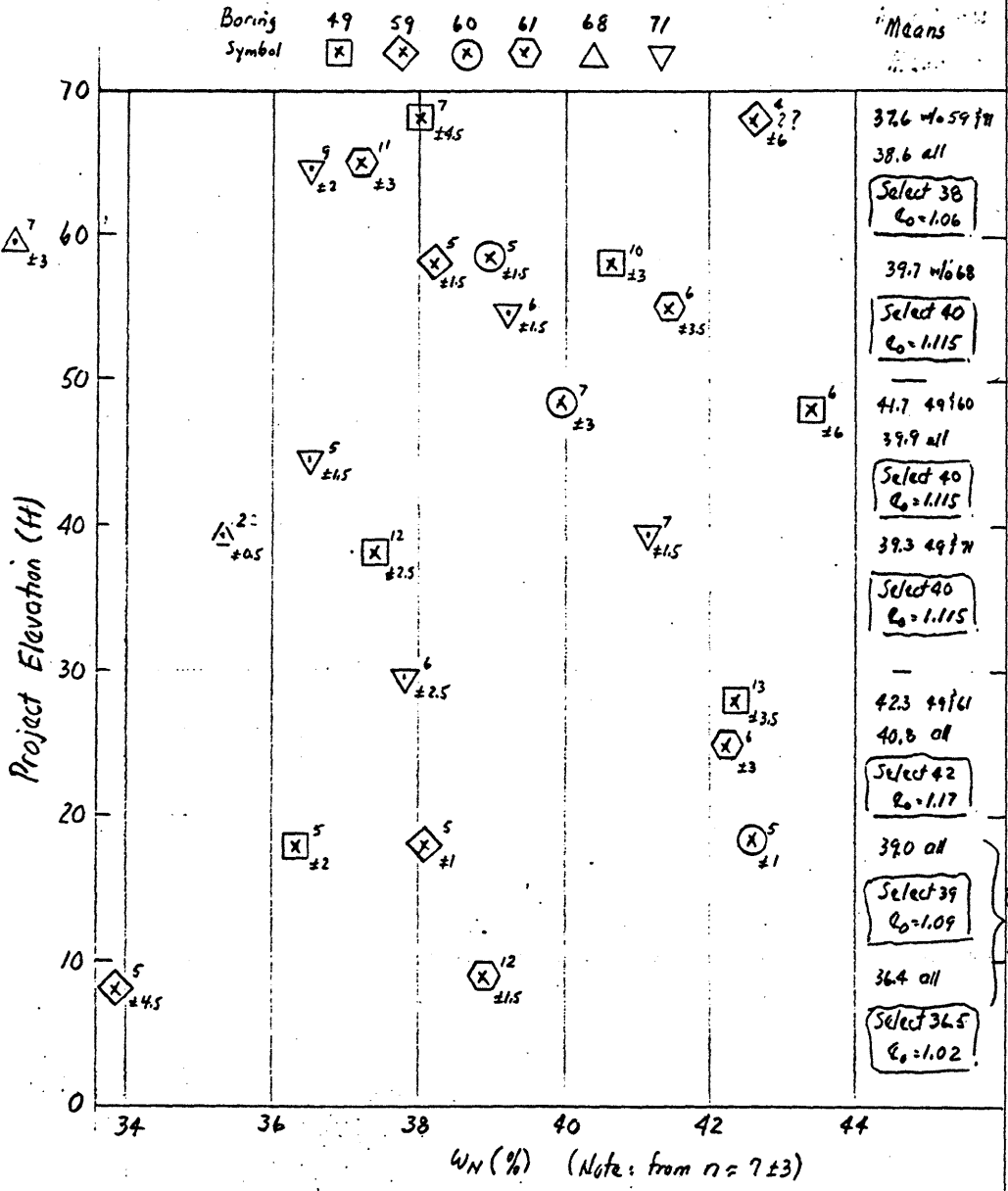
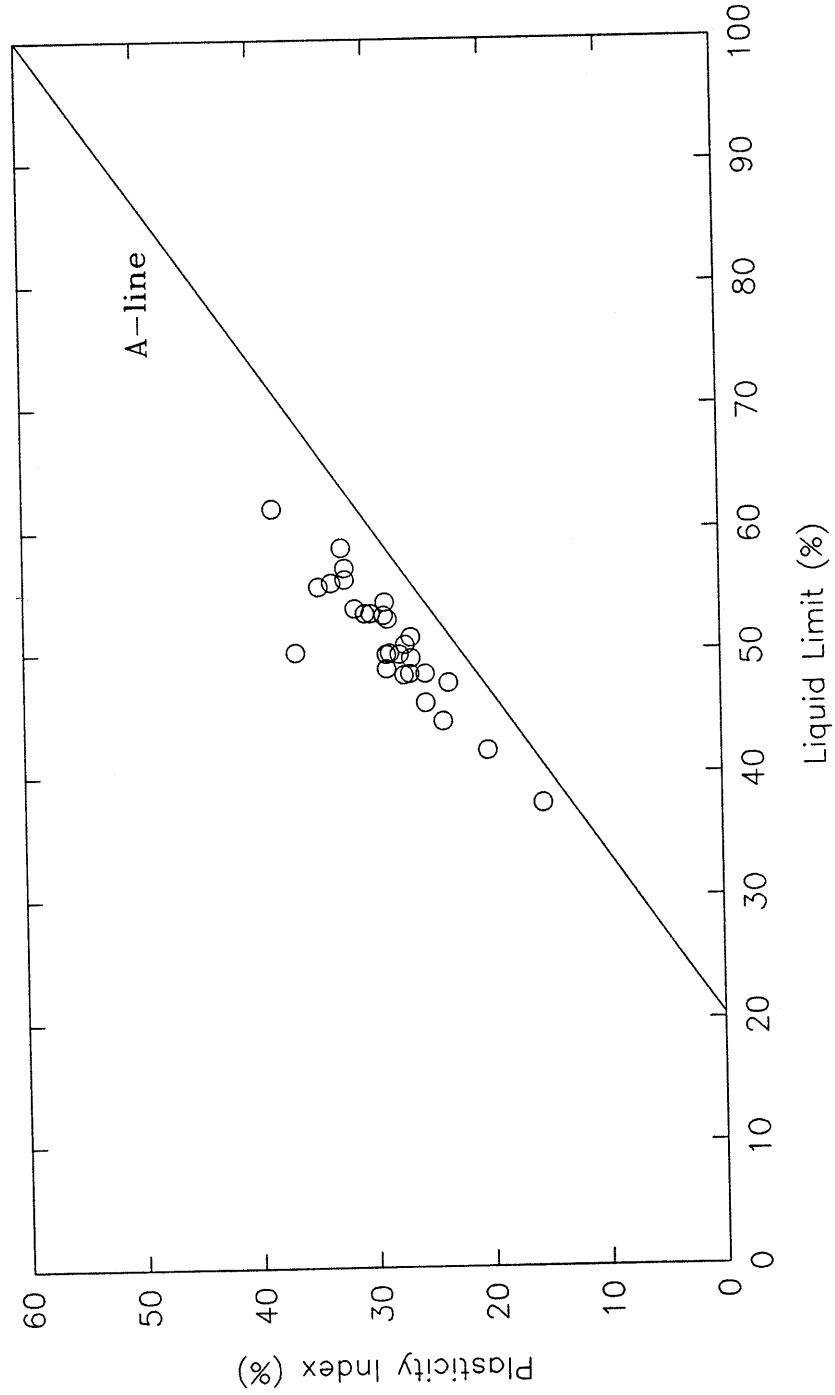
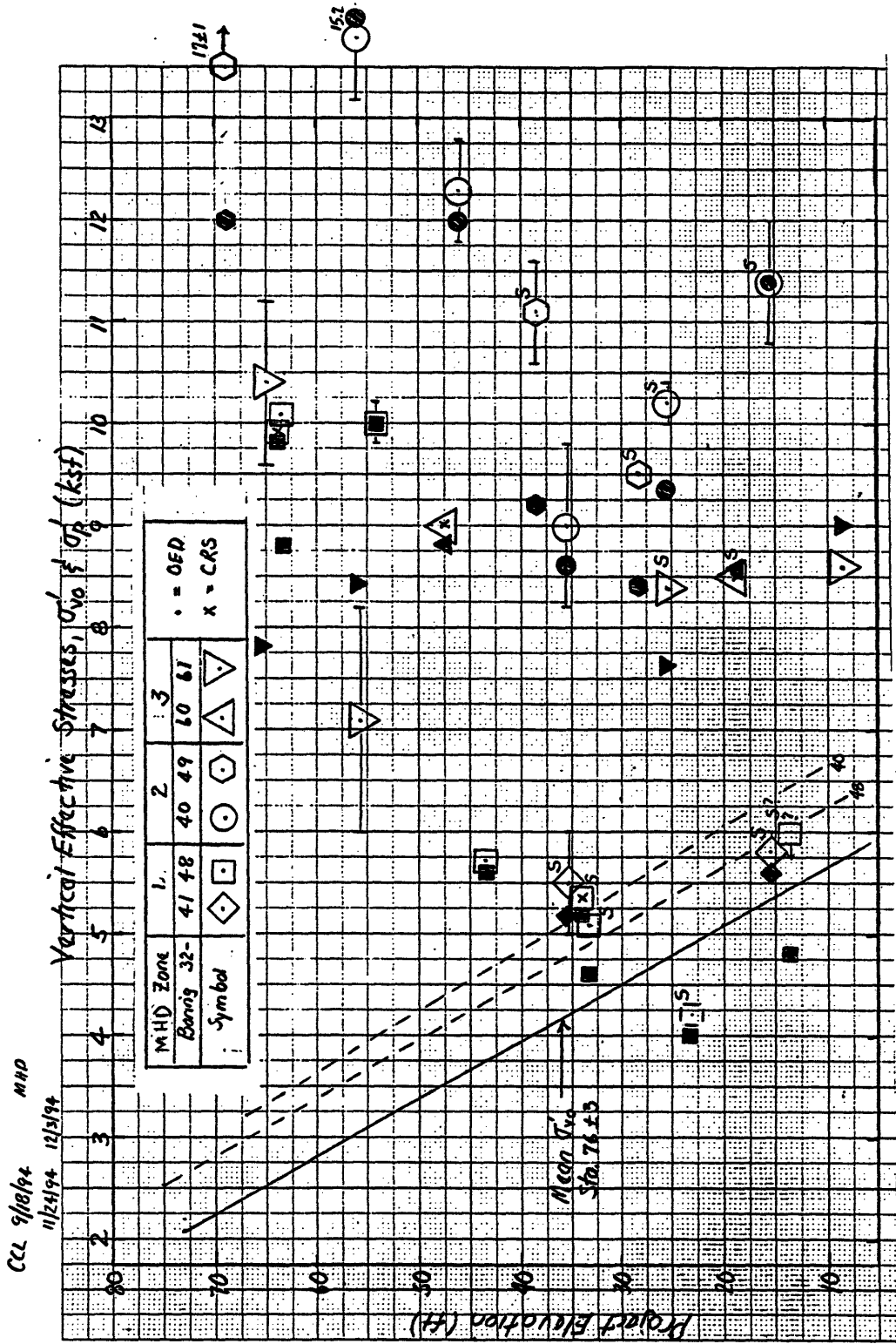


Fig. 5 Elevation vs. Mean Natural Water Content from Borings Around ISS-4

Plotted data is from borings B2-48,49,50,59,60,61, and 68.

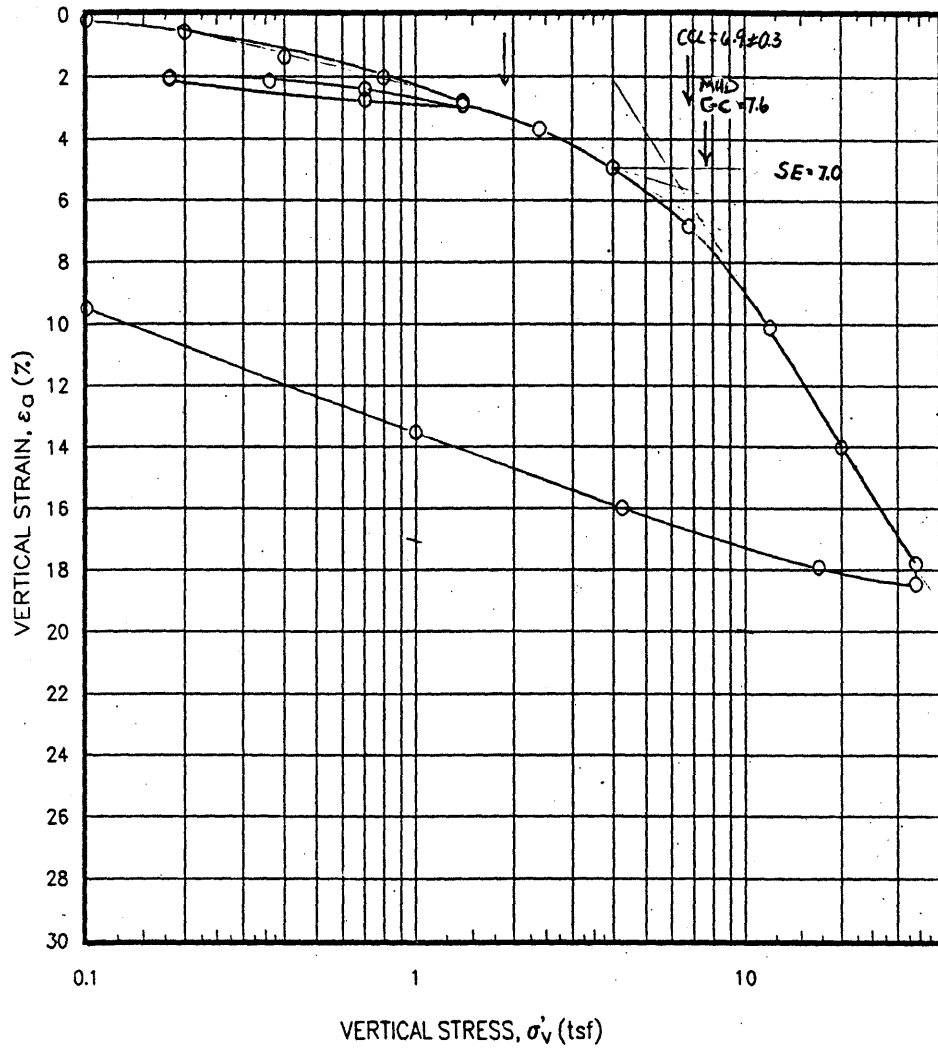


Plasticity Chart (Liquid Limit vs. Plasticity Index) Showing Range of Atterberg Limits for BBC in the Region Surrounding ISS-4.



NOTE: σ'_p from Casagrande Technique; MIT = Open Symbols; MHD GC = Solid Symbols
Boston : Sta. 71 to Sta. 79

CCL 9/10 9/24



Boring No. : 82-40
 Sample No. : U02
 Depth (ft.) : 60.1
 Test No. : OED14

Atterberg Limits (%)

W_L : 50.2
 W_p : 23.8
 I_p : 26.4

C_{v0} = 1.92

Sample Description : Gray green CLAY and silt

	Water Content (%)	Void Ratio, e
Initial :	37.84	1.210
Final :	33.81	1.033

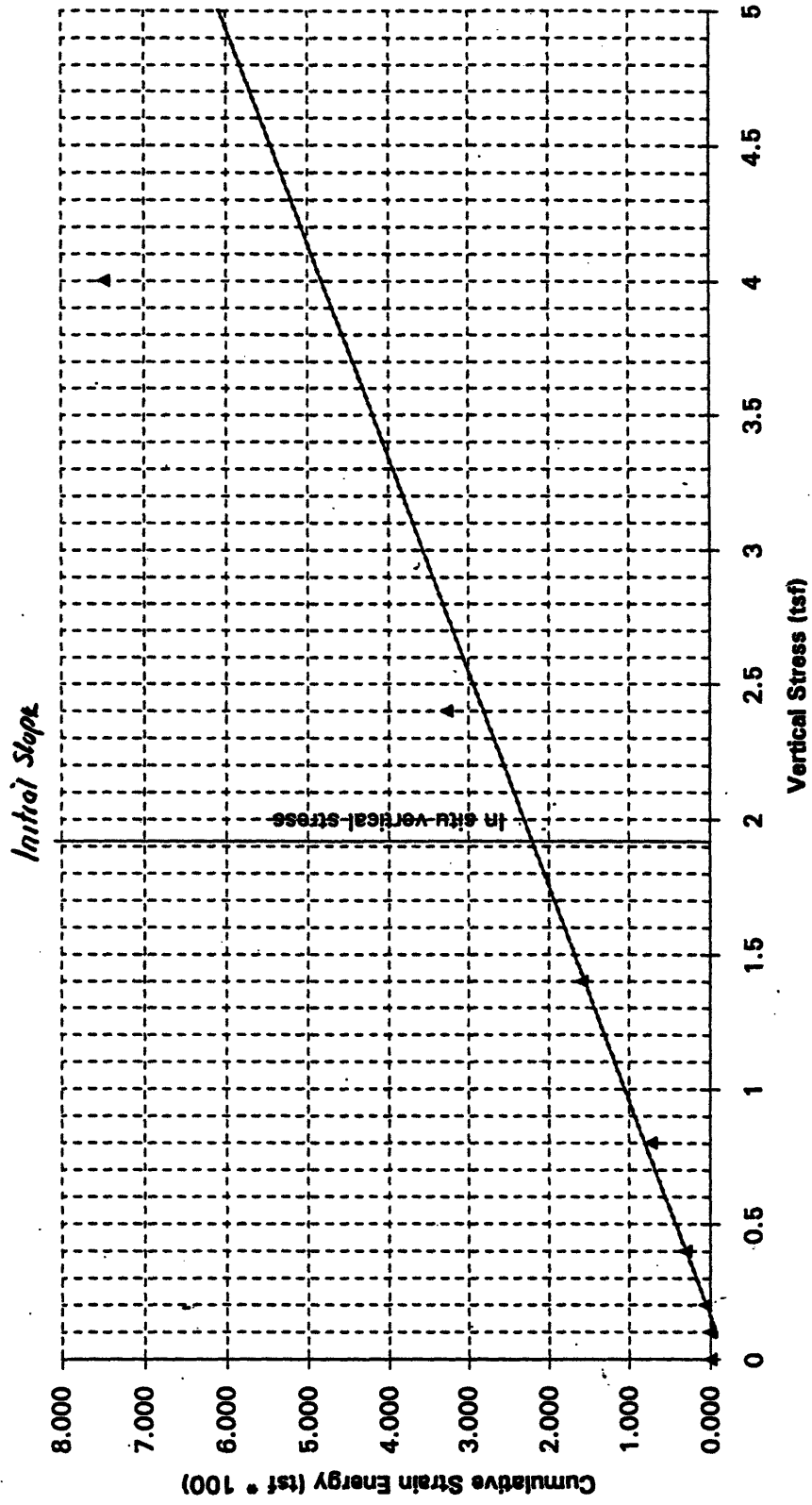
Preconsolidation Pressure (tsf) : 7.6
 Compression Ratio, CR : 0.176
 Recompression Ratio, RR : 0.012

29-Jun-90 : GUD120

MHD GEOTECHNICAL CONSULTANT	
CONSOLIDATION TEST	
FILE NO. 10360-32	FEB 1990

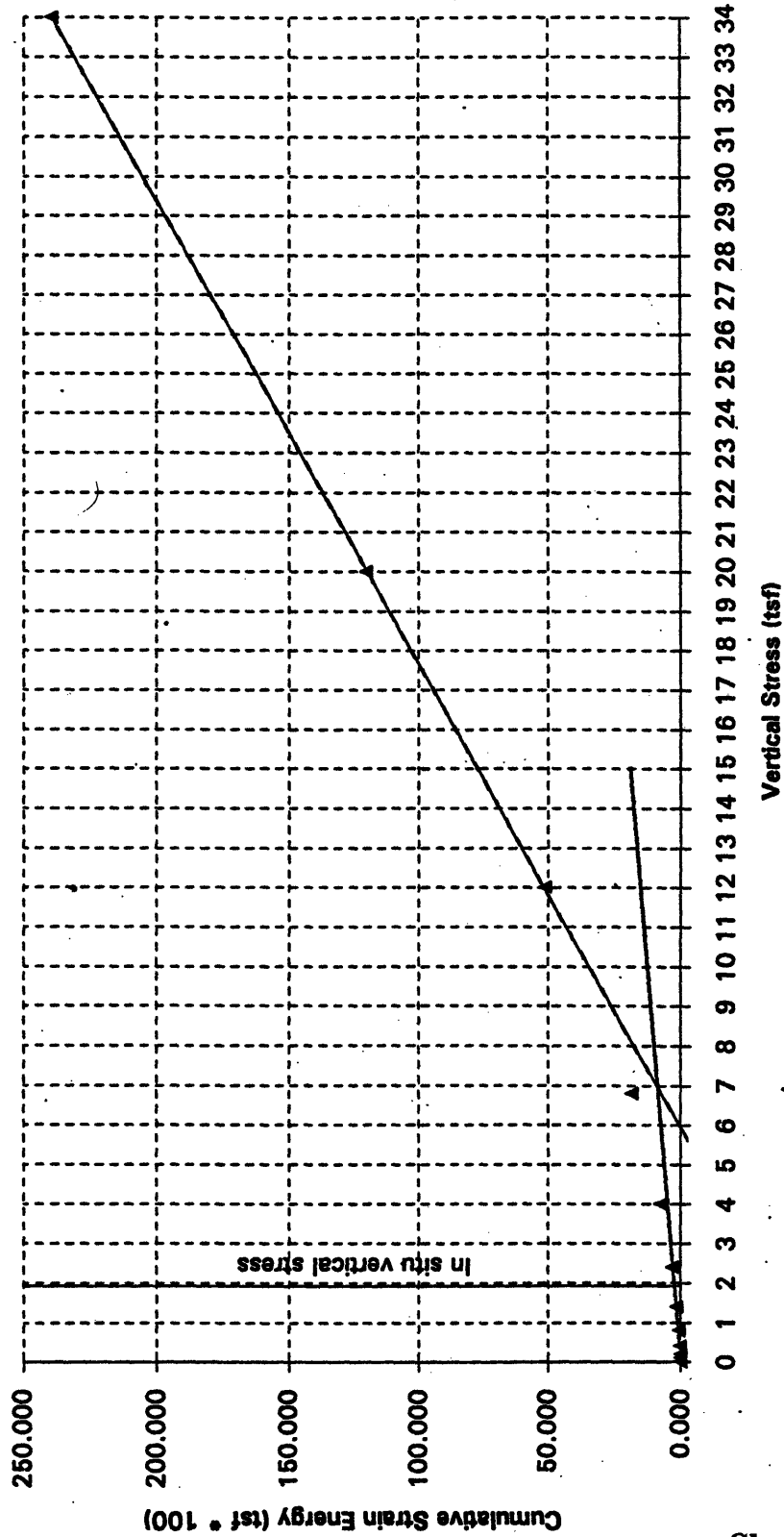
CCL 11/22/94

Recompression Strain Energy Plot: OED-14



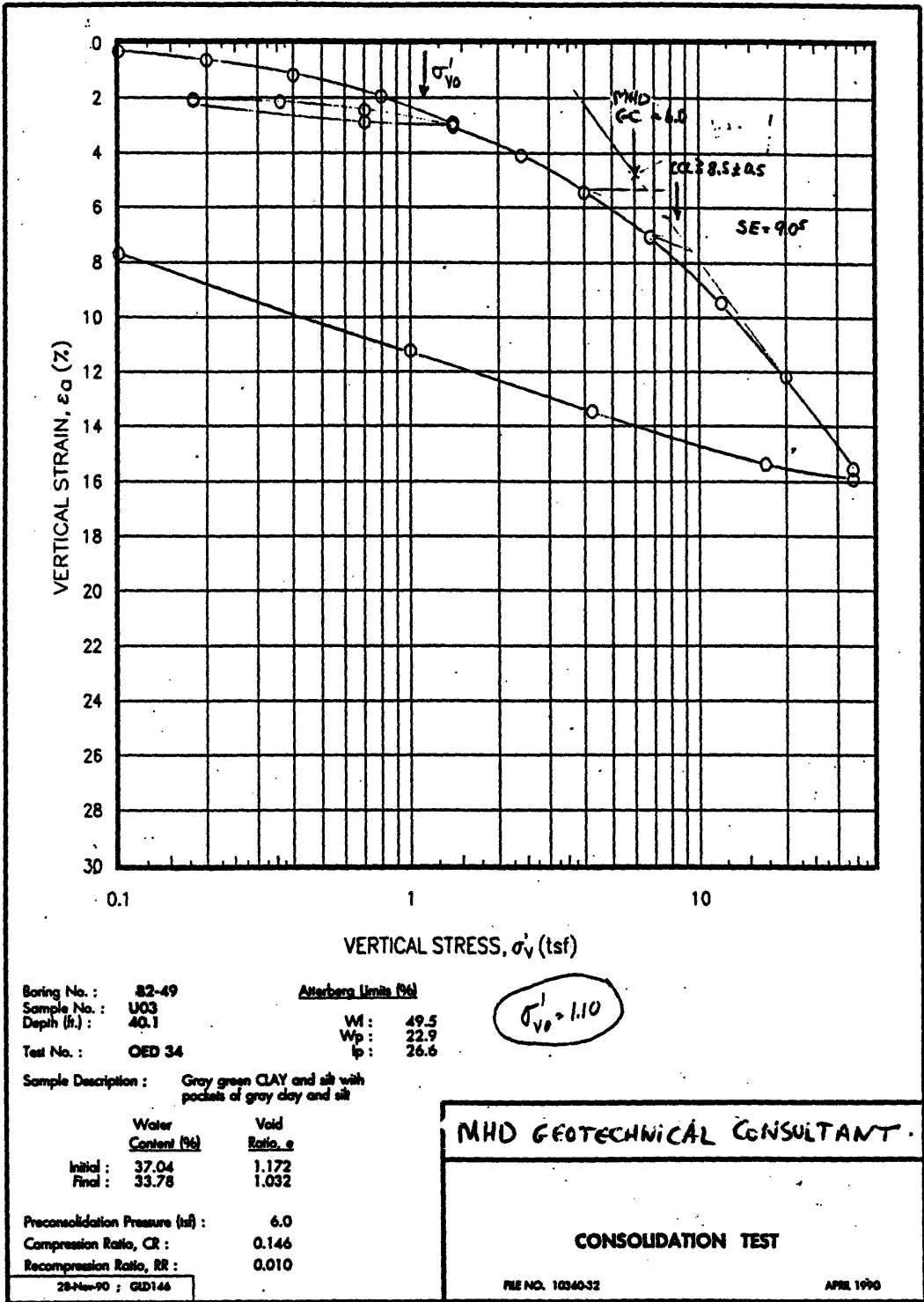
CCL 11/22/94

Strain Energy plot: OED-14



$\sigma_p'(SE) = 7.0 TSF = 14.0 ksf$

CEL 9/18



Boring No. : 82-49
 Sample No. : U03
 Depth (ft.) : 40.1
 Test No. : OED 34

Atterberg Limits (%)
 W_L : 49.5
 W_p : 22.9
 I_p : 26.6

$\sigma'_{v0} = 1.10$

Sample Description : Gray green CLAY and silt with pockets of gray clay and silt

	Water Content (%)	Void Ratio, e
Initial :	37.04	1.172
Final :	33.78	1.032

Preconsolidation Pressure (tsf) : 6.0
 Compression Ratio, CR : 0.146
 Recompression Ratio, RR : 0.010

MHD GEOTECHNICAL CONSULTANT.

CONSOLIDATION TEST

28-Nov-90 ; GUD146

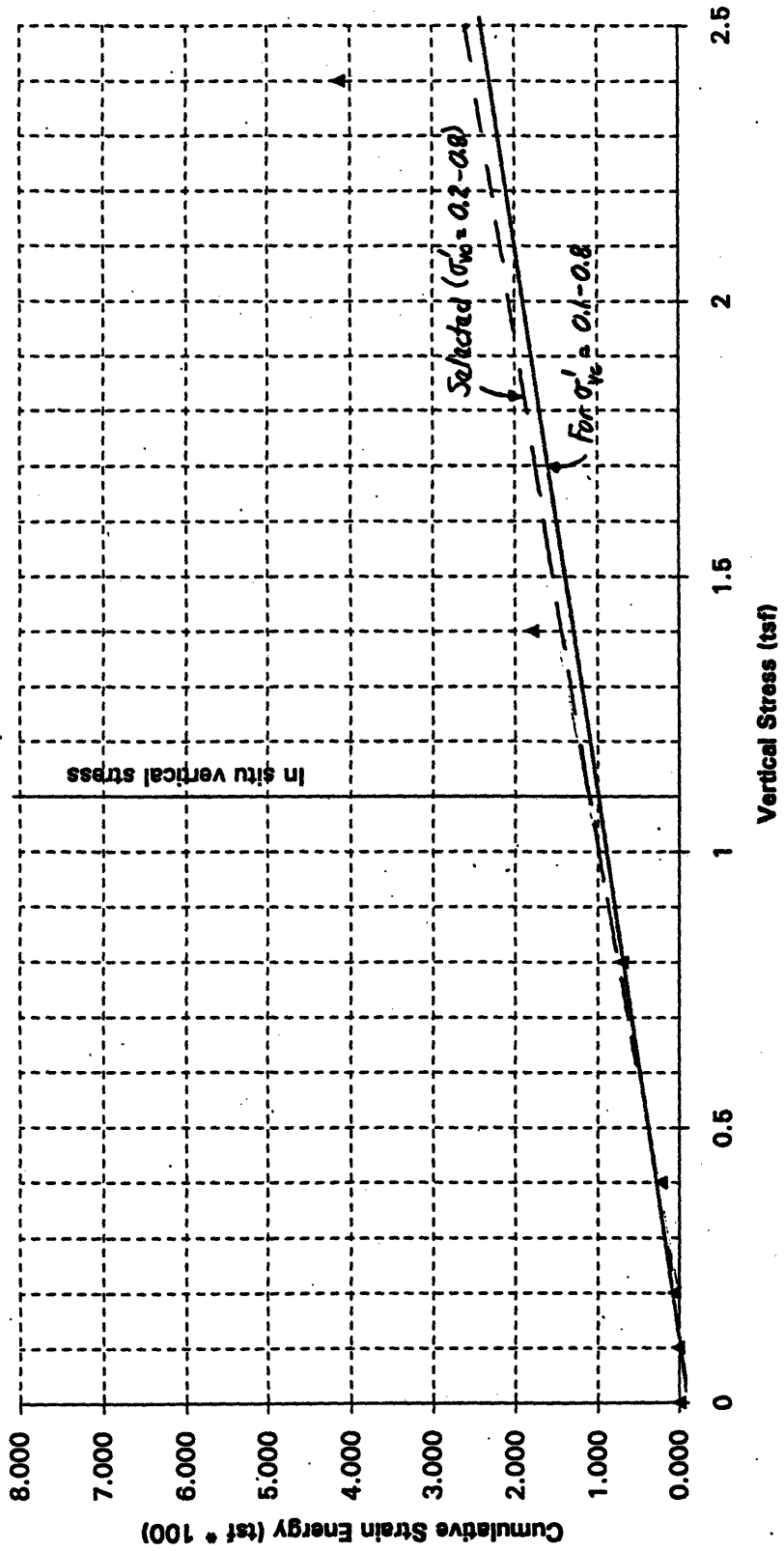
FILE NO. 10340-32

APRIL 1990

CCL 11/22/94

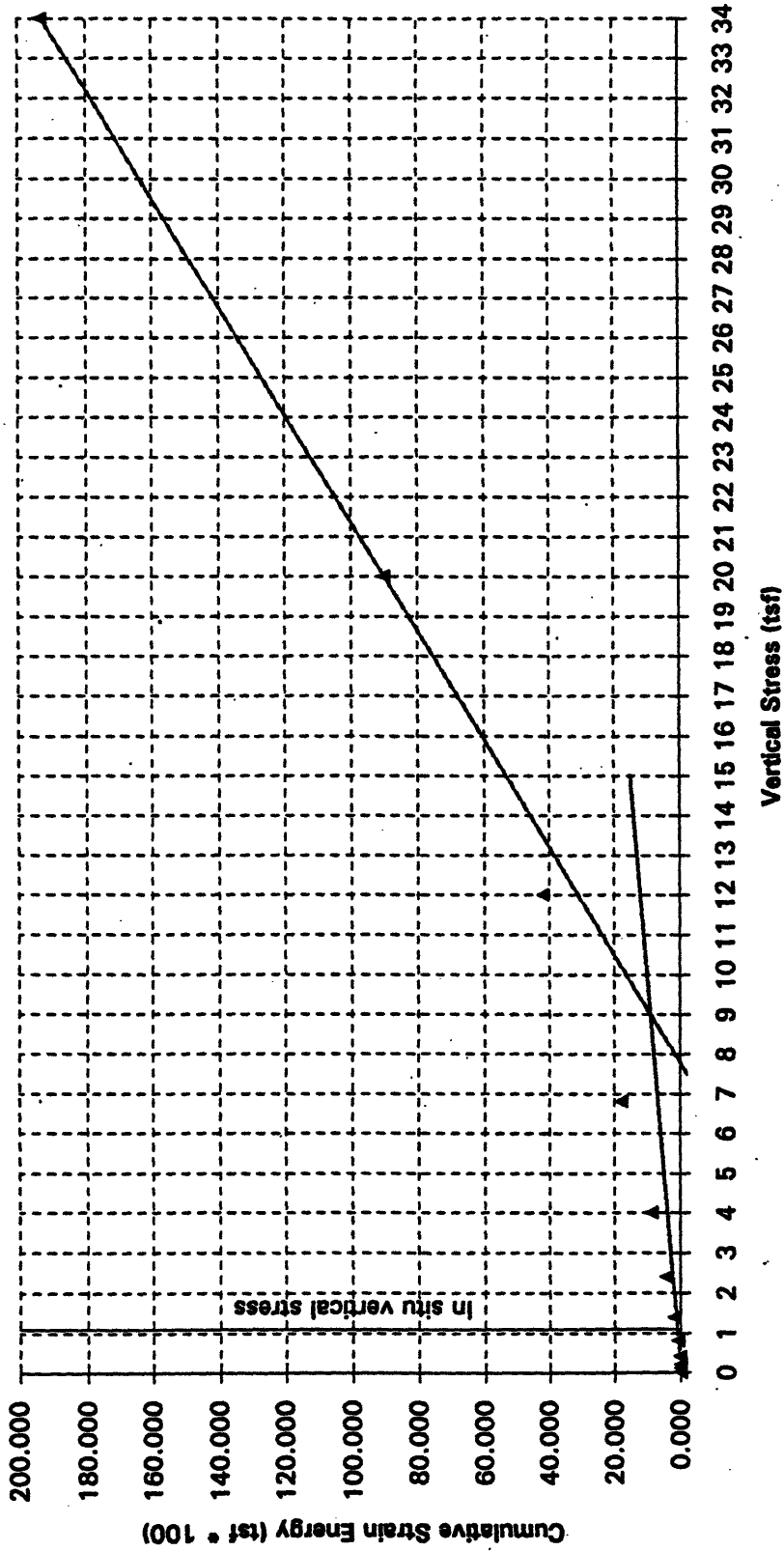
Recompression Strain Energy Plot: OED-34

Initial Slope



CCC 11/22/97

Strain Energy Plot: OED-34



$$\sigma'_p (SE) = 9.05 \pm 0.05 + 18.1 \pm 0.1 \text{ ksf}$$

MHD
 CCL 11/28/94

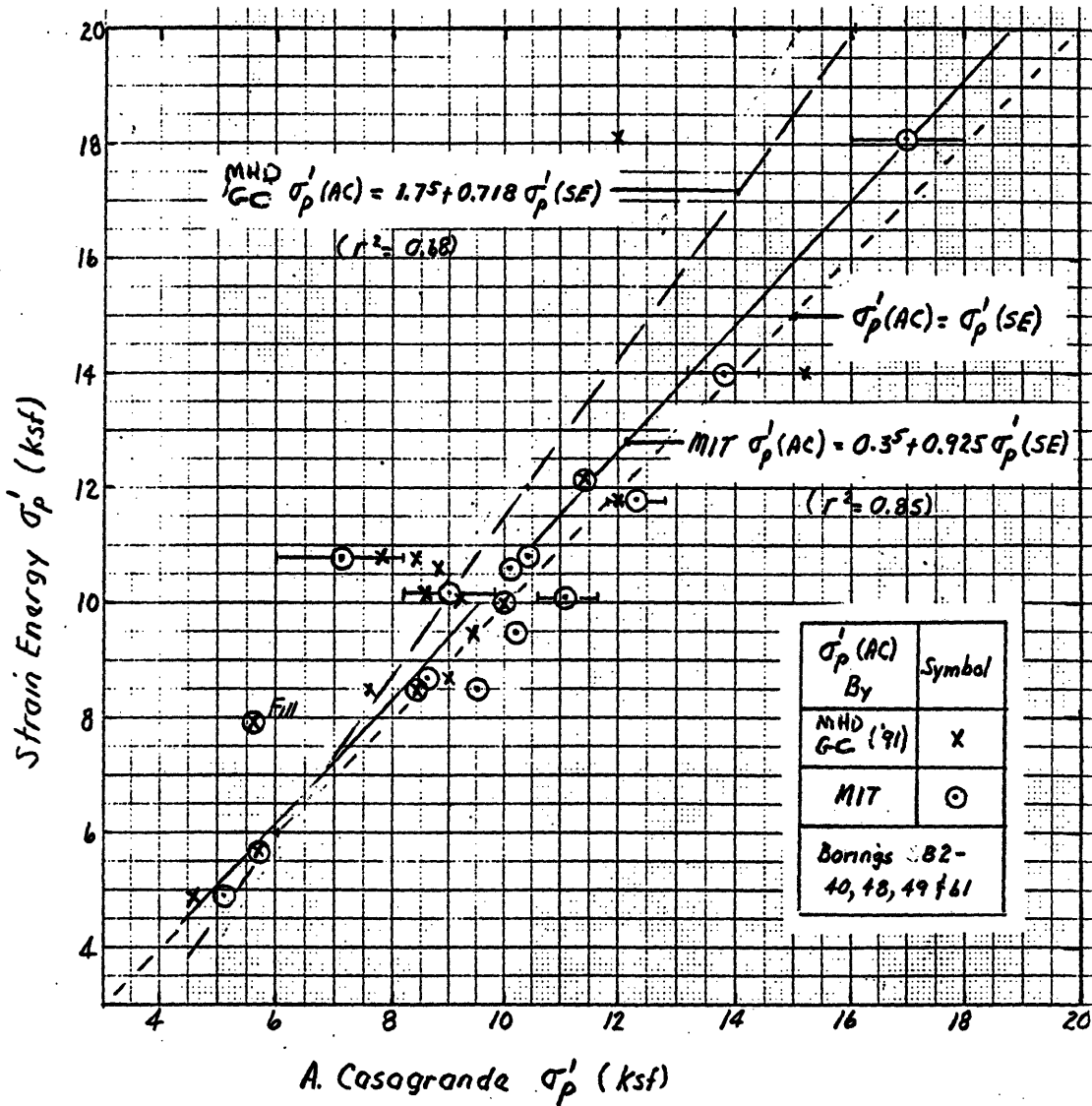
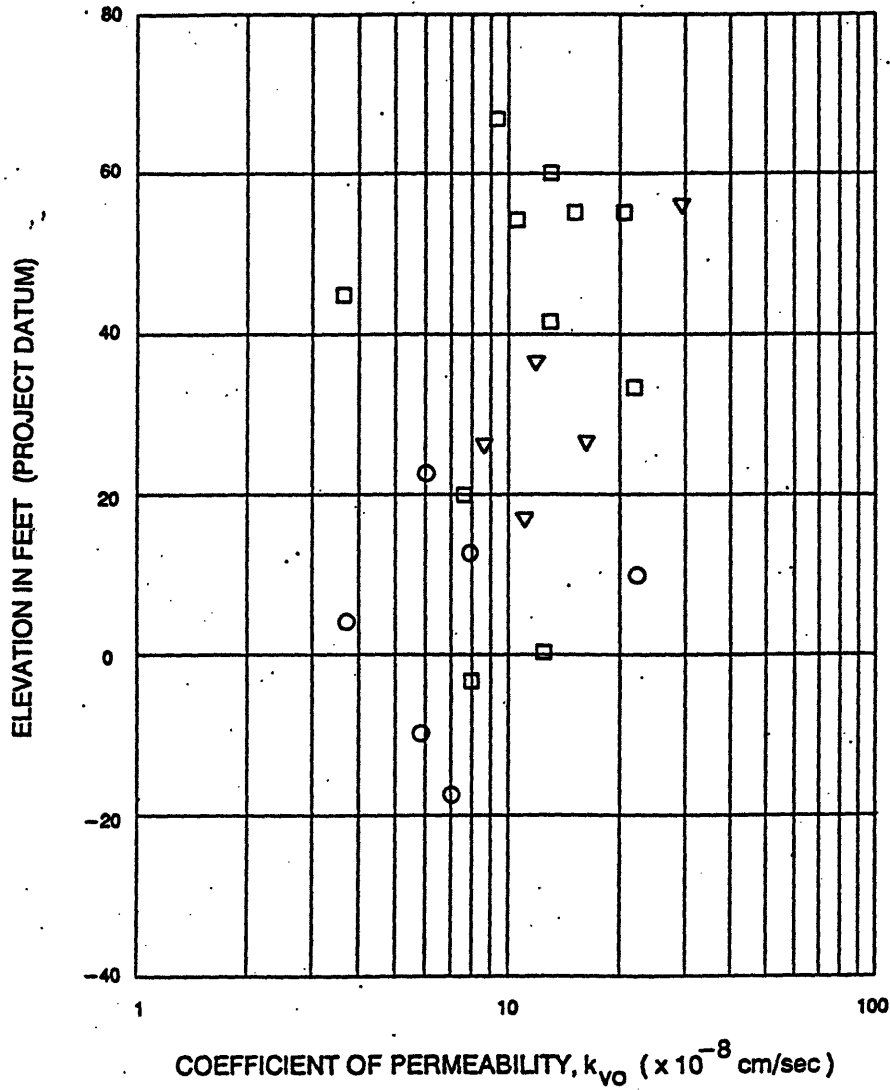


Fig.1 Comparison of Preconsolidation Pressures Estimated From Casagrande and Strain Energy Techniques for 17 Oedometer Tests on BBC (Fixed piston samples)

CCL 12/9/94



NOTE: DATA FROM CRSC TESTS ONLY

LEGEND:

- BOSTON - BLOCK
- BOSTON - TUBE
- ▽ BOSTON - TUBE (other site)

07-MAR-94 FIG 12.SPW *CORRECTED VERSION*

MHD GEOTECHNICAL CONSULTANT

SPECIAL TESTING PROGRAM
COEFFICIENT OF PERMEABILITY FOR
VERTICAL SEEPAGE vs. ELEVATION

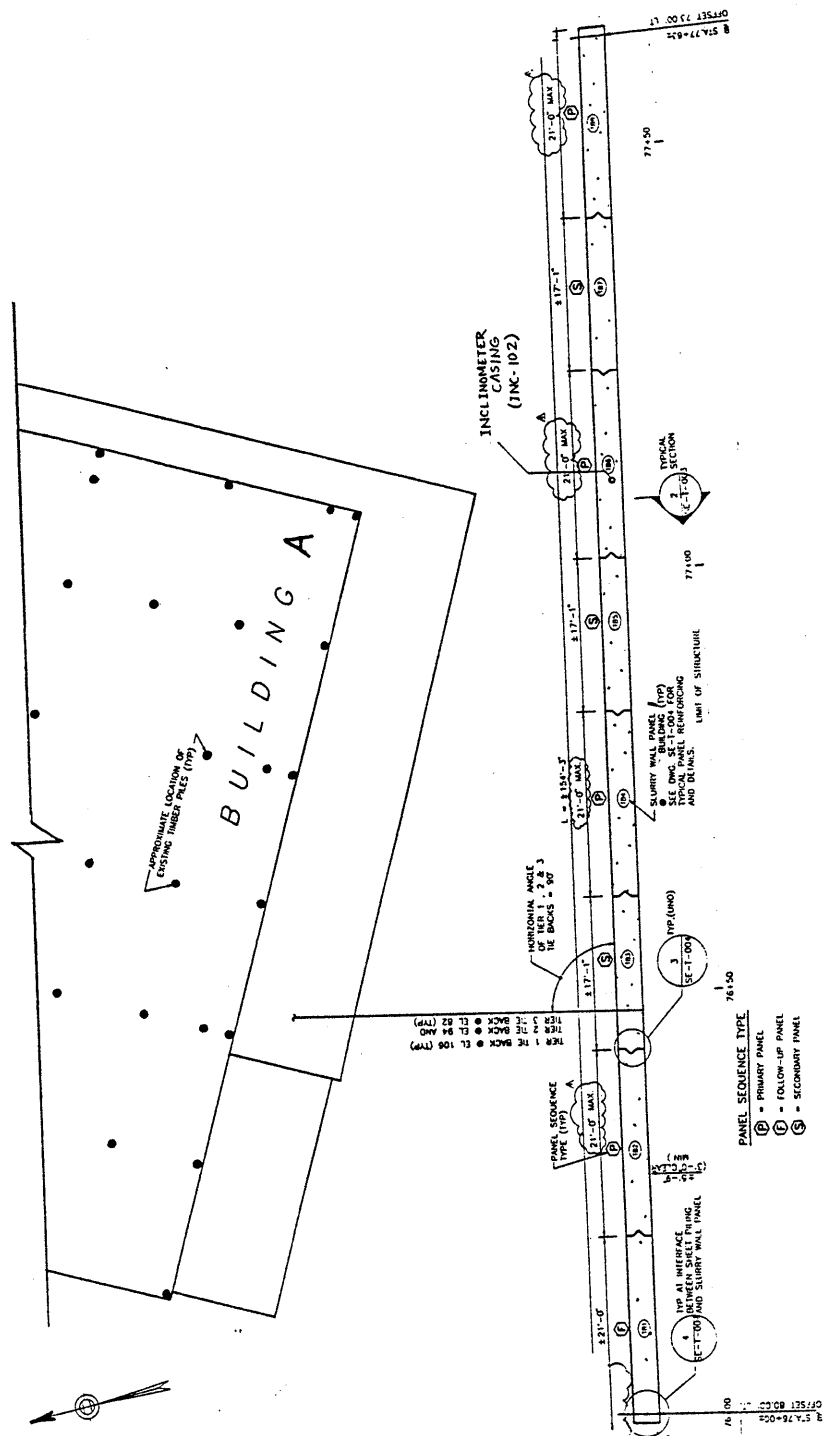
FILE NO. 10380-40

MARCH 1994

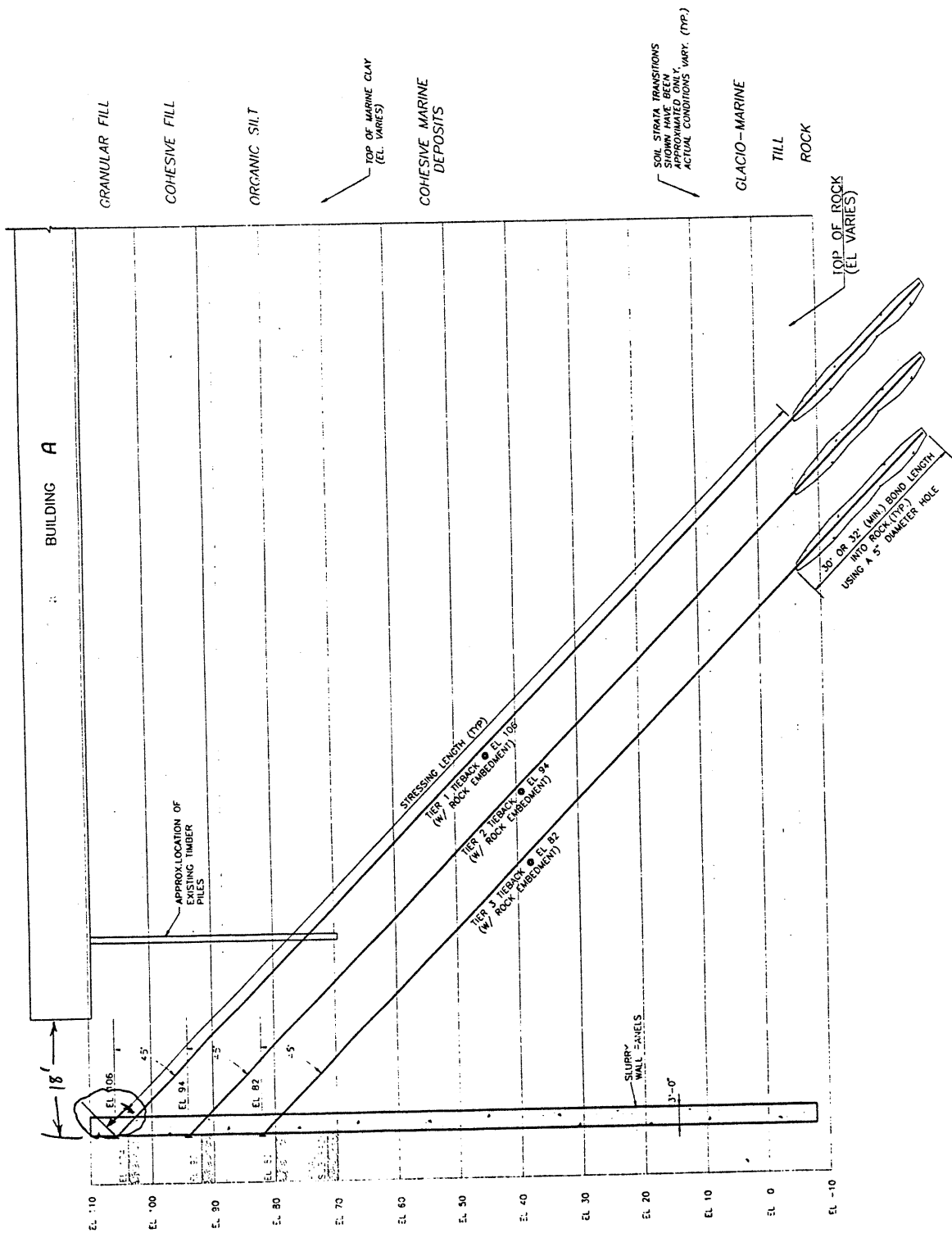
Sheet B18

APPENDIX C. Excavation Support System: SOE Walls and Tiebacks

Sheet C1. Plan View of Diaphragm Wall A and Building A.	296
Sheet C2. Elevation View of Diaphragm Wall A and Tiebacks.	297
Sheet C3. Placement of Reinforcing Steel Bars Within Diaphragm Wall A.	298
Sheet C4. Face-on View of Diaphragm Wall A, showing Tieback Locations, Embedment Depths of Wall Panels, and Dates of Concrete Pours.	299
Sheet C5. Face-on View of the Sheetpile Wall along the South side of ISS-4, showing Tieback Locations and Embedment Depth.	300
Sheet C6. Stress-Strain Plot for Tieback Tier 1 on the North Diaphragm Wall.	301
Sheet C7. Stress-Strain Plot for Tieback Tier 2 on the North Diaphragm Wall, Anchors 1-16.	302
Sheet C8. Stress-Strain Plot for Tieback Tier 2 on the North Diaphragm Wall, Anchors 17-24.	303
Sheet C9. Stress-Strain Plot for Tieback Tier 3 on the North Diaphragm Wall, Anchors 1-16.	304
Sheet C10. Stress-Strain Plot for Tieback Tier 3 on the North Diaphragm Wall, Anchors 17-24.	305
Sheet C11. Stress-Strain Plot for Tieback Tier 1 on the South Sheetpile Wall.	306
Sheet C12. Stress-Strain Plot for Tieback Tier 2 on the South Sheetpile Wall, page 1 of 3.	307
Sheet C13. Stress-Strain Plot for Tieback Tier 2 on the South Sheetpile Wall, page 2 of 3.	308
Sheet C14. Stress-Strain Plot for Tieback Tier 2 on the South Sheetpile Wall, page 3 of 3.	309
Sheet C15. Stress-Strain Plot for Tieback Tier 3 on the South Sheetpile Wall, page 1 of 3.	310
Sheet C16. Stress-Strain Plot for Tieback Tier 3 on the South Sheetpile Wall, page 2 of 3.	311
Sheet C17. Stress-Strain Plot for Tieback Tier 3 on the South Sheetpile Wall, page 3 of 3.	312
Sheet C18. Tabulation of Two Independently Estimated Tieback Moduli, and Selected Values.	313

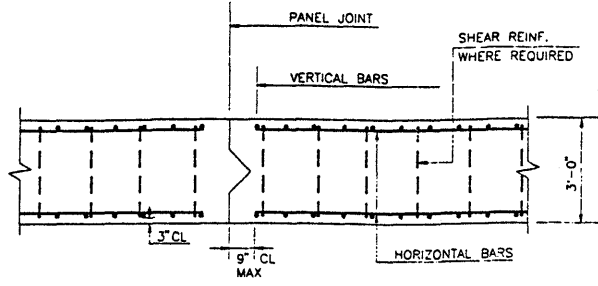
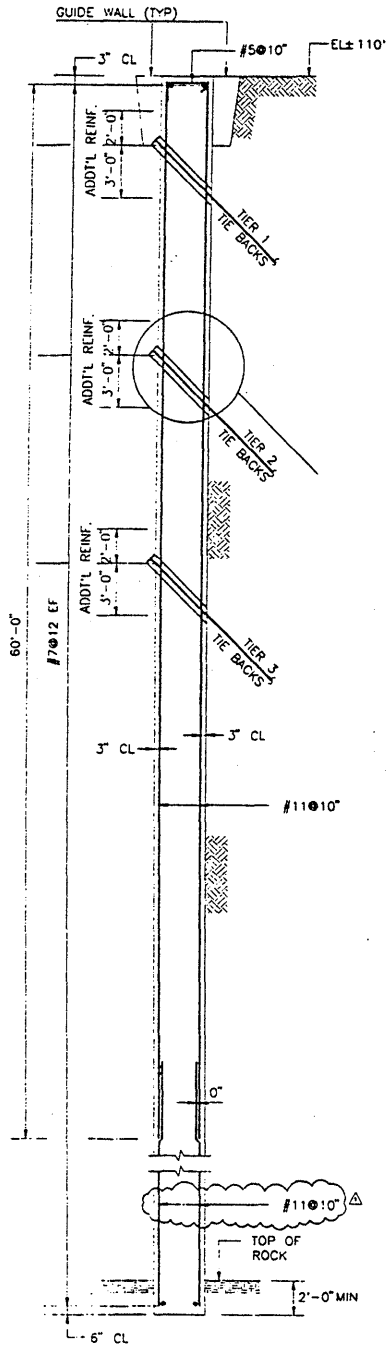


Sheet C1



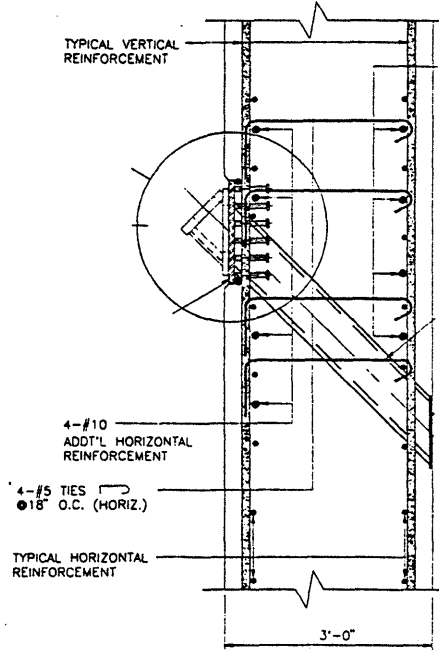
Sheet C2

ELEVATION VIEW

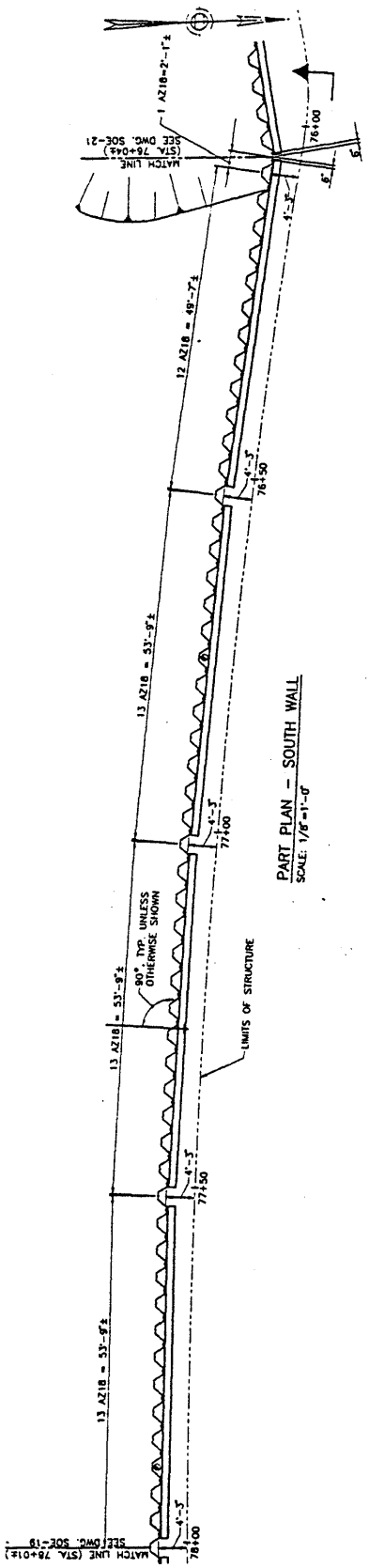


PLAN VIEW

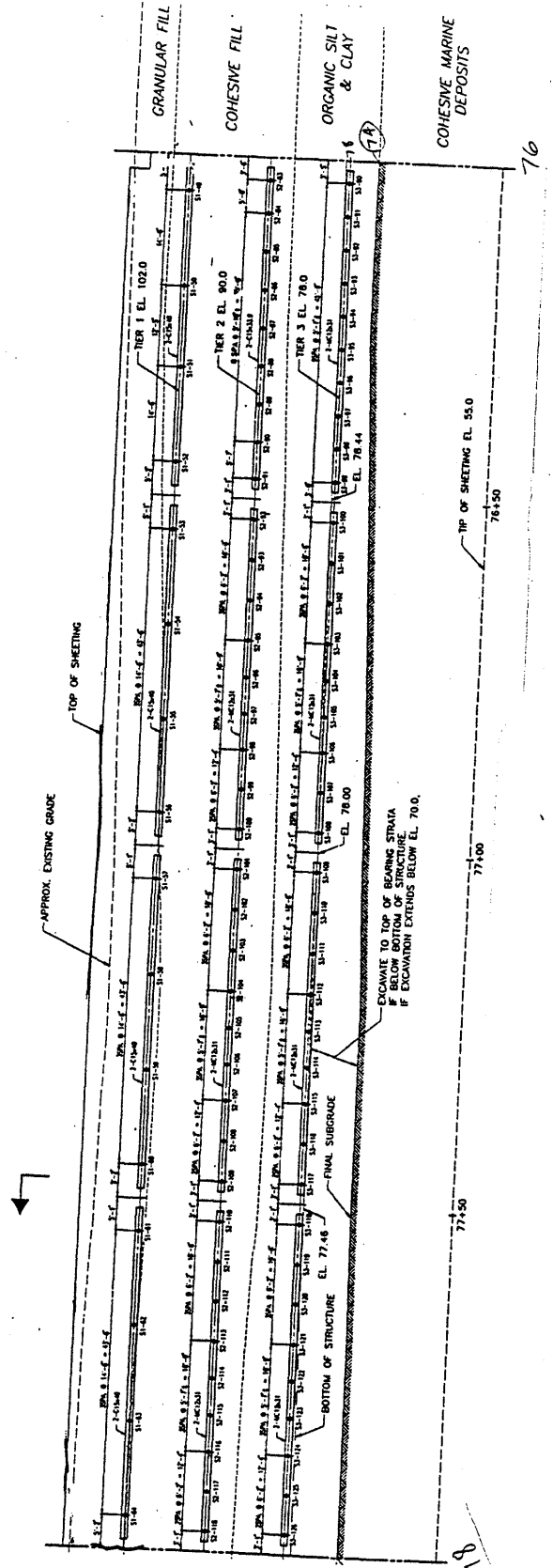
ELEVATION DETAIL

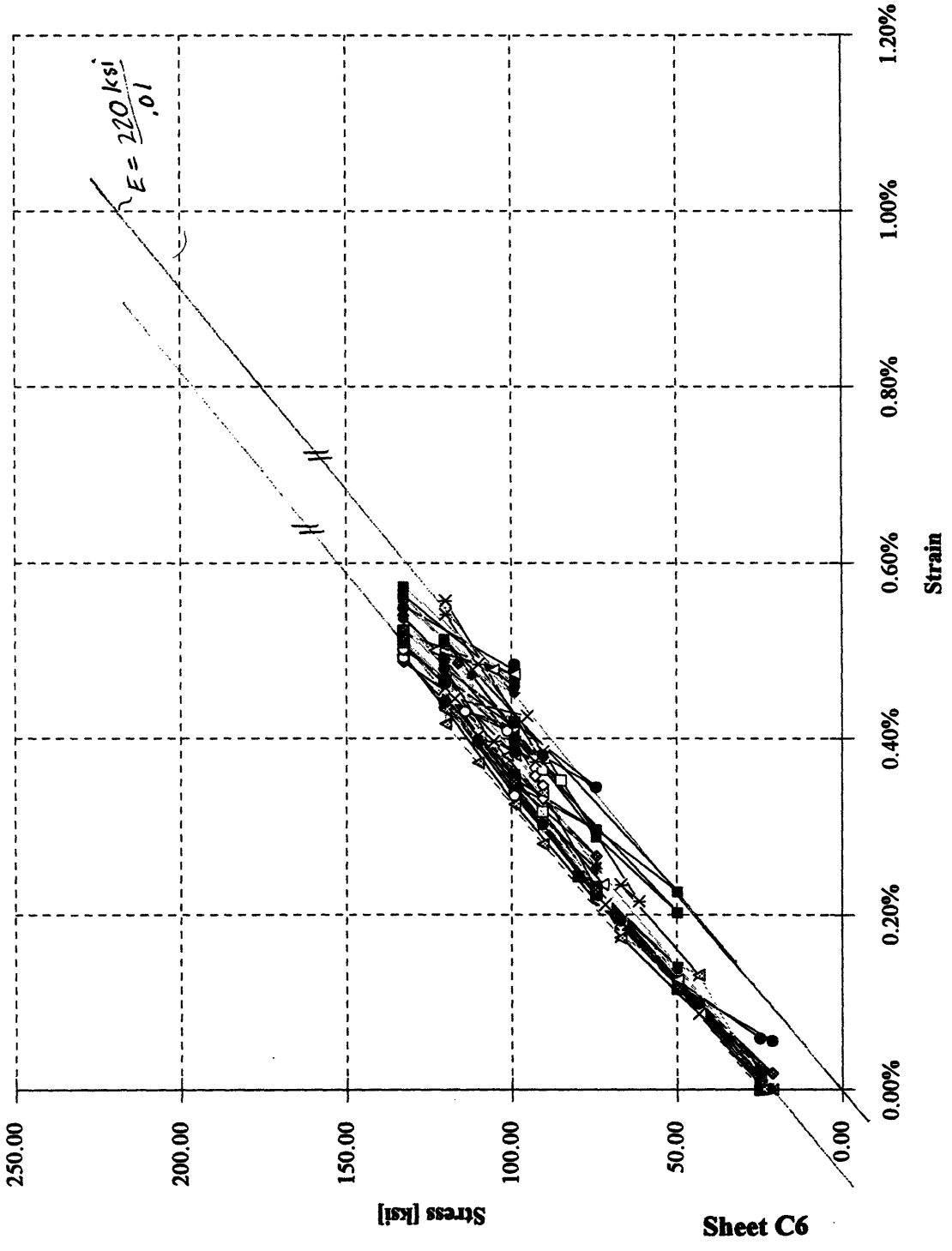


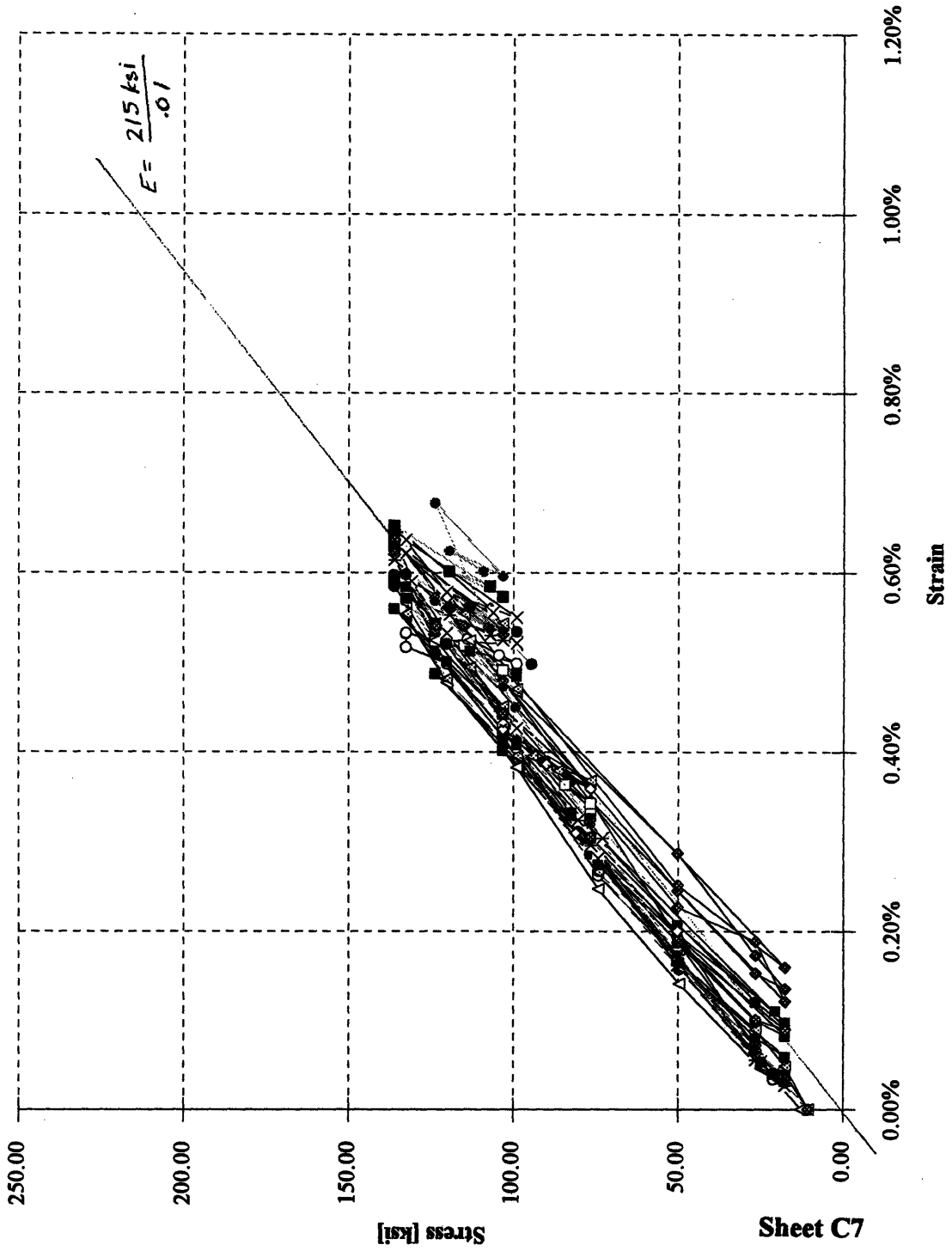
Sheet C3



PART PLAN - SOUTH WALL
SCALE: 1/8"=1'-0"

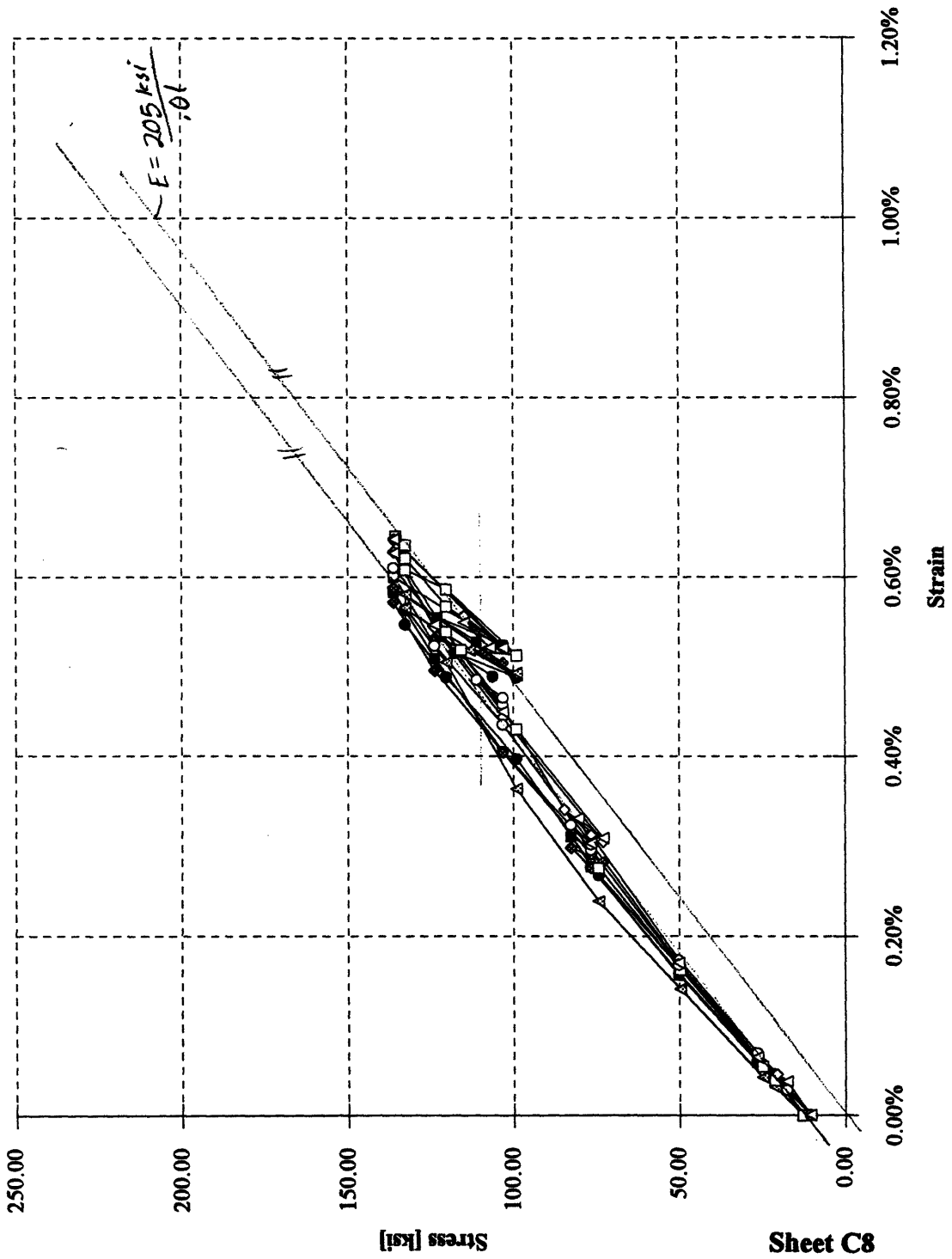


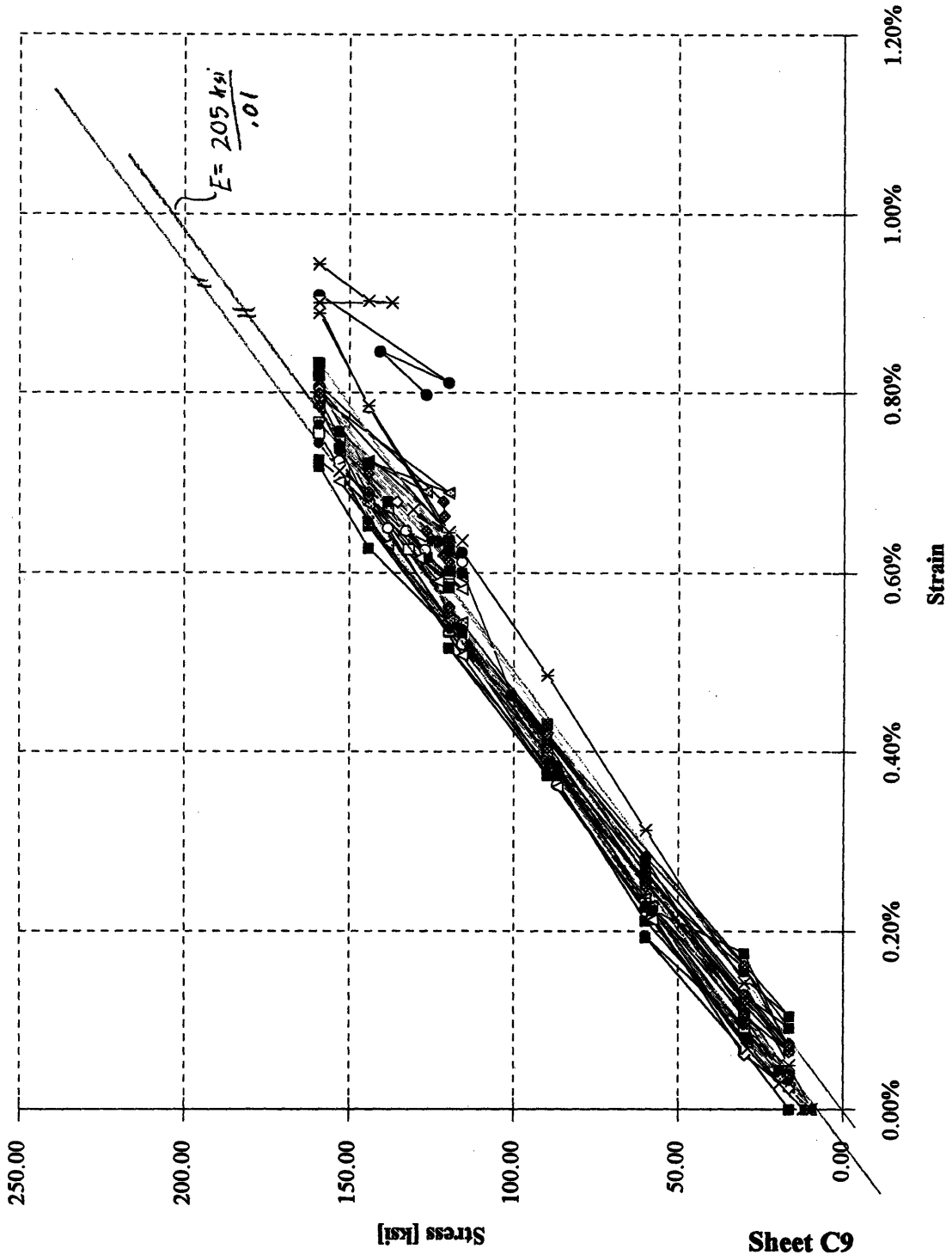




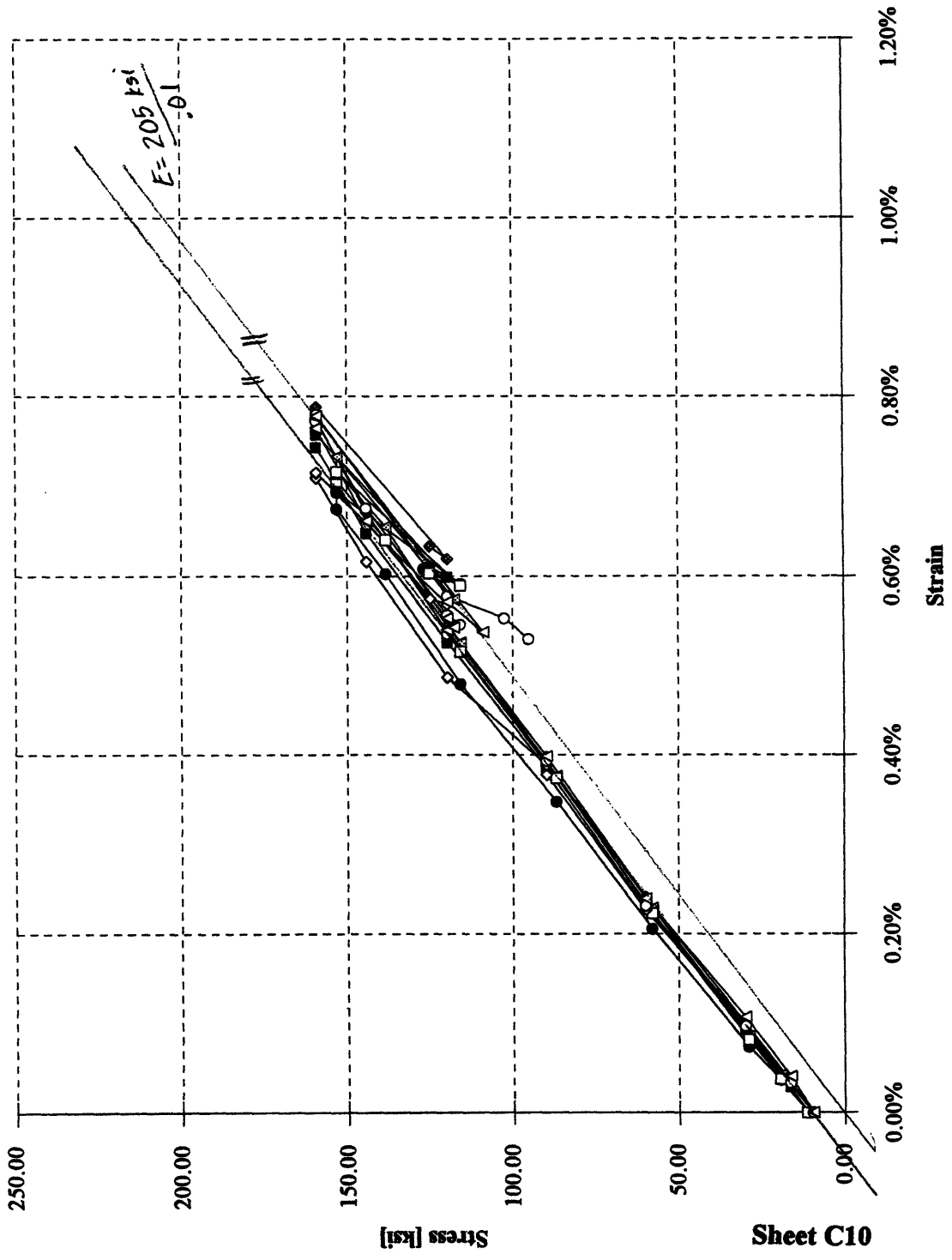
■	2-TB1
◆	2-TB2
●	2-TB3
△	2-TB4
□	2-TB5
◇	2-TB6
○	2-TB7
△	2-TB8
×	2-TB9
*	2-TB10
■	2-TB11
◆	2-TB12
●	2-TB13
△	2-TB14
■	2-TB15
●	2-TB16

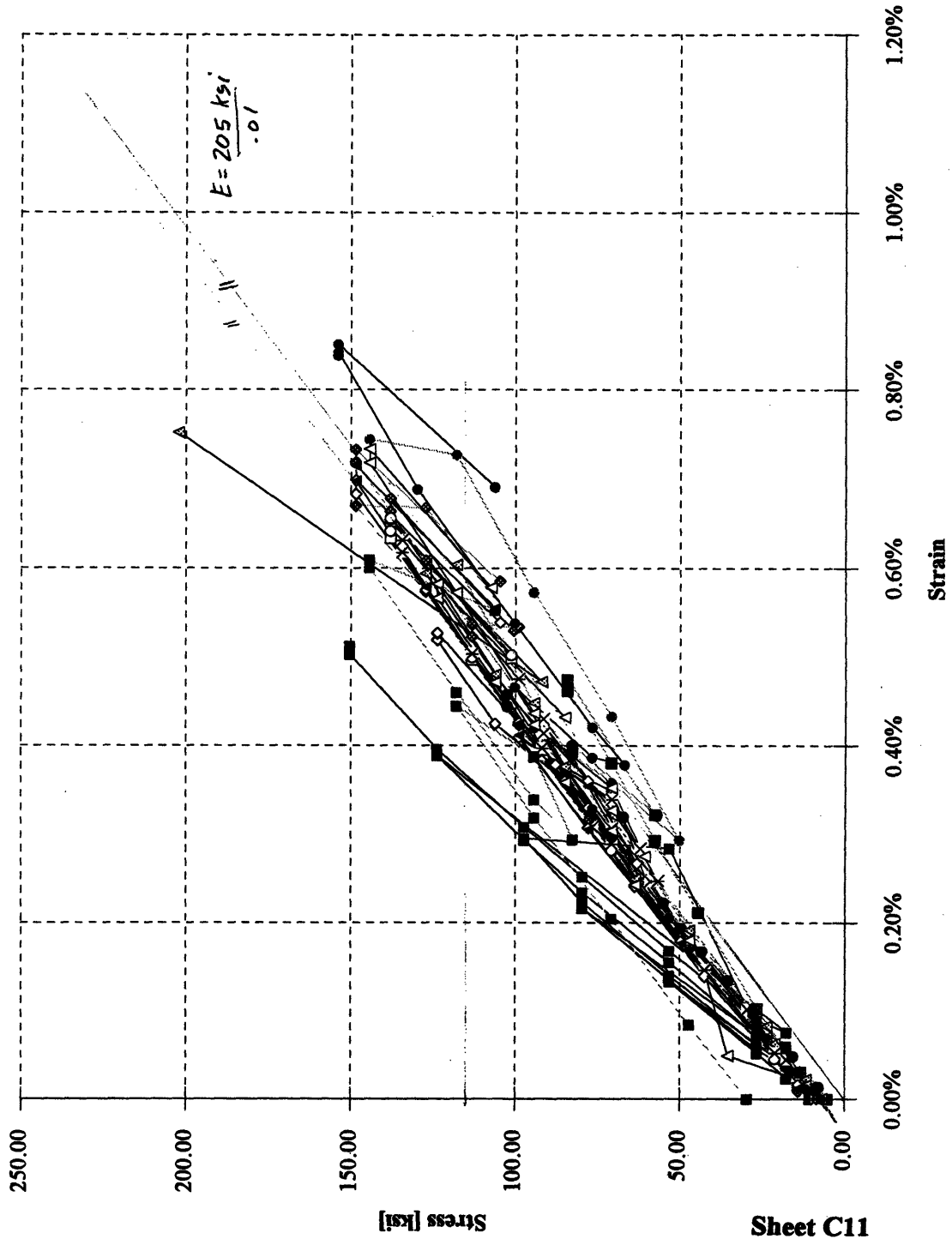
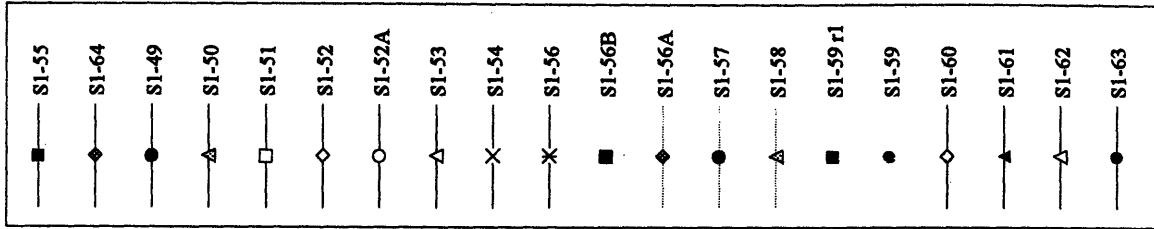
n = 16

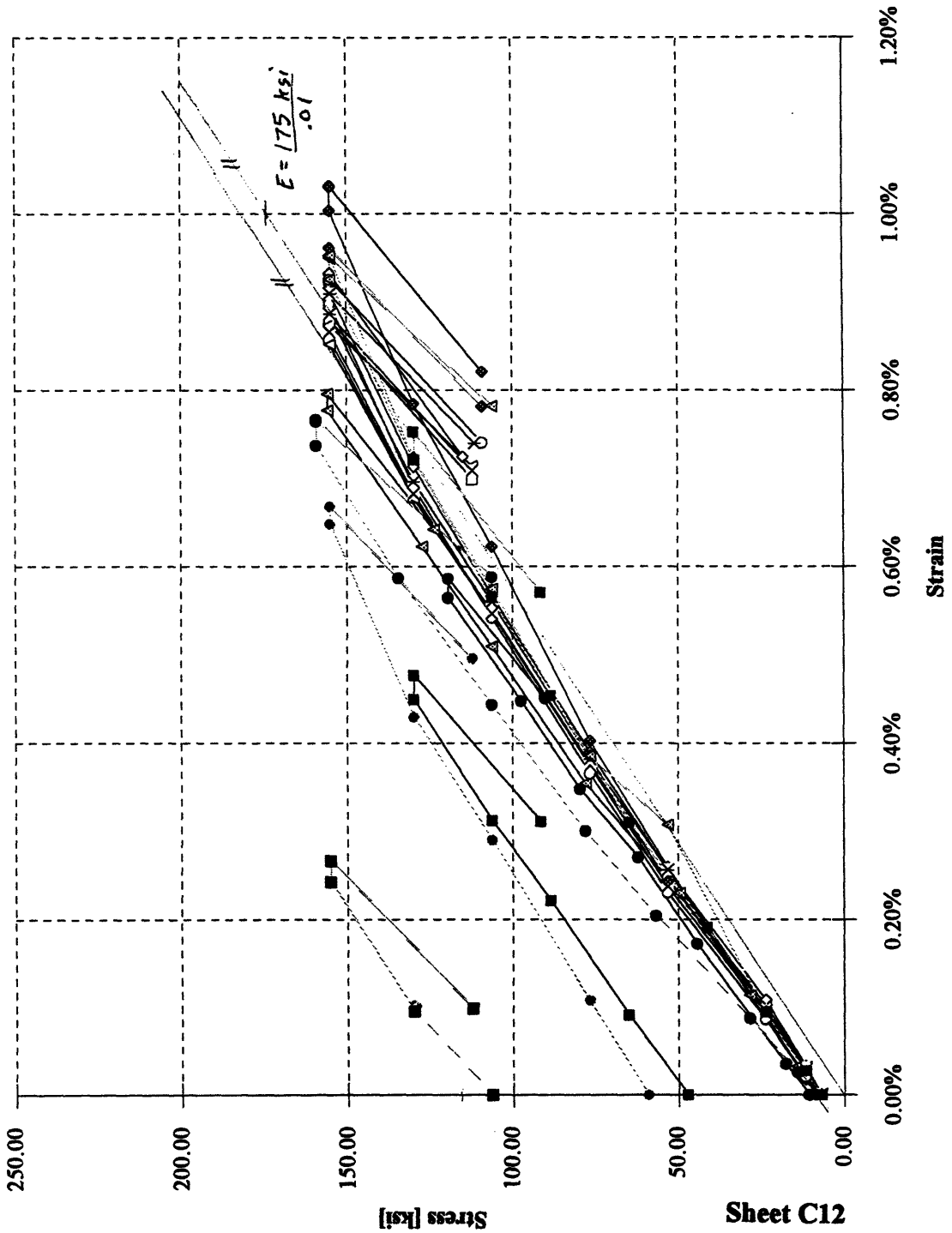




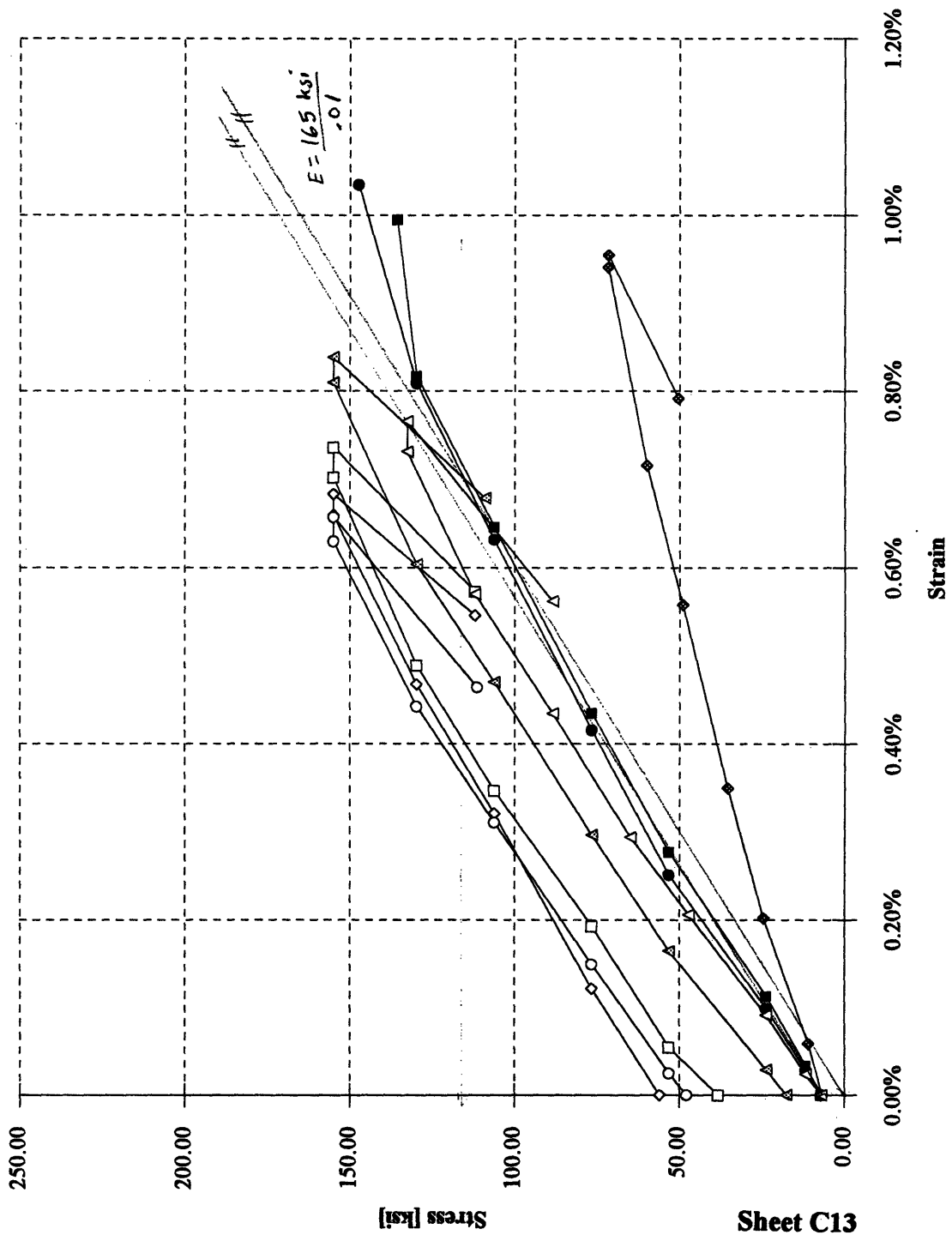
n = 16

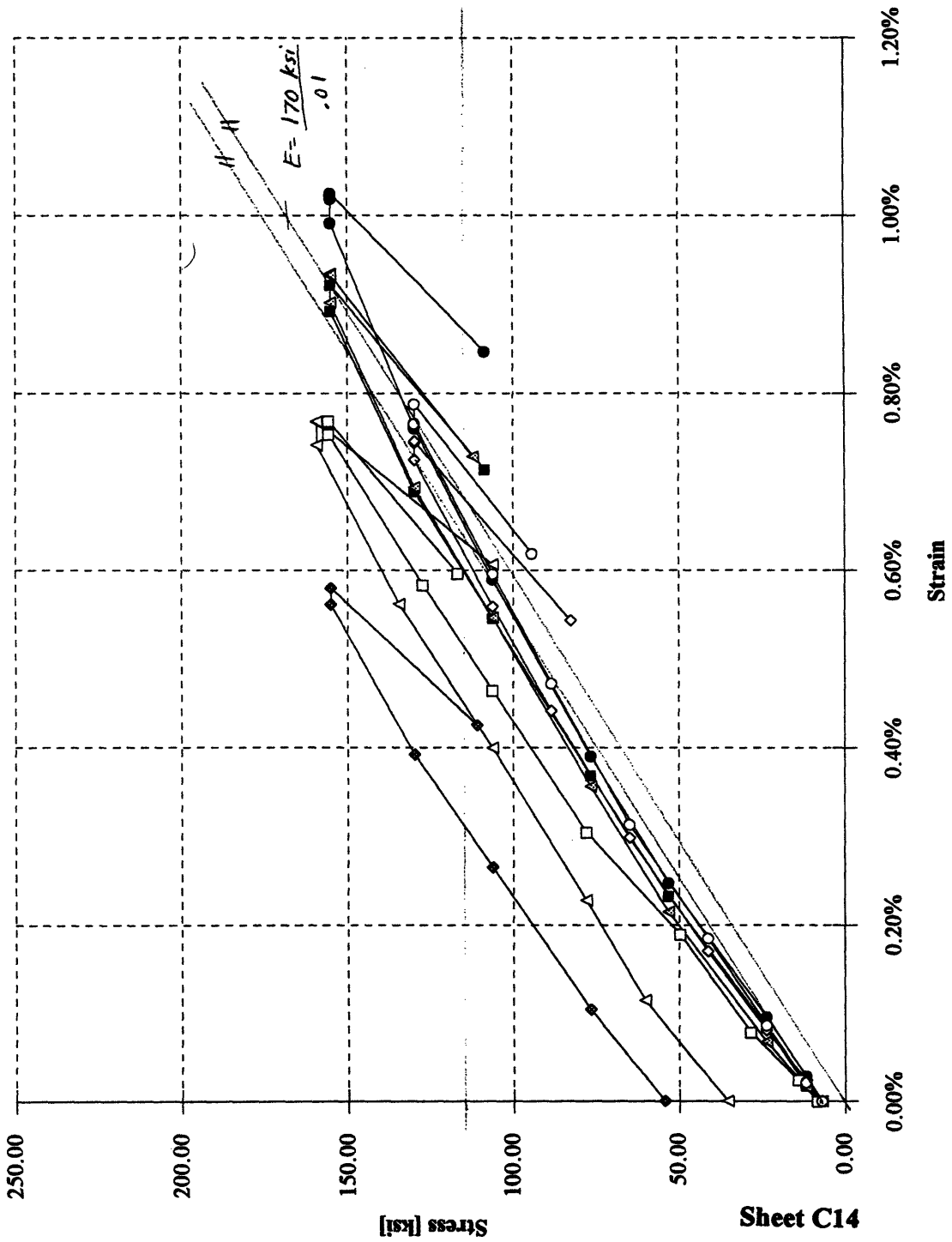


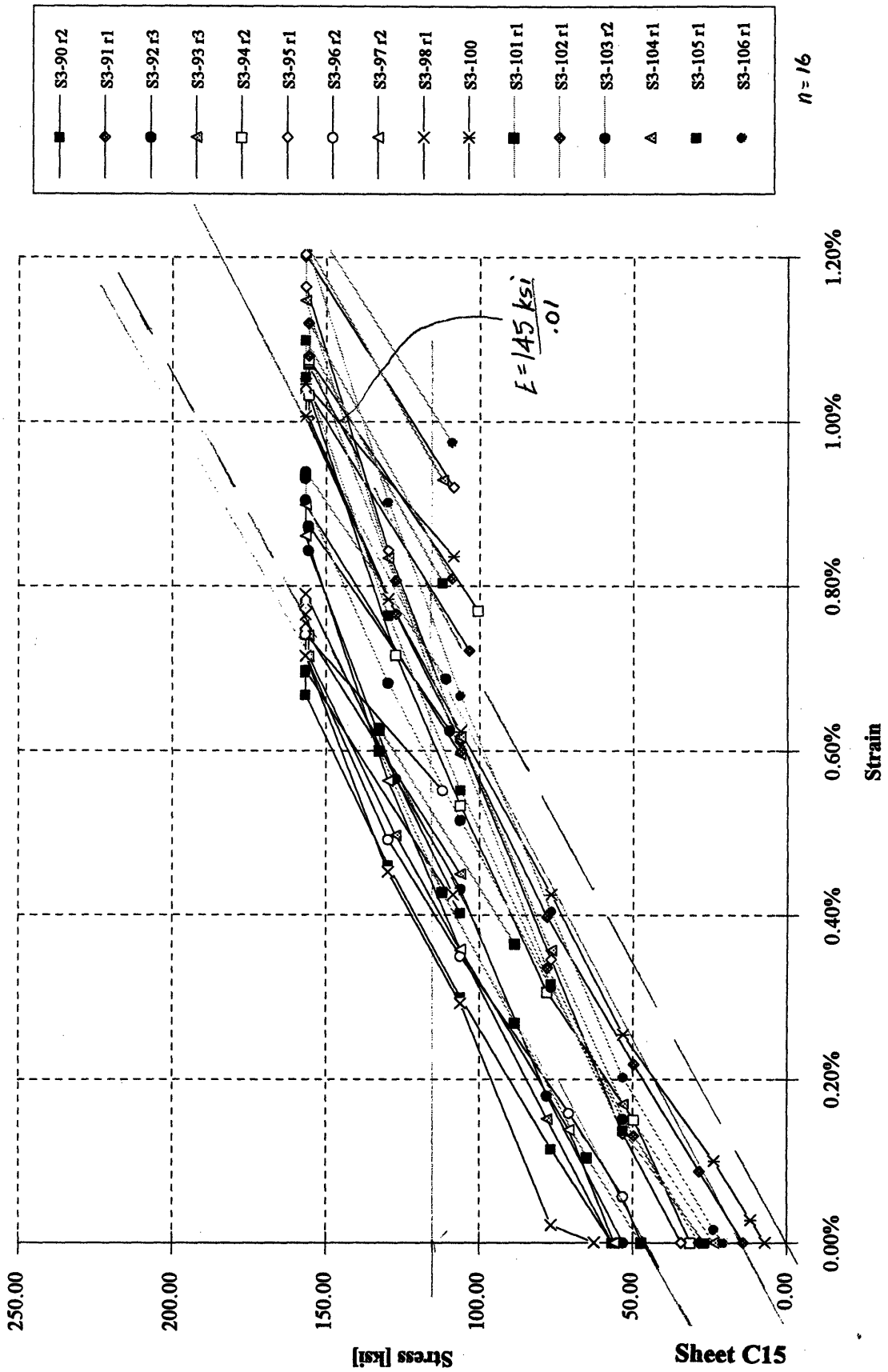


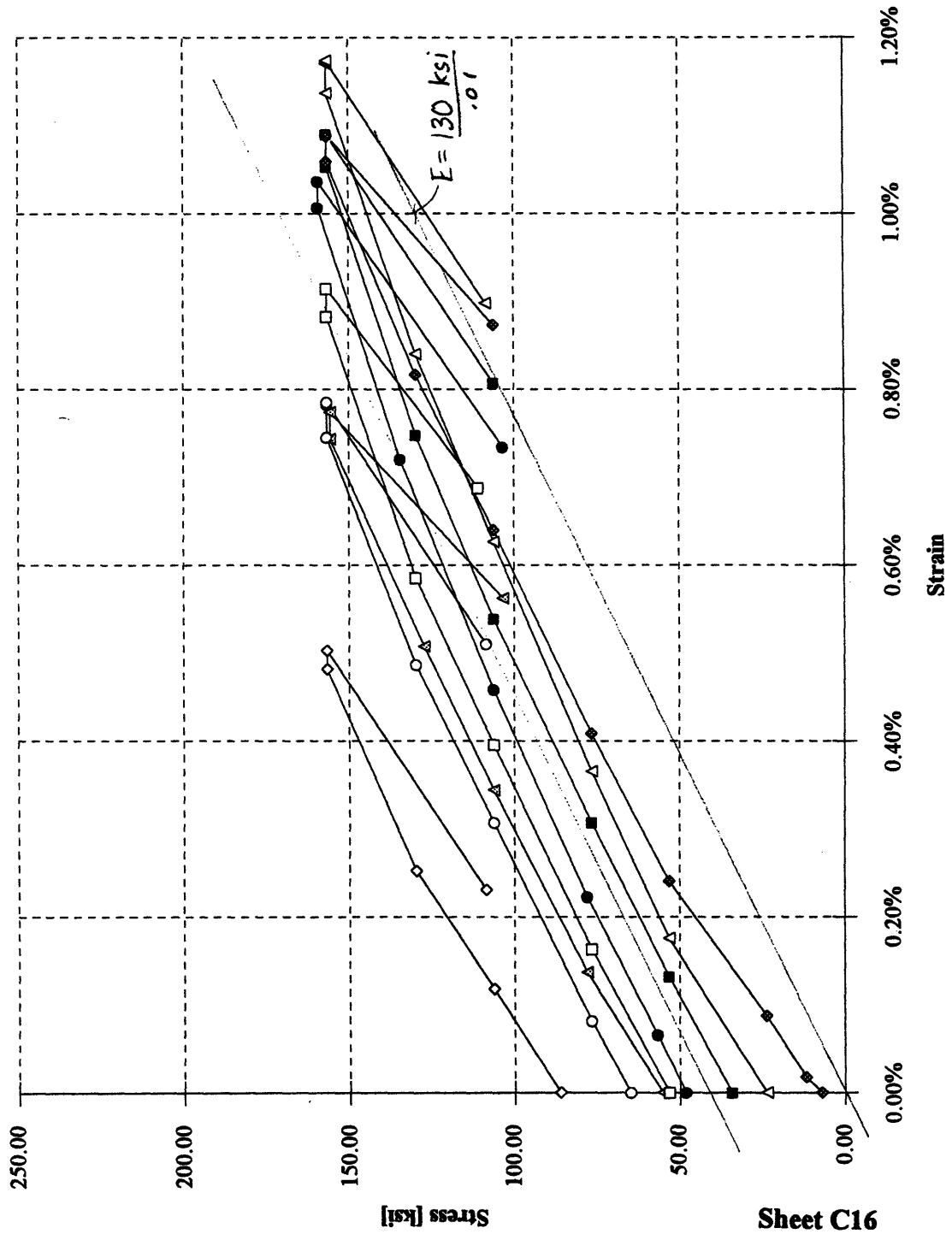


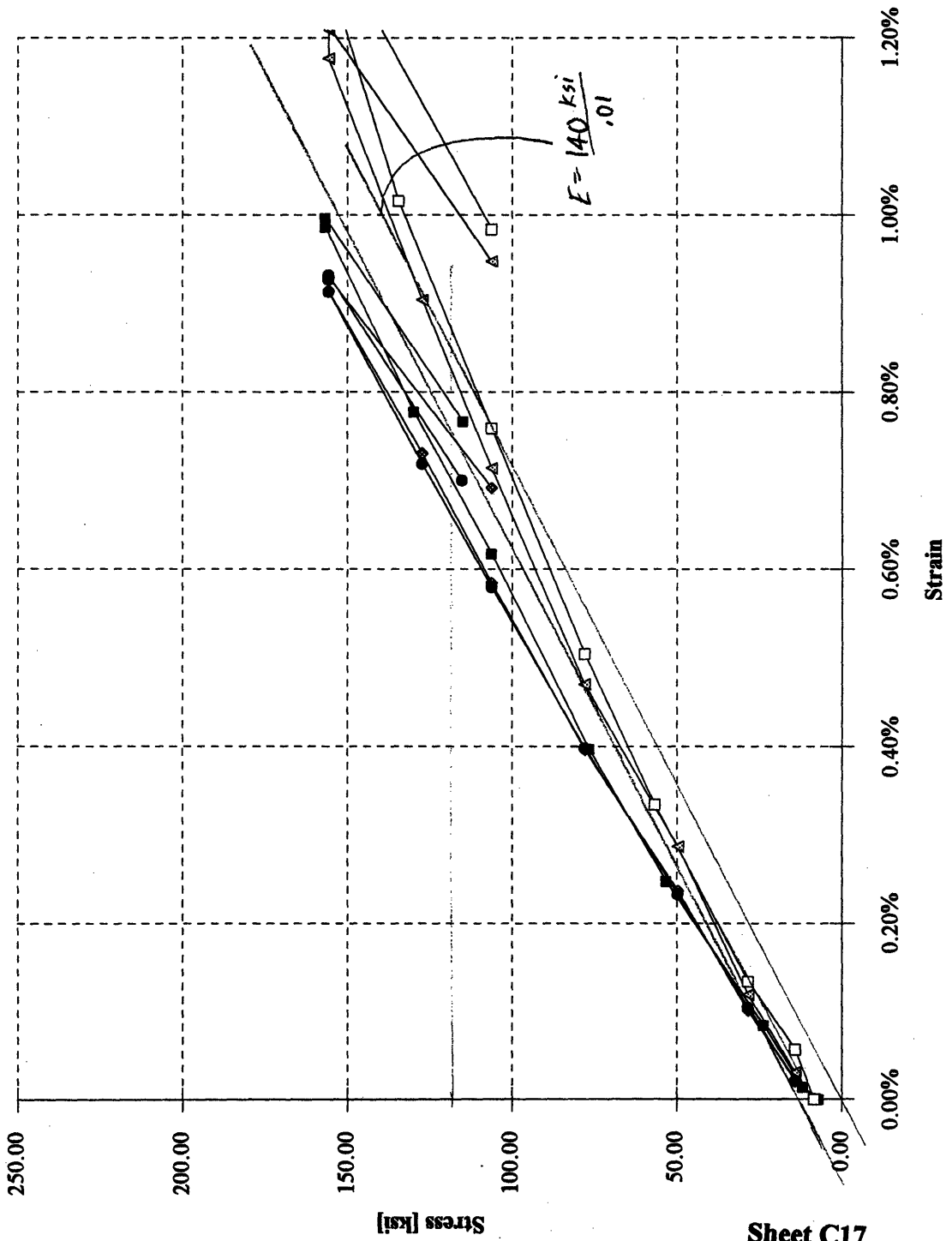
n = 16











Sheet C17

Estimates of Tieback Modulus of Elasticity

Tier #	Estimated E (ksi)		Selected Value	
	by MPW	by LCJ	(ksi)	(x10 ⁹ psf)
<i>North (Slurry) Wall</i>				
1	22,000	22,500	22,200	3.20
2	21,200	21,000	21,100	3.04
3	20,500	20,000	20,200	2.91
<i>South (Sheetpile) Wall</i>				
1	20,500	20,500	20,500	2.95
2	17,125	16,000	16,600	2.39
3	14,000	14,500	14,200	2.04

Sheet C18

APPENDIX D. Available Information on Excavation History

Sheet D1. Construction Activity Table, page 1 of 2 (from Weekly Geotechnical Summary Reports). 316

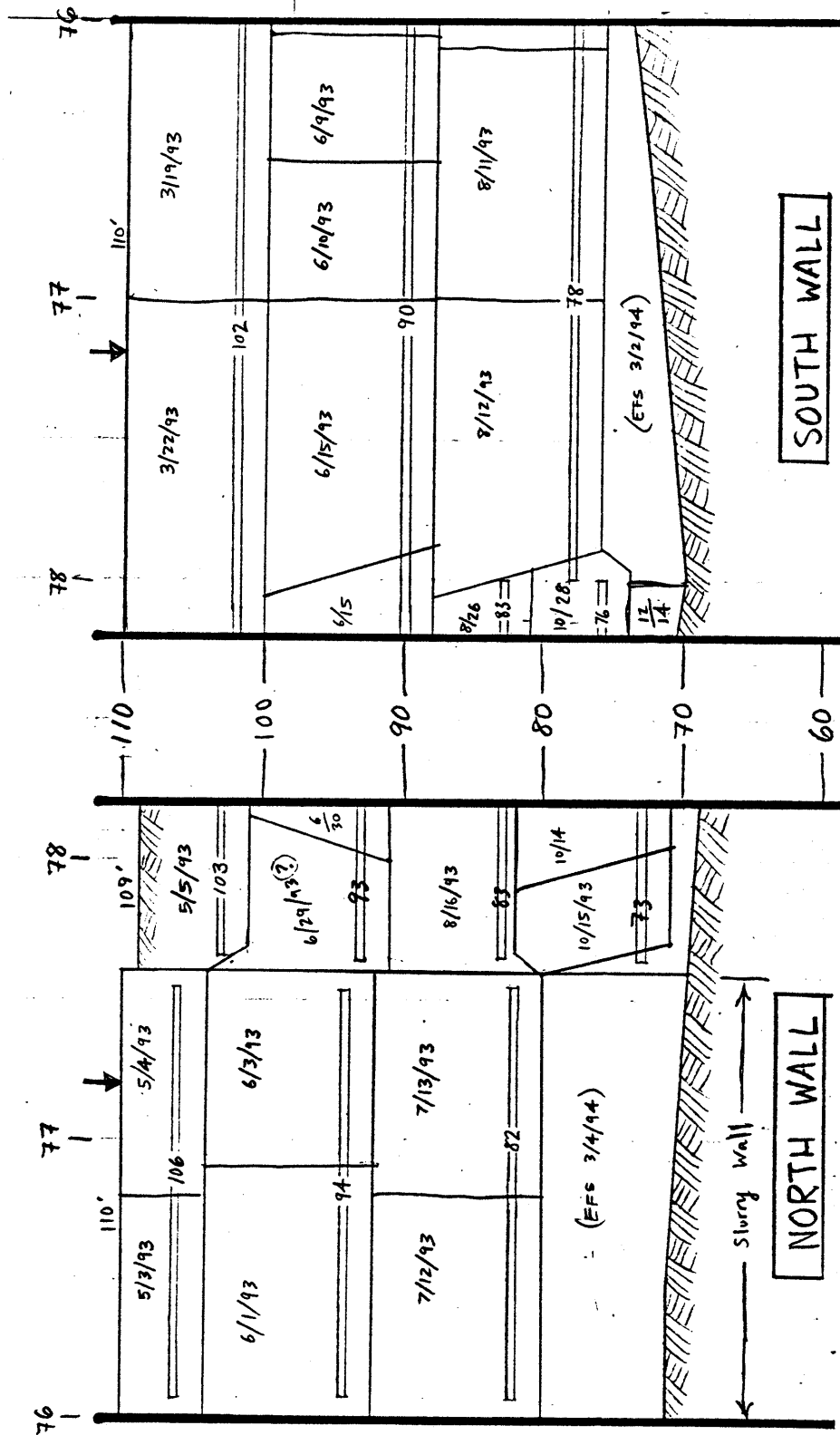
Sheet D2. Construction Activity Table, page 2 of 2..... 317

Sheet D3. Recopied Form of Large-Sheet SOE Wall Plans, provided by Contractor. 318

Sheet D4. Recopied Form of a Construction Progress Plan, showing dates of excavation of various lifts. (from Weekly Geotechnical Instrumentation Reports)..... 319

INSTRUMENT	STATION	TIER 1			TIER 2			TIER 3		
		EXCAV.	INSTALL	LOCK-OFF	EXCAV.	INSTALL	LOCK-OFF	EXCAV.	INSTALL	LOCK-OFF
IPE-103	72+50(N)	1/14/93	1/26/93	2/9/93	2/16/93	2/22/93	3/2/93	3/10/93	3/11/93	4/30/93
IPE-104	74+25(S)	1/26/93	2/17/93	3/2/93	5/10/93	5/20/93	6/9/93	6/11/93	6/21/93	7/7/93
IPE-105	74+25(N)	1/11/93	1/20/93	2/1/93	5/27/93	6/2/93	6/15/93	6/29/93	7/9/93	7/29/93
IPE-106	74+25(N)	1/11/93	1/20/93	2/1/93	5/27/93	6/2/93	6/15/93	6/29/93	7/9/93	7/29/93
IPE-107	71+00(S)	1/20/93	2/5/93	2/17/93	2/24/93	3/1/93	3/11/93	3/18/93	3/24/93	4/13/93
IPE-108	71+09(N)	1/18/93	1/28/93	2/12/93	2/18/93	2/24/93	3/5/93	3/12/93	3/18/93	4/5/93
IPE-109	73+25(S)	1/25/93	2/12/93	2/26/93	4/9/93	4/23/93	5/13/93	6/8/93	6/17/93	7/6/93
IPE-110	73+25(N)	1/12/93	1/22/93	2/22/93	2/12/93	5/25/93	6/11/93	6/28/93	7/9/93	7/28/93
IPE-111	8LDC B	7/7/93	8/16/93	9/10/93	12/17/93	1/14/94	1/20/94	1/24/94	2/4/94	2/14/94
IPE-113	77+01(S)	3/22/93	4/13/93	6/5/93	6/15/93	7/1/93	7/31/93	8/12/93	8/16/93	9/20/93
IPE-114	72+50(S)	1/22/93	2/10/93	2/12/93	2/23/93	3/3/93	3/12/93	3/24/93	3/26/93	4/14/93
IPE-115	71+00(S)	1/20/93	2/5/93	2/17/93	2/24/93	3/1/93	3/11/93	3/18/93	3/24/93	4/13/93
IPE-116	71+09(N)	1/18/93	1/28/93	2/12/93	2/18/93	2/24/93	3/5/93	3/12/93	3/18/93	4/5/93
INC-101	77+01(S)	3/22/93	4/13/93	6/5/93	6/15/93	6/30/93	7/31/93	8/12/93	8/16/93	9/20/93
INC-102	8LDC A	5/4/93	5/19/93	5/28/93	6/3/93	6/7/93	7/2/93	7/12/93	8/5/93	8/20/93
INC-103	81+94(S)	7/6/93	7/30/93	8/23/93	8/27/93	9/3/93	9/29/93	10/29/93	11/9/93	11/22/93
INC-104	8LDC B	7/7/93	8/12/93	9/10/93	9/24/93	10/1/93	10/25/93	10/26/93	2/3/94	2/16/94
INC-105	8LDC D	8/18/93	9/15/93	10/8/93	10/19/93	11/2/93	11/16/93	12/2/93	12/20/93	1/7/94
INC-109	71+70(S)	1/21/93	2/8/93	2/17/93	2/23/93	3/3/93	3/12/93	3/23/93	3/26/93	4/14/93
INC-110	78+31(S)	3/22/93	4/21/93	6/7/93	6/15/93	7/7/93	8/24/93	8/26/93	8/31/93	10/1/93
INC-111	78+65(N)	5/5/93	5/28/93	6/18/93	6/30/93	7/16/93	8/16/93	8/17/93	8/20/93	10/7/93
INC-112	79+99(S)	6/22/93	8/4/93	8/24/93	8/27/93	9/8/93	9/23/93	9/27/93	10/27/93	11/8/93
INC-113	80+55(N)	6/22/93	7/19/93	8/16/93	8/20/93	8/26/93	9/11/93	9/22/93	9/28/93	10/19/93
INC-114	82+98(S)	7/6/93	7/26/93	9/7/93	9/17/93	9/21/93	10/13/93	10/23/93	11/12/93	11/24/93
INC-115	83+52(S)	8/19/93	8/20/93	9/8/93	9/20/93	9/23/93	10/18/93	10/23/93	11/15/93	11/24/93
INC-116	84+48(N)	7/7/93	7/28/93	12/6/93	12/9/93	12/15/93	12/27/93	1/7/94	1/13/94	1/31/94
INC-117	86+22(N)	8/25/93	8/30/93	9/7/93	10/15/93	10/20/93	11/2/93	11/8/93	11/22/93	12/7/93
INC-118	87+30(N)	5/4/93	5/6/93	6/1/93	6/14/93	6/28/93	7/13/93	11/9/93	11/29/93	12/14/93
INC-119	88+59(S)	5/7/93	5/18/93	6/2/93	9/9/93	9/29/93	11/19/93	4/12/94	4/22/94	5/6/94
INC-120	88+76(N)	5/4/93	6/1/93	7/13/93	9/9/93	10/1/93	10/28/93	3/29/94	4/8/94	4/21/94
INC-121	89+55(S)	9/9/93	10/5/93	10/25/93	5/9/94	5/10/94	5/23/94	5/31/94	6/2/94	6/13/94
INC-122	89+93(N)	3/7/94	3/15/94	4/8/94	4/11/94	4/14/94	5/2/94	5/4/94	5/9/94	5/20/94
INC-502	72+50(N)	1/14/93	1/26/93	2/9/93	2/16/93	2/22/93	3/2/93	3/10/93	3/11/93	4/30/93

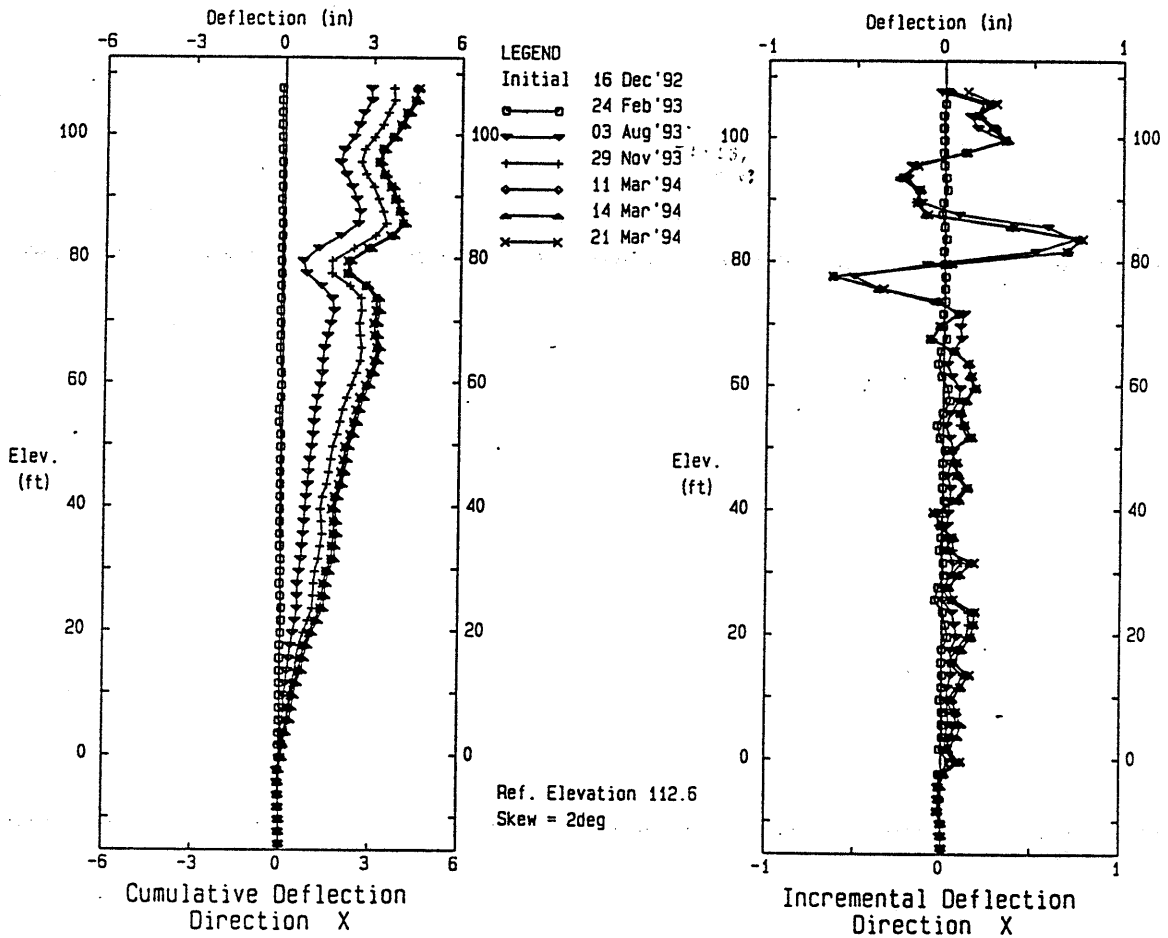
INSTRUMENT	STATION	TIER 4			TIER 5			FINAL SUBGRADE	
		EXCAV.	INSTALL	LOCK-OFF	EXCAV.	INSTALL	LOCK-OFF	EXCAV.	POUR INV.
PE-103	72+50(N)	N/A	N/A	N/A	N/A	N/A	N/A	8/9/93	3/24/94
PE-104	74+25(S)	N/A	N/A	N/A	N/A	N/A	N/A	1/4/94	4/6/94
PE-105	74+25(N)	N/A	N/A	N/A	N/A	N/A	N/A	1/3/94	3/22/94
PE-106	74+25(N)	N/A	N/A	N/A	N/A	N/A	N/A	1/3/94	3/22/94
PE-107	71+00(S)	N/A	N/A	N/A	N/A	N/A	N/A	4/27/93	6/4/93
PE-108	71+09(N)	N/A	N/A	N/A	N/A	N/A	N/A	6/24/93	8/6/93
PE-109	73+25(S)	N/A	N/A	N/A	N/A	N/A	N/A	8/9/93	2/16/94
PE-110	73+25(N)	N/A	N/A	N/A	N/A	N/A	N/A	9/8/93	1/29/94
PE-111	BLOC B	2/16/94	2/22/94	3/9/94	N/A	N/A	N/A	3/22/94	
PE-113	77+01(S)	N/A	N/A	N/A	N/A	N/A	N/A	3/2/94	
PE-114	72+50(S)	N/A	N/A	N/A	N/A	N/A	N/A	6/9/93	7/23/93
PE-115	71+00(S)	N/A	N/A	N/A	N/A	N/A	N/A	4/27/93	6/4/93
PE-116	71+09(N)	N/A	N/A	N/A	N/A	N/A	N/A	6/24/93	8/6/93
INC-101	77+01(S)	N/A	N/A	N/A	N/A	N/A	N/A	3/2/94	
INC-102	BLOC A	N/A	N/A	N/A	N/A	N/A	N/A	3/4/94	
INC-103	81+94(S)	12/13/93	1/4/94	2/1/94	N/A	N/A	N/A	3/17/94	
INC-104	BLOC B	2/17/94	2/28/94	3/12/94	N/A	N/A	N/A	3/16/94	
INC-105	BLOC D	1/11/94	2/17/94	3/17/94	N/A	N/A	N/A	4/3/94	
INC-109	71+70(S)	N/A	N/A	N/A	N/A	N/A	N/A	6/4/93	6/21/93
INC-110	78+31(S)	10/28/93	11/16/93	1/12/94	N/A	N/A	N/A	4/21/94	
INC-111	78+65(N)	10/14/93	10/20/93	11/9/93	N/A	N/A	N/A	4/21/94	
INC-112	79+99(S)	11/16/93	11/22/93	12/6/93	N/A	N/A	N/A	4/29/94	
INC-113	80+55(N)	10/21/93	11/2/93	11/12/93	12/9/93	12/17/93	1/25/94	4/14/94	
INC-114	82+98(S)	12/23/93	1/7/94	3/24/94	N/A	N/A	N/A	3/24/94	
INC-115	83+52(S)	12/27/93	1/11/94	3/15/94	N/A	N/A	N/A	3/24/94	
INC-116	84+48(N)	2/1/94	2/10/94	2/25/94	2/28/94	3/9/94	3/30/94	4/1/94	
INC-117	86+22(N)	1/8/94	1/18/94	2/18/94	2/28/94	3/17/94	4/8/94	4/21/94	
INC-118	87+30(N)	1/10/94	1/21/94	2/17/94	2/19/94	3/17/94	4/20/94	4/21/94	
INC-119	88+59(S)								
INC-120	88+76(N)	?	5/5/94						
INC-121	89+55(S)								
INC-122	89+93(N)								
INC-502	72+50(N)	N/A	N/A	N/A	N/A	N/A	N/A	8/9/93	3/24/94



Sheet D3

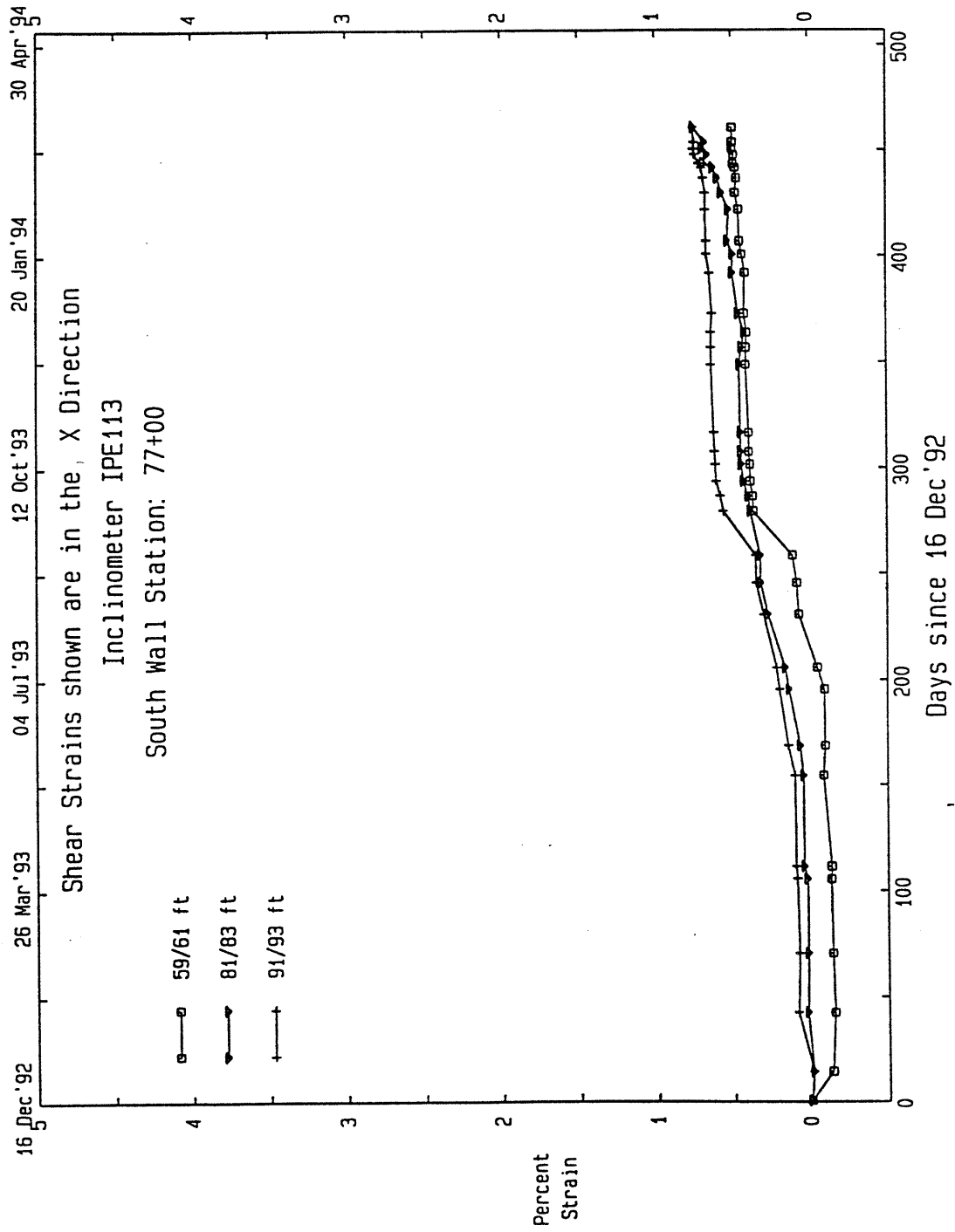
APPENDIX E. Data Plots Provided by Contractor

Sheet E1. <i>Inclinometer</i>: Deflection vs. Depth, from GTILT.....	322
Sheet E2. <i>Inclinometer</i>: Shear Strain vs. Time, from GTILT	323
Sheet E3. <i>DMP</i>:Settlement vs. Time.....	324
Sheet E4. <i>MPHG</i>:Settlement / Heave vs. Depth.....	325
Sheet E5. <i>IPE</i>:Settlement / Heave vs. Depth.....	326
Sheet E6. <i>Observation Well</i>:Tabulated Data.....	327
Sheet E7. <i>Observation Well</i>: Graph of Data vs. Time	328
Sheet E8. <i>VWPZ</i>:Tabulated Data.....	329
Sheet E9. <i>VWPZ</i>: Graph of Data vs. Time	330



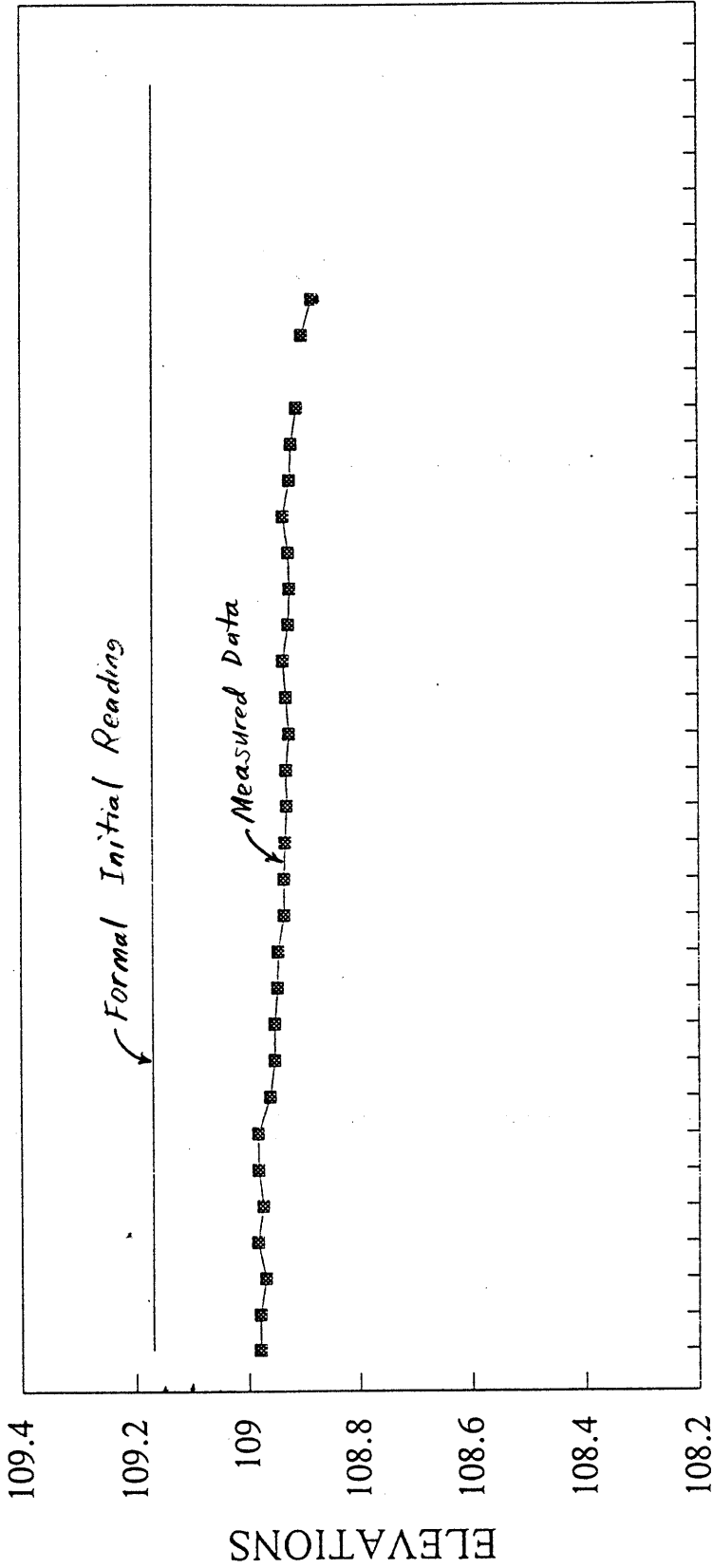
Inclinometer IPE113
South Wall Station: 77+00

Sheet E1



Sheet E2

DMP4-118



8/17 8/31 9/15 9/28 10/12 10/26 11/9 11/23 12/7 12/20 1/7 1/21 2/9 2/25 3/11
 8/27 9/8 9/21 10/5 10/19 11/2 11/16 11/30 12/13 12/28 1/12 1/28 2/17 3/4 3/16
 DATE

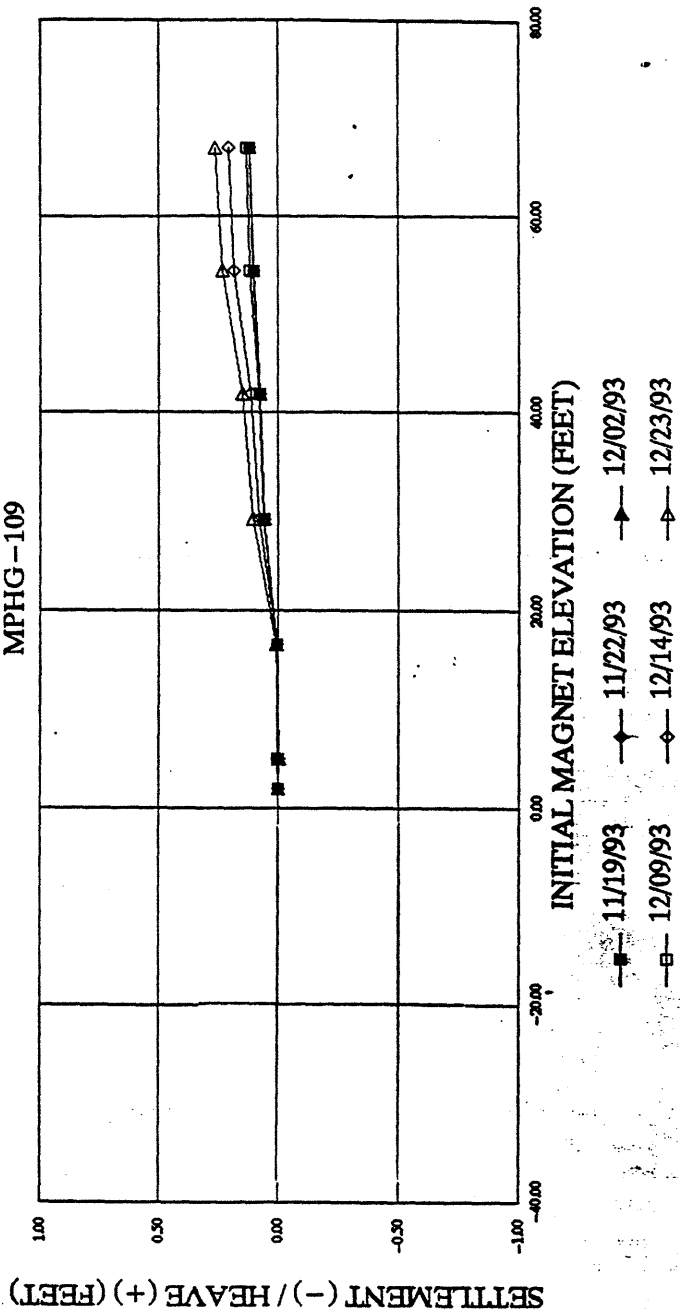
—■— ELEVATION — F.I.R.

SPIDER MAGNET DATA SUMMARY
INST NO: MPHG-109

MAGNET NUMBER	DATE	INITIAL MAGNET ELEV (FEET)	09/30/93		10/07/93		10/10/93		10/21/93		10/26/93		11/04/93		11/11/93		11/19/93		11/22/93		12/02/93		12/09/93		12/14/93		12/23/93		
			CHANGE FROM INITIAL (FEET)	INITIAL (FEET)	CHANGE FROM INITIAL (FEET)	INITIAL (FEET)	CHANGE FROM INITIAL (FEET)	INITIAL (FEET)	CHANGE FROM INITIAL (FEET)	INITIAL (FEET)	CHANGE FROM INITIAL (FEET)	INITIAL (FEET)	CHANGE FROM INITIAL (FEET)	INITIAL (FEET)	CHANGE FROM INITIAL (FEET)	INITIAL (FEET)	CHANGE FROM INITIAL (FEET)	INITIAL (FEET)	CHANGE FROM INITIAL (FEET)	INITIAL (FEET)	CHANGE FROM INITIAL (FEET)	INITIAL (FEET)	CHANGE FROM INITIAL (FEET)	INITIAL (FEET)	CHANGE FROM INITIAL (FEET)	INITIAL (FEET)	CHANGE FROM INITIAL (FEET)	INITIAL (FEET)	
1		2.01	0.00	2.01	0.00	2.01	0.00	2.01	0.00	2.01	0.00	2.01	0.00	2.01	0.00	2.01	0.00	2.01	0.00	2.01	0.00	2.01	0.00	2.01	0.00	2.01	0.00	2.01	0.00
2		5.02	-0.00	5.02	-0.00	5.02	-0.00	5.02	-0.00	5.02	-0.00	5.02	-0.00	5.02	-0.00	5.02	-0.00	5.02	-0.00	5.02	-0.00	5.02	-0.00	5.02	-0.00	5.02	-0.00	5.02	-0.00
3		18.51	0.00	18.51	0.00	18.51	0.00	18.51	0.00	18.51	0.00	18.51	0.00	18.51	0.00	18.51	0.00	18.51	0.00	18.51	0.00	18.51	0.00	18.51	0.00	18.51	0.00	18.51	0.00
4		29.17	0.06	29.23	0.06	29.23	0.06	29.23	0.06	29.23	0.06	29.23	0.06	29.23	0.06	29.23	0.06	29.23	0.06	29.23	0.06	29.23	0.06	29.23	0.06	29.23	0.06	29.23	0.06
5		41.78	0.08	41.86	0.08	41.86	0.08	41.86	0.08	41.86	0.08	41.86	0.08	41.86	0.08	41.86	0.08	41.86	0.08	41.86	0.08	41.86	0.08	41.86	0.08	41.86	0.08	41.86	0.08
6		54.95	0.10	55.05	0.10	55.05	0.10	55.05	0.10	55.05	0.10	55.05	0.10	55.05	0.10	55.05	0.10	55.05	0.10	55.05	0.10	55.05	0.10	55.05	0.10	55.05	0.10	55.05	0.10
7		68.92	0.11	69.03	0.11	69.03	0.11	69.03	0.11	69.03	0.11	69.03	0.11	69.03	0.11	69.03	0.11	69.03	0.11	69.03	0.11	69.03	0.11	69.03	0.11	69.03	0.11	69.03	0.11

HEAVE/SETTLEMENT PROFILE

MPHG-109

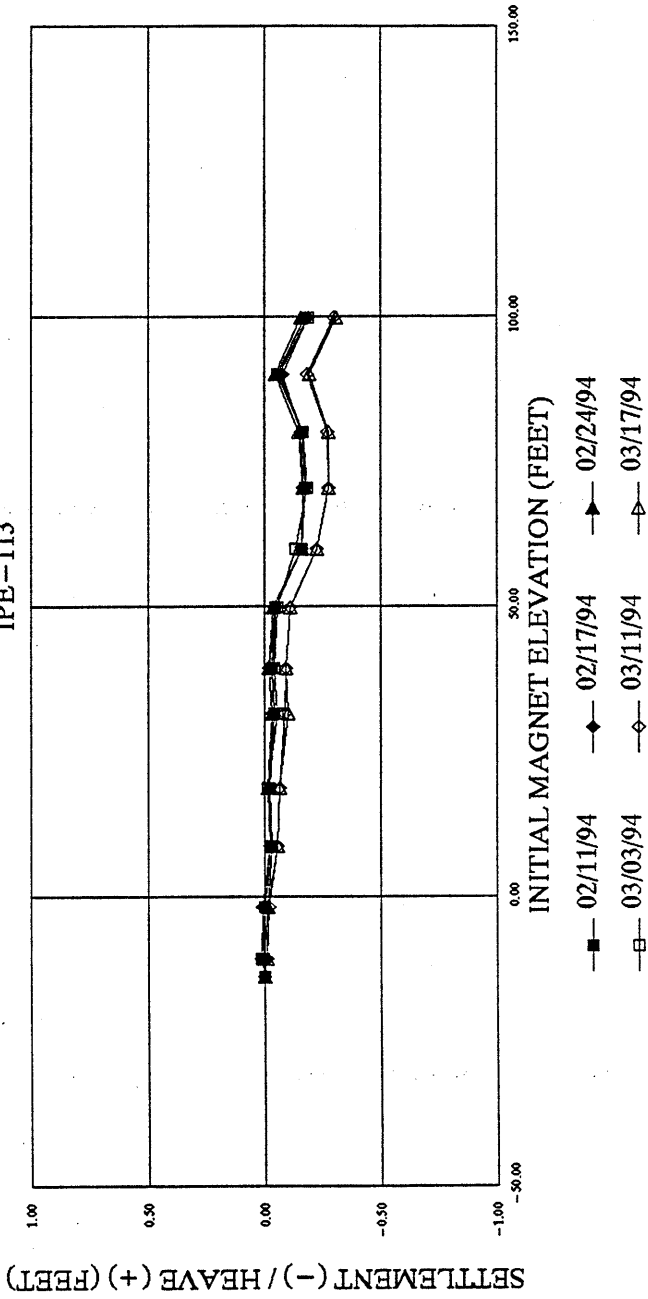


SPIDER MAGNET DATA SUMMARY
INST NO: IPE-113

MAGNET NUMBER	INITIAL MAGNET ELEV (FEET)	12/29/93		12/29/93		01/05/94		01/13/94		01/20/94		01/27/94		02/03/94		02/11/94		02/17/94		02/24/94		03/03/94		03/11/94		03/17/94	
		CHANGE FROM INITIAL (FEET)	INITIAL (FEET)	CHANGE FROM INITIAL (FEET)	INITIAL (FEET)	CHANGE FROM INITIAL (FEET)	INITIAL (FEET)	CHANGE FROM INITIAL (FEET)	INITIAL (FEET)	CHANGE FROM INITIAL (FEET)	INITIAL (FEET)	CHANGE FROM INITIAL (FEET)	INITIAL (FEET)	CHANGE FROM INITIAL (FEET)	INITIAL (FEET)	CHANGE FROM INITIAL (FEET)	INITIAL (FEET)	CHANGE FROM INITIAL (FEET)	INITIAL (FEET)	CHANGE FROM INITIAL (FEET)	INITIAL (FEET)	CHANGE FROM INITIAL (FEET)	INITIAL (FEET)	CHANGE FROM INITIAL (FEET)	INITIAL (FEET)	CHANGE FROM INITIAL (FEET)	INITIAL (FEET)
1	-13.68	0.00	0.00	0.00	0.00	0.00	0.00	0.00	0.00	0.00	0.00	0.00	0.00	0.00	0.00	0.00	0.00	0.00	0.00	0.00	0.00	0.00	0.00	0.00	0.00	0.00	0.00
2	-10.69	-0.03	0.01	-0.01	0.00	-0.02	0.01	-0.01	0.00	-0.02	0.01	-0.01	0.00	-0.01	0.00	-0.01	0.00	-0.01	0.01	-0.01	0.00	-0.01	0.00	-0.01	0.00	-0.01	0.00
3	-1.74	-0.04	0.01	-0.01	-0.00	-0.02	0.01	-0.01	-0.01	-0.02	0.01	-0.01	-0.00	-0.01	0.00	-0.01	0.00	-0.01	0.01	-0.01	0.00	-0.01	0.00	-0.01	0.00	-0.01	0.00
4	8.84	-0.07	0.00	-0.02	-0.04	-0.02	-0.02	-0.01	-0.01	-0.02	-0.01	-0.01	-0.01	-0.01	-0.01	-0.01	-0.01	-0.01	-0.01	-0.01	-0.01	-0.01	-0.01	-0.01	-0.01	-0.01	-0.01
5	18.87	-0.05	0.01	-0.02	-0.04	-0.02	-0.02	-0.01	-0.01	-0.02	-0.01	-0.01	-0.01	-0.01	-0.01	-0.01	-0.01	-0.01	-0.01	-0.01	-0.01	-0.01	-0.01	-0.01	-0.01	-0.01	-0.01
6	31.51	-0.05	0.00	-0.02	-0.03	-0.02	-0.02	-0.01	-0.01	-0.02	-0.01	-0.01	-0.01	-0.01	-0.01	-0.01	-0.01	-0.01	-0.01	-0.01	-0.01	-0.01	-0.01	-0.01	-0.01	-0.01	-0.01
7	39.37	-0.05	0.00	-0.02	-0.03	-0.02	-0.02	-0.01	-0.01	-0.02	-0.01	-0.01	-0.01	-0.01	-0.01	-0.01	-0.01	-0.01	-0.01	-0.01	-0.01	-0.01	-0.01	-0.01	-0.01	-0.01	-0.01
8	49.84	-0.05	0.00	-0.02	-0.04	-0.02	-0.02	-0.01	-0.01	-0.02	-0.01	-0.01	-0.01	-0.01	-0.01	-0.01	-0.01	-0.01	-0.01	-0.01	-0.01	-0.01	-0.01	-0.01	-0.01	-0.01	-0.01
9	58.68	-0.15	-0.08	-0.11	-0.11	-0.11	-0.11	-0.11	-0.11	-0.11	-0.11	-0.11	-0.11	-0.11	-0.11	-0.11	-0.11	-0.11	-0.11	-0.11	-0.11	-0.11	-0.11	-0.11	-0.11	-0.11	-0.11
10	70.26	-0.16	-0.13	-0.15	-0.15	-0.15	-0.15	-0.15	-0.15	-0.15	-0.15	-0.15	-0.15	-0.15	-0.15	-0.15	-0.15	-0.15	-0.15	-0.15	-0.15	-0.15	-0.15	-0.15	-0.15	-0.15	-0.15
11	79.91	-0.13	-0.09	-0.12	-0.12	-0.12	-0.12	-0.12	-0.12	-0.12	-0.12	-0.12	-0.12	-0.12	-0.12	-0.12	-0.12	-0.12	-0.12	-0.12	-0.12	-0.12	-0.12	-0.12	-0.12	-0.12	-0.12
12	90.03	-0.03	-0.01	-0.03	-0.03	-0.03	-0.03	-0.03	-0.03	-0.03	-0.03	-0.03	-0.03	-0.03	-0.03	-0.03	-0.03	-0.03	-0.03	-0.03	-0.03	-0.03	-0.03	-0.03	-0.03	-0.03	-0.03
13	99.84	-0.14	-0.11	-0.14	-0.14	-0.14	-0.14	-0.14	-0.14	-0.14	-0.14	-0.14	-0.14	-0.14	-0.14	-0.14	-0.14	-0.14	-0.14	-0.14	-0.14	-0.14	-0.14	-0.14	-0.14	-0.14	-0.14

HEAVE/SETTLEMENT PROFILE

IPE-113



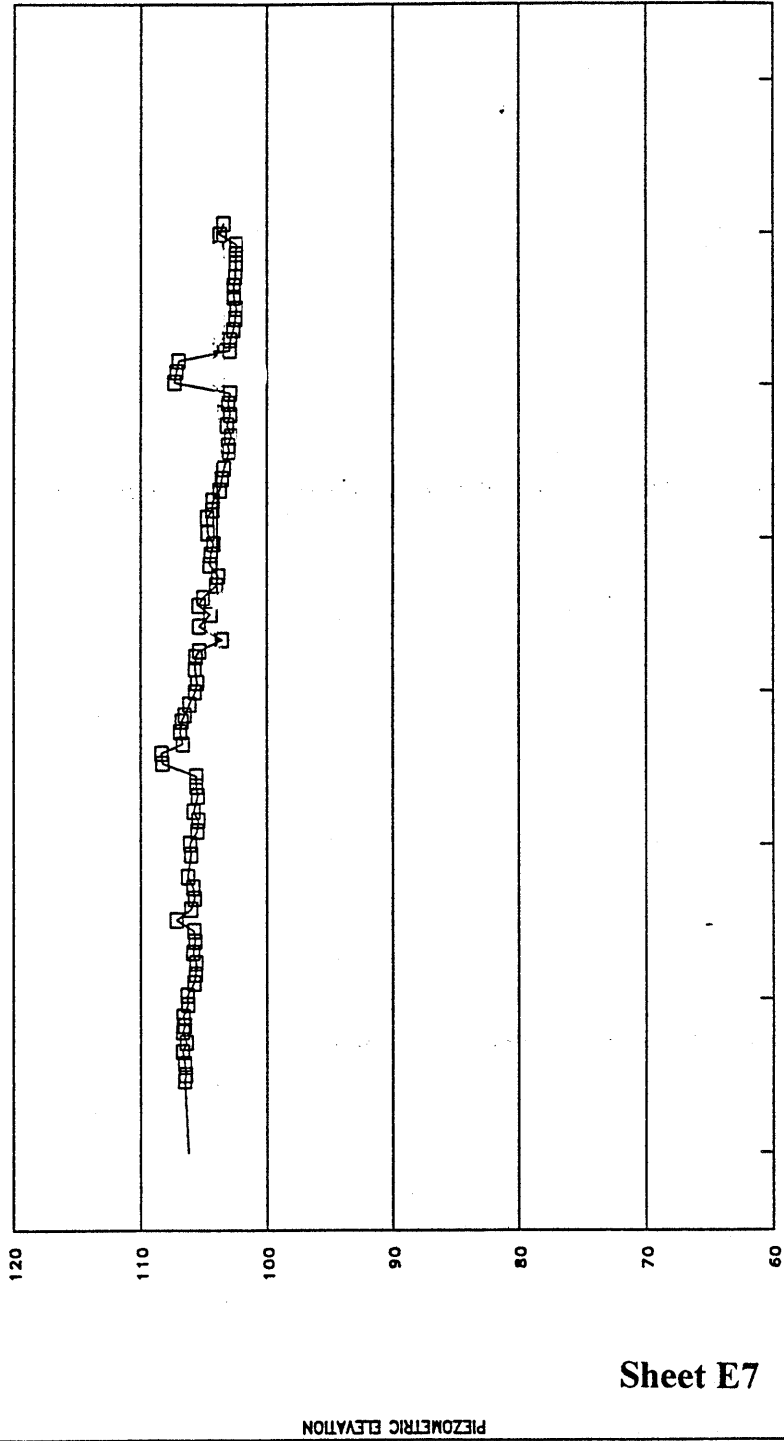
Sheet E5

TABLE FOR OPEN STAND PIPE PIEZOMETERS						
Project: Boston, Massachusetts				FILE NO. 12974		
GENERAL PIEZOMETER INFORMATION			FIELD DATA		INITIAL PIEZOMETER VALUES	
Instrument No.	OW-016		Top of SP Elev (ft)	108.4	Installation:	
Loc. Coords. N	2951834		RESPONSE VALUES		Date	09/04/91
E	780773		Threshold		Time	14:52
Station / Offset	77+40.0/115.0 R		Limiting		Zero Read	3.60
GENERAL			GROUND WATER DATA		PERSONNEL/REMARKS	
Date	Time	Elapsed Days	Depth to Water Below Ref. Point (ft)	Ground Water Elevation (ft)	Read By (init)	Remarks
09/23/91	10:52	19	3.10	106.30	H&A	
10/22/91	07:59	48	3.30	106.10	H&A	
09/04/92	10:30	274	3.40	106.00	H&A	
09/31/92	10:45	362	2.85	106.55	BWR	
09/04/92	07:15	366	2.97	106.43	BWR	
09/11/92	15:50	373	2.88	106.52	BWR	
09/19/92	07:15	381	2.72	106.66	BWR	
09/25/92	15:35	387	3.00	106.40	BWR	
10/02/92	12:50	394	2.69	106.71	BWR	
10/06/92	09:22	398	2.88	106.52	BWR	
10/12/92	08:58	404	2.78	106.62	BWR	
10/20/92	08:33	412	3.13	106.27	BWR	
10/26/92	10:22	418	3.10	106.30	BWR	
11/03/92	10:30	426	3.61	105.79	BWR	
11/09/92	07:56	432	3.76	105.64	BWR	
11/16/92	07:40	439	3.77	105.63	BWR	
11/23/92	08:36	446	3.53	105.87	BWR	
11/30/92	08:31	453	3.73	105.67	BWR	
12/07/92	10:43	460	3.63	105.77	BWR	
12/14/92	07:26	467	2.22	107.18	BWR	
12/21/92	09:58	474	3.38	106.02	BWR	
12/28/92	09:02	481	3.65	105.75	BWR	
01/04/93	08:43	488	3.51	105.89	BWR	
01/11/93	09:00	495	3.14	106.26	BWR	
01/18/93	10:25	502			BWR	Covered w/ice
01/25/93	10:08	509	3.37	106.03	BWR	
02/01/93	08:04	516	3.29	106.11	BWR	
02/09/93	11:02	524	3.87	105.53	BWR	
02/16/93	09:32	531	3.93	105.47	BWR	
02/22/93	10:52	537	3.59	105.81	BWR	
03/04/93	09:54	547	3.92	105.48	BWR	
03/10/93	08:31	553	3.77	105.63	BWR	
03/17/93	10:33	560	3.77	105.63	BWR	
03/25/93	10:28	568	1.14	108.26	BWR	
04/01/93	12:28	575	1.02	108.38	TJC	
04/07/93	09:58	581	2.72	106.68	TJC	
04/15/93	09:58	589	2.52	106.88	TJC	
04/22/93	10:15	596	2.65	106.75	TJC	
04/26/93	12:30	600	2.90	106.50	BWR	
05/03/93	12:37	607	3.24	106.16	BWR	
05/11/93	09:45	615	3.68	105.72	TJC	
05/17/93	12:45	621	3.87	105.53	TJC	

Sheet E6

Project: **Boston, Massachusetts**
GRAPH FOR OPEN STAND PIPE PIEZOMETERS- G.W. ELEV. VS. DATE
FILE NO. 12974

GENERAL PIEZOMETER INFORMATION		FIELD DATA		RESPONSE VALUES	INITIAL PIEZOMETER VALUES	FILE DATA
Instrument No.	4A-OW-016	Top of SP El (ft)	109.4	Threshold	Installation:	File
Loc. Coords. N	2951834	Station	77+40.0	Limiting	Date	OW-016.DAT
E	780773	Offset (ft)	115.0 ft		Zero Reading	Date Printed
-OW-016						



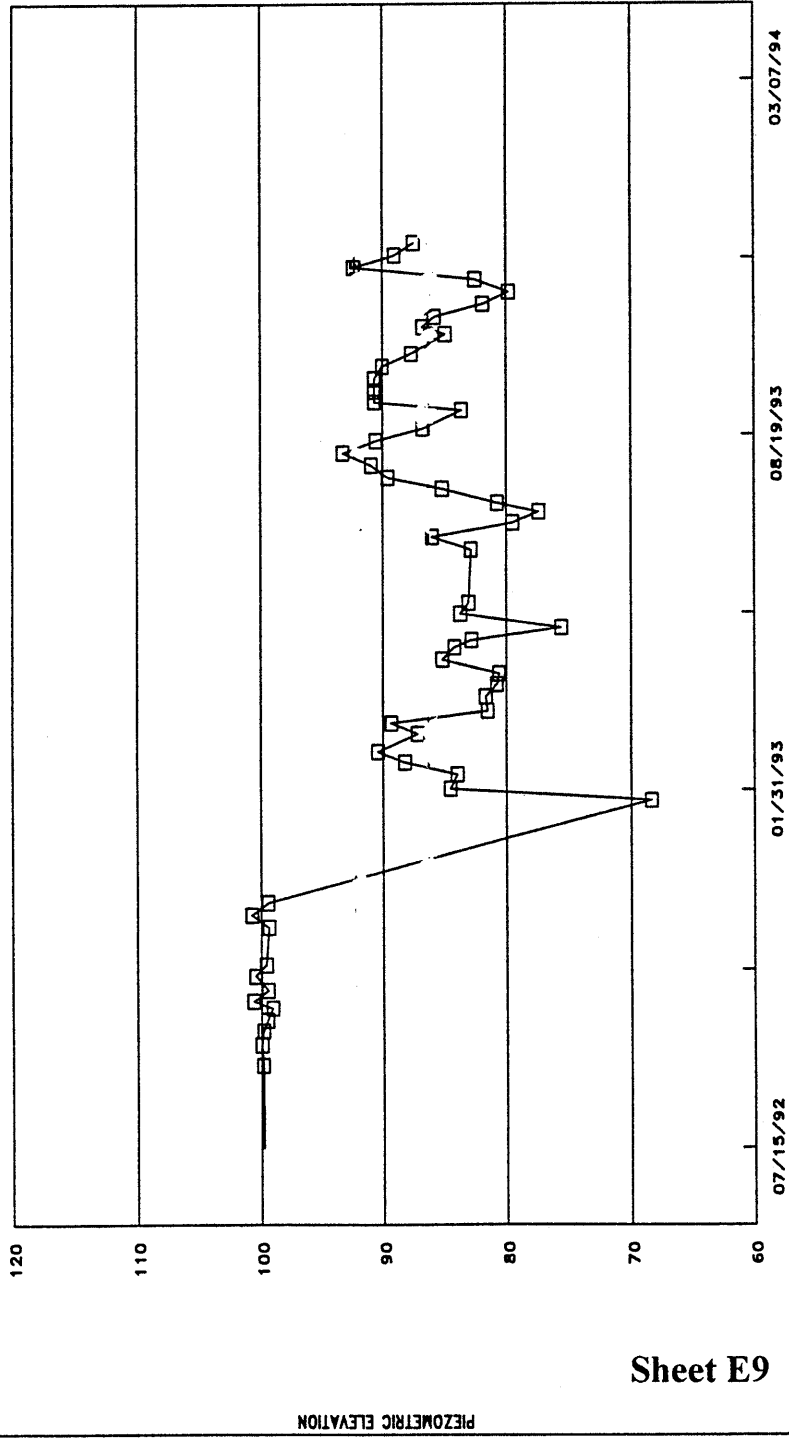
Sheet E7

TABLE FOR VIBRATING WIRE PIEZOMETERS									
Project: Boston, Massachusetts								FILE NO. 12974	
GENERAL PIEZOMETER INFORMATION			VIBRATING WIRE TRANSDUCER DATA				INITIAL PIEZOMETER VALUES		
Instrument No.	VWPZ-053		Cal Factor(C)	0.01641 psi/digit		Installation:			
Piez Serial No.	11473		Thermal Factor (K)	-0.01605 psi/C rise		Date	04/04/90		
Loc. Coords. N	2951001		Threshold			Time	07:50		
E	780636		Limiting			Zero Read	9503		
Station / Offset (ft)	78+30.0 / 40.0 ft		Piez Tip Elev (ft)	1.5		Temp (°C)	6.4		
GENERAL			VIBRATING WIRE TRANSDUCER				PERSONNEL/REMARKS		
Date	Time	Elapsed Days	Trans Reading	Temp. °C	Piez Press (psi)	Piez Head (ft)	Piez Elev (ft)	Read By (init)	Remarks
05/11/93	10:02	1133	7324	11.3	35.67	82.2	83.7	TJC	
05/17/93	13:00	1139	7341	11.3	35.39	81.6	83.0	TJC	
05/26/93	07:55	1148						MEV	Buried
06/02/93	13:10	1155						MEV	Buried
06/10/93	07:20	1163						MEV	Buried
06/16/93	09:44	1169	7346	11.3	35.31	81.3	82.8	MEV	
06/23/93	11:26	1176	7263	11.4	36.67	84.5	86.0	MEV	
07/01/93	10:45	1184	7435	11.3	33.65	78.0	79.5	MEV	
07/07/93	11:07	1190	7490	11.4	32.94	75.9	77.4	MEV	
07/12/93	09:14	1195	7402	11.3	34.39	79.2	80.7	MEV	
07/20/93	11:30	1203	7285	11.3	36.31	83.7	85.2	BWR	
07/26/93	09:56	1209	7168	11.3	38.23	88.1	89.6	MEV	
08/02/93	11:03	1216	7132	11.4	38.82	89.4	90.9	BWR	
08/08/93	13:45	1223	7070	11.4	39.84	91.8	93.3	BWR	
08/16/93	12:49	1230	7142	11.3	38.66	89.1	90.6	BWR	
08/23/93	09:20	1237	7244	11.2	36.98	85.2	86.7	BWR	
08/30/93	13:14	1247	7326	11.3	35.64	82.1	83.6	BWR	
09/07/93	09:02	1252	7139	11.2	38.71	88.2	90.7	BWR	
09/13/93	11:12	1258	7139	11.2	38.71	89.2	90.7	MEV	
09/20/93	09:01	1265	7139	11.2	38.71	89.2	90.7	MEV	
09/27/93	09:10	1272	7156	11.5	38.42	88.5	90.0	MEV	
10/04/93	09:19	1279	7218	12.1	37.39	86.2	87.7	MEV	
10/15/93	09:34	1290	7291	12.1	36.20	83.4	84.9	MEV	
10/19/93	11:54	1294	7242	12.1	37.00	85.2	86.7	MEV	
10/25/93	09:51	1300	7267	12.2	36.50	84.3	85.8	MEV	
11/01/93	09:13	1307	7370	12.9	34.89	80.4	81.9	MEV	
11/08/93	09:06	1314	7426	12.2	33.98	78.3	79.8	MEV	
11/15/93	08:42	1321	7355	12.0	35.15	81.0	82.5	MEV	
11/22/93	10:07	1328	7093	12.1	36.45	80.9	82.4	MEV	
11/29/93	09:08	1335	7182	12.1	37.98	87.5	89.0	MEV	
12/06/93	08:39	1342	7223	12.1	37.31	86.0	87.5	MEV	
12/13/93	09:13	1349	7172	12.0	38.15	87.9	89.4	MEV	
12/20/93	08:25	1356	7177	12.2	38.06	87.7	89.2	MEV	
12/27/93	09:32	1363	7104	12.1	39.28	90.5	92.0	MEV	
01/03/94	10:13	1370	7103	12.1	39.28	90.5	92.0	MEV	
01/10/94	09:25	1377						MEV	Under ice
01/17/94	08:43	1384	7109	12.1	39.18	90.3	91.8	MEV	
01/24/94	10:10	1391						MEV	Decommissioned
02/01/94	10:27	1399						MEV	Decommissioned
02/07/94	10:18	1405						MEV	Decommissioned
02/16/94	08:31	1414						MEV	Decommissioned
02/22/94	08:10	1420						MEV	Decommissioned
02/28/94	10:46	1426						MEV	Decommissioned
03/07/94	08:28	1433						MEV	Decommissioned
03/14/94	08:44	1440						MEV	Decommissioned
03/21/94	11:36	1447						MEV	Decommissioned

Project: . . . Boston, Massachusetts
 GRAPH FOR VIBRATING WIRE PIEZOMETERS - PIEZ. ELEV. vs DATE
 FILE NO. 12974

GENERAL PIEZOMETER INFORMATION		VIBRATING WIRE TRANSDUCER DATA		RESPONSE VALUES		INITIAL PIEZOMETER VALUES		FILE DATA	
Instrument No.	.VWPZ-053	Piez Tip El (ft)	1.5	Threshold	Installation:	Date	04/04/90	File	VWPZ-053.DAT
Loc. Coords. N	2951001	Station		40.0 ft Limiting	Zero Piez. Elev			Date Printed	12/18/93
E	790636	Offset (ft)							

4A-VWPZ-053



Sheet E9

APPENDIX F. Analysis of Consolidation and Settlement

Sheet F1. Settlement Calculation Spreadsheet S320-O.WKS, page 1 of 3.	332
Sheet F2. Settlement Calculation Spreadsheet S320-O.WKS, page 2 of 3.	333
Sheet F3. Settlement Calculation Spreadsheet S320-O.WKS, page 3 of 3.	334
Sheet F4. Settlement Calculation Spreadsheet S320-OC.WKS, page 1 of 3.....	335
Sheet F5. Settlement Calculation Spreadsheet S320-OC.WKS, page 2 of 3.....	336
Sheet F6. Settlement Calculation Spreadsheet S320-OC.WKS, page 3 of 3.....	337
Sheet F7. Settlement Summary Table, page 1 of 2	338
Sheet F8. Settlement Summary Table, page 2 of 2	339

SETTLEMENT ANALYSIS

File: S320-O.WKS

Organic thickness is changed to make equiv. Cv

t= 320 days
 Cv= 1.1 sq.ft/day
 T= 0.1394
 H (drain)= 50.25
 2H (drain)= 100.5

RECTANGULAR WEDGE (L&W, p.408)
 T= 0.1394

Elev.	Soil Type	Thick-ness	Initial S'vo	S'p	Initial Excess PWE	Z	Uz	Dissipated PWE
107.5			697	1184.9	3.5	0.00	1	3.5
92.5	Coh.Fill	15	1402	2383.4	3.5	0.30	0.55	1.925
92.5			1402	3500	3.5	0.30	0.55	1.925
71.5	Organics	21 <i>Increased</i>	2077	3500	3.5	0.72	0.18	0.63
71.5			2077	12000	3.5	0.72	0.18	0.63
65	BBC	6.5	2459.75	10600	3.5	0.85	0.14	0.49
55	BBC	10	3048.25	9600	3.5	1.04	0.11	0.385
45	BBC	10	3636.75	9000	3.5	1.24	0.16	0.56
35	BBC	10	4225.25	8700	3.5	1.44	0.27	0.945
25	BBC	10	4813.75	8600	3.5	1.64	0.47	1.645
15	BBC	10	5402.25	8650	3.5	1.84	0.76	2.66
7	BBC	8	5873	8750	3.5	2.00	1	3.5

Sheet F1

TRIANGLE WEDGE (L&W, p.413)

T= 0.1394

Total PWE= 15

Initial Excess PWE	Z	Uz	Uz x Tot.PWE	Dissipated PWE	Total Dissipated PWE	Total Dissipated U	S'vo	S'vf	S'p	Average S'vo
0.00	0.00	1	15.00	0.00	3.50	220.5	697.0	917.5	1184.9	1049.50
2.24	0.30	0.85	12.75	-0.01	1.91	120.6	1402.0	1522.6	2383.4	
2.24	0.30	0.85	12.75	-0.01	1.91	120.6	1402.0	1522.6	3500	
5.37	0.72	0.64	9.60	-0.03	0.60	38.0	2077.0	2115.0	3500	1739.50
5.37	0.72	0.64	9.60	-0.03	0.60	38.0	2077.0	2115.0	12000	
6.34	0.85	0.6	9.00	0.34	0.83	52.5	2459.8	2512.2	10600	2268.38
7.84	1.04	0.55	8.25	1.09	1.47	92.7	3048.3	3140.9	9600	2754.00
9.33	1.24	0.53	7.95	2.28	2.84	178.8	3636.8	3815.6	9000	3342.50
10.82	1.44	0.57	8.55	4.37	5.32	334.9	4225.3	4560.2	8700	3931.00
12.31	1.64	0.67	10.05	7.36	9.01	567.5	4813.8	5381.3	8600	4519.50
13.81	1.84	0.83	12.45	11.26	13.92	876.7	5402.3	6279.0	8650	5108.00
15.00	2.00	1	15.00	15.00	18.50	1165.5	5873.0	7038.5	8750	5637.63

At any depth, the Dissipated PWE from the Triangular wedge is found as follows:

$$\text{Dissipated PWE} = (Uz \times 15) - (15 - \text{Init. Excess PWE})$$

where -

Uz, the consolidation ratio, is read from Figure 27.6 in Lambe & Whitman (1969).
 Init. Excess. PWE = $(107.5' - \text{Elev.}) * (15' / 2H)$, based on a triangular distribution.

Average Sv _f	Average S _p	After Cons: OC/NC	RR	CR	ACTUAL Elev.	Soil Type	ACTUAL Thickness	Settlements (inches)		
								Recomp Range	Virgin Range	Total Sett.
1220.03	1784.15	OC	0.025	0.17	101.5 86.5	Coh.Fill	15	0.294		0.29
1818.78	3500.00	OC	0.02	0.24	86.5 71.5	Organics	15	0.070		0.07
2313.62	11300.00	OC	0.025	0.165	71.5 65	BBC	6.5	0.017		0.02
2826.58	10100.00	OC	0.025	0.175	55	BBC	10	0.034		0.03
3478.24	9300.00	OC	0.025	0.175	45	BBC	10	0.052		0.05
4187.86	8850.00	OC	0.025	0.25	35	BBC	10	0.082		0.08
4970.72	8650.00	OC	0.025	0.25	25	BBC	10	0.124		0.12
5830.12	8625.00	OC	0.025	0.21	15	BBC	10	0.172		0.17
6658.73	8700.00	OC	0.025	0.21	7	BBC	8	0.174		0.17

Total Settlement (in) =	1.02
Clay Settlement (in) =	0.65

Total Settlement (in) =
Clay Settlement (in) =

SETTLEMENT ANALYSIS File: S320-OC.WKS
Organic & Cohesive Fill thicknesses changed to make equiv. Cv

t= 320 days
 Cv= 1.1 sq.ft/day
 T= 0.17577
 H (drain)= 44.75
 2H (drain)= 89.5

RECTANGULAR WEDGE (L&W, p.408)
 T= 0.1758

Elev.	Soil Type	Thick-ness	Initial Svo	Sp	Z	Uz	Dissipated PWE
96.5			697	1184.9	0.00	1	3.5
92.5	Coh.Fill	4 <i>Reduced</i>	1402	2383.4	0.09	0.91	3.185
92.5			1402	3500	0.09	0.91	3.185
71.5	Organics	21 <i>Increased</i>	2077	3500	0.56	0.36	1.26
71.5			2077	12000	0.56	0.36	1.26
65	BBC	6.5	2459.75	10600	0.70	0.27	0.945
55	BBC	10	3048.25	9600	0.93	0.2	0.7
45	BBC	10	3636.75	9000	1.15	0.21	0.735
35	BBC	10	4225.25	8700	1.37	0.31	1.085
25	BBC	10	4813.75	8600	1.60	0.5	1.75
15	BBC	10	5402.25	8650	1.82	0.76	2.66
7	BBC	8	5873	8750	2.00	1	3.5

TRIANGLE WEDGE (L&W, p.413)

T= 0.1758

Total PWE= 15

Initial Excess PWE	Z	Uz	Uz x Tot.PWE	Dissipated PWE	Total Dissipated PWE	Total Dissipated U	S'vo	S'vf	S'p
0.00	0.00	1	15.00	0.00	3.50	220.5	697.0	917.5	1184.9
0.67	0.09	0.96	14.40	0.07	3.26	205.1	1402.0	1607.1	2383.4
0.67	0.09	0.96	14.40	0.07	3.26	205.1	1402.0	1607.1	3500
4.19	0.56	0.72	10.80	-0.01	1.25	78.7	2077.0	2155.7	3500
4.19	0.56	0.72	10.80	-0.01	1.25	78.7	2077.0	2155.7	12000
5.28	0.70	0.67	10.05	0.33	1.27	80.3	2459.8	2540.0	10600
6.96	0.93	0.6	9.00	0.96	1.66	104.3	3048.3	3152.5	9600
8.63	1.15	0.56	8.40	2.03	2.77	174.3	3636.8	3811.0	9000
10.31	1.37	0.59	8.85	4.16	5.24	330.3	4225.3	4555.5	8700
11.98	1.60	0.68	10.20	7.18	8.93	562.8	4813.8	5376.5	8600
13.66	1.82	0.83	12.45	11.11	13.77	867.5	5402.3	6269.7	8650
15.00	2.00	1	15.00	15.00	18.50	1165.5	5873.0	7038.5	8750

Sheet F5

At any depth, the Dissipated PWE from the Triangular wedge is found as follows:

$$\text{Dissipated PWE} = (Uz \times 15) - (15 - \text{Init. Excess PWE})$$

where -

Uz, the consolidation ratio, is read from Figure 27.6 in Lambe & Whitman (1969).
 Init. Excess. PWE = (107.5' - Elev.) * (15' / 2H), based on a triangular distribution.

Average S _{vo}	Average S _{vf}	Average Sp	After Cons: OC/NC	RR	CR	ACTUAL Elev.	Soil Type	ACTUAL Thickness	Settlements (inches)		
									Recomp Range	Virgin Range	Total Sett.
1049.50	1262.29	1784.15	OC	0.025	0.17	101.5 86.5	Coh.Fill	15	0.361		0.36
1739.50	1881.42	3500.00	OC	0.02	0.24	86.5 71.5	Organics	15	0.123		0.12
2268.38	2347.89	11300.00	OC	0.025	0.165	71.5 65	BBC	6.5	0.029		0.03
2754.00	2846.28	10100.00	OC	0.025	0.175	55	BBC	10	0.043		0.04
3342.50	3481.78	9300.00	OC	0.025	0.175	45	BBC	10	0.053		0.05
3931.00	4183.27	8850.00	OC	0.025	0.25	35	BBC	10	0.081		0.08
4519.50	4966.03	8650.00	OC	0.025	0.25	25	BBC	10	0.123		0.12
5108.00	5823.13	8625.00	OC	0.025	0.21	15	BBC	10	0.171		0.17
5637.63	6654.11	8700.00	OC	0.025	0.21	7	BBC	8	0.173		0.17

Total Settlement (in) =
Clay Settlement (in) =

1.16
0.67

Settlements Summary Table

Instrument	Distance from wall (ft)	FIR (El.)	Excav. Lift 1 (El.)	Excav. Lift 1 (settl)	Exc. Final Subgrd. (El.)	Exc. Final Subgrd. (settl)	Pour Invert (El.)	Pour Invert (settl)	EFS-2 (El.)	Settlements for "Pour Invert"				
										Normalized to depth: dist.	Normalized to Max. sett.: Max sett	Normalized to Max. sett.: Norm sett		
ISS-2 North				37										
DMP4-138	15	105.11	104.9	2.52	104.42	8.28	104.19	11.04	104.23	10.56	0.41	2.49	11.76	0.94
PBEX-502	20	98.05			97.72	3.96	97.42	7.56	97.45	7.2	0.54	1.7		0.64
PE-103	20	100.99	100.95	0.48	100.73	3.12	100.4	7.08	100.42	6.84	0.54	1.59		0.6
DMP4-139	31	104.2	104.17	0.36	103.79	4.92	103.57	7.56	103.59	7.32	0.84	1.7		0.64
DMP4-106	58	109.72	109.69	0.36	109.08	7.68	108.74	11.76	108.78	11.28	1.57	2.65		1
DMP4-107	83	110.03	110	0.36	109.59	5.28	109.27	9.12	109.3	8.76	2.24	2.05		0.78
DMP4-108	104	109.98	109.93	0.6	109.64	4.08	109.47	6.12	109.48	6	2.81	1.38		0.52
ISS-3 North				32										
PE-105	22	104.05	104.02	0.36	103.97	0.96	103.75	3.6			0.69	0.94		0.68
DMP4-140	31	104.18	104.16	0.24	103.97	2.52	103.9	3.36			0.97	0.88		0.64
PE-106	40	102.61	102.55	0.72	102.54	0.84	102.36	3			1.25	0.78		0.57
DMP4-113	65	109.32	109.29	0.36	108.88	4.44	108.88	5.28			2.03	1.37		1
DMP4-114	82	109.13	109.1	0.36	108.78	4.2	108.72	4.92			2.56	1.28		0.93
DMP4-115	106	109.14	109.12	0.24	108.89	3	108.85	3.48			3.31	0.91		0.66
ISS-4 North				39										
DMP2-006	22	115.21	115.15	0.72	114.71	6	114.68	6.36			0.56	1.36		1
DMP2-107	32	114.43	114.406	0.288	113.99	5.28	113.97	5.52			0.82	1.18		0.87
DMP4-120	38	108.95	108.87	0.96	108.47	5.76	108.44	6.12			0.97	1.31		0.96
DMP2-105	90	111.05	111.039	0.132	110.8	3	110.79	3.12			2.31	0.67		0.49
DMP2-104	139	110.22	110.21	0.12	110.13	1.08	110.11	1.32			3.56	0.28		0.21
DMP2-070	160	111.08	111.04	0.48	110.98	1.2	110.96	1.44			4.1	0.31		0.23
ISS-5 North				47										
DMP2-022	38	112.47	112.46	0.12	112.23	2.88	112.18	3.48			0.81	0.62		n/a
DMP2-038			n/a		n/a		n/a							
ISS-6 North				50										
DMP4-124	23	110.8	110.72	0.96	110.35	5.4	110.32	5.76			0.46	0.96		0.96
PE-111	23	86.02	86.03	-0.12	85.61	4.92	85.52	6			0.46	1		1
DMP2-037	39	111.95	111.92	0.36	111.71	2.88	111.67	3.36			0.78	0.56		0.56
DMP4-126	48	110.69	110.6	1.08	110.32	4.44	110.25	5.28			0.96	0.88		0.88
DMP2-036	79	111.93	111.9	0.36	111.8	1.56	111.75	2.16			1.58	0.36		0.36
DMP4-127	110	110.38	110.35	0.36	110.26	1.44	110.18	2.4			2.2	0.4		0.4
DMP2-034	131	112.21	112.19	0.24	112.15	0.72	112.11	1.2			2.62	0.2		0.2
ISS-7 North				53										
DMP4-130	49	110.46	110.24	2.64	109.99	5.64	109.93	6.36			0.92	1		0.91
DMP4-131	63	110.32	110.26	0.72	110.04	3.36	109.98	4.08			1.19	0.64		0.59
DMP4-132	92	110.36	109.94	5.04	109.84	6.24	109.78	6.96			1.74	1.09		1

Settlements Summary Table, continued

Instrument	Distance from wall (ft)	FIR (El.)	Excav. Lift 1 (El.)	Excav. Lift 1 (sett)	Exc. Final Subgrd. (El.)	Exc. Final Subgrd. (sett)	Pour Invert (El.)	Pour Invert (sett)	Settlements for "Pour Invert"				
									Normalized to depth: dist.	Normalized to depth: Norm sett	Normalized to Max. sett.: Max sett Norm sett		
ISS-2 South				38									
PBEX-501	18	101.43	??		101.09	4.08	101.09	4.08	0.47	0.89	6.24	0.65	
DMP4-103	40	116.59	116.52	0.84	116.15	5.28	116.07	6.24	1.05	1.37		1	
DMP4-102	65	118.15	118.09	0.72	117.85	3.6	117.79	4.32	1.71	0.95		0.69	
IFE-114	72	95.51	dne		95.41	1.2	95.42	1.08	1.89	0.24		0.17	
DMP4-101	139	113.12	113.07	0.6	113.04	0.96	113.03	1.08	3.66	0.24		0.17	
ISS-3 South				36									
IFE-104	20	103.75	103.69	0.72	103.56	2.28	103.35	4.8	0.56	1.11	4.8	1	
DMP4-111	40	115.26	115.2	0.72	114.94	3.84	114.87	4.68	1.11	1.08		0.98	
DMP4-110	64	115.56	115.5	0.72	115.28	3.36	115.2	4.32	1.78	1		0.9	
DMP4-109	105	117.29	117.24	0.6	117.07	2.64	117.01	3.36	2.92	0.78		0.7	
ISS-4 South				38									
IFE-113	31	99.84	99.85	-0.12	99.65	2.28	99.53	3.72	0.82	0.82	3.84	0.97	
DMP4-118	41	109.2	109.12	0.96	108.91	3.48	108.88	3.84	1.08	0.84		1	
DMP4-117	55	109.61	109.52	1.08	109.36	3	109.32	3.48	1.45	0.76		0.91	
DMP4-116	85	110.38	110.31	0.84	110.21	2.04	110.18	2.4	2.24	0.53		0.62	
ISS-5 South				45									
DMP4-122	84	109.67	109.65	0.24	109.51	1.92	109.46	2.52	1.87	0.47	2.52	1	
DMP4-121	106	110.15	110.14	0.12	110.07	0.96	110.02	1.56	2.36	0.29		0.62	
DMP2-016	131	112.34	112.32	0.24	112.26	0.96	112.24	1.2	2.91	0.22		0.48	
DMP2-015	143	111.25	111.22	0.36	111.18	0.84	111.16	1.08	3.18	0.2		0.43	
DMP2-014	184	111.53	111.5	0.36	111.48	0.6	111.48	0.6	4.09	0.11		0.24	
ISS-6 South				49									
DMP2-041	133	114.66	114.65	0.12	114.62	0.48	114.62	0.48	2.77	0.08			
DMP2-040	202	114.59	114.57	0.24	114.55	0.48	114.55	0.48	4.21	0.08			
ISS-7 South				51									
DMP4-129	18	109.92	109.63	3.48	109.46	5.52	109.44	5.76	0.35	0.94	5.76	1	
DMP4-128	34	109.89	109.81	0.96	109.63	3.12	109.59	3.6	0.67	0.59		0.62	
DMP2-043			n/r	n/r	n/r	n/r	n/r	n/r					

NOTE: "dne" stands for "does not exist"

APPENDIX G. Analysis Using MOVEX

Sheet G1. Definition of Input Parameters: ISS-4 Soil Profile and Vertical Stresses.	342
Sheet G2. Calculation of Input Undrained Shear Strengths, page 1 of 2.	343
Sheet G3. Calculation of Input Undrained Shear Strengths, page 2 of 2.	344
Sheet G4. Calculation of Wall Stiffnesses for Diaphragm Wall and Sheetpile.....	345
Sheet G5. Calculation of Strut Stiffnesses for Tiebacks Behind Sheetpile Wall.	346
Sheet G6. Calculation of Strut Stiffnesses for Tiebacks Behind Diaphragm Wall.	347
Sheet G7. Summary of MOVEX Results from “Best Estimate” Analyses.	348
Sheet G8. Summary of MOVEX Parametric Analyses, page 1 of 2.	349
Sheet G9. Summary of MOVEX Parametric Analyses, page 2 of 2.	350
Sheet G10. MOVEX Input File for ISS-4 Sheetpile Wall, page 1 of 3.....	351
Sheet G11. MOVEX Input File for ISS-4 Sheetpile Wall, page 2 of 3.....	352
Sheet G12. MOVEX Input File for ISS-4 Sheetpile Wall, page 3 of 3.....	353
Sheet G13. MOVEX Input File for ISS-4 Diaphragm Wall, page 1 of 3.....	354
Sheet G14. MOVEX Input File for ISS-4 Diaphragm Wall, page 2 of 3.....	355
Sheet G15. MOVEX Input File for ISS-4 Diaphragm Wall, page 3 of 3.....	356

11/25/94, 1/7/95

CALCULATION OF UNDRAINED SHEAR STRENGTHS

① Miscellaneous Fill-Dry $\gamma_T = 110 \text{ pcf}$ $H = 4'$

$S_u = \sigma_v' K_o \tan \phi$

At top (El. 110') $S_u = 0 \text{ psf}$
 At base (El. 106') $S_u = (440 \text{ psf})(0.50) \tan 32^\circ = 137 \text{ psf}$

Top $S_u = \boxed{0}$ $\frac{dS_u}{dd} = \frac{137}{4} = \boxed{34.25}$

② Miscellaneous Fill-Saturated $\gamma_T = 120 \text{ pcf}$ $H = 4.5'$

At top (El. 106') $S_u = 137 \text{ psf}$
 At base (El. 101.5') $S_u = (697 \text{ psf})(0.50) \tan 32^\circ = 218 \text{ psf}$

Top $S_u = \boxed{137}$ $\frac{dS_u}{dd} = \frac{81}{4.5} = \boxed{18}$

③ Cohesive Fill $\gamma_T = 110 \text{ pcf}$ $H = 15'$

$S_u = 0.2 \sigma_p' = 0.2 (1.7) \sigma_v'$ (for DSS shearing mode)

At top (El. 101.5') $S_u = 0.2 (1.7) (697 \text{ psf}) = 237 \text{ psf}$
 At base (El. 86.5') $S_u = 0.2 (1.7) (1402 \text{ psf}) = 477 \text{ psf}$

Top $S_u = \boxed{237}$ $\frac{dS_u}{dd} = \frac{240}{15} = \boxed{16}$

④ Organic Silt $\gamma_T = 108 \text{ pcf}$ $H = 15'$

At top (El. 86.5') $S_u = 730 \text{ psf}$
 At base (El. 71.5') $S_u = 790 \text{ psf}$ } estimated by CCL

Top $S_u = \boxed{730}$ $\frac{dS_u}{dd} = \frac{60}{15} = \boxed{4.00}$

⑤ Boston Blue Clay $\gamma_T = 116 \text{ pcf}$

⑧

S_u profile based on SHANSEP 'average' parameters $S = .205$, $m = .77$ and σ_p' determined by Casagrande and Strain Energy.

H=6.5' ⑤ Top $S_u = \boxed{1645}$ $\frac{dS_u}{dd} = \frac{-95}{6.5} = \boxed{-14.62}$

H=20' ⑥ Top $S_u = \boxed{1550}$ $\frac{dS_u}{dd} = \frac{-50}{20} = \boxed{-2.5}$

H=20' ⑦ Top $S_u = \boxed{1500}$ $\frac{dS_u}{dd} = \frac{40}{20} = \boxed{2.0}$

H=18' ⑧ Top $S_u = \boxed{1540}$ $\frac{dS_u}{dd} = \frac{95}{18} = \boxed{5.28}$

See prev. page and Figure 5.9

9) Glaciomarine

$\gamma_T = 135 \text{ pcf}$

$H = 7'$

$S_u = \sigma'_v K_o \tan \phi$

At top (El. 7') $S_u = (5873 \text{ psf})(1.1) \tan 42^\circ = 5817 \text{ psf}$
 At base (El. 0') $S_u = (6377 \text{ psf})(1.1) \tan 42^\circ = 6316 \text{ psf}$

Top $S_u = \boxed{5817}$ $\frac{ds_u}{dd} = \frac{499}{7} = \boxed{71.29}$

10) Glacial Till

$\gamma_T = 145 \text{ pcf}$

$H = 9'$

At top (El. 0') $S_u = (6377)(1.0) \tan 45^\circ = 6377 \text{ psf}$
 At base (El. -9') $S_u = (7115)(1.0) \tan 45^\circ = 7115 \text{ psf}$

Top $S_u = \boxed{6377}$ $\frac{ds_u}{dd} = \frac{738}{9} = \boxed{82.0}$

REMOVE - PART OF "FIRM" LAYER.

Depth to Firm Layer (if bedrock): $110' + 9' = \boxed{119'}$

Depth to Firm Layer (if Glaciomarine): $110' - 7' = \boxed{103'}$

Wall Stiffness (EI) = $\boxed{5.04 \times 10^7 \frac{\text{lb-ft}^2}{\text{LF}}}$ for AZ-18 sheeting (see p.4)

50,400,000

= $\boxed{1.33 \times 10^9 \frac{\text{lb-ft}^2}{\text{LF}}}$ for Diaphragm Wall (see p.4)

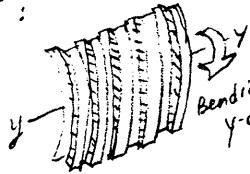
11/19/94

• WALL STIFFNESS (EI)

- For SHEETPILE WALL (Arbed AZ-18 sheeting)

E of steel = $29 \times 10^6 \text{ psi} = 4.2 \times 10^9 \text{ psf}$

I :



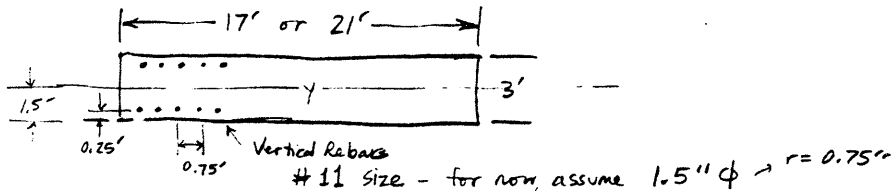
Bending about y-axis: use $I_y = 250.4 \frac{\text{in}^4}{\text{LF}}$

$EI = (29 \times 10^6 \frac{\text{lb}}{\text{in}^2}) (250.4 \frac{\text{in}^4}{\text{LF}}) (\frac{1}{144} \frac{\text{ft}^2}{\text{in}^2}) = 5.04 \times 10^7 \frac{\text{lb-ft}^2}{\text{LF}}$
 (see Smith, p.158) & p.168 for comparison to PE-32

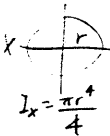
- For DIAPHRAGM WALL :

E of concrete = $3.5 \times 10^6 \text{ psi}$ (assumed, "typical" modulus)
 E of steel re-bar = $29 \times 10^6 \text{ psi}$ Xanthakos used 3×10^6

Typical D/W panel:



$I_{y, \text{conc}} = \frac{1}{12} \frac{b h^3}{b} = \frac{1}{12} \frac{(1') (3')^3}{1'} = \frac{2.25 \text{ ft}^4}{\text{LF}} = 4.6 \times 10^4 \frac{\text{in}^4}{\text{LF}}$



In each linear foot, there are $\frac{1}{0.75} = 1.3$ bars on each side.

From parallel-axis theorem,

$I_{\text{rebar}} = 2(I_c + Ad^2) = 2 \left(\left[\frac{1.3 \pi (0.75)^4}{4} \right] + \left[1.3 \pi (0.75)^2 (15'')^2 \right] \right)$
 due to rebar to either side
 $= 2(0.323 + 516.9) = 1034 \frac{\text{in}^4}{\text{LF}}$

$(EI)_{D/W} = (EI)_{\text{conc}} + (EI)_{\text{rebar}}$

$= (3.5 \times 10^6)(4.6 \times 10^4) + (29 \times 10^6)(1034) = 1.61 \times 10^{10} + 3.0 \times 10^{10}$

$= 1.91 \times 10^{10} \frac{\text{lb-in}^2}{\text{LF}} = 1.33 \times 10^9 \frac{\text{lb-ft}^2}{\text{LF}}$

about 26x stiffer than sheeting.

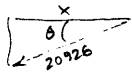
STRUT STIFFNESS - SHEETPILE WALL

= $\frac{AE}{L}$ per unit length of wall. (see p. 6 and 7)

① Tier 1: $A = 5.5(.283 \text{ in}^2) = 1.56 \text{ in}^2 = .0108 \text{ ft}^2$
 $E = 20,500 \text{ ksi} = 2.95 \times 10^9 \text{ psf}$
 $L = 85' + \frac{1}{2}(40') = 105'$
 $d_c = 14.5'$
 $\frac{AE}{Ld_c} = \frac{(.0108)(2.95 \times 10^9)}{(105)(14.5)} = \boxed{20926 \frac{\text{lb/ft}}{\text{LF}}}$ (FL + 1/2 BL) (FL) (FL + BL)
 25850 17578

② Tier 2: $A = 6(.283 \text{ in}^2) = 1.698 \text{ in}^2 = .0118 \text{ ft}^2$
 $E = 16,600 \text{ ksi} = 2.39 \times 10^9 \text{ psf}$
 $L = 54' + \frac{1}{2}(40') = 74'$
 $d_c = 6'$
 $\frac{AE}{Ld_c} = \frac{(.0118)(2.39 \times 10^9)}{(74)(6)} = \boxed{63518 \frac{\text{lb/ft}}{\text{LF}}}$ (FL + 1/2 BL) (FL) (FL + BL)
 87043 50004

③ Tier 3: $A = 6(.283 \text{ in}^2) = 1.698 \text{ in}^2 = .0118 \text{ ft}^2$
 $E = 14,200 \text{ ksi} = 2.04 \times 10^9 \text{ psf}$
 $L = 24' + \frac{1}{2}(40') = 44'$
 $d_c = 6'$
 $\frac{AE}{Ld_c} = \frac{(.0118)(2.04 \times 10^9)}{(44)(6)} = \boxed{91182 \frac{\text{lb/ft}}{\text{LF}}}$ (FL + 1/2 BL) (FL) (FL + BL)
 167167 62688

Correction for Inclination Angle  $X = 20926 \cos \theta$

① $\theta = 22^\circ$	$\frac{AE'}{Ld_c} = 20926 \cos 22^\circ = \boxed{19402 \frac{\text{lb/ft}}{\text{LF}}}$	23968	16298
② $\theta = 22^\circ$	$\frac{AE'}{Ld_c} = 63518 \cos 22^\circ = \boxed{58893 \frac{\text{lb/ft}}{\text{LF}}}$	80705	46363
③ $\theta = 20^\circ$	$\frac{AE'}{Ld_c} = 91182 \cos 20^\circ = \boxed{85683 \frac{\text{lb/ft}}{\text{LF}}}$	157086	58907
	(FL + 1/2 BL)	(FL)	(FL + BL)

Sheet G5

11/28, 1/7/95

STRUT STIFFNESS - DIAPHRAGM WALL

From page (4), wall stiffness (EI) = $1.33 \times 10^9 \frac{\text{lb}\cdot\text{ft}^2}{\text{LF}}$.

STRUT STIFFNESS - D/W

strand Area = .217 in² each.

EI. 106'

① Tier 1: 9.5 strands E = 22,200 ksi = 3.20×10^9 psf

$A = 9.5(.217 \text{ in}^2) = 2.06 \text{ in}^2 = .0143 \text{ ft}^2$ $d_L = 10.5'$

$L = 167' + \frac{1}{2}(30') = 182'$

10.5 str
d: 6.5

$\frac{AE}{Ld_L} = \frac{(.0143 \text{ ft}^2)(3.20 \times 10^9 \text{ psf})}{(182)(10.5)} = 23946 \frac{\text{lb/ft}}{\text{LF}}$

11.5 str
d: 6.5

Correction for inclination: $23946 \cos 45^\circ = \boxed{16932 \frac{\text{lb/ft}}{\text{LF}}}$

EI. 94'

② Tier 2: 10.5 strands E = 21,100 ksi = 3.04×10^9 psf

$A = 10.5(.217 \text{ in}^2) = 2.28 \text{ in}^2 = .0158 \text{ ft}^2$ $d_L = 6.5'$

$L = 150' + \frac{1}{2}(30') = 165'$

$\frac{AE}{Ld_L} = \frac{(.0158)(3.04 \times 10^9)}{(165)(6.5)} = 44785 \frac{\text{lb/ft}}{\text{LF}}$

Correction for inclination: $44785 \cos 45^\circ = \boxed{31668 \frac{\text{lb/ft}}{\text{LF}}}$

EI. 82'

③ Tier 3: 11.5 strands E = 20,200 ksi = 2.91×10^9 psf

$A = 11.5(.217 \text{ in}^2) = 2.50 \text{ in}^2 = .0173 \text{ ft}^2$ $d_L = 6.5'$

$L = 128' + \frac{1}{2}(30') = 143'$

$\frac{AE}{Ld_L} = \frac{(.0173)(2.91 \times 10^9)}{(143)(6.5)} = 54161 \frac{\text{lb/ft}}{\text{LF}}$

Correction for inclination: $54161 \cos 45^\circ = \boxed{38298 \frac{\text{lb/ft}}{\text{LF}}}$

1/7/95

"Best Estimate" MOVEX Analyses

MOVEX: SHEETPILE WALL RESULT

File = 'SW-1.DAT'

<u>Stage</u>	<u>Strut Elev.</u>	<u>Max. SH Elev.</u> ^①	<u>FSBH</u>	<u>Max. SH</u>		<u>Max. Sv</u>
1	102'	100'	6.8871	.042'	=	.50"
2	90'	88'	3.1708	.108'	=	1.30"
3	78'	76'	2.2374	.283'	=	3.40"
4	72'	70'	2.0027	.384'	=	4.61"

MOVEX: DIAPHRAGM WALL RESULT

File = "DW-1.DAT"

<u>Stage</u>	<u>Strut Elev.</u>	<u>Max. SH Elev.</u> ^①	<u>FSBH</u>	<u>Max. SH</u>		<u>Max. Sv</u>
1	106'	104'	13.8337	.014'	=	.17"
2	94'	92'	3.7947	.065'	=	.78"
3	82'	80'	2.4580	.149'	=	1.79"
4	70'	68'	1.9223	.275'	=	3.30"

① - Assume 2' below strut or subgrade elev.

Sheet G7

1/7/95

PARAMETRIC ANALYSES USING MOVEX

Using "Base Case" file = SW-1.DAT
 which incorporates "best-estimate" S_u profile and
 "corrected" strut stiffnesses. - Sheetpile wall. -

- Parameters to vary:
- Depth to "firm" layer.
 - Anisotropic Strength Ratio.
 - Effective strut length.
 - Initial cantilever movement.
 - Excavation width.

1. Depth to Firm Layer.

		<u>δ_{MAX}</u>	
Base Case	Firm layer = Glaciomarine	.3844'	4.6"
FL-BR.DAT	Firm layer = Bedrock	.2164'	2.6"

2. Anisotropic Strength Ratio.

		<u>δ_{MAX}</u>	
Base Case	ASR = 1.0	.3844'	4.6"
ASR-05.DAT	ASR = 0.5	.6103'	7.3"
ASR-125.DAT	ASR = 1.25	.3422'	4.1"

3. Effective Strut Length.

		Tier	$\frac{AE \cos \theta}{L_d}$ - see p. 5	<u>δ_{MAX}</u>	
Base Case	L = FL + $\frac{1}{2}$ BL	1	19402	.3844'	4.6"
		2	58893		
		3	85683		
ESL-1.DAT	L = FL	1	23968	.3559'	4.3"
		2	80705		
		3	157,086		
ESL-2.DAT	L = FL + BL	1	16298	.4019'	4.8"
		2	46363		
		3	58907		

4. Cantilever Movement.

Based on the 5/5 and 5/19 traces of INC-101, the initial cantilever
 has magnitude = 1" (= .083') and hinge point at E1.85'
 Depth = 110' - 85' = 25'

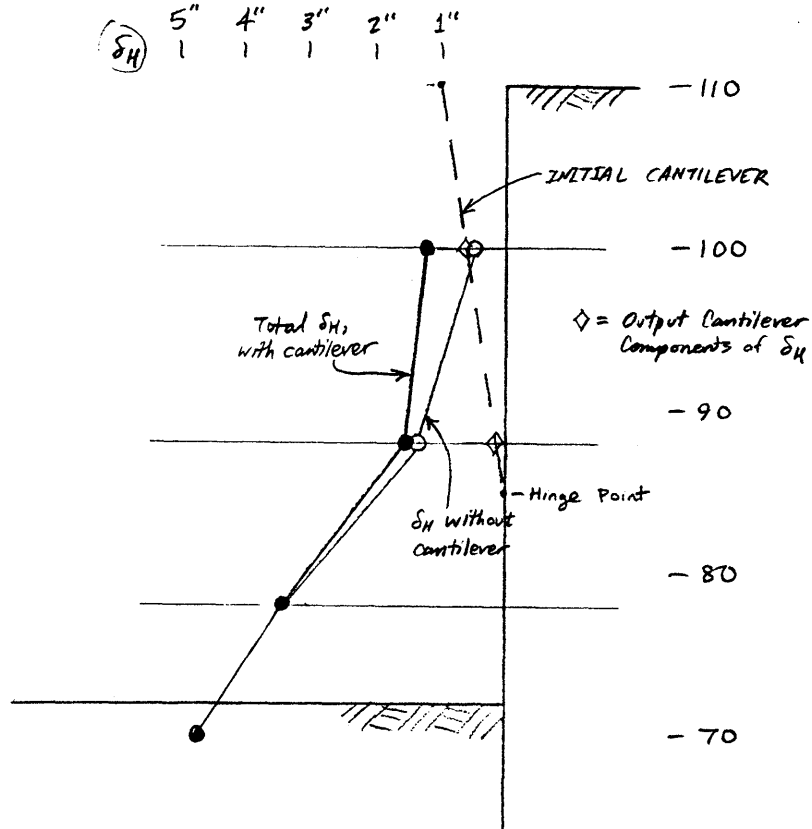
File Name: "CANT.DAT"

Stage	<u>δ_H, Wall</u>	<u>δ_H, Cantilever</u>	<u>TOTAL δ_H</u>
1	.042' = .50"	.056' = .67"	.098' = 1.18"
2	.108' = 1.30"	.017' = .20"	.125' = 1.50"
3	.283'	0	.283' = 3.40"
4	.384'	0	.384' = 4.61"

Sheet G8

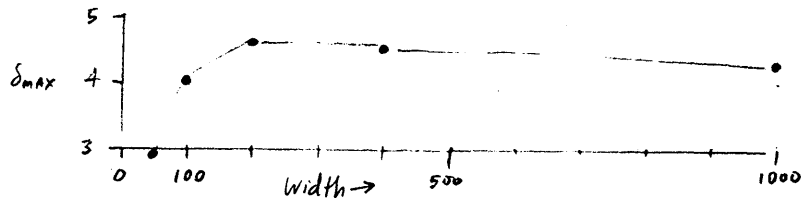
PARAMETRIC ANALYSES, continued.

4. Cantilever Movement, con't.



5. Excavation Width

	Width	S_{MAX}	
Base Case	Width = 200'	.3844'	4.61"
WIDTH-1.DAT	Width = 100'	.3354'	4.02"
WIDTH-4.DAT	Width = 400'	.3778'	4.53"
WIDTH-05.DAT	Width = 50'	.2444'	2.93"
WIDTH-10.DAT	Width = 1000'	.3579'	4.29"



1 PROGRAM MOVEX

+

, ISS-4 South Wall (Sheetpile)

0 The system of units used is English

, The units of length are - feet

, The units of stress are - psf

0 CONTROL DATA

+

, Number of soil layers 8

, Number of struts 3

, Design Option 0

, Anisotropic Strength Ratio 1.000

0 CANTILEVER EFFECT

+

0 No Cantilever Movements are Anticipated

0 SOIL LAYER DATA

+

0 Layer number 1

Thickness 4.00 Cohesion .00

Unit Weight 110.00 Coh. Increase 34.25

0 Layer number 2

Thickness 4.50 Cohesion 137.00

Unit Weight 120.00 Coh. Increase 18.00

0 Layer number 3

Thickness 15.00 Cohesion 237.00

Unit Weight 110.00 Coh. Increase 16.00

0 Layer number 4

Thickness 15.00 Cohesion 730.00

Unit Weight 108.00 Coh. Increase 4.00

0 Layer number 5

Thickness 6.50 Cohesion 1645.00

Unit Weight 116.00 Coh. Increase -14.62

0 Layer number 6

Thickness 20.00 Cohesion 1550.00

Unit Weight 116.00 Coh. Increase -2.50

0 Layer number 7

Thickness 20.00 Cohesion 1500.00

Unit Weight 116.00 Coh. Increase 2.00

0 Layer number 8

Thickness 18.00 Cohesion 1540.00

Unit Weight 116.00 Coh. Increase 5.28

0 Depth to firm layer from ground surface 103.000

0 WATER TABLE DATA

+

, Unit weight of water 63.00

0 EXCAVATION GEOMETRY

+

, Total width of excavation 200.00

, Total length of excavation 2000.00

, Final depth of excavation 38.00
 , Surcharge next to excavation .00
 Wall Stiffness (EI) .504E+08

0 STRUT DATA

Strut	Depth	Stiffness
1	8.00	.1940E+05
2	20.00	.5889E+05
3	32.00	.8568E+05

1 MOVEMENT CALCULATIONS

+
 0 Average Strut Spacing = 10.00
 Nondimensional System Stiffness = 80.00
 0 Excavation stage 1

Height of excavation is 8.000
 Factor of safety against basal heave is 6.8871
 Minimum factor of safety between stages is 6.8871
 0 Average Strut Stiffness = 19402.00
 Alpha D = 1.00
 Alpha B = 1.70
 Alpha S = 1.27
 0 Lateral Wall Movement at this Stage is .042
 Overall Maximum Lateral Wall Movement is .042
 0 Est. Distribution of Ground Surface Movement
 0 Dist. fr. Wall Vert. Disp. Lat. Disp.

.00	.0418	.0150
4.00	.0418	.0301
8.00	.0397	.0384
12.00	.0313	.0409
16.00	.0251	.0393
20.00	.0188	.0342
24.00	.0125	.0271
28.00	.0104	.0209

0 Excavation stage 2

Height of excavation is 20.000
 Factor of safety against basal heave is 3.1708
 Minimum factor of safety between stages is 3.1708
 0 Average Strut Stiffness = 39147.50
 Alpha D = 1.00
 Alpha B = 1.70
 Alpha S = 1.32
 0 Lateral Wall Movement at this Stage is .108
 Overall Maximum Lateral Wall Movement is .108
 0 Est. Distribution of Ground Surface Movement
 0 Dist. fr. Wall Vert. Disp. Lat. Disp.

.00	.1083	.0390
-----	-------	-------

10.00	.1083	.0780
20.00	.1029	.0997
30.00	.0813	.1062
40.00	.0650	.1018
50.00	.0488	.0888
60.00	.0325	.0704
70.00	.0271	.0542

0 Excavation stage 3

Height of excavation is 32.000
 Factor of safety against basal heave is 2.2374
 Minimum factor of safety between stages is 2.2374

0 Average Strut Stiffness = 54659.33
 Alpha D = 1.00
 Alpha B = 1.70
 Alpha S = 1.35

0 Lateral Wall Movement at this Stage is .283
 Overall Maximum Lateral Wall Movement is .283

0 Est. Distribution of Ground Surface Movement
 0 Dist. fr. Wall Vert. Disp. Lat. Disp.

.00	.2826	.0650
16.00	.2826	.1414
32.00	.2684	.2117
48.00	.2119	.2310
64.00	.1695	.1875
80.00	.1272	.1444
96.00	.0848	.1148
112.00	.0706	.0862

0 Excavation stage 4

Height of excavation is 38.000
 Factor of safety against basal heave is 2.0027
 Minimum factor of safety between stages is 2.0027

0 Average Strut Stiffness = 54659.33
 Alpha D = 1.00
 Alpha B = 1.70
 Alpha S = 1.38

0 Lateral Wall Movement at this Stage is .384
 Overall Maximum Lateral Wall Movement is .384

0 Est. Distribution of Ground Surface Movement
 0 Dist. fr. Wall Vert. Disp. Lat. Disp.

.00	.3844	.0693
19.00	.3844	.1563
38.00	.3652	.2411
57.00	.2883	.2467
76.00	.2306	.1882
95.00	.1730	.1358
114.00	.1153	.1027
133.00	.0961	.0726

```

1 PROGRAM MOVEX
+
, ISS-4 North Wall (Diaphragm/Slurry)
0 The system of units used is English
, The units of length are - feet
, The units of stress are - psf
0 CONTROL DATA
+
, Number of soil layers      8
, Number of struts           3
, Design Option              0
, Anisotropic Strength Ratio 1.000
0 CANTILEVER EFFECT
+
0 No Cantilever Movements are Anticipated
0 SOIL LAYER DATA
+
0 Layer number 1
  Thickness  4.00 Cohesion    .00
  Unit Weight 110.00 Coh. Increase 34.25
0 Layer number 2
  Thickness  4.50 Cohesion   137.00
  Unit Weight 120.00 Coh. Increase 18.00
0 Layer number 3
  Thickness 15.00 Cohesion   237.00
  Unit Weight 110.00 Coh. Increase 16.00
0 Layer number 4
  Thickness 15.00 Cohesion   730.00
  Unit Weight 108.00 Coh. Increase 4.00
0 Layer number 5
  Thickness  6.50 Cohesion  1645.00
  Unit Weight 116.00 Coh. Increase -14.62
0 Layer number 6
  Thickness 20.00 Cohesion  1550.00
  Unit Weight 116.00 Coh. Increase -2.50
0 Layer number 7
  Thickness 20.00 Cohesion  1500.00
  Unit Weight 116.00 Coh. Increase 2.00
0 Layer number 8
  Thickness 18.00 Cohesion  1540.00
  Unit Weight 116.00 Coh. Increase 5.28
0 Depth to firm layer from ground surface 103.000
0 WATER TABLE DATA
+
, Unit weight of water      63.00
0 EXCAVATION GEOMETRY
+
, Total width of excavation 200.00
, Total length of excavation 2000.00

```

Final depth of excavation 40.00
 Surcharge next to excavation .00
 Wall Stiffness (EI) .133E+10

0 STRUT DATA

Strut	Depth	Stiffness
1	4.00	.1693E+05
2	16.00	.3167E+05
3	28.00	.3830E+05

1 MOVEMENT CALCULATIONS

Average Strut Spacing = 12.00
 Nondimensional System Stiffness = 1018.09
 Excavation stage 1

Height of excavation is 4.000
 Factor of safety against basal heave is 13.8337
 Minimum factor of safety between stages is 13.8337
 Average Strut Stiffness = 16932.00
 Alpha D = 1.00
 Alpha B = 1.70
 Alpha S = 1.14
 Lateral Wall Movement at this Stage is .014
 Overall Maximum Lateral Wall Movement is .014
 Est. Distribution of Ground Surface Movement

Dist. fr. Wall	Vert. Disp.	Lat. Disp.
.00	.0136	.0049
2.00	.0136	.0098
4.00	.0129	.0125
6.00	.0102	.0133
8.00	.0081	.0128
10.00	.0061	.0111
12.00	.0041	.0088
14.00	.0034	.0068

0 Excavation stage 2

Height of excavation is 16.000
 Factor of safety against basal heave is 3.7947
 Minimum factor of safety between stages is 3.7947
 Average Strut Stiffness = 24300.00
 Alpha D = 1.00
 Alpha B = 1.70
 Alpha S = 1.37
 Lateral Wall Movement at this Stage is .065
 Overall Maximum Lateral Wall Movement is .065
 Est. Distribution of Ground Surface Movement

Dist. fr. Wall	Vert. Disp.	Lat. Disp.
.00	.0650	.0234

8.00	.0650	.0468
16.00	.0618	.0598
24.00	.0488	.0637
32.00	.0390	.0611
40.00	.0293	.0533
48.00	.0195	.0423
56.00	.0163	.0325

0 Excavation stage 3

Height of excavation is 28.000
 Factor of safety against basal heave is 2.4580
 Minimum factor of safety between stages is 2.4580

0 Average Strut Stiffness = 28966.00

Alpha D = 1.00

Alpha B = 1.70

Alpha S = 1.45

0 Lateral Wall Movement at this Stage is .149

Overall Maximum Lateral Wall Movement is .149

0 Est. Distribution of Ground Surface Movement

0 Dist. fr. Wall Vert. Disp. Lat. Disp.

.00	.1487	.0535
14.00	.1487	.1071
28.00	.1413	.1368
42.00	.1115	.1457
56.00	.0892	.1398
70.00	.0669	.1219
84.00	.0446	.0967
98.00	.0372	.0744

0 Excavation stage 4

Height of excavation is 40.000
 Factor of safety against basal heave is 1.9223
 Minimum factor of safety between stages is 1.9223

0 Average Strut Stiffness = 28966.00

Alpha D = 1.00

Alpha B = 1.70

Alpha S = 1.52

0 Lateral Wall Movement at this Stage is .275

Overall Maximum Lateral Wall Movement is .275

0 Est. Distribution of Ground Surface Movement

0 Dist. fr. Wall Vert. Disp. Lat. Disp.

.00	.2749	.0473
20.00	.2749	.1069
40.00	.2612	.1631
60.00	.2062	.1610
80.00	.1649	.1222
100.00	.1237	.0874
120.00	.0825	.0642
140.00	.0687	.0440

2556-1